



U.S. DEPARTMENT OF
ENERGY

Office of
Science

Program and Abstracts for the
2013
Experimental Condensed Matter Physics

Principal Investigators' Meeting

Hilton Washington DC North/Gaithersburg
Gaithersburg, Maryland
September 23–25, 2013

Materials Sciences and Engineering Division
Office of Basic Energy Sciences
US Department of Energy

This document was produced under contact number DE-AC05-06OR23100 between the U.S. Department of Energy and Oak Ridge Associated Universities.

The research grants and contracts described in this document are supported by the U.S. DOE Office of Science, Office of Basic Energy Sciences, Materials Sciences and Engineering Division.

Foreword

This book contains abstracts for presentations made at the 2013 Experimental Condensed Matter Physics Principal Investigators' Meeting sponsored by the Materials Sciences and Engineering Division of the US Department of Energy, Office of Basic Energy Sciences (DOE-BES). The purpose of the meeting is to bring together scientists supported by the DOE-BES program in Experimental Condensed Matter Physics to present the most exciting, new research accomplishments and proposed future research directions in their BES supported project. The meeting also affords PIs in the program an opportunity to see the broad range of research that is currently being supported. We hope that the meeting fostered a collegial environment that stimulated the discussion of new ideas and provided unique opportunities to develop or strengthen collaborations among PIs. In addition, the meeting provides valuable feedback to DOE-BES in their assessment of the state of the program and identifying future programmatic directions. The meeting was attended by more than 100 scientists giving both oral and poster presentations on their research. We were also pleased to have Dr. Eric Rohlffing, Acting Director for Technology at ARPA-E, present an overview of the ARPA-E program.

The Experimental Condensed Matter Physics Program covers a broad range of research activities, supporting experimental research aimed at gaining a fundamental understanding of the relationships between electronic structure, particularly in the case of strong correlation among electrons, and the properties of complex materials such as superconductors, magnetic materials and topological insulators. A particular emphasis in the program is placed on investigating the physics of one- and two-dimensional systems, including nanostructures, as well as studies of the electronic structure of materials under extreme conditions such as ultra-low temperatures and ultra-high magnetic fields. The program has a major investment in research to understand unconventional superconductors including cuprates and iron-based superconductors. In the last few years the program has increased support for research in the area of spin physics, nano-magnetism and cold atom research to provide new insights into the evolution of correlated electron behavior in condensed matter systems from atomic constituents. Improving the understanding of the electronic behavior of complex materials on the atomic scale is relevant to the DOE mission, as these materials offer enhanced properties that could lead to dramatic improvements in a broad range of technologies needed for efficient energy generation, conversion, storage, delivery, and use.

The meeting was organized into ten sessions that cover the broad range of activities supported by the program. These areas included research on correlated electrons, superconductivity, magnetism, spin physics, nano-systems, semiconductors, two dimensional electron systems, and photonics. We thank all the participants for their investment of time and for their willingness to share their ideas with the meeting participants. We also want to gratefully acknowledge the excellent support provided by Ms. Tammy Click and Ms. Joreé O'Neal of the Oak Ridge Institute for Science and Education and by Ms. Teresa Crockett of BES, for their efforts in organizing the meeting.

Dr. Andrew Schwartz
Senior Technical Advisor
Energy Frontier Research Centers
Program Manager, Expt. Condensed Matter
Physics Basic Energy Sciences

Dr. James Horwitz
Team Lead, Condensed Matter and Materials Physics
Division of Materials Sciences and Engineering
Basic Energy Sciences

Table of Contents

Foreword	i
Table of Contents	iii
Agenda	xii
Session 1	
 Atomic Engineering Oxide Heterostructures: Materials by Design	
<i>Harold Hwang, C. Bell, Y. Hikita, and S. Raghu</i>	3
 Artificially Layered Superlattice of Pnictide by Design	
<i>Chang-Beom Eom</i>	7
 Charge Inhomogeneity in Correlated Electron Systems	
<i>Barrett O. Wells</i>	11
 Interfaces in Epitaxial Complex Oxides	
<i>Hans M. Christen, H. N. Lee, T. Z. Ward, G. Eres, C. M. Rouleau, and M. Chi</i>	15
Session 2	
 Mapping the Electron Response of Nanomaterials: Probing the Electronic Structure and Dynamics of Low-Dimensional Condensed-Matter Systems Using Femtosecond Probes	
<i>R. M. Osgood and Andy Millis.....</i>	21
 Nanostructure Studies of Strongly Correlated Materials	
<i>Douglas Natelson.....</i>	25
 Probing the Origins of Conductivity Transitions in Correlated Solids: Experimental Studies of Electronic Structure in Vanadium Oxides	
<i>Kevin E. Smith.....</i>	29
 Nanostructured Materials: From Superlattices to Quantum Dots	
<i>Ivan K. Schuller</i>	33
 Spectroscopic Investigations of Novel Electronic and Magnetic Materials	
<i>Janice L. Musfeldt</i>	37

Session 3

Transport Studies of Quantum Magnetism: Physics and Methods	
<i>Minhyea Lee.....</i>	43
Thermalization of Artificial Spin Ice and Related Frustrated Magnetic Arrays	
<i>Peter Schiffer, Vincent Crespi, and Nitin Samarth.....</i>	47
Spin Wave Interactions in Metallic Ferromagnets	
<i>Kristen Buchanan.....</i>	51
Crystallite Size Effects in Permanent Magnet Materials	
<i>George C. Hadjipanayis and David J. Sellmyer.....</i>	55
Spin Physics	
<i>S.-C. Zhang, D. Goldhaber-Gordon, H. C. Manoharan, and J. Orenstein.....</i>	59

Session 4

Quantum Criticality and Unconventional Superconductivity	
<i>M. C. Aronson.....</i>	65
Emerging Materials	
<i>J. F. Mitchell, K. E. Gray, and B. J. Kim</i>	69
Understanding Iron Superconductors/Focus on Nodal Behavior	
<i>G. R. Stewart.....</i>	73
Unconventional Superconductivity in Strongly Correlated Materials	
<i>W. P. Halperin, D. Van Harlingen, A. Kapitulnik, M. R. Eskildsen, P. Dai, P. Canfield, and M. Greven</i>	77

Session 5

Optical Spectroscopy of Defects and Dopants in Nanocarbon Materials	
<i>Lukas Novotny.....</i>	83
Spectroscopy of Degenerate One-Dimensional Electrons in Carbon Nanotubes	
<i>Junichiro Kono.....</i>	87
Controlling Electronic Structure and Photophysics of Graphene	
<i>Feng Wang.....</i>	91
Infrared Optical Study of Graphene in High Magnetic Fields	
<i>Dmitry Smirnov and Zhigang Jiang.....</i>	95

Investigation of the Quantum Limit Transport Phenomena in Graphene	
<i>Philip Kim.....</i>	99

Session 6

Electronic and Optical Properties of Novel Semiconductors for Energy Applications	
<i>Angelo Mascarenhas.....</i>	105

Photonic Systems

<i>Joseph Shinar, Kai-Ming Ho, Costas Soukoulis, Rana Biswas, and Viatcheslav Dobrovitski.....</i>	109
--	-----

Ultrafast Studies of Hydrogen and Related Defects in Semiconductors and Oxides

<i>N. H. Tolk, L. C. Feldman, and G. Liipke</i>	113
---	-----

Session 7

Quantum Coherence and Random Fields at Mesoscopic Scales	
<i>Thomas F. Rosenbaum</i>	119

Spin Effects in Magnetic and Non-Magnetic Correlated Insulators

<i>Philip W. Adams.....</i>	123
-----------------------------	-----

Spin-Coherent Transport under Strong Spin-Orbit Interaction

<i>Jean J. Heremans.....</i>	127
------------------------------	-----

Magnetic Films and Nanomagnetism

<i>Axel Hoffmann</i>	131
----------------------------	-----

Nonlinear Transport in Mesoscopic Structures in the Presence of Strong Many-Body Phenomena

<i>Jonathan Bird</i>	135
----------------------------	-----

Session 8

Magneto-transport in GaAs Two-dimensional Hole Systems	
<i>M. Shayegan</i>	141

Integrated Growth and Ultra-Low Temperature Transport Study of the 2nd Landau Level of the Two-Dimensional Electron Gas

<i>Gabor Csathy and Michael Manfra</i>	145
--	-----

Experiments on Quantum Hall Topological Phases in Ultra Low Temperatures

<i>Rui-Rui Du.....</i>	149
------------------------	-----

Engineering Topological States of Matter and Search for Majorana Fermions	
<i>Leonid P. Rokhinson</i>	153

Session 9

High-Bandwidth Scanning Hall Probe Imaging of Driven Vortices in Periodic Potentials	
<i>Stuart Field</i>	159

Study of Multiband and Topological Superconductors through Electron Tunneling	
<i>Qi Li</i>	163

Thermodynamics of Strongly Correlated Fermi Gases	
<i>John E. Thomas</i>	167

Science of 100 Tesla	
<i>N. Harrison, R. D. McDonald, V. Zapf, J. Singleton, and M. Jaime</i>	171

Novel Behavior of Ferromagnet/Superconductor Hybrid Systems	
<i>Norman O. Birge and William P. Pratt, Jr.</i>	175

Session 10

Probing Nanocrystal Electronic Structure and Dynamics in the Limit of Single Nanocrystals	
<i>Moungi Bawendi</i>	181

Electromagnetic Response of Correlated Electron Systems	
<i>D. N. Basov</i>	185

Linear and Nonlinear Optical Properties of Metal-Nanoparticle Composites	
<i>Richard F. Haglund, Jr.</i>	189

Poster Sessions

Poster Session I	195
-------------------------------	-----

Poster Session II	197
--------------------------------	-----

Poster Abstracts

Experimental Studies of Correlations and Topology in Two Dimensional Electron Systems and Hybrid Structures	
<i>Eva Y. Andrei</i>	201

Novel Temperature Limited Tunneling Spectroscopy of Quantum Hall Systems <i>Raymond Ashoori</i>	205
Phase Diagram of Fe-Based Superconductors and Related Compounds at High Fields: Possible Field-Induced and Chiral Superconducting States <i>Luis Balicas</i>	209
Digital Synthesis: A Pathway to New Materials at Interfaces of Complex Oxides <i>Anand Bhattacharya and Sam Bader</i>	213
Raman Spectroscopy of Iron Oxypnictide Superconductors <i>Girsh Blumberg</i>	217
Cold Exciton Gases in Semiconductor Heterostructures <i>Leonid Butov</i>	221
Complex States, Emergent Phenomena and Superconductivity in Intermetallic and Metal-Like Compounds FWP <i>P. Canfield, S. Bud'ko, Y. Furukawa, D. Johnston, A. Kaminski, V. Kogan, R. Prozorov, and M. Tanatar</i>	225
Towards a Universal Description of Vortex Matter in Superconductors <i>L. Civale</i>	229
Quantum Materials at the Nanoscale <i>Peter Abbamonte, Alexey Bezryadin, Raffi Budakian, S. Lance Cooper, James N. Eckstein, Eduardo H. Fradkin, Laura H. Greene, Taylor Hughes, Anthony J. Leggett, Nadya Mason, Dale J. Van Harlingen, and Smitha Vishveshwara</i>	233
Spin Polarized Electron Transport through Aluminum Nanoparticles <i>Dragomir Davidovic</i>	237
Spectroscopic Imaging STM and Complex Electronic Matter <i>J. C. Séamus Davis</i>	241
Competing Interactions in Complex Transition Metal Oxides <i>L. E. De Long, Gang Cao, J. Todd Hastings, and S. S. Seo</i>	245
Infrared Hall Effect in Correlated Electronic Materials <i>H. Dennis Drew</i>	249
Microwave Spectroscopy of Electron Solids: Fractional Quantum Hall Effect and Controlled Disorder <i>Lloyd W. Engel</i>	253

Symmetries, Interactions, and Correlation Effects in Carbon Nanotubes	
<i>Gleb Finkelstein</i>	257
Magnetic Materials	
<i>P. Fischer, C. S. Fadley, F. Hellman, J. B. Kortright, W. Chao, E. H. Anderson, E. M. Gullikson, and P. Naulleau</i>	261
Tunneling and Transport in Nanowires	
<i>Allen M. Goldman</i>	265
Conductivity and Magnetism in Strongly Coupled Quantum Dot Solids	
<i>Philippe Guyot-Sionnest</i>	269
Investigation and Manipulation of Nanoscale Molecular Superconductivity	
<i>Saw Wai Hla</i>	273
Quantum Transport in Topological Insulator Nanoelectronic Devices	
<i>Pablo Jarillo-Herrero</i>	277
Electron Spectroscopy	
<i>P. D. Johnson and C. Homes</i>	281
Superconductivity and Magnetism	
<i>W.-K. Kwok, U. Welp, A. E. Koshelev, V. Vlasko-Vlasov, G. W. Crabtree, and Z. L. Xiao</i>	285
Spontaneous and Field-Induced Symmetry Breaking in Low Dimensional Nanostructures	
<i>Chun Ning (Jeanie) Lau and Marc Bockrath</i>	289
Experimental Study of Severely Underdoped Ultrathin Cuprate Films	
<i>Thomas R. Lemberger</i>	293
Probing High Temperature Superconductors with Magnetometry in Ultrahigh Magnetic Fields	
<i>Lu Li</i>	297
Engineering of Mixed Pairing and Non-Abelian Quasiparticle States of Matter in Chiral <i>p</i>-wave Superconductor Sr₂RuO₄	
<i>Ying Liu</i>	301
Time-Resolved Spectroscopy of Insulator-Metal Transitions: Exploring Low-Energy Dynamics in Strongly Correlated Systems	
<i>Gunter Lüpke</i>	305

Magnetotransport Studies of the Low Dimensional Electron System	
<i>R. G. Mani</i>	309
Superconductivity and Magnetism in d- and f-electron Materials	
<i>M. Brian Maple</i>	313
Quantum Materials	
<i>Joseph W. Orenstein, Robert Birgeneau, Edith Bourret, Alessandra Lanzara, Dung-Hai Lee, Joel Moore, Ashvin Vishwanath, Ramamoorthy Ramesh, and James Analytis</i>	317
Exploring Photon-Coupled Fundamental Interactions in Colloidal Semiconductor Based Hybrid Nanostructures	
<i>Min Ouyang</i>	321
Non-Centrosymmetric Topological Superconductivity	
<i>Johnpierre Paglione</i>	325
Quantum Electronic Phenomena and Structures	
<i>W. Pan, M. P. Lilly, J. L. Reno, G. T. Wang, R. Prasankumar, E. A. Shaner, and D. C. Tsui</i>	329
Magnetic Nanostructures and Spintronic Materials	
<i>Michael Pechan</i>	333
Artificially Structured Semiconductors to Model Novel Quantum Phenomena	
<i>A. Pinczuk, S. J. Wind, and V. Pellegrini</i>	337
Correlated and Complex Materials	
<i>B. C. Sales, D. Mandrus, M. A. McGuire, C. Cantoni, and L. A. Boatner</i>	341
Origin of Superconductivity in Structurally Layered Materials	
<i>Athena S. Sefat</i>	345
Fundamental Studies of Anisotropic Nanomagnets	
<i>David J. Sellmyer, Ralph Skomski, and George Hadjipanayis</i>	349
Spin-Polarized Scanning Tunneling Microscopy Studies of Nanoscale Magnetic and Spintronic Nitride Systems	
<i>Arthur R. Smith and Jeongihm Pak</i>	353
Electronic Complexity of Epitaxial Rutile Heterostructures	
<i>H. H. Weitering, P. C. Snijders, and P. R. C. Kent</i>	357
Imaging Electrons in Atomically Layered Materials	
<i>R. M. Westervelt</i>	361

Investigation of Spin Physics in Semiconductor Nanowire-Based Heterostructures <i>Fengyuan Yang and Ezekiel Johnston-Halperin</i>	365
Probing Correlated Superconductors and Their Phase Transitions on the Nanometer Scale <i>Ali Yazdani</i>	369
Novel sp²-Bonded Materials and Related Nanostructures <i>A. Zettl, C. Bertozi, M. L. Cohen, M. Crommie, A. Lanzara, S. Louie, and F. Wang</i>	373
Emergent Phenomena in Quantum Hall Systems Far From Equilibrium <i>Michael Zudov</i>	377
Author Index	383
Participant List	387

Experimental Condensed Matter Physics Principal Investigators' Meeting

AGENDA

Monday, September 23, 2013

7:30 – 8:15 am	***** <i>Breakfast</i> *****
8:15 – 8:35 am	BES Welcome Andy Schwartz and Jim Horwitz <i>Program Managers, Experimental Condensed Matter Physics and Condensed Matter and Materials Physics</i>
Session 1	Chair: Athena Sefat, ORNL
8:35 – 8:55 am	Harold Hwang (SLAC) <i>Atomic Engineering Oxide Heterostructures: Materials by Design</i>
8:55 – 9:15 am	Chang-Beom Eom (Wisconsin) <i>Artificially Layered Superlattice of Pnictide by Design</i>
9:15 – 9:35 am	Barrett Wells (Connecticut) <i>Charge Inhomogeneity in Correlated Electron Systems</i>
9:35 – 9:55 am	Hans Christen (ORNL) <i>Interfaces in Epitaxial Complex Oxides</i>
9:55 – 10:25 am	***** <i>Break</i> *****
Session 2	Chair: Nadya Mason, Illinois
10:25 – 10:45 am	Richard Osgood (Columbia) <i>Mapping the Electron Response of Nanomaterials: Probing the Electronic Structure and Dynamics of Low-Dimensional Condensed-Matter Systems Using Femtosecond Probes</i>
10:45 – 11:05 am	Douglas Natelson (Rice) <i>Nanostructure Studies of Strongly Correlated Materials</i>
11:05 – 11:25 am	Kevin Smith (Boston Univ.) <i>Probing the Origins of Conductivity Transitions in Correlated Solids</i>
11:25 – 11:45 am	Ivan Schuller (UCSD) <i>Nanostructured Materials: From Superlattices to Quantum Dots</i>
11:45 – 12:05 pm	Jan Musfeldt (UTK) <i>Spectroscopic Investigations of Novel Electronic and Magnetic Materials</i>

12:05 – 1:30 pm ******* Working Lunch *******

Session 3	Chair: Michael Pechan, Miami of Ohio
1:30 – 1:50 pm	Minhyea Lee (Colorado) <i>Transport Studies of Quantum Magnetism: Physics and Methods</i>
1:50 – 2:10 pm	Peter Schiffer (UIUC) <i>Thermalization of Artificial Spin Ice and Related Frustrated Magnetic Arrays</i>
2:10 – 2:30 pm	Kristen Buchanan (Colorado State) <i>Spin Wave Interactions in Metallic Ferromagnets</i>
2:30 – 2:50 pm	George Hadjipanayis (Delaware) <i>Crystallite Size Effects in Permanent Magnet Materials</i>
2:50 – 3:10 pm	David Goldhaber-Gordon (SLAC) <i>Spin Physics</i>
3:10 – 3:40 pm	***** Break *****

Session 4	Chair: Brian Maple, UCSD
3:40 – 4:00 pm	Meigan Aronson (BNL) <i>Quantum Criticality and Unconventional Superconductivity</i>
4:00 – 4:20 pm	John Mitchell (ANL) <i>Emerging Materials</i>
4:20 – 4:40 pm	Greg Stewart (Florida) <i>Understanding Iron Superconductors/Focus on Nodal Behavior</i>
4:40 – 5:00 pm	William Halperin (Northwestern) <i>Unconventional Superconductivity in Strongly Correlated Materials</i>
5:10 - 5:40 pm	Poster Introductions
5:40 – 6:00 pm	***** Break *****
6:00 – 7:30 pm	***** Working Dinner *****
7:30 – 9:30 pm	Poster Session I

Tuesday, September 24, 2013

7:30 – 8:30 am

***** **Breakfast** *****

Session 5

Chair: Alex Zettl, LBNL

8:30 – 8:50 am

Lukas Novotny (Rochester)

Optical Spectroscopy of Defects and Dopants in Nanocarbon Materials

8:50 – 9:10 am

Junichiro Kono (Rice)

Spectroscopy of Degenerate One-Dimensional Electrons in Carbon Nanotubes

9:10 – 9:30 am

Feng Wang (UC Berkeley)

Controlling Electronic Structure and Photophysics of Graphene

9:30 – 9:50 am

Dmitry Smirnov

Infrared Optical Study of Graphene in High Magnetic Fields

9:50 – 10:10 am

Philip Kim (Columbia)

Investigation of the Quantum Limit Transport Phenomena in Graphene

10:10 – 10:40 am

***** **Break** *****

Session 6

Chair: Aron Pinczuk, Columbia

10:40 – 11:00 am

Angelo Mascarenhas (NREL)

Electronic and Optical Properties of Novel Semiconductors for Energy Applications

11:00 – 11:20 am

Joseph Shinar (Ames)

Photonic Systems

11:20 – 11:40 am

Norman Tolk (Vanderbilt)

Ultrafast Studies of Hydrogen and Related Defects in Semiconductors and Oxides

11:40 – 12:00 pm

Invited talk:

Eric Rohlfsing (Acting Director for Technology)

An Overview of ARPA-E

12:00 – 1:30 pm

***** **Working Lunch** *****

Session 7

Chair: Art Smith, Ohio

1:30 – 1:50 pm

Thomas Rosenbaum (Chicago)

Quantum Coherence and Random Fields at Mesoscopic Scales

1:50 – 2:10 pm	Philip Adams (LSU) <i>Spin Effects in Magnetic and Non-Magnetic Correlated Insulators</i>
2:10 – 2:30 pm	Jean Heremans (Virginia Tech) <i>Spin-Coherent Transport under Strong Spin-Orbit Interaction</i>
2:30 - 2:50 pm	Axel Hoffmann (Bader) (ANL) <i>Magnetic Films and Nanomagnetism</i>
2:50 - 3:10 pm	Jonathan Bird (Buffalo) <i>Nonlinear Transport in Mesoscopic Structures in the Presence of Strong Many-Body Phenomena</i>
3:10 - 3:40 pm	***** Break *****

Session 8	Chair: Ray Ashoori (MIT)
3:40 – 4:00 pm	Mansour Shayegan (Princeton) <i>Magneto-transport in GaAs Two-dimensional Hole Systems</i>
4:00 – 4:20 pm	Gabor Csathy (Purdue) <i>Integrated Growth and Ultra-Low Temperature Transport Study of the 2nd Landau Level of the Two-Dimensional Electron Gas</i>
4:20 – 4:40 pm	Rui-Rui Du (Rice) <i>Experiments on Quantum Hall Topological Phases in Ultra Low Temperatures</i>
4:40 – 5:00 pm	Leonid Rokhinson (Purdue) <i>Engineering Topological States of Matter and Search for Majorana Fermions</i>
5:00 - 5:40 pm	Poster Introductions
5:40 – 6:00 pm	***** Break *****
6:00 – 7:30 pm	***** Working Dinner *****
7:30 – 9:30 pm	Poster Session II

Wednesday, September 25, 2013

7:30 – 8:30 am

***** **Breakfast** *****

Session 9

Chair: Dennis Drew, UMD

8:30 – 8:50 am

Stuart Field (Colorado State)

High-Bandwidth Scanning Hall Probe Imaging of Driven Vortices in Periodic Potentials

8:50 – 9:10 am

Qi Li (Penn State)

Study of Multiband and Topological Superconductors through Electron Tunneling

9:10 – 9:30 am

John Thomas (NC State)

Thermodynamics of Strongly Correlated Fermi Gases

9:30 – 9:50 am

Neil Harrison (LANL)

Science of 100 Tesla

9:50 – 10:10 am

Norman Birge (Michigan State)

Novel Behavior of Ferromagnet/Superconductor Hybrid Systems

10:10 – 10:40 am

***** **Break** *****

Session 10

Chair: Zeke Johnston-Halperin, Ohio State

10:40 – 11:00 am

Moungi Bawendi (MIT)

Probing Nanocrystal Electronic Structure and Dynamics in the Limit of Single Nanocrystals

11:00 – 11:20 am

Dmitri Basov (UCSD)

Electromagnetic Response of Correlated Electron Systems

11:20 – 11:40 am

Richard Haglund (Vanderbilt)

Linear and Nonlinear Optical Properties of Metal-Nanoparticle Composites

11:40 – 12:00 pm

BES Conclusion

Andy Schwartz and Jim Horwitz

Program Managers, Experimental Condensed Matter Physics and Condensed Matter and Materials Physics

12:00 – 1:00 pm

Lunch, Open Discussions, and Adjourning Comments

(Optional Box Lunches Available)

Session 1

Program Title: Atomic Engineering Oxide Heterostructures: Materials by Design

Principle Investigator: H. Y. Hwang^{1,2*}; Co-PIs: C. Bell¹, Y. Hikita¹, and S. Raghu^{1,3}

¹*Stanford Institute for Materials & Energy Sciences, SLAC National Accelerator Laboratory, Menlo Park, CA 94025*

²*Department of Applied Physics, Stanford University, Stanford, CA 94305*

³*Department of Physics, Stanford University, Stanford, CA 94305*

*hyhwang@slac.stanford.edu

Program Scope

A central aim of modern materials research is the control of materials and their interfaces to atomic dimensions. In the search for emergent phenomena and ever greater functionality in devices, transition metal oxides have enormous potential. They host a vast array of properties, such as orbital ordering, unconventional superconductivity, magnetism, and ferroelectricity, as well as (quantum) phase transitions and couplings between these states. Our broad objective is to develop the science and technology arising at interfaces between these novel materials. Using atomic scale growth techniques we explore the synthesis and properties of novel interface phases. Magnetotransport, x-ray, and scanning probes are used to determine the static and dynamic electronic and magnetic structure. Heterostructures with low-density superconductors are developed to explore new regimes of low-dimensional superconductivity, particularly in the presence of tunable spin-orbit coupling. Surface and interface couplings are used to engineer band alignments and control their physical properties. The experimental efforts are guided and analyzed theoretically, particularly with respect to x-ray scattering, superconductivity, and new states of emergent order. A wide set of tools, ranging from analytic field theory methods to exact computational treatments, are applied towards the rational design of heterostructures.

Recent Progress

- We performed first spectroscopic studies of the magnetism at the LaAlO₃/SrTiO₃ interface using element-specific techniques, including x-ray magnetic circular dichroism and x-ray absorption spectroscopy, along with corresponding model calculations. We find direct evidence for in-plane ferromagnetic order at the interface, with Ti³⁺ character in the d_{xy} orbital of the anisotropic t_{2g} band. These findings establish a striking example of emergent phenomena at oxide interfaces, since no bulk analog of magnetism exists in the constituent materials. They further have important implications for other LaAlO₃/SrTiO₃ interface properties, such as the nature of the coexisting superconducting state, which must occur in the presence of this polarized orbital. We pursue a combined theoretical and experimental understanding of aspects of interfacial superconductivity.
- We developed a theory of the Kerr effect in the pseudogap regime of the cuprates which shows explicitly that time-reversal symmetry breaking is not a necessary ingredient. Instead, density wave orders (charge density waves, spin density waves, d-density waves) can produce the Kerr response provided that there is a chirality associated with these orders. This phenomenological work resolves a five year old mystery in the field and helps synthesize the Kerr measurements in the pseudogap regime with the observation of Fermi surface

reconstruction, anomalous Nernst effects, and observation of incommensurate density wave order in soft x-ray studies as well as in NMR.

- Extensive investigations were performed in the fine control and mobility optimization of the interface electrons in $\text{LaAlO}_3/\text{SrTiO}_3$. Approaches include the variation in the cation stoichiometry of the grown LaAlO_3 film, the modification of the surface via surface charge writing using an AFM as well as surface adsorbates, and the development of top-gate device geometries. We find universal scaling of the mobility with electron density.
- We developed a theoretical strategy to enhance the superconducting transition temperature of unconventional superconductors by coupling metallic screening agents capacitively to the correlated metal that hosts superconductivity. The metallic screening layer weakens the role of longer range repulsive forces between electrons resulting in higher transition temperatures.
- We have initiated a project which involves close interplay between experiments and theoretical modeling to understand the role of spin-orbit coupling and orbital degeneracy in semiconductor perovskites. Initial focus is on doped SrTiO_3 , but can be readily extended to KTaO_3 and other materials. Simplified effective tight-binding descriptions are developed to model recent high resolution quantum oscillation measurements.
- We have studied the band alignment at heterointerfaces across the metal-insulator transition of $(\text{La},\text{Sr})\text{MnO}_3$, both in terms of their electrical properties (I-V, C-V) and spectroscopically (internal/core-level photoemission, electron energy-loss). A clear crossover is observed, corresponding to reconstructions of the polar discontinuity evolving to metallic screening.
- We developed well-controlled quantum field theory descriptions of 3 dimensional metals near a ferromagnetic quantum critical point. We show how the fermionic quasiparticles have a life-time much smaller than their energy, making the system a genuine non-Fermi liquid. Current work shows promising new renormalization group fixed points below 3 dimensions, which have implications for 2d metals near quantum critical points.
- Bilayer superconducting heterostructures based on delta-doped SrTiO_3 have been systematically investigated in terms of the angular variation of the upper critical field. Systematic coupling between the superconductors has been observed, from the decoupled limit at wide separations, to increasing coupling on the length scale of the superconducting coherence length. This suggests a novel approach to designing multicomponent superconductivity using the subband structure in quantum wells.

Future Plans

Further experimental development of these materials systems, as well as the anatase/perovskite interface we have recently explored, are planned. Theoretical progress is expected on understanding non-Fermi liquid metals and the physics of the half-filled Landau level. Increasing efforts combining theory and experiment are planned to analyze quantum oscillations measurements in oxide interfaces and heterostructures. In addition, a new mutual inductance probe will be developed to measure the superfluid density in thin films structures.

Numerical quantum Monte Carlo studies of Hubbard and Kondo models are planned, to examine dynamical properties, and continue work on interfacial enhancement of superconducting Tc. X-ray probes of magnetic reconstructions in ultrathin magnetic oxide films are planned, first to examine static properties, and eventually dynamical response. Increasing efforts to study magnetotransport in oxides on mesoscopic length scales are planned.

Publications

1. M. Kim, C. Bell, Y. Kozuka, M. Kurita, Y. Hikita, and H. Y. Hwang, "Fermi Surface and Superconductivity in Low-Density High-Mobility δ -Doped SrTiO₃," *Phys. Rev. Lett.* **107**, 106801 (2011). NPG Asia Materials featured highlight doi:10.1038/asiamat.2011.171.
2. B. Kim, D. Kwon, T. Yajima, C. Bell, Y. Hikita, B. G. Kim, and H. Y. Hwang, "Reentrant Insulating State in Ultrathin Manganite Films," *Appl. Phys. Lett.* **99**, 092513 (2011).
3. J. A. Bert, B. Kalisky, C. Bell, M. Kim, Y. Hikita, H. Y. Hwang, and K. A. Moler, "Direct Imaging of the Coexistence of Ferromagnetism and Superconductivity at the LaAlO₃/SrTiO₃ Interface," *Nature Phys.* **7**, 767 (2011). N & V by A. J. Millis, *Nature Phys.* **7**, 749 (2011).
4. Y. W. Xie, Y. Hikita, C. Bell, and H. Y. Hwang, "Control of Electronic Conduction at an Oxide Heterointerface Using Surface Polar Adsorbates," *Nature Commun.* **2**, 494 (2011).
5. M. Takizawa, S. Tsuda, T. Susaki, H. Y. Hwang, and A. Fujimori, "Electronic Charges and Electric Potential at LaAlO₃/SrTiO₃ Interfaces Studied by Core-Level Photoemission Spectroscopy," *Phys. Rev. B* **84**, 245124 (2011).
6. H. Y. Hwang, Y. Iwasa, M. Kawasaki, B. Keimer, N. Nagaosa, and Y. Tokura, "Emergent Phenomena at Oxide Interfaces," *Nature Mater.* **11**, 103 (2012).
7. Y. Kozuka, A. Tsukazaki, D. Maryenko, J. Falson, C. Bell, M. Kim, Y. Hikita, H. Y. Hwang, and M. Kawasaki, "Single-Valley Quantum Hall Ferromagnet in a Dilute Mg_xZn_{1-x}O/ZnO Two-Dimensional Electron System," *Phys. Rev. B* **85**, 075302 (2012).
8. P. D. C. King, R. H. He, T. Eknapakul, S.-K. Mo, Y. Kaneko, S. Harashima, Y. Hikita, M. S. Bahramy, C. Bell, Z. Hussain, Y. Tokura, Z.-X. Shen, H. Y. Hwang, F. Baumberger, and W. Meevasana, "Subband Structure of a Two-Dimensional Electron Gas Formed at the Polar Surface of the Strong Spin-Orbit Perovskite KTaO₃," *Phys. Rev. Lett.* **108**, 117602 (2012).
9. B. Kalisky, J. A. Bert, B. B. Klopfer, C. Bell, H. K. Sato, M. Hosoda, Y. Hikita, H. Y. Hwang, and K. A. Moler, "Critical Thickness for Ferromagnetism in LaAlO₃/SrTiO₃ Heterostructure," *Nature Commun.* **3**, 922 (2012).
10. T. Tachikawa, M. Minohara, Y. Nakanishi, Y. Hikita, M. Yoshita, H. Akiyama, C. Bell, and H. Y. Hwang, "Metal-to-Insulator Transition in Anatase TiO₂ Thin Films Induced by Growth Rate Modulation," *Appl. Phys. Lett.* **101**, 022104 (2012).
11. J. R. Kirtley, B. Kalisky, J. A. Bert, C. Bell, M. Kim, Y. Hikita, H. Y. Hwang, J. H. Ngai, Y. Segal, F. J. Walker, C. H. Ahn, and K. A. Moler, "Scanning SQUID Susceptometry of a Paramagnetic Superconductor," *Phys. Rev. B* **85**, 224518 (2012).
12. S. Raghu, R. Thomale, and T. H. Geballe, "Optimal T_c of Cuprates: Role of Screening and Reservoir Layers," *Phys. Rev. B* **86**, 094506 (2012).
13. B. Kalisky, J. A. Bert, C. Bell, Y. W. Xie, H. K. Sato, M. Hosoda, Y. Hikita, H. Y. Hwang, and K. A. Moler, "Scanning Probe Manipulation of Nanomagnetism at the LaAlO₃/SrTiO₃ Heterointerface," *Nano Lett.* **12**, 4055 (2012).

14. J. A. Bert, K. C. Nowack, B. Kalisky, H. Noad, J. R. Kirtley, C. Bell, H. K. Sato, M. Hosoda, Y. Hikita, H. Y. Hwang, and K. A. Moler, "Measurements of the Gate Tuned Superfluid Density in Superconducting $\text{LaAlO}_3/\text{SrTiO}_3$," *Phys. Rev. B(RC)* **86**, 060503 (2012). Editors' Suggestion.
15. M. Kim, Y. Kozuka, C. Bell, Y. Hikita, and H. Y. Hwang, "Intrinsic Spin-Orbit Coupling in Superconducting δ -Doped SrTiO_3 Heterostructures," *Phys. Rev. B* **86**, 085121 (2012).
16. E. Flekser, M. Ben Shalom, M. Kim, C. Bell, Y. Hikita, H. Y. Hwang, and Y. Dagan, "Magnetotransport Effects in Polar versus Non-polar SrTiO_3 Based Heterostructures," *Phys. Rev. B(RC)* **86**, 121104 (2012).
17. T. Higuchi and H. Y. Hwang, "General Considerations of the Electrostatic Boundary Conditions in Oxide Heterostructures," in *Multifunctional Oxide Heterostructures*, edited by E. Tsymbal, C. B. Eom, R. Ramesh, and E. Dagotto, pp. 183-213, Oxford University Press (2012) (arXiv: 1105.5779).
18. K. G. Rana, T. Yajima, S. Parui, A. F. Kemper, T. P. Devereaux, Y. Hikita, H. Y. Hwang, and T. Banerjee, "Hot Electron Transport in a Strongly Correlated Transition Metal Oxide," *Scientific Reports* **3**, 1274 (2013).
19. C. Bell, M. S. Bahramy, H. Murakawa, J. G. Checkelsky, R. Arita, Y. Kaneko, Y. Onose, M. Tokunaga, Y. Kohama, N. Nagaosa, Y. Tokura, and H. Y. Hwang, "Shubnikov-de Haas Oscillations in the Bulk Rashba Semiconductor BiTeI," *Phys. Rev. B(RC)* **87**, 081109 (2013).
20. M. Sakano, M. S. Bahramy, A. Katayama, T. Shimojima, H. Murakawa, Y. Kaneko, W. Malaeb, S. Shin, K. Ono, H. Kumigashira, R. Arita, N. Nagaosa, H. Y. Hwang, Y. Tokura, and K. Ishizaka, "Strongly Spin-Orbit Coupled Two-Dimensional Electron Gas Emerging near the Surface of Polar Semiconductors," *Phys. Rev. Lett.* **110**, 107204 (2013).
21. M. Hosoda, C. Bell, Y. Hikita, and H. Y. Hwang, "Composition and Gate Tuned Interfacial Conductivity in $\text{LaAlO}_3/\text{LaTiO}_3/\text{SrTiO}_3$ Heterostructures," *Appl. Phys. Lett.* **102**, 091601 (2013).
22. P. Hosur, A. Kapitulnik, S. A. Kivelson, J. Orenstein, and S. Raghu, "Kerr Effect as Evidence of Gyrotropic Order in the Cuprates," *Phys. Rev. B* **87**, 115116 (2013).
23. J.-S. Lee, Y. W. Xie, H. K. Sato, C. Bell, Y. Hikita, H. Y. Hwang, and C.-C. Kao, "Titanium d_{xy} Ferromagnetism at the $\text{LaAlO}_3/\text{SrTiO}_3$ Interface," *Nature Mater.* DOI: 10.1038/NMAT3674 (2013).
24. S. Chakraverty, X. Yu, M. Kawasaki, Y. Tokura, and H. Y. Hwang, "Spontaneous B-Site Order and Metallic Ferrimagnetism in LaSrVMO_6 Grown by Pulsed Laser Deposition," *Appl. Phys. Lett.* **102**, 222406 (2013).
25. Y. W. Xie, C. Bell, Y. Hikita, S. Harashima, and H. Y. Hwang, "Enhancing Electron Mobility at the $\text{LaAlO}_3/\text{SrTiO}_3$ Interface by Surface Control," *Adv. Mater.* DOI: 10.1002/adma.201301798 (2013).
26. H. K. Sato, C. Bell, Y. Hikita, and H. Y. Hwang, "Stoichiometry Control of the Electronic Properties of the $\text{LaAlO}_3/\text{SrTiO}_3$ Heterointerface," *Appl. Phys. Lett.* **102**, 251602 (2013).
27. Y. Yamada, H. K. Sato, Y. Hikita, H. Y. Hwang, and Y. Kanemitsu, "Measurement of the Femtosecond Optical Absorption of $\text{LaAlO}_3/\text{SrTiO}_3$ Heterostructures: Evidence for an Extremely Slow Electron Relaxation at the Interface," *Phys. Rev. Lett.* **111**, 047403 (2013).
28. S. Harashima, C. Bell, M. Kim, T. Yajima, Y. Hikita, and H. Y. Hwang, "Coexistence of Two- and Three-Dimensional Shubnikov-de Haas Oscillations in Ar^+ -Irradiated KTaO_3 ," *Phys. Rev. B* **88**, 085102 (2013).

Program Title: Artificially Layered Superlattice of Pnictide by Design

Principle Investigator: Chang-Beom Eom

Mailing Address: Room 2164 ECB, 1550 Engineering Drive, University of Wisconsin-Madison, Madison, WI 53706

E-mail: eom@engr.wisc.edu

Program Scope

The goals of the program are to grow artificially engineered superlattices of pnictide materials by atomic layer-controlled growth, and to understand how structure property-relationships interact with the novel superconductivity in the pnictides so as to develop new understanding, applications, and devices. The critical scientific issues we will address include growth mechanisms, interaction between superconductivity and magnetism, interfacial superconductivity and physics of flux pinning in pnictide thin film heterostructures. We expect that this goal will also enable an understanding of the fundamental heteroepitaxial growth of intermetallic systems on oxide surfaces and role of interfacial layers in a sufficiently general way that can be applied broadly to many different material systems.

The discovery of superconductivity with transition temperatures of 20K-50K in iron-based materials has initiated a flurry of activity to understand and apply these novel materials. The superconducting mechanism, the structural transitions, the magnetic behavior above and below T_c , the doping dependence, and the critical current and flux-pinning behavior have all been recognized as critical to progress toward understanding the pnictides. A fundamental key to both basic understanding and applications is the growth and control of high-quality epitaxial thin films and superlattices with atomic layer control. The ability to control the orientation, the strain state, defect and pinning site incorporation, the surface and interfaces, and the layering at the atomic scale, are crucial in the study and manipulation of superconducting properties.

An important characteristic of the Co-doped BaFe₂As₂ (Ba-122) material is the relatively low values of doping required to produce superconductivity. This leads to homogeneous films, and similar lattice constants between differently doped films, and great potential for epitaxial superlattices. The 122 materials share the fundamental iron-containing planes that are believed to be responsible for superconductivity, and they potentially all share the same basic mechanism of superconductivity, with a leading candidate being s^+ pairing between electron and hole pockets at the zone center and boundary. All share the five Fe 3d-orbitals important in the electronic structure, leading to a richness that has great potential for manipulation. In addition, the likely coexistence of magnetism and superconductivity for low-doping, and the nearby structural transitions in the intermediate-doping region, offer great flexibility in the design of new superlattices of, for instance, doped 122 and perovskite oxides, 122 layers of different doping levels, and doped 122 layers with the semi-metallic undoped parent compound.

We are guided to the main goals by our understanding developed over the last three years in relating pnictide structural and superconducting properties. The new film growth methods used in this project enables us to not only resolve these uncertainties, but also to design and synthesize new pnictide atomic layered structures that explore the limits of this material's superconducting properties. The **thrusts** of our project are:

- (1) *Atomic-layer-controlled growth of artificially engineered superlattice synthesis*
- (2) *Designing interfacial superconductivity at pnictide and FeSe interfaces.*
- (3) *Investigation of interaction between superconductivity and magnetism by proximity effect*
- (4) *Understanding and control of flux-pinning mechanisms*
- (5) *Study of growth mechanisms of heteroepitaxial superlattices and artificial pinning centers*

Recent Progress

Artificial layered superlattices offer unique opportunity towards tailoring superconducting properties and understanding the mechanisms of superconductivity by creating model structures which do not exist in nature. We have successfully demonstrated the growth of two different types of artificially engineered superlattices of pnictide superconductor by pulsed laser deposition. First, we have grown a structurally modulated SrTiO_3 (STO) / Co-doped Ba-122 superlattice with sharp interfaces. The epitaxial crystalline quality and modulation wavelength (Λ) of the superlattices were determined by four-circle x-ray diffraction (XRD). Figure 1a shows the θ - 2θ scan of the $(\text{STO}_{1.2 \text{ nm}} / 8 \% \text{ Co-doped Ba-122}_{13 \text{ nm}})^n$ ($n=24$) superlattice (STO SL) on 40 nm STO templates deposited on (001) $(\text{La},\text{Sr})(\text{Al},\text{Ta})\text{O}_3$ (LSAT) substrates. Figure 1(b) is a magnification of Fig. 1(a) close to the 002 reflection of the STO SL which clearly shows satellite peaks with calculated modulation length $\Lambda = 14 \text{ nm} \pm 2 \text{ nm}$ the same as the nominal Λ . We have also grown oxygen-rich undoped BaFe_2As_2 (Ba-122) / Co-doped Ba-122 compositionally modulated superlattices.

To investigate the microstructure of STO and O-Ba-122 SLs, transmission electron microscopy (TEM) was used. Figure 2a, b show cross sectional low and high magnification high-angle annular dark field (HAADF) images of STO SL. In Fig. 1(c), bright and dark layers correspond to 13 nm Co-doped Ba-122 layer and 1.2 nm STO layer, respectively. We can clearly see that there are 24 STO / Co-doped Ba-122 bi-layers and Λ is 14 nm in accordance with our design and the modulation wavelength determined by x-ray diffraction. Figure 2d is a cross-sectional TEM image of the O-Ba-122 SL, which clearly shows 24 bilayers and the modulation wavelength $\Lambda=16 \text{ nm}$. The interface O-Ba-122 layers have grown as laterally aligned but discontinuous second phase nano particles of several nm size. The structure of the O-Ba-122 SL is more desirable than the structure of the STO SL for flux pinning, since the O-Ba-122 SL has structural defects in both *c*- and *ab*-axis directions.

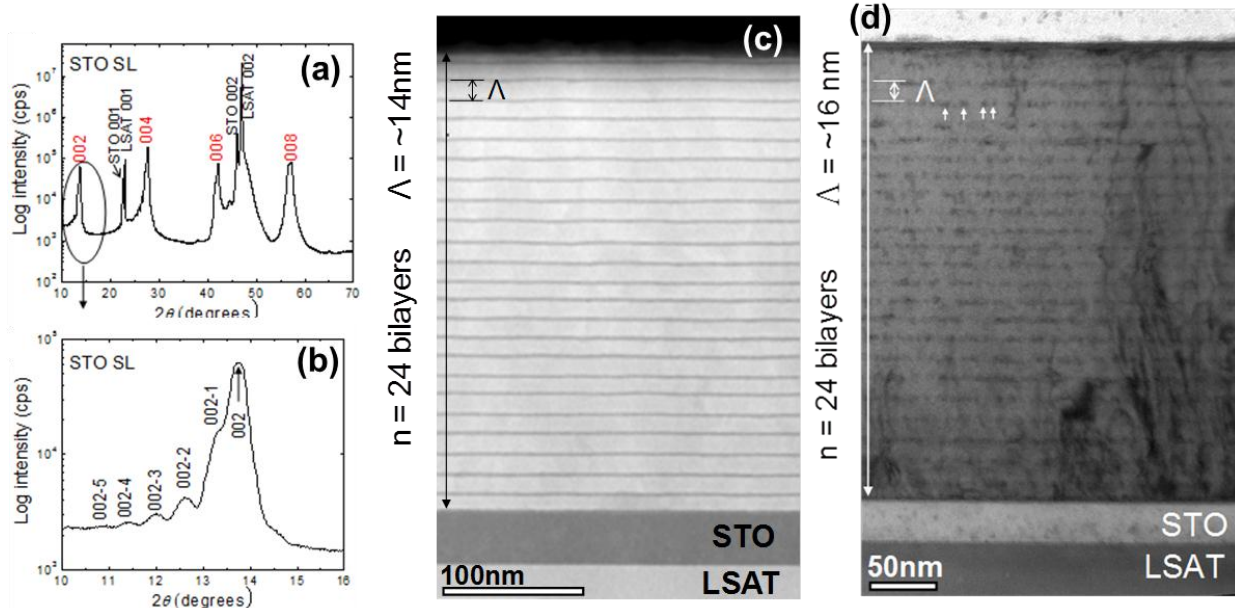


Figure 1. XRD patterns obtained on STO inserted Co-doped BaFe_2As_2 superlattices (a), Out-of-plane θ - 2θ XRD pattern of $(\text{STO}_{1.2 \text{ nm}}/\text{Co-doped Ba-122}_{13 \text{ nm}})^{\times 24}$. (b), Magnified at near 002 reflection of $(\text{STO}_{1.2 \text{ nm}}/\text{Co-doped Ba-122}_{13 \text{ nm}})^{\times 24}$. (c) HAADF image of the $<100>$ projection of $(\text{STO}_{1.2 \text{ nm}}/\text{Co-doped Ba-122}_{13 \text{ nm}})^{\times 24}$. (d) Cross-sectional TEM image of the $<100>$ projection of $(\text{O-Ba-122}_{3 \text{ nm}}/\text{Co-doped Ba-122}_{13 \text{ nm}})^{\times 24}$. Arrows indicate nano particle arrays in the O-Ba-122 layer along *ab*-axis.

In order to understand the effect of this nanostructural engineering on J_c and H_{irr} we made extensive characterizations at various temperatures, fields and field orientations to the crystal axes. Figure 2(a) shows $J_c(H)$ for $H//c$ at 4.2K far from T_c . It is immediately clear that the two samples with *c*-axis nanorod

pinning defects have much higher $J_c(H)$ and $H_{irr}(T)$. The influence of the ab -plane defects is revealed in Fig. 2(b) where the J_c anisotropy for the O-Ba-122 SL and Co-doped Ba-122 single layers at 16K for perpendicular ($H//c$) and parallel ($H//ab$) configurations is compared. Despite these data being affected by their T_c differences, both samples have the same $H_{irr} \sim 11$ T for H parallel to the c -axis, a result consistent with the lower density of c -axis pinning centres in O-Ba-122 SL compared to the single layer Co-doped Ba-122. But the really striking result is that the inverted H_{irr} anisotropy seen for the single layer film with only c -axis defects (H_{irr} for $H//ab$ is less than for $H//c$) is corrected when ab -plane pins are present in the O-Ba-122 SL film. It is clear that H_{irr} for $H//ab$ ($H_{irr,ab}$) of O-Ba-122 SL is approximately doubled from 9 to ~ 19 T, restoring the expected anisotropy of H_{irr} and $J_c(H)$ without any degradation to the c -axis properties. This enhancement is due to the presence of the ab -plane aligned nanoparticles in the O-Ba-122 SL shown in Fig. 1.

The angular transport J_c of the STO SL, O-Ba-122 SL, and Co-doped Ba-122 single layer shown in Fig. 2(c) evaluated at a constant reduced temperature $T/T_c \sim 0.6$ provides further insight into the pinning effects of the nanoparticles. The Co-doped Ba-122 single layer shows only the strong c -axis pinning produced by the correlated, self-assembled nanopillars, while the J_c of the STO SL shows only a sharp, few-degrees wide peak when the magnetic field is aligned with the ab -plane STO superlattice. The $J_c(\theta)$ of O-Ba-122 SL is higher than the other two samples and shows both strong ab -plane and c -axis peaks, which is quite consistent with the ab -plane aligned second-phase nanoparticles of the bilayer and its c -axis aligned defects, seen in Fig. 1(d).

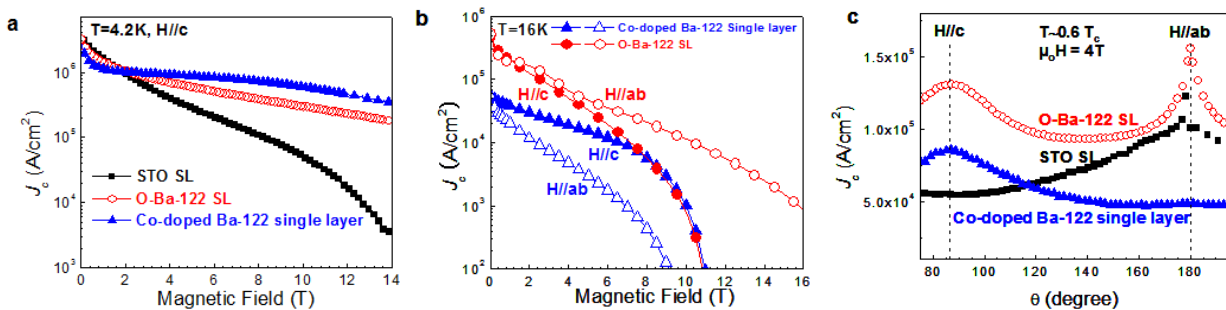


Figure 2. J_c as a function of magnetic field. a, Magnetization J_c as a function of magnetic field at 4.2K with the field applied perpendicular to the plane of all three films. b, Transport J_c as a function of magnetic field at 16K with the field applied perpendicular and parallel to the plane of $(\text{O-Ba-122}_{3\text{ nm}}/\text{Co-doped Ba-122}_{13\text{ nm}}) \times 24$ and Co-doped Ba-122 single layer thin films. c, Angular dependence of transport J_c at 4T for all three films at a reduced temperature of $T/T_c = \sim 0.6$.

Future Plans

(1) Superconductivity and magnetism at atomically abrupt Pnictide interfaces

The interaction between magnetism and superconductivity is central to the physics of pnictide superconductors, as well as other modern superconductors with potential applications. We have demonstrated that epitaxial heterostructures with sharp interfaces can be made between the optimally-doped material $\text{Ba}(\text{Fe},\text{Co})_2\text{As}_2$ and other doping levels, as well as insulators such as SrTiO_3 , and metallic ferromagnets such as Ni, Co, and Fe.

We will compare two different Normal Metal (N) / Superconductor (S) configurations, using the same superconducting layer and changing the N layer properties to determine the interfacial interaction of superconductivity and magnetism. The SC material will be fixed at optimal doping $\text{Ba}(\text{Fe}_{0.92}\text{Co}_{0.08})_2\text{As}_2$ ($x=0.08$), with maximum T_c (see Fig. 3, the phase diagram for Ba-122 with Co doping). In the first N_u

(undoped normal metal) /S (superconductor) interface, the normal metal (N_u) will be undoped BaFe₂As₂ in which the AFM-SDW correlations dominate. In the second N_o (overdoped normal metal) /S (superconductor) interface, the normal metal (N_o) will be heavily doped Ba122 ($x=0.20$), a paramagnetic metal with no AFM ordering and no SC transition. In Fig. 3 the blue, purple and red arrows represent, respectively, the low doping, optimally doping and over-doping Ba-122 compounds, whose relative interaction we propose to study. Any weakening or enhancement of superconductivity in these systems (i.e., seen as a decrease or increase of T_c) will provide a straightforward demonstration of the competitive nature or coexistence of the two long-range orders. The comparison between the two heterostructures will also determine if magnetism has an important role as mediator in the interaction that drives superconductivity in pnictides.

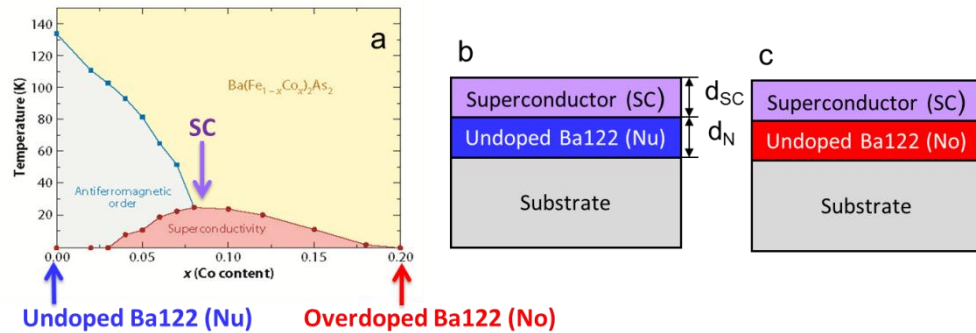


Figure 3. (a) Co-Ba 122 phase diagram, with heterostructure layer doping levels indicated, (b) and (c) two different S/N configurations with undoped ($x=0$) and overdoped ($x=0.2$) normal metals .

(2) Understanding and control of flux-pinning mechanisms in Pnictide

Pnictide superconductors have potential for high-field superconductivity. The existence of nano-scale columnar second phases and nanoparticles in our artificially engineered superlattices allows a direct probe of fundamental flux-pinning mechanisms in our films as shown in Figure 14(a). We would like to understand the nature of the pinning centers, their origin and growth mechanism, and from that understanding elucidate the physics of flux pinning in pnictide superconductors.

We will address (1) What is the nature of pinning centers in pnictide superlattices? (chemical, structural, and electrical characteristics) (2) What are the intrinsic limits to J_c and pinning force in pnictides? (3) How do we control the nucleation and growth of pinning centers (4) How do we achieve an ideal pinning center geometry (i.e. optimum size, volume fraction and density of the pinning) to reach a maximum and/or isotropic J_c ? We propose to answer these questions by controllably altering the nature of pinning in the films, and correlate the electromagnetic and structural characterizations.

References (which acknowledge DOE support)

1. "Artificially engineered superlattices of pnictide superconductors" S. Lee, C. Tarantini, P. Gao, J. Jiang, J. D. Weiss, F. Kametani, C. M. Folkman, Y. Zhang, X. Q. Pan, E. E. Hellstrom, D. C. Larbalestier, and C. B. Eom, *Nature Materials*, **12**, 392, doi:10.1038/nmat3575 (2013)
2. "Evidence for charge–vortex duality at the LaAlO₃/SrTiO₃ interface" *Nature Communications*, **3**, 955, doi:10.1038/ncomms1959 (2012)
3. "Artificial and self-assembled vortex-pinning centers in superconducting Ba(Fe_{1-x}Co_x)₂As₂ thin films as a route to obtaining very high critical-current densities" C. Tarantini, S. Lee, F. Kametani, J. Jiang, J.D. Weiss, J. Jaroszynski, C.M. Folkman, E.E. Hellstrom, C. B. Eom, D. C. Larbalestier, *Physical Review B*, **86**, 214504 (2012)

Program Title: Charge Inhomogeneity in Correlated Electron Systems

Principle Investigator: Barrett O. Wells

Mailing Address: Department of Physics, University of Connecticut, Storrs, CT 06269

E-mail: wells@phys.uconn.edu

Program Scope

This program is aimed at understanding the role of inherently inhomogenous charge distribution in high temperature superconductors. Our strategy is to explore materials in which dopants can be controlled in a manner that leads to particularly interesting and illuminating properties. The materials we study are both bulk and film samples grown in our lab, and we pursue a variety of experiments in collaboration with other groups to best answer the questions posed by the materials at hand. Of particular interest to our group are comparative doping strategies, comparing oxygen doping to cation substitution of different types. In the cases we study, oxygen can be incorporated topotactically, at lower temperatures within an already formed crystalline network.

The systems we study include both cuprates and Fe-based superconductors. In the cuprates we study $\text{La}_{2-x}\text{Sr}_x\text{CuO}_{4+y}$ (LSCO+O), investigating doping holes via excess oxygen in comparison to the more usual process of doping via the substitution of Sr or Ba for La. LSCO/LBCO is known for being an optimally doped superconductor at $x=0.16$, having a special phase with reduced superconductivity and interdependent charge density/spin density waves at $x=0.125$, and having substantial reports of nanoscale charge inhomogeneity. Superoxygenated LSCO+O at sufficiently high hole doping levels electronically phase separates to large regions with optimally doped superconductivity and other regions with no superconductivity but a well-developed spin density wave. The difference appears to be associated with the high mobility of the oxygen dopants, achieving annealed levels of disorder down to approximately 200 K. Mixing Sr/O dopants at a given charge density allows for a study of the effects of different sorts of disorder on superconductivity.

Our study of Fe-based superconductors aims to understand the exact role of dopants in producing a superconductor from a parent compound. Generally, both isovalent and heterovalent dopants can be used to create a superconductor from a parent compound, and sometimes pressure without doping will do the same. While one role of the doping process involves suppressing ordered magnetism, just how that happens is unclear; so, for example, exactly why FeTe is a parent compound while FeSe is a superconductor is not well understood. We study the co-doped system $\text{FeTe}_{1-x}\text{Se}_x\text{O}_y$. Either isovalent doping of Se onto Te sites or charge doping with excess oxygen will produce a superconductor from the parent FeTe. Oxygen doping of FeTe is difficult as oxygen mobility is very low, but can be accomplished in thick films. Superconductivity in these films is robust with considerable Meissner signals. Superconducting FeTeO_y has some intriguing properties. Unlike most Fe-superconductors, the valence state of Fe changes substantially with Fe doping. Yet, the compound retains a magnetic ordering as in FeTe and conductivity remarkably similar to the parent compound. These features may indicate some electronic phase separation, though at this time no clear signal has been found.

Recent Progress

1. Determining the phases of phase-separated LSCO+O

We have conducted a careful analysis of both neutron diffraction and muon spin resonance to examine the phases present in phase separated LSCO+O. [1] We studied three samples of LSCO,

with $x=0.04$, 0.065 , and 0.09 plus enough excess oxygen to make each sample superconducting with $T_C=40\text{K}$, though each is magnetic as well. High transverse field muon spectroscopy reveals magnetic and superconducting volume fractions as well as information about the nature of the superconducting state as the relaxation rate is characteristic of the vortex lattice state at particular dopings. We found that magnetic phase fractions in these samples ranged from 20 to 60%, whereas the superconducting phase for each phase matched the characteristics measured for optimally doped $\text{La}_{0.85}\text{Sr}_{0.15}\text{CuO}_4$.^[6] The neutron diffraction study of the magnetic peaks revealed that the magnetic fraction of each sample displayed peaks at the same locations in q -space and reflective of identical ordered moments, each consistent with LNSCO or LBCO with $x=1/8$.^[7] Taken together, these observations prove that a long-range electronic phase separation occurs in LSCO+O between a $1/8$ stripe-like magnetic phase and a superconducting phase which is similar to optimally doped LSCO.

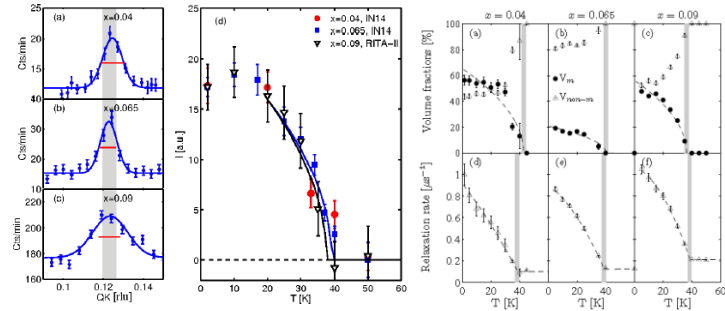


Figure 1. Left Panel: Magnetic neutron diffraction peaks for three phase separated LSCO+O samples, with $x = 0.04$, 0.065 , 0.09 plus enough oxygen to be in the phase separated region ($0.125 < nh < 0.16$). Middle Panel: Normalized peak intensities versus temperature for the same three samples. Right Panel: High field μSR derived phase fractions and relaxation rates for the same three samples.

2. FeTeO_y lattice anomaly at T_C

In recent studies, we demonstrated that incorporating oxygen into FeTe or FeSe creates Fe in a $3+$ -like valence state throughout the thickness of the films.^[2,3] However, to understand the role of the dopant ions, we also need to investigate what structural changes are induced by the oxygen dopant ions. Thus, we performed a high-resolution, temperature dependent study of the lattice structure of superconducting FeTeO_y .^[4] While the detailed lattice constants differ, the basic structures are the same as in the parent FeTe compound: tetragonal at high temperature and monoclinic at lower temperatures. The structural differences induced by oxygen are modest, and oxygen doping in this compound may represent something closer to charge doping without a change in structure than is usually seen in Fe-superconductors. A further significant feature of the structure is a large change in the c-axis thermal expansion near the superconducting T_C , characterized by a notable downturn in the c lattice constant. This change appears to be a thermodynamic effect seen at second order phase transitions determined by the Ehrenfest relationship. Typically, such changes are small, and usually studied using highly sensitive dilatometry techniques. In FeTeO_y the effect is large enough to be seen in diffraction, close to ten times larger than in other Fe-superconductors.^[8] Thus FeTeO_y has a particularly large lattice dependence on the condensation energy and the result indicates that synthesizing highly strained FeTeO_y films may be particularly effective at inducing a large increase in T_C .

Future Plans

1. Charge and spin density wave in LSCO+O

As we have shown in recent work, the magnetic phase of LSCO+O has a spin density wave that appears to be essentially identical to that of $\text{La}_{7/8}\text{Ba}_{1/8}\text{CuO}_4$, with particularly sharp magnetic peaks. If this magnetism is really the result of interdependent spin and charge density-wave order, there should be concomitant charge order peaks. Given recent developments in

finding charge order in related cuprates, [9] it would seem that soft x-ray resonant diffraction would be the best method for finding such charge order peaks.

While some technical issues mean that this search is not yet exhaustive, our preliminary measurements have failed to find such charge order peaks. If in fact we have a phase with well defined, $1/8^{\text{th}}$ doped magnetic phase with suppressed superconductivity but without any associated charge ordering then this would have implications on the underlying nature of the ordering, or at least the driving mechanism for such spin order.

2. FeTeO_y magnetism

As a general issue, the relationship between magnetism and superconductivity in high temperature superconductors is a central theme. In FeTeO_y, the interaction appears to be quite strong in that superconducting samples appear to still have some amount of ordered magnetism. In fact, measuring small moment, spin density wave magnetism in films is a challenge where we are making progress. We have preliminary data on magnetism using neutron diffraction and Mossbauer spectroscopy. Both methods indicate that there is ordered magnetism in superconducting FeTeO_y, and neutron results indicate the suppression of the magnetism at the onset of superconductivity. Our preliminary neutron data were taken at the SINQ source at the Paul Scherrer Institute, and we have a follow up experiment scheduled for December at the NOMAD beamline of the Spallation Neutron Source at ORNL where we expect at least an order of magnitude improved signal. Our preliminary Mossbauer spectra were taken at a lab source with Dr. Ercan Alp of Argonne National Laboratory, see figure 2. We are currently awaiting results from a proposal based upon these results to pursue synchrotron based Mossbauer at the Advanced Photon Source.

3. Universal aspects of electronic phase separation in doped Mott insulators

A comparison of the work done here on phase separation in LSCO+O and work on a separate NSF supported project examining magnetic oxide materials reveals interesting parallels with respect to doping via immobile cation substitution versus highly mobile oxygen intercalation. LSCO shows signs of nannoscale phase separation, glassy behavior, but ultimately smoothly varying properties between magnetism and superconductivity as a function of the degree of charge doping. In contrast, LSCO+O shows large scale separation and overall coexistence of magnetic and superconducting regions associated with different mobile valence hole densities. Similarly, perovskite La_{1-x}Sr_xCoO₃ shows signs of nannoscale phase separation, glassy behavior, but ultimately smoothly varying properties between different magnetic phases as a function of the degree of charge doping. In contrast, SrCoO_y with highly mobile oxygen vacancies shows large scale separation and overall coexistence of differing magnetic regions associated with different mobile valence charge densities. [10] The similarities of the phase diagrams are striking, shown in figure 3. In addition, a common feature of the stable phases in both systems is an ordered arrangement of valence charge revealed by techniques such as resonant diffraction at the transition metal L edge. We believe that this may reveal a broad

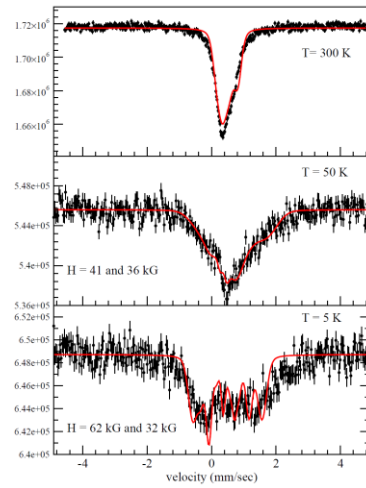


Figure 2. Conventional Mossbauer spectroscopy on a superconducting FeTeO_y film. While better statistics are still needed, a magnetic sextet appears at low temperature.

characteristic of charge doped Mott insulators, and that the mobility of the dopant ions may be a way to tune the disorder, and thus size of phase separated regions, in a manner similar to that suggested by Dagotto in theories for colossal magneto-resistance in manganites. [11] We are developing experiments to further explore the similarities between these systems, and to search for other materials with similar phase separation properties.

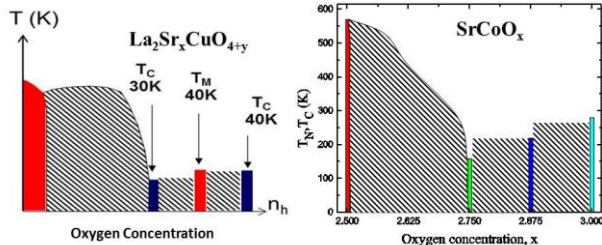


Figure 3. Schematic phase diagrams for $\text{La}_2\text{CuO}_{4+y}$ (left) and SrCoO_y (right). Solid bars are line electronic phases, either superconducting or magnetic. Dashed areas are two-phase regions.

References/Publications acknowledging DOE-BES support

1. L. Udby, J. Larsen, N. B. Christensen, M. Boehm, Ch. Niedermayer, H. E. Mohottala, T. B. S. Jensen, R. Toft-Petersen, F. C. Chou, N. H. Andersen, K. Lefmann, B. O. Wells, "Direct proof of unique magnetic and superconducting phases in superoxygenated high-T_c cuprates" submitted to *Phys. Rev. Lett.* and arXiv:1306.2155.
2. D. Telesca, Y. Nie, J. I. Budnick, B. O. Wells, and B. Sinkovic, "Impact of valence states on the superconductivity of iron telluride and iron selenide films with incorporated oxygen" *Phys. Rev. B* **85**, 214517 (2012).
3. D. Telesca, Y. Nie, J.I. Budnick, B.O. Wells, B. Sinkovic, "Surface valence states and stoichiometry of non-superconducting and superconducting FeTe films" *Suf. Sci.* **606**, 1056–1061 (2012).
4. L. K. Narangammana, X. Liu, Y. F. Nie, F. J. Rueckert, J. I. Budnick, W. A. Hines, G. Gu, and B. O. Wells, "Low temperature crystal structure and large lattice discontinuity at T_c in superconducting FeTeO_x films" submitted to *Appl. Phys. Lett.*
5. Y.F. Nie, D.Telesca, J.I.Budnick, B.Sinkovic, R.Ramprasad, B.O.Wells, "Superconductivity and properties of FeTeO_x films" *J. Phys. Chem. Solids* **72**, 426–429 (2011).

References (other)

6. Y.J. Uemura et al., "Systematic variation of magnetic-field penetration depth in high-T_c superconductors studied by muon-spin relaxation" *Phys. Rev. B* **38**, 909 (1988).
7. J.M. Tranquada et al., "Evidence for stripe correlations of spins and holes in copper oxide superconductors" *Nature* **375**, 561 (1995).
8. S. Bud'ko et al., "Anisotropic thermal expansion of $\text{Fe}_{1.06}\text{Te}$ and $\text{FeTe}_{0.5}\text{Se}_{0.5}$ single crystals" *Phys. Rev. B* **80**, 134523 (2009).
9. G. Ghirengelli et al., "Long-Range Incommensurate Charge Fluctuations in $(\text{Y},\text{Nd})\text{Ba}_2\text{Cu}_3\text{O}_{6+x}$ " *Science* **337**, 821 (2012).
10. Y. F. Nie, D. Telesca, J. I. Budnick, B. Sinkovic, and B. O. Wells, "Superconductivity induced in iron telluride films by low-temperature oxygen incorporation" *Phys Rev B* **82**, 020508-R (2010).
11. E. Dagotto "Open questions in CMR manganites, relevance of clustered states and analogies with other compounds including the cuprates" *New J. Phys.* **7**, 67 (2005).

Program Title: Interfaces in Epitaxial Complex Oxides**Principle Investigator: Hans M. Christen;****Co-PIs: H.N. Lee, T.Z. Ward, G. Eres, C.M. Rouleau, and M. Chi****Mailing Address: Materials Science and Technology Division, Oak Ridge National Laboratory,
Oak Ridge, TN 37831****E-mail: christenhm@ornl.gov****Program Scope**

The desire to create functional materials for specific applications motivates much of today's research in materials sciences and condensed-matter physics. At the forefront of these approaches are efforts to create materials without bulk analogs. The goal of this project is to create, understand, and utilize interfaces in epitaxial complex oxides in order to obtain desired functional properties. In particular, we treat not just the layers of materials as the building blocks in complex-oxide heterostructures but regard the interfaces themselves as fundamental constituents in epitaxial assemblies. This approach provides unprecedented freedom in the formation of materials with enhanced properties for applications (such as energy conversion and energy storage) and as highly controlled model systems in which we can explore fundamental physical mechanisms (including correlated-electron behavior, multiferroicity, coupled electronic and ionic transport, etc.). This research simultaneously addresses three objectives: first, to tune functional properties in epitaxially stabilized oxides; second, to manipulate properties that emerge at epitaxial interfaces; and third, to understand the mechanisms of epitaxial interface formation.

Tuning the properties of materials via interfacial constraints has the goal of creating new properties (strain-tuning of materials) and new materials (strain-stabilization of meta-stable phases), as well as utilizing strain and symmetry as a probe to interrogate the properties of complex materials. At the same time, the knowledge gained is a prerequisite for the second objective, namely the study of properties that specifically emerge at an interface: to properly interpret the origin of functional behaviors that are different from those found in the constituent materials, the properties of the constituent materials under the constraints of strain and symmetry must first be properly understood.

Past work that has shown that the behavior of a (nearly) two-dimensional interfacial region between two oxides is often fundamentally different from that found in the constituent materials (such as the conducting interface found between two insulators, or a ferromagnetic sheet forming between two paramagnetic oxides, etc.). We are now at a point where this research can be expanded to carefully tailor the properties of single-unit-cell layers within an epitaxial matrix via compositional tuning, or to manipulate the interactions between separate two-dimensional "sheets" by adjusting the thickness and physical properties of the material that separates them. This vastly enhances the possibilities to create macroscopic properties that result directly from interfacial behaviors.

Research performed by this team and others around the world has shown that synthesis parameters and functional properties at interfaces in complex-oxide materials are intimately linked, and that stabilization of certain structures and polymorphs is possible only by a very careful tuning of the synthesis conditions. This illustrates the urgent need to understand how epitaxial materials nucleate, crystallize, and grow, which is our third objective. Until recently, approaches to determine the appropriate synthesis conditions remained largely empirical due to the lack of quantitative in-situ monitoring of growth. Reflection high energy electron diffraction (RHEED) provides reliable feedback for many growth experiments, but lacks the quantitative nature of x-ray scattering. By combining both surface x-ray diffraction (SXRD) and RHEED, we aim to go far beyond previous approaches to understand and control the mechanisms of epitaxial interface formation.

Recent Progress

While the results presented at this meeting will focus on the rich variety of strain-induced polymorphs in BiFeO_3 [1,2], work within the project as a whole has led to results in a much broader field of research.

For example, in the case of the interface between LaAlO_3 and SrTiO_3 , the use of synchrotron surface x-ray diffraction in combination with scanning transmission microscopy and optical transmission spectroscopy has led to the demonstration that a single unit cell layer of LaAlO_3 grown at a relatively high oxygen pressure fundamentally alters the properties of such structures grown at low pressure [3]. This demonstrates the importance of unit-cell control in the synthesis of interfacial systems, and more generally the necessity to understand and monitor how epitaxial systems form. Significant progress has been made in understanding the interplay between interfacial constraints (strain) and oxygen stoichiometry precisely in those materials where the link between oxygenation and functional properties (magnetism, surface catalytic properties) are extremely pronounced: here, SrCoO_{3-x} is a particularly attractive example, as control over stoichiometry leads to a topotactic phase transformation between the brownmillerite $\text{SrCoO}_{2.5}$ with ordered oxygen vacancy channels and the ferromagnetic perovskite SrCoO_3 [4]. The transformation is seen to be fast and reversibly, and occurs at temperatures as low as 200°C - 300°C [5].

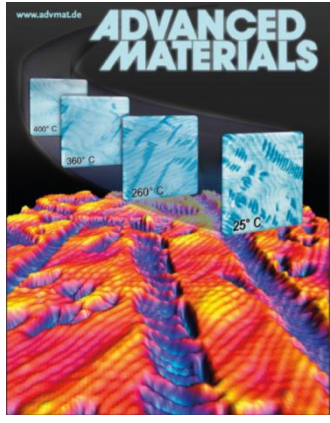


Figure 1. Strained BiFeO_3 films on LaAlO_3 substrates form a complex “stripe” structure, which is identified in this work as the coexistence of two polymorphs, both different from the structures that form under weaker compressive strain, and appearing only upon cooling after growth. (Image: Journal frontispiece from [1]).

have been available much earlier [7] than high-quality single crystals [8]. In addition to its multiferroic properties, BiFeO_3 is particularly interesting because of its response to strain. BiFeO_3 is rhombohedral in bulk but becomes monoclinic in epitaxial films under mild compressive strain [9], leading to a rotation of the polarization [10,11]. However, much more drastic changes are observed with large compressive strain in BiFeO_3 : The transition from a bulk-like phase to a (monoclinic) highly axial form was observed early on [12-13] and is associated with an *increase* in unit cell volume, i.e. it is not a simple Poisson-like distortion of the unit cell but a polymorphic transformation. In addition, a complex stripe pattern emerges (see Fig. 1), and our work shows that these stripes form after growth as a consequence of additional stress due to thermal expansion differences between film and substrate. More importantly, we demonstrate that these stripes are a prerequisite to ferroelectric switching, i.e. they enable the functional properties of the material. Understanding the details of the unit cell symmetry is motivated by the fact that ferroelectricity is a structural phenomenon, and therefore intimately linked structural changes. In this work, we use temperature-dependent 4-circle x-ray diffraction to monitor structural phase transitions as a function of temperature for films on different substrates (i.e., for different strain states). Elastic neutron scattering is shown to be a

Epitaxial constraints are a powerful tool to stabilize crystalline phases that would not otherwise be found. In fact, using epitaxial stabilization, we have been able to stabilize the hexagonal form of LuFeO_3 and demonstrate its multiferroic nature at room temperature [6]. This indicates that h- LuFeO_3 is the second material known to exhibit multiferroic properties at room temperature, together with the much more thoroughly studied example of BiFeO_3 .

BiFeO_3 is a particularly good example of the importance of epitaxial stabilization, as films

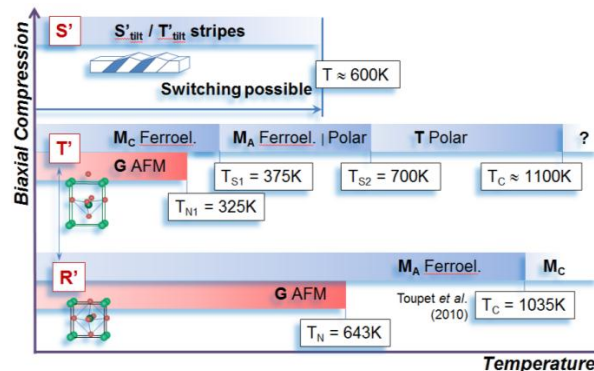


Figure 2. Phase diagram of epitaxial BiFeO_3 films, based on x-ray diffraction, neutron scattering, piezoresponse microscopy, and Raman data. R' , T' , and S' denote the polymorphs that form on SrTiO_3 substrates, LaAlO_3 substrates, and in the stripe patterns, respectively. From [2].

powerful tool for these studies of epitaxial films, allowing for the accurate determination of the Néel temperature and spin structure. In combination, these results lead to the establishment of a complete strain-temperature phase diagram for epitaxial BiFeO₃ films (see Fig. 2).

Future Plans

With synthesis techniques for epitaxial oxides having reached a point where perovskite heterostructures can be grown with a quality comparable to that achieved in semiconductor technology, opportunities for exploring interfacial effects in these complex materials abound. There is an increasing awareness that electronic and ionic transport are intimately linked, that oxygen stoichiometry in particular can change as consequence of electric fields or strains, and that the coherence of the octahedral tilt patterns across an interface strongly couples to functional properties (ferroelectricity, magnetism). This forces us to re-think some of the simplest models of “electronic reconstruction” at interfaces, and provides additional degrees of freedom with which to tune the functional properties of complex-oxide heterostructures.

References (* indicates papers supported by this work)

- [1]* C. Beekman, W. Siemons, T. Z. Ward, M. Chi, J. Howe, M. D. Biegalski, N. Balke, P. Maksymovych, A. K. Farrar, J. B. Romero, P. Gao, X. Q. Pan, D. A. Tenne, and H. M. Christen, “Phase transitions, phase coexistence, and piezoelectric switching behavior in highly strained BiFeO₃ films,” *Advanced Materials*, DOI: 10.1002/adma.201302066 (2013).
- [2]* W. Siemons, C. Beekman, G.J. MacDougall, J.L. Zarestky, S.E. Nagler, and H.M. Christen, “A complete strain-temperature phase diagram for BiFeO₃ films,” *Invited review, J. Phys. D.*, submitted (2013).
- [3]* W. S. Choi, C. M. Rouleau, S. S. A. Seo, Z. Luo, H. Zhou, T. T. Fister, J. A. Eastman, P. H. Fuoss, D. D. Fong, J. Z. Tischler, G. Eres, M. F. Chisholm, and H. N. Lee, “Atomic layer engineering of perovskite oxides for chemically sharp heterointerfaces,” *Adv. Mater.* **24**, 6423 (2012).
- [4]* H. Jeen, W.S. Choi, J.W. Freeland, H. Ohta, C.U. Jung, and H.N. Lee, “Topotactic phase transformation of brownmillerite SrCoO_{2.5} to perovskite SrCoO_{3-δ},” *Adv. Mater.* **25**, 3651 (2013).
- [5]* H. Jeen, W. S. Choi, M. D. Biegalski, C. M. Folkman, I. C. Tung, D. D. Fong, J. W. Freeland, D. Shin, H. Ohta, M. F. Chisholm, and H. N. Lee, “Reversible redox reactions in an epitaxially stabilized SrCoOx oxygen sponge,” *Nature Materials*, DOI: 10.1038/NMAT3736 (2013).
- [6]* W. Wang, J. Zhao, W. Wang, Z. Gai, N. Balke, M. Chi, H. N. Lee, W. Tian, L. Zhu, X. Cheng, D. J. Keavney, J. Yi, T. Z. Ward, P. C. Snijders, H. M. Christen, W. Wu, J. Shen, and X. Xu, “Room-temperature multiferroic hexagonal LuFeO₃ films,” *Phys. Rev. Lett.* **110**, 237601 (2013).
- [7] J. Wang, J.B. Neaton, H. Zheng, V. Nagarajan, S.B. Ogale, B. Liu, D. Viehland, V. Vaithyanathan, D.G. Schlom, U.V. Waghmare, N.A. Spaldin, K.M. Rabe, M. Wuttig, and R. Ramesh, “Epitaxial BiFeO₃ Multiferroic Thin Film Heterostructures,” *Science* **299**, 1719 (2003).
- [8] D. Lebeugle, D. Colson, A. Forget, and M. Viret, “Very large spontaneous electric polarization in BiFeO₃ single crystals at room temperature and its evolution under cycling fields,” *Appl. Phys. Lett.* **91**, 022907 (2007).
- [9] H.W. Jang, D. Ortiz, S.-H. Baek, C.M. Folkman, *et al.*, “Domain Engineering for Enhanced Ferroelectric Properties of Epitaxial (001) BiFeO₃ Thin Films,” *Adv. Mater.* **21** 817 (2009).
- [10]* D.H. Kim, H.N. Lee, M.D. Biegalski, and H.M. Christen, “Effect of epitaxial strain on ferroelectric polarization in multiferroic BiFeO₃ films,” *Appl. Phys. Lett.* **92**, 012911 (2008).
- [11] H.W. Jang, S.H. Baek, D. Ortiz, C.M. Folkman, *et al.*, “Strain-Induced Polarization Rotation in Epitaxial (001) BiFeO₃ Thin Films.” *Phys. Rev. Lett.* **101**, 107602 (2008)
- [12] R.J. Zeches, M.D. Rossell, J.X. Zhang, A.J. Hatt *et al.*, “A Strain-Driven Morphotropic Phase Boundary in BiFeO₃,” *Science* **326**, 977 (2009).
- [13] H. Béa, B. Dupé, S. Fusil, R. Mattana *et al.*, “Evidence for Room-Temperature Multiferroicity in a Compound with a Giant Axial Ratio,” *Phys. Rev. Lett.* **102**, 217603 (2009).

Publications resulting from work supported by this program

(This list includes papers that were published in print during the 24 months between July 2011 and June 2013)

July-Dec. 2011

- G. Eres, J. Z. Tischler, C. M. Rouleau, B. C. Larson, H. M. Christen, and P. Zschack, “Real-Time Studies of Epitaxial Film Growth Using Surface X-Ray Diffraction,” Chapter 9, p. 239–273 in *In Situ Characterization of Thin Film Growth*, ed. by Gertjan Koster and Guus Rijnders, Woodhead Publishing Limited, Oxford, 2011.
- G. Eres, J. Z. Tischler, C. M. Rouleau, P. Zschack, H. M. Christen, and B. C. Larson, “Quantitative determination of energy enhanced interlayer transport in pulsed laser deposition of SrTiO₃,” *Phys. Rev. B* **84**, 195467 (2011).
- N. M. Murari, S. Hong, H. N. Lee, and R. S. Katiyar, “Direct Observation of Fatigue in Epitaxially Grown Pb(Zr,Ti)O₃ Thin Films Using Second Harmonic Piezoresponse Force Microscopy,” *Appl. Phys. Lett.* **99**, 052904 (2011).

- W. Siemons, M. D. Biegalski, J. H. Nam, and H. M. Christen, "Temperature Driven Structural Phase Transition in Tetragonal-Like BiFeO₃," *Appl. Phys. Express* **4**, 095801 (2011).
- P. Yordanov, A. V. Boris, J. W. Freeland, J. J. Kavich, J. Chakhalian, H. N. Lee, and B. Keimer, "Far-Infrared and dc Magnetotransport of CaMnO₃-CaRuO₃ Superlattices," *Phys. Rev. B* **84**, 045108 (2011).
- D. Xiao, W. Zhu, Y. Ran, N. Nagaosa, and S. Okamoto, "Interface engineering of quantum Hall effects in digital transition metal oxide heterostructures," *Nat. Commun.* **2**, 596 (2011).

Jan.-Dec. 2012

- P. Chen, J. Y. Jo, H. N. Lee, E. M. Dufresne, S. M. Nakhmanson, and P. G. Evans, "Domain and symmetry transition origins of reduced nanosecond piezoelectricity in ferroelectric/dielectric superlattices," *New J. Phys.* **14**, 013034 (2012).
- T. Choi, L. Jiang, S. Lee, T. Egami, and H. N. Lee, "High rectification and photovoltaic effect in oxide nanojunctions," *New J. Phys.* **14**, 093056 (2012).
- W. S. Choi and H. N. Lee, "Band gap tuning in ferroelectric Bi₄Ti₃O₁₂ by alloying with LaTMO₃ (*TM* = Ti, V, Cr, Mn, Co, Ni, and Al)," *Appl. Phys. Lett.* **100**, 132903 (2012).
- W. S. Choi, M. F. Chisholm, D. J. Singh, T. Choi, G. E. Jellison, Jr., and H. N. Lee, "Wide bandgap tunability in complex transition metal oxides by site-specific substitution," *Nat. Commun.* **3**, 689 (2012).
- W. S. Choi, S. Lee, V. R. Cooper, and H. N. Lee, "Fractionally δ -doped oxide superlattices for higher carrier mobilities," *Nano Lett.* **12**, 4590 (2012).
- W. S. Choi, J.-H. Kwon, H. Jeen, J. E. Hamann-Borrero, A. Radi, S. Macke, R. Sutarto, F. He, G. A. Sawatzky, V. Hinkov, M. Kim, and H. N. Lee, "Strain-induced spin states in atomically ordered cobaltites," *Nano Lett.* **12**, 4966 (2012).
- W. S. Choi, C. M. Rouleau, S. S. A. Seo, Z. Luo, H. Zhou, T. T. Fister, J. A. Eastman, P. H. Fuoss, D. D. Fong, J. Z. Tischler, G. Eres, M. F. Chisholm, and H. N. Lee, "Atomic layer engineering of perovskite oxides for chemically sharp heterointerfaces," *Adv. Mater.* **24**, 6423 (2012).
- L. Jiang, W. S. Choi, H. Jeen, T. Egami, and H. N. Lee, "Strongly coupled phase transition in ferroelectric/correlated electron oxide heterostructures," *Appl. Phys. Lett.* **101**, 042902 (2012).
- Y. M. Kim, J. He, M. D. Biegalski, H. Ambaye, V. Lauter, H. M. Christen, S. T. Pantelides, S. J. Pennycook, S. V. Kalinin, and A. Y. Borisevich, "Local measurements of oxygen vacancy concentration and homogeneity in solid oxide fuel cell cathode materials on the (sub) unit cell level," *Nat. Mater.* **11**(10), 888 (2012).
- D. Lee, S. M. Yang, T. H. Kim, B. C. Jeon, Y. S. Kim, J.-G. Yoon, H. N. Lee, S. H. Baek, C. B. Eom, and T. W. Noh, "Multilevel data storage memory using deterministic polarization control," *Adv. Mater.* **24**, 402 (2012).
- G. J. MacDougall, H. M. Christen, W. Siemons, M. D. Biegalski, J. L. Zarestky, S. Liang, E. Dagotto, and S. E. Nagler, "Antiferromagnetic transitions in tetragonal-like BiFeO₃," *Phys. Rev. B* **85**, 100406(R) (2012).
- W. Siemons, M. A. McGuire, V. R. Cooper, M. D. Biegalski, I. N. Ivanov, G. E. Jellison, L. A. Boatner, B. C. Sales, and H. M. Christen, "Dielectric-constant-enhanced Hall mobility in complex oxides," *Adv. Mater.* **24**, 3965 (2012).
- W. Siemons, G. J. MacDougall, A. A. Aczel, J. L. Zarestky, M. D. Biegalski, S. Liang, E. Dagotto, S. E. Nagler, and H. M. Christen, "Strain dependence of transition temperatures and structural symmetry of BiFeO₃ within the tetragonal-like structure," *Appl. Phys. Lett.* **101**, 212901 (2012).
- W. Wang, Z. Gai, M. Chi, J. D. Fowlkes, J. Yi, L. Zhu, X. Cheng, D. Keavney, P. C. Snijders, T. Z. Ward, J. Shen, and X. Xu, "Growth diagram and magnetic properties of hexagonal LuFe₂O₄ thin films," *Phys. Rev. B* **85**, 155411 (2012).

Jan.-June 2013

- C. Beekman, W. Siemons, T. Z. Ward, J. D. Budai, J. Z. Tischler, R. Xu, W. Liu, N. Balke, J. H. Nam, and H. M. Christen, "Unit cell orientation of tetragonal-like BiFeO₃ thin films grown on highly miscut LaAlO₃ substrates," *Appl. Phys. Lett.* **102**, 221910 (2013).
- H. W. Guo, D. Sun, W. Wang, Z. Gai, I. I. Kravchenko, J. Shao, L. Jiang, T. Z. Ward, P. C. Snijders, L. F. Yin, J. Shen, and X. Xu, "Growth diagram of La_{0.7}Sr_{0.3}MnO₃ thin films using pulsed laser deposition," *J. Appl. Phys.* **113**, 234301 (2013).
- H. W. Guo and T. Z. Ward, "Fabrication of spatially confined complex oxides," *Journal of Visualized Experiments (JoVE)* **77**, e50573 (2013).
- A. Kumar, D. Leonard, S. Jesse, F. Ciucci, E. A. Eliseev, A. N. Morozovska, M. Biegalski, H. M. Christen, A. Tselev, E. Mutoro, E. Crumlin, D. Morgan, Y. Shao-Horn, A. Borisevich, and S. V. Kalinin, "Spatially resolved mapping of oxygen reduction/evolution reaction on solid-oxide fuel cell cathodes with sub-10 nm resolution," *ACS Nano* **7**, 3808 (2013).
- D. N. Leonard, A. Kumar, S. Jesse, M. Biegalski, H. M. Christen, E. Mutoro, E. Crumlin, Y. Shao-Horn, S. V. Kalinin, and A. Borisevich, "Nanoscale probing of voltage activated oxygen reduction/evolution reactions in nanopatterned (La_xSr_{1-x})CoO_{3-δ} cathodes," *Adv. Energy Mat.* **3**, 788 (2013).
- J. Park, B.-G. Cho, K. D. Kim, J. Koo, H. Jang, K.-T. Ko, J.-H. Park, K.-B. Lee, J.-Y. Kim, D. R. Lee, C. A. Burns, S. S. A. Seo, and H. N. Lee, "Oxygen vacancy-induced orbital reconstruction of Ti ions at the interface of LaAlO₃/SrTiO₃ heterostructures: a resonant soft x-ray scattering study," *Phys. Rev. Lett.* **110**, 017401 (2013).
- A. Tselev, P. Ganesh, L. Qiao, W. Siemons, Z. Gai, M. Biegalski, A. P. Baddorf, and S. V. Kalinin, "Oxygen control of atomic structure and physical properties of SrRuO₃ surfaces," *ACS Nano* **7**, 4403 (2013).
- W. Wang, J. Zhao, W. Wang, Z. Gai, N. Balke, M. Chi, H. N. Lee, W. Tian, L. Zhu, X. Cheng, D. J. Keavney, J. Yi, T. Z. Ward, P. C. Snijders, H. M. Christen, W. Wu, J. Shen, and X. Xu, "Room-temperature multiferroic hexagonal LuFeO₃ films," *Phys. Rev. Lett.* **110**, 237601 (2013).

Session 2

Program Title: Mapping the Electron Response of Nanomaterials: Probing the Electronic Structure and Dynamics of Low-Dimensional Condensed-Matter Systems Using Femtosecond Probes

Principle Investigator: R. M. Osgood; Co-PI: Andy Millis

Mailing Address: Departments of Applied Physics and Applied Mathematics, Columbia University, New York City, N. Y. 10027

E-mail: osgood@columbia.edu

Program Scope

The scope of this program is to understand the physics of emergent properties in artificially nanostructured materials. In our case, emergent behavior is due to the role of confinement - both lateral and vertically - in evolving new and unexpected materials response. Our focus is emergent properties in *surface* systems. Surfaces enable the use of the powerful tools of momentum-resolved photoemission (ARUPS) for probing electron motion and the tuning of a system by altering of the surface composition, reconstruction, or confinement. Use of femtosecond photoemission, particularly two-photon photoemission [3], allows our program to have a growing emphasis on measuring time-dependent dynamic phenomena. In addition, we use, where necessary, scanning tunneling microscopy to examine the atomic structure and density of states of our nanomaterials.

The main strategy that we are using to realize our goals consists of using self-assembly to form 1D nanosystems [2, 11] and to use exfoliation methods to form pristine two-dimensional crystals [1, 7, 10, 12]. In addition, we are initiating our work on quasi-2D crystals [9] by working on complex crystals, via colleagues at BNL and at Columbia. Continuing instrumentation upgrades at Columbia and at Brookhaven have and will continue to enhance our measurement capabilities. These include advanced tunable laser sources, improved manipulators, sample transfer methods, improved low-temperature STM (at BNL), and use of SPELEEM. Using these advanced techniques, we seek to answer such questions as:

- Are there new electronic phases near surfaces in one-atom-wide wires or in nanoparticles, and can theoretical constructs be developed to examine such systems?

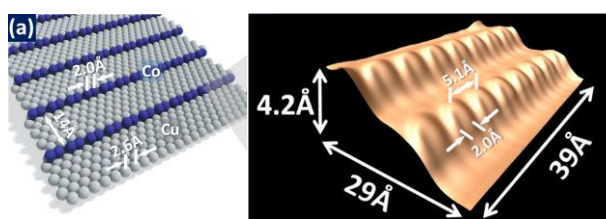


Fig. 1 (left) Model of a Co wire system under a CDW instability on a Cu(775) substrate. (right) LT-STM measurement of a CDW instability in monatomic Co wires, performed at T=5K.

understanding the emergent properties of nanomaterials as their dimensions and dimensionality are changed. These properties may be studied using time-resolved, ultrafast photoemission, nanometer photoemission, and proximal probes – all coupled with state of the art theoretical tools. Our research in this area has focused on 1D atomic chains [2, 5, 6, 8, 11] and on the use of layered crystals so that atomic-layer-thick single-crystal sheets may be formed using exfoliation methods.

- What are the emergent dynamic properties arising from lateral confinement in 1D and 2D confined systems?
- How do the properties of 2D materials vary with as the thickness of the samples increases from 1-4 MLs?
- How does the addition of a 2D layer on a single-crystal-metal surface affect electron dynamics as well as its self-energy?

Recent Progress

Background: A major emphasis in recent condensed matter research has been in

coupling theory and experiment to understand the properties of low-dimensional systems.

Theory: Theoretical calculations have shown that

the properties of 2D materials vary with as the thickness of the samples increases from 1-4 MLs.

How does the addition of a 2D layer on a single-crystal-metal surface affect electron dynamics as well as its self-energy?

Experiment: Experimental measurements have shown that

the properties of 2D materials vary with as the thickness of the samples increases from 1-4 MLs.

How does the addition of a 2D layer on a single-crystal-metal surface affect electron dynamics as well as its self-energy?

CDW Instabilities in 1D Atomic Chains: The goal of this effort [2] is to show that magnetic interactions can give rise to CDW behavior using relatively small atomic number transition metal atoms. We have recently shown experimentally that a 1-D magnetic atomic-Co-wire system that is aligned along a step edge undergoes a structural phase transition, in which a charge density wave (CDW) instability arises for $T < 85\text{K}$. Our original paper in this area included the development of synthetic methods and the development of a stepped template, and then, later, experimental observation of the CDW structure using a low-drift 5K STM. We have now used this experimental system as a test bed to see whether several theoretical techniques can correctly predict the ground state of this system [8]. These theoretical techniques included DFT (both LDA and GGA), DFT+U, DFT+HF, and DFT+DMFT. For each of these techniques, we found the same qualitative difference relative to experiment, namely that they did not predict a CDW instability. In order to resolve this problem, we have now used a cluster expansion analysis, which allowed separation of the magnetic contribution from the elastic (or non-magnetic) contribution of the total system energy. This approach allowed us to determine that for the DFT technique, the magnetic energy term was predicted to be weaker while the elastic term stiffer for the experimentally realized system of a Co wire on a vicinal Cu substrate. For the case of DFT+U, on the other hand, the point of failure was an unfavorable prediction of orbital filling of the Co d-orbitals, compared to regular DFT, which consequently inhibits the rise of a structural instability. Generally, these two sources of inaccuracy were also the cause of discrepancy in the more advanced techniques of DFT+HF and DFT+DMFT. Thus our experimental results provide an interesting test bed for the development of future theoretical techniques.

Nanoprobing of Electronic Structure of 1ML Layered Materials: Molybdenum disulfide: MoS₂ is a layered transition-metal dichalcogenide that can be fabricated as an atomically thin two-dimensional (2D) crystal. The fabrication uses exfoliation and relies on the fact that S-Mo-S slabs in bulk MoS₂ have a layered 2H crystal structure, and are weakly bonded by van der Waals (vdW) interactions. Given the broad current appeal of this and other 2D materials and their potential applications, we have carried out a series of measurements to determine the evolution of the thickness-dependent electronic band structure of this two-dimensional material. Specifically, we have performed micrometer-scale angle-resolved photoemission spectroscopy of mechanically exfoliated and chemical-vapor-deposition-grown crystals of MoS₂ [1]. These measurements provided direct evidence for the shifting of the valence band maximum from $\bar{\Gamma}$ to \bar{K} , for the case of MoS₂ having more than one layer, to the case of single-layer MoS₂, as predicted by density functional theory. This evolution of the electronic structure from bulk to few-layer to monolayer MoS₂ had earlier been predicted to arise from quantum confinement of the *d*-bands. Furthermore, one of the consequences of this progression in the electronic structure is the dramatic increase in the hole effective-mass, in going from bulk to monolayer MoS₂ at its Brillouin zone center, which is known as the cause for the decreased carrier mobility of the monolayer form compared to that of bulk MoS₂.

Electronic Structure of Correlated-Electron Layered Materials: 2H-NbSe₂ is a layered transition metal dichalcogenide, which exhibits both superconductivity and an incommensurate charge density wave (CDW) phase. In collaboration with the Pasupathy Group (Columbia), who used scanning tunneling microscopy (STM) and scanning tunneling spectroscopy (STS), we, in collaboration and Valla at BNL, used angle-resolved photoemission spectroscopy (ARPES) to measure the electronic structure of both pristine 2H-NbSe₂ and its light isovalently doped equivalent (NbSe_{1.99}S_{0.01}) [9]. To compare the two materials, we applied a tight-binding model to their rich band structure and quasiparticle scattering. Our results indicated the absence of Fermi

surface nesting at the CDW vector in pristine NbSe₂. In addition, the S impurities resulted in a shift of the Fermi energy, but without affecting the band structure of NbSe₂, and as a result, significantly enhanced the quasiparticle interference. Our observations rule out the presence of Fermi surface nesting and support electron-phonon coupling as the driving mechanism for the CDW phase in NbSe₂.

Excited Electron Dynamics for a Coupled Metal/Graphene Single-Crystal System: Gr/Ir(111):

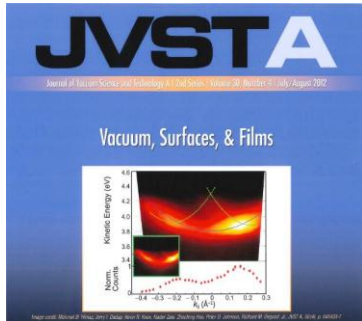


Fig 2: Cover page of our manuscript on photoemission band mapping with a tunable femtosecond source using nonequilibrium absorption resonances.

potential states. The weak interaction between Ir and graphene permits observation of resonant transitions from an unquenched Shockley-type surface state of the Ir substrate to graphene/Ir image-potential states. The image-potential-state lifetimes are comparable to those of mid-gap clean metal surfaces, indicating that the Gr acts only as a phase shifter for the image electrons' wave function. We also measure evidence of localization of the excited electrons on single-atom-layer graphene islands through the use of coverage-dependent measurements.

Instrumentation: A major effort was made to acquire time-resolved capability for our two-photon-photoemission effort. For this effort, experiments were conducted under monochromatic and bichromatic 2PPE modes. For the monochromatic setup, the laser system uses an ultrafast Ti:Sapphire oscillator, the pulses of which are amplified in a regenerative amplifier, and then used to drive our OPA to provide a tunable source of visible light. The visible output pulses are then frequency-doubled in a nonlinear crystal (β -BaB₂O₄), producing a train of tunable UV, 90 fs pulses, with photon energies in the 3.8 to 4.9 eV range at 250 kHz repetition rate and pulse energies of the order of 10 nJ. The bichromatic 2PPE measurements were carried out by overlapping the fundamental Ti:Sapphire oscillator output (IR: $1.51 < h\nu < 1.62$ eV) with its third harmonic (UV) generated by a β -BaB₂O₄ crystal. The lifetime, i.e., time-resolved measurements, were carried out by changing the time delay between the IR and UV pulses.

Future Plans

First, our immediate future plans will involve measurements at the Elettra Microbeamline in Trieste. Our experiments involve gated dichalcogenides and the use of suspended films on microstructured substrates. The higher resolution of this beamline will allow us to examine more closely information on spin-orbit splitting and other more subtle effects than in our initial studies. Recently we spent several months developing the sample handling systems for this work. Gating of the device will allow study of variably doped samples. Following this work, we will examine other dichalcogenide materials; these crystals will allow us to examine samples with larger spin-

orbit splitting. Second, our future experiments will involve unoccupied-state photoemission using fs lasers in order to probe thin layers of correlated-electron materials. We anticipate that our initial experiments will involve topological insulators. In order to carry out these experiments we must rework the UHV chamber to enable sample, *in-situ* cleaving, and high-quality vacuum. Third, we will build a new manipulator structure, which has a better vacuum level, sample cooling, and *in-situ* cleaving. We have now designed this manipulator and are formulating plans for fabrication.

References (which acknowledge DOE support)

1. W. Jin, P.-C. Yeh, N. Zaki, D. Zhang, J. T. Sadowski, A. Al-Mahboob, A. M. van der Zande, D. A. Chenet, J. I. Dadap, I. P. Herman, P. Sutter, J. Hone, R. M. Osgood, Jr., "Direct Measurement of the Thickness-Dependent Electronic Band Structure of MoS₂ Using Angle-Resolved Photoemission Spectroscopy." Phys. Rev. Lett. (Accepted, 2013)
2. N. Zaki, C. A. Marianetti, D. P. Acharya, P. Zahl, P. Sutter, J. Okamoto, P. D. Johnson, A. J. Millis, R. M. Osgood, "Experimental Observation of Spin-Exchange-Induced Dimerization of an Atomic One-Dimensional System." Phys. Rev. B: Rapid Communication 87, 16, 161406 (2013)
3. M. B. Yilmaz, J. I. Dadap, K. R. Knox, N. Zaki, Zhaofeng Hao, P. D. Johnson, R. M. Osgood, Jr., "Photoemission Band Mapping with a Tunable Femtosecond Source Using Nonequilibrium Absorption Resonances." J. Vac. Sci. Technol. A 30, 041403 (2012)
4. D. Niesner, Th. Fauster, J. I. Dadap, N. Zaki, K. R. Knox, P.-C. Yeh, R. Bhandari, R. M. Osgood, M. Petrovic, M. Kralj "Trapping Surface Electrons on Graphene Layers and Islands." Phys. Rev. B 85, 081402 (2012)
5. J. Okamoto and A. J. Millis, "One-dimensional physics in transition-metal nanowires: Renormalization group and bosonization analysis." Phys. Rev. B 85, 115406 (2012)
6. J. Okamoto and A. J. Millis, "One-dimensional physics in transition-metal nanowires: Phases and elementary excitations," Phys. Rev. B 84, 205433 (2011)
7. K.R. Knox, A. Locatelli, M.B. Yilmaz, D. Cvetko, T.O. Mentes, M.A. Nino, P. Kim, A. Morgante, and R.M. Osgood, Jr. "Making Angle-Resolved Photoemission Measurements on Corrugated Monolayer Crystals: Suspended Exfoliated Single-Crystal Graphene" Phys. Rev. B 84, 115401 (2011)
8. N. Zaki, R. Osgood, A. Millis, C. Marianetti, "The failure of DFT computations: stepped-substrate-supported monatomic highly-correlated wire system." Sub. Phys. Rev. B.
9. C. Arguello, E. Andrade, E. Rosenthal, S. Chockalingam, L. Zhao, C. Gutierrez, W. Chung, W. Jin, P.-C. Yeh, T. Valla, R. Fernandes, S. Jia, R. Osgood, A. Millis, R. Cava, A. Pasupathy "Scanning Tunneling Spectroscopy to probe the origin of Charge Density Waves in NbSe₂." (Submitted, PRL)

Other References

10. K.R. Knox, S. Wang, A. Morgante, D. Cvetko, A. Locatelli, T.O. Mentes, M.A. Niño, P. Kim, and R.M. Osgood, Jr., "Spectromicroscopy of Single and Multilayer Graphene Supported by a Weakly Interacting Substrate." Phys. Rev. B (Rapid Communications), 78, 201408 (2008)
11. N. Zaki, D. Potapenko, P.D. Johnson, and R.M. Osgood, Jr., "Atom-Wide Co Wires on Cu(775) at Room Temperature." Phys. Rev. B 80, 15, 155419 (2009)
12. Locatelli, K.R. Knox, D. Cvetko, T.O. Mentes, M.A. Niño, S. Wang, M.B. Yilmaz, P. Kim, R.M. Osgood, Jr., A. Morgante, "Corrugation in Exfoliated Graphene: An Electron Microscopy and Diffraction Study." ACS Nano 4, 8, 4879 (2010)

Program Title: Nanostructure Studies of Strongly Correlated Materials

Principal Investigator: Douglas Natelson

Mailing Address: Department of Physics and Astronomy, Rice University, MS 61, 6100 Main St., Houston, TX 77005

E-mail: natelson@rice.edu

Program Scope:

There are many materials in which strong electron-electron and electron-phonon interactions lead to rich phenomena associated with the competition between various ordered phases, including unconventional superconductivity, metal-insulator transitions, and colossal magnetoresistance. Great progress has been made in our understanding of these systems through bulk studies, spectroscopies, and nanoscale imaging such as scanning tunneling microscopy. This program employs nanostructure techniques, largely developed and applied to conventional semiconductors, to examine the properties of correlated materials, with a particular emphasis on systems that undergo metal-insulator transitions (for example, VO_2 and NdNiO_3). Nanostructure methods enable specific inquiries that are not possible with macroscopic samples:

- Electrodes with nanoscale separations allow the application of large electric fields even at modest voltages; this is important for delineating between true electric field effects and processes caused by energetic electrons.
- Electrodes separated at the nanoscale enable studies of correlated materials at length scales comparable to intrinsic and extrinsic inhomogeneities of the systems.
- Contact effects, often neglected or deliberately avoided, are most readily studied in nanostructures. In correlated materials with excitations that differ markedly from the weakly interacting quasiparticles of ordinary metals, contact effects can provide insights into the nature of the correlated state and its excitations.
- Field effect doping, the electrostatic modulation of the carrier density, is most readily performed in micro- or nanoscale device structures. This alters the electronic population at fixed disorder, to influence the competition between different ordered phases.
- In materials where elastic strain can strongly alter the balance between competing phases, nanoscale materials (*e.g.*, VO_2 single crystal nanobeams) allow studies in a controlled strain environment.

This program's efforts are currently directed toward two main material systems, VO_2 and NdNiO_3 , with additional plans to examine manganites and the charge density wave (CDW) system TiSe_2 . Both VO_2 and NdNiO_3 exhibit metal-insulator transitions, at 338 K and around 200 K, respectively. VO_2 has been studied for decades, with the first-order transition separating a high- T rutile (somewhat correlated) metallic R phase from a low- T insulating M1 monoclinic phase. The relative importance of Mott physics (from the half-filled V d -band) and Peierls physics (manifested in the dimerization of V chains in the M1 phase) has been a subject of much controversy. NdNiO_3 undergoes a first-order transition between a high- T paramagnetic metal and a low- T antiferromagnetic insulator, also associated with a structural distortion. In both cases, the overarching goal is to understand better the transition mechanism and the nature of the correlated states. This award supports two graduate students, and has resulted in five publications over the last two years¹⁻⁵.

Recent Progress:

Vanadium dioxide – Working with single-crystal VO_2 nanobeams grown through physical vapor deposition, we found that this material may be doped readily with atomic-hydrogen via catalytic spillover using Au, Cu, or Pd electrodes³. While chemically hydrogenated VO_2 had been demonstrated previously, this investigation was the first to examine the process in detail, identify that the doping process is reversible (at least in the presence of a catalyst for hydrogen splitting), and show that hydrogenation stabilized a metallic phase down to cryogenic temperatures with a structure similar to that of the rutile phase. Hydrogen doping in VO_2 proceeds through highly anisotropic diffusion of atomic H, with diffusion enhanced along the rutile *c*-axis compared to the transverse directions, analogous to what has been observed for atomic H in rutile TiO_2 . Strain strongly influences the diffusion rate; it is challenging to assess the strain-free material response.

We also performed experiments⁴ attempting to use ionic liquids for electrolytic gating of VO_2 nanowires, with the idea of tuning the metal-insulator transition via a gate potential. In agreement with work on VO_2 films at Harvard and IBM⁶, we found no large gating effect that was not electrochemical in origin.

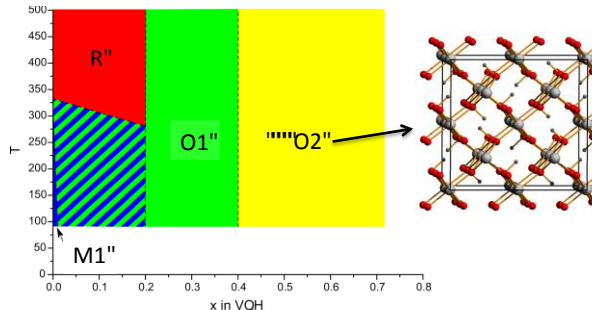


Figure 2. Phase diagram for $\text{H}_x \text{VO}_2$, with inferred structure of O2 phase ($\text{V} = \text{gray}$; $\text{O} = \text{red}$; $\text{H} = \text{black}$).

act as catalyst, with hydrogenation taking place *in situ* under a pressurized H_2 atmosphere. He has also performed neutron powder diffraction on analogously prepared deuterated samples. The results, in preparation for publication, are shown in Fig. 1. We now know that there are multiple hydrogen-containing phases of different symmetries. As hydrogen concentration is increased to intermediate values ($0.2 < x < 0.4$), $\text{H}_x \text{VO}_2$ goes from the distorted rutile $P4_2/mnm$ symmetry to the orthorhombically deformed $Pnnm$ symmetry **O1 phase**, in which the hydrogen atom positions are disordered along the vanadium *c* axis direction; each hydrogen is bound to an oxygen, forming a hydroxyl group. At higher hydrogen occupancies, there is ordering of the hydrogen positions, as the material's unit cell doubles to $2a$, $2b$, $2c$ compared to the O1 phase, becoming the **O2 phase** with $Fdd2$ symmetry. Both the O1 and O2 phases are stable down to cryogenic temperatures and appear to be paramagnetic. Preliminary evidence is that these phases

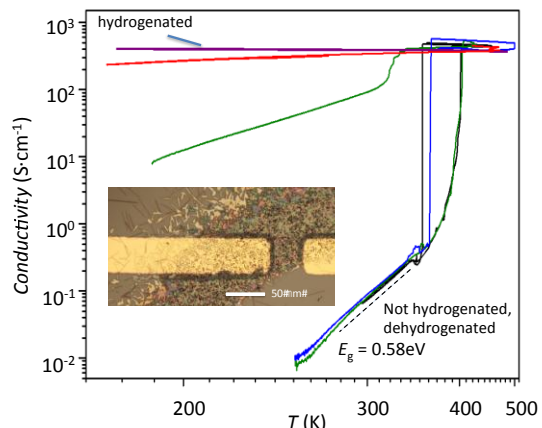


Figure 1. Conductivity vs. T for VO_2 nanobeam at various hydrogenation conditions. Inset: hydrogenation by spillover is visible in VO_2 in contact with Au pads.

The hydrogenation result has led to us pursuing three avenues of research regarding VO_2 . First, we have been collaborating with the group of Yaroslav Filinchuk of Université Catholique de Louvain (UCL), with the goals of understanding the detailed structure of $\text{H}_x \text{VO}_2$, quantifying hydrogen content, and mapping out the structural phase diagram of the $\text{H}_x \text{VO}_2$ system. Prof. Filinchuk has applied synchrotron methods to examine nominally strain-free powders of VO_2 mixed with (< 1% mass fraction) Pd nanoparticles to

are metallic, with the vanadium *d* band crossing the Fermi level. Note that metallicity even in the presence of unit cell doubling as in the O₂ phase suggests that Peierls physics is not dominant in the hydrogen-doped system.

To better understand the hydrogenation process and to perform low temperature transport experiments in the now-stabilized metallic state, we collaborated with Prof. Darrell Schlom of Cornell University and Prof. Jiang Wei of Tulane University, both of whom have sent us epitaxial VO₂ films (rutile *c*-axis as growth direction) on TiO₂ substrates. We have used direct low-*T* (~ 100 C and below) exposure to atomic H as well as catalytic spillover (Pd nanoparticles + H₂ exposure) to dope these strained films. In summary, we find: (1) Hydrogenation kinetics are much more rapid in the R phase than in the M1 phase; (2) hydrogenation is still possible and detectable in the M1 phase in these thin films; (3) de-hydrogenation is greatly hastened by the presence of catalyst particles; (4) When highly hydrogenated, the films can be extremely conductive at room temperature (a few Ohms per square), and remain conductive at cryogenic temperatures (hundreds of Ohms per square), but never show a metallic temperature dependence. This last point requires greater study – is this an effect of strain in the film, or an intrinsic property due to the underlying conduction mechanism? This work is in preparation for publication.

We have also worked with VO₂ nanobeams and atomic hydrogenation, including collaboration with Prof. Andriy Nevidomskyy of Rice via a shared undergraduate student, to try to quantify the diffusion process and compare with results of *ab initio* calculations. Calculations estimating the difference in activation energies for hydrogen hopping along the rutile *c*-axis for the R and M1 phases are encouraging, yielding results close to the experimental numbers (diffusion constant in R approximately 60 times higher than that in M1 for temperatures near the transition). Additional efforts have included an undergraduate project using an inductive method to assess the electronic properties of VO₂ powder in a non-contact configuration, and another undergraduate effort on the transfer of VO₂ nanosheets onto predefined nanogap electrodes.

Nickelates – Using films provided by Prof. Suzanne Stemmer of UCSB, we have been performing transport measurements on NdNiO₃ thin film (12–16 nm thick) devices on length scales from tens of microns down to ~ 200 nm. While it took some time to perfect the fabrication technique, we have now been able to observe the metal-insulator transition and the onset of the gap for transport. In particular, we find a crossover from ordinary resistive transport (differential conductance at zero bias scaling inversely with the length of the device) even well into the resistive state (20 K) to a regime at lower temperatures that looks much more like field-driven breakdown of the insulating state (differential conductance as a function of dc electric field showing a single functional form; *I*-*V* characteristics well described by a theoretical expression⁷ for Landau-Zener breakdown in a correlated system). Preliminary results are shown in Fig. 3.

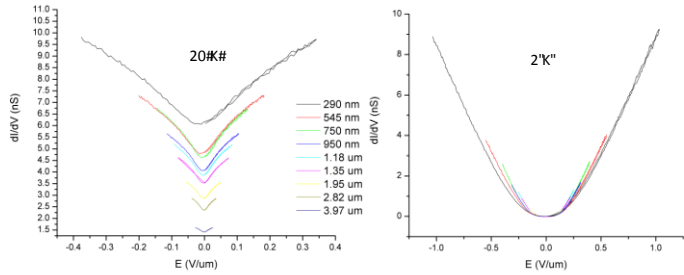


Figure 3. dI/dV vs. V/L for NdNiO₃ film devices.

Future Plans:

Vanadium dioxide – We will continue to perform transport experiments in the stabilized O₂ state in both films and nanobeams to examine the transport mechanism at work. In undoped nanogap

devices we plan to examine the evolution of the differential conductance into the nonlinear regime above and below the transition, to better understand the nature of the transition. We remain interested in measurements of the optical conductivity of H_xVO_2 , to assess the importance of correlations in this conducting state, though there are practical issues associated with performing optical characterization in low strain films. Finally, we will begin performing noise measurements in nanoscale junctions on VO_2 in its various phases. Of particular initial interest are the metallic, undoped R phase and the stabilized metallic O1 and O2 phases, where correlations may lead to renormalization of the noise when compared with a conventional metal.

Nickelates – We plan to continue our examination of the gapped state in and away from equilibrium in $NdNiO_3$. Of particular interest is the evolution of the gap in transport as a function of external magnetic field, H ; preliminary measurements show an enhanced conductance and decreased gap at cryogenic temperatures and large H . The hope is that the nonequilibrium response as found through transport will be an additional means of learning about the nature of the correlated state. Close collaboration with theory would be of great benefit here, and we are hopeful of developing such links.

Other materials – We will be branching out to examine exfoliated $TiSe_2$, known to exhibit a CDW transition, and known to exhibit superconductivity when doped with Cu as an intercalant. We plan to examine ionic liquid gating in this material as well as conventional field effect, and will similarly look at the evolution of the gapped state via nonequilibrium transport. Similarly, we will begin working with Prof. Charles Ahn of Yale University on $La_xCa_{1-x}MnO_3$ films, looking specifically at the evolution of the gapped state and its stability at large in-plane electric fields.

References acknowledging DOE support in previous two years:

1. D. Natelson and M. Di Ventra, "[Ion motion and electrochemistry in nanostructures](#)", [MRS Bulletin](#) **36**(11), 914-920 (2011).
2. Fursina, R. G. S. Sofin, I. V. Shvets, and D. Natelson, "[Statistical distribution of the electric field driven switching of the Verwey state in \$Fe_3O_4\$](#) ", [New Journal of Physics](#) **14**, 013019 (2012).
3. J. Wei, H. Ji, W. Guo, A. Nevidomskyy, and D. Natelson, "[Hydrogen stabilization of metallic \$VO_2\$ in single-crystal nanobeams](#)", [Nature Nano.](#) **7**, 357-362 (2012).
4. H. Ji, J. Wei, and D. Natelson, "[Modulation of the electrical properties of \$VO_2\$ nanobeams using an ionic liquid as a gating medium](#)", [Nano Lett.](#) **12**, 2988-2992 (2012).
5. E. Morosan, D. Natelson, A. H. Nevidomskyy, and Q. M. Si, "[Strongly Correlated Materials](#)", [Adv. Mater.](#) **24**, 4896-4923 (2012).

Other references:

6. J. Jeong, N. Aetukuri, T. Graf, T. D. Schladt, M. G. Samant, & S. S. P. Parkin, "Suppression of Metal-Insulator Transition in VO_2 by Electric Field-Induced Oxygen Vacancy Formation", [Science](#) **339**, 1402-1405 (2013).
7. Oka, T. & Aoki, H. Ground-State Decay Rate for the Zener Breakdown in Band and Mott Insulators. [Phys Rev Lett](#) **95**, 137601 (2005).

Program Title: **Probing the Origins of Conductivity Transitions in Correlated Solids: Experimental Studies of Electronic Structure in Vanadium Oxides.**

Principal Investigator: Kevin E. Smith,

Mail: Department of Physics, Boston University, 590 Comm. Ave., Boston, MA 02215.

e-mail: ksmith@bu.edu

Program Scope:

There is enormous scientific interest in understanding and controlling solid state electronic conductivity transitions. The switching of the electrical properties of a material between those of a metal and those of a non-metal is the very basis of the electronics industry. These transitions can be driven by many external and internal mechanisms, including electric and magnetic fields, chemical doping, defects, disorder, pressure, dimensionality, and temperature.

Vanadates display particularly complex and fascinating electronic phenomena. Whether as simple binary oxides or as ternary compounds with substituted metal cations, vanadates are replete with complex conductivity transitions, as well as charge ordering transitions, structural phase transitions, frustrated spin structures, superconductivity, and unusual magnetic properties. As such, vanadates are a prototypical class of correlated material.

The goal of this program is to measure the electronic properties of vanadates, and to use the knowledge gained to provide a deeper understanding of the origins of conductivity transitions in correlated materials. This in turn facilitates the control of these transitions. The experimental tools used are soft x-ray emission spectroscopy (XES), soft x-ray absorption spectroscopy (XAS), resonant inelastic soft x ray scattering (RIXS), x-ray photoemission spectroscopy (XPS), angle resolved photoemission spectroscopy (ARPES), and soon spectroscopic photoemission low energy electron microscopy (SPELEEM). The use of this highly diverse suite of electron and photon techniques enables a very wide range of physically important vanadates to be studied, since we can measure electronic structure in samples that are electrical conductors or electrical insulators, and in samples that are single crystals, thin films, polycrystalline powders, or nanoparticles. This degree of flexibility is unusual and highly advantageous. Through these conductivity transitions, we measure (and test against theory), band structures, densities of states, Fermi surfaces, many body correlations, charge states, valence band hybridization, valence excitations.¹⁻¹²

Recent Progress:

Rapid progress has been made over the last two years.¹⁻¹² Highlights include:

- The discovery of a new form of VO₂, namely a ***rutile insulating phase***;⁹
- The identification of the significant role played by ***V-O hybridization*** in the metal-insulator transition in VO₂;¹⁰
- The discovery of a ***dimensional-induced metal-to-insulator transition*** in CaVO₃;⁴
- The determination of ***orbital anisotropy and low-energy excitations*** in the quasi one-dimensional conductor β-Sr_{0.17}V₂O₅;¹¹
- The discovery of ***surface enhanced*** electron correlation in Sr_xCa_{1-x}VO₃;¹

- The determination of the electronic structure of the *kagomé staircase compounds*, $\text{Ni}_3\text{V}_2\text{O}_8$ and $\text{Co}_3\text{V}_2\text{O}_8$;²
- The development of a data analysis program for the *maximum entropy deconvolution* of resonant inelastic x-ray scattering spectra;¹²

A unifying theme of our vanadate work was the exploration of the effect of externally engineered factors on conductivity transitions. *Specifically, we have attempted to understand how mechanical strain and chemical doping can be used to precisely control these transitions.*

Future Plans:

We will continue definitive study of vanadates, involving measurement of their electronic structure as temperature, chemical composition, atomic and orbital order, defect concentration, physical form, and dimensionality, are varied. Our plans involve four related thrust areas:

1: Mechanical control of conductivity transitions: Whereas the mechanism of the conductivity transition in bulk VO_2 is understood as an orbital-assisted collaborative Mott-Peierls transition (or associated variants),^{13,14} the situation is less clear under large applied strain. Furthermore, our earlier XES and XAS studies of the metal-to-insulator transition in strained VO_2 revealed the importance of V-O orbital hybridization.¹⁰ We have performed experiments on heavily strained VO_2 thin films that led us to a startling discovery, namely a decoupling of the conductivity transition from the structural phase transition.⁹ Specifically, we observe a transition of VO_2 from a metal to an insulator, while the lattice remains in a rutile-like structure. This could have important implications for functional material engineering of VO_2 , suggesting a route towards circumventing the structural bottleneck in the ultrafast timescale of the metal-to-insulator transition.⁹ The remarkable observation of a new *static* phase of pure VO_2 forms the basis for a set of proposed experiments on other strained vanadate thin films, where we will look for additional cases of where a metal-to-insulator transition can be driven towards a purely electronic transition by the application of mechanical strain.⁹ We will examine both V_2O_3 and Cr-doped V_2O_3 films. This latter vanadate displays a rich phase diagram in the bulk, with two metal-to-insulator transitions, only one of which is associated with a structural phase transition.

2: Many body interactions: We performed a combined photoemission spectroscopy (PES) and XES study on $\text{Sr}_x\text{Ca}_{1-x}\text{VO}_3$, and made a remarkable discovery, namely surface enhanced electron correlation.¹ Our XES results are in much closer agreement with DMFT calculations than the photoemission results,¹⁵ and illustrate the powerful application that XES can have in addressing correlated electron behavior, particularly when comparisons can be directly made with ARPES measurements. We plan to confirm this observation by measuring hard x-ray PES at $h\nu \sim 4$ keV, allowing us to probe the electronic structure much deeper into the bulk of the material. Once we have completed our study of the $\text{Sr}_x\text{Ca}_{1-x}\text{VO}_3$ ($0 \leq x \leq 1$) system, we propose to more broadly explore this important observation of surface enhanced electron correlation. One promising class of vanadate to study in this context is the vanadium oxide β -bronzes, which show metal to non-metal transitions accompanied by charge ordering.^{16,17} Their chemical formula is $\beta\text{-}A_x\text{V}_2\text{O}_5$ (A : Li^+ , Na^+ , Ag^+ or Ca^{2+} , Sr^{2+} , Pb^{2+}) and they have a mixed valence of $\text{V}^{4+}(d^1)$ and $\text{V}^{5+}(d^0)$. As layered materials, they are ideal for study using ARPES.

3. Orbital and spin degrees of freedom: There is great interest in the coupling between orbital and spin degrees of freedom in correlated solids.¹⁸ While interatomic orbital *mixing* determines lattice distortions in many metal oxides (PbO, etc),¹⁹ the *ordering* of orbitals can also lead to lower symmetry lattice distortions. Materials with significant coupling between the orbital and spin degrees of freedom can display complex phenomena, including changes in conductivity with applied fields. The unique sensitivity of XES to hybrid states allows us to measure directly the detailed electronic structure of the orbitals of interest in such materials, while the element specificity of RIXS allows excitations from particular orbitals to be probed. We propose to study vanadates that exhibit orbital ordering effects and conductivity transitions, specifically orthovanadates RVO_3 (R = rare earth), and kagomé staircase vanadates $\text{M}_3\text{V}_2\text{O}_8$ (M = transition metal). We have made initial experiments in both of these areas, showing the feasibility of our approach.

4. Phase separation: The importance of phase separation and spatial inhomogeneity is increasingly recognized in vanadate conductivity transitions. The latter is reflected in the microstructure of VO_2 thin film surfaces, which exhibit microdomains of the order of a few μm .⁹ Consequently, there are obvious benefits to ARPES recorded from micron-sized areas of the sample surface (μARPES). A second question is the nature of the emergence of the metallic phase. In the low-temperature insulating phase, VO_2 adopts the M_1 monoclinic structure, whereas the tetragonal rutile (R) structure hosts the metallic phase. IR microscopy measurements indicate the percolation of ‘metallic nanopuddles’ at the transition into macroscopic metallic domains.²⁰ There is a recent report of the observation of striped M_1 and R phases in VO_2 thin films through the transition.²¹ We plan a combination of XPEEM, μXPS and μARPES to study of the electronic structure of VO_2 , and related vanadates, in an effort to understand the evolution in electronic structure across the transitions in real and reciprocal space.

References since 2011 which acknowledge DOE support:

1. J. Laverock, B. Chen, K.E. Smith, R.P. Singh, G. Balakrishnan, M. Gu, J.W. Lu, S.A. Wolf, R.M. Qiao, W. Yang, and J. Adell, "Resonant soft x-ray emission as a bulk probe of correlated electron behavior in metallic $\text{Sr}_x\text{Ca}_{1-x}\text{VO}_3$ ", Phys. Rev. Lett. (*in press*) (2013).
2. J. Laverock, B. Chen, A.R.H. Preston, K.E. Smith, G. Balakrishnan, P.-A. Glans, and J.-H. Guo, "Electronic structure of the kagomé staircase compounds $\text{Ni}_3\text{V}_2\text{O}_8$ and $\text{Co}_3\text{V}_2\text{O}_8$ ", Phys. Rev. B **87**, 125133 (2013).
3. S. Kittiwatanakul, J. Laverock, D. Newby, K.E. Smith, S.A. Wolf, and J. Lu, "Transport behavior and electronic structure of phase pure VO_2 thin films grown on *c*-plane sapphire under different O_2 partial pressure", J. Appl. Phys. **114**, 053703 (2013).
4. M. Gu, J. Laverock, B. Chen, K.E. Smith, S.A. Wolf, and J.W. Lu, "Metal-insulator transition induced in CaVO_3 thin films", J. Appl. Phys. **113**, 133704 (2013).
5. B. Chen, J. Laverock, L.F.J. Piper, A.R.H. Preston, S.W. Cho, A. DeMasi, K.E. Smith, D.O. Scanlon, G.W. Watson, R.G. Egddell, P.-A. Glans, and J.-H. Guo, "Band structure of WO_3 and non-rigid band behaviour in $\text{Na}_{0.67}\text{WO}_3$ from soft x-ray spectroscopy and density functional theory", Journal of Physics, Cond. Mat. **25**, 165501 (2013).
6. V.B.R. Boppana, F. Jiao, D. Newby, J. Laverock, K.E. Smith, J.C. Jumas, G. Hutchings, and R.F. Lobo, "Analysis of Visible-Light-Active Sn(II)-TiO₂ Photocatalysts", Phys. Chem. Chem. Phys. **15**, 6185 (2013).

7. J. Laverock, D. Newby Jr., E. Abreu, R.D. Averitt, K.E. Smith, R.P. Singh, G. Balakrishnan, J. Adell, and T. Balasubramanian, "Determination of the k -resolved susceptibility function of 2H-TaSe₂ from angle-resolved photoemission measurements", Phys. Rev. B **88**, 035108 (2013).
8. L.F.J. Piper, N.F. Quackenbush, S. Sallis, D.O. Scanlon, G.W. Watson, K.W. Nam, X.Q. Yang, K.E. Smith, F. Omenya, N.A. Chernova, and M.S. Whittingham, "Elucidating the nature of pseudo Jahn-Teller distortions in Li_xMnPO₄: Combining density functional theory with soft and hard x-ray spectroscopy", J. Phys. Chem. C **117**, 10383 (2013).
9. J. Laverock, A.R.H. Preston, D. Newby, K.E. Smith, S. Sallis, L.F.J. Piper, S. Kittiwatanakul, J. Lu, S.A. Wolf, M. Leandersson, and T. Balasubramanian, "Photoemission evidence for crossover from Peierls-like to Mott-like transition in highly strained VO₂", Phys. Rev. B **86**, 195124 (2012).
10. J. Laverock, L.F.J. Piper, A.R.H. Preston, B. Chen, J. McNulty, K.E. Smith, S. Kittiwatanakul, J.W. Lu, S.A. Wolf, P.A. Glans, and J.H. Guo, "Strain dependence of bonding and hybridization across the metal-insulator transition of VO₂", Phys. Rev. B **85**, 081104 (R) (2012).
11. J. Laverock, A.R.H. Preston, L.F.J. Piper, B. Chen, J. McNulty, K.E. Smith, P.A. Glans, J.H. Guo, C. Marin, E. Janod, and V. Ta Phuoc, "Orbital anisotropy and low-energy excitations of the quasi-one dimensional conductor β -Sr_{0.17}V₂O₅", Phys. Rev. B **84**, 155103 (2011).
12. J. Laverock, A.R.H. Preston, D. Newby, Jr., K.E. Smith, and S.B. Dugdale, "Maximum entropy deconvolution of resonant inelastic x-ray scattering spectra", Phys. Rev. B **84**, 235111 (2011).

Other References:

13. M.W. Haverkort, Z. Hu, A. Tanaka, W. Reichelt, S.V. Streltsov, M.A. Korotin, V.I. Anisimov, H.H. Hsieh, H.J. Lin, C.T. Chen, D.I. Khomskii, and L.H. Tjeng, "Orbital-assisted metal-insulator transition in VO₂", Phys. Rev. Lett. **95**, 196404 (2005).
14. C.d. Weber, D.D. O'Regan, N.D.M. Hine, M.C. Payne, G. Kotliar, and P.B. Littlewood, "Vanadium Dioxide: A Peierls-Mott Insulator Stable against Disorder", Phys. Rev. Lett. **108**, 256402 (2012).
15. I.A. Nekrasov, G. Keller, D.E. Kondakov, A.V. Kozhevnikov, T. Pruschke, K. Held, D. Vollhardt, and V.I. Anisimov, "Comparative study of correlation effects in CaVO₃ and SrVO₃", Phys. Rev. B **72**, 155106 (2005).
16. T. Yamauchi, M. Isobe, and Y. Ueda, "Charge order and superconductivity in vanadium oxides", Solid State. Sci. **7**, 874 (2005).
17. T. Yamauchi, Y. Ueda, and N. Môri, "Pressure-Induced Superconductivity in β -Na_{0.33}V₂O₅ beyond Charge Ordering", Phys. Rev. Lett. **89**, 057002 (2002).
18. K. Adachi, T. Suzuki, K. Kato, K. Osaka, M. Takata, and T. Katsufuji, "Magnetic-Field Switching of Crystal Structure in an Orbital-Spin-Coupled System: MnV₂O₄", Phys. Rev. Lett. **95**, 197202 (2005).
19. D.J. Payne, R.G. Egisdóttir, G. Paolicelli, F. Offi, G. Panaccione, P. Lacovig, G. Monaco, G. Vanko, A. Walsh, G.W. Watson, J. Guo, G. Beamson, P.-A. Glans, T. Learmonth, and K.E. Smith, "Nature of electronic states at the Fermi level of metallic β -PbO₂ revealed by hard x-ray photoemission spectroscopy", Phys. Rev. B **75**, 153102 (2007).
20. M.M. Qazilbash, M. Brehm, B.-G. Chae, P.-C. Ho, G.O. Andreev, B.-J. Kim, S.J. Yun, A.V. Balatsky, M.B. Maple, F. Keilmann, H.-T. Kim, and D.N. Basov, "Mott Transition in VO₂ Revealed by Infrared Spectroscopy and Nano-Imaging", Science **318**, 1750 (2007).
21. M. Liu, M. Wagner, E. Abreu, S. Kittiwatanakul, A. McLeod, Z. Fei, M. Goldflam, S. Dai, M. Fogler, J. Lu, S.A. Wolf, R.D. Averitt, and D.N. Basov, "Anisotropic electronic state via spontaneous phase separation in strained vanadium dioxide films", (*in preparation*) (2013).
22. T. Schmidt, S. Heun, J. Slezak, J. Diaz, K.C. Prince, G. Lilienkamp, and E. Bauer, "SPELEEM: Combining LEEM and Spectroscopic Imaging", Surf. Rev. Lett. **5**, 1287 (1998).

Program Title: “**Nanostructured Materials: From Superlattices to Quantum Dots**”
Principle Investigator: Ivan K. Schuller
Mailing Address: Physics Department, UCSD, La Jolla, Ca. 92093
E-mail: ischuller@ucsd.edu

Program Scope

This project is dedicated to important issues, which arise when materials are nanostructured in one, two and three dimensions. This comprehensive project includes preparation of nanostructures using thin film (Sputtering and MBE) and lithography (electron beam, Focused Ion Beam and self assembly) techniques, characterization using surface analytical, scanning probe microscopy, scattering (X-ray and Neutron) and microscopy techniques and measurement of physical properties (magneto-transport, magnetic and magneto-optical). The important physical properties investigated include confinement, a variety of proximity effects in hybrids, and induced phenomena by the application of external driving forces such as time varying electric and magnetic fields, light and other types of radiation. This has lead and will possibly produce and/or uncover unique new physical phenomena and devices. In particular, this research has major impact in the area of nanomagnetism a major basic forefront research area world-wide which has important implications for technologies such as energy storage and conversion. Specific physical problems investigated include important basic research issues in: exchange bias in magnetic bilayers; confinement of magnetism by geometric boundaries; proximity effects between ferromagnets/antiferromagnets, metals/oxides, organics/metals; and their behavior at ultrafast times. Moreover, some of the techniques (especially structural characterization) developed under this project are supplied free of charge to other researchers in a wide variety of related areas.

This research has direct impact on DOE’s Five Challenges for Science and Imagination and develops the basic research foundation of many technologies important for the nation. Moreover, this research has potential impact on new applications in important areas of applied research for DOE such as energy storage and conversion, sensors, novel electronics and data storage. Thus development and patenting important ideas are crucial ingredients in this project.

An important and crucial ingredient in this project is the education of the next generation scientists and technologists in state of the art forefront instrumentation, experimental and theoretical techniques. Many young researchers educated in this area have been traditionally employed in industries in the high technology area, have become independent researchers at major research and/or industrial organizations or educators in universities and/or colleges.

In addition to in-house research, collaborations, which crucially rely on materials and devices developed under this project, are underway at major DOE facilities (synchrotrons and neutron), at UCSD and other research universities. Thus this project is a source of materials and devices used by researchers all across the US and internationally, principally at other DOE funded institutions.

Recent Progress

Recently, we have performed extensive experiments, which are directly related to the aims of this project. Our studies have focused recently on understanding the behavior of hybrid materials that have properties, which are unlike that of either constituent. Thus the proximity between ferromagnets and antiferromagnets, ferromagnets and oxides, oxides and oxides, may develop properties, which are unlike either of the constituents.

In the field of Exchange Bias (i.e. the shift of the hysteresis loop) we performed several experiments, which help us identify the origin of the phenomenon. This is an important unsolved problem in the field. By preparing hybrid ferromagnetic/antiferromagnetic samples with nanostructured antidots prepared by Focused Ion Beams (FIB) we generated bulk uncompensated pinned spins and showed that they play a major role on Exchange Bias. [1] Interestingly and contrary to commonly held beliefs, the bulk of the antiferromagnet (not only the interface with the ferromagnet) plays a crucial role in the development of the Exchange Bias. This opens up new ways to engineer exchange-biased systems and explains many controversial issues in the field.

Through a detailed structural and magnetic study we have been able for the first time to observe the connection between exchange bias and the so-called “Verwey transition” in Fe_3O_4 . [2] The two series of experiments mentioned above may have important implication for the development of novel exchange biased systems in which the interaction of dissimilar magnetic materials fundamentally modifies their behavior.

We have performed, in collaboration with Los Alamos scientists, a detailed study of the ferromagnetism of one-dimensional chains in organic metallo-phthalocyanine films. This study addresses one of the fundamental issues related to the effect of dimensionality and magnetism. Using a combination of magneto-optical Kerr effect, SQUID magnetometry and Magnetic Circular Dichroism we were able to investigate the regimes in which weak inter-chain magnetic interaction produce nontraditional paramagnetic behavior whereas in the regime where the inter chain interaction is strong traditional magnetic behavior is recovered. [3]

In a tour-de-force experiment, [4] in collaboration with scientists at the Los Alamos National Labs, we have put an upper limit on the ferromagnetism at the interfaces of $\text{LaAlO}_3/\text{SrTiO}_3$. This is a major development since all measurement to date claiming spectacular effects at this interfaces were based on bulk or local magnetic measurements and only neutron scattering could ascertain unequivocally the origin of the fleeting magnetic signals encountered. This is an interesting and unique application of neutron scattering showing the importance and power of this major facility based technique.

The properties of oxide-magnetic hybrids are very interesting particularly when ferromagnets (FM) are in proximity to materials that undergo a metal-insulator (MIT) and

structural phase transition (SPT). The stress associated with the SPT produces a magnetoelastic anisotropy in proximity coupled FM films that allows controlling the magnetic properties without magnetic fields. Canonical examples are the vanadium oxides; VO₂ and V₂O₃. VO₂ undergoes a metal/rutile to an insulator/monoclinic phase transition at 340 K. In V₂O₃ the 160 K transition is from a metallic/rhombohedral to an insulating/ monoclinic phase. We have investigated the magnetic properties of different combinations of ferromagnetic (Ni, Co and Fe) and vanadium oxide thin films. The (0.32%) volume expansion in VO₂ or the (1.4 %) volume decrease in V₂O₃ across the MIT produce an interfacial stress in the FM overlayer. The coercivities and magnetizations of the FM grown on vanadium oxides are strongly affected by the phase transition. The coercivity change can be as large as 170 % and occur in a very narrow temperature interval. These effects are controlled by the thickness and deposition conditions. For VO₂/FM bilayers the large coercivity change occurring above room temperature opens the possibilities for important technological applications. It also opens up the road towards bulk applications in which a material that undergoes a phase transition is intimately mixed with a magnetic material. [5]

Importance of findings

The above-mentioned research shows in a clear fashion that the proximity between dissimilar, nanoscaled materials can change their properties in a fundamental fashion. Moreover, it also shows avenues for controlling and engineering properties of materials, which are not available in nature. This can be accomplished by the application of external stimuli, such as time varying light, magnetic, electric field. In this fashion, it is possible to engineer new properties and or manipulate other properties in a useful and interesting fashion. Moreover, it allows investigating time dependent properties, which in many cases have major relevance in a broad range of fields including catalysis, photolysis, magnetism and transport. These studies clearly provide the scientific underpinning of a variety of disrupting technologies related to energy production, sensor and electronics.

Future Plans

We will continue our studies of spin propagation in materials that undergo metal insulator transitions (MIT). This may allow manipulation of spin propagation in ways not yet done to date, mostly because the MITs provide large effects which occur close to room temperature in a whole broad range of materials. This may reduce the energy consumption needed for switching magnetic devices in a variety of applications.

We will continue the study of the effect of nanostructuring on Exchange Bias. In addition we will investigate the production of pinned moments in the bulk of the antiferromagnet using ion irradiation. This will allow us to address what is probably the key issue in the field; where are the spins that produce the effect? This will also have important implications for applied areas in the field of spintronics and energy transformation.

We will study the effect of the nanostructuring on a variety of Non Local (NL) effect such as NL spin valves, local and NL planar Hall effect etc... By studying nanostructured materials we can access the fundamental physics, for instance of single magnetic domain walls which are not generally available by performing more global measurements.

We will perform further studies at synchrotron and neutron facilities to map out the 3 dimensional spin concentration when magnetic and non-magnetic materials are in proximity and/or are driven by external stimuli. This will include, magnetic-normal, magnetic-oxide, and magnetic-antiferromagnetic etc. heterostructures in a variety of configuration and/or subject to electric field and or light. We will also investigate novel collective states developed at interfaces between oxides. In addition, we will expand our studies to investigate time dependent properties of materials, which exhibit collective, strongly interacting behavior. This will be done in collaborations with scientists at major DOE facilities; neutron and synchrotron facilities. This is an ideal symbiotic relationship in which samples and materials, which are developed in a single investigator laboratory, are studied using large DOE facilities, which provide atomic scale physical, chemical and magnetic structure. Many of the preliminary measurements and in some cases the major discoveries are accomplished prior to taking samples to major facilities thus assuring that the later are used in a most efficient way. In this fashion, interesting new physics is uncovered and its use in possible novel applications maybe developed.

Selected References (which acknowledge DOE support)

- [1] *Mirror Symmetry in Magnetization Reversal and Coexistence of Positive and Negative Exchange Bias in Ni/FeF₂ Heterostructures*, M. Kovylina, M. Erekhinsky, R. Morales, I.K. Schuller, A. Labarta, and X. Batlle, *Appl. Phys. Letts.* 98, 152507 (2011).
- [2] *Exchange Bias Induced by the Fe₃O₄ Verwey Transition*. J. de la Venta, M. Erekhinsky, S. Wang, K. West, R. Morales, and I. K. Schuller, *Phys. Rev. B*, 85, 134447 (2012).
- [3] *Substrate Controlled Ferromagnetism in Iron Phthalocyanine Films due to One-Dimensional Iron Chains*, T. Gredig, C. N. Colesniuc, S. A. Crooker, and I. K. Schuller, *Phys. Rev. B*, 86, 014409 (2012).
- [4] *Upper Limit to Magnetism in LaAlO₃/SrTiO₃ Heterostructures*, M. R. Fitzsimmons, N. W. Hengartner, S. Singh, M. Zhernenkov, F. Y. Bruno, J. Santamaria, A. Brinkman, M. Huijben, H. J. A. Molegraaf, J. delaVenta, and I. K. Schuller, *Phys. Rev. Lett.*, 107, 217201(2011).
- [5] *Control of Magnetism Across Metal to Insulator Transitions*, J. de la Venta, S. Wang, J.G. Ramirez and I.K. Schuller, *App. Phys. Lett.* 102, 122404 (2013).

Program title: Spectroscopic investigations of novel electronic and magnetic materials

Principle Investigator: Janice L. Musfeldt

Affiliation: Department of Chemistry, University of Tennessee, Knoxville TN 37996

Contact: (865) 974-3392 or musfeldt@utk.edu

Program scope

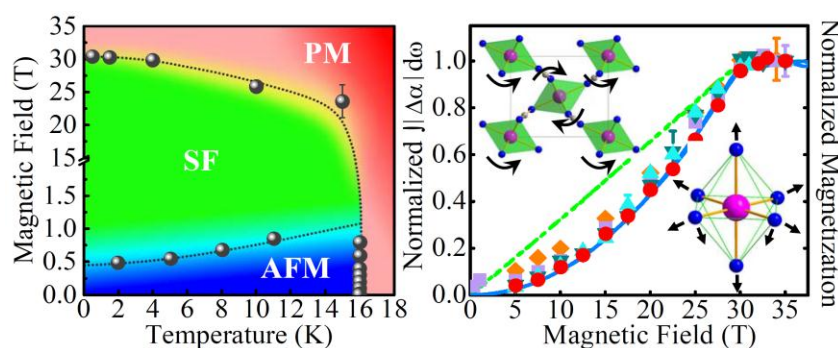
The goal of our research program is to develop a fundamental understanding of the mechanisms underlying the interplay between charge, structure, and magnetism in complex materials. This insight will facilitate the development of tunable multifunctional solids and nanomaterials, which are scientifically and technologically important. Our main strategy involves investigating the dynamic response of functional materials such as multiferroics and frustrated systems under external stimuli such as high magnetic fields, under unusual chemical and photochemical activation, and at very small sizes where quantum confinement becomes apparent. This allows us to learn about the relationships between different ordered and emergent states, explore the dynamic aspects of coupling, and gain insight into the generality of these phenomena and their underlying mechanisms. In addition to broadening the understanding of novel solids under extreme conditions, multifunctional materials and their assemblies are of interest for light harvesting, spintronic, and solid state lubrication applications.

Recent progress

Our team is well known for spectroscopic work on complex materials in high magnetic fields, under unusual chemical and photochemical activation, and at very small sizes where quantum confinement becomes apparent. In our Department of Energy-supported program, we recently used high magnetic fields to drive quantum critical transitions in $\text{Mn}[\text{N}(\text{CN})_2]_2$ and $\text{Ni}_3\text{V}_2\text{O}_8$ to reveal amplified magnetoelastic and charge-spin interactions that lead to field-induced local lattice distortions and color changes. We also discovered the Burstein-Moss effect in Re-substituted MoS_2 nanoparticles and identified spectroscopic signatures of the superparamagnetic transition and surface spin disorder in CoFe_2O_4 nanoparticles. These efforts are detailed below.

Quantum critical transition amplifies magnetoelastic coupling in $\text{Mn}[\text{N}(\text{CN})_2]_2$: Quantum phase transitions and associated quantum-critical points present a rich and challenging research area that is of current fundamental interest. In contrast to classical phase transitions governed by thermal fluctuations, quantum phase transitions are driven by an external parameter such as magnetic field, pressure, or composition. One case where field works as a quantum tuning parameter is in the suppression of antiferromagnetic order by applied magnetic field where the resulting quantum critical point separates the antiferromagnetic state from the fully polarized

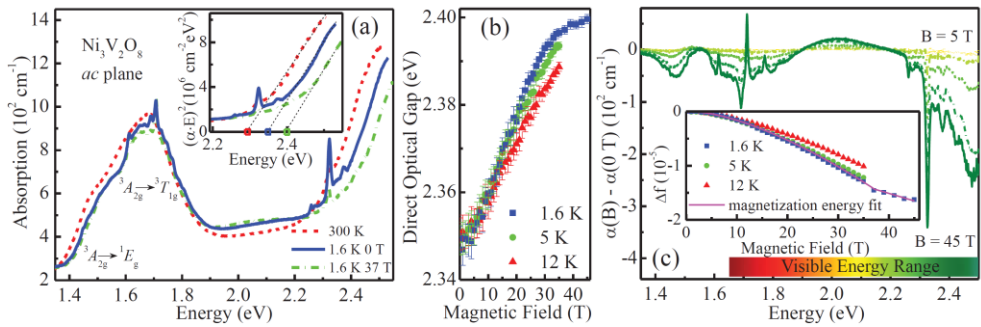
Fig. 1: The 30 T magnetic quantum critical transition in $\text{Mn}[\text{N}(\text{CN})_2]_2$ drives an antiferromagnetic to fully polarized state crossover with amplified magnetoelastic coupling. Important mode behaviors are overlaid on magnetization squared.



paramagnetic state. We recently reported the discovery of a magnetic quantum critical transition in $\text{Mn}[\text{N}(\text{CN})_2]_2$, the complete magnetic field-temperature phase diagram, and enhanced magnetoelastic coupling through the field-driven transition that we analyzed in terms of local lattice distortions (Fig. 1). The latter reveals a combined MnN_6 octahedra distortion + counter-rotation mechanism that reduces antiferromagnetic interactions and stabilizes the fully polarized state. Similar local lattice distortions underpin the remarkable properties of photomagnetic cyanides, ferroelectrics, and correlated oxides. These findings advance the fundamental understanding of quantum phase transitions, provide insight into higher energy scale materials, and are relevant to more complicated processes in which field acts as a tuning parameter like multiferroicity, multiple magnetization plateaus, and skyrmion lattice development.

Magnetic field-induced shift of the optical band gap in multiferroic $\text{Ni}_3\text{V}_2\text{O}_8$: The band gap is one of the most important electronic energy scales in a solid. It determines a variety of physical properties including *dc* resistivity, and it is vital to a number of applications like light harvesting. In both traditional semiconductors and complex oxides, the gap can be manipulated by chemical substitution, temperature, and pressure. Magnetic field also drives changes in the electronic properties. This effect can be as simple as the textbook case of Zeeman splitting of an isolated atom or as unexpected as amplified spin-charge interactions due to a collective phase transition in a solid. We recently investigated the interaction of spin ordering with charge excitations through the magnetic phase transition in frustrated $\text{Ni}_3\text{V}_2\text{O}_8$ with special emphasis on the color properties (Fig. 2). Our measurements reveal field-induced blue shifts of the band gap that are much larger than those driven by temperature, anticipating a more greenish appearance in the fully polarized state. This color change is verified with direct photographic images and emanates from charge density differences around the Ni and O centers in high field. These findings reveal that key electronic energy scales like the charge gap can be tuned to a surprising extent with external stimuli, and that when major charge excitations appear in the visible range, field-induced shifts can induce color property modifications.

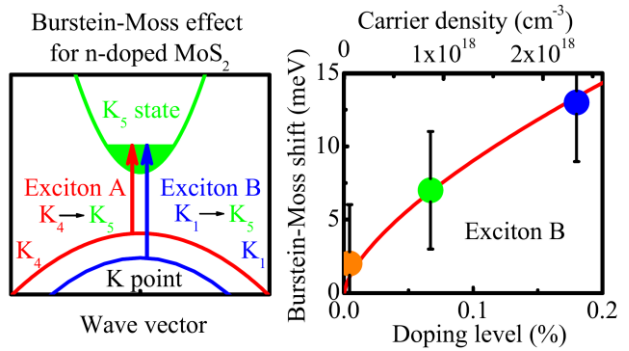
Fig. 2: (a) $\alpha(E)$ and gap analysis. (b) Gap vs. field at a few temperatures. (c) Absorption difference spectra [$\alpha(B) - \alpha(B = 0 \text{ T})$] at 1.6 K for $B//b$ axis at selected fields.



Discovery of a Burstein-Moss shift in Re-substituted metal dichalcogenide nanoparticles: The Burstein-Moss shift arises from the Pauli exclusion principle and describes how adding electrons or holes to traditional semiconductors like CdSe and ZnO controls carrier concentration, modifies the band gap, and enables control over the electronic structure. This is an enormously important issue for conventional bulk semiconductors and quantum dots because the Burstein-Moss model provides a framework under which a quantitative relationship between dopant concentration and carrier density can be established. Layered transition metal dichalcogenides like the hexagonal molybdenum disulfide (2H-MoS₂) are also candidates for investigation. The fact that nanoscale analogs reveal ambipolar transistor behavior, superconductivity under gating,

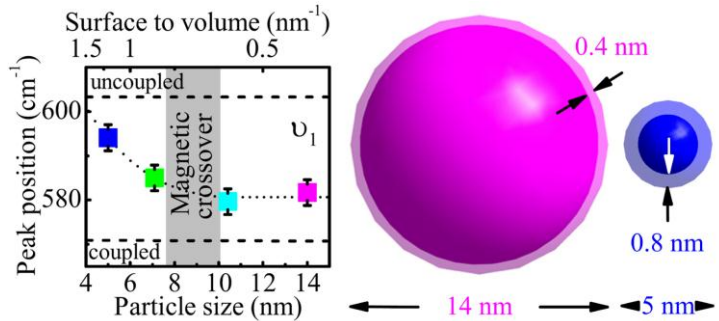
and enhanced tribological properties adds to the contemporary interest. We recently discovered a Burstein-Moss shift in a nanoscale transition metal dichalcogenide (Fig. 3). Our measurements reveal that small size softens the exciton positions and reduces spin-orbit coupling whereas doping has the opposite effect. Based on exciton and oscillator strength trends, we extract doping-induced changes in spin-orbit coupling and demonstrate that the carriers are bound rather than free. Taken together, these findings establish the relevance of the Burstein-Moss model to low dimensional metal dichalcogenide nanomaterials, extend the relationship between nominal and actual Re concentration to include a quantitative connection to carrier density, and highlight the unique electronic character of Re-substituted MoS₂ nanoparticles which is important for realizing the potential of transition metal dichalcogenides for chalcogenide-based electronics and solid state lubrication applications.

Fig. 3: (a) Schematic view of the Burstein-Moss effect in electron doped MoS₂ nanoparticles. (b) Measured blue-shift of exciton B as a function of Re substitution compared with predictions of the model. This agreement establishes a quantitative connection between actual dopant concentration and carrier density for nanoscale metal dichalcogenides.



Spectroscopic signature of the superparamagnetic transition and surface spin disorder in CoFe₂O₄ nanoparticles: Phonons are exquisitely sensitive to finite length scale effects in a wide variety of materials because they are intimately connected to charge, structure, and magnetism, and a quantitative analysis of their behavior can reveal microscopic aspects of chemical bonding. To investigate confinement in combination with strong magnetoelastic interactions, we measured the infrared vibrational properties of CoFe₂O₄ nanoparticles and compared our results to trends in the coercivity over the same size range and to the response of the bulk material. Remarkably, the spectroscopic response is sensitive to the size-induced crossover to the superparamagnetic state, which occurs between 7 and 10 nm (Fig. 4). This is because magnetoelastic coupling in the confined system makes the mode position sensitive to the superparamagnetic transition. A spin-phonon coupling analysis supports the core-shell model. Moreover, it provides an estimate of the magnetically disordered shell thickness, which increases from 0.4 nm in the 14 nm particles to 0.8 nm in the 5 nm particles, demonstrating that the associated local lattice distortions take place on the length scale of the unit cell (0.8391 nm for bulk CoFe₂O₄). These findings are important for understanding finite length scale effects in this and other correlated magnetic oxides where

Fig. 4: Peak position of metal-oxygen stretching mode as a function of particle size. The gray shaded area indicates the transition regime (from ferrimagnetic at large particle sizes to superparamagnetic at small sizes). Schematic view of our findings from the core-shell model in the 14 and 5 nm particles, respectively.



magnetoelastic interactions are important. They are also unique in that they verify the core-shell model from the spectroscopic point of view.

Future plans

Several exciting efforts are planned for the coming year. Briefly, they include (i) investigating field-induced color changes and magnetism in frustrated $R(\text{In},\text{Mn})\text{O}_3$ to test the role of combined frustration and spin-orbit interactions on the field-induced color change mechanism, (ii) probing the spectroscopic signatures of various topological structures like stripes and vortices on the dynamics of ErMnO_3 and BiFeO_3 to understand the dynamics of topological domains in multiferroics, (iii) measuring the optical properties of spinel ferrites with a focus on high temperature gap trends, the impact of finite length scale effects, and as superlattices, and their photoconductive response under broad band illumination to reveal charge-spin coupling, and (iv) Investigating nanoscale hematite to explore finite length scale effects on vibronic coupling.

Publications emanating from this grant (2012 – 2013)

1. *Magnetic field induced color change in $\alpha\text{-Fe}_2\text{O}_3$ single crystals*, P. Chen, N. Lee, S. McGill, S. -W. Cheong, and J. L. Musfeldt, Phys. Rev. B. **85**, 174413 (2012).
2. *Spectroscopic signature of the superparamagnetic transition and surface spin disorder in CoFe_2O_4 nanoparticles*, Q. -C. Sun, C. S. Birkel, J. Cao, W. Tremel, and J. L. Musfeldt, ACS Nano **6**, 4876 (2012).
3. *Spin spiral quenching in Nd^{3+} -substituted BiFeO_3* , P. Chen, O. Gunaydin-Sen, W. J. Ren, Z. Qin, T. V. Brinzari, S. McGill, S. -W. Cheong, and J. L. Musfeldt, Phys. Rev. B. **86**, 014407 (2012).
4. *Absorption-controlled growth of LuFe_2O_4 by molecular-beam epitaxy*, C. M. Brooks, R. Mirsra, J. A. Mundy, L. A. Zhang, B. S. Holinsworth, K. R. O'Neal, T. Heeng, W. Zander, J. Schubert, J. L. Musfeldt, Z. -K. Liu, D. A. Muller, P. Schiffer, and D. G. Schlom, Appl. Phys. Lett. **101**, 132907 (2012).
5. *Novel optical band gap hierarchy in a magnetic oxide: electronic structure of NiFe_2O_4* , Q. -C. Sun, H. Sims, D. Mazumdar, J. X. Ma, B. S. Holinsworth, K. R. O'Neal, W. H. Butler, A. Gupta, and J. L. Musfeldt, Phys. Rev. B. **86**, 205106 (2012).
6. *Observation of a Burstein-Moss shift in Re-substituted MoS_2 nanoparticles* Q. -C. Sun, L. Yadgarov, R. Rosentsveig, G. Seifert, R. Tenne, and J. L. Musfeldt, ACS Nano. **7**, 3506 (2013).
7. *Quantum critical transition amplifies magnetoelastic coupling in $\text{Mn}[\text{N}(\text{CN})_2]_2$* T. V. Brinzari, P. Chen, Q. -C. Sun, J. Liu, L. -C. Tung, Y. J. Wang, J. A. Schlueter, J. Singleton, J. L. Manson, M. -H. Whangbo, A. P. Litvinchuk, and J. L. Musfeldt, Phys. Rev. Lett. **110**, 237202 (2013).
8. *Spectroscopic determination of phonon lifetimes in Re-substituted MoS_2 nanoparticles* Q. -C. Sun, L. Yadgarov, R. Rosentsveig, R. Tenne, and J. L. Musfeldt, Nano Lett. **13**, 2803 (2013).
9. *Chemical tuning of the optical band gap in spinel ferrites: CoFe_2O_4 vs NiFe_2O_4* , B. S. Holinsworth, D. Mazumdar, H. Sims, M. K. Yurtisigi, S. Sarter, A. Gupta, W. H. Butler, and J. L. Musfeldt, Appl. Phys. Lett. **103**, 082406 (2013).
10. *Magnetic field-induced shift of the optical band gap in $\text{Ni}_3\text{V}_2\text{O}_8$* , P. Chen, B. S. Holinsworth, K. R. O'Neal, T. V. Brinzari, D. Mazumdar, Y. Q. Wang, S. McGill, R. J. Cava, B. Lorenz, and J. L. Musfeldt, submitted, Phys. Rev. Lett.

Session 3

Program Title: Transport Studies of Quantum Magnetism: Physics and Methods

Principal Investigator: Minhyea Lee

Mailing Address: 390 UCB, Department of Physics, University of Colorado Boulder, Boulder CO 80309-0390

Email: minhyea.lee@colorado.edu

(i) Program Scope

A part of our research program explores the spin chirality or non-trivial spin texture within a long-range ordered phase to characterize a novel magnetic state via magnetotransport measurements. Especially, transverse transport measurements - e.g. Hall effect and Nernst effect - provide a unique sensitivity to the existence of broken time-reversal symmetry, as manifested in such as anomalous Hall effect of ferromagnets or the edge state of quantum Hall systems. Recent works in our group are focused on a new type of magnetically ordered state to form a lattice from vortex-like objects in the spin texture, so-called Skyrmions [1]. Two-dimensional Skyrmion lattices are stabilized in the presence of an external magnetic field and thermal fluctuations near the Curie temperature (T_C), occupying a small pocket in the temperature (T) - magnetic field (B) phase diagram. They orient perpendicular to the applied field B (along z direction), and have been directly observed with small angle neutron scattering [1] and Lorentz tunneling electron microscopy [2], exclusively in B20-structures with cubic symmetry (space group P2₁3). Celebrated examples include the itinerant ferromagnet MnSi, semiconductors Fe_xCo_{1-x}Si, and FeGe, and insulator Cu₂SeO₃. The B20 crystal structure lacks inversion symmetry, allowing a new energy scale (D), the Dzyaloshinsky-Moriya interaction, to compete with the conventional exchange interaction (J). This results in a helically ordered magnetic ground state with well defined pitch λ , whose length is proportional to J/D . The length scale for the unit cell of a Skyrmion crystal is also set by λ [5], which runs from a few nm to a few tens of nm, depending on the compound. Hexagonal skyrmion lattices, however, are merely one example of a variety of possible non-collinear or non-coplanar spin structures. It is the non-coplanarity of these spin textures that can give a rise to an emergent magnetic field b_r .

$$b_r^i = \frac{\Phi_0}{8\pi} \epsilon_{ijk} \hat{n} \cdot (\partial_j \hat{n} \times \partial_k \hat{n})$$

where ϵ_{ijk} is the Levi-Civita symbol whose indices run over x, y , and z and $n(\mathbf{r})$ is a unit vector of the magnetization $M(\mathbf{r})$, and $\Phi_0 = h/e$ is the single electron flux quantum. Physically, the field arises in the strong Hund coupling limit, where the spin of conduction electrons orients parallel to the local magnetization, twisting to follow it as they move through the material. This results in the acquisition of an extra phase factor in their wave functions, represented by the line integral of a vector potential, analogous to the Aharonov-Bohm effect. The curl of that vector potential is the quantity given in equation above, which acts on conduction electrons in a similar way as the physical magnetic field, and causes the topological Hall effect (THE). Especially, the area integral b_r over the magnetic unit cell is quantized to an

integer number of flux quanta Φ_0 , which allows estimation of the upper bound for the average topological magnetic field induced by the spin texture, i. e. b_r proportional to Φ_0/λ^2 , where λ^2 corresponds to the area of the magnetic unit cell. The scale of this emergent field is as large as tens of Tesla for the conduction electron traveling through the spin-texture, which requires only a couple of tenth of Tesla of physical magnetic field to generate. Direct access to such large field via electronic transport opens up possibilities to incorporate such materials into technological application where a large field is required. The goals of our research program lie in understanding the discrepancy between the theoretical upper bound and actually measured one via Hall effect, and searching for new materials among vast variety of frustrated magnets, other than B20 crystal structure.

(ii) Recent Progress

Motivated to tune the skyrmion size, set by the helical pitch length λ and thus control the magnitude of the theoretical emergent field b_r , we have recently studied the Hall effect in Fe doped MnSi with samples with 6% and 9% Fe contents, and compare to that of pure MnSi under pressure. The primary effect of increasing Fe content is a suppression of T_C and the saturated magnetic moment m_S , both of which monotonically go to zero, vanishing at the critical doping concentration $x_c \simeq 15\text{--}19\%$ [4]. Previous studies have shown that Fe doping leads to a linear decrease in J while leaving D unchanged, resulting in a decrease in λ observed in scattering experiments [5]. Pressure also gradually suppresses T_C to zero at the $P_C \simeq 15$ kbar, however at $P = P_C$, m_S remains at $2/3$ of the value at $P = 0$, instead of vanishing to zero. Moreover, the helical pitch length also remains constant under pressure [6].

In our study, we discovered that the topological contribution in the sample with 9% Fe content is enhanced by a factor of 5 compared to pure MnSi. Unique B dependence of Hall resistivity ρ_{yx} , in which the topological Hall signal is marked unambiguously with the sharp peak within narrow range of T and B , that is known as A-phase.

We compare this with the Hall effect of pure MnSi under pressure, where large enhancement of the THE was also reported [3]. In addition to the changes magnitude, the sign of the THE was found to change as Fe doping, accordingly to that of normal Hall coefficient R_H , always remaining opposite to the sign of R_H . We compared the theoretical upper bound of the

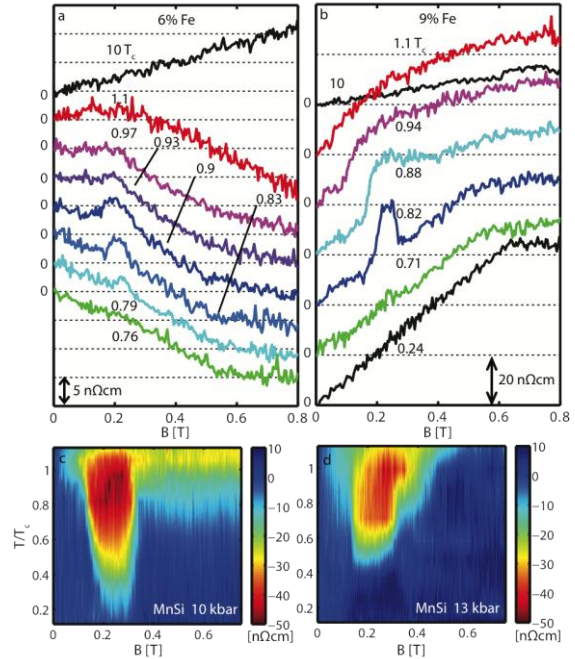


Figure 1 Hall resistivities as a function of B for the 6% (a) and 9% (b) sample. The different traces correspond different fixed T_c , indicated as a fraction of T_c . Color plots of the Hall resistivity of pure MnSi under pressure are shown at 10 kbar(c) and 13 kbar (d).

emerge field b_r from Φ_0/λ^2 to the measured B_{eff} from the relation $\rho_{yx}^C = R_H B_{\text{eff}}$, where the topological Hall resistivity (ρ_{yx}^C) is parsed from ρ_{yx} as a function of applied field B (for detailed see [8]), shown in Figure 1. The ratio $f = b_r/B_{\text{eff}}$ ranges between 0.2 and 0.4 for both Fe-doped and pressurized samples, while for pure MnSi at ambient pressure the ratio is much lower, only 0.05. Interestingly, despite the large size of the THE in pure MnSi under pressure, f remains more or less similar to the 9% Fe sample. We suggest three physical considerations that will be reflected in the value of f : (i) The strength of the coupling between conducting carriers and the spin texture. Only in the limit of strong Hund coupling, where the spin of conduction electrons tightly follows the spin-texture, can f approach unity. (ii) Alteration of the band structure and/or the shape of the Fermi surface via Fe doping and pressure is expected to modify the ratio of conduction electrons with majority to minority spins. This changes the magnitude of the THE, as electron with opposite spin feel opposite fields. (iii) The presence of strong fluctuations in the spin texture on much shorter time scales than our measurement period (in 10^{-3} second) is expected to reduce the time-averaged value of the emergent field B_{eff} . Magnetoresistances in both Fe-doped samples and pure MnSi under pressure demonstrate horn-like feature in A-phase, which implies the scattering rate gets modified by the spin-texture, yet rather small changes in magnitude confirm that the large emergent field can only contribute to the transverse conductivity.

We begin to obtain preliminary data on the magnetotransport measurement under pressure of 9% Fe-doped. At low pressure (up to 4 kbar), the THE signal is indeed increased then gets reduced rapidly as increasing P . This contrasts with the greatly enhanced THE signal in pure MnSi under pressure, which gets little diminished as P approach P_C . Based on this observation, we conclude that the spin fluctuation effect, likely strong chiral fluctuation plays important role in enhancing the THE signal of pure MnSi under pressure.

(iii) Future Plans

We will continue to study the evolution of skyrmion lattice and related spin texture, and the resulting changes of the emergent field as increasing the Fe doping. We are keen to observe how suppressing the magnetic long range order either via pressure or doping alters the spin texture, and thus the strength of emergent field reflected on the THE signal. Such results are expected to provide a guideline to search for other materials harboring non-trivial spin textures that generate the emergent field with large magnitude. In turn, it will also provide a steppingstone for utilizing such large field in technological application. Our investigations will be focused searching for other materials with the helical magnetic order originating from lacking the inversion symmetry, other than B20 structure. For example, $\text{Cr}_{1/3}\text{NbS}_2$ satisfies those conditions: While its magnetic anisotropy is larger than MnSi, moderate applied field (~ 2 T) seems enough to remove such anisotropy. $\text{Pr}_2\text{Ir}_2\text{O}_7$ is another example of non-coplanar spin configuration, which is believed to lead to non-zero Hall signal even in the zero applied field [7]. Both systems are under their way in our group. In fact, it will be worthwhile to re-visit non-collinear or non-coplanar spin structures, ubiquitously observed in metallic

frustrated magnets, where such non-trivial spin texture may be responsible for the strong B dependent Hall resistivity.

(iv) References

- [1] S. Muhlbauer, et al., *Science* **323**, 915 (2009).
- [2] X. Yu et al., *Nature* **465**, 901 (2010).
- [3] Minhyea Lee *et al.*, *Phys. Rev. Lett.* **102**, 186601 (2009)
- [4] A. Neubauer et al., *Phys.Rev.Lett.* **102** , 186602 (2009).
- [5] S.V. Grigoriev et al., *Phys.Rev.B* **79** , 144417 (2009).
- [6] B.A. Fak et al., *J. Phys: Cond. Matt.* **17**,1635 (2005)
- [7] S. Nakatsuji, et al., *Nature* **463**, 210 (2010)

(v) Publications (which acknowledge DOE support)

- [8] Benjamin J. Chapman, Maxwell G. Grossnickle, Thomas Wolf and Minhyea Lee, *Large enhancement of emergent magnetic fields in MnSi with impurities and pressure*, submitted to *Phys.Rev.Lett.* (2013).
- [9] □Xiaoqing Zhou, Lafe Spietz, Jose Aumentado and Minhyea Lee, *Resolution limits of the shot noise thermometer*, submitted to *J. App. Phys.* (2013).

Thermalization of artificial spin ice and related frustrated magnetic arrays

Principal Investigator: Peter Schiffer, University of Illinois at Urbana-Champaign, Urbana, IL (pschiffe@illinois.edu)

Co-Investigators: Vincent Crespi and Nitin Samarth, Pennsylvania State University, University Park, PA

Project Scope

This program encompasses experimental and theoretical studies of lithographically fabricated arrays of nanometer-scale single-domain ferromagnetic islands in which the array geometry results in frustration of the magnetostatic interactions between the islands. Such geometrical frustration can lead to multiple energetically equivalent configurations for the magnetic moments of the islands and a variety of associated novel collective behavior. These systems are analogs to a class of magnetic materials in which the lattice geometry frustrates interactions between individual atomic moments, and in which a wide range of novel physical phenomena have been recently observed. The advantage to studying lithographically fabricated samples is that they are both designable and resolvable: i.e., we can control all aspects of the array geometry, and we can also observe how individual elements of the arrays behave. In previous work, we have demonstrated that we can fabricate and probe frustrated magnet arrays, including some geometries that are directly analogous to the “spin ice” materials. We have designed frustrated lattices, controlled the strength of interactions by changing the spacing of the islands, and demonstrated that the island magnetic moment orientation is controlled by the inter-island interactions. Current work is focusing on thermal annealing of these arrays at temperatures above the Curie point of the ferromagnetic permalloy, a technique that allows better access to the low-energy ground state of these many-body systems.

Recent Progress

The past two years of this program has involved finishing some ongoing projects and initiating some new efforts. All work has been done in close collaboration with the group of Chris Leighton at the University of Minnesota and that of Cristiano Nisoli at Los Alamos National Laboratory.

Thermal annealing of artificial spin ice: Because of the large magnetic energy scales of the ferromagnetic islands in artificial spin ice, workers in the field have been unable to thermally anneal artificial spin ice into desired thermodynamic ensembles. Previous studies of artificial spin ice have either applied alternating magnetic fields or focused on the as-grown state of the systems, neither of which allowed consistent study of the ground state of the arrays (such as ordering of magnetic monopolar charges). We have demonstrated a method for thermalizing artificial spin ice arrays by heating them above the Curie temperature of the constituent material. This effectively allows us to reach the ground state of square ice and see charge ordering in

kagome ice. We find excellent agreement between experimental data and Monte Carlo simulations of emergent charge–charge interactions [2].

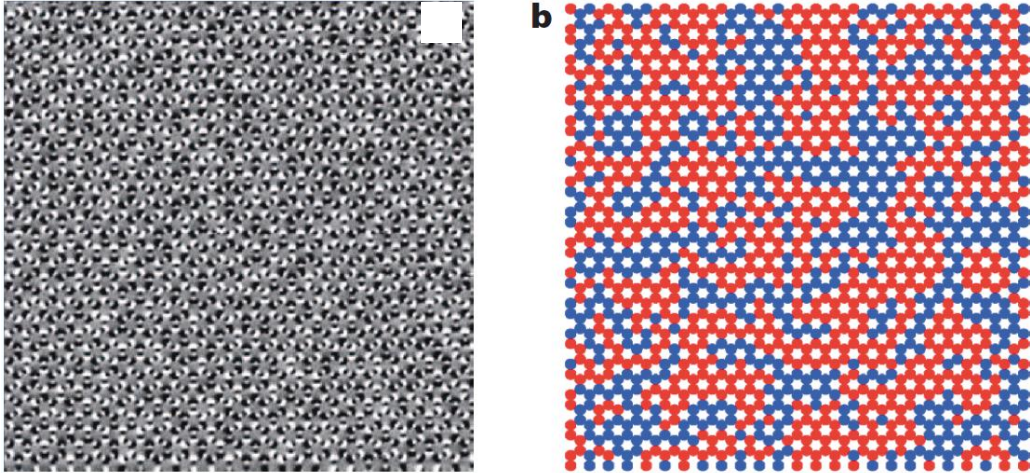


Figure 1 magnetic force microscope image of kagome artificial spin ice array on right and a representation of the magnetic charge order on left. The red and blue colors show complementary ordering of the effective magnetic charges. [figure from reference 2]

Perpendicular anisotropy artificial spin ice: We have studied artificial frustrated magnets consisting of single-domain ferromagnetic islands with magnetization normal to the plane, contrasting with all other studies that focused on moments in-plane. The measured pairwise spin correlations of these lattices can be reproduced by models based solely on nearest-neighbor correlations. Our study included a kagome lattice array with qualitatively different magnetostatics but identical lattice topology to previously-studied in-plane moment systems. The two systems show striking similarities in the development of moment pair correlations, demonstrating a level of universality in artificial spin ice behavior that is independent of specific realization in a particular material system [3].

The role of collective interactions in nanomagnet assemblies: We have studied the moment correlations within triangular lattice arrays of single-domain co-aligned nanoscale ferromagnetic islands. Independent variation of lattice spacing along and perpendicular to the island axis tunes the magnetostatic interactions between islands through a broad range of relative strengths. For certain lattice parameters, the sign of the correlations between near-neighbor island moments is opposite to that favored by the pair-wise interaction. This finding, supported by analysis of the total correlation in terms of direct and convoluted indirect contributions (a modified Ornstein-Zernike equations), indicates that indirect interactions and/or those mediated by further neighbors can be dominant, with implications for the wide range of systems composed of interacting nanomagnets [4].

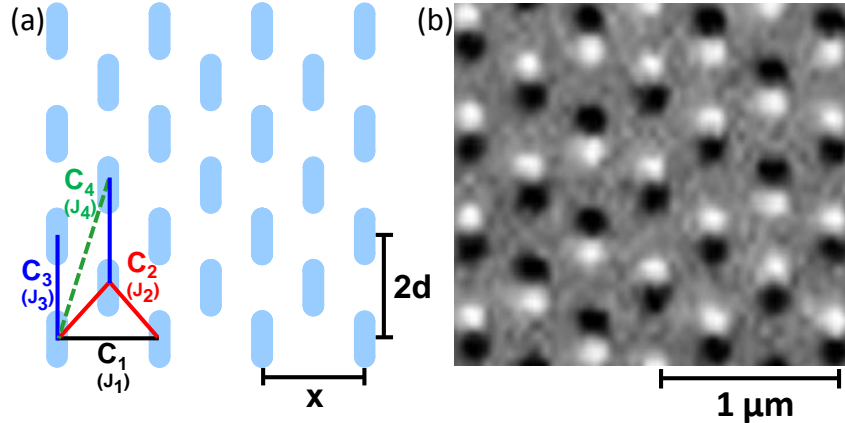


Figure 2 (a) Schematic of triangular lattice arrays of single domain nanomagnets with frustrated magnetostatic interactions. The near-neighbor pair types are labeled C1, C2, C3, and C4, and the convolution of all four pairs can affect moment correlations. (b) MFM image of a section of one triangular lattice array ($x = 680$ nm, $d/x = 0.4$). Black and white halves represent the north and south poles of each ferromagnetic island. [4]

Magneto-optical Kerr effect studies of square artificial spin ice: We have performed a magneto-optical Kerr effect study of the collective magnetic response of artificial square spin ice. We find that the anisotropic inter-island interactions lead to a non-monotonic angular dependence of the array coercive field, and comparisons with micromagnetic simulations indicate that the two perpendicular sublattices exhibit distinct responses to changing magnetic field that drive the magnetization reversal process. Furthermore, such comparisons demonstrate that island shape disorder plays a hitherto unrecognized but essential role in the collective behavior of these systems. This technique holds promise for a range of extended studies of artificial frustrated magnets, including frequency-dependent ac measurements. [6]

Future Plans:

Future plans for this research program include a number of different thrusts, in particular exploration of the consequences of thermalization for a range of different lattices and the effects of defects in a fully thermalized state. We also plan the development of MOKE microscopy for single-island imaging of the arrays with better time resolution than MFM allows. We also will explore electrical transport in systems consisting of interconnected ferromagnetic nanowire links.

References and Publications Acknowledging DOE support:

1. “Artificial Spin Ice: Controlling Geometry, Engineering Frustration,” Cristiano Nisoli, Roderich Moessner, and Peter Schiffer, *Reviews of Modern Physics* (in press, 2013).
2. “Crystallites of magnetic charges in artificial spin ice”, Sheng Zhang, Ian Gilbert, Cristiano Nisoli, Gia-Wei Chern, Michael J. Erickson, Liam O’Brien, Chris Leighton, Paul E. Lammert, Vincent H. Crespi and Peter Schiffer, *Nature* (in press, 2013).

3. “Ignoring Your Neighbors: Moment Correlations Dominated by Indirect or Distant Interactions in an Ordered Nanomagnet Array,” Sheng Zhang, Jie Li, Jason Bartell, Xianglin Ke, Cristiano Nisoli, Paul E. Lammert, Vincent H. Crespi, and Peter Schiffer Physical Review Letters **107**, 117204 – 1-4 (2011).
4. “Perpendicular Magnetization and Generic Realization of the Ising Model in Artificial Spin Ice,” Sheng Zhang, Jie Li, Ian Gilbert, Jason Bartell, Michael J. Erickson, Yu Pan, Paul E. Lammert, Cristiano Nisoli, K. K. Kohli, Rajiv Misra, Vincent H. Crespi, Nitin Samarth, C. Leighton, and Peter Schiffer, Physical Review Letters **109**, 087201 – 1-4 (2012).
5. “Magnetization states and switching in narrow-gapped ferromagnetic nanorings,” Jie Li, Sheng Zhang, Chris Grigas, Rajiv Misra, Jason Bartell, Vincent H. Crespi, and Peter Schiffer AIP Advances **2**, 012136 – 1-6 (2012).
6. “Magneto-optical Kerr effect studies of square artificial spin ice”, K. K. Kohli, Andrew L. Balk, Jie Li, Sheng Zhang, Ian Gilbert, Paul E. Lammert, Vincent H. Crespi, Peter Schiffer, and Nitin Samarth Physical Review B **84**, 180412(R) – 1-5 (2011).

Program Title: Spin wave interactions in metallic ferromagnets

Principle Investigator: Kristen Buchanan

Mailing Address: Department of Physics, Colorado State University, Fort Collins, CO
80523

E-mail: kristen.buchanan@colostate.edu

Program Scope

Spintronics and magnonics are two areas of active research in condensed matter physics and important connections between the two are beginning to emerge. The former refers to a new paradigm for electronic devices that make use of not only the charge but also the spin property of the electron. The latter refers to new ideas for how to utilize spin waves to transmit and process information. Both areas are attracting interest not only because they encompass a range of basic physics topics but also because of their potential to inspire new technologies. The interplay between spin dynamics, spin currents, and, more recently, heat transfer, are rich areas of basic physics research. Recent work has shown that spin dynamics is not only useful as a means to quantify spin Hall effects in materials, but also that the interactions of spin waves with spin accumulation at interfaces may provide a means to control the spin dynamics in a magnetic material. Furthermore, the study of the thermal effects on magnons may also help to provide insight into thermally-driven spin phenomena. This project will look at how dynamic processes in magnetic materials are affected by spin accumulation and thermal effect in order to gain new insight into these processes.

The main technique used for this project is Brillouin Light Scattering (BLS). The BLS technique has grown to become a powerful method for investigating dynamic excitations in magnetic materials and multilayers as well as patterned magnetic structures nanostructures [1]. Photons interact with spin waves or magnons in magnetic materials such that they are either created or annihilated in the scattering process. These are inelastic scattering processes so the scattered photon gains or loses energy in the process, which results in a small but measurable shift in frequency that is equal to the magnon frequency. BLS is capable of detecting spin waves at frequencies of approximately 1-120 GHz with diffraction-limited spatial resolution with a micro-BLS setup (Fig. 1) and temporal resolution of ~250 ps can be obtained through time-of-flight measurements. It is sensitive enough to measure thermally-generated spin waves [2]. The use of a magneto-optical probe to measure the magnetic state of the sample ensures that the magnetization is undisturbed during the

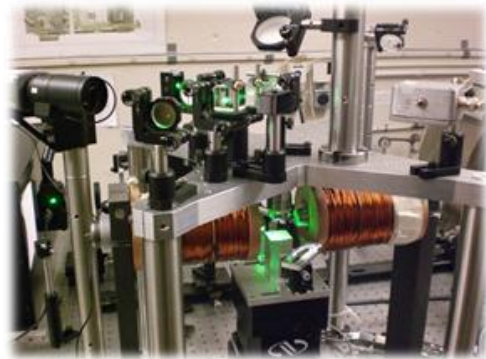


Fig. 1: Photo of the micro-BLS. The laser is focused down to a spot size of approximately 300 nm. The sample sits on an XYZ positioning stage with ~10 nm positioning accuracy and the sample position and focus are continuously stabilized using feedback from a camera. An electromagnetic provides a DC magnetic field and high frequency probes deliver microwaves to the sample. The scattered light is directed into a Fabry Perot Interferometer to determine the frequencies of the inelastically scattered photons.

measurement, providing a distinct advantage over techniques that employ magnetic probes, and it can be used effectively under a wide range of measurement conditions.

Recent Progress

Spin wave propagation in bilayer metallic/ferromagnet nanowires: One of the broad goals of this project is to study how spin waves interact with spin accumulations in an adjacent nonmagnetic material. As a first step towards this goal we have studied spin wave propagation in bilayer nanowires (FM/NM) that consist of 30 nm of Permalloy with an underlayer of 50 nm of gold (Fig. 2a). This sample design provides a starting point to study the effects of current on spin wave propagation for a simple situation where spin Hall effects should be small due to both the large thickness of the gold and the small spin Hall angle for this material. Electrical contacts were attached to each side of a 2.5- μm wide FM/NM nanowire and a microwave antenna was patterned on top to generate spin waves in the nanowire.

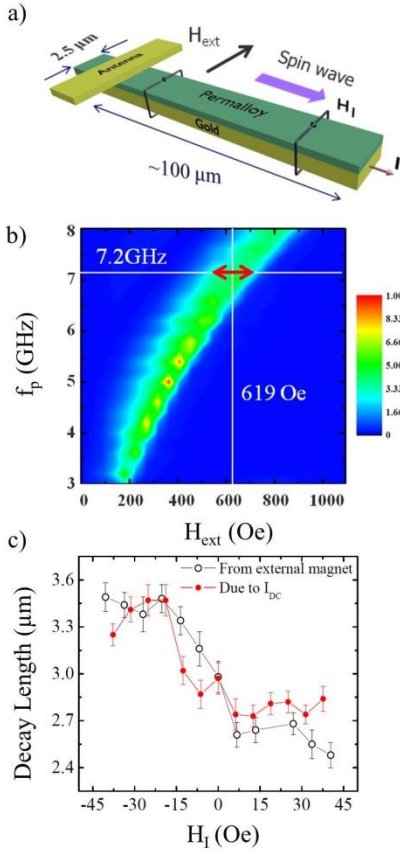


Fig. 2: a) Diagram of the sample geometry. b) BLS intensity as a function of f_p and H_{ext} measured 2 μm from the antenna. c) Decay constants extracted from spatial scans along the nanowire as a function of the Oersted field H_I due to the d.c. current I_{dc} through the nanowire at fixed $H_{ext} = 619$ Oe and $f_p = 7.19$ GHz. Measurements made at an equivalent H_{ext} with $I_{dc} = 0$ are shown for comparison. This sample was fabricated at the CNM at Argonne by collaborators H. Schultheiss and K. Vogt.

Micro-BLS measurements of the spin waves excited in the nanowire are shown in Fig. 2b. The external magnetic field H_{ext} is applied perpendicular to the nanowire, a configuration known as the Damon Eschbach (DE) geometry that is used to generate propagating surface waves. Measurements of the BLS intensity as a function of the pumping frequency f_p and H_{ext} at a fixed location show that the frequencies of the excited magnons increases as a function of H_{ext} as expected. One- and two-dimensional scans were also performed at selected frequency/field combinations to probe the spin wave decay and spatial propagation patterns, respectively, with and without a dc current I_{dc} applied through the FM/NM nanowire. As shown in Fig. 2c, the spin wave decay length changes measurably as a function of I_{dc} . When plotted as a function of the Oersted field H_I that is generated by the current flowing through the nanowire, the measured decay lengths match those obtained from the field scan in Fig. 2b with no current at all but the highest I_{dc} values. The decay length changes with H_{ext} because the field shifts the magnon dispersion curve resulting in the excitation of different k-vectors for a given f_p , which can lead to changes in the spin wave group velocity and hence the propagation distance. The results suggest that the primary function of the dc current for this gold thickness is that of an additional bias magnetic field that is generated by the current,

which flows primarily through the gold and generates a strong internal magnetic field. The only significant differences between the dc current and the external field measurements are observed at large currents where Joule heating effects likely come into play. There is no appreciable enhancement or suppression of spin wave propagation due to the dc current, which is not surprising since the spin Hall effect in gold is small and both the Permalloy and gold are thick compared to films reported to show large spin Hall effects.

It is important to note that the 1D scans show that the decay is not purely exponential in character. More detailed 2D scans show propagation patterns that are well described by theoretical calculations of interference patterns of the first and third spin waves modes in the wire (only odd modes are excited in this geometry; the antenna field does not couple to the even modes). The interfering modes are quantized due to the confined geometry along the width of the wire. The 2D propagation patterns agree well with previous results on spin wave interference patterns in metallic nanowires [3].

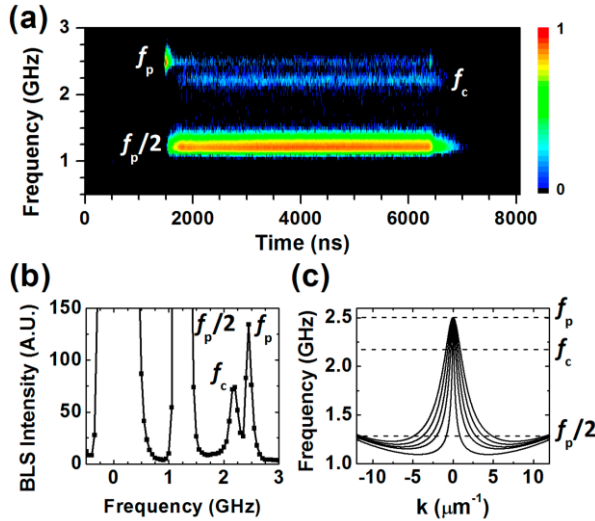


Fig. 2: FIG. 2. (a) Time-resolved and (b) standard BLS spectra obtained for a YIG film in the MSBVW configuration where the external magnetic field, in this case $H = 337$ Oe, is applied parallel to the direction of propagation. The spectra show strong signals at the pumping frequency f_p , at $f_p/2$, which is due to the parametrically pumped magnons, and a confluence signal is observed at frequency f_c . The spectra were measured at a distance of 2.75 mm away from the input antenna. (c) Calculated MSBVW dispersion curves for the YIG film showing the first 5 modes.

both with frequencies of close to $f_p/2$, through a process known as three magnon splitting. This process is important for this project because it can be used as a means to generate magnons with higher k -vectors, hence can be used to investigate the k -vector dependence of spin wave processes. The three magnon splitting and confluence processes, that is the subsequent recombination of the parametrically pumped magnons, were observed previously in YIG films using Brillouin light scattering (BLS) in both the magnetostatic surface wave (MSW) and the backward volume wave (MSBVW) configurations [4]. These experiments were done using continuous wave microwave excitations, however, and no time-resolved information was

Three-magnon splitting and confluence in yttrium iron garnet: Yttrium iron garnet (YIG) exhibits a combination of properties including high magneto-optical Kerr rotation values and extremely low damping that have made it a model system for spin wave propagation studies, including studies of nonlinear dynamic processes. Many of the concepts now being studied in metallic magnetic nanowires were first studied in YIG where the propagation distances are typically measured in millimeters, as compared to propagation distances of tens of micrometers or less in metals. At high pumping powers, one of the processes that often occurs is known as parametric pumping. This process involves the conversion of magnons at the pumping frequency f_p into two magnons,

obtained. Here we use time-resolved BLS to examine the temporal aspects of the splitting and confluence processes.

Figure 2 shows measurements made using time-resolved BLS that show the time-evolution of the splitting and confluence processes in the MSBVW configuration where the magnetic field is applied along the direction of the spin wave propagation. Propagating spin waves were excited in the YIG film using pulsed microwave excitations from a microstrip transducer at a frequency of f_p . Since there are available magnon states at a frequency of $f_p/2$ (see the dispersion curve for this geometry shown in Fig. 2c), the pumped magnons can split into two magnons with frequencies close to $f_p/2$ provided both energy and momentum are conserved. The spectra show the expected peaks in the frequency spectra at f_p , the parametrically excited half-frequency $f_p/2$, and the confluence frequency f_c . Examination of the arrival times of the scattered photons shows that there are subsequent time delays between the f_p and $f_p/2$ signals, and between the $f_p/2$ and f_c signals. Magnons at $f_p/2$ are detected long after the other signals have died out, indicating that these magnons have a wide distribution of group velocities. Time-resolved BLS scans as a function of distance from the antenna have been conducted as well, which provides additional information on where the splitting and confluence processes occur.

Future Plans

Going forward, BLS and BLS microscopy (micro-BLS) combined with analytical and numerical modeling will be used to explore spin wave propagation in magnetic nanowires and films, including the interplay between spin waves and spin currents in patterned magnetic nanowires and thermal effects on spin wave processes. The measurements on the bilayer nanowire shown above are an important first step since they provide a baseline as to what to expect in the absence of significant SHE. The next step is to vary the thickness and composition of the FM/NM bilayer nanowires to study how the SHE modifies spin wave propagation in magnetic nanowires. We plan to move towards thinner layers and materials such as Pt and Ta that are expected to exhibit a large SHE. We have also designed a sample holder that will be used to apply thermal gradients to magnetic films to study how the thermal landscape can affect spin waves.

References

1. B. Hillebrands, "Brillouin Light Scattering Spectroscopy" in Modern techniques for characterizing magnetic materials, edited by Y. Zhu (Kluwer Academic Publishers, Boston, 2005).
2. C. Matthieu, H. J. Liu, K. S. Buchanan, and V. R. Inturi, *J. Appl. Phys.* 111, 07A306 (2012).
3. V. E. Demidov, S. O. Demokritov, K. Rott, P. Krzysteczko, and G. Reiss, *Phys. Rev. B* 77 064406 (2008).
4. C. Ordonez-Romero, B. A. Kalinikos, P. Krivosik, W. Tong, P. Kabos, and C. E. Patton, *Phys. Rev. B* 79, 144428 (2009).

Publications

Publications on the work mentioned above are in preparation.

Program Title: Crystallite Size Effects in Permanent Magnet Materials

Principle Investigator: George C. Hadjipanayis; Co-PI: David J. Sellmyer

Mailing Address: Department of Physics and Astronomy, University of Delaware, Newark, DE, 19716

E-mail: hadji@udel.edu

Program Scope

Our DOE-supported research at the University of Delaware is focused on the following two topics: (i) the investigation of size/surface effects in magnetically hard rare earth transition metal particles (with a size in the range below one micron down to a few nanometers) which is important for the development of rare earth-lean exchange-coupled nanocomposite magnets consisting of a fine mixture of hard and soft magnetic phases and (ii) the effect of particle/grain size on two important structural/microstructural transformations, the spinodal decomposition and precipitation hardening; these two transformations determine the hard magnetic properties of Alnico and Sm-Co 2:17 precipitation-hardened magnets, respectively.

Recent Progress

BACKGROUND

Sm-Co and Nd-Fe-B Particles: Magnetically hard nanoparticles produced by milling have attracted great interest in the past few years because of their potential application in the development of high-performance nanocomposite magnets. Submicron size particles are also desired for the fabrication of high coercivity sintered magnet; these magnets can replace the Dy-substituted magnets and decrease our dependence of Dy which is one of the scarcest rare earths. For these applications, the particles must have a room-temperature (RT) coercivity higher than 10 kOe. The milling techniques allow for fabrication of larger amounts of particle powders that are needed for the additional processing (hot compaction/sintering) required to make a bulk magnet with high density. Recent studies reported a considerable progress in the synthesis of Nd-Fe-B and Sm-Co nanoparticles via surfactant-assisted ball milling. However, the coercivity of these particles decreases substantially with the particle size (FIG. 1). In fact, the RT coercivity of the as-synthesized Nd-Fe-B particles with a size below 30 nm does not exceed 3 kOe, which is not large enough for the bottom-up fabrication of exchange-coupled nanocomposite magnets. For the smaller particles with a size approaching their superparamagnetic limit, thermal effects are mainly responsible for the low coercivity. However, thermal effects alone cannot account for the low coercivity of the larger particles. This behavior could be due to an intrinsic size effect or to some kind of surface disorder induced by the technique used. The aim of the presented work is to understand the origin of lower coercivities that are observed in of Nd-Fe-B and Sm-Co particles with a size lower than one micron. A better understanding of the size-microstructure-property relationship would allow us to make the necessary adjustments in processing to

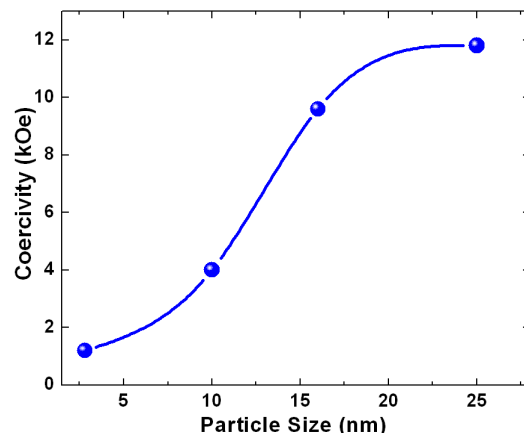


FIG. 1 Coercivity of $\text{Nd}_2\text{Fe}_{14}\text{B}$ nanoparticles as a function of particle size at 50 K.

fabricate Sm-Co and Nd-Fe-B particles with the proper size and the desired properties.

Effect of Particle/Grain Size on Spinodal Decomposition in Alnico-type Magnets: Recently, the Alnico magnets have been the subject of several studies because of the urgent need to develop a high-performance rare-earth-free magnet due to recent problems related to the export and shortages of rare earths. The rare-earth-free Alnico magnets have a high magnetization, excellent corrosion resistance, very good mechanical strength and temperature characteristics, but their coercivity is low. This coercivity is attributed to the shape anisotropy of fine and elongated Fe-Co rich precipitates embedded in a non-magnetic Ni-Al matrix, which develop through spinodal decomposition. The coercivity of an assembly of elongated particles undergoing coherent magnetization reversal should follow the relation $H_c = (1 - p)(N_b - N_a)M_s$, where p is the packing fraction, M_s the saturation magnetization and N_a and N_b the demagnetization factors along the major and minor axes of the particles. Assuming an M_s of 1.7 - 1.9 kG, $N_b - N_a = 2\pi$ and $p = 0.4 - 0.6$, the expected H_c is 4 - 6 kOe and the maximum energy product $(BH)_{max}$ is 30 - 35 MGOe. This theoretical $(BH)_{max}$ is comparable to that of the Sm-Co high-temperature magnets, and the temperature stability and mechanical strength of the Alnico magnets are far superior. Despite efforts to optimize the coercivity of Alnico, it was never found to be greater than 2 kOe with an energy product of 13 MGOe. This low coercivity has been attributed to a non-ideal two phase microstructure with crosslinks between the Fe-Co precipitates. The aim of the presented study is to investigate the development of spinodal decomposition and coercivity in Alnico thin films and melt-spun ribbons looking to build a basic understanding and the basis for manipulating the spinodal decomposition at the nanoscale to elucidate the materials requirements for reaching the potential of Alnico.

Effect of Particle/Grain Size on Precipitation Hardening in Sm-Co 2:17 Magnets: The hard magnetic properties of the precipitation-hardened Sm-Co-Fe-Cu-Zr magnets originate from a fine cellular microstructure that develops after treatment at 800 - 850 °C followed by a slow cooling. The 50 - 100 nm cells have the rhombohedral Th₂Zn₁₇-type structure; they are surrounded by thin, crystallographically coherent cell boundaries of the hexagonal CaCu₅-type structure. The cells are enriched in Fe, whereas the cell boundaries are rich in Cu. The latter enrichment leads to domain wall pinning at the cell boundaries, and the resulting coercivity is very sensitive to the microstructure and nanochemistry of the magnets. The presented project is aimed to investigate the precipitation hardening transformation in nanostructured Sm-Co alloys (melt-spun ribbons, nanoparticles and thin films) in order to (i) determine any intrinsic size effects on the precipitation hardening mechanism in small 2:17 crystals and (ii) learn how to control better the nanochemistry and microstructure of the thin films and nanoparticles critical for their coercivity. The high-coercivity nanoparticles are needed for the bottom-up assembly of anisotropic nanocomposites, whereas the information on tuning the microstructure and nanochemistry is needed for improvement of the bulk high-temperature magnets.

DISCUSSION OF FINDINGS

Single crystal SmCo₅ nanoparticles with an average size of 3.5 nm were prepared by cluster-beam deposition. The characterization of the particles revealed the importance of interparticle exchange interactions for the effective anisotropy and coercivity. As-prepared 5 nm particles are superparamagnetic with a blocking temperature T_B of 145 K and they have negligible RT coercivity (FIG. 2). Dispersing these particles in a C matrix led to an increase of T_B above RT and an increase of coercivity to 12 kOe (FIG. 3). This behavior can be explained by the random-

anisotropy model according to which exchange inter-particle interactions lead to a decrease of the overall effective anisotropy of the particles and therefore a decrease of coercivity.

Nd-Fe-B particles in the range of 5 - 500 nm were prepared using two different techniques, the surfactant-assisted high-energy milling and the mechanochemical synthesis. The latter technique, in which crystallization follows application of high mechanical energy, allows us to avoid crystalline disorder and microstructure defects. We were able to fabricate for the first time by the mechanochemical synthesis technique Nd-Fe-B nanoparticles with size around 100 nm and a coercivity exceeding 6 kOe.

The very recent preliminary studies in Alnico thin films with thickness in the range of 100 - 300 nm failed to show the formation of rod-like microstructure which is characteristic of spinodal decomposition. Instead, formation of faceted grains has been observed which is usually associated with nucleation and growth. This behavior could be attributed to the very small grain size (5 nm) in the as-made films which is lower than the critical wavelength λ_c above which spinodal decomposition takes place. Therefore, spinodal decomposition is suppressed by the nucleation and growth mechanism. Our current studies are focused on melt-spun ribbons with controlled grain size over a range that covers λ_c . The grain size of the samples was varied by changing the wheel speed from 5 - 60 m/s. Spinodal decomposition was induced by subjecting the samples to 900 C for 30 min followed by a slow cooling to 600 C where they were held for 4 hours. The microstructure of as-spun and annealed samples was studied by SEM and TEM. SEM micrographs show clearly that spinodal decomposition takes place in the annealed samples. The size of spinodal structures observed are in the range 45-80 nm with the larger size corresponding to the higher wheel speed samples. The coercivity was also found to depend strongly on the size of spinodal structures with the highest value obtained in the sample with the finer spinodal size. Further annealing and processing experiments especially in the presence of a magnetic field are under progress.

Melt-spun $\text{Sm}(\text{Co},\text{Fe},\text{Cu},\text{Zr})_z$ alloys were also found to exhibit a grain-size-sensitive precipitation-hardening behavior.

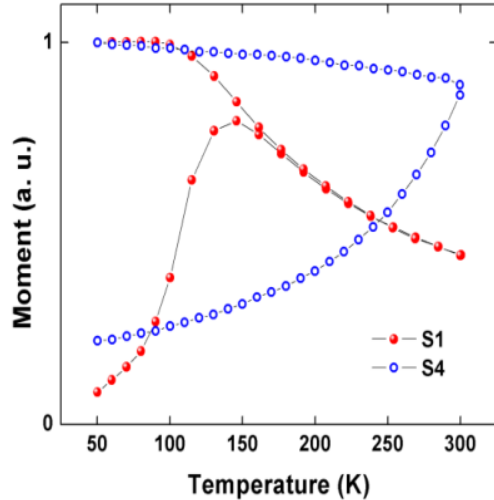


FIG. 2 ZFC and FC curves at 150 Oe for as-made SmCo_5 nanoparticles (S1) and nanoparticles embedded in a carbon matrix (S4).

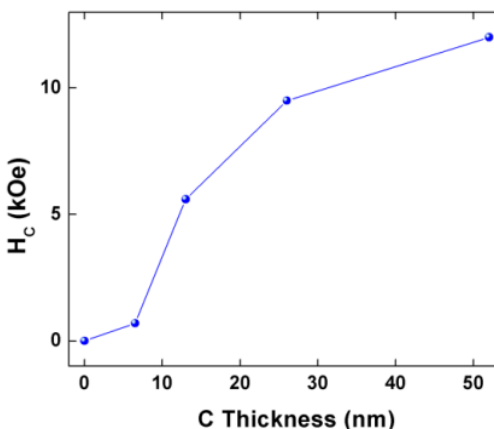


FIG. 3 Coercivity of SmCo_5 nanoparticles as a function of carbon thickness.

Future Plans

The work on grain/particle size effects on the spinodal decomposition and precipitation hardening are rather new that have started this summer and the experiments are under progress. The ongoing experiments with the $\text{Sm}(\text{Co},\text{Fe},\text{Cu},\text{Zr})_z$ alloys ($6.5 < z < 8.5$) will be extended to the $\text{Sm}(\text{Co},\text{Cu})_z$ alloys with $z > 5$. The graduate student supported with this grant will continue her experiments on the submicron Nd-Fe-B particles and model their hysteresis behavior with micromagnetic modeling.

Publications

1. O. Akdogan, W. Li, G.C. Hadjipanayis, D.J. Sellmyer, Synthesis of Single-Crystal Sm-Co Nanoparticles By Cluster Beam Deposition, *Journal of Nanoparticle Research* **13**, 7005 (2011).
2. O. Akdogan, W. Li, R. Skomski, D.J. Sellmyer, G.C. Hadjipanayis, One-Step Fabrication of fct FePt Nanocubes and Rods by Cluster Beam Deposition, *Journal of Applied Physics* **111**, 07B535 (2012).
3. O. Akdogan, W. Li, G. C. Hadjipanayis, High Coercivity of Alnico Thin Films: Effect of Si Substrate and the Emergence of a Novel Magnetic Phase, *Journal of Nanoparticle Research* **14**, 891 (2012).
4. O. Akdogan , W. Li , B. Balasubramanian , D. J. Sellmyer , and G. C. Hadjipanayis, Effect of Exchange Interactions on the Coercivity of SmCo_5 Nanoparticles Made by Cluster Beam Deposition, *Advanced Functional Materials* 1-6 (2013).

Presentations

1. Alnico Thin Films with High Coercivities up to 6.9 kOe, *ICM 2009* (Karlsruhe, Germany).
2. SmCo_5 Nanoparticles by Cluster Beam Deposition, *MMM 2010* (Atlanta, SC, USA).
3. Confinement effects on the A1 to L10 phasetransformation in FePt nanoparticles, *Intermag 2012* (Vancouver, Canada).
4. Novel GdCo_5 & SmCo_5 Nanoparticles by Cluster Beam Deposition, *Euromat 2011* (Montpellier, France).
5. One-Step Fabrication of fct FePt Nanocubes and Rods by Cluster Beam Deposition, *MMM 2011* (Scottsdale, AZ, USA).
6. Intrinsic Magnetic Properties of fct FePt Nanocubes and Rods by Cluster Beam Deposition, *APS 2012* (Boston, MA, USA).
7. Novel Technique for Self Assembly of Magnetic Nanoparticles by Cluster Beam Deposition, *ICM 2012* (Busan, Korea).

FWP Program Title: Spin Physics

Principle Investigator: S.-C. Zhang (SIMES); **Co-PIs:** D. Goldhaber-Gordon (SIMES), H. C. Manoharan (SIMES), and J. Orenstein (LBNL)

Mailing Address: Stanford Institute for Materials and Energy Sciences, SLAC National Accelerator Laboratory, Menlo Park, CA 94025

Program Scope

The main goals of this FWP are to discover new states of quantum matter and novel physical effects associated with the electron spin, to observe and to manipulate quantum spin degrees-of-freedom at the microscopic scale, and to design and predict materials with tailored functionality.

The Spin Physics program investigates novel phenomena arising from spin-orbit coupling in solids. In conventional semiconductors, spin-orbit coupling gives the possibility of electric manipulation of the spin degrees of freedom, which can be used for data storage and information processing. More recently, it is realized that spin-orbit coupling can lead to a fundamentally new state of matter, the topological insulator. These materials have an energy gap in the bulk, and a conducting topological state on the surface. The spin program develops theoretical concepts and experimental tools to investigate these novel effects.

Recent Progress

Extensive investigations of spin physics, especially those carried out within this FWP, strongly motivated the discovery of topological insulators. Two frontier topics in this area are spin transport associated with the topological surface states (most measurements to date are charge-based) and the interplay between spin-orbit coupling and correlation effects.

Discovery of topological insulators has also motivated the search for topological superconductors [Qi2011]. Topological superconductors have a full pairing gap in the bulk, and gapless quasiparticle states on the edge or surface which are Majorana modes. Majorana modes are self-conjugate with respect to the particle-hole transformation, and the point-like Majorana zero modes could be useful for topological quantum computation. A number of proposals involve proximity effects between an *s*-wave superconductor with either topological surface states or a spin-orbit coupled quantum wire. Promising results have already been obtained within these approaches [Mourik2012]; however, serious challenges and difficulties with

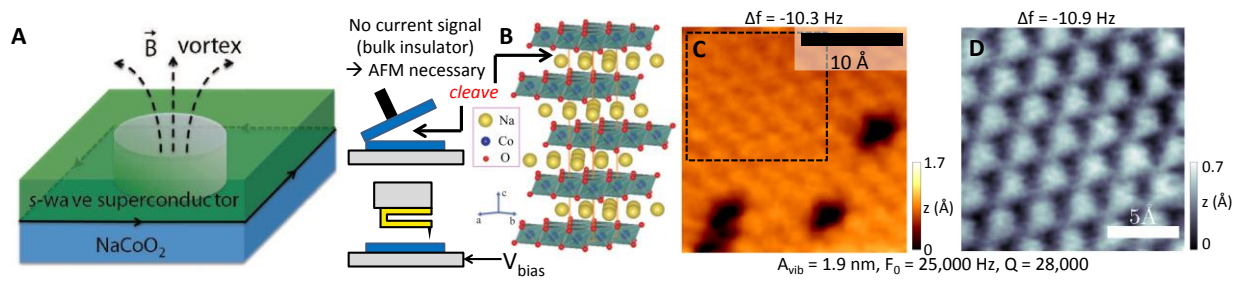


Figure 1. (A) Theoretical proposal for realizing Majorana modes without the need for an external magnetic field, by using half-metallic surface states of sodium cobaltate in proximity to an *s*-wave superconductor. (B) Atomic-resolution AFM experimental scheme for investigating the surface of bulk-insulating NaCo₂, which cleaves to expose a Na layer. (C) AFM image revealing Na atoms and vacancies. (D) Zoomed scan on dashed square region of (C), showing 100% Na coverage.

interpretations also remain [Liu2012]. Zhang has recently proposed another scenario, involving proximity coupling between an *s*-wave superconductor with a half-metal [Weng2011]. In particular, we predict theoretically that the bulk band insulator NaCoO₂ contains a half-metallic surface state. The half-metallic surface state contains a single-spin non-degenerate Fermi surface, due to the Pauli principle. Any proximity-induced pairing must be p_x+ip_y wave like, and it is therefore a topological superconductor. In particular, a vortex in the proximity induced half-metallic superconductor should contain a Majorana zero mode which can be detected by STM (Fig. 1A). Manoharan has been working on observing these modes in stages, with the first preliminary steps already completed successfully. Manoharan has now imaged the stoichiometric compound NaCoO₂ which is a bulk insulator, and thus not accessible by STM tunneling. To address this challenge, Manoharan used a new tuning-fork AFM technique which does not rely on tunnel current but measures the frequency shift of the tuning fork in proximity to an insulating surface (Fig. 1B). Since a sharp tip is still used, atomic precision can be obtained as shown in Fig. 1C. The cleavage plane is relevant (Fig. 1B) since it exposes a Na-doped surface, and the Na concentration effects the magnetism needed for creating a spin-polarized surface state. Since each Na atom can be counted in this experiment (Fig. 1D), an accurate count of this doping can be performed and hence the magnetism quantified in collaboration with theory. The experiments indicate that there are accessible regions with 100% Na coverage, which corresponds to the ideal phase of the theory [Weng2011]. We are investigating this first and then studying the nature of the surface state itself. By making a special sample holder that contacts only the surface, while still allowing cleaving, Manoharan has recently demonstrated a conducting surface state exists on the bulk insulator. This was accomplished in experiment by using the tuning fork to first image the bulk insulator, and then biasing the tip to flow current through the surface contact only in a hybrid STM/AFM mode. We plan to get further statistics and information on the scattering in this surface state, and then begin to combine the surface state with a superconductor. This last phase of the experiment is now possible via a superconducting-scanned-tip measurement, recently demonstrated in a collaboration between Manoharan (experiment) and Devereaux (SIMES theory) investigating scanning superconducting Pb-vacuum-Pb junctions and bosonic modes (Fig. 2). These experiments prove the integrity of the superconducting tip in both tunneling and point-contact geometries. Both of these geometries will be used with NaCoO₂ experiment in order to create a proximity effect in the surface state, and experiments will probe for *p*-wave-like pairing, the experimentally realized parameter ranges, and ultimately zero modes expected from Majorana physics.

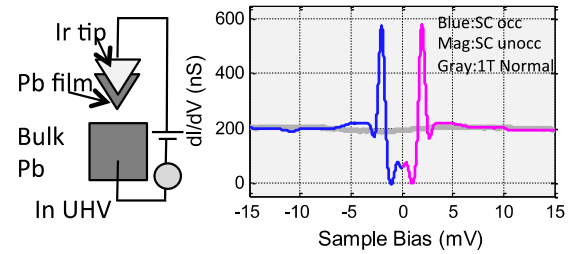


Figure 2. STM experiment demonstrating feasibility of stable scanning superconducting-vacuum-superconducting tunneling, in addition to simultaneous external magnetic field to quench superconductivity. Setup is now extended to TI experiments.

Kerr rotation experiments by Orenstein have recently shown direct evidence for the magnetic surface state of NaCoO₂ using the same samples studied by STM. Orenstein has also begun to investigate the magnetization of MBE grown thin (*n*-quintuple layer where $n \leq 5$) films of 3D topological insulators doped with magnetic ions, for example Cr. To detect the possible time-reversal breaking states resulting from the impurity ions, Orenstein used a sensitive coherent

optical polarimeter that is ultimately designed for ultrafast time-resolved Kerr effect measurements. In this detection system, each pulse from Ti:Sapphire laser is split into two pulses with orthogonal linear polarization. Before focusing onto the sample, the pulses pass through a quarter-wave plate, converting the two linearly polarized pulses to left and right circularly polarized ones. After reflection from the sample surface, the pulses propagate backwards through the optical system to a photodetector. Coherent heterodyne detection leads to a detector output voltage proportional to the phase difference, $\Delta\varphi_{LR}$, between the reflection coefficient of the sample for left and right polarization. This phase difference is directly proportional to the Kerr effect $\Delta\theta_K$, which is the rotation of the plane of polarization that would be experienced by linearly polarized light reflected from the sample. To further enhance the sensitivity of the system, we modulate the temperature of the sample at a low frequency, on the order of 100 Hz, and utilize lock-in detection to measure $d\Delta\theta_K/dT$.

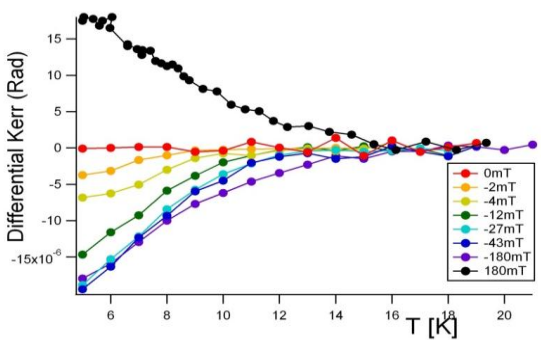


Figure 3. Differential Kerr rotation measurements on magnetically doped topological insulator thin films.

The data clearly reveal the onset of a strong magnetic response at approximately 15 K. Sensitivity to the sign of the applied field indicates a ferromagnetic or magnetoelectric response and rules out chiral symmetry breaking as the origin of the effect.

Future Plans

We plan detailed temperature-dependent measurements of Kerr rotation and STS of the NaCoO_2 surface state, which in preliminary data show a transition temperature around 20 K. For the magnetically doped TI's, although the onset of magnetization is quite clear, the temperature dependence is quite different from that expected for a mean-field transition. However, it also appears that the data are not consistent with a non-symmetry breaking paramagnetic response, as the magnetization is seen to saturate at an extremely low field of about 30 mT. Therefore, we plan measurements of hysteresis loops to unequivocally demonstrate time-reversal symmetry breaking. Future measurements will focus on control of the phase-transition temperature by varying the carrier concentration using electrical gating. We intend to extend this suite of surface measurements to topological p - n junctions and other ternary and tetradymite compounds.

2-Year Publication List (which acknowledge DOE support)

1. C. Brüne, A. Roth, H. Buhmann, E. M. Hankiewicz, L. W. Molenkamp, J. Maciejko, X.-L. Qi, S.-C. Zhang, "Spin polarization of the quantum spin hall edge states," *Nature Physics* **8**, 485-490 (2012).

2. K. K. Gomes, W. Ko, W. Mar, P. Guinea, H. C. Manoharan, "Designer Dirac fermions and topological phases in molecular graphene," *Nature* **483**, 306-310 (2012). [Also selected for cover article and News & Views feature].
3. Q. Liu, X.-L. Qi, S.-C. Zhang, "Stationary phase approximation approach to the quasiparticle interference on the surface of a strong topological insulator," *Physical Review B* **85**, 125314 (2012).
4. B. Yan, L. Muchler, X.-L. Qi, S.-C. Zhang, Claudia Felser, "Topological insulators in filled skutterudites," *Physical Review B* **85**, 165125 (2012).
5. L. Yang, J. Koralek, J. Orenstein, D. R. Tibbetts, J. L. Reno, M. P. Lilly, "Doppler velocimetry of spin propagation in a two-dimensional electron gas," *Nature Physics* **8**, 153-157 (2012).
6. X. Zhang, H. Zhang, C. Felser, S.-C. Zhang, "Actinide topological insulator materials with strong interaction," *Science* **335**, 1464-1466 (2012).
7. J. D. Koralek, L. Yang, D. R. Tibbetts, J. Orenstein, "Doppler velocimetry of spin and charge currents in the 2D Fermi gas," XVIIIth International Conference on Ultrafast Phenomena 8-12 July 2012, *EPJ Web of Conferences* **41**, 3017 (2013).
8. H. Zhang, C.-X. Liu, S. C. Zhang, "Spin-orbital Texture in Topological Insulators," *Physical Review Letters* **111**, 066801 (2013).
9. M. König, M. Baenninger, A. G. F. Garcia, N. Harjee, B. L. Pruitt, C. Ames, P. Leubner, C. Brüne, H. Buhmann, L. W. Molenkamp, D. Goldhaber-Gordon, "Spatially Resolved Study of Backscattering in the Quantum Spin Hall State," *Physical Review X* **3**, 021003 (2013).
10. M. Pelliccione, A. Sciambi, J. Bartel, A. Keller, D. Goldhaber-Gordon, "Design of a scanning gate microscope for mesoscopic electron systems in a cryogen-free dilution refrigerator," *Review of Scientific Instruments* **84**, 033703 (2013).
11. K. C. Nowack, E. M. Spanton, M. Baenninger, M. König, J. R. Kirtley, B. Kalisky, C. Ames, P. Leubner, C. Brüne, H. Buhmann, L. W. Molenkamp, D. Goldhaber-Gordon, K. A. Moler, "Imaging currents in HgTe quantum wells in the quantum spin Hall regime," *Nature Materials* **12**, 787-791 (2013).
12. M. Polini, F. Guinea, M. Lewenstein, H. C. Manoharan, V. Pellegrini, "Artificial honeycomb lattices for electrons, atoms and photons," *Nature Nanotechnology* (in press, scheduled to appear Sept. 2013), doi:10.1038/nnano.2013.161.

Literature cited

- [Qi2011] X. L. Qi, S. C. Zhang, "Topological insulators and superconductors," *Reviews of Modern Physics* **83**, 1057-1110 (2011).
- [Mourik2012] V. Mourik, K. Zuo, S. M. Frolov, S. R. Plissard, E. P. A. M. Bakkers, L. P. Kouwenhoven, "Signatures of majorana fermions in hybrid superconductor-semiconductor nanowire devices," *Science* **336**, 1003-1007 (2012).
- [Liu2012] J. Liu, A. C. Potter, K.T. Law, P. A. Lee, "Zero-bias peaks in spin-orbit coupled superconducting wires with and without majorana end-states," arXiv:1206.1276.
- [Weng2011] H. Weng, G. Xu, H. Zhang, S.-C. Zhang, X. Dai, Z. Fang, "Half-metallic surface states and topological superconductivity in NaCoO₂ from first principles," *Physical Review B*. **84**, 060408(R) (2011).

Session 4

Program Title: Quantum Criticality and Unconventional Superconductivity

Principle Investigator: M. C. Aronson

Mailing Address: Building 703, Brookhaven National Laboratory, Upton NY 11973

Email: maronson@bnl.gov

Program Scope The primary research focus of this program is the discovery of new transition metal-based systems where strong electronic correlations lead to unconventional ordered states, especially superconductivity (SC). Understanding how these correlations lead to a holistic phase diagram where superconductivity and magnetism are separate but ubiquitous regimes is a crucial first step towards their active control, transforming the traditional serendipitous exploration of materials into directed searches, where synthesis and theory are partnered to discover new materials with purpose-built functionality.

There is considerable evidence that associates unconventional SC in the cuprates and Fe-based pnictides with two different $T=0$ phase transitions. The first is the collapse of antiferromagnetic order to a quantum critical point (QCP) where $T_N=0$. The second is an electronic delocalization transition (EDT) that involves a change in the Fermi surface (FS) volume. The properties of systems near such QCPs are completely different from those of normal metals, underscoring the special conditions that are needed to foster unconventional superconductivity. The critical fluctuations for a $T=0$ phase transition reflect the full quantum mechanical nature of the system, linking both the spatial and temporal correlations in new ways, resulting in unusual and incompletely explored critical classes. The QC fluctuations can involve either conventional order parameter fluctuations, analogous to those found near finite temperature magnetic transitions, or can involve fluctuations that connect two critical FS with volumes that differ by one electron per unit cell. How these different critical fluctuations that are found near QCPs enable superconducting pairing remains an unanswered question of fundamental importance.

It is generally believed that only systems with sufficiently strong electron correlations display the full richness of behavior near QCPs, or alternatively that strong correlations are an inevitable outcome in interacting electron materials that are tuned to the vicinity of a QCP. It is remarkable that the signatures of the QCP are quite similar in systems like the f-electron based heavy electron compounds, where the correlations are among the largest ever identified, and compounds such as organic conductors where these correlations are much weaker. This research seeks to explicate the minimal physics of quantum criticality, by determining whether the global phase diagrams established in strongly interacting systems like heavy fermions, cuprates, and iron pnictides are also realized in classes of materials where these interactions are very weak, but where magnetic order can still be suppressed to zero temperature, forming a quantum critical point. The project involves exploratory synthesis of new Fe-based compounds where magnetic order is weak or vanishing. The characterization of these new systems includes lab-based measurements of their transport, magnetic, and thermal properties, complemented by in-depth neutron scattering and photoemission studies.

Recent Progress:

Quantum Criticality in New Families of Fe-Based Compounds/References 7,8,10,11]

BACKGROUND: In most cases, the suppression of magnetic order at a QCP requires fine tuning via charge doping, although disorder is especially disruptive near QCPs, or by the application of pressure or magnetic fields, although the associated sample environments may limit the use of powerful spectroscopic techniques. It is significant that we have identified a new family of Fe-based cage compounds RFe_2Al_{10} ($R=Y, La, Lu$) that are quantum critical at ambient pressure and in zero field, allowing full experimental access in very clean materials where disorder is unimportant.

DISCUSSION OF FINDINGS: Our detailed work on the low temperature magnetic and thermodynamic properties of the RFe_2Al_{10} has shown that critical fluctuations dominate, leading to divergencies that display no characteristic temperature scale, confirming that they are associated with phase transitions that occur strictly at $T=0$. Accordingly, Muon spin rotation measurements find that no order is present at temperatures above 20 mK. A crossover scale $T^*\sim H^{0.6}$ separates the strong QC behavior that is found at small H/T from the normal metallic behaviors at large H/T , demonstrating that it is the diverging quantum critical fluctuations that are responsible for the breakdown of the standard Fermi liquid description of metals in the RFe_2Al_{10} compounds. This QC behavior is strongest in YFe_2Al_{10} , where high precision scaling of the magnetization and specific heat reveals an underlying free energy that is QC in zero field, identical to the one found in Mott-Hubbard systems near their EDTS. Similar scaling is found in the NMR relaxation time T_1 and specific heat, indicating that the fluctuations are uniform ($q=0$). Since doping experiments have not driven YFe_2Al_{10} into an ordered state, the nature of the $T=0$ QCP remains unknown. The critical exponents found in this system are not consistent with any known magnetic model, and so it is tempting to believe that YFe_2Al_{10} is naturally poised on the verge of a EDT, involving both the destruction of its Fermi surface as well as the formation of long-lived Fe moments. Indeed, the electrical resistivity of this very clean system is strongly enhanced and shows an upturn at the lowest temperatures that supports this proposal.

Electronically Tuned Quantum Criticality in Itinerant Ferromagnets

BACKGROUND: Quantum criticality has emerged as a central feature of the phase diagrams for virtually every class of strongly correlated materials. It is almost always the case that there is no underlying model for the electronic structure, and for its transitions near the QCP. A noted exception to this is in certain classes of itinerant ferromagnets(FMs), where the Slater-Pauling rule predicts the sequence of FM order, replaced at a FM-QCP or first order transition by a half-metal and eventually an unpolarized metal as the electron count is decreased. This project seeks to determine if QC fluctuations, particularly of the FS-shredding type, are present in such a system, and whether they are connected to this well-established sequence of electronic modifications.

DISCUSSION OF FINDINGS: We have synthesized Fe- and Co-based Heusler FMs for the first time as single crystals, necessary for limiting the impact of disorder. An extensive study of the magnetic and thermal properties of these systems has been conducted, finding that FM order can

be suppressed by the removal of valence electrons. It has been theoretically predicted that the FM phase vanishes via a series of mean-field transitions at ever-lower temperatures, and our experiments confirm this prediction for the first time. While this lack of QC fluctuations would rationalize the eventual suppression of the FM phase in a first-order instability, this is avoided by the sudden appearance of an AF phase. Surprisingly, QC behavior in this system is associated with the suppression of the half-metallic phase, leading to divergencies in the specific heat and magnetic susceptibility once FM order has been suppressed.

IMPORTANCE OF FINDINGS: EXPERIMENTAL AND THEORETICAL PERSPECTIVES

Understanding the normal state is a necessary requirement for understanding how unconventional superconductivity is stabilized. Our results underscore how anomalous this normal state is. The RFe₂Al₁₀ are first in class materials, providing unprecedented access to the undoped, metallic side of a Mott transition, where unconventional superconductivity is generically expected. It is possible that we may find this superconductivity by compositionally modulating the distance from the QCP. We have performed the first exhaustive scaling analysis of such a T=0 system, and have identified the underlying free energy. These results provide experimental benchmarks for new and existing theories of Mott criticality, without the additional complication of doping or strong correlations, as in the cuprates.

Our results on the stability of FM order in the Heusler-based compounds confirm longstanding theoretical predictions, but at the same time have serious ramifications for the possibility of unconventional superconductivity. Setting aside the possible role of AF fluctuations, the apparent absence of FM critical fluctuations implies that superconductivity may be entirely driven in these systems by the density of states, accessible by virtue of their weak correlations to electronic structure calculations. We are exploring the possibility that these calculations can guide synthesis by identifying target compositions that may be more favorable for superconductivity, a practical realization of a 'Materials by Design' scheme.

Future Plans We have been successful in identifying new systems where quantum criticality can be studied in depth, and we have made considerable progress in developing an experimental methodology for characterizing and even controlling quantum criticality in several materials that may come to be considered prototypical. However, superconductivity remains elusive, and it seems likely that there are additional factors that may still need to be controlled, beyond QC behavior. So far, no connection has been made between the observed QC behavior and the underlying electronic structure that would guide future compositional modifications. Photoemission and x-ray absorption studies are much needed, as well as electronic structure calculations. It is possible that the incipient magnetic order in these systems is not suitable for superconducting pairing, but we will only have insight into this when neutron scattering studies reveal the properties of the low-energy magnetic excitations. On the materials side, we have not yet demonstrated the full range of behaviors, spanning these strongly correlated metals and

their erstwhile insulating counterparts, possibly separated by a QCP. New synthesis schemes that would strengthen these correlations, as well as a careful investigation of charge doping are needed to explore this connection.

References and Publications acknowledging DOE support:

- 1."Nanospheres of a New Intermetallic FeSn₅ Phase: Synthesis, magnetic properties, and anode performance in Li-ion batteries", Xiao-Liang Wang, Mikhail Feygenson, Haiyan Chen, Chia-Hui Lin, Wei Ku, Jianming Bai, Meigan C. Aronson, Trevor A. Tyson, and Wei-Qiang Han, Journal of the American Chemical Society **133**, 11213 (2011).
- 2.``Ionothermal Synthesis and Magnetic Studies of Novel Two-Dimensional Metal-Formate Frameworks", Paul J. Calderone, Paul M. Forster, Lauren A. Borkowski, Simon J. Teat, Mikhail Feygenson, Meigan C. Aronson, and John B. Parise, Inorganic Chemistry **50**, 2159 (2011).
- 3.``Towards a Reliable Synthesis of Strontium Ruthenate: Parameter Control and Property Investigation of Submicron Structures", Amanda Tiano, Alexander Santulli, Christopher Koenigsmann, Mikhail Feygenson, Meigan Aronson, Richard Harrington, John Parise, and Stanislaus Wong, Chemistry of Materials **23**,3277 (2011).
- 4.``HfFeGa₂and HfMnGa₂: New Itinerant Ferromagnets, C. Marques, Y. Janssen, M. S. Kim, L. Wu, P. Khalifah, S. X. Chi, J. W. Lynn, M. C. Aronson, Physical Review B **83**, 184435 (2011).
- 5.``Thermal and electrical transport in the Spin Density Wave Antiferromagnet CaFe₄As₃", M. S. Kim, Z. P. Yin, L. L. Zhao, E. Morosan, G. Kotliar, and M. C. Aronson, Physical Review B **84**, 075112 (2011).
- 6.``A Layered transition metal pnictide SrMnBi₂ with metallic blocking layer", J. K. Wang, L. L. Zhao, Q. Yin, G. Kotliar, M. S. Kim, M. C. Aronson, and E. Morosan, Physical Review B **84**, 064428 (2011).
- 7.``Quantum Critical Fluctuations in YFe₂Al₁₀", K. Park, L. S. Wu, Y. Janssen, M.-S. Kim, C. Marques, and M. C. Aronson, Physical Review B **84**, 094425 (2011).
- 8.``Crystal structure of aluminum iron yttrium (10/2/1), Al₁₀Fe₂Y", Alexander Kerkau, Liusuo Wu, Keesong Park, Yurii Prots, Manuel Brando, Meigan C. Aronson, and Guido Kreiner, Z. Kristallogr. NCS **227**, 289 (2012).
- 9.``Factors governing Yb magnetism in YbPtIn₂ and other MgCuAl₂ type structures", Andrew Malingowski, Moosung Kim, Liusuo Wu, Jonathan Hanson, Meigan Aronson and Peter Khalifah, Journal of Solid State Chemistry 198, 308 (2012).
- 10.``Field tuned critical fluctuations in YFe₂Al₁₀: Evidence from magnetization and NMR and NQR investigations", P. Khuntia, A. Strydom, L. S. Wu, M. C. Aronson, F. Steglich, and M. Baenitz, Phys. Rev. B **86**, 220401 (R) (2012). Editors' Suggestion.
- 11.``Erratum: Field tuned critical fluctuations in YFe₂Al₁₀: Evidence from magnetization and NMR and NQR investigations", P. Khuntia, A. Strydom, L. S. Wu, M. C. Aronson, F. Steglich, and M. Baenitz, Phys. Rev. B **88**, 019902 (E) (2013).

Program Title: Emerging Materials

Principal Investigator: J.F. Mitchell; Co-PIs: K.E. Gray, B.J. Kim

Mailing Address: Materials Science Division, Bldg 241, Argonne National Laboratory, 9700 S.

Cass Avenue, Argonne, IL 60439

E-mail: mitchell@anl.gov

Program Scope

The Emerging Materials research program tightly couples materials synthesis to insight-driven science as the most efficient pathway to achieve our goal of understanding discovery, creation and behavior of materials. Within this synthesis-science diad, our program goal is to understand the link between the distinct materials physics studies of $3d$ transition metal oxides—in which spin, charge, and orbital sectors are distinct, identifiable, and measurable—and $5d$ systems that lie beyond the regime of ‘delicately balanced and tightly coupled’ interactions found among $3d$ systems. Inspired by the novel Mott state of Sr_2IrO_4 , we grow single crystals to explore how relativistic spin orbit coupling entangles the spin-, charge-, and orbital-order parameters to expose new quantum phases in the presence of electron correlation in $5d$ oxides. Specifically, we explore metal insulator transitions and search for links to unconventional superconductivity; we create frustrated lattice structures in both $3d$ and $5d$ compounds to expose spin-sector and spin-lattice sector interactions for insights into control of magnetic short-range order; we use reduced dimensionality to test the generality of magnetic and electronic phase segregation; and we explore nonequilibrium transport effects in both $3d$ and $5d$ systems. Areas of current research focus include:

- Exploring how a spin-orbit coupling induced Mott insulator evolves into a metal and potentially into an unconventional superconductor by surface and/or bulk doping
- Understanding the role of dimensionality on the spin, orbit and spin-orbit states of iridium oxides.
- Assessing if strong electron correlation effects or geometric frustration in $5d$ iridates can unveil new topological states e.g., a quantum spin liquid, through synthesis of new materials
- Exploring the competition of one-electron and correlated electron interactions in spin dimerization in three-dimensional lattices of $4d$ and $5d$ compounds.
- Creating and understanding novel materials structures to reveal new exemplars of geometric frustration of magnetism.

Our approach is to synthesize targeted materials and produce single crystals by zone, flux, or vapor growth methods where possible. These specimens are then subjected to rigorous measurements within our group, among various collaborative groups within the Argonne community (including the APS), or among a wide network of international research teams that value both our specimens and our insights.

Recent Progress

Iridates: Large crystals of Ruddlesden-Popper (R-P) phases (e.g., Sr_2IrO_4 , $\text{Sr}_3\text{Ir}_2\text{O}_7$) are now being grown and have been used to (a) discover a dimensionality controlled spin-flop transition

in R-P iridates. Our RIXS spectroscopy first showed conclusively that the Ir moment flips from in plane for $n=1$ in the Ruddlesden-Popper series $\text{Sr}_{n+1}\text{Ir}_n\text{O}_{3n+1}$ to c -axis parallel for $n=2$. The nature of this spin-flip was traced to two factors: a substantially decreased band gap as n increases and the importance of dipolar interactions. (b) identify striking similarities in magnon dispersion between Sr_2IrO_4 and cuprates, leading further strength to possibility of superconductivity in this system. In particular, we found that the magnon dispersion follows qualitatively that of 214 cuprates, and can be fit to a Heisenberg dispersion. Additionally, we identified what we consider to be a spin-orbit exciton in Sr_2IrO_4 (Fig. 1a). This represents an excitation from $j_{\text{eff}}=1/2$ to $j_{\text{eff}}=3/2$ states, dispersing with a bandwidth of ~ 300 meV.[15]

We are now growing crystals of a number of iridate systems, and have found ways to ‘dope’ Sr_2IrO_4 (doping mechanism unknown); our results differ from those of Cao, who finds a metal-insulator transition with either La- or K-doping; our crystals are all insulating, albeit more metallic than the undoped parent. Investigating these samples via resonant inelastic x-ray scattering and other techniques will be a future activity. We have grown crystals of a number of pyrochlore iridates that range from metallic to insulating and will study them using transport and ARPES. We have also succeeded in growing the first single crystals of Li_2IrO_3 (Fig 1b) without any Na content; this material is believed to be closer to the Kitaev ground state than the Na variant. Our crystals, however, do show a transition at 15 K that is believed to be to an antiferromagnetic state, presumably the same ‘stripy’ phase as reported for Na_2IrO_3 .

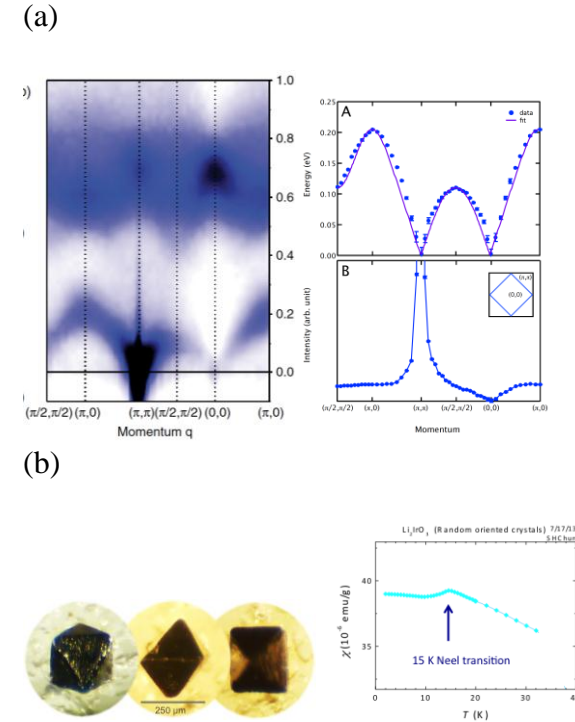


Fig. 1 (a) RIXS measurement of Sr_2IrO_4 single crystals showing low-energy dispersing mode (magnon branch) and a high energy spin-orbit-exciton. At right is a fit of the magnon dispersion to a Heisenberg model similar to cuprate physics. (b) Single crystals of pure Li_2IrO_3 . This ‘honeycomb lattice’ material is posited to be a candidate for a Kitaev quantum spin-liquid, but our data suggest a long-range ordered antiferromagnet below 15 K.

New Geometrically Frustrated Topologies: Cobalt oxides of general formul RBaCo_4O_7 (‘114’) are topological relatives of canonical pyrochlore frustrated magnets, with a trigonal bipyramidal rather than a tetrahedron as the fundamental building block of the magnetic sublattice. We have found that when the oxygen sublattice is stoichiometric the Y member of this series undergoes a structural phase transition that breaks the geometric frustration, ultimately leading to a long-range ordered antiferromagnet.[16] The spin structure has motifs typical of Kagome or triangular lattice systems. Introduction of small ($\sim 1.5\%$) interstitial O completely suppresses to 1.4 K both structural and magnetic transitions. A model for the spin structure has been

developed that links the unique topology of the trigonal bipyramidal to magnetic exchange, a model verified by diffuse magnetic neutron scattering from single crystals. We have also found that certain of these materials are magnetoelectric. We have prepared large single crystals of $\text{CaBaCo}_4\text{O}_7$, which had been shown in powders to be weakly magnetoelectric. Our collaborators in Caen claim that their measurements on our crystals demonstrate this material has among the highest magnetoelectric response known in the class of ‘improper ferroelectrics.’

Future Plans

Iridates: Future activities will focus on both deeper understanding of known materials (e.g., Ruddlesden-Popper phases) and discovery synthesis of novel iridates. As an example, we will extend the range of ‘honeycomb’ lattice materials that have been suggested theoretically as a basis for Kitaev quantum spin liquids. The A_2IrO_3 ($\text{A}=\text{Na}, \text{Li}$) compounds are nominally related to 3d analogs containing Mn that are electrochemically active. We propose to explore the phase diagrams of the $\text{A}_{1-x}\text{IrO}_3$ systems using single crystals and controlled oxidative deintercalation. While this is speculative, it is not unreasonable to draw an analogy between this system and the known $\text{Na}_{1-x}\text{CoO}_2$ analog, for which endmember band and Mott insulators bookend a range of magnetic and electronic phases, including of course, superconducting hydrates.

Cobaltites: ISIS collaborators have predicted based on symmetry arguments that a chiral spin liquid is possible in YBaCo_4O_7 if it is in a hexagonal (*i.e.*, undistorted) form. As discussed above, we have stabilized this hexagonal form by adding a slight (1.5%) excess of O and have seen a weak magnetic hysteresis. This hysteresis is a necessary but not sufficient condition, and we will pursue this. We also need to understand the dynamics of the spin arrangements to fully characterize this ‘114’ topology. First, we will use the large crystals for inelastic neutron scattering. This will allow direct access to the low energy excitations from either the ordered state (stoichiometric) or spin liquid state (O doped). Second, with collaborators at the magnet lab (M. Hoch) we will extend NMR studies on the stoichiometric specimens to the O doped crystals. In the $\text{CaBaCo}_4\text{O}_7$ system, we will determine the underlying fundamental mechanism for how the strong magnetoelectric coupling occurs and explore for other high response materials in related compounds.

References (FY12-13 supported by DOE-BES)

1. Pressure-induced volume collapse and structural phase transitions in SrRuO_3 , Zhernenkov, M., *et al.*, *Journal of Solid State Chemistry* **205**(0), 177-182 (2013).
2. Measuring 3D magnetic correlations during the photo-induced melting of electronic order in $\text{La}_{0.5}\text{Sr}_{1.5}\text{MnO}_4$, Tobey, R.I., *et al.*, *EPJ Web of Conferences* **41**, 03003 (2013).
3. Unusual evolution of the magnetism on oxygen in $\text{La}_{1-x}\text{Sr}_x\text{CoO}_3$, Medling, S., *et al.*, *Physica Status Solidi C*, **10**(2), 254-258 (2013).
4. Quantifying magnetic exchange in doubly-bridged Cu-X-2-Cu ($X = \text{F}, \text{Cl}, \text{Br}$) chains enabled by solid state synthesis of CuF_2 (pyrazine), Lapidus, S.H., *et al.*, *Chemical Communications* **49**(34), 3558-3560 (2013).
5. Observation of Electronic Inhomogeneity and Charge Density Waves in a Bilayer $\text{La}_{2-2x}\text{Sr}_{1+2x}\text{Mn}_2\text{O}_7$ Single Crystal, Kim, J., *et al.*, *Physical Review Letters* **110**(21) (2013).
6. Evidence for an internal-field-induced spin-flop configuration in the extended kagome YBaCo_4O_7 , Hoch, M.J.R., *et al.*, *Physical Review B* **87**(6) (2013).

7. Antiferromagnetic domain structure in bilayer manganite, Garcia-Fernandez, M, *et al.*, *Physical Review B* **88**(7), 075134 (2013).
8. Evolution of three-dimensional correlations during the photoinduced melting of antiferromagnetic order in $\text{La}_{0.5}\text{Sr}_{1.5}\text{MnO}_4$, Tobey, R.I, *et al.*, *Physical Review B* **86**(6) (2012).
9. Nonmonotonic Fermi surface evolution and its correlation with stripe ordering in bilayer manganites, Sun, Z, *et al.*, *Physical Review B* **86**(20) (2012).
10. Evolution of the spin-state transition with doping in $\text{La}_{1-x}\text{Sr}_x\text{CoO}_3$, Smith, R.X, *et al.*, *Physical Review B* **86**(5) (2012).
11. Understanding Fluxes as Media for Directed Synthesis: In Situ Local Structure of Molten Potassium Polysulfides, Shoemaker, D.P, *et al.*, *Journal of the American Chemical Society* **134**(22), 9456-9463 (2012).
12. Evolution of Magnetic Oxygen States in Sr-Doped LaCoO_3 , Medling, S, *et al.*, *Physical Review Letters* **109**(15) (2012).
13. Vapor Growth and Chemical Delithiation of Stoichiometric LiCoO_2 Crystals, Lin, Q.Y, *et al.*, *Crystal Growth & Design* **12**(3), 1232-1238 (2012).
14. Dimensionality Driven Spin-Flop Transition in Layered Iridates, Kim, J.W, *et al.*, *Physical Review Letters* **109**(3) (2012).
15. Magnetic Excitation Spectra of Sr_2IrO_4 Probed by Resonant Inelastic X-Ray Scattering: Establishing Links to Cuprate Superconductors, Kim, J, *et al.*, *Physical Review Letters* **108**(17) (2012).
16. Spin-ordering and magnetoelastic coupling in the extended kagome system YBaCo_4O_7 , Khalyavin, D.D, *et al.*, *Physical Review B* **85**(5) (2012).
17. Interplay between intrinsic and stacking-fault magnetic domains in bi-layered manganites, Hossain, M.A, *et al.*, *Applied Physics Letters* **101**(13), 132402 (2012).
18. Tetragonal $\text{YBaFe}_4\text{O}_{7.0}$: A stoichiometric polymorph of the "114" ferrite family, Duffort, V, *et al.*, *Journal of Solid State Chemistry* **191**, 225-231 (2012).
19. Pressure-induced tuning of a magnetic phase separation in $\text{Nd}_{0.53}\text{Sr}_{0.47}\text{MnO}_3$, Baldini, M, *et al.*, *Physical Review B* **86**(9) (2012).
20. Kinetic control of structural and magnetic states in $\text{LuBaCo}_4\text{O}_7$, Avci, S, *et al.*, *Physical Review B* **85**(9) (2012).
21. Cascade of Magnetic Field Induced Spin Transitions in LaCoO_3 , Altarawneh, M.M, *et al.*, *Physical Review Letters* **109**(3) (2012).
22. Surface melting of electronic order in $\text{La}_{0.5}\text{Sr}_{1.5}\text{MnO}_4$, Wilkins, S.B, *et al.*, *Physical Review B* **84**(16) (2011).
23. Response of Acoustic Phonons to Charge and Orbital Order in the 50% Doped Bilayer Manganite $\text{LaSr}_2\text{Mn}_2\text{O}_7$, Weber, F, *et al.*, *Physical Review Letters* **107**(20) (2011).
24. Synthesis of Homogeneous Pt-Bimetallic Nanoparticles as Highly Efficient Electrocatalysts, Wang, C, *et al.*, *ACS Catalysis* **1**(10), 1355-1359 (2011).
25. Structure and properties of rhombohedral CePd_3Ga_8 : A variant of the cubic parent compound with BaHg_{11} structure type, Macaluso, R.T, *et al.*, *Journal of Solid State Chemistry* **184**(12), 3185-3189 (2011).
26. Driving magnetic order in a manganite by ultrafast lattice excitation, Forst, M, *et al.*, *Physical Review B* **84**(24) (2011).

Understanding Iron Superconductors/Focus on Nodal Behavior

G. R. Stewart, Dept. of Physics, University of Florida, Gainesville, FL 32611

Program Scope

Our goal in this project is to understand the superconductivity in iron pnictide and chalcogenide (FePn/Ch) superconductors, potentially technologically useful materials. This goal is addressed on several fronts, of which two are listed here:

- 1.) Using single crystals of $\text{Ba}(\text{Fe}_{1-x}\text{Co}_x)_2\text{As}_2$ grown in our own lab and annealed optimally after an intensive annealing study (see Fig. 1), we have performed two studies.

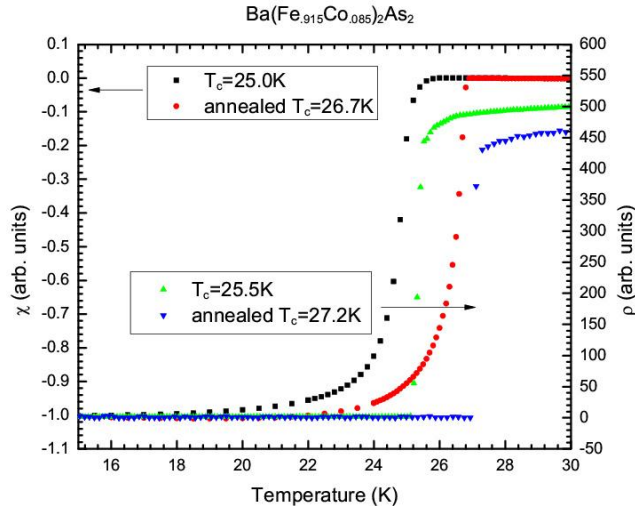


Fig. 1 Comparison of magnetic susceptibility χ and resistivity ρ for annealed and unannealed $\text{Ba}(\text{Fe}_{1-x}\text{Co}_x)_2\text{As}_2$, $x=0.085$ (nominal composition). Note T_c^{onset} of 27.2 K.

First, we have investigated the temperature dependence of the resistivity in 17 different compositions between underdoped ($T_c \approx 8$ K) and overdoped ($T_c \rightarrow 0$), with a focus around optimally doped (x_{opt}), to look for non-Fermi liquid behavior and the possible quantum

critical point under the superconducting dome. Second, we have looked at the specific heat discontinuity at T_c , ΔC , as a function of composition for both underdoped and overdoped material to compare its behavior with T_c and compare to theoretical predictions.

- 2.) Using specific heat in field as a function of angle, $C(H, \Theta)$, at temperatures below 0.1 T_c , we are looking for nodal behavior in several Fe pnictide (FePn) superconductors to

understand the pairing symmetry. Strong candidates for the states with the nodal structure in the iron superconductors now believed to have $\Delta \rightarrow 0$ on the Fermi surface (including $\text{BaFe}_{2-x}\text{Co}_x\text{As}_2$) include nodal s_+ states (where the dominant spin fluctuation interaction involves pair scattering between hole and electron Fermi surface ‘pockets’) and d-wave states. The variation with angle of the electronic density of states at the Fermi energy (proportional to the γ coefficient in the specific heat, $C(T \rightarrow 0) = \gamma T + \beta T^3$) for various nodal symmetries is shown in the figure at the left. Knowledge of the nodal structure

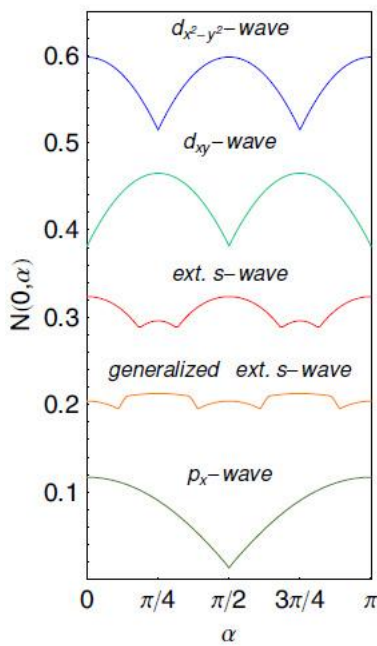


Fig. 2: Predictions [1] for $\gamma(H)$ for field in the nodal plane of FePn superconductors of various pairing symmetries.

(presence or absence of gaps and the symmetry of the nodes, i. e. where the energy gap Δ goes to zero on the Fermi surface) is a central question for understanding the parameters important for the pairing in a superconductor. [For a discussion, see several reviews,

refs. 2-4.] There are a number of probes of the nodal structure of a superconductor; none of the probes gives a stand-alone answer, in the sense that multiple probes offer both mutual confirmation as well as additional information not obtainable from one probe.

Recent Progress

We have mostly finished the studies of annealed single crystals of $\text{Ba}(\text{Fe}_{1-x}\text{Co}_x)_2\text{As}_2$, with the ΔC already published (publication #4) and the resistivity/search for the quantum critical point in submission. We discuss the latter study here as **Part 1** of recent progress.

Part 1: Resistivity of Annealed $\text{Ba}(\text{Fe}_{1-x}\text{Co}_x)_2\text{As}_2$ – Evidence for a Broad Composition Range of non-Fermi Liquid Behavior

Background

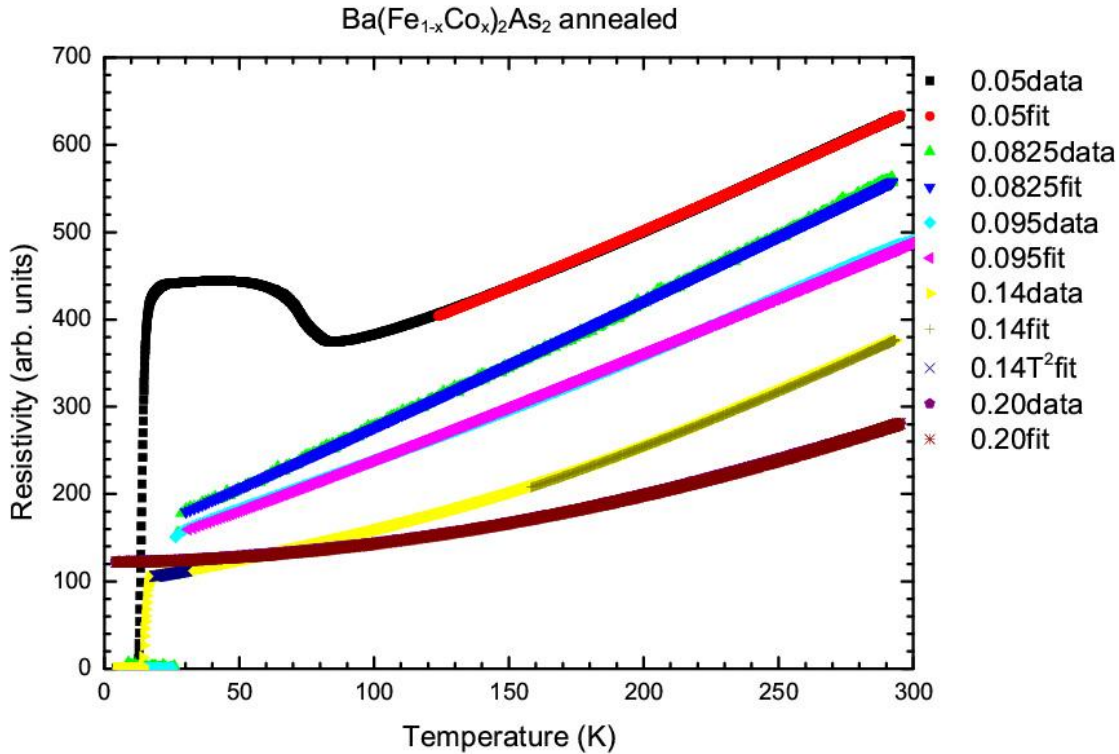
One of the theories [2-4] for the underlying mechanism of the superconductivity in the FePn (and Fe chalcogenides, FeCh) is the exchange of magnetic spin fluctuations. Such a scenario would be strengthened in probability if the oft-looked-for quantum critical point (QCP) in these materials could be more concretely proven. There seems rather solid evidence for such a QCP in $\text{BaFe}_2(\text{As}_{1-x}\text{P}_x)_2$ (a known nodal superconductor) [5], and we therefore studied $\text{Ba}(\text{Fe}_{1-x}\text{Co}_x)_2\text{As}_2$ using straightforward resistivity measurements to look above the superconducting dome for the temperature dependence, a good indicator of whether there is an underlying QCP. It is worthwhile to note that recently a theoretical argument has been advanced [6] that the QCP in $\text{BaFe}_2(\text{As}_{1-x}\text{P}_x)_2$ is *not* where the magnetic transition, T_{SDW} , extrapolates to $T=0$.

Discussion of Findings

Above any transition, either superconducting or structural for $x < x_{opt}$, the low temperature resistivity behaves approximately linearly with temperature from $x=0.05$ up to at least $x=0.095$ (see Figure 3 for some examples), with $\rho \propto T^2$ starting for $x=0.14$. The apparent constancy of the temperature dependence over a broad composition range argues strongly for the presence of a quantum critical point (QCP) underneath the superconducting dome. However, the temperature dependences measured down to T_c leave the exact location of the QCP open. Interestingly, although the transition temperature, T_c , rises by ≈ 1.5 K with annealing (Fig. 1), the temperature dependence of ρ appears unaffected by annealing, i. e. the QCP appears insensitive to small amounts of lattice disorder. Figure 3 shows five selected (nominal) compositions, with the following temperature ranges for the fits and the resultant exponents in $\rho = \rho_0 + aT^\alpha$: **x=0.05**: $\alpha=1.18(1)$ (fit range 125-300 K), **x=0.0825**: $\alpha=1.05(0)$ (30-300 K), **x=0.095**: $\alpha=1.06(9)$ (30-300 K), **x=0.14**: $\alpha=2$ (19-30 K)/ $\alpha=1.49$ (160-300 K), and **x=0.20**: $1.88(1)$ (50-300 K).

Fig. 3: ρ data for $\text{Ba}(\text{Fe}_{1-x}\text{Co}_x)_2\text{As}_2$ **x=0.05** (black), **0.0825** (green), **0.095** (light blue), **0.14** (yellow) and **0.20** (purple.) Clearly, in the neighborhood of the composition, x_{opt} , for the peak T_c , the temperature dependence of the resistivity remains fairly constant at about T^1 over a wide range of temperature. To get an idea of the possible practical error bar for these fits, if the fit for $x=0.095$ is restricted to 70-220 K rather than the 30-300 K shown here, $\alpha=1.05(5)$ rather than $1.06(9)$ for the whole range. The temperature

ranges of the various fits (red for $x=0.05$, blue for $x=0.0825$, pink for $x=0.095$, and blue/green for low and high temperatures respectively for $x=0.14$), are listed in the text.



Importance of Findings

Although the temperature dependence of the resistivity in $\text{Ba}(\text{Fe}_{1-x}\text{Co}_x)_2\text{As}_2$ around the peak of the superconducting dome has been long known to be about T^1 , we have now shown the extent as a function of composition of this non-Fermi liquid behavior. Thus, the theoretical argument for $\text{BaFe}_2(\text{As}_{1-x}\text{P}_x)_2$ that [6] the QCP may *not* be at x_{opt} where (approximately) $T_{\text{SDW}} \rightarrow 0$ is entirely consistent with our results here – i. e. the broad range of $\rho \sim T^1$ seen in our data on $\text{Ba}(\text{Fe}_{1-x}\text{Co}_x)_2\text{As}_2$ implies that the QCP could be somewhere different than x_{opt} in the range (nominal) of $x=0.05$ to 0.095.

Part 2: Angle resolved specific heat, $C(H,\Theta)$, as a probe of nodal structure and pairing symmetry. (Background has been covered in the introduction)

Discussion of Progress

Our instrumental ability to suppress scatter in $C(H,\Theta)$ has now been improved to $\pm 0.3\%$. We currently have an annealed sample of $\text{Ba}(\text{Fe}_{1-x}\text{Co}_x)_2\text{As}_2$ under measurement.

Future Plans

Finish measurements of $C(H,\Theta)$ on both over- and under-doped $\text{Ba}(\text{Fe}_{1-x}\text{Co}_x)_2\text{As}_2$ and then attempt the more difficult (due to the lower T_c) pure KFe_2As_2 (our sample has RRR=650) – based on some experimental work consistent with being a d-wave superconductor.

References

1. S. Graser, G. R. Boyd, Chao Cao, H.-P. Cheng, P. J. Hirschfeld and D. J. Scalapino, Phys. Rev. B **77**, 180514(R) (2008).
2. G. R. Stewart, Rev. Mod. Phys. 83, 1589 (2011).
3. D. C. Johnston, Adv. Phys. **59**, 803 (2010).
4. J. P. Paglione and R. L. Greene, Nat. Phys. **6**, 645 (2010).
5. K. Hashimoto, K. Cho, T. Shibauchi, S. Kasahara and Y. Mizukami, Science **336**, 1554 (2012).
6. D. Chowdhury, B. Swingle, E. Berg, and S. Sachdev, arXiv1305.2918.

Publications acknowledging BESS support (last 2 years since Aug. 21, 2011)

1. S. Khim, B. S. Lee, J. W. Kim, E. S. Choi, G. R. Stewart and K. H. Kim, " Pauli-limiting effects in the upper critical fields of a clean LiFeAs single crystal," Phys. Rev. B **84**, 104502 (2011).
2. Y. Wang, G. R. Stewart, J.S. Kim, P.J. Hirschfeld, S. Graser, S. Kasahara, T. Shibauchi, T. Terashima, Y. Matsuda, and I. Vekhter, "Volovik effect in a highly anisotropic multiband superconductor: experiment and theory," Phys. Rev. B **84**, 184524 (2011).
3. J. S. Kim, B. D. Faeth, Y. Wang, P. J. Hirschfeld, G. R. Stewart, K. Gofryk, F. Ronning, A. S. Sefat, K. Y. Choi and K. H. Kim, " Specific Heat To H_{c2} : Evidence for Nodes or Deep Minima in the Superconducting Gap of Under- and Overdoped $\text{BaFe}_{2-x}\text{Co}_x\text{As}_2$ ", Phys. Rev. B **86**, 014513 (2012).
4. J. S. Kim, B. D. Faeth, and G. R. Stewart, "Specific Heat Discontinuity vs T_c in Annealed $\text{Ba}(\text{Fe}_{1-x}\text{Co}_x)_2\text{As}_2$," Phys. Rev. B **86**, 054509 (2012).
5. J. S. Kim, G. R. Stewart, L.Y. Xing, X.C. Wang and C. Q. Jin, "Specific Heat vs Field of $\text{LiFe}_{1-x}\text{Cu}_x\text{As}$," Journal of Physics: Condens. Matter **24**, 475701 (2012).
6. M. B. Silva Neto, A. H. Castro Neto, J. S. Kim, and G. R. Stewart, "d and f hybridization and quantum criticality in weakly-itinerant ferromagnets", Journal of Physics: Condens. Matter. **25**, 025601 (2013).
7. J. S. Kim, T. Stürzer, D. Johrendt, and G. R. Stewart, " Specific Heat of the Electron-Doped La-1038 Compound $(\text{Ca}_{0.85}\text{La}_{0.15})_{10}(\text{FeAs})_{10}(\text{Pt}_3\text{As}_8)$ ", Journal of Physics: Condensed Matter **25**, 135701 (2013).
8. J. S. Kim, L.Y. Xing, X.C. Wang, C. Q. Jin and G. R. Stewart, " LiFeP – a Nodal Superconductor with an Unusually Large $\Delta C/T_c$," Phys. Rev. B**87**, 054504 (2013).
9. J. S. Kim, K. Zhao, C. Q. Jin, and G. R. Stewart, "Specific Heat of $\text{Ca}_{0.33}\text{Na}_{0.67}\text{Fe}_2\text{As}_2$ in Zero and Applied Field," submitted to Phys. Rev. B, their code BB12251.
10. J. S. Kim and G. R. Stewart, "UHg₃ – A Heavy Fermion Antiferromagnet 'By Design,'" submitted to Phys. Rev. Lett.
11. G. N. Tam, B. D. Faeth, J. S. Kim, and G. R. Stewart, "Resistivity of Annealed $\text{Ba}(\text{Fe}_{1-x}\text{Co}_x)_2\text{As}_2$ – Evidence for a Broad Composition Range of nFL Behavior" submitted to Phys. Rev. B.

Program Title: Unconventional Superconductivity in Strongly Correlated Materials
Principal Investigator: W.P. Halperin; co-PI's D. Van Harlingen, A. Kapitulnik, M.R. Eskildsen, P. Dai, P. Canfield and M. Greven
Mailing Address: Department of Physics and Astronomy, Northwestern University, Evanston IL, 60208
E-mail: w-halperin@northwestern.edu

Program Scope:

We investigate correlated fermionic excitations of novel materials that lead to quantum condensed states of superconductivity and magnetism and the competition between them. The general consensus is that the existence of unconventional pairing (broken symmetries not manifest in the normal state beyond gauge symmetry) is firmly established in superfluid ^3He , cuprate superconductors, the heavy fermion superconductors, UPt₃, and Sr₂RuO₄. There is particular interest in possible spontaneously broken time reversal symmetry and/or chiral symmetry which are relevant to the competition between magnetism and superconductivity and topologically protected surface states. In some instances a firm identification of the quantum state of the superconductor is missing. This is the case for the class of odd-parity superconductors that includes UPt₃ (possibly *f*-wave) and Sr₂RuO₄ (possibly *p*-wave) which are the best candidates we know for exhibiting chirality that, in principle, can be exploited for quantum computation. Similarly there is an unusual duality, or coexistence, between multiband superconductivity and spin density wave magnetism in both hole and electron-doped pnictides. Although our work covers experimental investigations over a broad range of these systems, our DOE/BES program¹⁻¹⁰ has two clear parts. It focuses on the use of high magnetic field NMR to study the normal and mixed states of superconductors and the behavior of vortices in the limit where the vortex density becomes very high at high magnetic fields; and secondly on crystal growth and characterization of UPt₃ as a part of collaborations with other DOE/BES programs employing, neutron scattering (SANS,¹ polarized elastic,⁵ and inelastic¹⁷), coherent tunneling,¹⁴ and polar Kerr rotation experiments.¹⁶

Underlying this program is the necessity to investigate very high quality single crystals and, depending on the system, these crystals are grown or processed in-house including UHV annealing (UPt₃), doping (HgBa₂CuO_{4+d}, Bi₂Sr₂CaCu₂O_{8+d}), isotope exchange (HgBa₂CuO_{4+d}, Bi₂Sr₂CaCu₂O_{8+d}), and UHV zone refining and crystal growth (UPt₃).

Recent progress:

We grow high quality large single crystals of UPt₃ which, together with our collaborators, have recently narrowed the uncertainty in the identification of the order parameter of this candidate chiral superconductor to support the prediction of E_{2u} symmetry.^{1,5,11,14,15} There are three vortex phases (A, B, and C) with thermodynamic transitions between them in the field-temperature plane. Nodal structure in the A-phase has been unambiguously determined¹⁴ from directional tunneling experiments; and phase sensitive Josephson Interference with corner junctions measurements¹⁴ are consistent with this symmetry classification. However theory for thermal conductivity measurements claim E_{1u} is more appropriate. E_{2u} has the B-phase as a unique chiral phase and E_{1u} is non-chiral. It has been an important issue to confirm one or the other of these results and their theoretical basis. Consequently, we have measured the temperature dependence of the penetration depth using a novel but high precision technique that

probe the bulk of the superconductor using small angle neutron scattering (SANS). This method obviates criticism of traditional measurements that are inherently surface sensitive. Within the context of the London theory the temperature dependences of the components of the penetration depth tensor are all found to be linear in temperature in the low temperature limit $T \ll T_c$ ($= 0.56$ K) consistent with equatorial *ab*-plane nodes and *c*-axis point nodes which open with quadratic dispersion. These results¹ are accurately consistent with E_{2u} symmetry. However, temperature dependence arguments are generally not as convincing as phase sensitive measurements or direct probes of nodal structure as have been performed by Van Harlingen's group.¹⁴ The characterization of the spin part of the order parameter is, however, not in such good shape.¹¹ There is a disparity between anisotropy of the upper critical field which indicates Pauli limiting for fields in the *ab*-plane and temperature independence of the spin susceptibility (NMR Knight shift) for fields along the *c*-axis. Since the NMR measurements are within a penetration depth of the surface, and spin-orbit interaction is expected to be strong, it has been argued⁵ that surface scattering might affect the NMR results. However, the critical field experiments are performed with a bulk acoustic probe. Consequently we have undertaken measurements using polarized neutron spin-flip scattering techniques to directly measure the magnetization internal to the superconductor and our results⁵ for all current orientations concur with the NMR experiments that were interpreted in terms of a triplet spin-state for UPt₃ with very weak spin-orbit interaction. The conflict with theoretical interpretation of Pauli limiting and spin-orbit effects is now a theoretical issue. Recent, as yet unpublished Kerr effect measurements from Aharon Kapitulnik,¹⁶ show Kerr rotation onsets at the transition from the A to the B-phase indicating broken time reversal symmetry consistent with a chiral order parameter in that phase.

Using high field ¹⁷O NMR, up to 30 T at the National High Magnetic Field Laboratory, we have investigated vortex behavior and structure in Bi₂Sr₂CaCu₂O_{8+d}. (Bi2212) There is broad interest in the interplay between magnetism and superconductivity in high T_c cuprates. The vortex core states arise from a singular response to competition between the high magnetic fields and the pairing interaction for spin-singlet superconductors. NMR is an ideal probe of the bulk superconductor behavior and it gains great sensitivity to core states at high magnetic fields where the vortex density increases proportionately. Furthermore, there are immediate applications of these materials for construction of high field magnets for NMR/MRI that depend on pinning of vortices at high density and for which a leading candidate is Bi2212 in the form of round wire. For basic scientific understanding of vortex physics at high field and its applications we have been investigating Bi2212 using ¹⁷O NMR where we do isotope exchange and doping on crystals from Uchida at the University of Tokyo. We have discovered¹⁰ theoretically, along with consistent experimental results that the pancake vortex structure that forms in strongly anisotropic materials such as Bi2212, has a weak three dimensional structure that is inherently unstable in high magnetic fields in the presence of vortex charging, *i.e.* transfer of electrical charge to the vortex core. Recent predictions show that this charging should be more pronounced for cuprates compared to low T_c materials by a factor of $(D/E_F)^2$ giving charge transfer to a pancake $\sim 10^{-3}$ e which our calculations show have an instability field of ~ 10 T. This field corresponds well with our observation of a field dependent collapse in the NMR linewidth which we identify with this phenomenon.¹⁰ At much higher magnetic fields we have found⁹ a spin-density wave emanating from the vortex core using a combination of spin-lattice relaxation measurements to image the vortex environment, and frequency shifts that correlate with an oscillating local field near the vortex core.

In collaboration with Martin Greven's group we have performed precision ^{17}O NMR frequency shift measurements² on underdoped $\text{HgBa}_2\text{CuO}_{4+\delta}$ ($\text{Hg}1201$). At the apical oxygen site we find absence of local fields posited to exist from orbital loop currents which have been inferred¹² from neutron scattering experiments to produce two orders of magnitude larger local field than our resolution.²

The discovery of superconductivity in pnictide compounds by Hosono in 2008 has led to a rapid and explosive investigation of this unusual multi-band system of materials. The key questions have been: i) What is the symmetry of the superconducting state? Is it $S+/+$ or $S+/-$? ii) How is this informed from impurity and magnetic field studies? and iii) Is there microscopic coexistence of spin-density wave (SDW) and superconducting order parameters in the range of overlap of these phases? In our four recent papers using ^{75}As and ^{23}Na NMR we have studied electron and hole-doped single crystals from Canfield's group⁸ and Dai's group.^{3,4,6} We have found that the interplay between impurity effects and the temperature dependence of the Knight shift and relaxation rates is sufficiently ambiguous that clear indications of the symmetry are difficult to determine⁸ since sufficient control and characterization of impurity concentrations is not straightforward to investigate experimentally, except potentially in the extremely clean limit. However, this is not the case for the combination of magnetic field and temperature dependence, where both can be varied continuously.^{6,8} Our observations of relaxation rates over a very wide range of temperature in electron doped $\text{Ba}(\text{Fe}_{0.93}\text{Co}_{0.07})_2\text{As}_2$ (BaCo122) aided by theoretical calculations from Vorontsov are consistent with $S+/-$ symmetry.^{5,8} In the class of 111 compounds $\text{NaFe}_{1-x}\text{Co}_x$ we have found exceedingly narrow ^{75}As and ^{23}Na linewidths and their absence of temperature dependence in the normal state is a strong indication of high homogeneity and absence of impurities. These spectra are even narrower than in $\text{Hg}1201$! The crystals from Dai's group ($x=0.025$) allowed measurements of the Knight shift from which we determined the penetration depth, and spin-lattice relaxation giving the order parameter amplitude in the zero temperature limit. Both are consistent with ~weak coupling BCS theory, but are agnostic vis-à-vis symmetry of the order parameter. However for the $x=0.017$ crystals we observe simultaneous microscopic coexistence of a spin density wave and superconductivity which requires the order parameter to be $S+/-$ as inferred from the theory. Interesting for this doping there appear to be two amplitudes for the SDW easily resolved through our combination of ^{75}As and ^{23}Na NMR.

Future Plans:

We are collaborating with the Grenoble high magnetic field NMR group of Julien to study charge ordering in the pseudogap phase of $\text{Hg}1201$. Their work on underdoped YBCO has identified charge order as a characteristic of this family of cuprates. The question remains whether this result is ubiquitous for cuprates as a whole. Since Greven's crystals are of such high quality (extremely narrow NMR lines even in underdoped material) it remains to do isotope exchange and dope them appropriately. This will require some very detailed processing studies. In parallel we will investigate the vortex structures in underdoped $\text{Hg}1201$ using spectrally resolved spin lattice relaxation in high magnetic fields. The role of magnetic interactions becomes more prevalent for underdoped cuprates and so with these new materials the vortex interactions at high density and vortex core states can be probed for the first time.

The usual two-component spin density wave we have found in Na111 pnictides will be extended to different dopings in the overlapping region of SDW and superconductivity to determine how each of these condensed states is modified by competing orders.

Directional probe experiments will be performed on UPt₃ to explore the dispersion near the nodes in the B and C-phases and continuing Kerr rotation experiments will require new crystals prepared with suitable facets. We have recently discovered in SANS experiments a splitting of the diffraction pattern in the B-phase which is completely unexpected and requires further work, although it is most likely related to two chiral order parameter domains. We also plan inelastic neutron scattering experiments to study the relation between superconductivity and magnetism at very high energy resolution, < 0.1 meV.¹⁷

References (Publications from past two years acknowledging DOE/BES support):

1. *Temperature Dependence of the Magnetic Penetration Depth and Nodal Gap Structure of UPt₃ from Small Angle Neutron Scattering*, W. J. Gannon, W. P. Halperin, C. Rastovski, K. J. Schlesinger, J. Hlevyack, C. Steiner, M. R. Eskildsen, J. Gavilano, U. Gasser, G. Nagy, arXiv:1302.4144
2. *Absence of Static Orbital Current Magnetism at the Apical Oxygen Site in HgBa₂CuO_{4+d} from NMR*, A.M. Mounce, Sangwon Oh, Jeongseop A. Lee, W.P. Halperin, A.P. Reyes, P.L. Kuhns, M.K. Chan, C. Dorow, L. Ji, D. Xia, X. Zhao, M. Greven, arXiv:1304.6415, submitted to Phys. Rev. Lett.
3. *Microscopic Coexistence of a Two-component Incommensurate Spin Density Wave with Superconductivity in Underdoped NaFe_{0.983}Co_{0.017}As*, Sangwon Oh, A. M. Mounce, Jeongseop A. Lee, W. P. Halperin, C. L. Zhang, S. Carr, Pengcheng Dai, A. P. Reyes, P. L. Kuhns, arXiv:1307.5366
4. *Spin Pairing and Penetration Depth Measurements from Nuclear Magnetic Resonance in NaFe_{0.975}Co_{0.025}As*, S. Oh, A.M. Mounce, J.A. Lee, W.P. Halperin, C.L. Zhang, S. Carr, P. Dai, Phys. Rev. B 87, 174517 (2013).
5. *Magnetization in the Superconducting State of UPt₃ from Polarized Neutron Diffraction*, W.J. Gannon, W.P. Halperin, C. Rastovski, M.R. Eskildsen, Pengcheng Dai, and A. Stunault, Phys. Rev. B 86, 104510 (2012).
6. *Magnetic Field Dependence of Spin-lattice Relaxation in the s± state of Ba_{0.67}K_{0.33}Fe₂As₂*, S. Oh, A.M. Mounce, W.P. Halperin, C.L. Zhang, P. Dai, A.P. Reyes, and P.L. Kuhns, Phys. Rev. B 85, 174508 (2012).
7. *Nuclear Magnetic Resonance Studies of Vortices in High Temperature Superconductors*, A.M. Mounce, S. Oh, and W.P. Halperin, Frontiers of Physics, 6, 450-462 (2011).
8. *⁷⁵As NMR of Ba(Fe_{0.93}Co_{0.07})₂As₂ in High Magnetic Field*, Sangwon Oh, A. M. Mounce, S. Mukhopadhyay, W. P. Halperin, A. B. Vorontsov, S. L. ko, P. C. Canfield, Y. Furukawa, A. P. Reyes, and P. L. Kuhns, Phys. Rev. B 83, 214501 (2011).
9. *Spin-density Wave Near the Vortex Cores in the High-temperature Superconductor Bi₂Sr₂CaCu₂O_{8+d}*, A.M. Mounce, S. Oh, S. Mukhopadhyay, W.P. Halperin, A.P. Reyes, P.L. Kuhns, K. Fujita, M. Ishikado, S. Uchida, Phys. Rev. Lett. 106, 057003 (2011).
10. *Charge Induced Vortex Lattice Instability*, A.M. Mounce, S. Oh, S. Mukhopadhyay, W.P. Halperin, A.P. Reyes, P.L. Kuhns, K. Fujita, M. Ishikado, S. Uchida, Nature Physics 7, 125 (2011).

Other References:

11. M. R. Norman, (2013), in *Novel Superfluids*, Volume 2, International Series of Monographs on Physics, edited by K.H. Bennemann and J.B. Ketterson (Oxford University Press, Oxford, United Kingdom, 2013) Chap. 12, arXiv:1302.3176v1.
12. S. Lederer and S.A. Kivelson, Phys. Rev. B 85, 155130 (2012).
13. J.A. Sauls, *Surface states, Edge Currents, and the Angular Momentum of Chiral p-wave Superfluids*, Phys. Rev. B, **84**, 214509, (2011).
14. J.D. Strand, D.J. Bahr, D.J. Van Harlingen, J.P. Davis, W.J. Gannon, W.P. Halperin, *The Transition Between Real and Complex Superconducting Order Parameter Phases in UPt₃*, Science, 328 (5984), 1368 (2010); also J.D. Strand *et al.*, Phys. Rev. Lett., **103**, 197002 (2009).
15. Y. Tsutsumi, K. Machida, T. Ohmi, and M. Ozaki, J. Phys. Soc. of Japan **81**, 074717 (2012).
16. A. Kapitulnik, private communication
17. W.J.Gannon *et al.* PhD thesis, Northwestern University, and to be published

Session 5

Optical Spectroscopy of Defects and Dopants in Nanocarbon Materials

DOE Grant Number: DE-FG02-05ER46207

Lukas Novotny (novotny@optics.rochester.edu)

University of Rochester, The Institute of Optics, Rochester, NY, 14627.

1. Program Scope

We study the optoelectronic properties of nano carbon materials, such as carbon nanotubes and graphene. The physical properties of these nanocarbon materials are strongly affected by impurities and structural defects. In the past we have studied individual defects and dopants in carbon nanotubes using near-field Raman scattering, a technique which allowed us to optically and spectroscopically resolve features on the order of 10 nm. More recently, we have studied the symmetry breaking nature of graphene edges and associated local electronic effects. Using a novel defocusing technique we were able to measure the electron coherence length at variable temperatures with a spatial resolution of a few nanometers.

2. Recent Progress

In the last project period we invested time and effort to develop an efficient graphene transfer technique in order to deposit a graphene sheet onto a selected region of a substrate. Graphene has demonstrated promise for future semiconductor and photonic technologies, but many applications, such as photovoltaic devices, organic LEDs, photodetectors, touch screens, and flexible smart windows, rely on the precise deposition of graphene on processed substrates. Thus far, considerable effort has been invested into procedures to transfer graphene between substrates. In the standard chemical transfer procedure, a graphene flake is transferred to the target substrate using Poly(methyl methacrylate) (PMMA). The PMMA is dissolved using acetone, leaving the graphene flake on the desired substrate. While this is a straightforward procedure, the acetone treatment frequently fails to fully remove the PMMA, leaving a residue on the graphene surface and the substrate.

The procedure that we have developed starts by overcoating a substrate with deposited graphene flake with PMMA. By using a sodium hydroxide solution, the graphene-PMMA stack is lifted from the initial substrate and placed onto the target substrate. Finally, the PMMA is dissolved using acetone. After transfer to the target substrate, the graphene-PMMA stack is placed in acetic acid for 24 hours. Afterwards, the sample is cleaned in methanol. We have characterized transferred graphene samples using differential optical contrast microscopy (DIC), Raman spectroscopy, and atomic force microscopy (AFM). We have compared the quality of our transfer technique with previous approaches and used fluorescence quenching to further illustrate the improvement in the quality of our acetic acid method.

Figure 1 shows a comparison between acetone and acetic acid based transfer methods. (a) and (b) are optical images recorded with DIC light microscopy, and (c) and (d) are topographic images recorded with AFM. (e) and (f) are representative Raman spectra that feature several characteristic phonon modes. For either transfer method we observed no folding or tearing of the

graphene layer.

The Raman spectra were acquired by placing the samples on an inverted microscope. The sample was excited with a 532 nm laser through an air objective ($NA = 0.7$), which was also used for collection. The signal was sent to either an avalanche photodiode (APD) or a combination of spectrometer and charge-coupled device (CCD). The samples were raster scanned through the focus with an x-y piezo scan stage to form a confocal Raman 2D band image. Using this confocal image, the laser was moved to specific locations on the graphene sample to obtain spectra.

Figure 1(e,f) show Raman spectra taken on an acetone and acetic acid cleaned sample, respectively. The Raman spectra exhibit the first-order bond stretching G band centered at $\sim 1580\text{ cm}^{-1}$, and the two-phonon 2D (or G') band centered at $\sim 2700\text{ cm}^{-1}$. Both spectra are

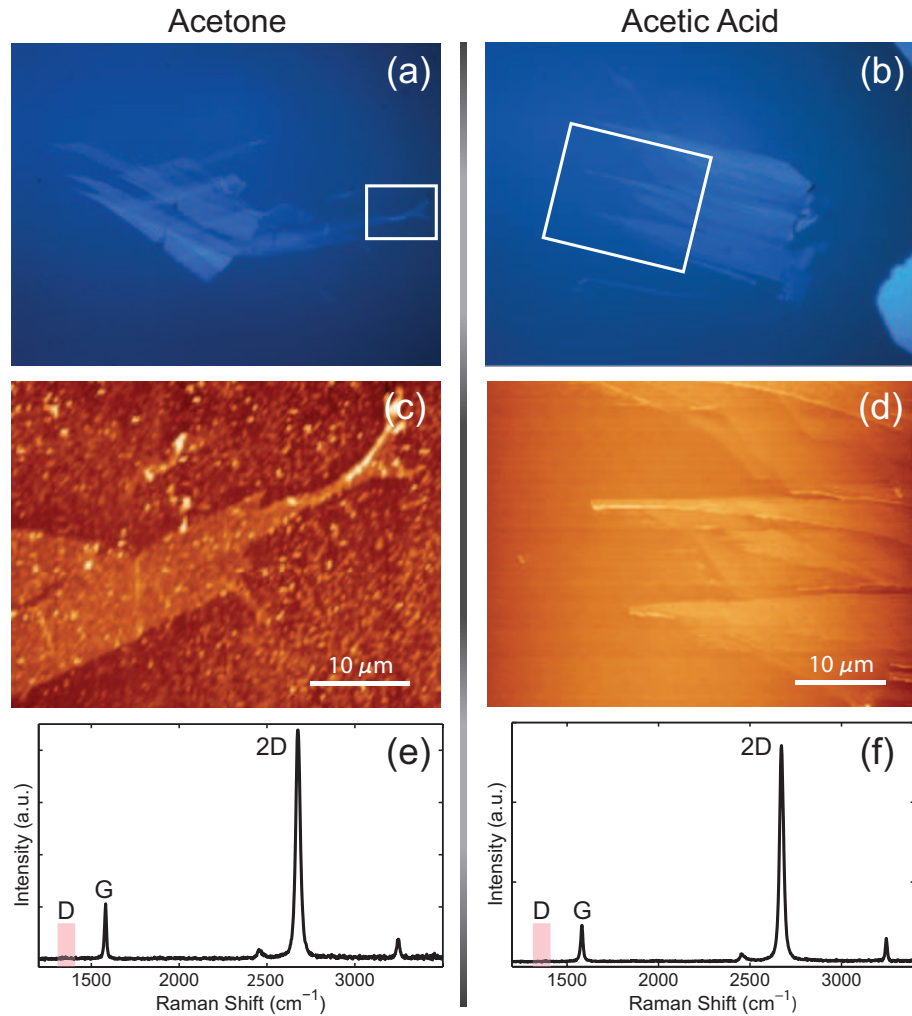


Figure 1: Comparison of graphene transfer methods. (a,c,d) Standard acetone based approach and (b,d,f) acetic acid method. The images show a graphene sample that has been transferred on a glass substrate. (a,b) Optical images viewed under a differential interference contrast (DIC) light microscope. (c,d) Topographic images recorded with AFM, and (e,f) Raman spectra. The red box indicates the D band frequency range.

characteristic of single layer graphene, as can be seen from the lineshape of the 2D band, and neither show additional peaks due to a chemical alteration of the graphene. It is also important to note the absence of the disorder-induced D band [red box in Fig. 1(e-f)] which indicates that neither transfer process damages the sp^2 bonds of the graphene flakes.

The residue from the acetone transfer method is not observable optically or spectroscopically, but is clearly visible in topography [Fig. 1(c)]. The topographic images were taken using a commercial AFM operating in semi-contact mode. The residue on this flake ranges in size from $\sim 0.2 - 2.0 \mu\text{m}$. By dissolving the PMMA in an acetic acid solution, we have been able to remove this residue from the graphene, as shown in Fig. 1(d).

To further illustrate the cleanliness of our acetic acid transfer method as well as demonstrate the effects of contaminants on the optical properties of a graphene flake, we acquired fluorescence quenching images of acetic acid and acetone cleaned samples. The total decay rate of the excited state of a fluorescent molecule (γ) can be written as $\gamma = \gamma_r + \gamma_{nr}$, where γ_r and γ_{nr} are the radiative and non-radiative rates, respectively. As a fluorescent molecule is brought closer to the graphene surface, γ increases due to the Purcell effect. However, the separation distance determines whether γ_r or γ_{nr} dominates. In the case of a metal film, for distances larger than $\approx 5 \text{ nm}$, γ_r dominates. If separation distance is less than 5 nm , then the decay process is primarily non-radiative ($\gamma_{nr} \gg \gamma_r$), which is known as fluorescence quenching. If there is a dielectric spacer between the molecule and the metal film then fluorescence is still observed and the thickness of the dielectric spacer determines the strength of the fluorescence signal. Therefore, a clean graphene flake coated with fluorescent dye should show uniform quenching, whereas in the presence of contaminants on the surface, the dye molecules can still fluoresce. We have recorded fluorescence and lifetime images of dye molecules deposited on several graphene samples and verified that acetic acid treated graphene is reasonably contamination free.

3. Future Plans

In our future work we will study the nonlinear optical properties of thin graphene films. It has been shown that the third-order susceptibility of graphene is particularly strong, which opens the door for investigating effects such as phase conjugation and negative refraction.

4. DOE sponsored publications 2008-2013

a. Papers which exclusively acknowledge DMSE support

- [1] H. Harutyunyan, R. Beams and L. Novotny, "Controllable optical negative refraction and phase conjugation in graphene ,," Nature Physics **9**, 423-425 (2013).
- [2] M. Her, R. Beams, and L. Novotny, "Graphene transfer with reduced residue," Phys. Lett. A **377**, 1455-1458 [(2013)].
- [3] D. Lopez-Mago and L. Novotny, "Quantum-optical coherence tomography with collinear entangled photons," Opt. Lett. **37**, 4077-4079 (2012).
- [4] D. Lopez-Mago and L. Novotny, "Coherence measurements with the two-photon Michelson interferometer," Phys. Rev. A **86**, 023820 (2012).
- [5] R. Beams, L. G. Cancado, and L. Novotny, "Low temperature Raman study of the electron coherence length near graphene edges," Nano Lett. **11**, 1177–1181 (2011).

- [6] L. G. Cançado, A. Jorio, A. Ismach, E. Joselevich, A. Hartschuh, and L. Novotny, "Mechanism of Near-Field Raman Enhancement in One-Dimensional Systems," *Phys. Rev. Lett.* **103**, 186101 (2009).
- [7] L. G. Cançado, A. Hartschuh, and L. Novotny, "Tip enhanced Raman scattering of carbon nanotubes," *J. Raman Spectrosc.* **40**, 1420–1426 (2009).
- [8] N. Anderson, A. Hartschuh, and L. Novotny, "Chirality changes in carbon nanotubes studied with near-field Raman spectroscopy," *Nano Lett.* **7**, 577–582 (2007).

b. Papers which acknowledge DMSE and other agency support

- [1] R. V. Maximiano, R. Beams, L. Novotny, A. Jorio, and L. G. Cancado, "Imaging physical phenomena with local probes," *Phys. Rev. B* **85**, 235434 (2012). **International collaboration. Near-field measurements done with DMSE support.**
- [2] D. A. Bonnell, D. N. Basov, M. Bode, U. Diebold, S. V. Kalinin, V. Madhavan, L. Novotny, M. Salmeron, U. D. Schwarz, and P. S. Weiss, "Imaging physical phenomena with local probes," *Rev. of Mod. Phys.* **84**, 1343–1381 (2012). **Review article.**
- [3] J. Soares *et al.*, "Modulating the electronic properties along carbon nanotubes via tube-substrate interaction," *Nano Lett.* **10**, 5043–5048 (2011). **International collaboration. Near-field measurements done with DMSE support.**
- [4] H. Qian, N. Anderson, C. Georgi, L. Novotny, and A. Hartschuh, in *Tip-enhanced optical microscopy, Nano-Optics and Near-Field Optical Microscopy*, A. Zayats and D. Richards, eds., (Artech House, 2009). **International collaboration. Near-field measurements done with DMSE support.**
- [5] A. Hartschuh, H. Qian, C. Georgi, and L. Novotny, "Tip-enhanced near-field optical microscopy of carbon nanotubes," *Anal. and Bioanal. Chem.* **394**, 1787 (2009). **International collaboration. Near-field measurements done with DMSE support.**
- [6] C. Georgi, M. Boehmler, H. Qian, L. Novotny, and A. Hartschuh, "Probing exciton propagation and quenching in carbon nanotubes with near-field optical microscopy," *Phys. Stat. Sol. B* **246**, 2683–2688 (2009). **International collaboration. Near-field measurements done with DMSE support.**
- [7] I. O. Maciel *et al.*, "Electron and phonon renormalization at defect/doping sites in carbon nanotubes," *Nature Mat.* **7**, 878 – 883 (2008). **International collaboration. Near-field measurements done with DMSE support.**
- [8] H. Qian, C. Georgi, N. Anderson, A. A. Green, M. C. Hersam, L. Novotny, and A. Hartschuh, "Exciton energy transfer in pairs of single-walled carbon nanotubes," *Phys. Stat. Sol. B* **245**, 2243–2246 (2008). **International collaboration. Near-field measurements done with DMSE support .**
- [9] H. Qian, P. T. Araujo, C. Georgi, T. Gokus, N. Hartmann, A. A. Green, A. Jorio, M. C. Hersam, L. Novotny, and A. Hartschuh, "Visualizing the local optical response of semiconducting carbon nanotubes to DNA-wrapping," *Nano Lett.* **8**, 2706–2711 (2008). **International collaboration. Near-field measurements done with DMSE support .**
- [10] H. Qian, C. Georgi, N. Anderson, A. A. Green, M. C. Hersam, L. Novotny, and A. Hartschuh, "Exciton transfer and propagation in carbon nanotubes studied by near-field optical microscopy," *Nano Lett.* **8**, 1363–1367 (2008). **International collaboration. Near-field measurements done with DMSE support.**
- [11] A. Hartschuh, H. Qian, A. J. Meixner, N. Anderson, and L. Novotny, "Tip-enhanced optical spectroscopy for surface analysis in biosciences," *Surface and Interface Analysis* **38**, 1472–1480 (2006). **International collaboration. Near-field measurements done with DMSE support .**

Program Title: Spectroscopy of Degenerate One-Dimensional Electrons in Carbon Nanotubes

Principle Investigator: Junichiro Kono

Address: Department of Electrical and Computer Engineering and Department of Physics and Astronomy, Rice University, Houston, Texas, U.S.A. E-mail: kono@rice.edu

Program Scope

We study degenerate one-dimensional (1D) electrons in single-wall carbon nanotubes (SWCNTs) using optical spectroscopies. Transport and optical studies on SWCNTs during the past decade have revealed some characteristic 1D features, but most of the predicted exotic properties of interacting 1D electrons have yet to be observed. Here, using spectroscopic methods from the terahertz to the optical ranges, we aim to achieve a fundamental understanding of correlations and many-body effects in 1D.

Recent Progress

1) Enrichment and Optical Spectroscopy of Armchair SWCNTs

We used density gradient ultracentrifugation (DGU) to produce aqueous suspensions enriched in armchair nanotubes. Through resonant Raman spectroscopy, we provided evidence that DGU can enrich armchair nanotubes. Furthermore, using optical absorption spectroscopy, we showed that interband absorption in armchair nanotubes is strongly excitonic. These findings lay the foundation for further spectroscopic studies to probe many-body physical phenomena in one dimension. See Refs. [3,8] for more detail.

2) Dephasing of G-band Phonons in SWCNTs

We performed coherent phonon spectroscopy of SWCNTs using ultrafast pump-probe spectroscopy. The temperature dependence of the observed dephasing rate clearly exhibited a thermally-activated component, indicating that the G-band phonon mode dephases via anharmonicity-induced coupling with a lower-frequency mode. See Refs. [6,7,9] for more detail.

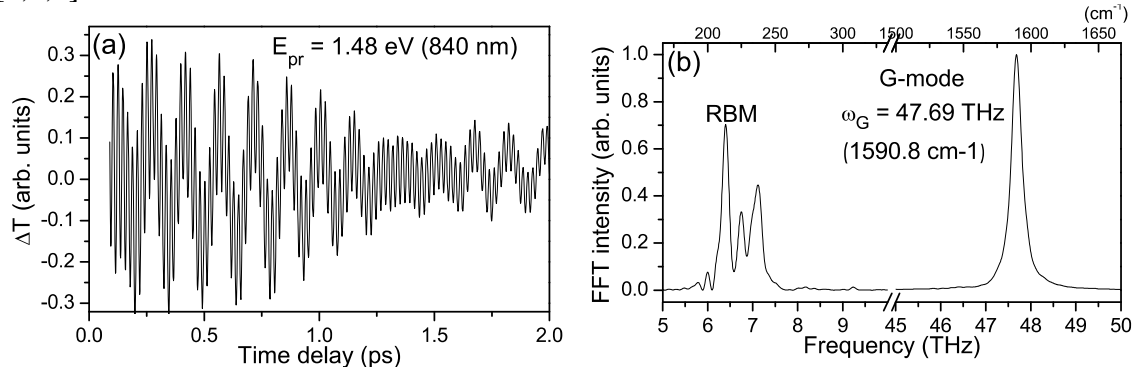


Figure 1: (a) Coherent phonon oscillations in SWCNTs, observed with pump-probe spectroscopy. (b) Corresponding Fourier-transformed spectrum showing radial-breathing modes (RBMs) at 6.0-7.5 THz ($200-250 \text{ cm}^{-1}$) and G-mode phonons at 47.69 THz (1590.8 cm^{-1}).

3) Enhancement of the Electron Spin Resonance of SWCNTs by Oxygen Removal

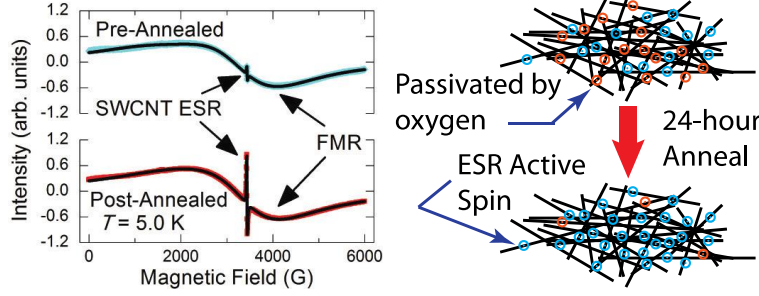


Figure 2: (Top left) ESR scan at 5.0 K of SWCNT sample before annealing (cyan), where the ESR signal is buried in the large FMR background. (Bottom left) ESR scan of SWCNT sample at 5.0 K after annealing (red), where the SWCNT ESR is the dominant feature.

We showed that adsorbed molecular oxygen has a considerable influence on the spin susceptibility of SWCNTs, while having only a small impact on spin movement. By looking at the electron spin resonance (ESR) of SWCNTs as a function of temperature both before and after thermal annealing, we were able to quantitatively evaluate the impact of adsorbed oxygen spins. Strikingly, we found that oxygen desorption increased the ESR signal by nearly a factor of 4. See Refs. [4,16] for more detail.

4) Collective Antenna Effects in the Terahertz Response of Aligned Carbon Nanotubes

We studied the THz and infrared response of highly aligned SWCNT films to elucidate the frequency and polarization dependence of transmission. The attenuation spectrum exhibits a pronounced peak around 450 cm^{-1} in the parallel polarization case. We take into account both the scattering and absorption contributions to the total attenuation of the THz wave. Although an individual nanotube is an inefficient radiator due to its small diameter, at long wavelengths a large number of aligned nanotubes in the film can be excited coherently and radiate in phase. See Refs. [1,2,11] for more detail.

5) Midinfrared Third Harmonic Generation from Aligned Ultralong SWCNTs

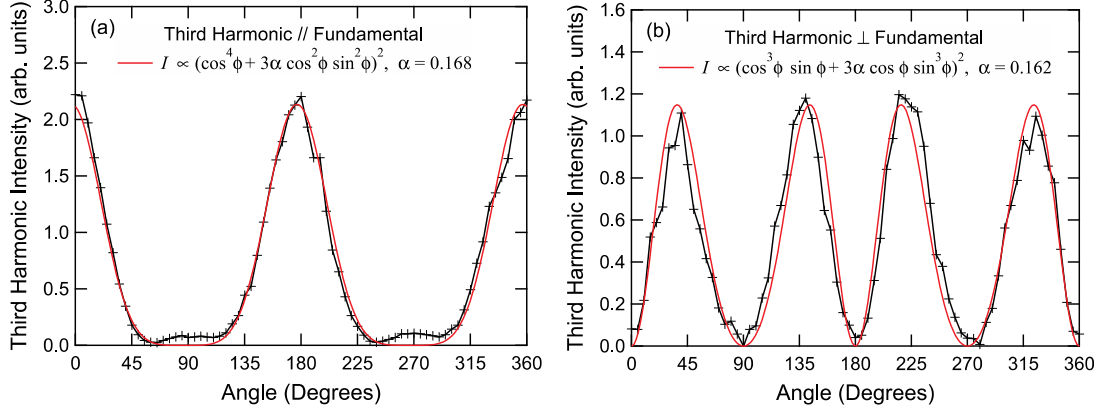


Figure 3: Experimental and theoretical angular dependence for a THG signal polarized (a) parallel and (b) perpendicular to the fundamental, considering the $\chi^{(3)}$ tensor contribution relationship is $\alpha \chi_{zzzz}^{(3)} = \chi_{zzxx}^{(3)}$. The theoretical fits (red) show ϕ dependence for $\alpha \approx 1/6$.

We observed strong third harmonic generation from a macroscopic array of aligned ultralong SWCNTs with intense midinfrared radiation and determined the absolute value of the third-order nonlinear optical susceptibility, $\chi^{(3)}$, to be 5.53×10^{-12} esu, three orders of magnitude larger than that of the fused silica reference we used. Furthermore, through polarization-dependent experiments, we extracted all the nonzero elements of the $\chi^{(3)}$ tensor. See Ref. [12] for more detail.

Future Plans

- To perform DC transport, THz conductivity, electron spin resonance, and optical pump-probe measurements on film samples of metallic-enriched SWCNT samples to obtain new insights to the dynamics of interacting 1-D electrons.
- To study photoluminescence from gated films of semiconductor-enriched SWCNT samples to understand under what the Fermi-edge singularity appears in 1-D systems.
- To fabricate device structures based on armchair SWCNTs for i) investigating the possibility of Peierls instability in small-diameter armchair tubes and ii) resistively detecting electron spin resonance on a single-tube level.
- To study light emission from highly excited semiconducting SWCNTs to observe an excitonic Mott transition in one dimension and to search for cooperative spontaneous emission (superfluorescence).

Publications

1. L. Ren, C. L. Pint, T. Arikawa, K. Takeya, I. Kawayama, M. Tonouchi, R. H. Hauge, and J. Kono, “Broadband Terahertz Polarizers with Ideal Performance Based on Aligned Carbon Nanotube Stacks,” *Nano Lett.* **12**, 787 (2012).
2. L. Ren, Q. Zhang, S. Nanot, I. Kawayama, M. Tonouchi, and J. Kono, “Terahertz Dynamics of Quantum-Confinement Electrons in Carbon Nanomaterials,” *J. Infrared, Millimeter and Terahertz Waves* **33**, 846 (2012).
3. E. H. Hároz, J. G. Duque, B. Y. Lu, P. Nikolaev, S. Areppalli, R. H. Hauge, S. K. Doorn, and J. Kono, “Unique Origin of Colors of Armchair Carbon Nanotubes,” *J. Am. Chem. Soc.* **134**, 4461 (2012).
4. W. D. Rice, R. T. Weber, A. D. Leonard, J. M. Tour, P. Nikolaev, S. Areppalli, V. Burka, A.-L. Tsai, and J. Kono, “Enhancement of the Electron Spin Resonance of Single-Walled Carbon Nanotubes by Oxygen Removal,” *ACS Nano* **6**, 2165 (2012).
5. S. Nanot, E. H. Hároz, J.-H. Kim, R. H. Hauge, and J. Kono, “Optoelectronic Properties of Single-Wall Carbon Nanotubes,” *Adv. Mat.* **24**, 4977 (2012).
6. J.-H. Kim, K.-J. Yee, Y.-S. Lim, L. G. Booshehri, E. H. Hároz, and J. Kono, “Dephasing of G-Band Phonons in Single-Wall Carbon Nanotubes Probed via Impulsive Stimulated Raman Scattering,” *Phys. Rev. B* **86**, 161415(R) (2012).
7. J.-H. Kim, A. R. T. Nugraha, L. G. Booshehri, E. H. Hároz, K. Sato, G. D. Sanders, K.-J. Yee, Y.-S. Lim, C. J. Stanton, R. Saito, and J. Kono, “Coherent Phonons in Carbon Nanotubes and Graphene,” *Chem. Phys.* **413**, 55 (2013).

8. E. H. Hároz, J. G. Duque, X. Tu, M. Zheng, A. R. Hight Walker, R. H. Hauge, S. K. Doorn, and J. Kono, “Fundamental Optical Processes in Armchair Carbon Nanotubes,” *Nanoscale* **5**, 1411 (2013).
9. G. D. Sanders, A. R. T. Nugraha, K. Sato, J.-H. Kim, J. Kono, R. Saito, and C. J. Stanton, “Theory of Coherent Phonons in Carbon Nanotubes and Graphene Nanoribbons,” *J. Phys.: Cond. Mat.* **25**, 144201 (2013).
10. S. Nanot, A. W. Cummings, C. L. Pint, A. Ikeuchi, T. Akiho, K. Sueoka, R. H. Hauge, F. Léonard, and J. Kono, “Broadband, Polarization-Sensitive Photodetector Based on Optically-Thick Films of Macroscopically Long, Dense, and Aligned Carbon Nanotubes,” *Sci. Rep.* **3**, 1335 (2013).
11. L. Ren, Q. Zhang, C. L. Pint, A. K. Wójcik, M. Bunney, T. Arikawa, I. Kawayama, M. Tonouchi, R. H. Hauge, A. A. Belyanin, and J. Kono, “Collective Antenna Effects in the Terahertz and Infrared Response of Highly Aligned Carbon Nanotube Arrays,” *Phys. Rev. B* **87**, 161401(R) (2013).
12. D. T. Morris, C. L. Pint, R. S. Arvidson, A. Lüttege, R. H. Hauge, A. A. Belyanin, G. L. Woods, and J. Kono, “Midinfrared Third Harmonic Generation from Macroscopically Aligned Ultralong Single-Wall Carbon Nanotubes,” *Phys. Rev. B* **87**, 161405(R) (2013).
13. S. Ushiba, S. Shoji, K. Masui, J. Kono, and S. Kawata, “3D Micro-Fabrication of Single-Wall Carbon Nanotube/Polymer Composites by Two-Photon Polymerization Lithography,” *Carbon* **59**, 283 (2013).
14. Y. Kim, J.-M. Poumirol, A. Lombardo, N. G. Kalugin, T. Georgiou, Y. J. Kim, K. S. Novoselov, A. C. Ferrari, J. Kono, O. Kashuba, V. I. Fal’ko, and D. Smirnov, “Measurement of Filling-Factor-Dependent Magnetophonon Resonances in Graphene Using Raman Spectroscopy,” *Phys. Rev. Lett.* **110**, 220402 (2013).
15. W. D. Rice, R. T. Weber, P. Nikolaev, S. Arepalli, V. Berka, A.-L. Tsai, and J. Kono, “Spin Relaxation Times of Single-Wall Carbon Nanotubes,” *Phys. Rev. B* **88**, 041401(R) (2013).
16. X. He, S. Nanot, X. Wang, R. H. Hauge, A. A. Kane, J. E. M. Goldsmith, F. Léonard, and J. Kono, “Photothermoelectric p-n Junction Photodetectors with Intrinsic Polarimetry Based on Macroscopic Carbon Nanotube Films,” *ACS Nano*, published online on June 30, 2013.
17. W. Gao, G. Shi, Z. Jin, Q. Zhang, P. M. Ajayan, J. Kono, and Q. Xu, “Excitation and Active Control of Propagating Surface Plasmon Polaritons in Graphene,” *Nano Lett.*, published online on July 29, 2013.

Program Title: Controlling Electronic Structure and Photophysics of Graphene

Principle Investigator: Feng Wang

**Mailing Address: Department of Physics, University of California at Berkeley,
Berkeley, CA 94720**

E-mail: fengwang76@berkeley.edu

Program Scope

The goals of this program are to develop fundamental understanding and control of electronic structure and photophysics in graphene. Graphene has an unusual electronic structure that can be tailored with a variety of approaches, which allows for active control of electrical, optical, and mechanical properties in graphene. Such control is of importance for both basic science and technology: it can open up exciting new opportunities for exploring two-dimensional physics, and it can lead to novel nanoelectronic and nanophotonic devices and impact a broad range of energy technologies.

Graphene, a one-atom thick sheet of carbon, is a multifunctional material with fascinating electrical, optical, and mechanical properties. And amazingly, electronic structure of graphene can be controlled through electrostatic gating, nanoscale patterning, graphene-graphene interactions, and graphene-substrate interactions. In earlier DOE supported work we have demonstrated that (i) optical absorption in monolayer graphene can be switched on and off by electrical gating[1], which can lead to efficient modulation of light[2], and (ii) a widely tunable bandgap can be achieved in dual-gated bilayer graphene[3]. In more recent work we have discovered that efficient control of electronic structure and optical responses can be achieved in graphene-boron nitride heterostructures and in graphene-nanophotonic hybrid structures[4,5]. We also realize control of not only linear optical properties, but also ultrafast responses in monolayer and bilayer graphene.

In this program I combine material synthesis and advanced nanofabrication with state-of-the-art laser spectroscopy to probe novel physical phenomena arising from the tunable electronic structure of graphene. These techniques are further complemented by scanning microscopy characterizations and by theoretical investigations through already established collaborations with other DOE-supported PIs at Berkeley.

Recent Progress

1. Hybrid graphene-nanophotonic structures

Nanophotonics enables efficient routing and manipulation of light at nanometer scale either through plasmonic metamaterials or photonic crystals. In many applications it is often desirable to be able to control the plasmon or photonic crystal cavity resonance *in situ* with electrostatic gating. Graphene, with its unique tunable optical properties and excellent compatibility with nanofabrication, provides an ideal material to integrate with nanophotonic structures for realizing such control.

Although graphene is only one monolayer thick, it can lead to efficient modulation of light due to enhanced light-matter interactions in a plasmonic structure or a photonic

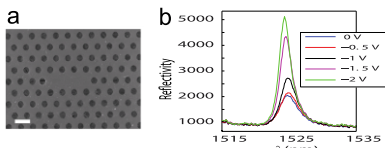


Fig. 1: (a) A hybrid graphene-PhC structure. (b) Electrical control of PhC resonance with graphene.

crystal. We demonstrated that electrical controlled plasmonic resonance can be achieved at near infrared using the hybrid graphene-gold nanorod structure as a model system[4]. We also demonstrated that efficient electrical modulation of a silicon photonic crystal cavity (PhC) with graphene (Fig. 1)[5]. Figure 1a illustrates the hybrid graphene-PhC structure, and Figure 1b shows that the PhC resonance linewidth

and the resonance reflection intensity can be modulated by several through electrostatic gating of graphene. This electro-modulation of the PhC resonance by graphene can be understood quantitatively through gate-variable optical transitions and the associated dielectric constant of graphene. The cavity resonance linewidth change is proportional to the real part of the conductivity of graphene, while the resonance shift is proportional to the imaginary part.

2. Control Graphene Hot Carrier Response from Metal-like to Semiconductor-like

“Hot” charge carriers generated by optical excitation play an important role in optoelectronic responses in graphene. Understanding and further control of the dynamic response of hot carriers can potentially lead to carrier multiplication, broad band photodetector, and new types of hot carrier-based graphene devices.

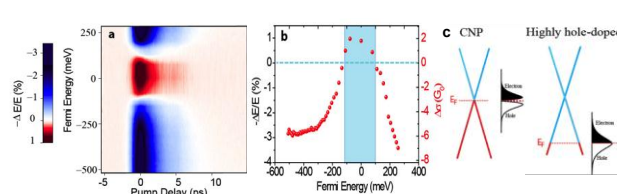


Fig. 2: (a) Transient THz transmission as a function of pump-probe delay and Fermi energy. (b) Pump-induced THz signal changes sign with Fermi energy. It corresponds to a transition from semiconductor-like response at CNP to metallic like response in doped graphene, as illustrated in (c).

energy. One salient feature is that the photo-induced THz response switches sign very close to the CNP, changing from positive (decrease of transmission) in undoped graphene to negative (increase of transmission) in highly doped graphene. Fig. 2b displays a vertical line cut of the two-dimensional plot at $\tau = 0$, showing the maximum THz transmission change as a function of Fermi energy. We observe that the photo-induced THz response changes sign in a window $\sim \pm 100$ meV away from CNP (shaded area).

This sign change in photo-induced THz transmission corresponds to a transition from semiconductor-like to metal-like behavior upon doping. This behavior is characteristic of hot carrier response in Dirac materials with zero bandgap, as we illustrate in Fig. 2c. At charge neutral point, higher electronic temperature leads to both more electrons and holes, similar to that in a semiconductor. The net carrier concentration increase leads to an increase in conductivity (i.e. absorption), and therefore lower transmission. In highly doped graphene, on the otherhand, higher electronic temperature mainly leads to a redistribution of charge carrier within the valence or conduction band with no net change of charge carriers, similar to that in a metal. In this case, carrier concentration does not

We employ optical pump-THz probe spectroscopy in electrostatically gated graphene to systematically probe graphene hot carrier responses at different carrier concentrations. Figure 2a shows a two-dimensional plot of the pump-induced THz field transmission change ($-\Delta E/E_0$) as a function of optical pump-THz probe time delay and the initial graphene Fermi

change, but the scattering rate increases with the electron temperature. As a result, we have a reduction in conductivity (i.e. absorption), and therefore higher transmission.

3. Graphene-boron nitride (BN) heterostructures

In bulk materials the electronic structure engineering requires a modification of strong covalent bonds like doping chemical elements or changing crystalline structure. However, in atomically thin graphene electronic properties can also be engineered through its coupling to the substrate because its electron waves are completely exposed and the inter-molecular electronic coupling becomes important. One unique combination is graphene on boron nitride, where both materials are atomically smooth and their quantum coupling leads to emerging phenomena from Van Hove singularity to Hofstadter butterfly.

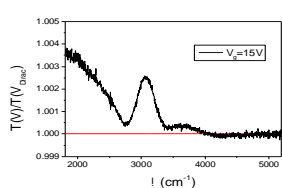


Fig. 3: IR transmission through gated graphene/BN heterostructure (normalized by the CNP) shows a new resonance peak.

The modified bandstructure of graphene on BN also leads to new optical phenomena. Figure 3 shows our preliminary data on gate-dependent optical absorption in a graphene/BN heterostructure. Unlike pristine graphene which is absent of any resonances in infrared frequencies, a clear absorption peak emerges at $\sim 3000 \text{ cm}^{-1}$ in the graphene/BN heterostructure. This absorption resonance is a signature of the modified electronic structure in graphene, and provides valuable information on the van der Waals coupling between the incommensurate graphene and boron nitride lattices.

Future Plans

(1) Resonantly enhanced light-matter interaction in hybrid graphene-nanophotonic structures

Light-matter interaction in graphene is greatly enhanced when it is coupled to nanophotonic structures, which leads to large modulation of optical signals even through a suspended monolayer graphene absorbs only 2.5% of light. I plan to explore new optical phenomena that are enabled by such enhanced light-matter interaction, including (a) power-efficient and high-speed electrical modulation of light in hybrid graphene-PhC structures and (b) strongly nonlinear optical response of graphene in hybrid graphene-plasmonic metamaterial structures.

(2) Ultrafast dynamics in monolayer and bilayer graphene

Based on improved understanding of hot carrier response, I plan to further investigate ultrafast dynamics in monolayer and bilayer graphene. In particular, bilayer graphene provides a unique system with a continuously variable semiconductor bandgap. I will focus on valley-related physics in bilayer graphene. It was predicted that K and K' valley of a finite-bandgap bilayer graphene will couple to different circularly polarized light. Ultrafast optical spectroscopy will allow us to create a finite valley polarization using circularly polarized light. It offers a unique opportunity for exploring both the dynamic evolution of the valley polarization as well as electrical transport associated with valley electrons such as valley Hall effect.

(3) Band-structure engineering with graphene heterostructures

I plan to investigate in detail electronic structure and optical responses in graphene/BN heterostructure arising from the incommeasurable van der Waals coupling. I will also examine the effects of electrical gating and many body interactions on the fine structure of optical absorption.

I also plan to explore other heterostructures composed of graphene. Two examples are 2D substrates with charge density waves below graphene and self-assembled molecules adsorbed on graphene. In both case a periodic modulation of potential will be imposed on graphene, forming a graphene superlattice structure without breaking any graphene chemical bond. It can lead to new ways to engineer the graphene electronic structure.

References:

1. F. Wang, Y. Zhang, C.S. Tian, C. Girit, A. Zettl, M.F. Crommie, Y.R. Shen, “*Gate-Variabe Optical Transitions in Graphene*”, Science, 320,206 (2008)
2. Ming Liu, Xiaobo Ying, Erick Ulin-Avila, Baisong Geng, Thomas Zentgraf, Long Ju, Feng Wang*, and Xiang Zhang*, “A graphene-based Broadband Optical Modulator”, Nature, 474, 64, (2011)
3. Y. Zhang, T.T. Tang, C. Girit, Z. Hao, M.C. Martin, A. Zettl, M.F. Crommie, Y.R. Shen and F. Wang, “*Direct Observation of a Widely Tunable Bandgap in Bilayer Graphene*”, Nature, 459, 820 (2009)
4. J. Kim, H. Son, D. Cho, B. Geng, W. Regan, S. Shi, K. Kim, A. Zettl, Y.R. Shen, and F. Wang, “Electrical Control of Optical Plasmon Resonance with Graphene”, Nano Lett., 12, 5598-5602 (2012)
5. A. Majumdar, J. Kim, J. Vuckovic, and F. Wang, “Electrical Control of Silicon Photonic Crystal Cavity by Graphene”, Nano Lett. 13, 515-518 (2013)

Publiations in the last two years:

1. J. Long, B. Beng, J. Horng, C. Girit, M. Martin, Z. Hao, H.A. Bechtel, X.G. Liang, A. Zettl, Y.R. Shen, F. Wang, “Graphene Plasmonics for Tunable Terahertz Metamaterials”, Nature Nanotech, 6, 630, (2011)
2. W. Regan, S. Byrnes, W. Gannett, O. Ergen, O. Vazquez-Mena, F. Wang, and A. Zettl, “Screening-Engineered Field Effect Solar Cells”, Nano Lett. 12, 4300 (2012)
3. Xiaoping Hong, Xinglai Shen, Mali Gong, and Feng Wang, “Broadly Tunable Mode-Hop-Free Mid-infrared Light Source with MgO:PPLN Continuous-Wave Optical Parametric Oscillator”, Optics Lett, 37, 4982 (2012)
4. Shiwei Wu, Weitao Liu, Xiaogan Liang, P. James Schuck, Feng Wang, Y. Ron Shen, and Miquel Salmeron, “Hot Phonon Dynamics in Graphene”, Nano Lett, 12, 5495-5499 (2012)
5. J. Kim, H. Son, D. Cho, B. Geng, W. Regan, S. Shi, K. Kim, A. Zettl, Y.R. Shen, and F. Wang, “Electrical Control of Optical Plasmon Resonance with Graphene”, Nano Lett., 12, 5598-5602 (2012)
6. A. Majumdar, J. Kim, J. Vuckovic, and F. Wang, “Electrical Control of Silicon Photonic Crystal Cavity by Graphene”, Nano Lett. 13, 515-518 (2013)

Project Title: Infrared Optical Study of Graphene in High Magnetic Fields

Principal Investigator: Dmitry Smirnov; Co-PI: Zhigang Jiang

Address: National High Magnetic Field Laboratory, Tallahassee, FL 32312

Email: smirnov@magnet.fsu.edu

Program Scope

The program focuses on magneto-optical study of graphene and its nanostructures, and on related Dirac-like or atomically thin 2D materials. Using a variety of optical techniques including infrared (IR) and Raman spectroscopies, the program aims at fundamental understanding of the electronic structure, low-energy excitations, and many-body effects in graphene and graphene inspired materials.

Recent Progress

1) Magneto-plasmons in quasi-neutral epitaxial graphene nanoribbons

Graphene plasmons are collective oscillations of Dirac fermions enabling strong enhancement of light-matter interaction. Multilayer epitaxial graphene (MEG) grown on the C-face of SiC is an ideal system for studying magneto-plasmons: (i) graphene nanoribbons (GNRs) can be patterned in a large area, leading to greater light-graphene coupling; (ii) the top layers of graphene formed on the C-face are quasi-charge-neutral, and behave like isolated monolayers; (iii) high mobility can be achieved in top layers even after ribbon patterning.

We fabricated large-scale epitaxial GNRs with various widths and studied the electrodynamic response in a magnetic field. We show that large- q graphene plasmons couple with the cyclotron

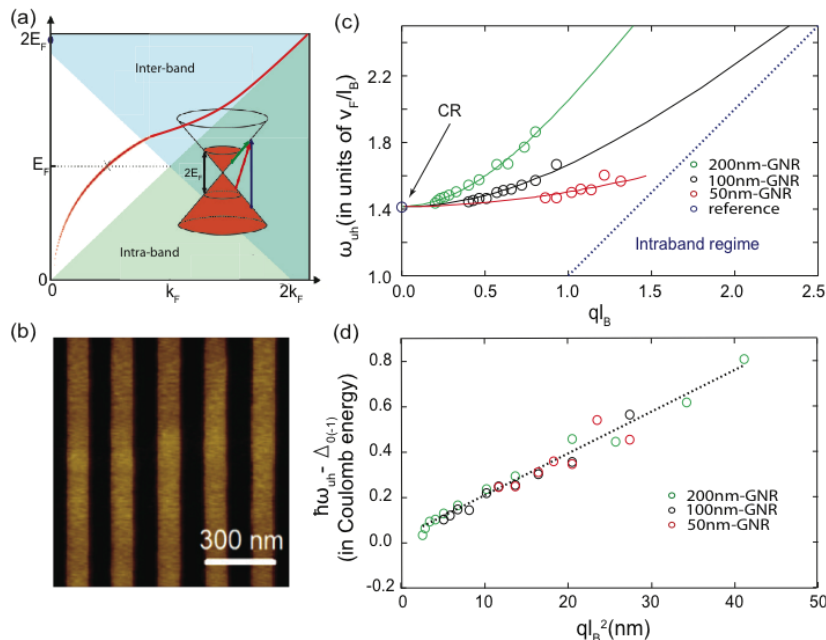


Fig. 1. Magneto-plasmons in GNRs [1]. (a) Plasmon dispersion in graphene. The plasmon is not damped in the white region. Once entering the inter-band scattering area (light blue), the plasmon lifetime is reduced by electron-hole pair formation. (b) AFM image of a 100nm-wide GNR sample. (c,d) Dispersion of the UHM as a function of ql_B^n . For quasi-neutral GNRs in the quantum regime, the energy of the UHM is blueshifted with respect to the CR of 2D graphene. The energy shift scales with ql_B^2 .

resonance (CR) modes forming an upper-hybrid mode (UHM). The resulting energy shift follows a peculiar scaling law, which distinguishes it from the UHM in conventional 2D electron systems and in highly doped graphene. Furthermore, we observe a wavelength shrinkage of ~ 165 , a value difficult to achieve in common plasmonic materials but in agreement with that predicted for graphene. See Ref. [1] for details.

2) Electron-phonon coupling in graphite: magneto-phonon resonance effects

We employed IR and Raman magneto-spectroscopy to explore electron-phonon coupling (EPC) in graphite. Besides graphite's unusual electronic structure which can be viewed as a combination of single- and bi-layer graphene like dispersion, its optical phonons strongly interact with the charge carriers (as that in graphene). In the presence of a strong magnetic field, a prominent manifestation of EPC is the magneto-phonon resonance (MPR) that occurs when the optical phonon energy matches the separation of two Landau levels (LLs). The MPR effect in graphene can be described as a resonant mixing of electronic and lattice excitations into a combined mode, leading to a splitting proportional to the EPC strength.

We observed that the E_{2g} phonon Raman line (G peak) shifts and splits as a function of magnetic field. This complex behavior is explained as MPRs caused by coupling of the E_{2g} phonons to both H -point (graphene like) and K -point (bilayer graphene like) inter-LL excitations. By investigating the field dependence of the MPR splitting and line broadening, we extracted EPC strength for K - and H -point carriers as well as E_{2g} phonon lifetime. See Ref. [2] for details. We also observed a series of purely electronic Raman excitations (i.e. emission of electron-hole pairs instead of phonons) which exhibit strongly temperature-dependent, asymmetric lineshape. The microscopic model developed in collaboration with A. Imambekov and J. Kono (Rice Univ.) shows that electron-electron interactions explain the observed results, through the 'shake-up' process known in the problem of X-ray (or Fermi-edge) singularities. See Ref. [4] for details.

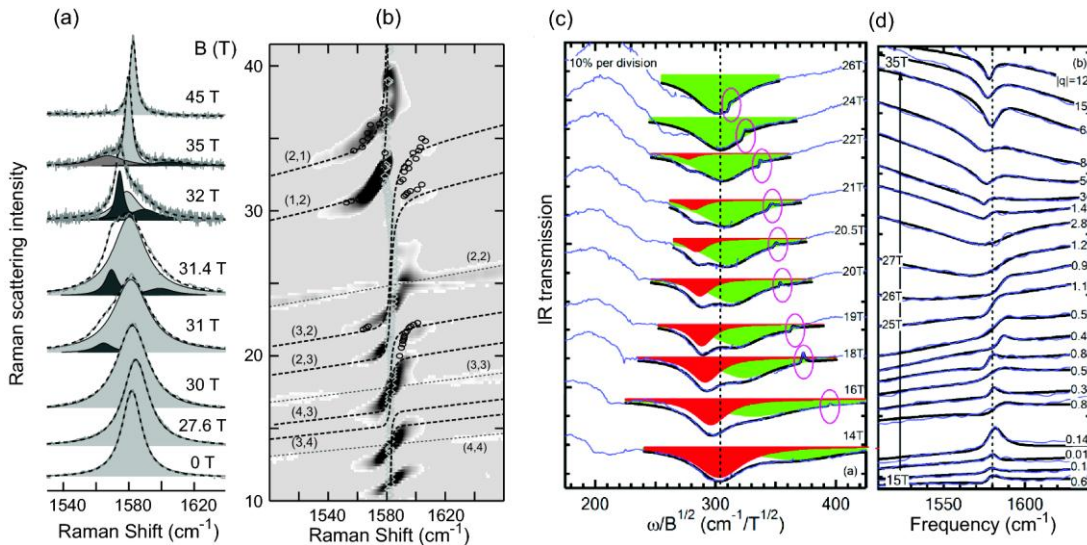


Fig. 2. MPRs in graphite probed by Raman (a,b) and IR (c,d) magneto-spectroscopy. (a) MPR structure of Raman G peak of graphite measured at different magnetic fields. (b) Second derivative Raman intensity map. Dash lines are calculated energies of coupled electron-phonon modes involving E_{2g} phonons. (c) Normalized IR magneto-transmission spectra of thin graphite flakes as a function of the scaled frequency near the MPR associated with K -point optical phonons. Vertical dash line represents the expected position of the H -point $-1 \rightarrow 0$ inter-LL transition in the absence of electron-phonon coupling. Colored Lorentzian lineshape illustrates the evolution of electron-phonon coupled modes. (d) Normalized IR magneto-transmission spectra near the $I-E_{1u}$ phonon energy (vertical dash line).

Using IR magneto-spectroscopy, we studied the EPC effects in graphite involving other optical phonon modes that were not probed with Raman scattering technique, namely the zone-boundary $K-A'_1$ phonons and the zone-center $\Gamma-E_{1u}$ phonons. In particular, we observed an anti-crossing splitting of the CR at ~ 19 T, when the $-1 \rightarrow 0$ inter-LL transition of the H -point carriers crosses the $K-\square_1'$ phonon mode. The magnitude of this splitting provides a direct measure of the effective EPC strength. In addition, we find a Fano resonance like behavior near the $\Gamma-E_{1u}$ phonon energy with asymmetric lineshape, which evolves from anti-resonance (enhanced transmission) to resonance (absorption), as the H -point $-1 \rightarrow 0$ transition is tuned to cross the energy of the $\Gamma-E_{1u}$ phonon mode.

3) Electron-phonon coupling in graphene: filling-factor- and polarization-dependent magneto-phonon resonances

A specific feature of MPR in graphene is the filling factor and polarization dependence of the anti-crossing fine structure of coupled electron and phonon modes. We performed polarization-resolved Raman spectroscopy on CVD-grown graphene in magnetic fields up to 45 T, demonstrating a strong dependence of the MPR lineshape on the Raman polarization and carrier density. By varying the carrier density via chemical doping, we identified different types of G peak magnetic-field dependencies, providing a comprehensive experimental evidence of MPRs on circularly polarized phonons. The deduced value of EPC strength is in a remarkable agreement with theoretical predictions. Also, we observed an unexpected increase of Raman intensity in the middle of the MPR anti-crossing gap. This observation is explained as a specific signature of MPR in strained graphene, reflecting mixing of electron-phonon coupled modes, caused by fluctuations of strain-induced pseudo-magnetic fields. See Ref. [3] for details.

Future Plans

- Magneto-plasmons in graphene nano-structures in the quantum regime. We plan to investigate further the IR plasmonic response in quasi-neutral epitaxial graphene nano-

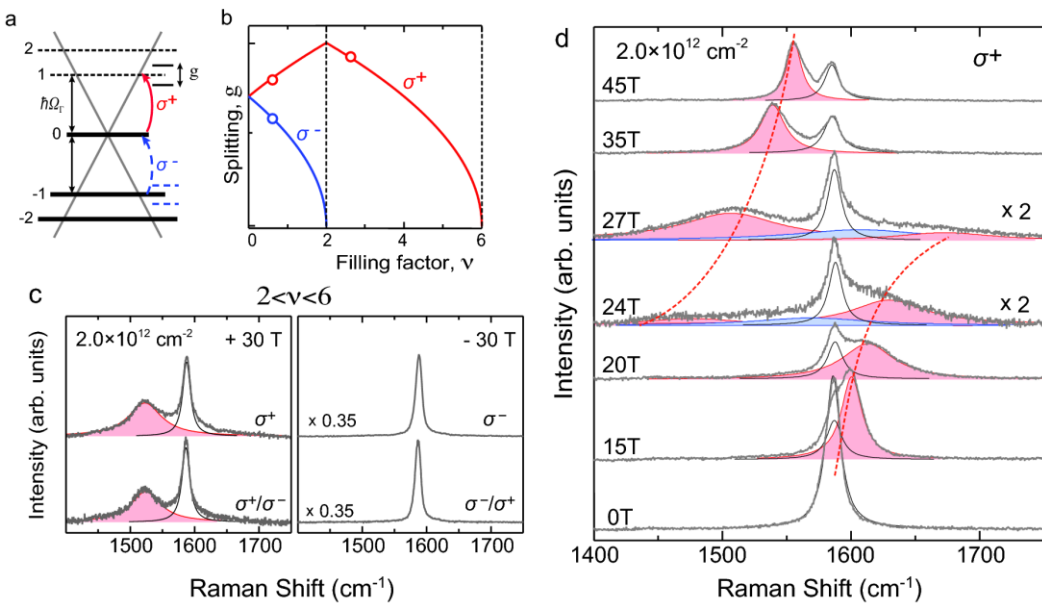


Fig. 3. (a) MPR mode splitting ensues in the vicinity of the resonance between the $0 \rightarrow 1$ electron-hole excitations and the E_{2g} phonons, for $B_{MPR} \sim 25\text{--}30$ T. (b) Calculated mode splitting, g , as a function of filling factor, v . Open circles indicate the filling factors probed in our experiment. (c,d) Circular-polarized magneto-Raman spectra at $2 < v < 6$. Dash lines are guides to the eye for the B dependence of electron-phonon coupled modes at the $0 \rightarrow 1$ MPR anti-crossing.

structures such as nanoribbons and nanodisks. High-density nanodisk arrays will also be utilized to study the effects of plasmon cross-talk, i.e., plasmon energy interchange between adjacent nano-structures.

- Magneto-Raman spectroscopy of gated graphene structures. Gated 1-, 2-, 3- or more layered graphene devices have shown exotic electronic transport properties. We plan to use polarization-resolved micro-Raman spectroscopy and continuous gate tuning to probe electronic structure, electron-phonon and electron-electron interactions in high-mobility samples in the quantum Hall regime.
- Magneto-optical study of WSe₂ field-effect-transistors (FETs). Transition metal dichalcogenides of TX₂ type (T: Mo, W, etc.; X: S, Se, Te, etc.) exhibit a wide range of electronic, optical, mechanical, chemical, and thermal properties. We plan to employ Raman and photoconductivity spectroscopy to characterize WSe₂ FETs as a function of the gate voltage and the number of layers and probe potential spin-valley coupling effects.

To reflect the program's expansion, for the next funding cycle we propose to change the project title to "*Magneto-optical study of correlated electron materials in high magnetic fields*".

Publications (2011-2013)

1. J. M. Poumirol, W. Yu, X. Chen, C. Berger, W. A. De Heer, M. L. Smith, T. Ohta, W. Pan, M. O. Goerbig, D. Smirnov, and Z. Jiang, "*Magnetoplasmons in Quasi-Neutral Epitaxial Graphene Nanoribbons*," Phys. Rev. Lett. **110**, 246803 (2013).
2. Y. Kim, Y. Ma, A. Imambekov, N. G. Kalugin, A. Lombardo, A. C. Ferrari, J. Kono, and D. Smirnov, "*Magnetophonon Resonance in Graphite: High-Field Raman Measurements and Electron-Phonon Coupling Contributions*," Physical Review B **85**, 121403(R) (2012).
3. Y. Kim, J. M. Poumirol, A. Lombardo, N. G. Kalugin, T. Georgiou, Y. J. Kim, K. S. Novoselov, A. C. Ferrari, J. Kono, O. Kashuba, V. I. Fal'ko, and D. Smirnov, "*Measurement of Filling-Factor-Dependent Magnetophonon Resonances in Graphene Using Raman Spectroscopy*," Phys. Rev. Lett. **110**, 227402 (2013).
4. Y. Ma, Y. Kim, N. G. Kalugin, A. Lombardo, A. C. Ferrari, J. Kono, A. Imambekov, and D. Smirnov, "*Effects of Electron-Electron Interactions on Electronic Raman Scattering of Graphite in High Magnetic Fields*," submitted to Phys. Rev. Lett. (arXiv:1304.5415).
5. L. C. Tung, P. Cadden-Zimansky, J. Qi, Z. Jiang, and D. Smirnov, "*Measurement of Graphite Tight-Binding Parameters Using High-Field Magnetoreflectance*," Physical Review B **84**, 153405 (2011).
6. Y. Kim, X. Chen, Z. Wang, J. Shi, I. Miotkowski, Y. P. Chen, P. A. Sharma, A. L. L. Sharma, M. A. Hekmaty, Z. Jiang, and D. Smirnov, "*Temperature Dependence of Raman-Active Optical Phonons in Bi₂Se₃ and Sb₂Te₃*," Appl. Phys. Lett. **100**, 071907 (2012).
7. M. Hajlaoui, E. Papalazarou, J. Mauchain, G. Lantz, N. Moisan, D. Boschetto, Z. Jiang, I. Miotkowski, Y. P. Chen, A. Taleb-Ibrahimi, L. Perfetti, and M. Marsi, "*Ultrafast Surface Carrier Dynamics in the Topological Insulator Bi₂Te₃*," Nano Lett. **12**, 3532 (2012).
8. X. Chen, H. D. Zhou, A. Kiswandhi, I. Miotkowski, Y. P. Chen, P. A. Sharma, A. L. L. Sharma, M. A. Hekmaty, D. Smirnov, and Z. Jiang, "*Thermal Expansion Coefficients of Bi₂Se₃ and Sb₂Te₃ Crystals from 10 K to 270 K*," Appl. Phys. Lett. **99**, 261912 (2011).

Project Title:

DE-FG02-05ER46215: Investigation of the Quantum Limit Transport Phenomena in Graphene

Principal Investigator: **Philip Kim**

Institution: Department of Physics, Columbia University

Email: pk2015@columbia.edu

Project Scope

The goal of this project is to investigate the exotic physical phenomena associated with the electron interaction in graphene. In particular, we have been focusing our research on fundamental transport properties in high quality graphene samples by probing its correlated electronic states. This effort has been greatly augmented by developing processes to yield high-mobility, homogeneous graphene and hybrid graphene structures utilizing novel substrate and dielectric engineering employing hexa boron nitride (hBN) to provide material platforms for investigations into possible emergent phenomena. The key scientific questions we are trying to address are: (i) searching for highly-correlated fractional quantum Hall effects in the extreme quantum limit; (ii) investigating excitonic correlations in double-layer graphene hybrid nanostructures; (iii) studying interaction-induced, quasi-relativistic, hydrodynamic thermoelectric transport in graphene at the quantum limit; and (iv) performing bulk magnetic moment measurements of graphene in the IQHE and FQHE regimes. Through this research effort we are seeking new insights into the unique correlated behavior of electrons in graphene. As the longer term and broader impact, we hope that the discoveries made in this project will provide the basis for making new, low-dimensional structures for electronic devices, and potentially provide insight into emergent properties that will be the basis for energy-efficient material applications.

Recent Progress

Investigation of spin and valley quantum Hall ferromagnetism in graphene: Electronic systems with multiple degenerate degrees of freedom can support a rich variety of broken symmetry states. In a graphene Landau level (LL), strong Coulomb interactions and the fourfold spin/valley degeneracy lead to an approximate SU(4) isospin symmetry. At partial filling, exchange interactions can break this symmetry, manifesting as additional Hall plateaus outside the normal integer sequence. In this period of time, we explore these unique and diverse quantum Hall ferromagnetism phenomena in different Landau levels. First, we reported on transport measurements of the insulating state that forms at the charge neutrality point of graphene in a magnetic field [1]. Using both conventional two-terminal measurements, sensitive to bulk and edge conductance, and Corbino measurements, sensitive only to the bulk conductance, we observed a vanishing conductance with increasing magnetic fields. By examining the resistance changes of this insulating state with varying perpendicular and in-plane fields, we probe the spin-active components of the excitations in total fields of up to 45 T. Our results indicate that the zero energy quantum Hall state in single layer graphene is not spin-polarized. Second, we also report the observation of a number of the quantum Hall isospin ferromagnetic (QHIFM) states in higher Landau levels, which we classify according to their real spin structure using tilted field magnetotrasport. The large activation gaps confirm the Coulomb origin of all the broken symmetry states, but the order depends strongly on LL index. In the high energy LLs, the Zeeman effect is the dominant aligning field, leading to real spin ferromagnets hosting

Skyrmionic excitations at half filling, whereas in the ‘relativistic’ zero LL, lattice scale interactions drive the system to a density wave.

Investigation of Evidence for a spin phase transition at charge neutrality in bilayer graphene: The quantum spin Hall effect is characterized by spin-polarized counter-propagating edge states. It has been predicted that this edge state configuration could occur in graphene when spin-split electron- and hole-like Landau levels are forced to cross at the edge of the sample. In particular, a quantum spin-Hall analogue has been predicted in bilayer graphene with a Landau level filling factor $v=0$ if the ground state is a spin ferromagnet. Previous studies have demonstrated that the bilayer $v=0$ state is an insulator in a perpendicular magnetic field, although the exact nature of this state has not been identified. In this period time we present measurements of the $v=0$ state in a dual-gated bilayer graphene device in a tilted magnetic field [3]. Our experiment is carried out in BLG samples with top and bottom gates in which thin single-crystal hexagonal boron nitride (hBN) serves as a high-quality dielectric on both sides. By controlling the top gate voltage and the bottom gate voltage we can adjust the carrier density and the perpendicular electric displacement field independently. Furthermore, tilting the sample in the magnetic field allows us to independently control the Coulomb energy in a Landau level. Employing this experimental setup, we can tune anisotropies and characterize the broken-symmetry quantum Hall states in the approximate SU(4) spin-pseudospin space. We map out a full phase diagram of the $v=0$ state as a function of experimentally tunable in-plane magnetic field and perpendicular electric field (Fig 1). At large in-plane magnetic field we observe a quantum phase transition to a metallic state with conductance of the order of $4e^2/h$, consistent with predictions for the ferromagnet.

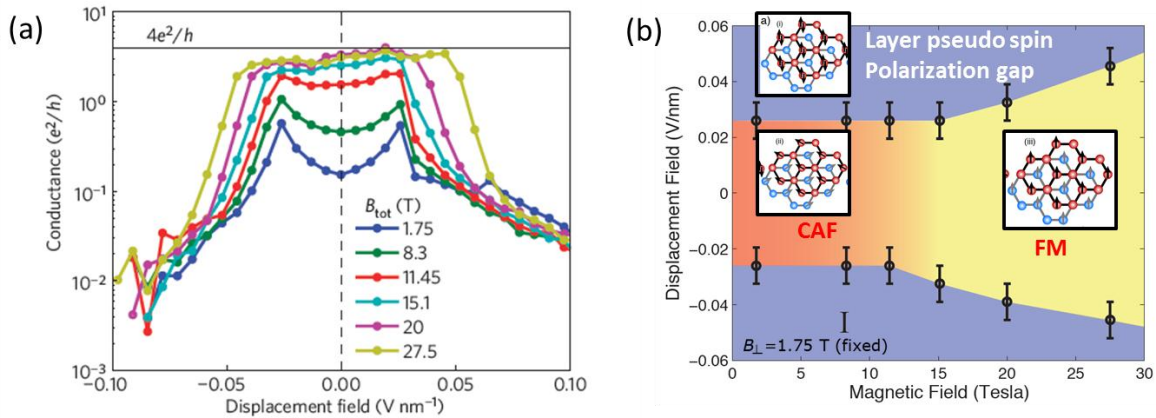


FIG. 1 (a) Four-terminal conductance at the charge neutrality point of bilayer graphene plotted against displacement field for a variety of total magnetic fields, with a fixed perpendicular magnetic field at 1.75 T. The dashed line indicates the zero displacement field points. The solid line marks the theoretically expected $4e^2/h$ conductance for the ferromagnetic phase. The data were taken at 350 mK. (b) Different phases of the $v=0$ state mapped as a function of displacement and total magnetic fields. At low magnetic field, the phase boundary between layer-polarized and canted antiferromagnetic (CAF) is determined by the conductance spike separating the two insulating phases. At large magnetic fields, the phase boundary between layer-polarized and ferromagnetic (FM) is determined by the point where conductance begins to exponentially decrease with displacement field.

Observation of Fractal quantum Hall effect showing Hofstadter’s butterfly energy spectrum in graphene and hBN moire superlattices: Electrons moving through a spatially periodic lattice potential develop a quantized energy spectrum consisting of discrete Bloch bands. In two

dimensions, electrons moving through a magnetic field also develop a quantized energy spectrum, consisting of highly degenerate Landau energy levels. In 1976 Douglas Hofstadter theoretically considered the intersection of these two problems and discovered that 2D electrons subjected to both a magnetic field and a periodic electrostatic potential exhibit a self-similar recursive energy spectrum¹. Known as Hofstadter's butterfly, this complex spectrum results from a delicate interplay between the characteristic lengths associated with the two quantizing fields, and represents one of the first quantum fractals discovered in physics. In the decades since, experimental attempts to study this expect have been limited by difficulties in reconciling the two length scales. Typical crystalline systems (< 1 nm periodicity) require impossibly large magnetic fields to reach the commensurability condition, while in artificially engineered structures (~ 100 nm), the corresponding fields are too small to completely overcome disorder. In this period of time, we demonstrate that moire superlattices arising in bilayer graphene coupled to hexagonal boron nitride provide a nearly ideal-sized periodic modulation, enabling unprecedented experimental access to the fractal spectrum [4]. We confirm that quantum Hall effect features associated with the fractal gaps are described by two integer topological quantum numbers, and report evidence of their recursive structure. Observation of Hofstadter's spectrum in graphene provides the further opportunity to investigate emergent behavior within a fractal energy landscape in a system with tunable internal degrees of freedom.

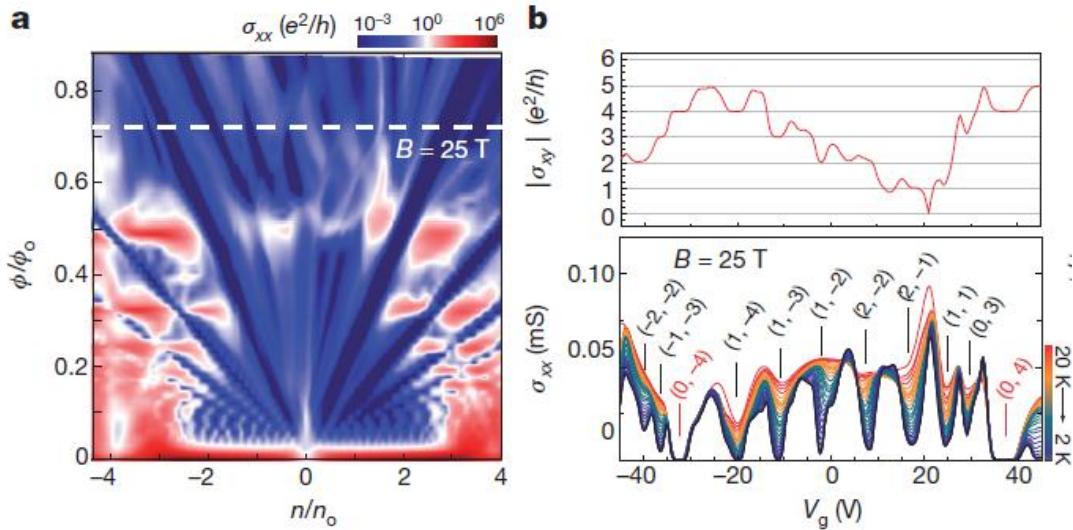


FIG. 1 (a) Landau fan diagrams measured in bilayer graphene on hBN with Moire superlattice with the unit cell dimension 11.6 nm. (b) Bottom: the evolution of magnetoconductivity with temperature varying between 2 and 20 K, acquired at constant magnetic field which corresponds to the line cut shown in (a). Top: the corresponding Hall conductivity at 5.2 K. The bracketed numbers label the two integer numbers (s, t) values of the corresponding fractal gaps according to the Diophantine equation.

Future Plan

Building on the successful progress described in the previous section, we plan to focus our interest on *investigation of the role of electron interactions in graphene* as described below:

Electric field tunable fractional quantum Hall effect in bilayer: The integration of bilayer graphene with the top and bottom gate electrode with hBN as gate dielectric allows to probe extremely high mobility bilayer graphene samples that can be tuned by vertical electric fields.

Bilayer graphene affords an even richer electronic system for the study of correlated quantum Hall effects, governed by the so-called Haldane pseudopotentials, which describe effective electronic interactions within a single Landau level. This unique feature allows us engineering of correlated electron states. We will explore the FQHE physic in bilayer graphene with full control of both the spin sector, through the Zeeman effect, and the valley sector, where the splitting is controlled by the applied out of plane electric field.

Electron correlation in double layer graphene nanostructures: Our recently demonstrated ability to transfer graphene without degradation of sample quality, together with high-quality BN, a complimentary wide band gap dielectric, opens the possibility of realizing novel graphene-based device architectures by alternately stacking the two materials. We will explore the Coulomb drag measurement in double layer grpahene/hBN/graphene heterostructures where we should probe the electron correlation across the two graphene layers electrically separated but correlated via Coulomb interaction.

Thermodynamic Self-Measurement in suspended graphene: Thermodynamic bulk probes of the QHE, such as magnetization, provide complementary information to that obtained from transport measurements. Exploiting the mechanical stability of graphene, we will develop a novel tool for measuring magnetization in graphene using a suspended sample as its own torque magnetometer. Atomically thin materials, with extremely small mass and high mechanical strength, offer a unique opportunity to build electro-magneto-mechanical devices, where new forms of coupling emerge between mechanical degrees of freedom to measure the chemical potential. We use a graphene mechanical resonator, via a novel coupling to electric and magnetic fields, and will porbe chemical potential and electronic compressibility by measuring the modulation of mechanical resonance frequency.

Interaction induced thermoelectric transport in graphene: Inheriting our successful demonstration of thermopower (TEP) and magneto-thermopower (MTEP) measurement in graphene, we plan to use TEP and MTEP measurement to probe the e-e interactions in high quality graphene samples with reduced disorder. This includes the the electron-hole plasma at high temperatures, which is described by hydrodynamics, and MTEP in the FQH regime.

Publications acknowledged the current DOE grant

- [1] Y. Zhao, P. Cadden-Zimansky, F. Ghahari, and P. Kim, “Magnetoresistance Measurements of Graphene at the Charge Neutrality Point,” Phys. Rev. Lett. **108**, 106804 (2012)
- [2] A. F. Young, C. R. Dean, L. Wang, H. Ren, P. Cadden-Zimansky, K. Watanabe, T. Taniguchi, J. Hone, K.L. Shepard, and P. Kim, “Spin and valley quantum Hall ferromagnetism in graphene,” Nature Physics, **8**, 553-556 (2012).
- [3] P. Maher, C. R. Dean, A. F. Young, T. Taniguchi, K. Watanabe, K. L. Shepard, J. Hone, and P. Kim, “Evidence for a spin phase transition at charge neutrality in bilayer graphene,” Nature Physics, **9**, 154-158 (2013)
- [4] C. R. Dean, L. Wang, P. Maher, C. Forsythe, F. Ghahari, Y. Gao, J. Katoch, M. Ishigami, P. Moon, M. Koshino, T. Taniguchi, K. Watanabe, K. L. Shepard, J. Hone, and P. Kim, “Hofstadter's butterfly in moire superlattices: A fractal quantum Hall effect,” Nature, **497**, 598-602 (2013).

Session 6

Electronic and Optical Properties of Novel semiconductors for Energy Applications

Principal Investigator: Angelo Mascarenhas

Mailing Address: National Renewal Energy Lab., Golden CO 80401

E-mail: angelo.mascarenhas@nrel.gov

Program Scope

Advanced energy technologies require high-performance materials, which in photovoltaics translates to new semiconductors to efficiently absorb sunlight, and in solid-state lighting(SSL), to new materials for direct conversion of electricity to white light. A goal of this project is fundamental materials research for the realization of semiconductors that transcend the existing limitations constraining present photovoltaic and solid-state lighting technologies. It specifically addresses the current unavailability of efficient high bandgap (2.1 eV) and low bandgap (1 eV) absorbers for photovoltaics, and efficient amber emitters for SSL, via technologies based on GaAs substrates. The key to transcending the present limitations is the understanding and control of fundamental electronic and optical processes in these materials. The project focuses on understanding the abnormal electronic structure and properties of isoelectronic dopants N and Bi in GaAs, and on the effects of spontaneous ordering on the band alignments in $\text{Al}_{1-x}\text{In}_x\text{P}$. Additionally, it addresses recent observations of new excitations in photogenerated bipolar plasmon gasses in semiconductors, with the goal of understanding these collective phenomena that could enable semiconductor alloys with novel, useful properties. The project combines growth, spectroscopy, and theory, and utilizes the user facilities at the CINT and the NHFML.

Recent Progress

1)The highest efficiency PV devices require materials for sub-cells with carefully selected bandgaps, that are lattice matched to Ge substrates. The ideal material for the middle sub-cell that meets both of these requirements is dilute $\text{GaAs}_{1-x}\text{N}_x$ ($x < 0.03$). However, the presence of N introduces electron traps that degrade the electrical properties of this material. By using magnetic fields up to 57 T (see Fig.1), we were able to controllably tailor the overlap of these trap states to tune carrier localization. The information provided by these measurements yields new understanding of how N clusters and superclusters degrade the carrier transport and suggest pathways for remediating the deleterious effects.

2) The signature of abnormalities in the light-scattering response of the dilute nitride alloy $\text{GaAs}_{1-x}\text{N}_x$ is contained in an asymmetric lineshape (Fig. 2) that arises due to a Fano interference phenomenon. E_w and $E_{w'}$ are the energies of a double resonance observed for the asymmetric lineshape in resonant Raman scattering studies on this material, and are associated with Nitrogen induced perturbations of the L-pont bandstructure. We observed that a discontinuity of E_w occurs precisely at the percolation threshold of $\text{GaAs}_{1-x}\text{N}_x$, showing that this technique can thus be

used to probe the evolution of the electronic structure of abnormal alloys.

3) We developed a new photoluminescence (PL) imaging technique to identify how photogenerated carriers interact with defects in polycrystalline semiconductors. Imaging poly-CdTe films showed that bound excitons recombine over very short distances, but networks of deep acceptor states enable carrier diffusion up to 10 μm from the point of photogeneration. The results provide clues to the fundamental reasons underlying low open circuit voltages in CdTe solar cells.

4) Using the precisely calibrated growth facilities at the CINT (Sandia), we able to grow samples at NREL so close to the Γ -X cross-over in $\text{Al}_x\text{Ga}_{1-x}\text{As}$ that it was possible to simultaneous optical transitions from both the Γ and X conduction bands. Knowing the precise value of x_c is crucial to realizing a Bragg mirror for electrons.

5) $\text{Al}_x\text{In}_{1-x}\text{P}$ is the ideal material for amber LEDs. Improved performance would enable highly efficient color-mixing red/amber/green/blue lamp designs that avoid the use of phosphors for solid state lighting applications. We have demonstrated that direct bandgap $\text{Al}_x\text{In}_{1-x}\text{P}$ can be grown metamorphically on GaAs substrates with low ($< 10^{-5} \text{ cm}^{-2}$) threading dislocation densities using the step-grading approach and have determined the precise direct-indirect crossover of $\text{Al}_x\text{In}_{1-x}\text{P}$. CuPt-type ordering shifts the bandgap as much as 250 meV. The ability to control spontaneous ordering in this alloy will thus make it possible to synthesize cladding layers for electrons in $\text{Al}_x\text{In}_{1-x}\text{P}$ and thus enable amber LEDs for solid-state lighting applications.

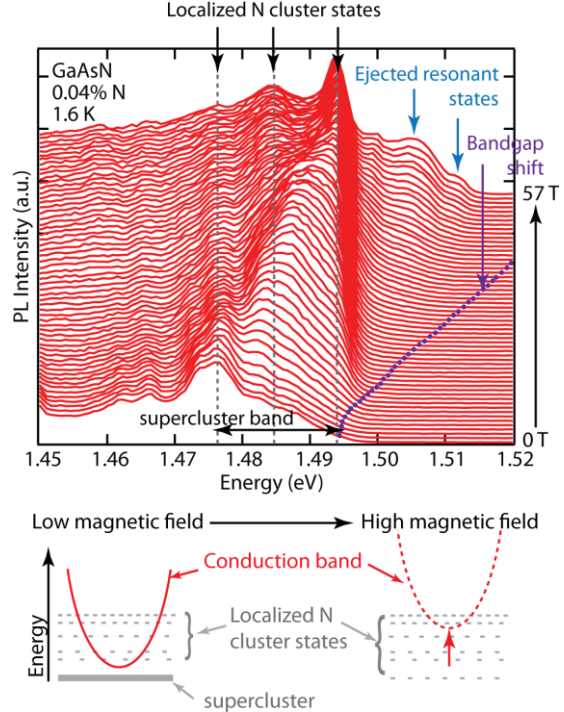


Fig. 1 The percolation of N superclusters is reversed under high magnetic fields, providing insight into how they form.

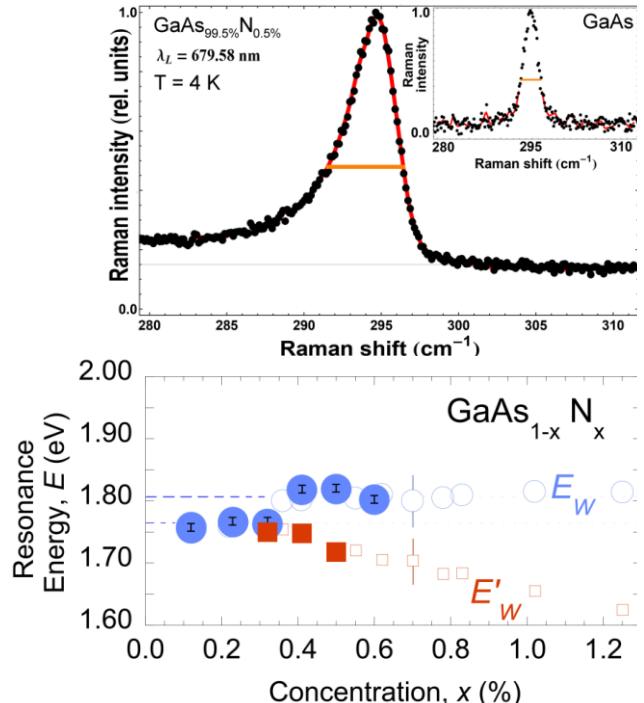


Fig. 2
Top: Assymmetric Fano lineshape of LO phonon
Bottom: Abrupt drop in E_W at the percolation threshold

Future Plans

High-magnetic fields will be used to probe the localized-delocalized transition in dilute GaP:N. The electronic properties of GaP:Bi will be explored using samples grown in a new Laser assisted MBE machine. The properties of isoelectronically co-doped GaAs and GaP with both nitrogen and Bismuth will be explored, (new samples grown by new laser assisted MBE). A time resolved PL imaging technique will be developed. The investigation on new excitations in photogenerated plasmon gasses in dilute GaAs:N will be continued. The ability for very high speed frequency modulation using a plasmon gas is being explored. The possibility of synthesizing an electron Bragg reflector using AlGaAs is currently being explored.

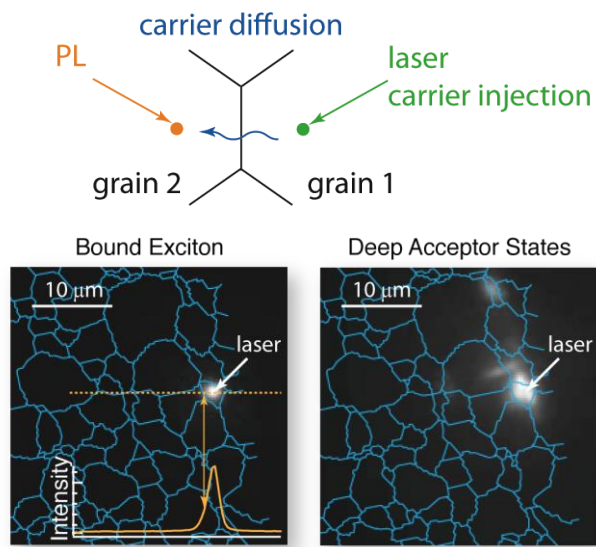


Fig. 3 Injecting carriers into one grain and observing PL from an adjacent grain indicates diffusion across the grain boundary (upper schematic). Images of bound exciton (lower left) and conduction band to acceptor state (lower right) PL in poly-CdTe reveal how grain boundary and impurity states affect carrier transport.

Publications since 2012.

1. “Magnetic field-induced delocalized to localized transformation in GaAs:N”, K. Alberi, S.A. Crooker, B. Fluegel, D.A. Beaton, A.J. Ptak, A. Mascarenhas. *Phys. Rev. Lett.* **110**, 156405 (2013).
2. “Raman Scattering Signature of a Localized-to-Delocalized Transition at the Inception of a Dilute Abnormal $\text{GaAs}_{1-x}\text{N}_x$ Alloy”, A.V. Mialitsin and A. Mascarenhas. *Appl. Phys. Express* **6**, 052401 (2013).
3. “Long-Range Carrier Diffusion across Multiple Grains in Polycrystalline Photovoltaics”, K. Alberi, B. Fluegel, R. Dhere, S.A. Crooker, and A. Mascarenhas, *accepted Nature Communications*. (2013).
4. “Growth, microstructure, and luminescent properties of direct-bandgap InAlP on relaxed InGaAs on GaAs substrates”, K. Mukherjee, D.A. Beaton, T. Christian, E.J. Jones, K. Alberi, A. Mascarenhas, M.T. Bulsara, E.A. Fitzgerald. *J. Appl. Phys.* **113**, 1183518 (2013).

5. “Precise Determination of the direct-indirect bandgap energy cross-over composition in $\text{Al}_x\text{Ga}_{1-x}\text{As}$ ”, D.A. Beaton, B. Fluegel, K. Alberi, A. Mascarenhas and J.L. Reno, *Appl. Phys. Express* **6**, 071201 (2013).
6. T. Christian, D.A. Beaton, K. Mukherjee, K. Alberi, E.A. Fitzgerald and A. Mascarenhas, accepted in *J. Appl. Phys.* (2013)
7. “Evolution of superclusters and delocalized states in GaAsN”, B. Fluegel, K. Alberi, D.A. Beaton, S.A. Crooker, A.J. Ptak, A. Mascarenhas, *Phys. Rev. B* **86**, 205203 (Nov 2012).
8. “Determination of the Direct to Indirect Bandgap Composition in $\text{Al}_y\text{In}_{1-y}\text{P}$ ”, D. A. Beaton, T. Christian, K. Alberi, and A. Mascarenhas, *Appl. Phys. Express* **114**, 074505 (2013).
9. “Evolution of superclusters and delocalized states in GaAsN”, B. Fluegel, K. Alberi, D.A. Beaton, S.A. Crooker, A.J. Ptak, A. Mascarenhas, , *Phys. Rev. B* **86**, 205203 (2012)..
10. “Localization-delocalization transition of electrons at the percolation threshold of semiconductor GaAsN alloys: the appearance of a mobility edge”, K. Alberi, B. Fluegel, D.A. Beaton, A.J. Ptak, A. Mascarenhas, *Phys. Rev. B (Rapid Comm.)* **86**, 041201 (2012).
11. “Shubnikov-de Haas measurement of electron effective mass in $\text{GaAs}_{1-x}\text{Bi}_x$ ” B. Fluegel, R. N. Kini, A. J. Ptak, D. Beaton, K. Alberi, A. Mascarenhas, *Appl. Phys. Lett.* **99**, 162108 (2012).
12. “Mechanism of asymmetric lineshape broadening in $\text{GaAs}_{1-x}\text{Nx}$ Raman spectra”, Aleksej Mialitsin, Brian Fluegel, Aaron Ptak, and Angelo Mascarenhas, *Phys. Rev. B* **86**, 045209 (2012).
13. “Eigenstate localization in an asymmetric coupled quantum well pair”, A. Mialitsin, S. Schmult, I. A. Solov'yov, B. Fluegel, and A. Mascarenhas, *Superlattices and Microstructures* **51**, 834 (2012).
14. “Quaternary bismide alloy BGaAsBi lattice matched to GaAs”, D.A. Beaton, A.J. Ptak, K. Alberi, A. Mascarenhas, *J. Crystal Growth*, **351**, 37 (2012).
15. “Growth of BGaAs by molecular-beam epitaxy and the effects of a bismuth surfactant”, A. Ptak, D. Beaton, and A. Mascarenhas *J. Cryst. Growth* **351**, 122 (2012).
16. “Elemental and magnetic sensitive imaging using x-ray excited luminescence microscopy”. R. A. Rosenberg, S. Zohar, D. Keavney, R. Divan, D. Rosenmann, A. Mascarenhas, and M. A. Steiner, *Rev. of Scientific Instr.* **83**, 073701 (2012).
17. “Kinetically limited growth of GaAsBi by molecular beam epitaxy”, A.J. Ptak, R. France, D.A. Beaton, K. Alberi, J. Simon, A. Mascarenhas, *J. Crystal Growth* **338**, 107 (2012).

Photonic Systems

Joseph Shinar, Kai-Ming Ho, Costas Soukoulis, Rana Biswas, and Viatcheslav Dobrovitski

Ames Laboratory – USDOE and Physics & Astronomy Dept, Iowa State University

Program Scope

This effort was created to address outstanding DOE challenges in efficient energy conversion and utilization through fundamental studies of photonic materials, structures, and devices. These include photonic crystals (PCs), organic semiconductors, organic light emitting diodes (OLEDs), and, in particular, novel systems combining these three.

PCs,^{1,2} or artificial periodic dielectric or metallic structures, have revolutionized control and manipulation of photons. The diffraction of photons by PCs has opened new vistas in the control of spontaneous emission, chemical reactions, optical communications, sensing, energy-efficient lighting, solar-energy utilization, and displays.^{3,4} In particular, new photonic materials, structures, and devices may improve solar cells and light emitting systems dramatically.

The knowledge gained from our previous studies of woodpile PCs,⁵⁻⁷ optically and electrically detected magnetic resonance (ODMR and EDMR, respectively)⁸⁻¹³ and other studies of organic semiconductors, OLEDs, and OLED-based sensors,¹⁴⁻¹⁸ and theoretical quantum dynamics and control of spins studies, form the basis for the development of photonic structures and devices with novel properties not found in naturally occurring materials. For example, our group pioneered the 3-dimensional (3-D) woodpile PC, from microwave to near-optical frequencies. Our patented structure has been so successful it has become the accepted standard for 3-D PCs, even at near-optical frequencies.¹⁹⁻²⁵ We also fabricated large-area woodpile PCs using a low-cost micro-transfer mold technique.²⁶ As another example, our ODMR studies highlighted quenching of singlet excitons (SEs) in OLEDs as a major cause of reduced efficiency at high brightness.⁸⁻¹³ The identification of these quenching mechanisms contributed to the development of tandem (stacked) OLED structures, which yield the most efficient OLEDs at high brightness reported to date.²⁷⁻²⁹ These, in turn, inspired the development of efficient tandem organic solar cells.³⁰⁻³³ In another example, the efforts to develop OLED-based luminescent sensors led to the incorporation of TiO₂ (nano)particles in such sensor films, which dramatically enhances their photoluminescence (PL).^{17,18} Such TiO₂-doped luminescent films could lead to random lasing at an extremely low excitation density; Soukoulis and coworkers^{34,35} have conducted extended theoretical studies of random lasing.

One outcome from this research is the creation of photonic structures with novel functionalities, e.g., increased light outcoupling from OLEDs.

Recent Progress – Highlights

1. ODMR and EDMR studies of polaron, singlet exciton (SE), and triplet exciton (TE) dynamics in luminescent π-conjugated materials and OLEDs. We published a comprehensive review of such studies (Fig. 1).¹³ These materials and devices typically exhibit both positive and negative spin 1/2 resonances due to polarons and bipolarons, respectively, and full- and half-field spin 1 TE resonances. The positive resonance is attributed to enhanced

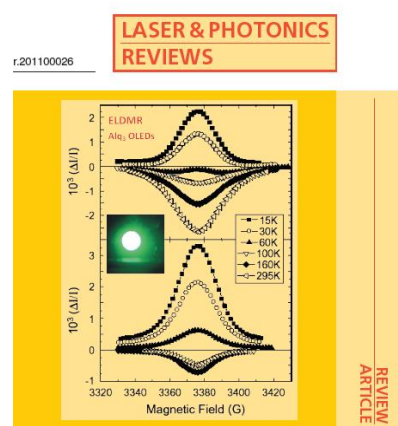


Fig. 1. Review on “Optically detected magnetic resonance studies of luminescence-quenching processes in π-conjugated materials and organic light-emitting devices.”¹⁶

quenching of TEs by polarons, which lowers the steady-state population of both species. This decreases the quenching rate of SEs by polarons and TEs, and the luminescence increases. These quenching processes are now universally recognized as responsible for the roll-off (drop) of OLED efficiency at high brightness. The negative resonance is attributed to enhanced formation of spinless bipolarons stabilized by a counterion apparently at specific sites. We are currently exploring the relationship between the behavior of these resonances, and the devices' efficiency and stability.

2. Comprehensive study of transient ns EL spikes (overshoots) in (guest-host) small molecule OLEDs, following a bias pulse, including in relatively efficient devices.³⁶ The spikes were strongly dependent on device materials, structure, temperature, etc. At low temperatures, all fluorescent devices exhibit the spikes at ~70-300 ns. At room temperature only those with a hole injection barrier, carrier-trapping guest-host emitting layer, and no strong electron-transporting and hole-blocking layer exhibit strong spikes. The results suggest that reduced electric field-induced dissociative quenching of SEs is responsible for the spikes' amplitude exceeding the on-pulse dc EL level. The spikes can serve as an important tool to identify the dominant emitting mechanisms in guest-host systems.

3. Extremely strong transient room temperature photocurrent (PC or I_{PC})-detected magnetic resonance (PCDMR) in ITO/O₂-baked poly(2-methoxy-5-(2'-ethyl)-hexoxy-1,4-phenylene vinylene) (MEH-PPV)/Al.³⁷ It is observed that $|\Delta I_{PC}/I_{PC}|$ peaks at values $\gg 1$, where ΔI_{PC} is the change in I_{PC} induced by magnetic resonance conditions (Fig. 2). Importantly, ΔI_{PC} and I_{PC} are of different origin. The mechanism most likely responsible for this effect is the spin-dependent formation of spinless bipolarons adjacent to negatively-charged deep traps, apparently induced, in particular, by oxygen centers to form triions.

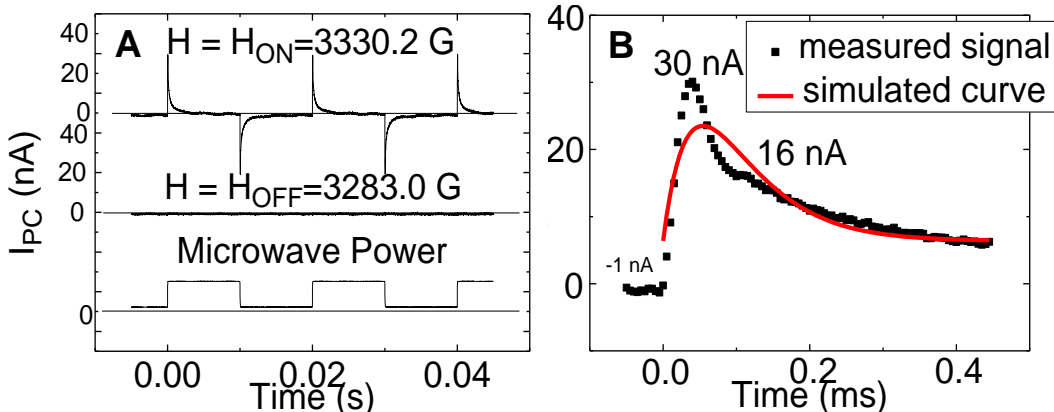


Fig. 2. Colossal spin-1/2 PCDMR in MEH-PPV single layer devices. The red line in B is the fit of the model based on bipolaron formation at negative oxygen centers

4. Extremely efficient ITO-free OLEDs.³⁸ ITO is currently the dominant transparent anode but (1) its index of refraction is high, which causes unwanted total internal reflection at the ITO/glass interface. (2) it is fragile and inflexible, (3) its surface is relatively rough, which could cause contact problems and energy loss, and (4) the supply of In is limited. In this work, we demonstrated extremely efficient ITO-free green phosphorescent OLEDs (PhOLEDs) with multilayered, highly conductive poly(3,4-ethylene dioxythiophene): poly(styrene sulfonate) (PEDOT:PSS) anodes on a glass substrate. Peak luminous efficiency $\eta_{L,max} = 127$ Cd/A, peak power efficiency $\eta_{P,max} = 118$ lm/W, and peak external quantum efficiency $\eta_{ext,max} = 40\%$ were achieved without outcoupling-enhancing structures (Fig. 3). These values are the highest among

ITO-free OLEDs and are significantly higher than those of the otherwise identical devices with ITO anodes fabricated on identical glass substrates under nominally identical conditions. Importantly, a quantitative optical simulation was developed, revealing that the optical enhancement is due mainly to a weak microcavity effect, specifically, the suppression of waveguide modes predicted in PEDOT:PSS-anode OLEDs. This work was featured in R& D Magazine.

Future Plans

We will develop PCs with new functionalities, including lasing and non-linear effects, and enhance light emission from OLEDs. We will also utilize low-cost methods to demonstrate large-area PC structures relevant to energy-related applications. The work will focus on

- (1) Studies of enhanced light emission, extraction, and carrier dynamics in light-emitting systems, utilizing novel photonic structures and top-emitting OLEDs.
- (2) Studies of OLED and OPV efficiency and stability in devices with heat-sinking components.
- (3) Quantum dynamics and control of spins in organic semiconductors.
- (4) Novel photonic structures, with surface beaming, supertransmission, and PC lasing.
- (5) Other photonic structures for energy-related applications.

References

1. E. Yablonovitch, *Phys. Rev. Lett.* **58**, 2059 (1987).
2. S. John, *Phys. Rev. Lett.* **58**, 2486 (1987).
3. C. M. Soukoulis, Editor, *Photonic Crystals and Light Localization in the 21st Century, NATO Science, Series C* **563** (Kluwer, Dordrecht, 2002).
4. J. D. Joannopoulos et al., *Photonic Crystals: Molding the Flow of Light*, Princeton University Press (Princeton, NJ, 1995).
5. K.M. Ho et al., *Solid State Comm.* **89**, 413 (1994).
6. E. Ozbay et al., *Phys. Rev. B* **50**, 1945 (1994).
7. S. Lin et al., *Nature* **394**, 251 (1998).
8. E. J. W. List et al., *Phys. Rev. B* **64**, 155204 (2001).
9. E. J. W. List et al., *Phys. Rev. B* **66**, 235203 (2002).
10. G. Li, C.-H. Kim, P. A. Lane, and J. Shinar, *Phys. Rev. B* **69**, 165311 (2004).
11. M.-K. Lee et al., *Phys. Rev. Lett.* **94**, 137403 (2005).
12. M. Segal et al., *Phys. Rev. B* **71**, 245201 (2005).
13. J. Shinar, *Laser & Photonics Reviews* **6**, 767 – 786 (2012).
14. L. Zou et al., *Appl. Phys. Lett.* **79**, 2282 (2001).
15. K. O. Cheon and J. Shinar, *Appl. Phys. Lett.* **83**, 2073 (2003).
16. G. Li and J. Shinar, *Appl. Phys. Lett.* **83**, 5359 (2003).
17. Z. Zhou, R. Shinar, A. J. Allison, and J. Shinar, *Adv. Func. Mat.* **17**, 3530 (2007).
18. J. Shinar and R. Shinar, *J. Phys. D: Appl. Phys.* **41**, 133001 (2008).
19. J. G. Fleming, S. Y. Lin, I. El-Kady, R. Biswas, and K. M. Ho, *Nature* **417**, 52 (2002).

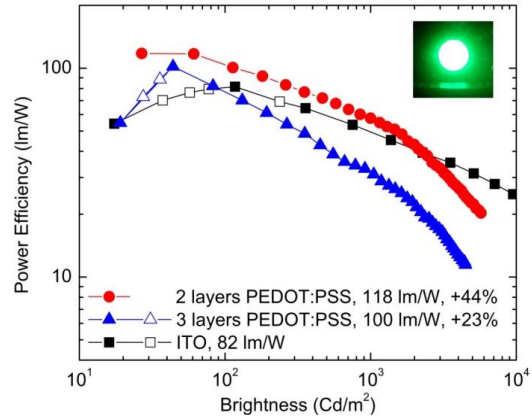


Fig. 4. Luminous power efficiency of $\text{Ir}(\text{ppy})_3$ -based green PhOLEDs fabricated on ITO and multilayered PEDOT:PSS anodes.

20. R. Biswas et al., *Photonic Band Gap Crystals*, Wiley Encyclopedia of Electrical and Electronics Engineering (John Wiley & Sons, 2007).
21. T. Katsuyama et al., *Photonics and Nanostructures* **4**, 54 (2006).
22. M. Hermatschweiler et al., *Adv. Funct. Mater.* **17**, 2273 (2007).
23. G. M. Gratson et al., *Adv. Mater.* **18**, 461 (2006).
24. N. Tétreault et al., *Adv. Mater.* **18**, 457 (2006).
25. M. Deubel et al., *Nat. Mater.* **3**, 444 (2004).
26. J.-H. Lee et al., *Appl. Phys. Lett.* **88**, 18112, (2006).
27. L. S. Liao, K. P. Klubek, and C. W. Tang, *Appl. Phys. Lett.* **84**, 167 (2004).
28. Fawen Guo and Dongge Ma, *Appl. Phys. Lett.* **87**, 173510 (2005).
29. Ting-Yi Cho, Chun-Liang Lin, and Chung-Chih Wu, *App. Phys. Lett.* **88**, 111106 (2006).
30. J. Y. Kim et al., *Science* **317**, 222 (2007).
31. D. W. Zhao et al., " *Appl. Phys. Lett.* **93**, 083305 (2008).
32. X. Guo et al., *Org. Electr.* **10**, 1174 (2009).
33. S. Sista et al., *Adv. Mat.* **21**, 1 (2009).
34. X. Jiang and C. M. Soukoulis, *Phys. Rev. Lett.* **85**, 70 (2000).
35. X. Jiang et al., *Phys. Rev. B* **69**, 104202 (2004).
36. R. Liu, Z. Gan, R. Shinar, and J. Shinar, *Phys. Rev. B* **83**, 245302 (2011).
37. Y. Chen, R. Liu, M. Cai, R. Shinar, and J. Shinar, *Phys. Rev. B* **86**, 235442 (2012).
38. M. Cai et al., *Adv. Mater.* **24**, 4337 (2012).

Selected Publications

1. Joseph Shinar, "Optically Detected Magnetic Resonance Studies of Luminescence-Quenching Processes in π -Conjugated Materials and Organic Light-Emitting Devices," *Laser & Photonics Reviews* **6**, 767 – 786 (2012). (invited review)
2. Rui Liu, Zhengqing Gan, Ruth Shinar, and Joseph Shinar, "Comprehensive Investigation of Transient Electroluminescence Spikes in Small Molecular Organic Light-Emitting Diodes," *Phys. Rev. B* **83**, 245302 (2011).
3. Ying Chen, Rui Liu, Min Cai, Ruth Shinar, and Joseph Shinar, "Extremely strong room temperature photocurrent-detected magnetic resonance in organic devices," *Phys. Rev. B* **86**, 235442 (2012).
4. Min Cai, Zhuo Ye, Teng Xiao, Rui Liu, Ying Chen, Robert W. Mayer, Rana Biswas, Kai-Ming Ho, Ruth Shinar, and Joseph Shinar, "Extremely efficient indium-tin-oxide-free green phosphorescent organic light-emitting diodes," *Adv. Mater.* **24**, 4337 – 4342 (2012).
5. Min Cai, Teng Xiao, Emily Hellerich, Ying Chen, Ruth Shinar, and Joseph Shinar, "High efficiency solution-processed small molecule electrophosphorescent organic light-emitting diodes," *Adv. Mater.* **23**, 3590–3596 (2011).
6. Joong-Mok Park, Zhengqing Gan, Wai Y. Leung, Zhuo Ye, Kristen Constant, Joseph Shinar, Ruth Shinar, and Kai-Ming Ho, "Soft lithography microlens fabrication for enhanced OLED light extraction," *Opt. Exp.* **19**, A786 – A792 (2011).
7. Rui Liu, Zhuo Ye, Joong-Mok Park, Min Cai, Ying Chen, Kai-Ming Ho, Ruth Shinar, and Joseph Shinar, "Microporous phase-separated films of polymer blends for enhanced outcoupling of light from OLEDs," *Opt. Exp.* **19**(S6), A1272 - A1280 (2011).
8. Rui Liu, Chun Xu, Rana Biswas, Joseph Shinar, and Ruth Shinar, "MoO₃ as Combined Hole Injection Layer and Tapered Spacer in Combinatorial Multicolor Microcavity Organic Light Emitting Diodes," *Appl. Phys. Lett.* **99**, 093305 (2011); *APL: Organic Electronics and Photonics* **4**, 093305 (2011)

Ultrafast Studies of Hydrogen and Related Defects in Semiconductors and Oxides

Principal Investigator: N. H. Tolk¹

Co-PIs: L. C. Feldman¹ and G. Lüpke²

¹ Department of Physics and Astronomy, Vanderbilt University, Nashville, TN

² Department of Applied Science, The College of William and Mary, Williamsburg, VA

E-mail: norman.tolk@vanderbilt.edu

Program Scope

Our research program addresses the roles of defects, interfaces, and dopants on the optical and electronic characteristics of semiconductor crystals. The primary methods in these studies are phonon generation by means of ultrafast coherent acoustic phonon (CAP) spectroscopy, nonlinear characterization using second harmonic generation (SHG), and ultrafast pump-and-probe reflectivity and absorption measurements. This program represents a broadening of our previous DOE-funded research efforts from hydrogen defects in silicon alone to other forms of defects such as interfaces and dopant layers, as well as to other important semiconducting systems. Even so, the emphasis remains on phenomena and processes far from equilibrium, such as hot electron effects and travelling localized phonon waves.

This program directly addresses two of the five grand challenges set forth by the Department of Energy: (1) to characterize and control matter away, especially very far away, from equilibrium; and ultimately (2) to design and perfect atom and energy-efficient synthesis of revolutionary new forms of matter with tailored properties. More specifically, non-equilibrium in these systems is achieved in the extraordinarily high free electron concentrations achieved in current high power lasers and the exploration of these excited sites via pump and probe techniques. Synthesis of new forms of matter are achieved: i) via the use of new applications of acoustic phonon propagation, and the effects of compression waves to mediate materials modification and ii) the identification of hydrogen sites applicable to quantum tunneling and the accompanying non-equilibrium transport.

Knowledge of the rates and pathways of vibrational and electronic energy flow in condensed matter is critical for understanding dynamical processes in solids including electronically, optically and thermally stimulated defect and impurity reactions and migrations. The ability to directly probe these pathways and rates allows tests of theory and scaling laws at new levels of precision. This research addresses issues of energy transfer and dissipation in solids, of fundamental importance to our understanding of solid-state properties and has numerous applications.

Recent Progress

Annealing Effect in Boron-Induced Interface Charge Traps in Si/SiO₂ Systems

We investigated annealing effects on the built-in interfacial DC electric field arising from boron-induced charge traps in Si/SiO₂ systems using a time-dependent SHG technique.¹ (See Figure 1). The observed initial time-dependent SHG signals suggest that the boron-induced charge traps are neutralized by annealing in non-oxygen environments (hydrogen, argon, and about 1 mTorr vacuum) at about 200 °C and 800 °C, and as well as 100 °C DI-water. Our data is most consistent with thermally assisted tunneling that modifies the charge states. We did not observe any

recovery of the initial SHG signals in the annealed samples for several months. This research will lead to a significant improvement in our understanding of the role of boron impurities in silicon-based devices and will help enhance device reliability and performance.

Effect of Hydrogen Desorption Kinetics on Thermionic Emission from Polycrystalline Chemical Vapor Deposited Diamond

We measured the time-dependent thermal emission from polycrystalline CVD diamond films at temperatures between 600 and 800 °C.² The rate of decrease of emission behavior as a function of both time and temperature followed a first-order rate equation, similar to that observed for the desorption of hydrogen from diamond surfaces in previous studies. The rate constants obtained showed Arrhenius behavior with activation energy $E_A = 1.23$ eV, in agreement with reported values of the C-H bond energies on diamond (100) and (111) surfaces. Our results suggest that at low temperatures, hydrogenated diamond surfaces show high thermionic emission because the C-H surface dipole field induces negative electron affinity. At elevated temperatures, hydrogen desorbs, the dipole disappears, leading to positive electron affinity and reduced thermionic emission. Thus, our study demonstrates that the decline of the thermionic emission current from diamond at elevated temperatures is due to the first-order desorption of hydrogen from the surface C-H bond termination thereby altering the emission behavior as the hydrogen becomes depleted. This study provides a basis for further exploration into the relationship between H-bonding and thermionic emission and insight into methods to achieve stable, higher temperature TEC operation.

Ion Implantation-Induced Modification of Optical Properties in Single-Crystal Diamond Studied by Coherent Acoustic Phonon Spectroscopy

Reliable fabrication of single-photon emitting centers and photonic devices in diamond will require a detailed understanding of the associated defects created within the lattice during the

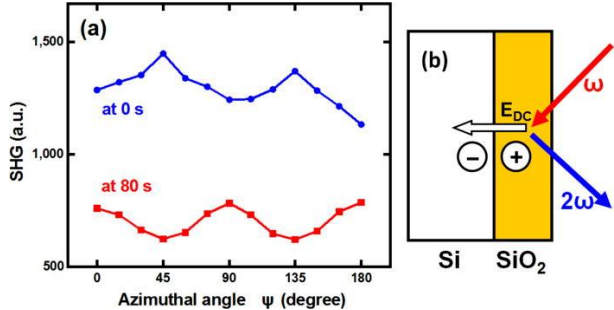


Figure 2: (a) Rotational anisotropic measurements of initial (at $t = 0$ s) and nearly saturated (at $t = 80$ s) SHG signals in an as-received boron-doped Si/SiO₂ sample with a laser beam power at 160 mW. $\Psi = 0^\circ$ corresponds to that the incident plane is parallel to $<110>$ silicon crystal plane. (b) Schematic diagram of SHG experiment and a boron-induced charge trap model.

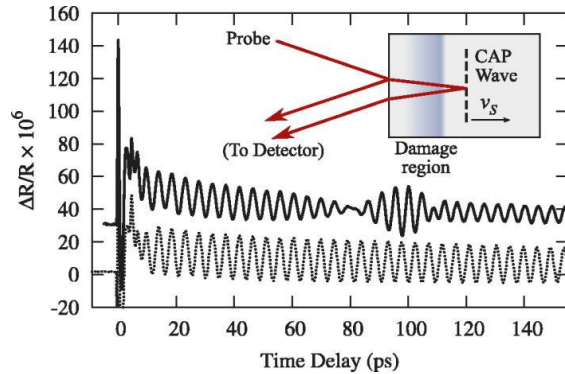


Figure 1: Typical pump-probe reflectivity responses for implanted (solid) and unimplanted (dotted) diamonds, vertically offset for clarity. Data are relevant to a sample implanted at a fluence of $3 \times 10^{15} \text{ cm}^{-2}$. Inset: CAP experiment configuration showing strain-wave induced self-interference in the probe reflectivity. The CAP wave is generated by the optical pump (not shown).

implantation process. In this study, single-crystal CVD diamond specimens were implanted with 1-MeV He⁺ ions at fluences ranging from 10^{14} to 10^{16} cm^{-2} and analyzed using coherent acoustic

phonon interferometry.³ The coherent acoustic phonon response varies greatly with implantation fluence and provides depth-dependent information about the implantation defect-induced modification of diamond's optical characteristics (Figure 2). The results indicate a decrease in the real part of the refractive index, an increase in the imaginary refractive index, and a sign reversal of the photoelastic coefficient at higher levels of implantation damage. These studies provide insight into the application of ion implantation to the fabrication of diamond-based photonic devices.

Experimental and Theoretical Determination of the Opto-Acoustic Spectrum of Silicon

Accurately predicting the opto-acoustic response of a material like Si(100) allows one to utilize the full power of first-principles calculations and go beyond Maxwellian analytical or phenomenological models in order to model the PE response in defected or disorder materials. We have demonstrated excellent agreement between *ab initio* first-principles calculations and CAP spectroscopic measurements of the opto-acoustic response in Si(100) substrates.⁴ Our calculation is shown to be consistent with the measured reflectivity behavior across the entire studied energy range of 1.4–3.5 eV (Figure 3), including the experimental observation that the CAP response increases by two orders of magnitude from 1.5 eV to 3.2 eV, the latter of which is in the vicinity of the $E_{\Gamma 1}$ direct band edge of silicon. We were also able to reproduce the time-domain reflectivity CAP response observed experimentally with good agreement. Our study motivates the extension to a theory-driven experimental study of dopant profiling, noninvasive nanometer-scale strain field analysis, and point-defect studies, among other applications.

Future Plans

- To use CAP spectroscopy to characterize the isolated depth profiles of specific hydrogen defect species in silicon crystals, revealing valuable information about the defect complexes in the silicon lattice, and demonstrating the usefulness of the technique as a general approach to targeted defect identification.
- To combine ultrafast carrier excitation with the local strain-induced band gap deformation associated with CAP waves to selectively activate thin layers of dopants in semiconductor crystals, providing a simple way to fabricate two-dimensional electron gases.

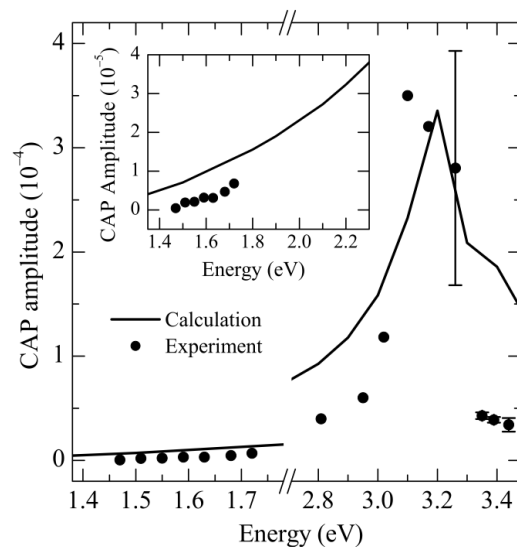


Figure 3: Comparison of theoretical (line) and experimental (dots) CAP amplitudes, showing overall agreement between theory and experiment. At some energies, more than one experimental result was obtained. In these cases, the mean value is presented, with error bars to indicate standard deviation. The inset presents an expanded view of the 1.4–2.3 eV range for the experimental and theoretical CAP responses.

- To characterize the interfaces between Si, SiO₂, and graphene using second harmonic generation, providing a quantitative description of carrier densities and dynamics at the device interfaces.
- To characterize the perturbation of the Si/SiO₂ interface in the presence of phonons by measuring the SHG signal of this interface as it is traversed by CAP waves.
- To use ultrafast spectroscopy to characterize ErAs:GaAs nanoparticle layers in order to understand the underlying electronic and plasmon-phonon relaxation processes, leading toward the development of optoelectronic devices with strong resonant absorption in the infrared.

References

- ¹ H. Park, B. Choi, A. Steigerwald, K. Varga, and N. Tolk, “Annealing effect in boron-induced interface charge traps in Si/SiO₂ systems,” Journal of Applied Physics, vol. 113, no. 2, p. 023711, 2013.
- ² W. F. Paxton, A. Steigerwald, M. Howell, N. Tolk, W. P. Kang, and J. L. Davidson, “The effect of hydrogen desorption kinetics on thermionic emission from polycrystalline chemical vapor deposited diamond,” Applied Physics Letters, vol. 101, no. 24, p. 243509, 2012.
- ³ J. Gregory, A. Steigerwald, H. Takahashi, A. Hmelo, and N. Tolk, “Ion implantation induced modification of optical properties in single-crystal diamond studied by coherent acoustic phonon spectroscopy,” Applied Physics Letters, vol. 101, no. 18, p. 181904, 2012.
- ⁴ H. Lawler, A. Steigerwald, J. Gregory, H. Krzyzanowska, and N. H. Tolk, “Experimental and theoretical determination of the opto-acoustic spectrum of silicon,” manuscript submitted to Physical Review Letters (2013).

Publications

- H. Park, B. Choi, A. Steigerwald, K. Varga, and N. Tolk, “Annealing effect in boron-induced interface charge traps in Si/SiO₂ systems,” Journal of Applied Physics, 113, 023711 (2013).
- W. F. Paxton, A. Steigerwald, M. Howell, N. Tolk, W. P. Kang, and J. L. Davidson, “The effect of hydrogen desorption kinetics on thermionic emission from polycrystalline chemical vapor deposited diamond,” Applied Physics Letters 101, 243509 (2012).
- J. Gregory, A. Steigerwald, H. Takahashi, A. Hmelo, and N. Tolk, “Ion implantation induced modification of optical properties in single-crystal diamond studied by coherent acoustic phonon spectroscopy,” Applied Physics Letters 101, 181904 (2012).
- Steigerwald, A. B. Hmelo, K. Varga, L. C. Feldman, and N. Tolk, “Determination of optical damage cross-sections and volumes surrounding ion bombardment tracks in GaAs using coherent acoustic phonon spectroscopy,” Journal of Applied Physics 112, 013514 (2012).
- T. C. Wade, D. W. Coffey, N. Ghosh, J. E. Wittig, W. P. Kang, L. F. Allard, K. A. Unocic, J. L. Davidson, and N. H. Tolk, “Nanostructure TEM analysis of diamond cold cathode field emitters,” Diamond and Related Materials 22, 29-32 (2012).
- H. Park, J. Qi, Y. Xu, G. Luepke, and N. Tolk, “Polarization-dependent temporal behaviour of second harmonic generation in Si/SiO₂ systems,” Journal of Optics 13, 055202 (2011).
- SVSN Rao, S. K. Dixit, G. Luepke, N. H. Tolk, and L. C. Feldman, “Reconfiguration and dissociation of bonded hydrogen in silicon by energetic ions,” Physical Review B 83, 045204 (2011).

Session 7

Program Title: Quantum Coherence and Random Fields at Mesoscopic Scales

Principal Investigator: Thomas F. Rosenbaum

Mailing Address: The James Franck Institute and Department of Physics, The University of Chicago, Chicago, IL 60637

E-mail: t-rosenbaum@uchicago.edu

Program Scope

Disorder and fluctuations can combine to produce novel and important electronic, magnetic, and optical effects. Inhomogeneous quantum systems are particularly appealing in this context because they have a proclivity for self-organization on the mesoscale and can exhibit pronounced fluctuations away from equilibrium. With the right choice of materials, there are manifest opportunities for tailoring the macroscopic response and for garnering insights into fundamental quantum properties such as coherence and entanglement.

We seek to explore and exploit model, disordered and geometrically frustrated magnets where spin clusters stably detach themselves from their surroundings, leading to extreme sensitivity to finite frequency excitations and the ability to encode information. Moreover, by tuning the spin concentration and/or the quantum tunneling probability, it should be possible to study the competition between quantum entanglement and random field effects. As one passes from the quantum to the classical limit, clear implications develop for magnetic storage architectures. Finally, extensions from quantum ferromagnets to quantum antiferromagnets promise new physics as well as tests of universality and general applicability.

A combination of ac susceptometry, dc magnetometry, noise measurements, hole burning, non-linear Fano experiments, and neutron diffraction as functions of temperature, magnetic field, frequency, excitation amplitude, dipole concentration, and disorder should address issues of stability, overlap, coherence, and control. We are especially interested in probing the evolution of the local order in the progression from spin liquid to spin glass to long-range-ordered magnet.

Recent Progress

Engineering Quantum States in Bulk Magnets: There have been indications in the literature that the spin liquid state in the dilute, disordered, model quantum magnet $\text{LiHo}_x\text{Y}_{1-x}\text{F}_4$ [1] may give way to a spin glass state in nominally identical crystals as a result of presently unknown differences [2]. This opens the possibility of inducing an actual transition from spin liquid to glass. The reason that such an effort is important is because the spin liquid state results from a manifestation of quantum entanglement on a mesoscopic length scale; controllable induction of such a state from the spin glass would involve controllable introduction (and dissolution) of quantum entanglement in a solid state system of visible extent.

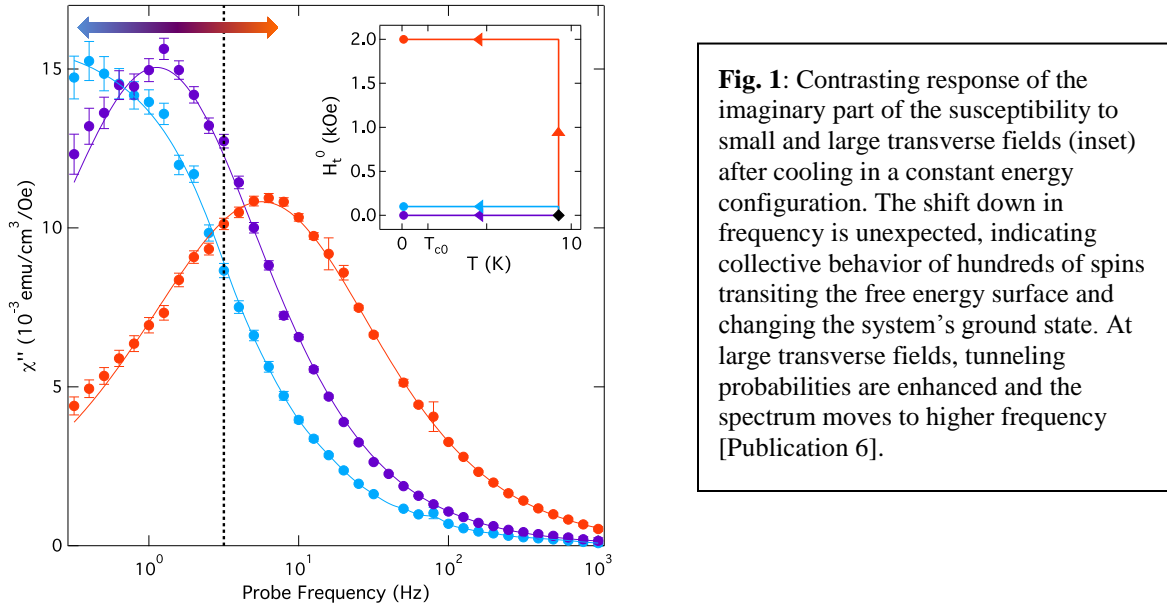
We believe that we have identified at least one such state-changing parameter: thermal coupling to the heat bath. The putative physical picture is that thermodynamics under constant energy conditions – poor coupling to the heat bath – favors quantum tunneling of blocks of spins, while thermodynamics under constant temperature conditions – strong coupling to the heat bath – favors classical excitations of individual spins over activation barriers. Cooling a crystal of

$\text{LiHo}_{0.045}\text{Y}_{0.955}\text{F}_4$, that is well connected to the heat bath yields an Arrhenius law for the peak value of the imaginary part of the magnetic susceptibility with activation energy $E_A = 1.54 \pm 0.03$ K, in close agreement with the result $E_A = 1.57$ K reported in Ref. 2. By contrast, in the isolated configuration we have observed deviations from Arrhenius law at $T \sim 120$ mK in good qualitative agreement with the results of Ref 1. While the deviations from the Arrhenius law in the isolated case may at first appear to be a symptom of sample heating, we find that the response of the system when cooled in a small transverse field rules out heating alone as the cause of the non-Arrhenius behavior. For cooling in transverse fields of 100 Oe or less, the spectrum actually moves *down* in frequency at constant base temperature, recapturing its Arrhenius form and apparently relaxing into the spin glass state (Fig. 1). Application of transverse field is expected to produce a net quantum speed-up that shifts the spectrum *up* in frequency at low temperature [3] as the quantum tunneling is enhanced. This effect emerges at sufficiently high transverse field, in this case ~ 1 kOe, also plotted in Fig. 1.

The spectral relaxation we have observed here at low cooling field is entirely new and unexpected. The small values of transverse field are orders of magnitude smaller than the field scales required to produce single-ion effects. Describing this system using the Hamiltonian for the Ising Model in transverse field,

$$H = -\sum_{i,j}^N J_{ij} S_i^z S_j^z - G \sum_i^N \sigma_i^x$$

where the σ 's are Pauli spin matrices and the J_{ij} 's are longitudinal couplings, permits a quantitative evaluation of the pertinent energies. Experiments and mean-field theory calculations find the mixing term Γ to be approximately quadratic in H_t for $H_t < 20$ kOe, with $\Gamma(1 \text{ kOe}) = 30$ mK. Clearly, in the single ion picture only transverse fields on the order of 1 kOe or more will be relevant at temperatures of order 1 K; however, we have observed unmistakable effects on the evolution of the magnetic system for transverse cooling fields as small as 10 Oe. We argue that in order for the interaction energy between a magnetic moment and a transverse field



this small to be relevant at $T \sim 0.1$ K, the moment must be comprised of order 100 spins adding coherently. As also deduced from the hole-burning results, the natural interpretation of this many-body effect is that clusters of spins are the relevant degrees of freedom. Indeed, the interaction energy of a field of 100 Oe with a single spin is ~ 3 mK, negligible compared to thermal fluctuations at $T = 90$ mK. These data therefore indicate that the field-cooled relaxation is a many-body effect in which clusters of spins act coherently, reacting to an applied field *en masse* in order to find a deeper local minima in the free-energy landscape as the sample cools. It also suggests a strategy to similarly enhance quantum relaxation in crystals of $\text{Li}(\text{Ho},\text{Y})\text{F}_4$ at higher dipole (Ho) concentration, where long-range magnetic order emerges.

Quantum Antiferromagnetism: The dipolar force between magnetic moments – the simple consequence of Maxwell's fundamental laws for electromagnetism – is present in all magnetic systems from classical to quantum magnets, from bulk materials to nanoparticles. However, while critical phenomena are well studied in systems with short range forces like the Heisenberg antiferromagnet RbMnF_3 , dipolar-coupled systems, especially antiferromagnetic ones, have received less scrutiny, mainly due to a dearth of physical realizations. We have undertaken a full suite of neutron scattering, specific heat, and magnetic susceptibility studies of LiErF_4 [Publication 3], establishing it as a model dipolar-coupled antiferromagnet with a quantum phase transition in applied field $H_c = 4.0 \pm 0.1$ kOe. For both the classical and quantum phase transitions we discover non-mean-field critical scaling. The intrinsic frustrated nature of the dipolar interaction appears to lead to an effective reduction in the dimensionality of the system, with implications for the study of magnetic thin films and nanomagnetic storage media and promise for testing longstanding theoretical predictions.

Future Plans

Geometrically-Frustrated Spin Liquids: The existence of coherent clusters of spins effectively decoupled from the surrounding magnetic environment (so-called “quantum protectorates”) can be interrogated using a magnetic hole-burning technique. The excited spins are removed from the magnetic relaxation spectrum in a process analogous to optical bleaching experiments, but we use an inductance loop at a few Hertz rather than a laser at TeraHertz frequency, with an excitation field of order the earth’s magnetic field. In the case of GGG ($\text{Gd}_3\text{Ga}_5\text{O}_{12}$), spin freezing is suppressed by geometrical frustration without the need for dilution. Frustration refers to the inability of complex systems to simultaneously satisfy all constraints, epitomized by the triangular antiferromagnet. If a spin on a particular triangle has two antiparallel neighbors, the latter two must be parallel and therefore do not satisfy their own pairwise preference for antiparallelism. The outcome for a large network of triangles is that the number of lowest energy spin configurations is not finite, as for a square lattice antiferromagnet, but grows linearly with the number of spins, resulting in a finite $T = 0$ entropy.

Exchange-coupled Gd ions lie on corner-sharing triangles in GGG and form two interpenetrating networks. The Weiss temperature, which is proportional to a combination of the exchange (1.5 K) and dipolar (~ 0.7 K) couplings between spins and measures where the system would ordinarily order antiferromagnetically, is 2 K [4]. The single ion anisotropy is less than 0.040 K [5], making this a Heisenberg system where spins in isolation can point along any spatial direction. There is acute sensitivity to applied ac magnetic field amplitude, with the onset of a

non-linear response below 1 Oe, corresponding to hundreds of spins that are labelled by frequency and locally addressable [6].

We plan to investigate the effects of disorder on the non-linear spin dynamics in GGG. We have on hand single crystals of GGG:Nd, with Nd dopings from 0.1% to 1% (Princeton Scientific). Preliminary results indicate that the Nd appears to create natural divisions between plaquettes of spins (perhaps self-organized around vacancies in pure GGG), leading to two resonances in the spectral response. We need to understand quantitatively if and how various degrees of disorder alter the nature of the quantum protectorate, and what that implies for coherence properties and control. The Nd ion is optically active and provides an additional means to probe the spin clusters.

References

1. S. Ghosh, R. Parthasarathy, T.F. Rosenbaum, and G. Aeppli, *Science* **296**, 2195 (2002); S. Ghosh, T.F. Rosenbaum, G. Aeppli, and S.N. Coppersmith, *Nature* **425**, 48 (2003); D.M. Silevitch, C.M.S. Gannarelli, A.J. Fisher, G. Aeppli, and T.F. Rosenbaum, *Phys. Rev. Lett.* **99**, 057203 (2007).
2. J.A. Quilliam *et al.*, *Phys. Rev. Lett.* **101**, 187204 (2008); M.J.P Gingras and P Henelius, *J. Phys.: Conf. Ser.* **320**, 012001 (2011).
3. J. Brooke, D. Bitko, T.F. Rosenbaum, and G. Aeppli, *Science* **284**, 779 (1999).
4. W.I. Kinney and W.P. Wolf, *J. Appl. Phys.* **50**, 2115 (1979).
5. A.P. Ramirez and R.N. Kleiman, *J. Appl. Phys.* **69**, 5252 (1991).
6. S. Ghosh, T.F. Rosenbaum and G. Aeppli, *Phys. Rev. Lett.* **101**, 157205 (2008).

Recent Publications (Supported by BES)

1. “Continuous and Discontinuous Quantum Phase Transitions in a Model Two-Dimensional Magnet,” S. Haravifard, A. Banarjee, J.C. Lang, G. Srager, D.M. Silevitch, B.D. Gaulin, H. Dabkowska, and T.F. Rosenbaum, *Proc. Nat. Acad. Sci.* **109**, 2286 (2012).
2. “Contribution of Spin Pairs to the Magnetic Response in a Dilute Dipolar Ferromagnet,” C.M.S. Gannarelli, D.M. Silevitch, T.F. Rosenbaum, G. Aeppli, and A.J. Fisher, *Phys. Rev. B* **86**, 014420 (2012).
3. “Dipolar Antiferromagnetism and Quantum Criticality in LiErF₄,” C. Kraemer, N. Nikseresht, J. O. Piatek, N. Tsyrulin, B. Dalla Piazza, K. Kiefer, B. Klemke, T. F. Rosenbaum, G. Aeppli, C. Gannarelli, K. Prokes, A. Podlesnyak, Th. Straessle, L. Keller, O. Zaharko, K. W. Kraemer, and H. M. Rønnow, *Science* **336**, 1416 (2012).
4. “Sub-Kelvin ac Magnetic Susceptometry,” M.A. Schmidt, D.M. Silevitch, N. Woo, and T.F. Rosenbaum, *Rev. Sci. Instrum.* **84**, 013901 (2013).
5. “Reversible Disorder in a Room Temperature Ferromagnet,” S.L. Tomarken, D.M. Silevitch, G. Aeppli, B.A.W. Brinkman, J. Xu, K. A. Dahmen, and T.F. Rosenbaum, *Nature Communications*, under review.
6. “Using Thermal Boundary Conditions to Engineer the Quantum State of a Bulk Magnet,” M.A. Schmidt, D.M. Silevitch, G. Aeppli, and T.F. Rosenbaum, submitted to *Nature Physics*.
7. A. Dutta, G. Aeppli, B.K. Chakrabarti, U. Divakaran, T.F. Rosenbaum, and D. Sen, *Quantum Phase Transitions in Transverse Field Models: From Statistical Physics to Quantum Information* (Cambridge University Press, under contract).

Program Title: Spin Effects in Magnetic and Non-Magnetic Correlated Insulators

Principle Investigator: Philip W. Adams

**Mailing Address: Department of Physics and Astronomy, Louisiana State University,
Baton Rouge, LA 70803**

Email: adams@phys.lsu.edu

Program Scope

This program focuses on the magneto-transport, non-equilibrium relaxation, and spin-resolved density-of-states properties of highly disordered two-dimensional paramagnetic, ferromagnetic, and superconducting systems. In addition, we are investigating proximity effects in bilayer hybrids of these systems with the aim of understanding and controlling the interface-induced exchange field in ferromagnetic/paramagnetic structures. Our specific research agenda is organized into three separate but related areas.

The first is a study of disorder and correlation effects in superconducting Al and V films that have been subjected to high Zeeman fields. We are primarily interested in what role local spin-triplet fluctuations play in determining the nature of the superconductor-insulator transition in these systems. We now have good evidence that a disordered Larkin-Ovchinnikov phase emerges near the Zeeman-limited transition and that this phase has a significant influence on the character of the transition. Thus, the spin behavior near the transition is much more complex than expected.

The second class of systems that we study is represented by ultra-thin CR₃ magnetic films (R = Ni, Co, Fe) formed via e-beam deposition from arc-melted buttons of these metastable, covalently bonded compounds. When made sufficiently thin, these films they exhibit a correlated insulator phase that is similar to what we have observed in homogeneously disordered, non-magnetic, Be films. In addition to the conductivity, we can follow the magnetic behavior via the anomalous Hall effect and spin polarized tunneling as the films are pushed to higher and higher sheet resistance.

The third class of systems is proximity structures comprised of non-magnetic/ferromagnetic bilayers. We have developed spin-resolved tunneling probes that give us a direct measure of the proximity-induced exchange field in non-magnetic component of the bilayers. Recently we have demonstrated that the magnitude of the exchange field can be modulated with an external gate, thereby producing a magnetoelectric response in the bilayers. We plan to optimize this mangetoelectric effect by getting a better understanding of the microscopic mechanism of the interface-induce exchange field, as well as improving the gate barriers and/or the bilayer interface quality. The ultimate goal is to develop a device such as a voltage-controlled superconducting switch or a spin- polarized electron source with a voltage-tunable Zeeman splitting.

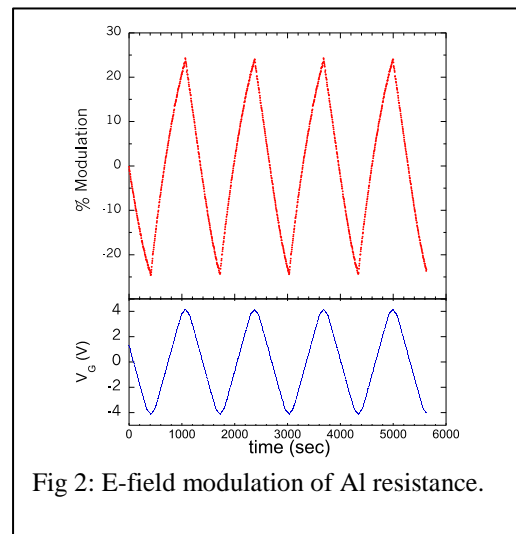
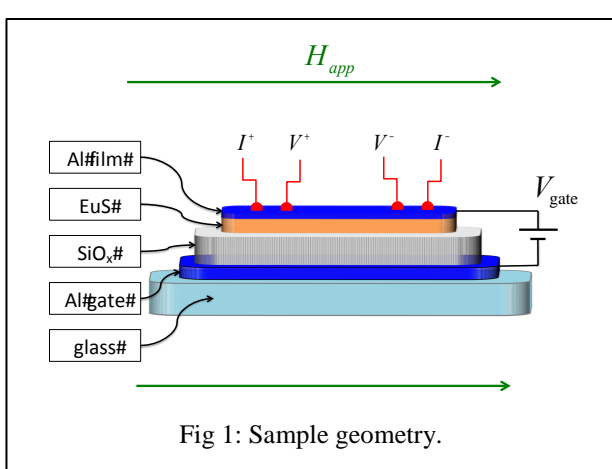
Recent Progress

Over the past decade significant progress has been made in understanding the nature of the SC order parameter in the proximity of a ferromagnetic-superconductor (FM-SC) interface [1,2]. Our interests in these proximity effect systems are primarily focused on

what happens on the SC side of the interface as a result of the interactions with the FM. Just as superconductivity is induced in the FM layer, magnetism is induced in the SC layer in the form of an exchange field. We have made a detailed study of this exchange field and showed that it is not static but has unexpected temperature and applied magnetic field dependencies that are not attributable to the temperature and/or field dependencies of the FM layer's magnetization

The development of a magnetic analog of the ubiquitous field-effect transistor (FET) has been a long-term goal of the materials research community. Indeed, the electrical manipulation of magnetism is central to the future development of spintronic applications [3]. In contrast to semiconducting FET's, which use gate-controlled electric fields to modulate a device's charge carrier concentration, a magnetic FET would use a gate to modulate the magnetism of a thin magnetic film. Recently, gating strategies have been employed to tune the magnetic properties in complex multiferroics and ferromagnetic semiconductors [4,5]. In these studies a magnetoelectric (ME) effect typically arises from the strain induced by the electric field and/or from the modulation of the carrier density itself. In a recent series of experiments we focused on ME effects that exploit the proximity-induced exchange field formed in ferromagnetic/superconductor bilayers. Using a MOSFET-type geometry we demonstrated that an exchange field of the order of several tesla can be modulated by a few percent with gate voltages $\sim \pm 5$ V. We used this effect to electrostatically tune the superconducting transition temperature of the Al layer in EuS/Al bilayers.

We can induce an electric field to the EuS-Al interface using the arrangement shown in the inset of Fig. 1. The 100-nm-thick SiO_x layer formed the gate barrier, and a voltage was applied across the upper and lower Al layers, which formed the gate electrodes. A gate voltage of ± 4 V produced a 20 mT modulation in the apparent parallel critical field, $H_{c||}$. Of course, what is actually being modulated is the exchange field in the Al layer. We have also explored ME effects at the midpoint of the critical field transition. In this case, the gate voltage was ramped linearly in time between ± 4 V, with the magnetic field set to the midpoint of the transition. Figure 2 shows the resulting time dependence of the bilayer resistance.



Future Plans

We are very excited by our initial success in modulating the exchange field in EuS/Al bilayers with a gate field. Now that we have shown that the strategy can work, we can proceed to optimize the modulation amplitude. Because the exchange field develops at the interface between the FM and SC layers, we believe that the interfacial characteristics are very important in determining both the magnitude of the exchange field and also its susceptibility to externally applied electric fields. Obviously, we would like to increase the magnitude of the electrostatic modulation of H_{ex} . One of our long-term goals is to produce a device in which the superconducting state is switched “on” and “off” with a relatively modest gate voltage. To achieve this goal we need a better dielectric barrier than what we have been using (SiO_x) and we need to explore other FM/PM interfaces.

One of the limiting factors in determining the magnitude of the exchange field modulation may be the strength of the gate electric field. Dielectric breakdown is an obvious problem, and we are now exploring the possibility of replacing the SiO_x barrier with Al_2O_3 , which has a significantly higher dielectric constant [6]. We also plan to begin depositing the bilayers on thin, commercially available, ferroelectric substrates, such as SrTiO_3 [7]. Utilizing a ferroelectric can, in principle, greatly increase the electric field at the EuS-Al interface. The idea, of course, is to determine if the modulation amplitudes in the EuS/Al system are limited by the electric field strength or by an intrinsic saturation of the effect.

In a separate project, my graduate student, Joe Prestigiacomo is studying non-equilibrium dynamics in the density of states of superconducting Al films that are near the Zeeman-limited critical field transition. For the first time we are observing macroscopic avalanches in the density of states spectrum. We have previously reported a statistical study of such avalanche behavior in transport [8], but we have never studied it as a function of disorder, nor have we studied avalanche behavior using tunneling. The avalanches are not due to quantized vorticity, because the films are in a carefully aligned parallel field. They, in fact, represent macroscopic regions of the films that suddenly undergoing a first-order phase transition. We believe that the non-equilibrium behavior of the films will give us insight into microscopic nature of the Zeeman-limited superconducting phase and perhaps shed some light on the disordered FFLO phase.

References

1. “Long Range Proximity Effects in Superconductor-Ferromagnet Structures”, F. S. Bergeret, A. F. Volkov, and K. B. Efetov, *Phys. Rev. Lett.* **86**, 4096 (2001).
2. “Spectroscopy and Critical Temperature of Diffusive Superconducting/Ferromagnetic Hybrid Structures with Spin-Active Interfaces”, A. Cottet, *Phys. Rev. B* **76**, 224505 (2007).
3. “Spintronics: Fundamentals and Applications”, I. Zutic, J. Fabian, and S. Das Sarma, *Rev. Mod. Phys.* **76**, 323 (2004).
4. “Electrostatic Modification of Novel Materials”, C.H. Ahn, A. Bhattacharya, M. Di Ventra, J.N. Eckstein, C.D. Frisbie, M.E. Gershenson, A.M. Goldman, I.H. Inoue, J. Mannhart, A.J. Mills, A.F. Morpurgo, D. Natelson, and J.M. Triscone, *Rev. Mod. Phys.* **78**, 1185 (2006).
5. “Multiferroic and Magnetoelectric Materials”, W. Eernstein, N.D. Mathur, and J.F. Scott, *Nature* **442**, 7104 (2006).

6. "Leakage Current and Breakdown Electric-Field Studies on Ultrathin Atomic-Layer-Deposited Al_2O_3 on GaAs", H.C. Lin, P.D. Ye and G.D. Wilk, *Appl. Phys. Lett.* **87**, 182904 (2005).
7. "Micromachined SrTiO_3 Single Crystals as Dielectrics for Electrostatic Doping of Thin Films", *Appl. Phys. Lett.* **85**, 997 (2004).
8. "Avalanches and Slow Relaxation: Dynamics of Thin-Film Granular Superconductors in Parallel Magnetic Field", Wenhao Wu and P.W. Adams, *Phys. Rev. Lett.* **74**, 610 (1995).

Publications (2011 - 2013)

1. "Origin of Excess Low Energy States in a Disordered Superconductor in a Zeeman Field", Y. L. Loh, N. Trivedi, Y. M. Xiong, **P. W. Adams**, and G. Catelani, *Phys. Rev. Lett.* **107**, 067003 (2011).
2. "The Comparison of Direct and Indirect Methods for Determining the Magnetocaloric Parameters in the Heusler Alloy $\text{Ni}_{50}\text{Mn}_{34.8}\text{In}_{14.2}\text{B}$ ", I. Dobenko, T. Samanta, A. Quetz, A. Kazakov, I. Rodionov, D. Mettus, S. Stadler, **P. Adams**, J. Prestigiacomo, A. Granovsky, A. Zhukov, and N. Ali, *Appl. Phys. Lett.* **100**, 192402 (2012).
3. "Structures and Phase Transitions of $\text{CePd}_{3+x}\text{Ga}_{8-x}$: New Variants of the BaHg_{11} Structure Type", M.C. Francisco, C.D. Malliakas, R.T. Macaluso, J. Prestigiacomo, N. Haldolaarachchige, **P.W. Adams**, D.P. Young, Y. Jia, H. Claus, K.E. Gray, and M.G. Kanatzidis, *J. Am. Chem. Soc.* **134**, 12998 (2012).
4. "Exchange Field-Mediated Magnetoresistance in the Correlated Insulator Phase of Be Films", T.J. Liu, J. C. Prestigiacomo, Y.M. Xiong, and **P.W. Adams**, *Phys. Rev. Lett.* **109**, 147207 (2012).
5. "The Adiabatic Temperature Changes in the Vicinity of the First-Order Paramagnetic-Ferromagnetic Transition in the Ni-Mn-In-B Heusler Alloy", I. Dobenko, T. Samanta, A. Quetz, A. Kazakov, I. Rodionov, D. Mettus, S. Stadler, **P.W. Adams**, J. Prestigiacomo, A. Granovsky, A. Zhukov, and N. Ali, *IEEE T. Magn.* **48**, 3738 (2012).
6. "Electrostatic Tuning of the Proximity-Induced Exchange Field in EuS/Al Bilayers", T. J. Liu, J. C. Prestigiacomo, and **P. W. Adams**, *Phys. Rev. Lett.* **111**, 027207 (2013).
7. " $\text{Mn}_{1-x}\text{Fe}_x\text{CoGe}$: A Strongly Correlated Metal in the Proximity of a Non-collinear Ferromagnetic State", T. Samanta, I. Dubenko, A. Quetz, J. Prestigiacomo, **P.W. Adams**, S. Stadler, and N. Ali, *Appl. Phys. Lett.* **103**, 042408 (2013).
8. "Field-pulse Memory in a Spin Glass", D.C. Schmitt, J.C. Prestigiacomo, **P.W. Adams**, D.P. Young, S. Stadler, and J.Y. Chan, *Appl. Phys. Lett.*, in press.

Program Title: Spin-Coherent Transport under Strong Spin-Orbit Interaction

Principal Investigator: Jean J. Heremans

Mailing Address: Department of Physics, Virginia Tech, Blacksburg, VA 24061

Email: heremans@vt.edu

Program Scope

The aim of the program is to gain fundamental insight in quantum-coherent spin-dependent phenomena arising from spin-orbit interaction, via experiments on nanolithographically fabricated mesoscopic solid-state samples. Spin-orbit interaction in the solid-state can open avenues for the generation of new quantum states of matter and for spin operations in quantum information processing. Presently the experiments, on electronic transport at mesoscopic length scales, allow a deeper understanding of spin phenomena and quantum-coherent spin-dependent electronic interactions. Also, under spin-orbit interaction the electric fields confining the carriers within the edges of the mesoscopic structure interact with the spin degree of freedom, of increasing fundamental and applied interest. Long-term, the ultimately magnetoelectric phenomena studied under the project are of interest for future magnetoelectronic and spintronics device functionalities.

The experiments use low-temperature quantum magnetotransport in structures at length scales approaching the mean free path and the quantum phase- and spin-decoherence lengths. Materials used comprise semiconductor and semimetal systems with specifically strong spin-orbit interaction and long quantum coherence: electron systems in the heterostructures and thin films of the narrow-bandgap semiconductors InAs, InGaAs and InSb [8], and carriers in thin-film semimetal bismuth and its surface states. The main in-lab tools are electronic transport measurements over variable temperatures and magnetic fields, electron beam lithography fabrication techniques adapted to various materials, and deposition of high-quality bismuth thin films. Semiconductor heterostructures result from collaborations with epitaxy groups.

Objectives include a study of the effect of reduced dimensions on spin coherence under spin-orbit interaction. Spin coherence is studied in quasi-one-dimensional wires, using antilocalization measurements (sensitive to quantum phase- and spin decoherence). It is found that the spin decoherence length increases with narrower wire width, a consequence of linear spin-orbit interaction and confinement of the wave function to the wire [2,3,7,9]. Objectives also comprise the characterization of the Aharonov-Casher quantum-mechanical phase and its associated vector potential, particularly as generated by the confining electric fields at the boundaries of mesoscopic spin-coherent samples. The Aharonov-Casher phase is the electromagnetic dual of the Aharonov-Bohm phase [10,11,4], and is obtained by exchanging the magnetic fields and electric charges appearing in the Aharonov-Bohm phase by electric fields and magnetic moments (spin). The Aharonov-Casher vector potential is equivalent to linear spin-orbit interaction (a specific case is Rashba spin-orbit interaction). The experiments explore the use of the Aharonov-Casher vector potential to generate effective gauge fields for creating new quantum states of matter and decoherence-free edge states (under broken time reversal symmetry, i.e. for fully aligned spins) [4]. The project also studies mesoscopic devices on the elemental semimetal bismuth, using its strongly spin-orbit coupled surface states. Bismuth is relatively unexplored as a material for mesoscopic structures, and the project hence aims at the fabrication and characterization of bismuth thin film mesoscopic devices, to explore the effect of the strong spin-orbit interaction in quantum coherent structures [2,3]. The project further studies

the interactions between surface electrons in the InAs accumulation layer and local magnetic moments deposited on the surface, using antilocalization measurements under strong spin-orbit interaction [1,5]. In the tunable artificial surface structure thus created interactions between electrons and local moments and surface magnetism can be studied

Recent Progress

Growth of bismuth thin films and mesoscopic structures:

To study the Bi surface states, predicted to have strong Rashba-like spin-orbit interaction [12], we refined the growth conditions for Bi thin films deposited in UHV conditions. We systematically optimized the quantum dephasing and spin decoherence lengths for quantum transport measurements. The films were processed into wires by electron beam lithography and wet etching. Antilocalization measurements show an increase in spin decoherence length in narrower wires, consistent with surface states with linear spin-orbit interaction (a first transport observation of the surface states of Bi) [2,3]. We observed the quantum dephasing length to decrease with decreasing wire width, an unexpected observation possibly due to dwell-time limited quantum coherence (Fig. 1).

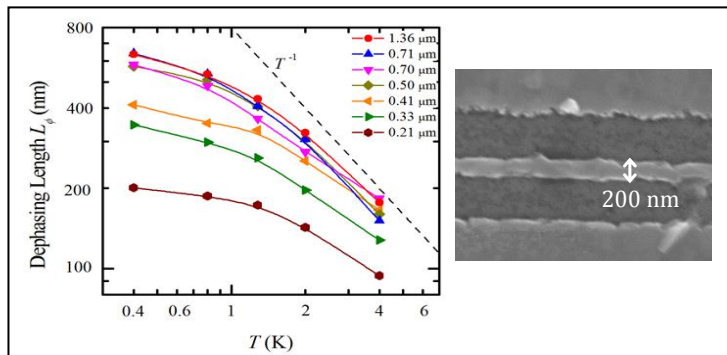


FIG. 1: Left: Quantum dephasing length L_ϕ as function of temperature in bismuth wires of widths 0.21 μm to 1.36 μm . The dephasing length is observed to decrease with decreasing wire width. Right: SEM micrograph of the 0.21 μm wide wire.

Confinement-induced spin-orbit interaction in narrow InGaAs channels:

The Aharonov-Casher vector potential, equivalent to linear spin-orbit interaction, suggests the use of effective gauge fields to generate new quantum states of matter, with special emphasis on edge states potentially robust against decoherence [4]. To characterize the strength and effects of the effective gauge fields, we study the spin-orbit interaction induced by the electric field laterally confining electrons to narrow lithographic channels. The channel magnetoresistance due to antilocalization can provide measurements of the confinement-induced spin-orbit interaction, if, as measurements indicate, the variation in conducting width of the channel is also taken into account. Samples consist of side-gated narrow channels of mesoscopic dimensions on InGaAs/InAlAs heterostructures. Figure 2 shows antilocalization magnetoresistance measurements parametrized in side-gate voltage, and the inset depicts a typical sample.

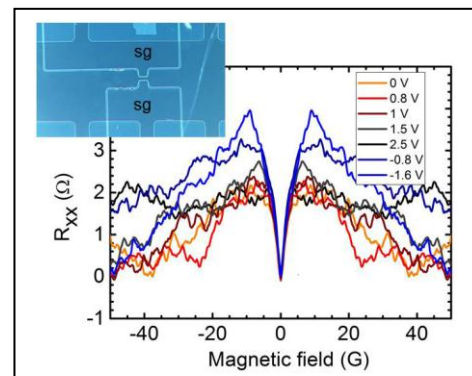


FIG. 2: Antilocalization measurements (0.4 K) on a side-gated channel on InGaAs/InAlAs, showing a systematic dependence on the side-gate voltage (electric field). Inset: Sample with the narrow channel, 2 μm wide, 4 μm long, between side gates (sg).

Quantum dephasing and amplitude modulation in mesoscopic interferometers:

Aharonov-Bohm oscillations in the magnetoresistance of mesoscopic interferometric rings patterned on an InGaAs/InAlAs heterostructure were investigated for their dependence on

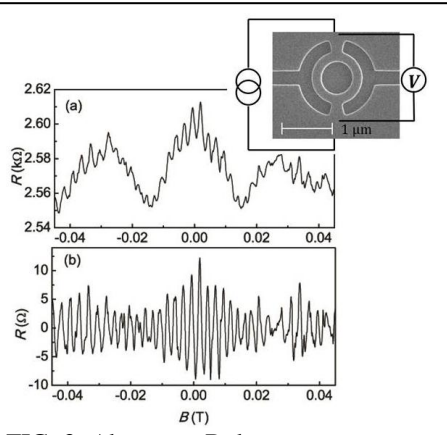


FIG. 3: Aharonov-Bohm magnetoresistance oscillations (0.4 K) in an InGaAs/InAlAs ring, with typical dimensions and layout in the inset micrograph. Panel (a) shows the raw data, (b) after background removal.

excitation current and temperature. The rings yield pronounced interference oscillations (Fig. 3), with an amplitude showing a quasi-periodic modulation with magnetic field. Analysis of the temperature and bias dependence of the interference oscillations provide the insight that the Thouless criterion for quantum dephasing has an important role, as does the time-reversal symmetry breaking due to the magnetic flux threading the finite width of the interferometer arms [13]. The comparative study of quantum-coherent phenomena at reduced dimensions in varied materials (InAs, InSb, InGaAs electron quantum wells, GaAs hole quantum wells, bismuth) also led to corollary insight into which interferometer configurations, designs and material parameters (role of carrier density and mobility) produce the strongest signals.

Interactions between InAs surface electrons and magnetic surface species:

In a series of comparative antilocalization experiments, we studied the spin interactions between electrons in the InAs surface accumulation layer, with local moments due to surface rare earth [1] or transition metal ions (Sm^{3+} , Gd^{3+} , or Ho^{3+} , and Fe^{3+} or Co^{2+} , some bound in phthalocyanines). We find that the presence of the ions modifies the spin-orbit interaction properties and the magnetic spin-flip rates of the surface electrons in this artificial structure. Sm^{3+} and Gd^{3+} induce temperature-independent electron spin-flip rates in proportion to their magnetic moments. Ho^{3+} induces a spin-flip rate increasing with temperature, resulting from transitions between finely split electronic levels on the surface (crystal fields effects and hyperfine splitting). We observe that the average spin-orbit interaction is increased by the heavy rare earths' proximity [1]. Co^{2+} and Fe^{3+} lead to a higher spin-flip rate due to their more exposed 3d shells compared to the 4f shells in lanthanides.

Future Plans

1) Spin-orbit interaction in narrow channels: The characterization of confinement-induced spin-orbit interaction in narrow channels is a stepping stone we have found necessary to study the electromagnetic duality between the Aharonov-Bohm and the Aharonov-Casher phases, which has deep implications for new quantum states of matter and quantum information processing. In mesoscopic narrow-channel geometries emphasizing edge phenomena, with length scales shorter than the spin decoherence length, we plan to extend the measurements to backscattering of edge states induced by the Aharonov-Casher effective gauge field (in analogy to their magnetic counterparts in the integer quantum Hall effect). Various accompanying effects (such as variable channel width) have to be understood and taken into account.

2) Mesoscopic and magnetoelectronic devices on bismuth and its surface states: The systematic lengthening of the spin decoherence length in Bi wires has technological implications for nanoscale spin-based electronics. The effect is consistent with the existence of spin-orbit coupled surface states on Bi. Yet, the quantum dephasing length decreasing with decreasing

wire width is not understood (provisionally ascribed to dwell-time limited quantum coherence). To achieve a deeper understanding of mesoscopic quantum transport in Bi, we will study narrow wires on other strongly spin-orbit coupled surface systems, will fabricate interferometric geometries on Bi thin films, and will use (already started) Bi single-crystals (which are not patternable but allow detailed macroscopic measurements for comparison). Thin film multilayers of CoFe with Bi (thin films and single-crystals) will be used to explore magnetoresistance effects similar to those observed on ferromagnet/semiconductor junctions. A collaborative study of Bi surfaces and surface states by low-temperature scanning tunneling microscopy is also planned.

Publications which acknowledge DOE support

1. Yao Zhang, R. L. Kallaher, V. Soghomonian, and J. J. Heremans, “Measurement by antilocalization of interactions between InAs surface electrons and local moments”, Physical Review B **87**, 054430 (2013).
2. M. Rudolph, and J. J. Heremans, “Electronic and quantum phase coherence properties of bismuth thin films”, Applied Physics Letters **100**, 241601 (2012).
3. M. Rudolph, and J. J. Heremans, “Spin-orbit interaction and phase coherence in lithographically defined bismuth wires”, Physical Review B **83**, 205410 (2011).
4. L. L. Xu, Shaola Ren, and J. J. Heremans, “Magnetoelectronics at edges in semiconductor structures: helical Aharonov-Casher edge states”, Integrated Ferroelectrics **131**, 36 (2011).
5. Yao Zhang, R. L. Kallaher, J. J. Heremans, and V. Soghomonian, “Spin interactions between InAs two-dimensional surface electrons and local magnetic moments determined by antilocalization measurements”, AIP Conference Proceedings **1416**, 168 (2011).
6. Yong-Jae Kim, M. Rudolph, R. L. Kallaher, and J. J. Heremans, “Spin-dependent transport in thin film InSb with ferromagnetic CoFe electrodes”, AIP Conference Proceedings **1416**, 158 (2011).
7. M. Rudolph, J. J. Heremans, R. L. Kallaher, N. Goel, S. J. Chung, M. B. Santos, W. Van Roy, and G. Borghs, “Dependence of the spin coherence length on wire width for quasi-1-dimensional InSb and InAs wires and Bi wire surface states”, AIP Conference Proceedings **1416**, 171 (2011).

Other References

8. R. L. Kallaher, J. J. Heremans, N. Goel, S. J. Chung, and M. B. Santos, “Spin-orbit interaction determined by antilocalization in an InSb quantum well”, Phys. Rev. B **81**, 075303 (2010).
9. S. Ketteman, “Dimensional control of antilocalization and spin relaxation in quantum wires”, Phys. Rev. Lett. **98**, 176808 (2007).
10. Y. Aharonov, and A. Casher, “Topological quantum effects for neutral particles”, Phys. Rev. Lett. **53**, 319 (1984).
11. H. Mathur, and D. A. Stone, “Quantum transport and the electronic Aharonov-Casher effect”, Phys. Rev. Lett. **68**, 2964 (1992).
12. Ph. Hofmann, “The surfaces of bismuth: Structural and electronic properties”, Prog. Surf. Sci. **81**, 191 (2006).
13. M. A. Castellanos-Beltran, D. Q. Ngo, W. E. Shanks, A. B. Jayich, and J. G. E. Harris, “Measurement of the Full Distribution of Persistent Current in Normal-Metal Rings”, Phys. Rev. Lett. **110**, 156801 (2013).

Magnetic Films and Nanomagnetism*
Materials Science Division, Argonne National Laboratory

Axel Hoffmann

Materials Science Division, Argonne National Laboratory, Argonne, IL 60439
Phone: (630) 252-5469; Fax: (630) 252-9595; Email: hoffmann@anl.gov

Program Scope

The issues our group addresses in nanomagnetism encompass (1) spin dynamics, (2) spin transport, and (3) the creation of new multilayer materials, based on metallic heterostructures. Our program in spin dynamics provides insights into artificial magnonic materials. The work advances our fundamental understanding of linear and nonlinear excitations in magnetic nanostructures. Our program in spin transport focuses on the physics of pure spin currents. Recently spin currents have been recognized as a way to communicate without charge currents, potentially eliminating wasted heat that impedes further transistor miniaturization. Due to this heat, information technology is an energy technology issue, as well as a U.S. economic competitiveness issue. Finally, the quest for new functional materials via nanoscale multilayering enables us to create systems that possess unusual synergistic properties that may otherwise be mutually exclusive. Such systems include exchange spring composites with low or no rare-earth content than can exceed today's commercial capabilities as used in electric motors and generators, or ferromagnetic-superconducting multilayers that support an exotic interfacial pairing even though the individual components can be as simple as elemental layers. Such multilayering also enables us to explore the energetics and transport mechanisms underlying organic spintronic heterostructures. These concepts and the materials explored within this proposal also provide samples worthy of advanced characterization at BES major characterization facilities.

Recent Progress:

For this presentation we will focus on our recent work related to spin Hall effects [4]. Spin Hall effects intermix spin and charge currents in non-magnetic materials and, therefore, offer the possibility to generate and detect spin currents without using ferromagnets. In order to understand the underlying physical mechanism and to identify technologically relevant materials, it is important to quantify the spin Hall angle γ , which is a direct measure of the charge-to-spin (and vice versa) conversion efficiency. Towards this end we developed an approach based on spin pumping, which enables us to quantify even small spin Hall angles with high accuracy [i,ii,2]. Spin pumping utilizes the microwave excitation in a ferromagnetic layer adjacent to a non-magnetic metal to generate over a macroscopic area a *dc* spin current [17]. This spin current can be quantified from the line-width of the ferromagnetic resonance, while the concomitant charge current from the inverse spin Hall effect can be measured through the associated electrical voltage. The ratio between the spin and charge current directly determines the spin Hall angle. In this geometry, the voltages from the inverse spin Hall effect scale with the device dimension and therefore large signal-to-noise ratios can be obtained even for materials with small spin Hall angles. We integrated ferromagnet/normal metal bilayers into a co-planar waveguide and determined the spin Hall angle for a variety of non-magnetic materials

* Work supported by the U.S. Department of Energy, Office of Science, Basic Energy Sciences, under contract No. DE-AC02-06CH11357.

(Pt, Pd, Au, and Mo) at room temperature. Of these materials Pt shows the largest spin Hall angle with $\gamma = 0.027 \pm 0.005$ [i,ii,2]. Furthermore, analyzing the data as a function of normal layer thickness enables the determination of the spin diffusion length independent of possible variations of normal metal resistivity and yields 5.5 ± 0.5 nm for Pd [2] and 1.1 ± 0.5 nm for Pt. Due to the very short spin diffusion length in Pt and the transverse nature of spin Hall effects, it is possible to obtain a high amplification of spin currents generated by charge currents, which can through spin-transfer torque generate [14] and modify magnetization dynamics in adjacent ferromagnets, including insulating ferromagnets such as yttrium iron garnet [32].

Future Plans

While our previous work focused mainly on spin Hall effects and homogenous magnetization dynamics, *i.e.*, ferromagnetic resonance, we plan to focus our future efforts on inhomogeneous magnetization dynamics, such as spin waves (magnons) [15,19]. In particular, high quality thin yttrium iron garnet thin films [1,32] will enable us to explore the influence of magnetic proximity effects, auto-oscillation of localized spin-wave modes, and modulation of spin-wave propagation via spin Hall effects. Towards this end our newly installed Brillouin light scattering microscope can detect the energy distribution of excited spin-wave modes with high spatial (250 nm) and temporal resolution (100 ps). This enables investigation of the energy flow due to spin waves, which is important for understanding the damping of magnetization dynamics and the connection between spin currents and heat currents. In addition using spatially modulated spin Hall effects may give rise to phase coherent amplification of specific spin wave modes. Furthermore, it has been recently shown that parametric pumping of magnons can result Bose-Einstein condensation (BEC) at room temperature. Ultimately, we intend to use spin Hall effects for electrical pumping of sufficiently high magnon densities for BEC in yttrium iron garnet. Successful demonstration of electrical driven BEC of magnons will then allow to spatially modulate the BEC for directly probing its quantum coherence.

References

- i. Quantifying spin Hall angles from spin pumping: Experiments and theory, O. Mosendz, J. E. Pearson, F. Y. Fradin, G. E. W. Bauer, S. D. Bader, and A. Hoffmann, Phys. Rev. Lett. **104**, 046601 (2010).
- ii. Detection and quantification of inverse spin Hall effect from spin pumping in permalloy/normal metal bilayers, O. Mosendz, V. Vlaminck, J. E. Pearson, F. Y. Fradin, G. E. W. Bauer, S. D. Bader, and A. Hoffmann, Phys. Rev. Lett. **104**, 046601 (2010).

List of Publications resulting from DOE sponsored research in FY12 and FY13

1. Damping in Nanometer-Thick Yttrium Iron Garnet Films Capped by Platinum, Y. Sun, H. Chang, M. Kabatek, Y.-Y. Song, Z. Wang, M. Jantz, W. Schneider, M. Wu, E. Montoya, B. Kardasz, B. Heinrich, S. G. E. te Velthuis, H. Schultheiss, and A. Hoffmann, Phys. Rev. Lett. (in press).
2. Dependence of spin pumping spin Hall effect measurements on layer thickness and stacking order, V. Vlaminck, J. E. Pearson, S. D. Bader, and A. Hoffmann, Phys. Rev. B (in press).
3. Magnetization dynamics through magnetoimpedance effect in isotropic Co₂FeAl/Au/Co₂FeAl full-Heusler alloy trilayer films, M. A. Corrêa, V. M. Escobar, O. Triguero-Neto, C. G. Bezerra, C. Chesman, J. E. Pearson, and A. Hoffmann, Appl.

- Phys. Exp. (in press).
4. Spin Hall Effects in Metals, A. Hoffmann, IEEE Trans. Mag. (in press), DOI:10.1109/TMAG.2013.2262947
 5. Ligand effect on magnetic properties in FePt-Fe₃O₄ core-shell nanoparticles, D-H. Kim, Y. Tamada, E. Rozhkova, J. Pearson, T. Ono, S. D. Bader, and V. Novosad, J. Nanosci. Nanotech. **13**, (in press, 2013).
 6. Influence of the thickness of the ferro- and antiferromagnetic phases on magnetic properties in epitaxial heterostructures based on exchange biased La-Ca-Mn-O system, M. E. Gomez, G. E. Campillo, S. Diez, A. Hoffmann, and W. Lopera, IEEE Trans. Mag. (in press).
 7. Unanticipated proximity behavior in ferromagnet/superconductor heterostructures with controlled magnetic non-collinearity, L. Y. Zhu, Yaohua Liu, F. S. Bergeret, J. E. Pearson, S. G. E. te Velthuis, S. D. Bader, and J. S. Jiang, Phys. Rev. Lett. **110**, 177001 (2013).
 8. Reconfigurable ground states in connected double-dot system, S. Jain, V. Novosad, F. Y. Fradin, J. E. Pearson, and S. D. Bader, Appl. Phys. Lett. **102**, 052401 (2013).
 9. Observation of microwave-assisted magnetization reversal in perpendicular recording media, L. Lu, M. Wu, M. Mallary, G. Bertero, K. Srinivasan, R. Acharya, H. Schultheiß, and A. Hoffmann, Appl. Phys. Lett. **103**, 042413 (2013).
 10. Two-dimensional quantum diffusion of Gd adatoms in nano-size Fe corrals, R. X. Cao, B. F. Miao, Z. F. Zhong, L. Sun, B. You, W. Zhang, D. Wu, A. Hu, S. D. Bader, and H. Ding, Phys. Rev. B **87**, 085415 (2013).
 11. Static and dynamic properties of Fibonacci multilayers, L. D. Machado, C. G. Bezerra, M. A. Correa, C. Chesman, J. E. Pearson, and A. Hoffmann, J. Appl. Phys. **113**, 17C102 (2013).
 12. Control and manipulation of the dynamic response of interacting spin vortices, (invited), S. Jain, V. Novosad, F. Y. Fradin, J. E. Pearson, V. Tiberkevich, A. N. Slavin, and S. D. Bader, IEEE Trans. Mag. **49**, 3081-3088 (2013).
 13. Magnetic field dependence of non-local lateral spin-valve signals beyond the Hanle effect, K. Výborný, G. Mihajlović, A. Hoffmann, and S. I. Erlingsson, J. Phys.: Cond. Matt. **25**, 216007 (2013).
 14. Make your Spins Spin, A. Hoffmann, Physics **6**, 39 (2013).
 15. Thermoelectric detection of spin waves, H. Schultheiß, J. E. Pearson, S. D. Bader, and A. Hoffmann, Phys. Rev. Lett. **109**, 237204 (2012).
 16. Effect of Interface-Induced Exchange Fields on Cuprate-Manganite Spin Switches, Y. Liu, C. Visani, N. M. Nemes, M. R. Fitzsimmons, L. Y. Zhu, J. Tornos, M. Garcia-Hernandez, M. Zhernenkov, A. Hoffmann, C. Leon, J. Santamaria, and S. G. E. te Velthuis, Phys. Rev. Lett. **108**, 207205 (2012).
 17. Mapping microwave field distributions via the spin Hall effect, V. Vlaminck, H. Schultheiß, J. E. Pearson, F. Y. Fradin, S. D. Bader, and A. Hoffmann, Appl. Phys. Lett. **101**, 252406 (2012).
 18. Growth and ferromagnetic resonance properties of nanometer-thick yttrium iron garnet films, Y. Sun, Y.-Y. Song, H. Chang, M. Kabatek, M. Jantz, W. Schneider, M. Wu, H. Schultheiß, and A. Hoffmann, Appl. Phys. Lett. **101**, 152405 (2012).
 19. Spin waves turning a corner, K. Vogt, H. Schultheiß, S. Jain, J. E. Pearson, A. Hoffmann, S. D. Bader, and B. Hillebrands, Appl. Phys. Lett. **101**, 042410 (2012).
 20. Non-collinear Fe spin structure in (Sm-Co)/Fe exchange-spring bilayers: Layer-resolved

- ⁵⁷Fe Mössbauer spectroscopy and electronic structure calculations, V. M. Uzdin, A. Vega, A. Khrenov, W. Keune, V. E. Kuncser, S. Jiang, and S. D. Bader, Phys. Rev. B **85**, 024409 (2012).
21. Coupled vortex oscillations in mesoscale ferromagnetic double-disk structures, S. Jain, H. Schultheiß, O. Heinonen, Y. Fradin, J. E. Pearson, S. D. Bader and V. Novosad, Phys. Rev. B **86**, 214418 (2012).
 22. Anomalous magnetoresistance in Fibonacci multilayers, L. D. Machado, C. G. Bezerra, M. A. Correa, C. Chesman, J. E. Pearson, and A. Hoffmann, Phys. Rev. B **85**, 224416 (2012).
 23. Quantum depinning of the magnetic vortex core in micron-size permalloy disks, R. Zarzuela, S. Velez, J. M. Hernandez, J. Tejada, and V. Novosad, Phys. Rev. B **85**, 180401 (2012).
 24. Optical transmission modulation by disk-shaped ferromagnetic particles, E. Vitol, V. Yefremenko, S. Jain, J. Pearson, E. A. Rozhkova, S. D. Bader, and V. Novosad, J. Appl. Phys. **111**, 07A945 (2012).
 25. Multifunctional ferromagnetic disks for modulating cell function (invited), E. Vitol, E. Rozhkova, and V. Novosad, IEEE Trans. Mag. **48**, 3269-3274 (2012).
 26. Vortex confinement in planar superconductor/ferromagnet hybrid structures (invited), M. Iavarone, A. Scarfato, F. Bobba, M. Longobardi, S. A. Moore, G. Karapetrov, V. Yefremenko, V. Novosad, and A. M. Cucolo, IEEE Trans. Mag. **48**, 3275-3279 (2012).
 27. Charge-Magnetic Interference Resonant Scattering Studies of Ferromagnetic Crystals and Thin Films (INVITED), D. Haskel, E. Kravtsov, Y. Choi, J. Lang, Z. Islam, G. Srayer, J. S. Jiang, S. D. Bader, and P. C. Canfield, Eur. J. Phys. Spec. Top. **208**, 141-155 (2012).
 28. Superconducting Vortex Pinning with Magnetic Dots: Does Size and Magnetic Configuration Matter?, A. Hoffmann, P. Prieto, V. Metlushko, and I. K. Schuller, J. Supercond. Nov. Magn. **25**, 2187 (2012).
 29. Visualizing vortex dynamics in Py/Nb thin film hybrids by low temperature Magnetic Force Microscopy, (invited), A. M. Cucolo, A. Scarfato, M. Iavarone, M. Longobardi, F. Bobba, G. Karapetrov, V. Novosad, and V. Yefremenko, J. Supercond. Nov. Magn., DOI 10.1007/s10948-012-1644-8 (2012).
 30. Nano-structured magnetic metamaterial with enhanced nonlinear properties, Y. Kobljanskyj, G. Melkov, K. Guslienko, V. Novosad, S. D. Bader, M. Kostylev, and A. Slavin, Scientific Reports **2**, DOI: 10.1038/srep00478 (2012).
 31. From chaos to selective ordering of vortex cores in interacting mesomagnets, S. Jain, V. Novosad, Y. Fradin, J. E. Pearson, V. Tiberkevich, A. N. Slavin and S. D. Bader, Nature Comm., DOI: 10.1038/ncomms2331 (2012).
 32. Electric control of magnetization relaxation in thin film magnetic insulators, Z. Wang, Y. Sun, Y.-Y. Song, M. Wu, H. Schultheiß, J. E. Pearson, and A. Hoffmann, Appl. Phys. Lett. **99**, 162511 (Oct. 2011).
 33. Magnetic-field enhancement of nonlocal spin signal in Ni₈₀Fe₂₀/Ag lateral spin valves, G. Mihajlović, S. I. Erlingsson, K. Výborný, J. E. Pearson, S. D. Bader, and A. Hoffmann, Phys. Rev. B **84**, 132407 (Nov. 2011).
 34. Structural Transitions and Magnetic Properties of Ni₅₀Mn_{36.7}In_{13.3} Particles with Amorphous-Like Phase, D. M. Liu, Z. H. Nie, Y. Ren, Y. D. Wang, J. Pearson, P. K. Liaw, and D. E. Brown, Metall. Mater. Trans. A – Phys. Metall. and Mater. Sci. **42A** 3062-3070 (Oct. 2011).

Nonlinear Transport in Mesoscopic Structures in the Presence of Strong Many-Body Phenomena

Jonathan Bird, University at Buffalo

Program Scope

On approaching the microscopic realm from the classical world one enters an intermediate, “mesoscopic”, regime, in which rich quantum-mechanical behavior may be manifested by systems with large numbers of interacting particles. The study of physics on this mesoscopic scale has a long history of informing the development of condensed-matter physics. At the same time, this field remains fertile for fundamental discovery, most notably by addressing issues at the nexus of two distinct fields – nonequilibrium quantum transport and many-body physics. It is the exploration of novel phenomena in these regimes that provides the overarching motivation for this project, which explores important fundamental questions such as: how are the many-body interactions of carriers modified when their motion is strongly confined on the nanoscale; how are the quantum states of isolated mesoscopic structures affected when they are coupled to an external environment; can such an environment mediate a coherent coupling between different structures, and; what is the nature of carrier transport in such systems under strongly-nonequilibrium conditions? To address these questions, we study mesoscopic transport in a variety of semiconductor nanostructures, which are implemented in high-quality gallium arsenide heterostructures, or by using an emergent material, graphene, as the carrier host.

Recent Progress

In my presentation I will focus on a discussion of recent studies that we have made of energy relaxation of hot carriers in graphene. The loss of excess energy by “hot” carriers, driven out of equilibrium by optical or electrical excitation, is critical to the operation of modern semiconductor devices. With the emergence of graphene as a promising new material for nanoelectronics, the need to understand the origins of its energy relaxation has stimulated significant theoretical and experimental activity. A key aspect of graphene is the large energy of its various optical modes, which ensures that these phonons are ineffective in cooling at all but the highest temperatures. While substrate phonons may provide a path for relaxation, the cooling of hot carriers is primarily achieved through their interaction with acoustic phonons (especially at the low temperatures of interest here). An important parameter for describing this cooling is the energy-relaxation time (τ_e), the typical time on which energy is lost by the carriers as a whole. The variation of this parameter with temperature and density can yield valuable insight into the mechanisms responsible for cooling, an issue that is of particular relevance to graphene, for which dis-

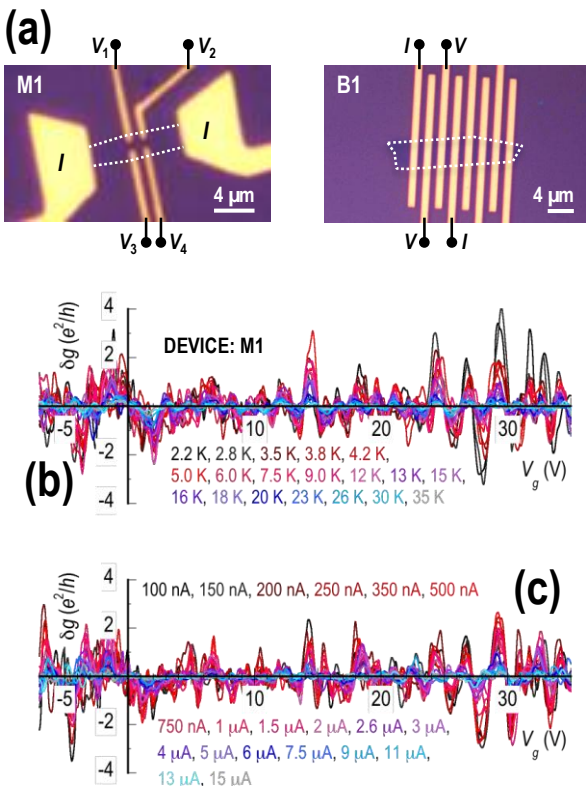


Fig. 1: (a) Optical micrographs of two of the devices studied. White dotted lines indicate the position of the graphene flake and current and voltage probes are indicated. (b) Conductance fluctuations in Device M1 as a function of gate voltage at various lattice temperatures (indicated). $I = 100$ nA RMS. (c) Corresponding fluctuations at a series of different RMS currents (indicated) for $T_L = 1.8$ K.

disordered [2] graphene predict exactly the opposite behavior, arguing that the relaxation rate should increase as the DP is approached. Particular attention has focused on Ref. 2, in which this surprising behavior was obtained by considering how disorder-mediated scattering may relax momentum-conservation constraints, allowing the full thermal-phonon distribution to be utilized in cooling. These “super-collisions” were found to become particularly effective as the DP is approached, where the Bloch-Gruneisen temperature becomes vanishingly small and one effectively enters the regime of high-temperature phonon scattering. Recent experiments performed using *pn*-junction photo-currents [3] and noise thermometry [4] appear to provide support for this mechanism.

As has long been known from the study of conventional semiconductors, a useful mechanism for investigating hot-carrier cooling involves using a large measurement current to raise the effective carrier temperature (T_e) above that of the lattice (T_L). In my presentation, I describe how we make use of this approach to investigate energy relaxation in graphene, working primarily in the high-density limit ($T_{BG} > T_L$) appropriate for many electronic-device applications. By

tinct, disorder-dependent, relaxation pathways have been predicted. We therefore determine the energy-relaxation time in this material, utilizing the carrier-heating approach that has previously been applied to conventional semiconductors.

Many of the novel properties of graphene derive from the peculiarities of its band-structure, whose linear energy bands intersect at so-called Dirac points (DPs) where the density of states also vanishes. In contrast to metals, with their large Fermi surfaces, a feature of acoustic-phonon scattering in graphene is that the boundary between its “high-” and “low-” temperature regimes is actually dependent upon carrier density, through the influence of this parameter on the Bloch-Gruneisen temperature (T_{BG}). As the Fermi level is swept towards the DP from either band, the phase space available for scattering shrinks and one might therefore expect hot-carrier cooling to slow significantly. However, recent theories for both clean [1] and

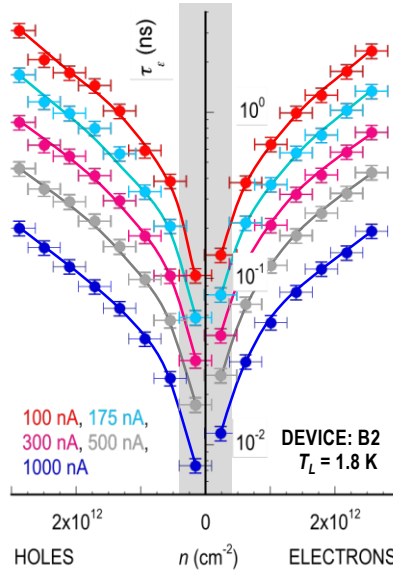


Fig. 2. Measured energy relaxation time for graphene at $T_L = 1.8$ K, and at various measurement currents (indicated).

requiring rapid energy relaxation that will have important consequences for the design of future devices that operate far from equilibrium in this material.

determining the energy-relaxation time from the dependence of T_e on input power, we demonstrate a pronounced increase in the cooling rate (i.e. $\tau_e \rightarrow 0$) as the DP is approached from either the electron or hole bands [5]. While this behavior is suggestive of recent theories for energy relaxation in graphene [1,2], our observations imply a stronger quantitative variation than that predicted by these models. At the same time, neither the variation of the power-loss rate, nor of the relaxation time, with temperature is found to be consistent with their predictions. Our results therefore suggest that the understanding of carrier cooling in this material is still incomplete, and we point to the known strong incompressibility of the electron-hole system at the DP as a possible reason for this. The incompressibility implies that excitation of carriers out of electron and hole puddles should be suppressed as the DP is approached,

Future Plans

Future research is focused on the manifestations of nonequilibrium transport in nanostructures, realized in both conventional semiconductors and in graphene. Motivated by the desire to be able to study energy-relaxation processes in real time, we will undertake measurements of electrical heating using (ns-scale) time-resolved measurement techniques. In graphene we will use these measurements to directly extract the energy-relaxation time, allowing us to verify the unusual behavior demonstrated in Fig. 2. In more conventional GaAs two-dimensional-electron-gas systems, we will use time-resolved measurements to study non-linear transport through quantum point contacts, focusing on the extreme nonlinear regime where the voltage bias is larger than all other energy scales in the problem. In this limit we have recently obtained evidence of an interesting “subband renormalization” that arises from the strongly-enhanced electron phonon interaction and leads to the formation of a protected ground-state subband that dominates the QPC conductance.

References

1. Kubakaddi, S. *Phys. Rev. B* **79**, 075417 (2009).
2. Song, J. C. W.; Reizer, M. Y.; Levitov, L. S. *Phys. Rev. Lett.* **109**, 106602 (2012).

3. Graham, M. W.; Shi, S.-F.; Ralph, D. C.; Park, J.; McEuen, P. L. *Nature Phys.* **9**, 103 – 108 (2013).
4. Betz, A. C.; Jhang, S. H.; Pallecchi, E.; Ferreira, R.; Fève, G.; Berroir, J-M.; Plaçais, B. *Nature Phys.* **9**, 109 – 112 (2013).
5. Somphonsane, R.; Ramamoorthy, H.; Bohra, G.; He, G.; Ferry, D. K.; Ochiai, Y.; Aoki, N.; Bird, J. P. *Nano Lett.*, under review.

Project-Related Publications: 2011 - 2013

1. T. Kim, R. V. Chamberlin, and J. P. Bird, “*Large magnetoresistance of nickel-silicide nanowires; Non equilibrium heating of magnetically-coupled dangling bonds*”, *Nano Letters* **13**, DOI: 10.1021/nl3044585 (2013).
2. S. Xiao, S. Xiang, Y. Yoon, M.-G. Kang, M. Kida, N. Aoki, J. L. Reno, Y. Ochiai, L. Mourokh, J. Fransson, and J. P. Bird, “*Talking through the continuum: New manifestations of Fano-resonance phenomenology realized with mesoscopic nanostructures*”, *Fortschritte der Physik* **61**, 348-359 (2013). *This invited paper was part of a special issue on non-Hermitian systems, for which PI Bird served as one of the guest editors.*
3. G. Bohra, R. Somphonsane, N. Aoki, Y. Ochiai, R. Akis, D. K. Ferry, and J. P. Bird, “*Non-ergodicity and microscopic symmetry breaking of the conductance fluctuations in disordered mesoscopic graphene*”, *Physical Review B* **86**, 161405(R) (2012).
4. Z. Chen, T.-Y. Lin, X. Wei, M. Matsunaga, T. Doi, Y. Ochiai, N. Aoki, and J. P. Bird, “*The magnetic Y-branch nanojunction: Domain-wall structure and magneto-resistance*”, *Applied Physics Letters* **101**, 102403 (2012).
5. G. Bohra, R. Somphonsane, N. Aoki, Y. Ochiai, D. K. Ferry, and J. P. Bird, “*Robust mesoscopic fluctuations in disordered graphene*”, *Applied Physics Letters* **101**, 093110 (2012).
6. Y. Yoon, M.-G. Kang, T. Morimoto, M. Kida, N. Aoki, J. L. Reno, Y. Ochiai, L. Mourokh, J. Fransson, and J. P. Bird, “*Coupling quantum states through a continuum: a mesoscopic multistate Fano resonance*”, *Physical Review X* **2**, 021003 (2012).
7. J. E. Han, S. F. Fischer, S. S. Buchholz, U. Kunze, D. Reuter, A. D. Wieck, and J. P. Bird, “*Many-body enhanced nonlinear conductance resonance in quantum channels*”, *Physical Review B* **84**, 193302 (2011).

Session 8

Program Title: Magneto-transport in GaAs Two-dimensional Hole Systems

Principal Investigator: M. Shayegan

Mailing Address: Department of Electrical Engineering, Princeton University, Princeton, NJ, 08544

E-mail: shayegan@princeton.edu

Program Scope

Two-dimensional (2D) carrier systems confined to modulation-doped semiconductor heterostructures provide a nearly ideal testing ground for exploring new physical phenomena. At low temperatures and in the presence of a strong magnetic field, these systems exhibit fascinating, often unexpected, many-body states, arising from the strong electron-electron interaction. Examples include the fractional quantum Hall liquid, the Wigner solid, and the newly discovered striped and bubble phases in the higher Landau levels.

Much of the work on the clean 2D systems has been performed on 2D *electrons* confined to a remotely-doped GaAs quantum well. The goal of this project is to study the materials science and physics of 2D *holes* confined to such wells. Compared to the 2D electrons in GaAs, the 2D holes possess a more complex energy band structure which not only depends on the quantum well width and 2D hole density, but it can also be tuned via perpendicular electric field (gate bias), parallel magnetic field, and strain. These characteristics add new twists and allow for insight into fundamental phenomena in confined, low-disorder carrier systems.

In our project we study 2D hole samples which are grown via state-of-the-art molecular beam epitaxy, and use low-temperature magneto-transport measurements to explore their novel physics. Among the problems we are addressing are the shapes of Fermi contours of 2D holes and of flux-hole composite Fermions in the presence of applied parallel magnetic field and/or strain. Also of interest are the fractional quantum Hall states, including the state at the even-denominator filling $v = \frac{1}{2}$, in 2D hole systems confined to wide GaAs quantum wells. In our work, we collaborate closely with Prof. Roland Winkler (Univ. of Northern Illinois), who is an expert in calculating the energy band structure and Landau levels in 2D hole systems, and Dr. Loren Pfeiffer who is a world expert in molecular beam epitaxy.

Recent Progress

A. Tuning and probing Fermi contours of 2D hole systems

A hallmark of the GaAs 2D holes is their complex band structure. Thanks to the spin-orbit interaction, the 2D hole bands are often split at finite values of wave vector (k) and also become anisotropic as k grows in different in-plane directions. One goal of our proposed research is to quantitatively probe these dispersions, both experimentally and theoretically. Experimental determination of the 2D hole dispersions has long been a subject of interest. It continues to be a subject of active research, thanks partly to the interest in spintronic devices and also the possibility that holes in confined structures might have a long spin coherence time (because of the lack of overlap of holes' *p*-type wave function with the nuclei) and be useful in quantum computing. We focused our recent efforts on tuning and probing the 2D holes' dispersions using magnetic field B_{\parallel} applied parallel to the 2D plane.

Figure 1 provides an example of the tunability, as well as complexity, of the 2D hole bands. Here we show the results of self-consistent calculations for the Fermi contours of 2D holes confined to a (001) GaAs square quantum well of width 17.5 nm, and subjected to a strong B_{\parallel} applied along the [110] direction. The splitting between the two $p+$ and $p-$ contours as well as the anisotropy of these contours is clear in Fig. 1 plots. Both the splitting and the anisotropy grow with the application of B_{\parallel} , leading to unusual Fermi contour shapes. Note that the finite thickness of the hole layer causes a coupling between B_{\parallel} and the holes' orbital motion. This coupling, combined with the spin-orbit interaction, lead to the unusual Fermi contour shapes seen in Fig. 1.

In our experiments we monitored the commensurability between the holes' quasi-classical orbits with a periodic potential modulation, induced by depositing an electron-beam resist grating. We were thus able to measure the size of the Fermi wave vector k_F along both [110] and [1̄10] as a function of B_{\parallel} . We used a novel technique that allows us to apply a large B_{\parallel} and a small perpendicular field to induce the commensurability oscillations. Our results, summarized in Fig. 2, agree semi-quantitatively with the numerical calculations given in Fig. 1. They demonstrate the *tuning* and *probing* of the GaAs 2D hole dispersions and Fermi contour anisotropy through the application of B_{\parallel} .

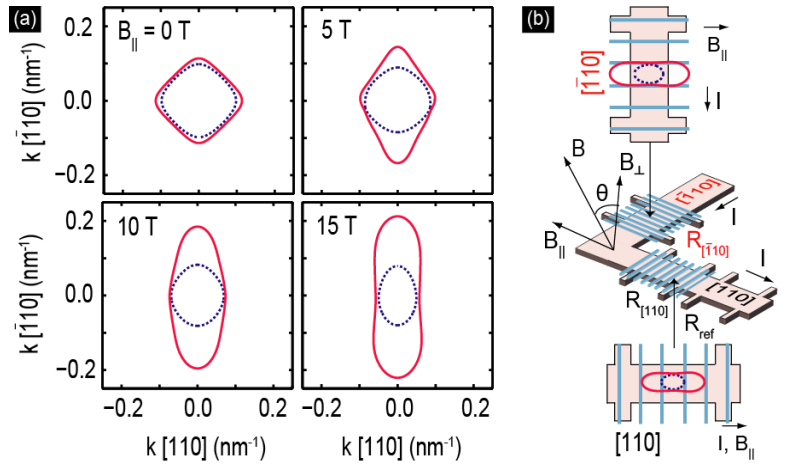


Fig. 1. (a) Fermi contours calculated for 2D holes confined to a 17.5-nm-wide, (001) GaAs quantum well at a density of $1.50 \times 10^{11} \text{ cm}^{-2}$. The contours for the majority ($p+$) and minority ($p-$) spin-subbands are shown by solid red and dotted blue curves, respectively. Each set of contours was calculated for the indicated value of parallel magnetic field applied along the [110] direction. (b) Schematic of the experimental setup, indicating the orientation of the Hall bar arms and the applied B_{\parallel} . The electron beam-resist grating covering the top surface of each Hall bar is shown as blue stripes. The orientations of the Hall bars and the resist gratings are chosen to probe the Fermi contours in the [110] and [1̄10] directions. (After Ref. 10.)

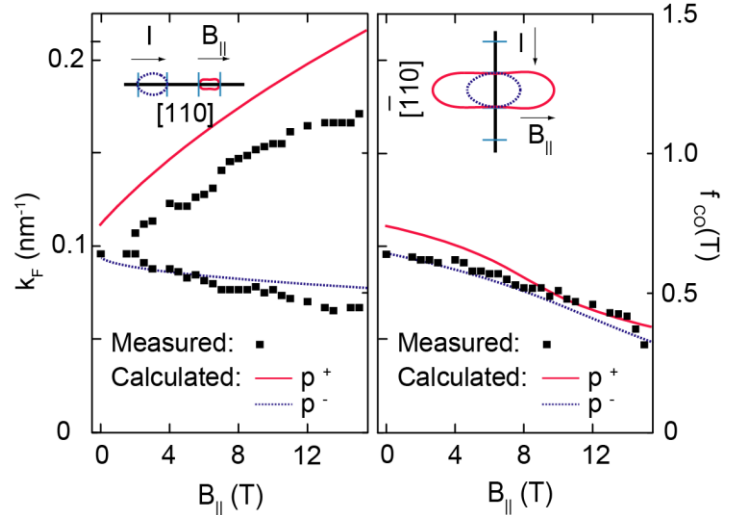


Fig. 2. (a), (b) Summary of the peak positions of the commensurability oscillations Fourier spectra for the two Hall bar arms. The left axis shows the deduced Fermi wave vectors k_F according to $k_F = e a f_{co} / \pi \hbar$. The experimental data are shown by square symbols. The lines represent the corresponding calculated values, based on k_F of the $p+$ and $p-$ contours. (After Ref. 10.)

B. Tuning and probing Fermi contours of hole-flux composite Fermions

The composite fermion (CF) formalism provides an extremely powerful yet very simple description of the interacting particles at high perpendicular magnetic fields. In the CF picture, an even number of flux quanta pair up with each carrier at high magnetic field to form quasi-particles which, at Landau level filling factor $v = \frac{1}{2}$, occupy a Fermi sea with a well-defined Fermi contour (Fig. 3). The existence of a CF Fermi contour raises the question whether fermionization preserves any low-field Fermi contour anisotropy (Fig. 3). To answer this fundamental question we determined, via measurements of commensurability oscillations, the shape of the hole-flux CF Fermi contour near filling factor $v = \frac{1}{2}$ as a function of applied B_{\parallel} . This is a very challenging experiment as it requires samples with extremely high quality 2D holes, as well as a very gentle and well-ordered periodic potential.

We measured the magnetoresistance along two perpendicular arms of an L-shaped Hall bar, shown in Figs. 4a and b, at different tilt angles (θ) of the sample. The periodic modulation produces strong CF commensurability resistance minima near filling factor $v = \frac{1}{2}$. When the magnetic field is purely perpendicular ($\theta = 0$), as shown in the bottom traces of the Fig. 4 panels, the observed positions of the minima agree with the positions anticipated for a circular CF Fermi contour (dashed green lines in Fig. 4). As the sample is tilted to increase B_{\parallel} , the minima move *away* (Fig. 4a) or *toward* (Fig. 4b) the magnetic field at $v = \frac{1}{2}$ position, depending on the orientation of the Hall bar. These shifts are a direct measure of the changes in the size of the CF Fermi contour wave vectors along and perpendicular to B_{\parallel} .

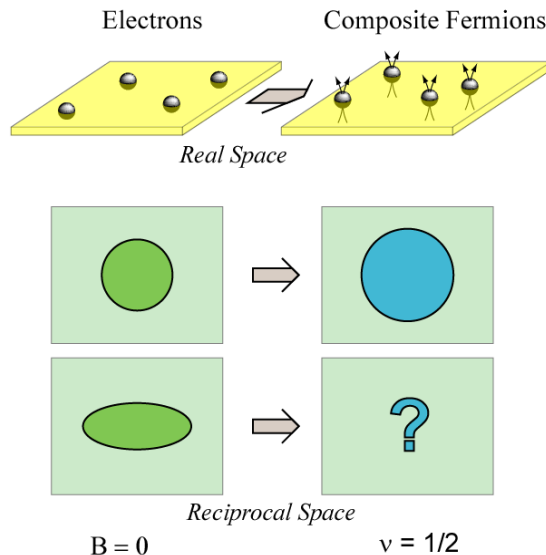


Fig. 3. Top panel: Schematic diagrams of 2D electrons (or holes) and composite Fermions (CFs) in real space. Lower panels: Schematic diagrams of isotropic and anisotropic Fermi contours for electrons (left) and the corresponding CFs (right).

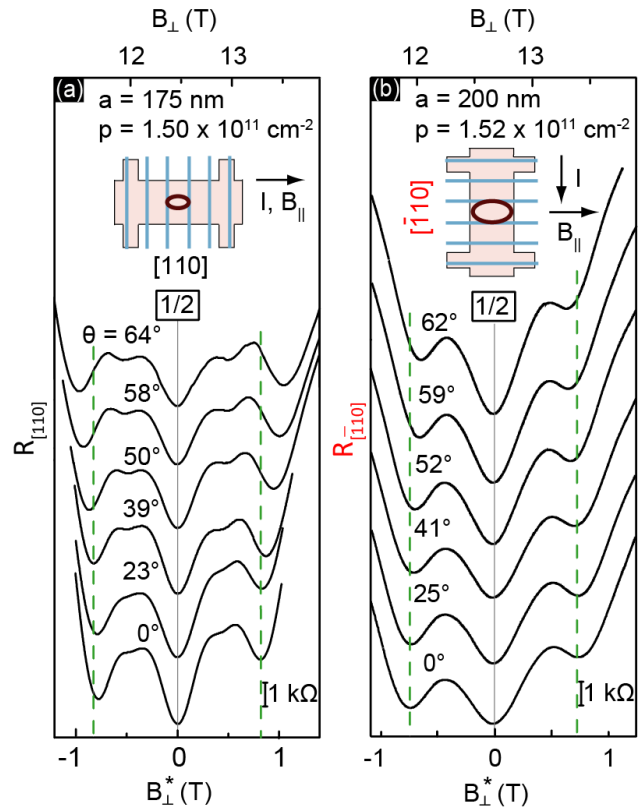


Fig. 4. CF commensurability minima near $v = \frac{1}{2}$ measured along the two arms of an L-shaped Hall bar. B_{\perp}^* is the effective magnetic field felt by the CFs. As the sample is tilted at an angle θ to introduce B_{\parallel} along [110], the resistance minima for the [110] Hall bar (a) move away from $v = \frac{1}{2}$ ($B_{\perp}^* = 0$) while those in the $\bar{[110]}$ Hall bar (b) move towards $v = \frac{1}{2}$. (After Ref. 12.)

Our results provide direct evidence that the hole-flux CF Fermi contour can be anisotropic. Moreover, they demonstrate that the anisotropy is tunable via the application of B_{\parallel} .

Future plans

We plan to concentrate on two areas. First, we will continue to study the relation between the anisotropy of the carrier and CFs' Fermi contours. We will measure the CFs' resistance as a function of B_{\parallel} . Combined with our Fermi contour measurements, the data should shed light on CFs' scattering time and effective mass. We also plan to utilize uniaxial strain, rather than B_{\parallel} , to induce Fermi contour anisotropy. The main advantage of using strain is that it eliminates the coupling of the out-of-plane motion (with B_{\parallel}). Second, we plan to study magnetotransport in holes confined to relatively wide GaAs quantum wells. Our preliminary data show a wealth of exciting new phenomena, including novel even-denominator fractional quantum Hall states.

References (which acknowledge DOE support)

1. Yang Liu, J. Shabani, and M. Shayegan, "Stability of the $q/3$ Fractional Quantum Hall States", Phys. Rev. B **84**, 195303 (2011).
2. Yang Liu, D. Kamburov, M. Shayegan, L.N. Pfeiffer, K.W. West, and K. Baldwin, "Anomalous Robustness of the $v = 5/2$ Fractional Quantum Hall Effect near a Sharp Phase Boundary," Phys. Rev. Lett. **107**, 176805 (2011).
3. YenTing Chiu, Medini Padmanabhan, T. Gokmen, J. Shabani, E. Tutuc, M. Shayegan, and R. Winkler, "Effective Mass and Spin Susceptibility of Dilute Two-Dimensional Holes in GaAs," Phys. Rev. B **84**, 155459 (2011).
4. A.L. Graninger, D. Kamburov, M. Shayegan, L.N. Pfeiffer, K.W. West, K.W. Baldwin, and R. Winkler, "Reentrant $v = 1$ Quantum Hall State in a Two-dimensional Hole System," Phys. Rev. Lett. **107**, 176810 (2011).
5. Yang Liu, J. Shabani, D. Kamburov, M. Shayegan, L.N. Pfeiffer, K.W. West, and K. Baldwin, "Evolution of the $v = 7/2$ Fractional Quantum Hall State in Two-subband Systems," Phys. Rev. Lett. **107**, 266802 (2011).
6. Yang Liu, C.G. Pappas, M. Shayegan, L.N. Pfeiffer, K.W. West, and K. Baldwin, "Observation of Reentrant Quantum Hall States in the Lowest Landau Level," Phys. Rev. Lett. **109**, 036801 (2012).
7. Z. Wang, Y.P. Chen, H. Zhu, L.W. Engel, D.C. Tsui, E. Tutuc, and M. Shayegan, "Unequal Layer Densities in Bilayer Wigner Crystal at High Magnetic Field," Phys. Rev. B **85**, 195408 (2012).
8. D. Kamburov, H. Shapourian, M. Shayegan, L.N. Pfeiffer, K.W. West, K. Baldwin, and R. Winkler "Ballistic Transport of (001) GaAs 2D Holes through a Strain-induced Lateral Superlattice," Phys. Rev. B **85**, 121305(R) (Rapid Communications) (2012).
9. D. Kamburov, M. Shayegan, L.N. Pfeiffer, K.W. West, and K.W. Baldwin, "Commensurability Oscillations of Hole-flux Composite Fermions," Phys. Rev. Lett. **109**, 236401 (2012).
10. D. Kamburov, M. Shayegan, R. Winkler, L.N. Pfeiffer, K.W. West, and K.W. Baldwin, "Anisotropic Fermi Contour of (001) GaAs Holes in Parallel Magnetic Fields," Phys. Rev. B **86**, 241302(R) (Rapid Communications) (2012).
11. Yang Liu, D. Kamburov, M. Shayegan, L.N. Pfeiffer, K.W. West, and K. Baldwin, "Spin and Charge Distribution Symmetry Dependence of Stripe Phases in Two-Dimensional Electron Systems Confined to Wide Quantum Wells," Phys. Rev. B **87**, 075314 (2013).
12. D. Kamburov, Yang Liu, M. Shayegan, R. Winkler, L.N. Pfeiffer, K.W. West, and K.W. Baldwin, "Composite Fermions with Tunable Fermi Contour Anisotropy," Phys. Rev. Lett. **110**, 206801 (2013).
13. Y. Liu, S. Hasdemir, M. Shayegan, L.N. Pfeiffer, K.W. West, and K.W. Baldwin, "Evidence for a $v = 5/2$ Fractional Quantum Hall Nematic State in Parallel Magnetic Fields," Phys. Rev. B **88**, 035307 (2013).

Title: Integrated growth and ultra-low temperature transport study of the 2nd Landau level of the two-dimensional electron gas

Principal Investigators: Gabor Csathy and Michael Manfra

Institution: Purdue University

Address: 525 Northwestern Ave., West Lafayette, IN 47907

E-mail of PIs: gcsathy@purdue.edu, mmanfra@purdue.edu

Program Scope

We have developed a synergistic experimental program based on systematic growth and ultra-low temperature measurement of high quality GaAs crystals tailored to answering outstanding questions concerning the collective behavior of the correlated electronic ground states of the two dimensional electron gas. Our primary focus is the study of the fractional quantum Hall states and exotic electronic solids of the second Landau level, i.e. corresponding to Landau level filling factors $2 \leq v \leq 4$. There is mounting theoretical and experimental evidence that several fractional quantum Hall states in this region are not well described by the model of non-interacting composite fermions. For example, the even denominator state at $v=5/2$ may result from an unusual pairing mechanism of the composite fermions described by the Pfaffian wavefunction. Because the pairing is believed to be p -wave, the $5/2$ state may resemble other condensed matter systems of current interest such as strontium ruthenate, certain fermionic atomic condensates, and the quantum liquid He-3. Moreover several odd denominator fractional states in the 2nd Landau level such as the $2+2/5$ and $2+6/13$ states are quite distinct from their well understood lowest Landau level ($v < 2$) counterparts.

The study of the $5/2$ state has been reenergized with the prediction that its excitations obey exotic non-Abelian statistics. The $v=5/2$ and other novel states in the 2nd Landau level are not only of fundamental interest as they may manifest behavior not seen in any other physical system, but also may find technological utility in fault-tolerant schemes for quantum computation. These exotic states are, however, fragile and hence they develop only in the highest quality GaAs host crystals and typically only at the lowest electron temperatures.

The goal of our program is to use incisive experimental techniques to generate new insight into the nature of the exotic correlated states of the 2nd Landau level. We carry out an integrated growth and experimental study of the two-dimensional electron gas in GaAs in the 2nd Landau level by focusing on:

- 1)** Growth of ultra-high quality GaAs/AlGaAs heterostructures specifically tailored to study the impact of various material parameters on the stability of the various fractional quantum Hall ground states in the 2nd Landau level.
- 2)** Application of novel techniques together with transport measurements in the most interesting but technologically difficult ultra low temperature regime ($T \sim 5\text{mK}$). As this regime is still largely unexplored, new and unanticipated results can be expected.

Recent Progress

This project builds on the ongoing collaboration of the PIs and unique experimental capabilities developed at Purdue University. *Our team has recently developed a unique combination of next generation growth and measurement capabilities needed to address several of the outstanding problems in the field of 2D electron physics.*

Manfra has designed and built a highly customized MBE chamber designed for the growth of ultra high mobility GaAs/AlGaAs heterostructures (see Fig.1). Over the past year, Manfra's DOE-related work has focused on 4 primary tasks: 1) improvement of 2DEG samples for examination of exotic 2nd Landau level physics, 2) growth and processing development of in-situ backgated ultra-high mobility 2DEGs, 3) growth and characterization of 2DEGs with controlled disorder, 4) growth of samples specifically designed for DOE-funded external collaborations. Towards these ends several accomplishments are noteworthy.

- a. electron samples with a record high stability of the exotic $v=5/2$ fractional quantum Hall state as measured by the largest energy gap of 569mK. This is an ongoing work, the first results are already published [1,2].
- b. samples in which the 2DEG density can be tuned with an in-situ backgate from $2 \times 10^{10} \text{ cm}^{-2}$ to $2.7 \times 10^{11} \text{ cm}^{-2}$ with a peak mobility of $17 \times 10^6 \text{ cm}^2/\text{Vs}$ at $T=0.3\text{K}$.
- c. a series of samples with different strength of the alloy disorder including samples with Al concentrations as low as 0.057% [4].
- d. Manfra's samples have been widely distributed to collaborators, including many DOE-funded researchers. Samples have been grown for approximately 15 independent research groups around the world. Manfra's work with Michael Zudov of the University of Minnesota is a prime example of his external collaborations with DOE-funded researchers [6-8].

Csathy has built a specialized ultra-low temperature refrigerator capable of cooling electrons in semiconductors to 5mK [9,10]. This setup not only cools the electrons but also allows for a reliable magnetic-field-independent temperature measurement of the local bath via He-3 viscometry. His immersion cell is shown in Fig.2. Notable results from his lab supported by this DOE award are:

- a. discovery of a unique experimental signature in the R_{xx} of the exotic electronic solids called the bubble phases [1].
- b. we have reported unexpected results of the bubble phases in the third Landau level [2].
- c. we have made significant progress with the measurements of samples with alloy disorder [4].

Our progress is evident in the observation of some of the most fragile fractional quantum Hall states [1, 2]. Our electron samples show extremely robust fractional quantum Hall ground states in the lower spin branch of the second Landau level near the filling factor $v=5/2$ [2]. The $v=5/2$

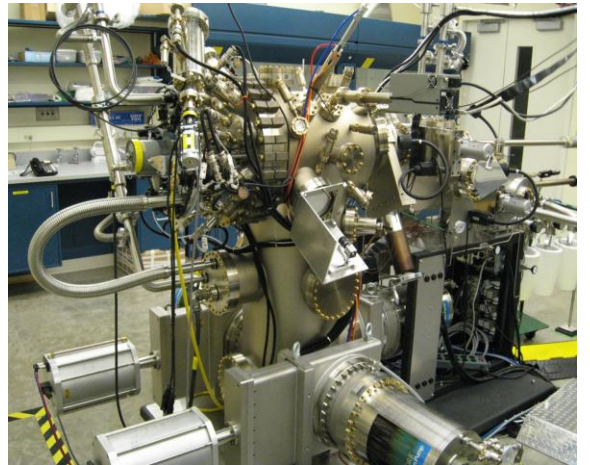


Fig.1. Manfra's custom-designed MBE installed at Purdue. This new machine is producing samples of record quality used not only in this current project but also distributed among colleagues, several of which are DOE supported.



Fig.2. Csathy's He-3 immersion cell allows reaching temperatures of 5mK (left). A sample mounted on sintered Silver heat sinks (right). Reliable temperature measurement is achieved using a novel quartz He-3 viscometry [9].

state in one sample grown by Manfra has the largest excitation gap ever reported – close to 0.6 Kelvin. The fine details of the transport features near $v=5/2$ are shown in Fig.3. In particular, we find a completely well-formed $v=2+2/5$ state. This feature has only been reported in 2 samples during the past 6 years, yet it appears quite strong in many of our samples.

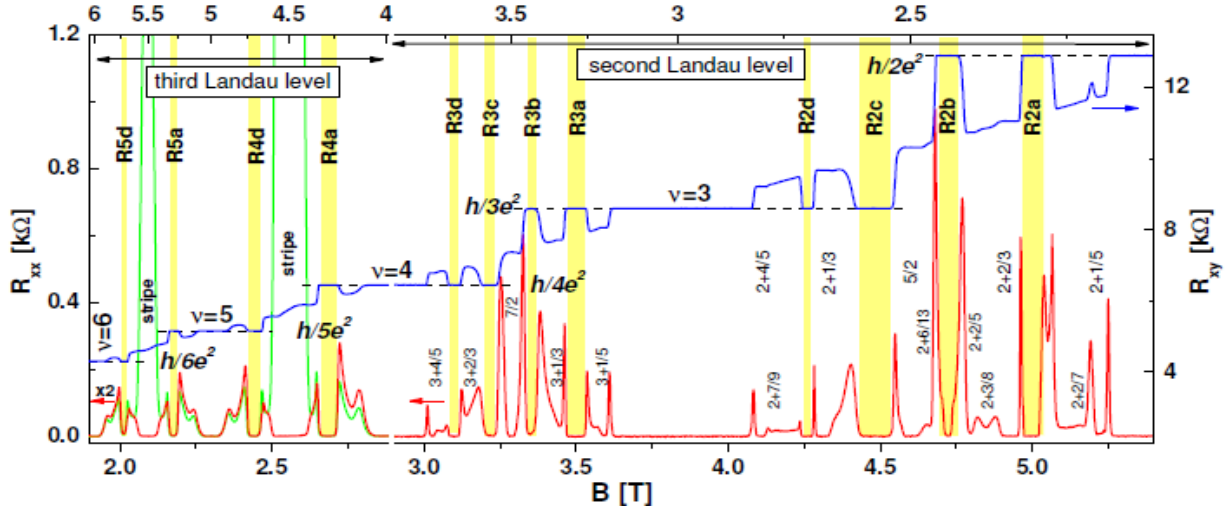


Fig.3 Magnetotransport in the second and third Landau levels showing the prominent reentrant integer states shaded in yellow and many fractional quantum Hall states marked by their quantum number. See reference [2] for more detail.

In addition, we see rich physics in the upper spin branch, near the quantum number $v=7/2$, and in the third Landau level, near $v=9/2$ and $11/2$. The exquisite quality of the data enabled us, for the first time, to investigate the reentrant integer quantum Hall states (RIQHS). In a recently published Phys. Rev. Lett. [1] we report an unexpected sharp peak in the R_{xx} versus temperature curve of the reentrant integer states, also called the bubble phases. We associated these peaks with the melting of the collective ground state. This allowed us, for the first time, to compare energy scales of various reentrant states [2]. We found that the onset temperatures scale with the Coulomb interaction energy. This comparison allowed us to conclude, that since the interaction energy plays a dominant role in the formation of these phases, the electrons are not randomly localized but form a strongly interacting phases, most likely an exotic electron solid. Furthermore, we found that, contrary to expectations, the onset temperature in the third Landau level is substantially higher than that in the second Landau level. This large discrepancy is not yet understood, but it shows us that there is still much to be learned about these states.

Available data suggests that the $5/2$ state responds differently to different types of disorder. However, in all prior measurements, disorder is uncontrolled as it is the residual disorder from the sample growth process. Manfra has grown a set of samples with deliberate introduction of a specific type of disorder: short range alloy disorder [4]. What is remarkable about these samples is that they host well-developed $5/2$ states even in the regime in which alloy disorder dominates. The low temperature transport measurements are currently under way.

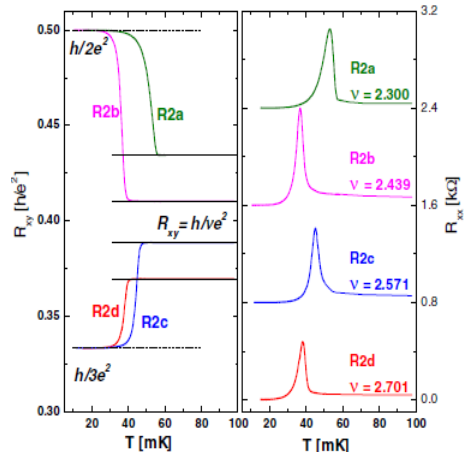


Fig.4 The prominent changes in both R_{xy} and R_{xx} signal the onset of the electronic bubble phases, see reference [1].

Under this program, Manfra has also grown high quality two-dimensional hole samples, for which he holds the record for mobility. Manfra's students found that the mobility exhibits an unexpected peak at the relatively low hole density of $\sim 6 \times 10^{10}/\text{cm}^2$. Their analysis of known scattering mechanisms was not able to account for the observed behavior leaving the possibility open for an underappreciated mechanism at high densities [3].

Future Plans

We will continue our effort in studying disorder effects by energy gap measurements in the presence of alloy disorder. We will then extend our studies to other types of well-controlled disorders. We are also investigating the spin polarization of the $v=5/2$ state. Finally, our recent result on the reentrant insulating states calls for their study in high Landau levels. Such investigations involve a coordinated effort between growth and ultra-low temperature measurement and are part of our long term effort aimed at exploring unconventional collective behavior in low-dimensional systems.

References acknowledging DOE support

1. N. Deng, A. Kumar, M.J. Manfra, L.N. Pfeiffer, K.W. West, and G.A. Csathy, "Collective Nature of the Reentrant Integer Quantum Hall States in the Second Landau Level", *Physical Review Letters* **108**, 086803 (2012)
2. N. Deng, J.D Watson, L.P. Rokhinson, M.J. Manfra, and G.A. Csathy, "Contrasting Energy Scales of the Reentrant Integer Quantum Hall States", *Rapid Communications, Physical Review B* **86**, 201301 (2012)
3. J.D. Watson, S. Mondal, G. Gardner, G.A. Csathy, and M.J. Manfra, "Exploration of the Limits to Mobility in Two-Dimensional Hole Systems in GaAs/AlGaAs Quantum Wells", *Physical Review B* **85**, 165301 (2012)
4. G.C. Gardner, J.D. Watson, S. Mondal, N. Deng, G.A. Csathy, and M.J. Manfra, "Growth and electrical characterization of $\text{Al}_{0.24}\text{Ga}_{0.76}\text{As}/\text{Al}_x\text{Ga}_{1-x}\text{As}/\text{Al}_{0.24}\text{Ga}_{0.76}\text{As}$ modulation-doped quantum wells with extremely low x ", *Applied Physics Letters* **102**, 252103 (2013)
5. E. Kleinbaum and G.A. Csathy, "A Transimpedance Amplifier for Remotely Located Quartz Tuning Forks", *Review of Scientific Instruments* **83**, 126101 (2012)
6. A.T. Hatke, M.A. Zudov, J.D. Watson, and M.J. Manfra, "Magnetoplasmon resonance in a Two-Dimensional; Electron System Driven into a Zero-Resistance State", *Physical Review B* **85**, 121306 (2012)
7. A.T. Hatke, M. A. Zudov, J. D. Watson, M. J. Manfra, L. N. Pfeiffer, and K. W. West, "Effective mass from microwave photoresistance measurements in GaAs/AlGaAs quantum wells", *Journal of Physics: Conference Series* **456**, 012040 (2013)
8. A.T. Hatke, M.A. Zudov, J.D. Watson, and M.J. Manfra, L.N. Pfeiffer, and K.W. West, "Evidence of Effective Mass Reduction in GaAs/AlGaAs Quantum Wells", *Physical Review Letters* **B 87**, 161307 (2013)

Other references

9. N. Samkharadze, A. Kumar, M.J. Manfra, L.N Pfeiffer, K.W. West, and G.A. Csathy, "Integrated Electronic Transport and Thermometry at milliKelvin Temperatures and in Strong Magnetic Fields", *Review of Scientific Instruments* **82**, 053902 (2011)
10. A. Kumar, G.A. Csathy, M.J. Manfra, L.N Pfeiffer, and K.W. West, "Nonconventional Odd Denominator Fractional Quantum Hall states in the Second Landau Level", *Physical Review Letters* **105**, 246808 (2010)

Program Title:

Experiments on Quantum Hall Topological Phases in Ultra Low Temperatures

Principal Investigator: Rui-Rui Du

Mailing Address: Department of Physics and Astronomy MS-61, William Marsh Rice University, 6100 Main Street, Houston, TX 77251-1892

Email: rrd@rice.edu

Program Scope

The goal of the program is to cool electrons in semiconductors to extremely low temperatures (a few millikelvin), and to study new states of matter formed by low-dimensional electrons. At such low temperatures (and with an intense magnetic field), electronic behavior differs completely from ordinary ones observed at room temperatures. Studies of electrons at such low temperatures would open the door for fundamental discoveries in condensed matter physics. Understanding low-temperature electron transport in low-dimensional and nanoscale devices is the foundation for developing next generation quantum information and quantum computation technologies.

The experimental program consists of the following components:

- 1) Experiments at ultra-low temperatures in the 5/2 fractional quantum Hall Effect and related quantum phases: Our goal is to understand the energy scale of competing quantum phases, by measuring the temperature-dependence of transport features. Focus will be placed on such issues as the energy gap of the 5/2 state, and those of 12/5 (and possible 13/5); resistive signature of instability near 1/2 at ultra-low temperatures.
- 2) Measurement of the 5/2 gaps in the limit of small or large Zeeman energies: Our goal is to gain physics insight of 5/2 state at limiting experimental parameters, especially those properties concerning the spin polarization.
- 3) Studies of screened fractional quantum Hall effect in double-layer 2D hole gas (2DHG). In addition, the PI and Dr. Pfeiffer have developed an experimental plan to explore induced superconductivity in GaAs/AlGaAs heterostructures. This ideal was initiated in Bell Labs during 90's but so far no experiments were attempted: if a layer of high density, metal-like 2DHG could be placed within a Fermi wavelength (~ 10 nm) to a high mobility, low density 2DHG which is in the charge density wave or plasmon state, BCS paring could be induced mediated by CDW or plasmons instead of phonons.
- 4) Ultralow temperature transport experiments on quantum spin Hall effect in InAs/GaSb composite QWs. Although this topic is not in the fractional quantum Hall effect area, its' underlying physics is connected to the topological quantum phases at 5/2. Part of our efforts is to fabricate Nb-InAs/GaSb junctions, where superconductivity can be proximity-induced in the 1D helical edge of the device. The novel transport properties related to the Andreev reflection and Majorana bound states will be measured into the ultralow temperature regime of a few milliKelvin using our demagnetization refrigerator.

Recent Progress

Here we highlight recent work supported by the program.

1) Enhanced 5/2 FQHE in a Small Tilted Magnetic Field

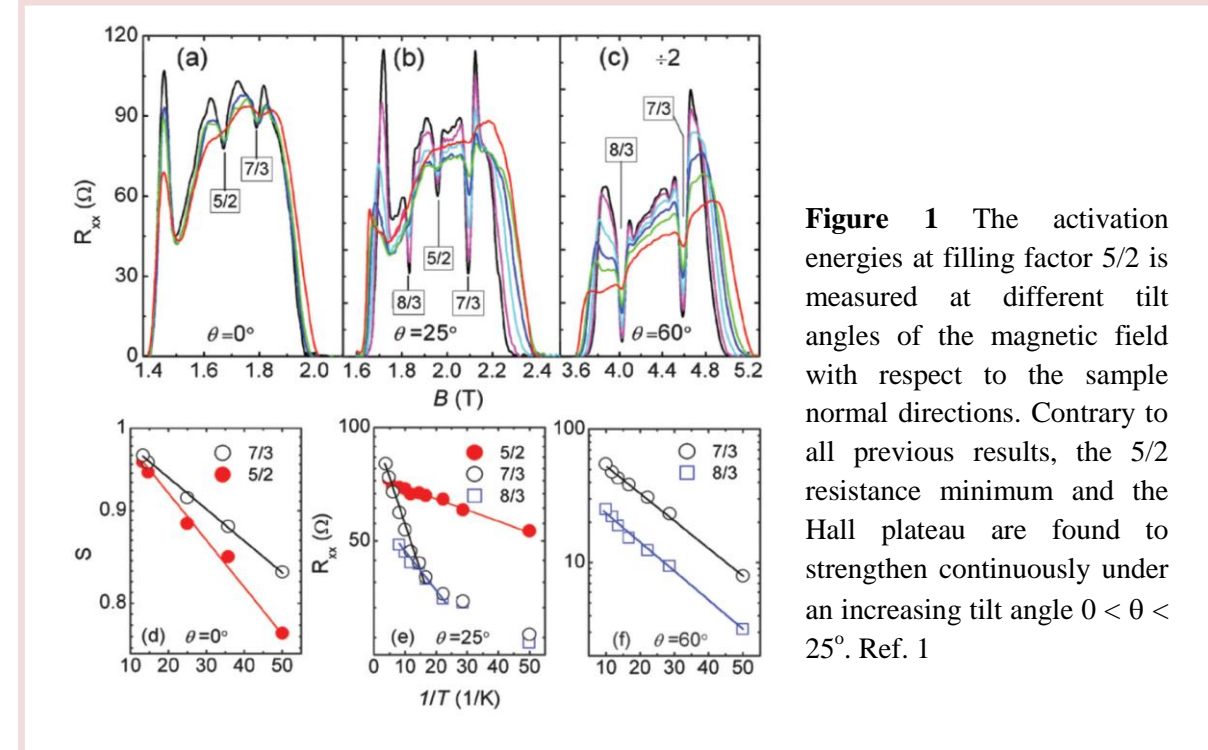


Figure 1 The activation energies at filling factor 5/2 are measured at different tilt angles of the magnetic field with respect to the sample normal directions. Contrary to all previous results, the 5/2 resistance minimum and the Hall plateau are found to strengthen continuously under an increasing tilt angle $0 < \theta < 25^\circ$. Ref. 1

Using a 50-nm-width ultraclean GaAs/AlGaAs quantum well, we have studied the Landau level filling factor 5/2 fractional quantum Hall effect in a perpendicular magnetic field $B = 1.7$ T and determined its dependence on tilted magnetic fields. Contrary to all previous results, the 5/2 resistance minimum and the Hall plateau are found to strengthen continuously under an increasing tilt angle $0 < \theta < 25^\circ$. In the same range of θ , the activation gaps of both the 7/3 and the 8/3 states are found to increase with tilt. The 5/2 state transforms into a compressible Fermi liquid upon tilt angle $\theta > 60^\circ$. Based on our results, we discuss the relevance of a Skyrmiон spin texture at 5/2 associated with small Zeeman energy in wide quantum wells, as proposed by Wojs et al. [Phys. Rev. Lett. 104, 086801 (2010)].

2) Observation of Robust Quantum Spin Hall States in InAs/GaSb Bilayers

Topological insulators (TIs) are a class of new state of matter with nontrivial surface or edge states. Time-reversal-symmetry (TRS) protected TIs are characterized by Z2 topological invariant and their helical property becomes lost in an applied magnetic field. Currently there exist extensive efforts to identify TIs that are protected by symmetries other than TRS. Here we show, in an inverted electron-hole bilayer engineered from indium arsenide - gallium antimony semiconductors, the quantum spin Hall effect can persist to very high magnetic fields. Helical edge modes with a wide plateau, quantized to $2e^2/h$ value, are observed; plateaus persist to 12T applied magnetic field without evidences for transition to other topological phases. Our finding

opens the way in engineering robust helical edge channels for spintronics and for creating and manipulating Majorana particles in solid states.

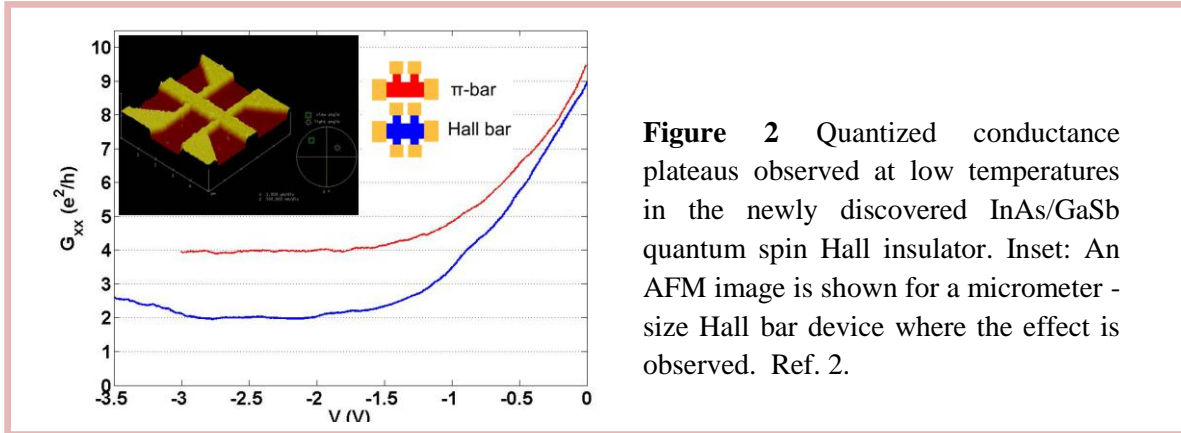


Figure 2 Quantized conductance plateaus observed at low temperatures in the newly discovered InAs/GaSb quantum spin Hall insulator. Inset: An AFM image is shown for a micrometer - size Hall bar device where the effect is observed. Ref. 2.

Our collaborator Dr. Loren Pfeiffer of Princeton has successfully grown high-quality double layer carbon-doped 2DHG for our experiments on screened fractional quantum Hall effect at mK temperatures. We have characterized these wafers and are preparing for systematic measurements. Presently we have fabricated samples (with individually contacted layers) and will look for low temperature signatures of pairing.

Future Plans

1. Experiments will focus on fractional quantum Hall effect in screened, very high mobility 2DHG, where the screening metallic layer is provided by adjacent (within a distance comparable to Fermi wavelength ~ 10 nm) high density 2DHG. Such highly sophisticated structures became available only recently, thanks to the effort by Dr. Loren Pfeiffer. It is proposed to use the screening layer to modify the electron-electron interaction pseudo-potential in the active layer, in particular to reduce the relative contribution from short-distance repulsion, in which case FQHE quasiparticle pairing could be favored.
2. In the same heterostructure system (in some cases even in the same set of samples), but under different conditions (for example, ultra low temperature, \sim a few mK, and zero magnetic field), seeking experimental evidences for Cooper pairing mediated by electronic mechanism. 1) and 2) has a good synergy in exploring new physics as well as in innovative experimental approaches.
3. Since we have successfully designed and grown (by our collaborator Dr. Gerard Sullivan in Teledyne Scientific & Imaging, Inc) the high-quality MBE InAs/GaSb quantum wells and observed the quantum spin Hall effect in gated devices, we plan to continue pursuing the interesting physics by low temperature transport in this novel materials system. These include the Nb-InAs/GaSb proximity coupled hybrid device for Majorana bound states, and the exciton insulator and exciton superfluidity in electron-hole bilayers. The details will be described in the renewal proposal.

Publications (which acknowledge BES support)

Ref.1. "Enhancement of the $v = 5/2$ Fractional Quantum Hall State in a Small In-Plane Magnetic Field", Guangtong Liu, Chi Zhang, D. C. Tsui, Ivan Knez, Aaron Levine, R. R. Du, L. N. Pfeiffer, and K. W. West, *Phys. Rev. Lett.* **108**, 196805 (2012).

Ref. 2. "Observation of Quantum Spin Hall States in InAs/GaSb Bilayers under Broken Time-Reversal Symmetry", Lingjie Du, Ivan Knez, Gerard Sullivan, Rui-Rui Du, arXiv:1306.1925, submitted to *Nature*, in review.

Invited Talks on works supported by DOE:

1. 2011 APS March Meeting Symposium on Transport in Topological Insulators (presented by graduate student Ivan Knez)
2. 31th Int'l Conf. on the Physics of Semiconductors (ICPS31), July 29-August 3, 2012, Zurich, Switzerland
3. Int'l Workshop on "Majorana Fermions in Condensed Matter", July 2-6, 2012, Leiden, The Netherland
4. Int'l Workshop on "Majoranas in Solid State", June 3-7, 2013, Beijing, China
5. Int'l Workshop on "Quantum Hall Effect and Related Topics", June 26-28, 2013, Max-Planck-Institute for Solid-State Research in Stuttgart, Germany
6. Int'l Workshop on "Majorana Physics in Condensed Matter", July 12-18, 2013, Elice, Italy
7. 16th International Conf. on Narrow Gap System, August 2-6, 2013, Hanzhou, China

Program Title: Engineering topological states of matter and search for Majorana fermions.

Principle Investigator: Leonid P. Rokhinson

Mailing Address: Department of Physics, Purdue University, West Lafayette, IN 47906

E-mail: leonid@purdue.edu

Program Scope

The goal of the program is to develop systems which support excitations with non-Abelian statistics and to study properties of these new unconventional states of matter. In such matter some quantum numbers of a many-particle condensate are encoded in the topology of the state and protected from small local perturbations. These protected degrees of freedom can be used to encode quantum information and are the basis of fault-tolerant topological quantum computer proposals, which presents a robust alternative to the conventional quantum computation where decoherence poses the major technological challenge.

The main strategy that we use to achieve our goals is to design synthetic hybrid topological superconductors from conventional semiconductors and s-wave superconductors, and to choose materials and geometries where phase space to observe topological superconductivity is maximized. We focus on InSb semiconductor, which has the best combination of parameters to observe Majorana fermions, and use planar MBE-grown structures where spin-orbit effects are further amplified by geometry. In case of InSb the Dresselhaus spin-orbit term depends on the thickness of the structure d , $E_{so} = \gamma(\frac{\pi}{d})^2 k$, and quantum wires fabricated from a thin quantum well will have spin-orbit energy enhanced by an order of magnitude compared to thick CVD-grown quantum wires. In order to minimize fabrication-induced damage we will adopt AFM local anodic oxidation techniques which is a low-energy alternative to the conventional high-energy e-beam lithography and dry etching. Development of AFM patterning of thin superconducting films will allow multi-layer structures being fabricated using this low energy technique with nanometer alignment capability.

Detection of non-Abelian excitation using dc spectroscopy raised a number of questions and is not unambiguous. We work on the development of a dedicated system which will allow detection of the fractional Josephson effect in a linear regime.

Recent Progress

The major efforts during the first year of the project were devoted to the growth and characterization of InSb heterostructures, design of an rf detection system, and development of an entirely new system where both Majorana fermions and higher order parafermions can be realized.

Growth of InSb heterostructures is performed in the laboratory of Prof. Furdyna in the University of Notre Dame, in close collaboration with Prof. Tomasz Wojtowicz from Polish Academy of Sciences. InSb layers grown on GaSb substrates suffer from large amount of strain-induced defects and high current leakage to the substrate. Recently we used high quality MgCdTe substrates, lattice matched to InSb, to grow high quality InSb films. The films have better stoichiometry and less corrugation than InSb/GaSb heterostructures but their flatness is still inferior to commercial GaAs wafers, see Figure 1. Flatness of the surface seems to affect AFM LAO lithography: the grown oxide lines are uniform on flat GaAs surfaces but have variable height on rough InSb. We suspect that unstable writing may be related to the fact that different crystallographic axes are exposed on InSb surface since oxygen diffusion is different along different axes. Currently we are adjusting growth conditions in order to have large (several micron) terraces with monolayer roughness.

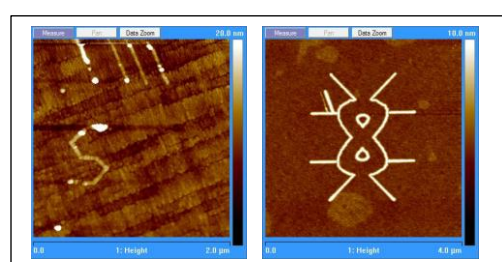


Figure 1. Left: AFM lithography on InSb grown on lattice matched MgCdTe substrate. Light lines are oxide. Right: AFM lithography on GaAs substrate.

Development of a new system which supports Majorana fermions and higher order parafermions. Recently several experiments [1-5] (including one from our group [1]) investigated synthetic topological superconductors, where Majorana fermions can be localized at the ends of a 1D wire. Unfortunately, neither experiment is unambiguously conclusive: tunneling experiments measured properties that are not unique to Majorana fermions, while experiments which probe Josephson relation were performed in a non-linear regime. No experiment even attempted to probe non-Abelian braiding statistics, the most exciting and technologically relevant property of Majorana fermions, and there is a serious challenge to extend 1D topological wires into a 2D network where statistic can be assessed. Over the last year we worked on the development of a new system which combines benefits and topological protection of an FQHE system with localization and electrostatic control of a 1D wire. In that system it should be possible to realize both Majorana fermions and parafermions, localize, manipulate, and braid (exchange) them and, hopefully, demonstrate non-Abelian statistics.

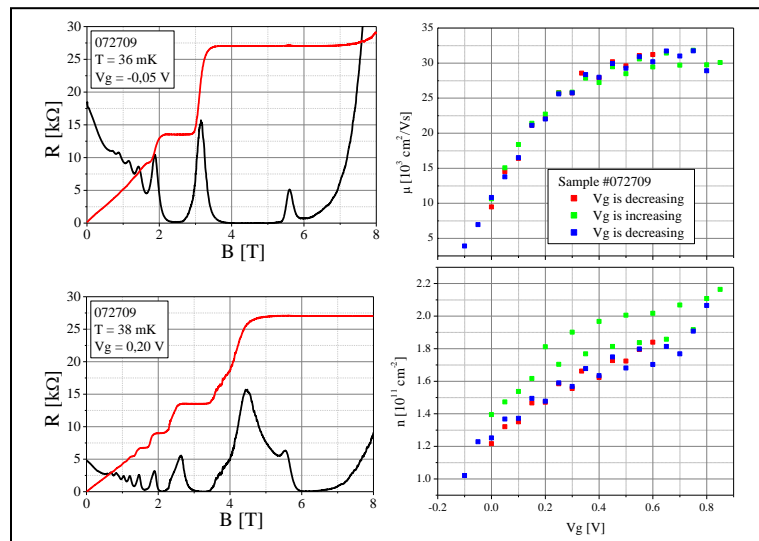


Figure 2: Left: Quantum Hall effect in gated quantum well at different gate voltages. A peak at 5.5 Tesla may indicate level crossing. Right: density and mobility dependence on gate voltage in a gated quantum well.

Several wafers with high mobility 2D electron gases have been grown from new materials and we successfully demonstrated gating and density tuning, see Figure 2. The heterostructures are very similar to the conventional III-V GaAs/AlGaAs quantum wells, except that we designed a system where Landé

g -factor changes sign at high magnetic fields. With properly designed heterostructures the crossing field for the two spin subbands can be controlled *in situ* by electrostatic gating, see Figure 3a.

In the QHE regime current is localized along sample edges (edge channels). If a top gate is tuned in such a way that Zeeman splitting changes sign under the gate, as shown in Figure 3b, there will be two topologically protected counter-propagating edge states with opposite polarization confined to the edge of the gate. It is possible to induce superconducting coupling in such a counter-propagating edge channel by a proximity effect from superconducting contacts. Zero-energy modes will be localized near the contacts, these modes will be ordinary fermions for $v = 2$,

Majorana fermions for $v = 1$, and parafermions for $v = 1/3$. When such Josephson junction is embedded into an ac SQUID device, the energy-flux relation will be 2π -periodic for $v = 2$, 4π -periodic for Majorana fermions and 12π -periodic for parafermions. Quasiparticle exchange can be achieved by a sequence of gating shown in Figure 3 (c), the sequence is easily generalized to more complex braiding and fusion which involves several pairs of quasiparticles. These exchanges in conjunction with ac SQUID spectroscopy will allow us to probe spectrum of parafermions, demonstrate non-Abelian statistics and design a fault-tolerant qubit.

Future Plans

Development of topological superconductors based on InSb. We continue working on the growth improvement of InSb heterostructures as well as on the AFM lithography of these materials. AFM-fabricated InSb wires will be fabricated and characterized. We will also characterize oxidation and post-oxidation stability of thin Nb and NbN films and reproducibility of AFM-fabricated Josephson junctions and work on subsequent oxidation of multi-layer semiconductor/superconductor structures.

Development of rf measurement system. We designed and assembled most components for the development of a sensitive heterodyne detection system which, ideally, should allow us to measure single photon absorption in a Josephson junction. Assembly and characterization of the system, as well as the design of the coupling scheme for the actual device measurements will be the highest priority.

Development of a novel topological system. In order to be able to tune the field at which spin-polarized levels cross we have to design special heterostructures. We performed detailed simulations of heterostructures devices with various gate biases and optimized heterostructures design. Now we expect that several iterations of growth and characterization will be needed in order to fine-tune the growth

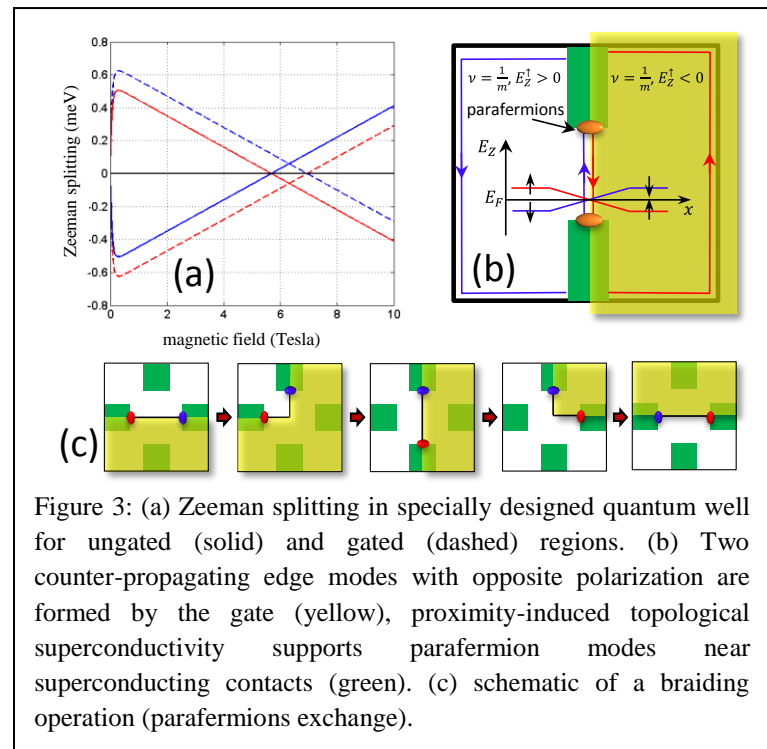


Figure 3: (a) Zeeman splitting in specially designed quantum well for ungated (solid) and gated (dashed) regions. (b) Two counter-propagating edge modes with opposite polarization are formed by the gate (yellow), proximity-induced topological superconductivity supports parafermion modes near superconducting contacts (green). (c) schematic of a braiding operation (parafermions exchange).

parameters. At the same time we will work on the development of low resistance contacts to these quantum wells using doping and superconducting materials with high critical fields. Further fabrication challenges will include development of low damage lithography of gates and gate insulation. The ultimate goal will be detection of proximity effects in gated structures at $\nu=1$ and $\nu=1/3$ quantum Hall regimes.

References

- [1] L. P. Rokhinson, X. Liu, J. K. Furdyna, *Observation of the fractional ac Josephson effect: the signature of Majorana particles*, Nature Physics **8**, 795 (2012)
- [2] V. Mourik, K. Zuo, S. M. Frolov, S. R. Plissard, E. P. A. M. Bakkers, and L. P. Kouwenhoven, Science **336**, 1003 (2012).
- [3] M. T. Deng, C. L. Yu, G. Y. Huang, M. Larsson, P. Caroff, and H. Q. Xu, Nano Lett. **12**, 6414 (2012).
- [4] A. Das, Y. Ronen, Y. Most, Y. Oreg, M. Heiblum, and H. Shtrikman, Nature Phys. **8**, 887 (2012).
- [5] A. D. K. Finck, D. J. Van Harlingen, P. K. Mohseni, K. Jung, and X. Li, Phys. Rev. Lett. **110**, 126406 (2013).

Session 9

High-Bandwidth Scanning Hall Probe Imaging of Driven Vortices in Periodic Potentials

Stuart Field, Department of Physics, Colorado State University, Fort Collins, CO 80523
field@lamar.colostate.edu

Program Scope

The goal of this project is to use a novel technique, *high-bandwidth scanning Hall probe microscopy*, to study the *local, real-time* dynamical states of current-driven vortices in artificially structured periodic potentials. This technique extends the frequency response of Hall probe microscopy from the usual 10–100 Hz used for imaging into the MHz range. Using this technique, the dynamics of driven vortices can be probed with an unprecedented combination of temporal and spatial resolutions, allowing a wealth of new physics, inaccessible to standard transport and magnetization measurements, to be uncovered.

Recent lithographic advances have made it possible to fabricate superconducting films that present a variety of *periodic* potentials to vortices in the film. Interesting effects of commensurability arise when the vortex spacing, easily adjusted by varying the magnetic field, matches the period of the underlying potential. These effects include strong increases in the critical current and dips in the resistance, indicating that vortices become particularly strongly pinned at these special matching fields. More recently, attention has turned to the *dynamics* of vortices driven across the film by the imposition of an external current. Again, commensurability has a profound effect on the depinning of vortices from their static configurations, and on the detailed nature of their dynamical trajectories.

In order to understand the nature of these states, this project makes use of high-bandwidth scanning Hall probe microscopy to image the trajectories of vortices moving in a periodic potential. The technique uses a powerful combination of standard low-bandwidth imaging with several high bandwidth (~5 MHz) imaging modes, including a method of making high-speed movies for vortices driven by an ac current in a periodic potential. Using these advanced imaging techniques, many of the outstanding questions concerning vortex dynamics in these systems can be directly addressed.

A number of specific experimental systems are being explored. Vortices in two-dimensional potentials have unique depinning signatures that can best be addressed by real-space imaging. Once vortices are moving, a variety of dynamical states are predicted, including simple channeled flow and several more complex disordered flows. There are also remarkable effects observed when vortices are driven, in addition to a dc current, a high-frequency ac current. The real-space, dynamical nature of all of these systems are best explored by a high-bandwidth imaging technique.

Recent Progress

The infrastructure for this project is largely being built from the ground up. Thus, in this first year of the project we have been working mainly on sample preparation, and the instrumentation necessary for making physics measurements. Significant progress has been made in all of the key areas of fabrication and instrumentation, as outlined below.

Cryocooler Development: We measure our superconducting samples in a closed-cycle cryocooler that is the centerpiece of our experimental measuring station. The critical temperatures of the ultra-low-pinning granular aluminum films we will use in our experiments are in the range of 1.6–2.0 K, below the base temperature of about 2.5 K achievable by our Cryomech PT403 pulse-tube cryocooler. In addition, the base temperature of the cooler head oscillates about its mean temperature with a peak-to-peak value of some 150 mK, far too large an excursion for our experiments. Thus, over the last year we have modified our commercial instrument, allowing it to reach lower and more stable temperatures, as shown in Figure 1. Here, helium gas from an external tank is precooled to 50 K, further cooled in a heat exchanger attached to the cryocooler's regenerator, then liquefied in a condenser attached to the second stage. After flowing through a capillary impedance, the liquid helium enters and fills a small pot. The pot is externally pumped, cooling the helium down just as in a conventional helium refrigerator. Because the pot contains only a few cm³ of liquid helium, the total helium used during a run is very small, only a few dollars' worth. Because the instrument uses no cryogenic fluids, we have experienced fast turnarounds and the efficient throughput of samples and experiments.

A cooldown takes overnight (about 12 h), because of the large thermal mass of the sample stage attached to the pot, and because the pot is only weakly coupled to the 2nd stage. Once the sample stage reaches ~5 K, helium gas is introduced and the sample stage quickly cools (about 3 min) to its base temperature of around 1.38 K. Near its base temperature, the cryocooler has a temperature stability significantly better than 1 mK, which is ideal for our experiments.

Sample Fabrication: A key requirement of the experiments is the fabrication of superconducting films with a periodic thickness modulation. This modulation leads to a corresponding modulation of the vortex potential. We are implementing a novel method to construct smooth and reproducible thickness modulations by angle-evaporating the superconducting film onto a substrate which itself has a modulation in its surface profile.

To fabricate these substrates, we use electron-beam lithography to create a grating pattern in chrome-on-glass wafers. The chrome serves as a mask for a subsequent HF wet etch. When the chromium is removed, we are left with a glass substrate with a square-wave profile, as shown in the AFM scans in Fig. 2. Subsequent thermal annealing near the glass transition temperature then smooths this square wave into the required sinusoidal profile.

Important progress has also been made in the growth of the superconducting films that will be used in our experiments. For our samples we are using granular aluminum films that have extremely low inherent pinning; low-pinning films are critical so that the vortex dynamics are dictated solely by the artificial thickness modulation, and not by random disorder in the films themselves.

High-quality granular aluminum films are deceptively difficult to fabricate. Their superconducting properties are extremely sensitive to growth conditions, particularly on the evaporation rate and the pressure of the oxygen in which these films are grown.

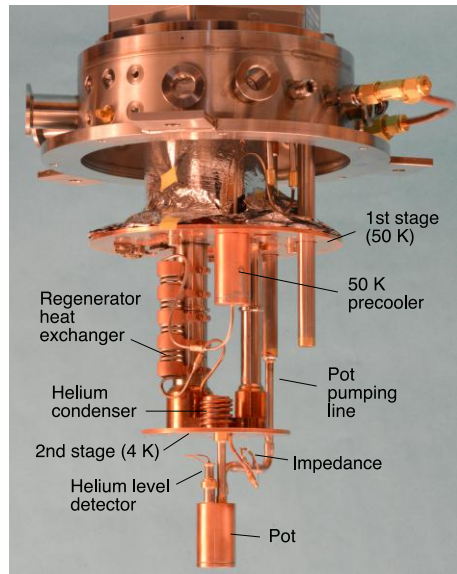


Figure 1. Closed-cycle cryocooler used for measuring superconducting samples.

In order to grow high-quality films we have completely rebuilt an older diffusion-pumped thermal evaporation system into a modern dry system, with a turbo pump backed by a scroll pump. This new system can reach a base pressure of 2.8×10^{-7} torr. We have also incorporated an oxygen flow controller to accurately set the oxygen pressure.

Exhaustive research into various types of evaporation sources, outgassing sources, and other details of the evaporation process have resulted in a highly controlled film growth process. Thin film samples with transition widths on the order of 5 mK can be grown using our system. Figure 3 shows a representative resistance-vs.-temperature curve.

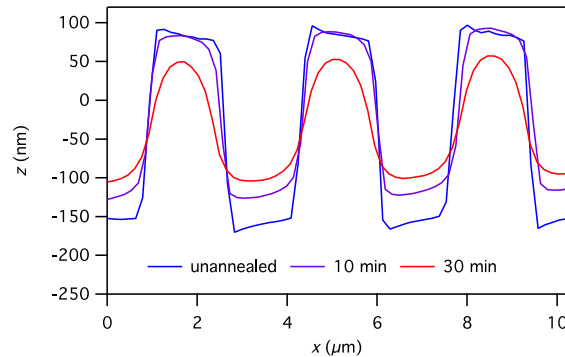


Figure 2. Annealing test of a Borofloat 33 substrate.

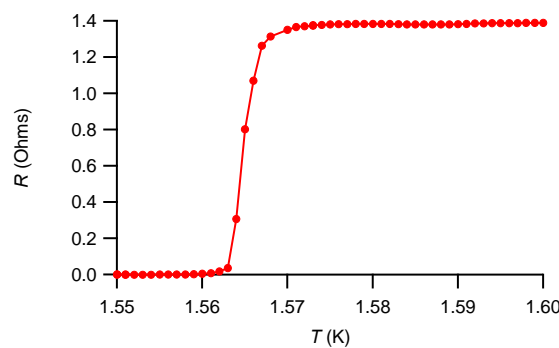


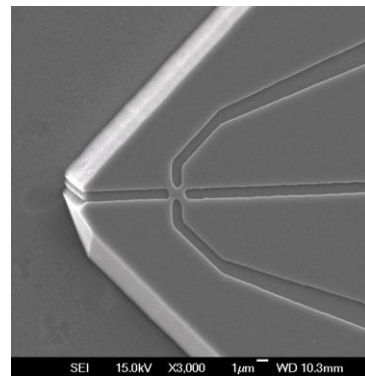
Figure 3. R vs. T curve for a granular aluminum sample.

Future Plans

Once the samples are complete, we will begin with a series of transport experiments designed to survey the phase space of temperature, magnetic field, and driving current. Here, we will look for transport signatures of the several dynamic vortex phases predicted in the theoretical literature. For example, we will drive the vortices with a dc current plus a small, high-frequency component. The resulting voltage response is expected to depend strongly on the underlying vortex state; for instance, we would expect to observe strong effects of commensurability and phase locking in ordered states in which the vortices move stepwise through the periodic potential, whereas these effects would presumably be greatly suppressed in the chaotic state predicted by several theoretical groups.

These transport measurements are, of course, preliminary to the overall goal of the project: high-bandwidth imaging studies of dynamical vortex states using scanning Hall probe microscopy. For this stage, we will need to incorporate the microscope into the cryocooler on a low-vibration stage, and we'll need to fabricate a new generation of Hall sensors.

Preliminary progress has been made on such sensors. Figure 4 shows a sensor fabricated on a GaAs chip; the corner of the sensor is lithographically defined by the deep trench to the left.



Publications

At this relatively early stage in this new project we do not yet have any science results or publications. However, we expect science experiments to start in the near future, and many interesting results over the next year.

Program Title: Study of multiband and topological superconductors through electron tunneling

Principle Investigator: Qi Li

Mailing Address: Department of Physics, Pennsylvania State University, University Park, PA 16802

e-mail: qil1@psu.edu

Project scope

The goal of the program is to use electron tunneling and point contact spectroscopy to study unconventional superconductors. Electron tunneling measurements can provide energy gap and quasiparticle spectroscopy information which are fundamental parameters for understanding superconductivity. For this purpose, high quality thin film samples will also be developed which are scientifically and technologically important. The focus of this project is on multiband superconductor MgB₂ and proximity induced topological superconductor NbSe₂/Bi₂Se₃ and MgB₂/Bi₂Se₃. Multiband superconductivity has gained tremendous attention recently owing to the discovery of superconductivity in MgB₂ and iron pnictides. Many new physical phenomena, such as the “Leggett mode”, interband interference, soliton, and Andreev bound state, have been proposed. In the previous project, very clean MgB₂ thin films have been achieved using hybrid physical chemical vapor deposition (HPCVD). The very clean samples as well as high T_c make MgB₂ an ideal model system for exploring multiband effects which can be easily smeared by the interband scattering. Topological superconductors are newly predicted new superconducting state after the discovery of topological insulators. Topological insulator is an insulator in bulk, but contains conducting surface states. The surface states can become superconducting when it is in contact with superconductors. One particularly significant effect is the possible presence of Majorana fermions, which are their own antiparticles and have potential applications in quantum information processing. In this project, Bi₂Se₃ thin films have been achieved by using HPCVD technique and bilayer of MgB₂/Bi₂Se₃ have also been fabricated *in situ*. Point contact and electron tunneling have been studied on MgB₂/Bi₂Se₃ as well as on MBE grown NbSe₂/Bi₂Se₃ bilayers (reference 1-11).

Recent Progress

Proximity-induced superconductivity in Bi₂Se₃ by point contact spectroscopy

We have successfully fabricated Bi₂Se₃ thin films using HPCVD technique⁵ which achieved similar carrier concentration and mobility as thin films grown using MBE technique. Epitaxial bilayers of MgB₂/Bi₂Se₃ have been grown using HPCVD and Bi₂Se₃ thin films have been grown on NbSe₂ single crystals in Prof. Samarth’s group at Penn State.

We have studied the point contact spectroscopy in NbSe₂ single crystal and NbSe₂/Bi₂Se₃ heterostructure samples by the so-called “soft” point contact technique¹² with silver planar contact about 50 – 100 μm. The point contact spectra on a 16 quintuple layer (QL) NbSe₂/Bi₂Se₃ heterostructure sample are shown in Fig. 1. At temperatures below the T_c (~7.1 K) of NbSe₂, the differential conductance (dI/dV) around zero bias increases as a result of the Andreev reflection process, similar to the bare NbSe₂ spectra. Strikingly, a

second differential conductance increase appears below ~ 5 K, corresponding to a proximity induced energy gap at the $\text{NbSe}_2/\text{Bi}_2\text{Se}_3$ interface.

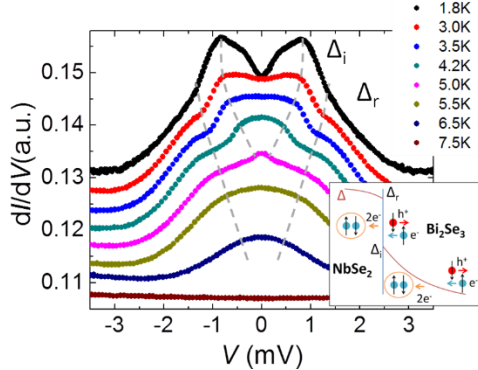


Fig. 1. Conductance v.s. voltage bias spectra of a silver point contact on a $\text{NbSe}_2/\text{Bi}_2\text{Se}_3$ bilayer at different temperatures. The gray dashlines mark the superconducting gap of NbSe_2 Δ_r and induced gap in Bi_2Se_3 Δ_i at $\text{NbSe}_2/\text{Bi}_2\text{Se}_3$ interface. The bottom right inset shows the two different Andreev reflection processes corresponding to Δ_r and Δ_i .

We obtain the NbSe_2 gap changing from 0 to ~ 1.3 mV from 7.1 K to 1.8 K. The induced gap changes from 0 to ~ 0.8 mV from 5.0 K to 1.8 K. The induced superconducting order parameter in Bi_2Se_3 decays within the proximity coherence length. Injected electrons from the point contact are Andreev reflected inside the superconducting Bi_2Se_3 proximity layer if their energies are lower than the energy gap in Bi_2Se_3 . When their energies are above the induced gap Δ_i , injected electrons are not affected by the order parameter in the Bi_2Se_3 layer but Andreev reflected at the $\text{NbSe}_2/\text{Bi}_2\text{Se}_3$ interface. There is an additional fine gap feature around 0.3 meV in the spectrum at 1.8 K. It could be due to the induced gap at the Bi_2Se_3 layer top surface. Together with the ARPES results, our data demonstrated that superconductivity was successfully induced in the 3D TI Bi_2Se_3 .¹¹

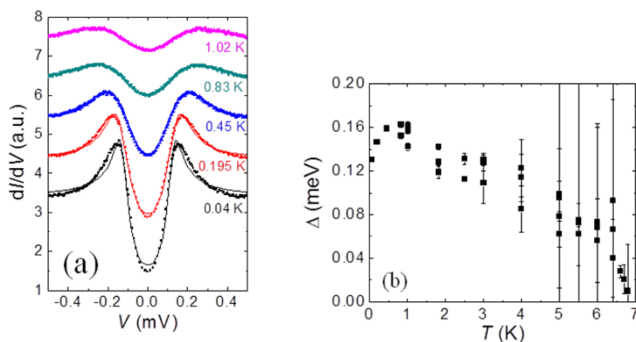


Fig. 2. (a) Conductance v.s. voltage spectra at different temperatures of a point contact junction. The lines are fitting curves using the BTK model. Curves are shifted vertically for clarity. (b) The superconducting gap value Δ from the single gap BTK fittings as a function of temperature T .

When the surface of Bi_2Se_3 has an oxide layer, the spectrum exhibits a tunneling behavior in certain point contact junctions. Fig. 2(a) plots the conductance spectra of a point contact junction on a 15QL $\text{NbSe}_2/\text{Bi}_2\text{Se}_3$ sample at different temperatures down to 40 mK and the fittings using the BTK model.¹³ Fig. 2(b) shows the fitted gap values as a function of temperature T . Because the sample is close to tunneling limit, the gap measured is from the top surface, which is much smaller than the gap at the interface Δ_i . Given the gap value ~ 0.8 meV at the bottom of the Bi_2Se_3 layer from Fig. 1 and assuming an exponential decay function for the induced gap value in the Bi_2Se_3 layer, the proximity coherence length is estimated to be ~ 8 nm at 3K in the Bi_2Se_3 layer.

It is important to note that the fitting curves using the standard BTK model deviate from the experimental data at temperatures below 0.45 K as shown in Fig. 2(a). Additionally, the gap value using a single gap from the fittings shows an abnormal decrease at low T ,

which is unusual as the superconductivity and proximity-coupling are usually enhanced with decreasing T . The conductance can be fitted with two gaps with one 0.16 meV and a smaller gap at 0.11 meV. ARPES measurement on similar samples showed that both the Bi_2Se_3 bulk state and the topological surface state became superconducting in the $\text{NbSe}_2/\text{Bi}_2\text{Se}_3$ heterostructure. Therefore, the second smaller gap could be a signature of the superconducting surface state at Bi_2Se_3 top surface while the main gap ~ 0.16 meV is due to the induced bulk superconducting state.

Momentum-dependent multiple gaps in MgB_2

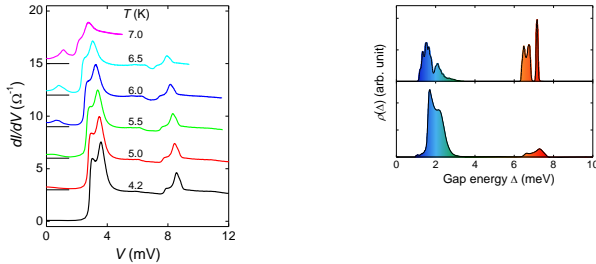


Fig. 3. (left) Tunneling spectrum of a $\text{MgB}_2/\text{native oxide}/\text{Pb}$ junction at different temperatures. Both π -gap feature and σ -gap feature show double peak structures. (right) The density of states and energy gap distribution of MgB_2 (top) calculated¹⁴ (bottom) derived from experimental data.

In MgB_2 , besides the widely-observed two superconducting energy gaps arising from the σ and π bands, theoretical calculations taking into account the fully anisotropic electron-phonon interaction further predict a distribution of gap values for both σ and π bands on the Fermi surface, which have not been observed before. Our results on very clean $\text{MgB}_2/\text{native oxide}/\text{Pb}$ junctions clearly show the distribution of energy gaps within one band in very clean samples. By deconvoluting the tunneling spectrum based on the density of state of Pb, we have derived the momentum-dependent energy gaps of MgB_2 , which are in good agreement with the anisotropic Eliashberg calculation.¹⁴ On samples with different amount disorders, the gap features become narrower with increasing disorder until it becomes a single gap. This is consistent with the theoretical prediction that scattering will smear out the multigap features.

Future plans

Topological superconductivity has gained tremendous attention recently owing to the unconventional nature and the possibility of observing Majorana fermions. We will continue to study the tunneling spectroscopy of the induced superconducting states, particular those features which may be from the surface superconducting states. We will focus on two systems on this study: MBE grown Bi_2Se_3 on superconducting substrates which offers the best crystal structure and atomically flat morphology of Bi_2Se_3 thin films; HPCVD grown $\text{MgB}_2/\text{Bi}_2\text{Se}_3$ which provides much higher T_c and wider range of temperature for the study. We have also recently grown Bi_2Te_3 nanotubes. We will first study the topological insulator state with much larger surface to bulk ratio in the nanotube structures. We will then induce superconductivity using superconducting contact leads. Magnetotransport measurement will be conducted to study the induced superconducting states in the nanotube structures.

Publications with DOE support

1. Wenqing Dai, V. Ferrando, A. V. Pogrebnyakov, R. H. T. Wilke, Ke Chen, Xiaojun Weng, Joan Redwing, Chung Wung Bark, Chang-Beom Eom, Y. Zhu, P. M. Voyles, Dwight Rickel, J. B. Betts, C. H. Mielke, A. Gurevich, D. C. Larbalestier, Qi Li and X. X. Xi, "High-field properties of carbon-doped MgB₂ thin films by hybrid physical-chemical vapor deposition using different carbon sources", *Supercond. Sci. Technol.* 24, 125014 (2011) . Selected as editor's choice of highlight for 2011.
2. H. B. Zhao, D. Talbayev, X. Ma, Y. H. Ren, A. Venimadhav, Qi Li, and G. Lüpke, Optical excitation of coherent spin precession via transient exchange field in La_{0.67}Ca_{0.33}MnO₃, *Phys. Rev. Lett.*, 107, 207205 (2011).
3. K. Chen, W. Dai, C. G. Zhuang, Qi Li, S. Carabello, J. G. Lambert, J. T. Mlack, R. C. Ramos, and X. X. Xi, "Momentum-dependent multiple gaps of MgB₂ probed by electron tunnelling spectroscopy on MgB₂/native oxide/Pb junctions", *Nature communication* 3, 619 (2012)
4. Kamron Fazel, Qi Li, and Kostadin Ivanov, "Effects of Superconductor Electron Screening on Fusion Reaction Rates" *Fusion Science and Technology* 61, 469 (2012).
5. Joseph E. Brom, Yue Ke, Renzhong Du, Dongjin Won, Xiaojun Weng, Kalissa Andre, Jarod C. Gagnon, Suzanne E. Mohney, Qi Li, Ke Chen, X. X. Xi, and Joan M. Redwing "Structural and electrical properties of epitaxial Bi₂Se₃ thin films grown by hybrid physical-chemical vapor deposition" *Appl. Phys. Lett.* 100, 162110 (2012)
6. Y. W. Yin, M. Raju, W.J. Hu, X.J. Weng, K. Zou, J. Zhu, X.G. Li, Z.D. Zhang, Qi Li "Multiferroic tunnel junctions" *FRONTIERS OF PHYSICS* 7, 380 (2012) (Cover page of the issue)
7. Wenqing Dai, Qi Li, Ke Chen, and X.X. Xi, "Tunneling investigation of the electron scattering effect on the momentum-dependent energy gap distribution in MgB₂", *J. Appl. Phys.* 113, 083902 (2013).
8. Y. W. Yin, J. D. Burton, Y.-M. Kim, A. Y. Borisevich, S. J. Pennycook, S. M. Yang, T. W. Noh, A. Gruverman, X. G. Li, E. Y. Tsymbal, and Q. Li, "Enhanced tunnelling electroresistance effect due to a ferroelectrically induced phase transition at a magnetic complex oxide interface", *Nature Materials* 12, 397 (2013)
9. T. P. Chen, K. Wu, S.Z. Wang, Qi Li, B. Chen, U. Tipparaach, C. J. Chen, Finite Size Effect On YBCO/PBCAO And YBCO/PECGO Nanometer Multilayers, *Int. J. Modern Phys B* 27, 1962009 (2013)
10. T.-P. Chen · K.Wu · Q. Li · B. Chen · H. Kandel, J.C. Chen, M. Mohammed, A. Al-Hilo, "2-D and Mott Transition Studies on Metal (M) Doped PrBa₂Cu₃O₇" *J. Low Temp. Phys.* (2013) DOI 10.1007/s10909-013-0893-7
11. Su-Yang Xu, Nasser Alidoust, Ilya Belopolski, Anthony Richardella, Chang Liu, Madhab Neupane, Song-Hsun Huang, Brian DellaBetta, Chen Fang, Wenqing Dai, Qi Li, Matthew J. Gilbert, Fangcheng Chou, Nitin Samarth, and M. Zahid Hasan, "Momentum space Cooper pairing in a half Dirac gas", submitted to *Science* (2013).

Other references

12. D. Daghero and R.S. Gonnelli, *Supercond. Sci. Technol.* **23**, 043001 (2010).
13. G. Blonder, M. Tinkham, and T. Klapwijk, *Phys. Rev. B* **25**, 4515 (1982).
14. H. Choi, D. Roundy, H. Sun, M.L. Cohen, and S.G. Louie, *Nature* **418**, 758 (2002).

Project Title: Thermodynamics of Strongly-Correlated Fermi Gases

Principal Investigator: John E. Thomas (Award # DE-SC0008646)

Mailing Address: Physics Department, North Carolina State University, Raleigh, NC 27695

E-mail: jethoma7@ncsu.edu

Program Scope

The purpose of the proposed program is the broad study of the thermodynamic properties of a strongly correlated Fermi gas of ^6Li atoms. The primary goals are (1) to make measurements away from (rather than on) a collisional (Feshbach) resonance, to understand the properties when the gas is no longer scale-invariant and (2) to explore a new ``relativistic'' regime of this unique quantum gas, by using optical fields to control the dispersion relation of the trapped interacting atoms. This novel cold atomic Fermi gas will be a paradigm for relativistic strongly correlated matter, from graphene to quark-gluon plasmas, and will bring trapped ultra-cold unitary gases a step closer to theoretical treatment by conformal field methods, which are difficult to apply to non-relativistic systems.

Our experiments employ an optically trapped cloud of ^6Li atoms in a mixture of the two lowest hyperfine states, which is tuned in bias magnetic field to a collisional (Feshbach) resonance at 834 G and cooled by evaporation. At resonance, where the s-wave scattering length diverges, the gas is universal, in the sense that the pressure p depends only on the local density and temperature. In this case, $p = \frac{2}{3} \varepsilon$, where ε is the local energy density, the same result that holds for an ideal gas. A remarkable property of this system is that it is tunable between two scale-invariant regimes, a non-interacting gas at 528 G and the most strongly interacting non-relativistic system known at 834 G. For this reason, an ultra-cold Fermi gas is ideally suited for studying scale invariance and the departure from scale invariance at finite scattering length, where the pressure-change $\Delta p \equiv p - \frac{2}{3} \varepsilon \neq 0$. The parameter $\Delta p / p$ serves as a dimensionless conformal symmetry breaking parameter.

Recent Progress

In the past few months, we made a major breakthrough in our studies: We performed the first precision measurements of scale invariance in *expanding* ultra-cold gases. Using two-cameras to measure the cloud profile in all three dimensions, we observed scale invariant flow and measured the bulk viscosity, which is found to be consistent with zero, as predicted for a scale-invariant system. We also investigated the departure from scale invariance, as a function of the conformal symmetry breaking parameter $\Delta p / p$. Our experiments are also the first to investigate thermodynamics in an expanding cloud, which enables a study of thermodynamic equilibrium in hydrodynamic *expansion*. This work connects our NSF program on hydrodynamic transport properties of strongly interacting Fermi gases, to our DOE program on thermodynamics.

In performing the experiments, we realized that bulk viscosity is most easily measured by releasing a Fermi gas cloud from an optical trap and monitoring the *sum* of the mean square cloud radii using two camera images taken along orthogonal directions. This *scalar* quantity eliminates entirely the effect of the shear viscosity, which is a rank two tensor. At a Feshbach resonance, where the bulk viscosity is expected to vanish, based on scale invariance, the mean square radius is then predicted to increase precisely as the square of the time after release, i.e., $\langle \mathbf{r}^2 \rangle = \langle \mathbf{r}^2 \rangle_0 + \frac{Et^2}{m}$, where E is the initial energy of the trapped cloud. This is an incredible result, since the individual cloud radii expand hydrodynamically, while the sum of squares of the three dimensional cloud radii expands ballistically! In Fig. 1, we show the x-y aspect ratio of the cloud as a function of time after release, for a resonantly interacting gas at 834 G, at four energies ranging from $E/E_F = 0.66$ to 1.5 (top to bottom), as determined from the size of the trapped cloud and measured trap parameters. As the energy increases, the time scale slows, due to increase in shear viscosity, used as the only free parameter in the solid theory curves. The fifth and lowest curve is for a ballistic gas (528 G) with $E/E_F = 1.8$. While the ballistic curve saturates to an aspect ratio of 1, the resonantly interacting data exhibits hydrodynamic “elliptic flow,” with the aspect ratio increasing to 1.5 as the cloud profile changes from a cigar to an ellipse. Fig. 2 shows $\langle \mathbf{r}^2 \rangle$ for the same data, demonstrating scale invariant flow.

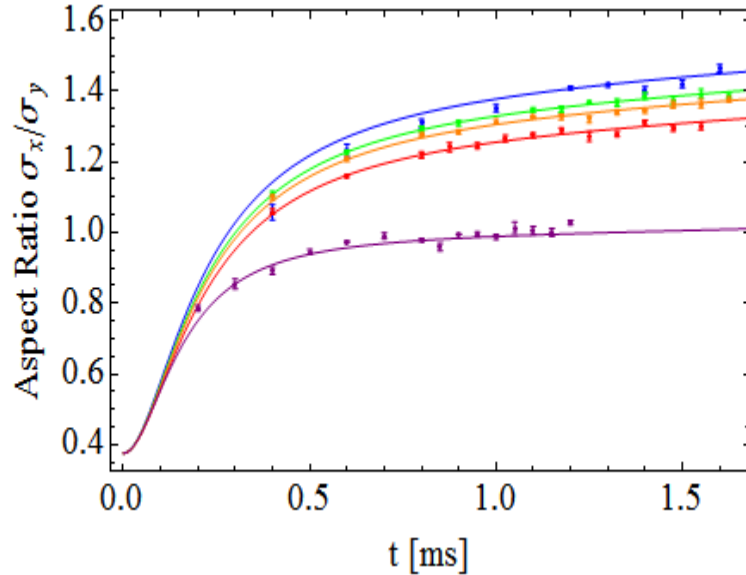


Fig. 1. Aspect ratio of the cloud in the x-y plane versus time after release from the optical trap. Top four curves: Resonantly interacting cloud, which exhibit energy-dependent elliptic flow, characteristic of a hydrodynamic system. The lowest curve is for an ideal Fermi gas, which exhibits ballistic flow, with the aspect ratio saturating to unity.

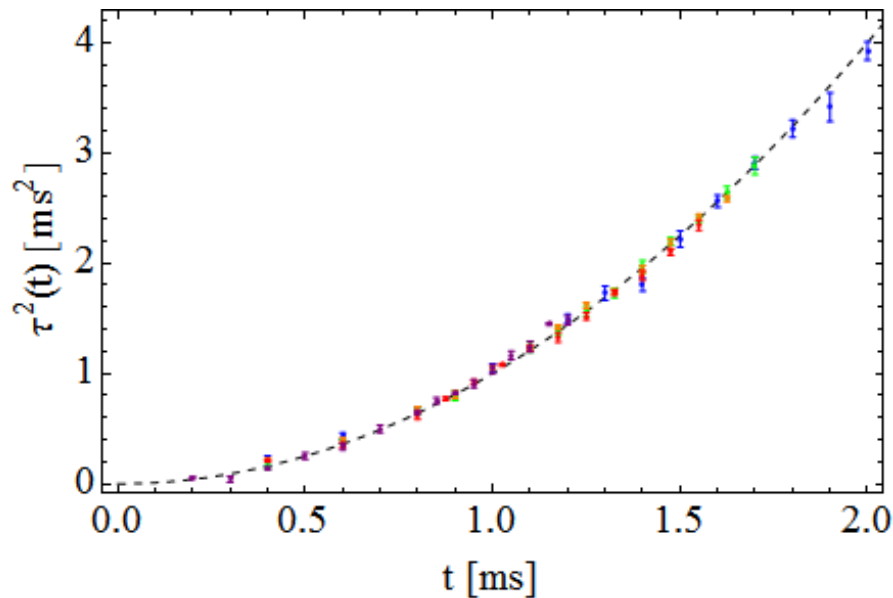


Fig. 2. Observation of scale-invariant hydrodynamic. Dots: Measured $\tau^2(t) \equiv m(\langle \mathbf{r}^2 \rangle - \langle \mathbf{r}^2 \rangle_0)/E$ for the data of Fig. 1 as a function of time after release. The data collapse onto a single t^2 curve, corresponding to ballistic flow of the mean square cloud size for both the resonantly- interacting hydrodynamic gas and for the non-interacting gas.

Future Plans

We are currently measuring the shear viscosity in the finite scattering length region and plan to explore both the thermodynamics and transport properties as a function of frequency, by modulating the trap depth. We are also implementing a bichromatic lattice system for optical control of the dispersion of a trapped Fermi gas.

References (which acknowledge DOE support).

- 1) E. Elliott, J. A. Joseph, and J. E. Thomas, "Scale invariance in expanding Fermi gases," submitted to *Science*.
- 2) A. Adams, L. D. Carr, T. Schäfer, P. Steinberg and J. E. Thomas, "Strongly correlated quantum fluids: Ultracold quantum gases, Quantum chromodynamic plasmas and Holographic duality," *New J. Phys.* **14** (2012) 115009 (121pp).
- 3) H. Wu and J. E. Thomas, "Optical control of Feshbach resonances in Fermi gases using molecular dark states," *Phys. Rev. Lett.* **108**, 010401 (2012).

- 4) Y. Zhang, W. Ong, I. Arakelyan, and J. E. Thomas, ``Polaron-to-polaron transitions in the radio-frequency spectrum of a quasi-two-dimensional Fermi gas," Phys. Rev. Lett. **108**, 235302 (2012).
- 5) H. Wu and J. E. Thomas, ``Optical control of the scattering length and effective range for magnetically tunable Feshbach resonances in ultracold gases," Phys. Rev. A **86**, 063625 (2012).

Program Title: Science of 100 Tesla

Principal Investigator: N. Harrison; Co-PIs: R. D. McDonald, V. Zapf, J. Singleton, M. Jaime

Mailing Address: Mail Stop E536, Los Alamos National Laboratory, Los Alamos, NM 87545

E-mail: nharrison@lanl.gov

Program Scope

The goal of this program is to conduct a coordinated research plan at the extremes of non-destructive high magnetic field, tackling pressing questions in condensed matter physics that only magnetic fields around 100 tesla can answer. Our scientific team ensures that the recent record delivery of non-destructive magnetic fields reaching 100 tesla (provided by the National High Magnetic Field Laboratory) is matched by an experimental program in the extremes of high magnetic field that is unparalleled by that any other laboratory—routinely publishing scientific results in fields extending to 100 tesla.

Magnetic fields manipulate matter either through a tunable nanometer length scale or a tunable magnetic energy scale (or sometimes both), enabling a great variety of different physical effects to be studied. For example; the magnetic lengthscale is important for pairing and cyclotron motion in unconventional superconducting materials, which constitutes one of our foremost research focus areas in 100 tesla magnetic fields. Work on unconventional superconductors includes the use of magnetic quantum oscillations to map the ground state of high T_c superconductors within the enigmatic pseudogap regime. The magnetic lengthscale can further be used for tuning commensurability phenomena in low dimensional materials, which constitutes another focus area of our program. Included here is the recent discovery of field-induced phases in two-dimensional frustrated quantum magnets and possible fractional states on the surface of topological insulators. The magnetic energy scale, meanwhile, is most relevant for tuning competing interactions or phase transitions in multifunctional magnetic materials, which is a further key focus area. The large intrinsic energy scales in multiferroic materials and materials susceptible to spin state transitions necessitates the use of 100 tesla magnetic fields.

Recent Progress

Recent experimental progress is centered on the recent achievement of non-destructive magnetic fields reaching 100 tesla for the first time, yielding several significant scientific results that have received much attention in the published literature and at international conferences. In the underdoped cuprate high T_c superconductors, for example, the increased range in inverse magnetic field has afforded unprecedented resolution in determining the Fermi surface topology [1]. The quantum oscillation beat pattern in Fig. 1a yields a distribution of several frequencies (see Fig. 1b) on performing a Fourier transform, each of which is associated with a unique cyclotron orbit on the Fermi surface. Rather than originating from three distinct sections of Fermi surface, the beat pattern and the frequency distribution can be fit (red and blue lines) to a simple model in which

carriers tunnel between bonding and antibonding Fermi surface sheets in strong magnetic fields.

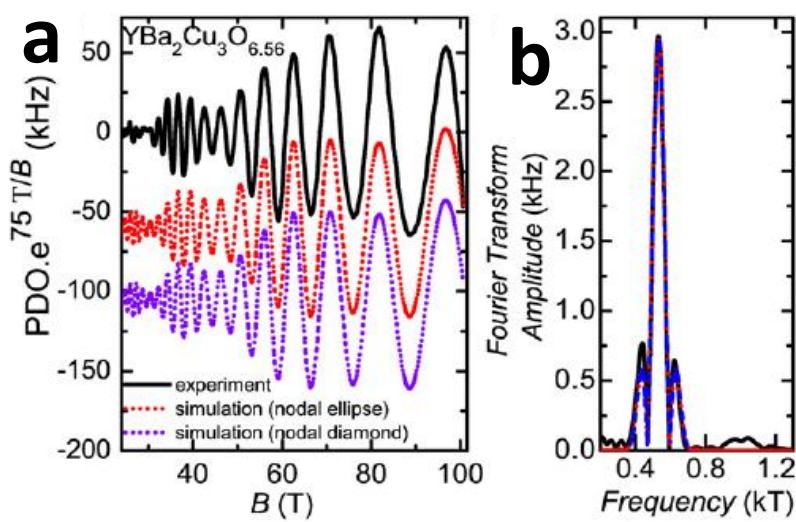


Fig. 1. **a**, Magnetic quantum oscillations measured in the underdoped high T_c superconductor $\text{YBa}_2\text{Cu}_3\text{O}_{6.56}$ to 100 tesla (black line). **b**, Fourier transform of the oscillations. Red and blue lines represent fits to Fermi surfaces with twofold and fourfold symmetry respectively.

In low dimensional materials, we now have hard thermodynamic evidence for long sought after field-stabilized phases in fields exceeding 85 tesla (both in the magnetization and magnetostriction) in the two-dimensional frustrated quantum magnet $\text{SrCu}_2(\text{BO}_3)_2$ [2] (see Fig. 2). As the magnetic field is increased above 20 tesla, the material undergoes a series of transitions into states with different magnetic superstructures, each of which is characterized by a uniform magnetization component that is a simple fraction of the fully saturated magnetization. Of particular importance is our discovery of the $\frac{1}{2}$ and $\frac{2}{5}$ phases, which correspond to the simplest possible superstructures against which proposed theoretical models can be rigorously tested. The $\frac{1}{2}$ phase had long been sought after in prior high magnetic field studies.

Further accomplishments in magnetic fields extending to 100 tesla include measurements of the upper critical field of optimally-doped high T_c pnictide superconductors [3], and the discovery of new forms of field-induced collective phenomena involving orbital ordering in the vicinity of a spin state transition in the perovskite LaCoO_3 [4].

Future Plans

Given the progress being made towards understanding the electronic structure of high T_c superconductors, this work will remain a key focus area. New high T_c sample compositions and dopings are only just becoming available, while the experimental techniques for conducting transport experiments are in the process of being upgraded. Preliminary measurements have indicated that the doping range over which quantum oscillations are seen can be doubled, providing information on the electronic structure much closer to the putative quantum critical point near optimal doping than previously obtained. The acquisition of 200 gigahertz – 1 terahertz extensions to our existing mm-

wave Vector Network Analyzer (MVNA) capability also opens up the opportunity for cyclotron resonance measurements to be performed on the cuprates and other strongly correlated materials, providing new and different information than what is currently gained through quantum oscillation measurements.

In magnetic materials, the availability of 100 tesla magnetic fields has inspired a renewed interest in spin state transitions and the search for new types of multiple functionality involving orbital ordering and lattice instabilities. In LaCoO_3 , the optical strain gauge method applied along different directions within the crystal relative to the magnetic field combined with measurements of the electric polarization will provide more specific information on the nature of the field-induced structural changes occurring above 60 tesla.

Finally, in low dimensional materials, the surface preparation of topological insulators has recently seen significant advancements at LANL, which we expect to significantly increase the quality of high magnetic field measurements.

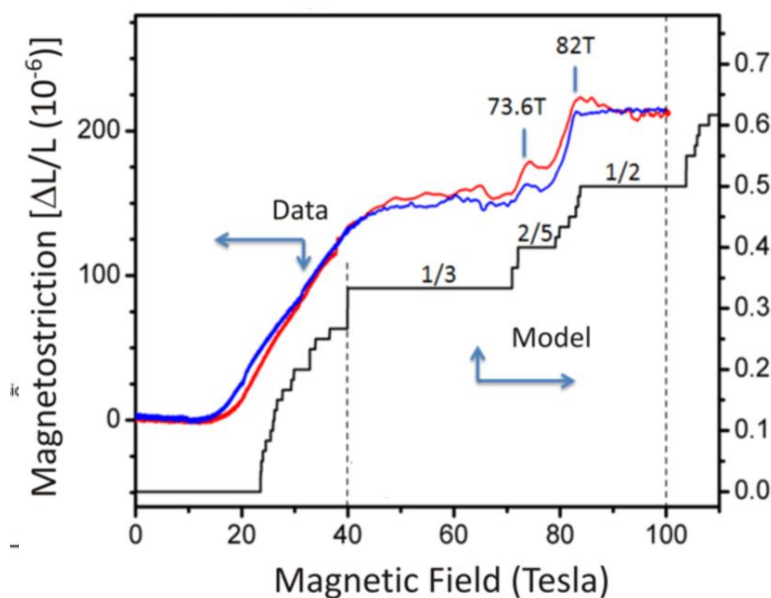


Fig. 2. Magnetostriiction measurements made using the fiber optical strain gauge method in the quantum magnet $\text{SrCu}_2(\text{BO}_3)_2$, revealing the discovery of field induced $\frac{1}{2}$ and $\frac{2}{5}$ phases. Red and blue curves correspond to rising and falling magnetic fields. The data are compared against a theoretical model (black curve).

References

- [1] S. E. Sebastian, N. Harrison, R.-X. Liang, D. A. Bonn, W. N. Hardy, C. H. Mielke, G. G. Lonzarich, *Physical Review Letters* **108**, 96403 (2012).
- [2] M. Jaime, R. Daou, S. A. Crooker, F. Weickert, A. Uchida, A. E. Feiguin, C. D. Batista, H. A. Dabkowska, B. D. Gaulin, *Proceedings of the National Academy of Science of the United States of America* **109**, 12404 (2012).

- [3] M. M. Altarawneh, G. W. Chern, N. Harrison, C. D. Batista, A. Uchida, M. Jaime, D. G. Rickel, S. A. Crooker, C. H. Mielke, J. B. Betts, J. F. Mitchell, M. J. R. Hoch, *Physical Review Letters* **109**, 037201 (2012).
- [4] E. Mun, N. Ni, J. M. Allred, R. J. Cava, O. Ayala, R. D. McDonald, N. Harrison, V. S. Zapf, *Physical Review B* **85**, 100502 (2012).
- [5] W. Kohn, *Physical Review* 123, 1242 (1961).

Publications fully supported by program over past 2 years:

Chemical potential oscillations from nodal Fermi surface pocket in the underdoped high-temperature superconductor $\text{YBa}_2\text{Cu}_3\text{O}_{6+x}$, Sebastian, SE; Harrison, N; Altarawneh, MM; Liang, RX; Bonn, DA; Hardy, WN; Lonzarich, GG, *NATURE COMMUNICATIONS* **2**, 471 (SEP 2011)

Near Doping-Independent Pocket Area from an Antinodal Fermi Surface Instability in Underdoped High Temperature Superconductors, Harrison, N, *PHYSICAL REVIEW LETTERS* **107**, 186408 (OCT 28 2011).

Anisotropic H_{c2} up to 92 T and the signature of multiband superconductivity in $\text{Ca}_{10}(\text{Pt}_4\text{As}_8)((\text{Fe}_{1-x}\text{Pt}_x)_2\text{As}_2)_5$, Mun, E; Ni, N; Allred, JM; Cava, RJ; Ayala, O; McDonald, RD; Harrison, N; Zapf, VS, *PHYSICAL REVIEW B* **85**, 100502 (MAR 5 2012).

Quantum Oscillations from Nodal Bilayer Magnetic Breakdown in the Underdoped High Temperature Superconductor $\text{YBa}_2\text{Cu}_3\text{O}_{6+x}$, Sebastian, SE; Harrison, N; Liang, RX; Bonn, DA; Hardy, WN; Mielke, CH; Lonzarich, GG, *PHYSICAL REVIEW LETTERS* **108**, 96403 (MAY 11 2012).

Cascade of Magnetic Field Induced Spin Transitions in LaCoO_3 , Altarawneh, MM; Chern, GW; Harrison, N; Batista, CD; Uchida, A; Jaime, M; Rickel, DG; Crooker, SA; Mielke, CH; Betts, JB; Mitchell, JF; Hoch, MJR, *PHYSICAL REVIEW LETTERS* **109**, 037201 (JUL 16 2012).

Magnetostriction and magnetic texture to 100.75 Tesla in frustrated $\text{SrCu}_2(\text{BO}_3)_2$, Jaime, M; Daou, R; Crooker, SA; Weickert, F; Uchida, A; Feiguin, AE; Batista, CD; Dabkowska, HA; Gaulin, BD, *PROCEEDINGS OF THE NATIONAL ACADEMY OF SCIENCES OF THE UNITED STATES OF AMERICA* **109**, 12404 (JUL 31 2012).

Fermi surface reconstruction from bilayer charge ordering in the underdoped high temperature superconductor $\text{YBa}_2\text{Cu}_3\text{O}_{6+x}$, Harrison, N; Sebastian, SE, NEW *JOURNAL OF PHYSICS* **14**, (SEP 27 2012).

Towards resolution of the Fermi surface in underdoped high- T_c superconductors, Sebastian, SE; Harrison, N; Lonzarich, GG, *REPORTS ON PROGRESS IN PHYSICS* **75**, 102501 (OCT 2012).

Program Title: Novel Behavior of Ferromagnet/Superconductor Hybrid Systems

Principle Investigator: Norman O. Birge; Co-PI: William P. Pratt, Jr.

**Mailing Address: Department of Physics and Astronomy, Michigan State University
567 Wilson Rd., East Lansing, MI 48824-2320**

E-mail: birge@pa.msu.edu

Program Scope

The interplay between superconductivity and ferromagnetism gives rise to a number of new and fascinating phenomena. The project focuses on the unusual proximity effects that arise when conventional superconducting (S) materials are placed in contact with conventional ferromagnetic (F) materials. Because of the strong exchange field, the electron pair correlations in F oscillate and decay rapidly with increasing distance from the S/F interface [1]. A decade ago, however, it was predicted that a new type of pair correlations, with spin-triplet symmetry, could be induced in S/F systems in the presence of certain kinds of magnetic inhomogeneity [2]. Those pair correlations penetrate deeply into ferromagnetic materials; hence they are sometimes called “long-range triplet correlations,” or LRTC.

Experimental verification of the LRTC took quite some time; there were hints of it as early as 2006, but convincing and reproducible confirmation had to wait until our results on S/F/S Josephson junctions published in 2010 [3]. (Shortly thereafter, several other groups also published strong evidence for the LRTC.) Since then, we have been deeply engaged in characterizing, optimizing, and controlling the LRTC. The objectives of this project are: i) to optimize generation of the LRTC in S/F/S Josephson junctions; ii) to fabricate sub-micron samples with single-domain magnetic layers, which will allow us to control the LRTC in a single sample; iii) to find a new signature of the LRTC in the tunneling density of states; iv) to measure the spatial decay of the LRTC over long distances, in planar samples patterned by e-beam lithography; and v) to explore the possibility of generating the LRTC under extreme non-equilibrium conditions, for example by magnetization precession.

The LRTC has scientific interest beyond simply giving rise to a long-range superconducting proximity effect in ferromagnetic materials. The handful of spin-triplet superconductors that occur in nature all have p-wave orbital angular momentum to satisfy the fermion anti-symmetry requirement of quantum mechanics. In contrast, the LRTC can have s-wave symmetry, which makes it more robust to disorder. In order not to violate quantum mechanics, the pair correlation function must then be odd under time-reversal, or equivalently, odd in Matsubara frequency. Although the idea of odd-frequency pair correlations dates back to a paper by Berezinski in 1974 [4], the LRTC is the first example of such correlations occurring in real physical systems, to our knowledge. The odd-frequency nature of the LRTC is predicted to give rise to a peak in the density of states at the Fermi level, which we are trying to measure by tunneling spectroscopy.

We view the training of students as an essential element of our work – as important as our contributions to the scientific knowledge base in our field. Three graduate students have received their PhD's working on this project, and three more are currently involved. Two visiting students from Germany and four MSU undergraduates have contributed to this project.

Recent Progress

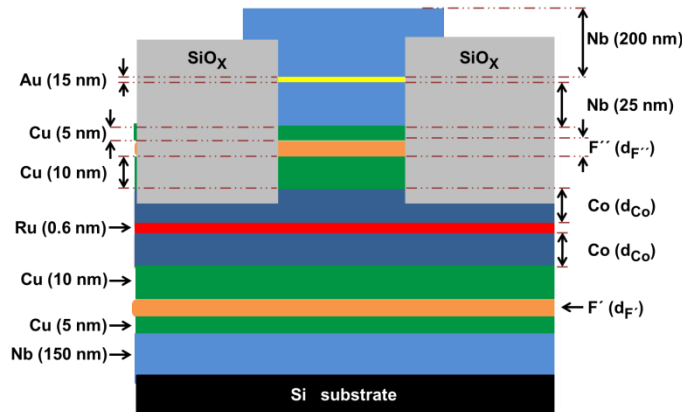


Figure 1: Schematic representation of our Josephson junction samples (not to scale). The current flows in the vertical direction.

coupled antiparallel to each other. The SAF cancels the intrinsic magnetic flux in the junctions, enabling us to characterize our junctions by measuring the “Fraunhofer patterns” of critical current vs applied in-plane magnetic field. (The supercurrent flows in the out-of-plane direction.)

Our first major advance since our initial discovery of the LRTC was the discovery that the amplitude of the spin-triplet supercurrent in our Josephson junctions could be enhanced by magnetizing the samples in a large in-plane magnetic field [6]. This discovery relied on a peculiar property of the Co/Ru/Co SAF. During application of a large in-plane field, the SAF undergoes a spin-flop transition, whereby the two Co layers point nearly perpendicular to the applied field direction. At the same time, the field magnetizes the F' and F'' layers in the field direction. The resulting situation, with the F layer magnetization perpendicular to the F' and F'' magnetizations, maximizes the conversion of spin-singlet to spin-triplet supercurrent [7]. More recently, we have replaced the Co/Ru/Co SAF with a [Co/Ni] multilayer with perpendicular magnetic anisotropy. The Josephson junctions containing the [Co/Ni] multilayers appear to have optimized spin-triplet supercurrent in the virgin state [8].

Control of the sign of the Josephson coupling: One of the most pressing unresolved issues is the theoretical prediction that the Josephson coupling can change sign depending on the relative orientations of the magnetizations of the F', F, and F'' layers [7]. Standard Josephson junctions have positive coupling, meaning that the phases of the superconducting condensates in the superconductors on either side of the junction are the same in equilibrium (in the absence of supercurrent). Such junctions are called “0” junctions. One can also have “ π ” junctions, where the phases of the condensates differ by π in equilibrium. In π junctions, the current-phase relation has a minus sign relative to the case in 0 junctions. The existence of π junctions has been demonstrated in S/F/S Josephson junctions that carry only short-range, spin-singlet, supercurrent [9], but in those systems the sign of the coupling oscillates with F-layer thickness. In spin-triplet junctions, in contrast, the sign of the Josephson coupling has been predicted to be controllable *in a single sample* by controlling the magnetic configuration of the sample. There

Background: The Josephson junction samples we used to observe the LRTC have the sandwich geometry shown in Figure 1, with the general structure S/F'/F/F''/S, where F' and F'' are thin ferromagnetic layers (\approx a few nm), whereas F can be quite thick – up to 50 nm so far. In our initial work [2] we used either PdNi or CuNi alloy for F' and F'', but we later found that pure Ni was even more effective at producing spin-triplet supercurrent [5]. For the F layer, we used a Co/Ru/Co “synthetic antiferromagnetic” (SAF), in which the magnetizations of the two Co layers are

have been no experimental reports concerning the sign of the Josephson coupling in spin-triplet junctions. (Our own attempts to garner phase information indirectly from the area-dependence of the critical current were inconclusive [10].)

To address this issue, we are fabricating S/F'/F/F''/S junctions where F' is a hard magnetic material with in-plane magnetization (thin Ni), F is either the Co/Ru/Co SAF or the [Co/Ni] multilayer with perpendicular magnetization, and F'' is a soft magnetic material with in-plane magnetization (for the moment, a dilute PdFe alloy). Magnetizing the samples with a large in-plane field should result in parallel magnetizations of the F' and F'' layers, while the magnetization of F remains perpendicular to those. Theory predicts that the Josephson junction should be in the π state under those conditions [7]. Application of a small in-plane field in the opposite direction should reverse the F'' magnetization without affecting the F' magnetization.

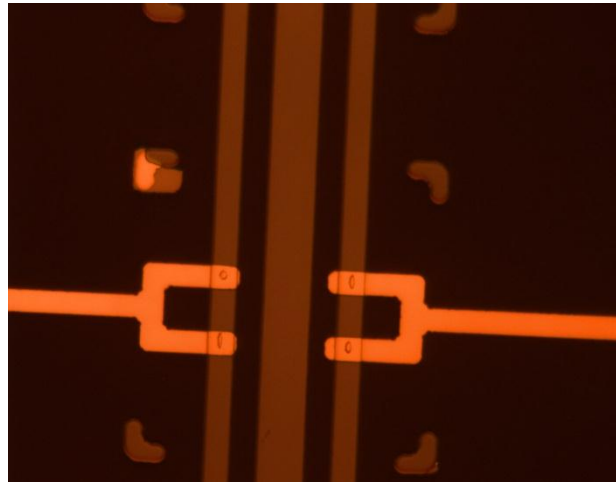


Figure 2: Two SQUID samples, each consisting of two S/F'/F/F''/S Josephson junctions of elliptical cross section. Current applied through the central dark line couples magnetic flux into the SQUIDs.

To stabilize the parallel and antiparallel configurations, the F'' layer is patterned into an elliptical nanomagnet using electron-beam lithography. To acquire information about the phase of the junctions, we measure two Josephson junctions in parallel, in a SQUID geometry as shown in Figure 2. The two junctions have different aspect ratios so that their F'' layers switch at different fields. Preliminary measurements of these samples are very promising; we have observed 0- π switching in the SQUID interference pattern of some samples, but the switching of the F'' layer is not yet under good control. We expect to have better results very soon – possibly even in time for the DOE-BES meeting in late September, 2013.

Future Plans

We are currently working on two projects in addition to the one described above:

1. Our sandwich-style Josephson junctions have total ferromagnetic layer thicknesses of a few tens of nanometers at most. When one speaks of a “long-range proximity effect,” however, one is usually thinking of hundreds of nanometers. An important goal is to understand the ultimate limits on the decay length of the spin-triplet correlations. Layer thicknesses in excess of 100 nm are not practical in the sandwich geometry (due to variations in growth morphology with increasing film thickness), but they are easily accessible in a planar geometry, using electron-beam lithography fabrication techniques. Given the peculiarities of sputtering deposition in tandem with lift-off processing, there have been a series of technical issues to overcome, but we are quite close to success. We have successfully fabricated and measured S/N/S Josephson junctions using the same deposition conditions that will be used for S/F/S samples. Results should be forthcoming soon.

2. We are pursuing tunneling measurements in the hope of observing the signature of the LRTC. In earlier work on samples of the form S/F/I/N, where I is a thin insulating tunnel barrier and N is a non-magnetic normal metal, we observed a series of oscillations in the proximity-induced features in the tunneling density of states as a function of F layer thickness [11]. Insertion of an additional F' layer, however, did not reveal the predicted signatures of the LRTC. We are currently fabricating samples with much smaller area than we used in [11], which should increase the signal-to-noise ratio of the experiment. The key issue is finding a fabrication recipe that produces tunnel barriers with a very flat tunneling density of states vs energy, so that the small LRTC signal will be visible above any background fluctuations.

References

- [1] See, for example, Proximity effects in superconductor-ferromagnet heterostructures, A.I. Buzdin, *Rev. Mod. Phys.* **77**, 935-976 (2005).
- [2] Josephson current in superconductor-ferromagnet structures with a nonhomogeneous magnetization, F.S. Bergeret, A.F. Volkov, and K.B. Efetov, *Phys. Rev. B* **64**, 134506 (2001).
- [3] Observation of spin-triplet superconductivity in Co-based Josephson junctions, T.S. Khaire, M.A. Khasawneh, W.P. Pratt, Jr., and N.O. Birge, *Phys. Rev. Lett.* **104**, 137002 (2010).
- [4] New Model of Anisotropic Phase of Superfluid He-3, V.L. Berezinskii, *JETP Lett.* **20**, 287-289 (1974).
- [5] Spin-triplet supercurrent in Co-based Josephson junctions, M.A. Khasawneh, T.S. Khaire, C. Klose, W.P. Pratt, Jr., and N.O. Birge, *Supercond. Sci. Technol.* **24**, 024005 (2011).
- [6] Optimization of spin-triplet supercurrent in ferromagnetic Josephson junctions, C. Klose, T.S. Khaire, Yixing Wang, W.P. Pratt, Jr., N.O. Birge, B.J. McMoran, T.P. Ginley, J.A. Borchers, B.J. Kirby, B.B. Maranville, and J. Unguris, *Phys. Rev. Lett.* **108**, 127002 (2012).
- [7] Long range triplet Josephson effect through a ferromagnetic trilayer, M. Houzet and A.I. Buzdin, *Phys. Rev. B* **76**, 060504(R) (2007).
- [8] Spin-triplet supercurrent in Co/Ni multilayer Josephson junctions with perpendicular anisotropy, E.C. Gingrich, P. Quarterman, Y. Wang, R. Loloe, W.P. Pratt, Jr., and N.O. Birge, *Phys. Rev. B* **86**, 224506 (2012).
- [9] Josephson junction through a thin ferromagnetic layer: Negative coupling, T. Kontos, M. Aprili, J. Lesueur, F. Genet, B. Stephanidis, and R. Boursier, *Phys. Rev. Lett.* **89**, 137007 (2002).
- [10] Area-dependence of spin-triplet supercurrent in ferromagnetic Josephson junctions, Y. Wang, W.P. Pratt, Jr., and N.O. Birge, *Phys. Rev. B* **85**, 214522 (2012).
- [11] Proximity-induced density-of-states oscillation in a superconductor/strong ferromagnet system, K. Boden, W.P. Pratt, Jr., and N.O. Birge, *Phys. Rev. B* **84**, 020510(R) (2011).

Publications from the past 2 years acknowledging DOE support include references [5], [6], [8], [10], and [11] from the above list, as well as:

- [12] Spin-memory loss at Co/Ru interfaces, M.A. Khasawneh, C. Klose, W.P. Pratt, Jr., and N.O. Birge, *Phys. Rev. B* **84**, 014425 (2011).

Session 10

Program Title: Probing Nanocrystal Electronic Structure and Dynamics in the Limit of Single Nanocrystals

Principle Investigator: Moungi Bawendi

Mailing Address: Dept. of Chemistry, MIT, Rm. 6-221, Cambridge, MA 02139

E-mail: mgb@mit.edu

Program Scope: Given the potential impact of devices that use NCs as a functional material in the energy field, it is crucial to understand *at a very basic level* the optical physics, both static and dynamic, of NCs of a variety of materials and morphologies. Without such understanding, designing novel structures, novel device architectures, and understanding the potential and limitations of present materials and devices is haphazard at best. A basic understanding of the optical physics of semiconductor NCs is the core aim of this program. We focus in large part on single NC spectroscopy to directly probe exciton and multiexciton spectroscopy and dynamics in a variety of NCs and NC hybrid structures.

The focus of our research consists of a set of critical studies of nanocrystal electronic structure and dynamics, largely at the level of single NCs, including: (1) utilizing a novel single molecule characterization technique that we have developed, Photon-Correlation Fourier Spectroscopy (PCFS), to reveal the intrinsic single NC spectrum and its dynamics at time scales from 30 nanoseconds to seconds and longer, as a function of temperature, directly in solution or fixed on a substrate, and using this to characterize interactions between single nanocrystals and their environment; (2) probing the dynamical and spectral properties of multiexcitons, as a function of temperature and through the development of solution and nth-order Photon Correlation Spectroscopy (nPCS) for higher order multiexcitons ($n > 2$); (3) applying PCFS and single NC Photon-Correlation Spectroscopies to Shortwave Infrared (SWIR) emitting NCs that have a band gap matched to the solar spectrum (e.g. PbS, PbSe, and InAs NCs) to extract fundamental intrinsic NC spectral and dynamical properties, using superconducting nanowire single photon detectors (SNSPDs); and (4) probing the dynamics of fluorescence intermittency to elucidate the effect of NC structure on fluorescence “blinking” and to understand mechanistically the connection between ensemble and single NC emission properties.

Recent Progress:

Development and applications of PCFS to single NCs

Our group has pioneered the development of two forms of PCFS, a new class of single-molecule spectroscopy that circumvents the limitations of conventional single-molecule methods. Single-NC PCFS measures the spectral correlation of a single NC immobilized on a substrate, revealing the previously inaccessible spectral dynamics of single NCs on timescales ranging from sub-microseconds to hundreds of milliseconds. Solution PCFS (S-PCFS) measures both the spectral correlation of the average single emitter within an ensemble *and* the autocorrelation of the ensemble spectrum itself by collecting emission from a dilute solution of emitters.

a) Direct observation of rapid discrete spectral diffusion events in single-NC fluorescence using single-NC PCFS

Our focus with low temperature PCFS has been in measuring the spectral diffusion of single-NC fluorescence. With PCFS, we can extract the intrinsic spectral lineshape of NC emission by comparing the energies of photon pairs spaced closely enough in time (*e.g.*<1 μ s) that they are drawn from the same quasi-static intrinsic spectrum. Our low temperature studies have measured single-NC linewidths on the order of 10 μ eV. Our single-NC studies open the door for a comprehensive survey of linewidth variability, a parameter unavailable to ensemble techniques. PCFS also allows us to access spectral dynamics across sub-millisecond timescales, enabling us to test standing hypotheses regarding the nature of spectral dynamics. Our latest manuscript under review (Beyler *et al*, 2013), directly reveals the underlying discrete spectral jumps that give rise to rapid spectral diffusion in single NCs (**Figure 1**).

b) Observation of batch-to-batch variations in the average single-NC linewidth using S-PCFS

Our focus with S-PCFS has been in measuring the spectral properties of single NCs at room temperature – the pertinent regime for NC applications. S-PCFS is the ideal tool to study the emission linewidths of NCs with large sample statistics and high signal-to-noise ratios, but without the selection bias unavoidable in conventional single-NC studies (Cui *et al*, 2013). Our investigations have revealed wide variations in the intrinsic linewidth of single NCs, which arise from excitonic coupling to phonons within the NC and to vibrations in the environment. In **Figure 2(a)**, we show the average single-NC and ensemble spectral correlations for NCs with three different core materials: CdSe, InP, and InAs. Surprisingly, these samples were found to have very similar single-NC linewidths. This result demonstrates that the broad ensemble spectra of InP and InAs core/shell particles are limited by sample polydispersity, and that the synthesis of monodisperse InP and InAs NCs could produce ensemble linewidths as narrow as modern CdSe samples. **Figure 2(b)** shows that the single-NC linewidth is dramatically broadened for CdSe particles undergoing CdS shell growth. These results suggest that the single-NC lineshape

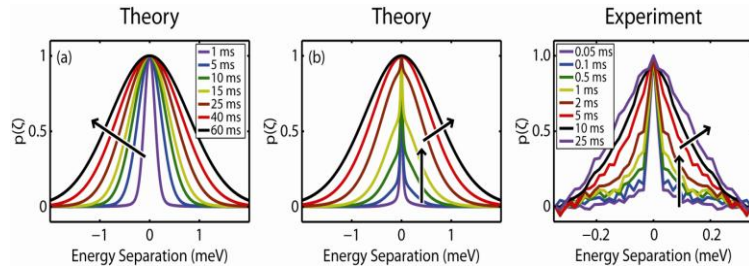


Figure 1. Modeled spectral correlations for a NC undergoing (a) continuous and (b) discrete spectral diffusion. The discrete behavior is distinguished by the presence of two distinct distributions that reflect whether spectral diffusion events occurred over the given time interval. (c) An experimental spectral correlation of an actual NC exhibits discrete spectral diffusion.

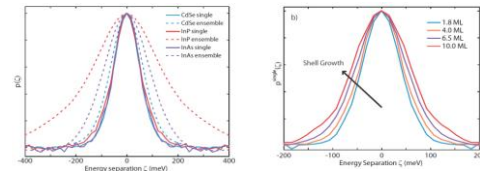


Figure 2. a) Single-NC (solid) and ensemble (dotted) spectral correlation functions for core/shell particles with CdSe, InP, and InAs cores. The differences between single-NC and ensemble spectral correlations are caused by spectral polydispersity. **b)** Shell growth broadens the single-NC spectral correlation in CdSe/CdS particles.

is defined by a delicate interplay between the various structural and compositional parameters.

Interrogating SWIR nanocrystals in the single molecule limit

We have successfully pushed the sensitivity of SWIR photon collection and detection to the ultimate limit – single photons from a single NC – using a unique detector that circumvents the intrinsic sensitivity problems of traditional technologies by relying on a radically different photon counting mechanism. We demonstrated the impact of this method (Correa *et al.*, 2012), by interrogating individual colloidal NCs composed of lead sulfide (PbS) and indium arsenide (InAs) with emission beyond 1100 nm, discovering that both systems exhibit significant fluorescence intermittency (**Figure 3**). In addition, we quantified the purity of the single photon stream from a PbS NC under ambient conditions using photon correlation obtaining an ‘antibunching’ dip of $g^{(2)}(0) = 0.19$ (**Figure 4**), a definitive proof that we had localized a single NC.

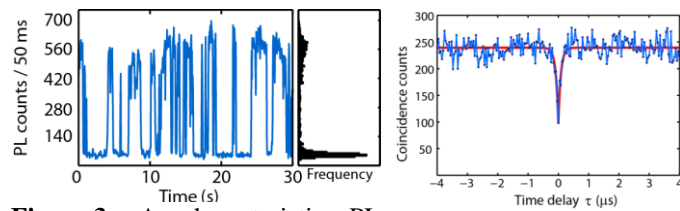


Figure 3: A characteristic PL blinking trace for a single PbS nanocrystal emitting at ~ 1150 nm.

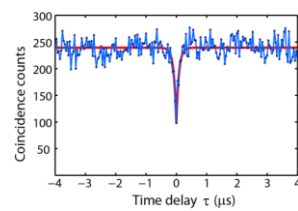


Figure 4: 2nd-order photon correlation for a PbS NC, with $g^{(2)}(0) = 0.19$ after background subtraction.

Correlation between biexciton QY and exciton blinking in CdSe/CdS NCs

This work represents our effort towards elucidating the mechanism behind biexciton recombination in a new generation of colloidal nanocrystals that we have recently developed (O. Chen *et al.* 2013). The novel core/shell NCs we used in this work have a high-quality relatively thin shell (~ 2.3 nm thick), a high PL ON fraction as measured from single NC blinking traces, and qualitatively different power law statistics for the ON and OFF times when compared to conventional CdSe NCs. These studies imply that the presence of a well-grown and relatively thin shell is capable of suppressing exciton blinking by limiting access to non-radiative pathways.

As reported in (Zhao *et al.* 2012), we explored the BX recombination mechanism in single NCs by studying the relationship between BX QYs and exciton blinking, as well as the excitation wavelength dependence of the BX QY. To achieve this, we utilized a novel method that we introduced (Nair *et al.* 2011) to directly measure the BX QY of single NCs using photon correlation at low flux, sidestepping problems inherent to previously used high flux ensemble techniques.

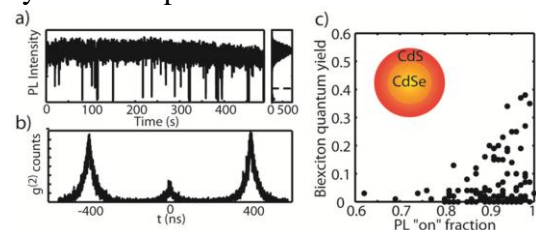


Figure 5: Representative a) PL blinking and b) antibunching traces for a single CdSe/CdS NC under mild, pulsed excitation. c) The weak correlation between the BX QY and ON fraction suggests that Auger recombination is not a shared mechanism.

Future Plans:

1. *Revealing the Intrinsic Single-Nanocrystal Spectrum and its Dynamics Using PCFS.* We plan to probe interactions between NC excitons and their environment using PCFS, coupled with a theoretical model to extract exciton-environment coupling parameters from the intrinsic single-NC linshape. We also plan to probe and understand the spectral dynamics of single NCs across all timescales and temperatures.
2. *Understanding Multiexciton States in Single Nanocrystals.* We plan to study the influence of many-body processes on nanocrystal relaxation by measuring the multiexciton quantum yield of single NCs, through the development of nth-order Photon Correlation Spectroscopy (nPCS).
3. *Probing Single-NC Spectral and Photon Correlations in the Shortwave Infrared (SWIR).* We plan on measuring the homogenous linewidth, spectral dynamics, and multiexciton properties of single lead chalcogenide NCs using PCFS, nPCS, and SNSPDs.

Publications with support from this DoE program in the last two years.

1. Nair, G.; Chang, L.-Y.; Geyer, S. M.; Bawendi, M. G. "Perspective on the prospects of a carrier multiplication nanocrystal solar cell" *Nano Letters* **2011**, *11*:2145–2151.
2. Nair, G.; Zhao, J.; Bawendi, M. G. "Biexciton Quantum Yield of Single Semiconductor Nanocrystals from Photon Statistics" *Nano Letters* **2011**, *11*: 1136-1140
3. Correa, R. E.; Dauler, E. A.; Nair, G.; Pan, S. H.; Rosenberg, D.; Kerman, A. J.; Molnar, R. J.; Hu, X.; Marsili, F.; Anant, V.; Berggren, K. K.; Bawendi, M. G. "Single photon counting from individual nanocrystals in the infrared" *Nano Letters* **2012**, *12*:2953–2958
4. Zhao, J.; Chen, O.; Strasfeld, D. B.; Bawendi, M. G. "Biexciton quantum yield heterogeneities in single CdSe (CdS) core (shell) nanocrystals and its correlation to exciton blinking" *Nano Letters* **2012**, *12*:4477–4483
5. Chen, O.; Zhao, J.; Chauhan, V. P.; Cui, J.; Wong, C.; Harris, D. K.; Wei, H.; Han, H.-S.; Fukumura, D.; Jain, R. K.; Bawendi, M. G. "Compact high-quality CdSe–CdS core–shell nanocrystals with narrow emission linewidths and suppressed blinking" *Nature Materials* **2013**, *12*:1–7.
6. Cui, J.; Beyler, A. P.; Marshall, L. F.; Chen, O.; Harris, D. K.; Wanger, D. D.; Brokmann, X.; Bawendi, M. G. "Single-Nanocrystal Emission Linewidth Variability and Synthetic Tunability Revealed with Ensemble-Level Statistics" *Nature Chemistry* **2013**, *5*:602–606
7. Beyler, A. P.; Marshall, L. F.; Cui, J.; Brokmann, X.; Bawendi, M. G. "Direct Observation of Rapid Discrete Spectral Diffusion Events in Single Colloidal Quantum Dots" (*under review, 2013*)

Program Title: Electromagnetic response of correlated electron systems

PI: D.N. Basov

Address: Department of Physics, UCSD, La Jolla CA92093

E-mail: dbasov@ucsd.edu

Program Scope

The physics of correlated electron systems is rich, and many phenomena discovered in these materials still elude a thorough understanding. The complexity of these solids is, at least in part, related to their tendency towards the formation of electronic and/or magnetic inhomogeneities at diverse length scales. The dynamical properties of individual electronic phases commonly coexisting in correlated electron matter on the nano-meter (nm) scale remain largely unexplored because methods appropriate to the study of charge dynamics (transport, infrared/optical, and many other spectroscopies) lack the required spatial resolution. This deficiency is fundamental, and ought to be remedied in order to make critically needed advances in our understanding of complex correlations phenomena. The challenges involved in elucidating the physics of correlated systems call for the development of novel experimental approaches. Work carried out by the PI is aimed at advancing new methods including infrared (IR) nano-spectroscopy, nano-imaging and most recently ultra-fast pump-probe nano-spectroscopy to significantly advance the present experimental understanding of correlated electrons.

The program is focused on two systems: transition metal oxides (TMO) and graphene. Both classes of materials feature a wealth of new physical phenomena which are yet to be understood. Both classes of materials also hold great promise for technological applications. The program that is being implemented by the PI is aimed at exploring and exploiting the complex and novel many-body effects arising in these systems. The goal of the proposed IR nanoscopy studies is the systematic investigation of the role of electronic phase separation in the insulator-to-metal transition regime of a variety of TMO systems. The second component of the program is focused on the methodical examination of the electronic and plasmonic response by means of infrared nano-scopy.

Recent Progress (selected highlights only)

- 1) *Mott Physics Near the Insulator-To-Metal Transition in NdNiO₃.* We employed a novel approach to investigate the physics behind the insulator-to-metal transition in a prototypical correlated oxide. The PI employed spectroscopic ellipsometry to monitor transformations of the electromagnetic response of ultrathin strained films of NdNdO₃. Our results point to the dominant role of strong correlations (Mott physics) in the insulator-to-metal transition phenomena thus resolving a long standing controversy surrounding nickelate systems¹.
- 2) *Infrared Plasmon Interferometry of Many-Body effects in graphene.* We proposed a novel experimental technique to probe surface conductivity of complex materials based on the advances in near field infrared nano-optics in our group. Using a metalized tip of an atomic force microscope we launch a plasmon wave on the surface of the studied specimens. This wave propagates radially away from the tip, eventually reaches the sample edge, bounces back from the edge and eventually returns to the launching tip. We were able to show theoretically and confirmed experimentally that the standing wave

formed by the launched and back-reflected plasmons contains complete information on the real and imaginary part of the optical constants of the studied specimen. Thus it became possible for the first time to extract this quantitative information directly from near field images. When applied to monolayer graphene, these data revealed marked deviations of the optical constants from models of non-interacting Dirac quasiparticles².

- 3) *Development of ultra-fast pump-probe infrared nano-scopy.* The PI has designed and constructed a unique facility for broad-band (THz to near IR) pump-probe spectroscopy and imaging with the nano-scale spatial resolution. Pump-probe spectroscopy is central for exploring ultrafast dynamics of fundamental excitations, collective modes and energy transfer processes: phenomena that are of utmost importance in all of natural sciences and engineering. Typically carried out using conventional diffraction-limited optics, pump-probe experiments inherently average over local chemical, compositional, and electronic inhomogeneities. The PI has circumvent this deficiency and introduce pump-probe IR spectroscopy with ~20 nm spatial resolution far beyond the diffraction limit, which is accomplished in a setting of a scattering scanning near-field optical microscope. First data for the nano-scale pump-probe response of graphene revealed an opportunity of all-optical control of plasmonic effects at fs time scales (submitted).
- 4) *Publications.* The PI has published several works in high impact venues including *Physical Review Letters*^{1,3}, *Nature*², *Reviews of Modern Physics*⁴ and several other articles^{5,6,7,8}.

Future Plans

- 1) Capitalizing on fundamentally novel experimental capabilities for pump-probe spectroscopy at the nano-scale the PI will perform a series of experiments aimed at control of phase transitions in correlated oxides.
- 2) The PI will continue the exploration of electronic and plasmonic phenomena in graphene using samples with ultra-high electronic mobility. These studies will be aimed at uncovering intrinsic properties of graphene and, specifically, at assessing the role of many body physics in the properties of graphene.
- 3) The PI will carry out studies of plasmonic and phonon polaritonic behavior in two-dimensional van-der-Waals crystals including boron nitride and molybdenum sulfide. Preliminary experiments carried out by the PI have uncovered rich polaritonic effects in the response of ultrathin BN crystals that are of interest in the context of confining and controlling electromagnetic radiation at the nanoscale.

References (acknowledging DOE support)

¹ M. K. Stewart, Jian Liu, M. Kareev, J. Chakhalian, and D. N. Basov “*Mott Physics near the Insulator-To-Metal Transition in NdNiO₃*” Phys. Rev. Lett. 107, 176401 (2011).

² Z. Fei, A. S. Rodin, G. O. Andreev, W. Bao, A. S. McLeod, M. Wagner, L. M. Zhang, Z. Zhao, M. Thiemens, G. Dominguez, M. M. Fogler, A. H. Castro Neto, C. N. Lau, F. Keilmann & D. N. Basov, “*Gate-tuning of graphene plasmons revealed by infrared nano-imaging*” Nature 487 82 (2012).

³ M. K. Liu, B. Pardo, J. Zhang, M. M. Qazilbash, Sun Jin Yun, Z. Fei, Jun-Hwan Shin, Hyun-Tak Kim, D. N. Basov, and R. D. Averitt “*Photoinduced Phase Transitions by Time-Resolved*

Far-Infrared Spectroscopy in V₂O₃" Phys. Rev. Lett. 107, 066403 (2011)

⁴ Dawn A. Bonnell, D. N. Basov, Matthias Bode, Ulrike Diebold, Sergei V. Kalinin, Vidya Madhavan, Lukas Novotny, Miquel Salmeron, Udo D. Schwarz, and Paul S. Weiss "Imaging physical phenomena with local probes: From electrons to photons" Rev. Mod. Phys. 84, 1343 (2012).

⁵ M. K. Stewart, Jian Liu, R. K. Smith, B. C. Chapler, C.-H. Yee, R. E. Baumbach, M. B. Maple, K. Haule, J. Chakhalian, and D. N. Basov "Optical probe of strong correlations in LaNiO₃ thin films" Journal of Applied Physics 110, 033514 (2011).

⁶ M. K. Stewart, D. Brownstead, S. Wang, K. G. West, J. G. Ramirez, M. M. Qazilbash, N. B. Perkins, I. K. Schuller, and D. N. Basov "Insulator-to-metal transition and correlated metallic state of V₂O₃ investigated by optical spectroscopy" Physical Review B 85, 205113 (2012).

⁷ T. J. Huffman, Peng Xu, M. M. Qazilbash, E. J. Walter, H. Krakauer, Jiang Wei, D. H. Cobden, H. A. Bechtel, M. C. Martin, G. L. Carr, and D. N. Basov "Anisotropic infrared response of vanadium dioxide microcrystals" Physical Review B 87, 115121 (2013).

⁸ T. Timusk, J. P. Carbotte, C. C. Homes, D. N. Basov, and S. G. Sharapov, "Three-dimensional Dirac fermions in quasicrystals as seen via optical conductivity" Phys. Rev. B 87, 235121 (2013).

PROGRAM TITLE: Linear and Nonlinear Optical Properties of Metal-Nanoparticle Composites

PRINCIPAL INVESTIGATOR: Richard F. Haglund, Jr.

MAILING ADDRESS: Department of Physics and Astronomy, 6301 Stevenson Center Lane, Vanderbilt University, Nashville, TN 37235-1807

E-MAIL: richard.haglund@vanderbilt.edu

I. PROGRAM SCOPE

Efficiently harvesting, modulating and transporting light is central to technologies ranging from photovoltaics to telecommunications. The science underpinning these technologies asks how energy delivered by photons to nanocomposites comprising both metallic and insulating elements can be stored, manipulated and exchanged in material structures with characteristic feature sizes smaller than the wavelength of the incident photons. The central objective of our program is to understand the energetics and dynamics of photon interactions with metals and insulators at the nanoscale. This necessarily also involves the coupling of *excitons* (the electron-hole excitation created by photon absorption in an insulator) to *plasmons* (the fundamental many-body excitation of metallic electrons). Our technical approach, illustrated in Section II, combines nanofabrication, microscopy and time- and space-resolved optical spectroscopies, and is augmented by computational and analytical insights that help to guide experiment and illuminate scaling.

II. RECENT PROGRESS

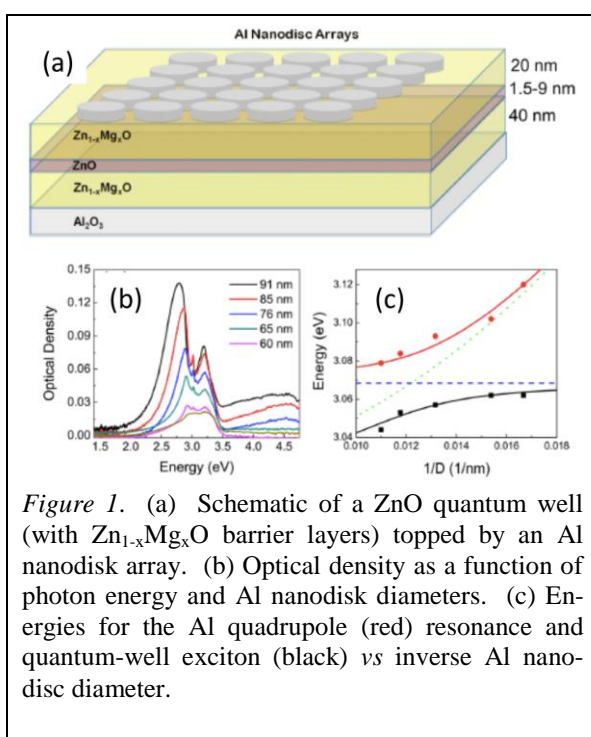


Figure 1. (a) Schematic of a ZnO quantum well (with $\text{Zn}_{1-x}\text{Mg}_x\text{O}$ barrier layers) topped by an Al nanodisk array. (b) Optical density as a function of photon energy and Al nanodisk diameters. (c) Energies for the Al quadrupole (red) resonance and quantum-well exciton (black) *vs* inverse Al nanodisk diameter.

Our technical approach is illustrated in a recent study [1] of the *quantum-well plasmonic heterostructure* shown in Fig. 1(a), designed to couple plasmons in Al nanodisks to the ultraviolet band-edge exciton in ZnO . The layered structure was fabricated by pulsed laser deposition in ultrahigh vacuum. After deposition of the barrier and quantum-well layers, aluminum (Al) nanodisc arrays with nanodisks of varying diameters were fabricated on top of the barrier layer by electron-beam lithography. Extinction measurements at 77K, shown in Figure 1(b), exhibit a sharp, size-dependent spectral feature superimposed on the broad plasmon resonance. Finite-difference, time-domain simulations of the spatial distribution of the electric field showed that the quadrupole field of the Al plasmons, rather than the dipole field, overlapped the band-edge emission from the ZnO quantum well. Interference between this broad plasmon resonance and the sharp emission resonance of the quantum well produces a Fano resonance on the blue side of the transmission spectrum. Plotting the dispersion of the exciton resonance peak as a function of the inverse nanoparticle diameter, one finds the avoided-crossing behavior typical of the Fano resonance and can calculate the exciton-plasmon coupling energy responsible for the phenomenon — in this case, 15 meV.

well produces a Fano resonance on the blue side of the transmission spectrum. Plotting the dispersion of the exciton resonance peak as a function of the inverse nanoparticle diameter, one finds the avoided-crossing behavior typical of the Fano resonance and can calculate the exciton-plasmon coupling energy responsible for the phenomenon — in this case, 15 meV.

The localized surface-plasmon resonance (LSPR) of Au nanodisk arrays can be used as a *nanoantenna to probe the insulator-to-metal transition* (IMT) in vanadium dioxide (VO_2), the prototypical quantum material. [2] Vanadium dioxide undergoes an insulator-to-metal transition at a critical temperature T_c near 340K, with a near-simultaneous structural transformation from the monoclinic, insulating ground state to the rutile, metallic metastable phase. The transformation from insulating band structure below the critical temperature T_c , to the metallic band structure above T_c is illustrated in Figure 2(a). The transition can also be initiated optically and electrically, thus VO_2 is being studied intensively as a potential switchable building block in electronic and opto-electronic devices.[3] We used a nano-disc array [Fig. 2(b)] to probe strong electron-electron correlations during the IMT, by observing the change in the energy and width of the LSPR. Figure 2(c) shows how the first-order phase transition is traced out by the hysteresis in LSPR energy, due to the changing dielectric function of the VO_2 as the $3d_{\parallel}$ band begins to overlap with the $3d_{\pi}$ band. The singular feature of the transition is the change in resonance width [Figure 2(d)] that occurs at the beginning and end of the hysteresis loop in Figure 2(c). Effective-medium calculations of this shift in resonance width shows that it can be fit by assuming a Lorentzian resonance at 1.4 eV, the interband transition energy — the same resonance needed to fit ellipsometric measurements of the VO_2 film.

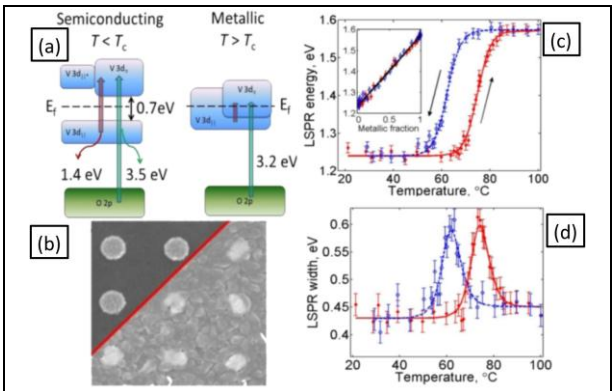


Figure 2. (a) Schematic band structures for the insulating and metallic states of VO_2 . (b) Array of Au nanodisks covered by a 60 nm film of VO_2 . (c) LSPR energy as a function of temperature showing the phase transition during the heating (red) and cooling (blue) cycles. (d) LSPR width during heating and cooling cycles; the smooth curve is a fit assuming a single resonant coupling with VO_2 at the interband transition.

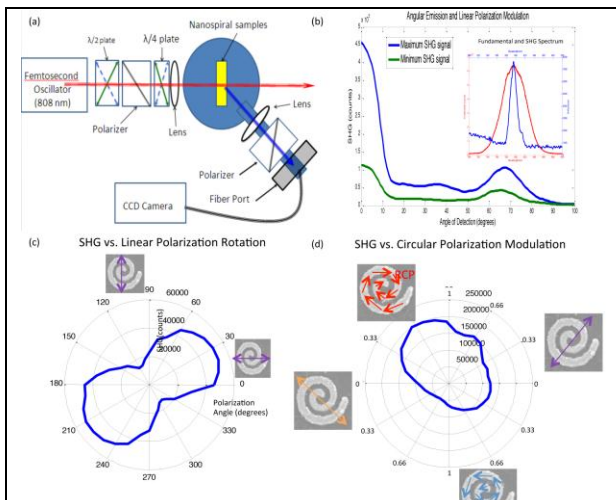


Figure 3. (a) Layout of SHG measurements. (b) SHG angular and spectral distributions. (c) SHG vs linear polarization angle. (d) SHG vs eccentricity for elliptically polarized light.

We are probing *ultrafast plasmon dynamics in asymmetric nanospiral geometries* by studying enhanced forward second-harmonic generation (SHG), forbidden in centrosymmetric structures.[4] Figure 3 exhibits SHG results from 4π Au nanospiral arrays, generated by an 800 nm oscillator with a pulse duration of 12 fs. Using the apparatus in Fig. 3(a), we measured angular distributions of SHG [Fig. 3(b)] and found an efficiency of order 10^{-11} for input powers up to the damage threshold of 45 mW; the blue curve is for the polarization angle optimized for SHG emission, the green curve for polarization rotated by 90° . The spectral distribution of the incident light and the SHG are shown in the inset. Figures 3(c) and 3(d) show polar plots of SHG emission as a function of linear polarization angle and eccentricity for elliptically polarized light.

III. FUTURE PLANS

Enhanced photoluminescence from ZnO excitons in the presence of metal nanoparticles results from both charge transfer and local-field enhancement. In ZnO quantum wells, we separated these mechanisms by using MgO spacer layers to vary the exciton-plasmon coupling strength.

We plan to follow this strategy for ZnO nanowires (NWs), with their manifold possibilities for nanoscale sensors and light sources. In preliminary studies, [5] we synthesized core-shell (ZnO/MgO) NWs and compared photoluminescence yields with and without decorating the NWs with metal nanoparticles. When ZnO NWs were coated with MgO [Fig. 4(a)], the core-shell structure enhanced the band-edge PL of the ZnO at specific MgO thicknesses, leaving the visible, defect PL unchanged. The band-edge PL enhancement is not accounted for by passivation of shallow ZnO defects. We think that the enhancement in Fig. 4(c) arises from spatially distinct, optical cavity modes [(1,1,0), (1,2,0)] in the NWs. When Ag nanoparticles were deposited onto the NWs [Fig. 4(b)], an even larger band-edge PL enhancement overall was seen [Fig. 4(d)], with an enhancement strongly dependent on MgO shell thickness. The difference between the two modes suggests that the (1,2,0) NW resonant mode couples more efficiently with the plasmon near-field.

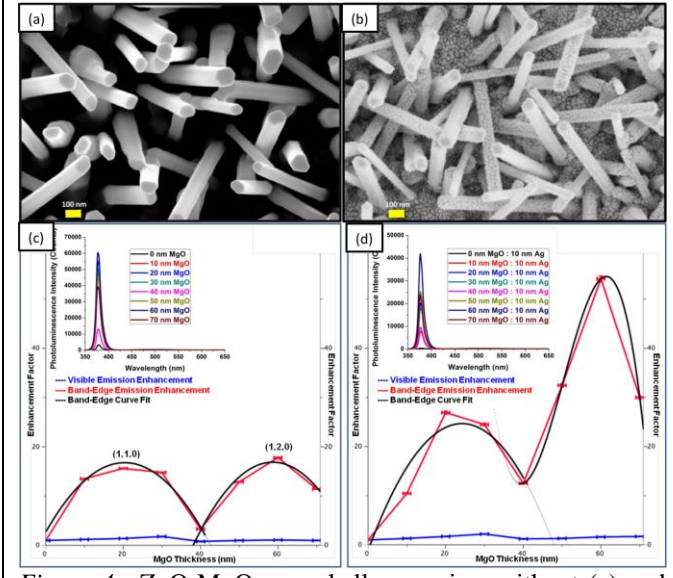


Figure 4. ZnO-MgO core-shell nanowires without (a) and (b) with Ag nanoparticles. Scale bars are 100 nm. Photoluminescence enhancement vs MgO thickness for sample (a) seen in (c) and for sample (b) in (d). Band-edge PL red, visible emission blue, fit black.

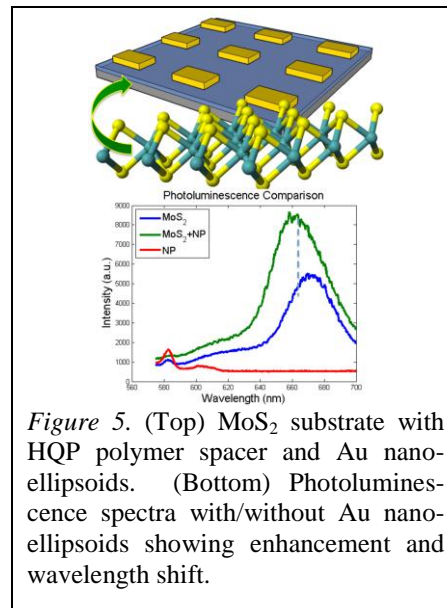


Figure 5. (Top) MoS₂ substrate with HQP polymer spacer and Au nanellipsoids. (Bottom) Photoluminescence spectra with/without Au nanellipsoids showing enhancement and wavelength shift.

We will also extend our studies of exciton-plasmon coupling to two-dimensional atomic-crystal materials (2DAs), such as the metal dichalcogenides. In recent work with colleagues at Vanderbilt [6, 7], we have studied electrical and strain control of the excitons in monolayer MoS₂, and have developed a technique for isolating a plasmonic control layer from monolayer MoS₂ by using the polymer HQP. We were able to shift the so-called A and B exciton resonances in the MoS₂ by choosing the dimensions of ellipsoidal Au nanorods to couple separately to each resonance. The preliminary results show that maximal photoluminescence enhancement of the excitons is achieved by exciting the corresponding plasmon resonance, while also shifting the exciton energy [Fig. 5], implying that we are tuning into the strong regime of exciton-plasmon coupling. These structures open up the possibility of plasmonically manipulated electro-optic devices in these 2DAs.

IV. REFERENCES

- [1] "Plasmon-exciton hybridization in ZnO-quantum well-Al nanodisc heterostructures," B. J. Lawrie, K.-W. Kim, D. P. Norton, R. F. Haglund, Jr., *Nano Letters* **12**, 6125-6157 (2012).
- [2] "Plasmon-electron coupling across the gold::vanadium dioxide interface," D. W. Ferrara, J. Nag, E. R. MacQuarrie, A. B. Kaye and R. F. Haglund, Jr., on line at *Nano Letters*, ASAP dx.doi.org/10.1021/nl401823r.
- [3] "An all-optical, reconfigurable, ultra-compact silicon ring resonator controlled by a semiconductor-to-metal transition," J. D. Ryckman, K. A. Hallman, R. E. Marvel, R. F. Haglund, Jr. and S. M. Weiss. *Optics Express* **21** (9), 10753-10763 (2013).
- [4] "Second harmonic generation from arrays of symmetric gold nanoparticles," M. D. McMahon, R. Lopez, R. F. Haglund, Jr., E. A. Ray and P. H. Bunton, *Physical Review B* **73**, 041401, *Rapid Communication* (2006).
- [5] "Surface-plasmon-mediated photoluminescence from Ag-coated ZnO-MgO core-shell nanowires," D. C Mayo, C. Marvinney, E. Bililign, R. Mu and R. F. Haglund, Jr., under review at *Thin Solid Films*, July 2013.
- [6] "Electrical control of optical properties of monolayer MoS₂," A. K. M. Newaz, D. Prasai, J. I. Ziegler, D. Caudel, S. Robinson, R. F. Haglund, Jr. and K. I. Bolotin, *Solid State Communications* **155**, 49-52 (2013).
- [7] "Bandgap Engineering of Strained Monolayer and Bilayer MoS₂," H. Conley, B. Wang, J. I. Ziegler, R. F. Haglund, Jr., S. T. Pantelides and K. I. Bolotin, on line at *Nano Letters* ASAP, dx.doi.org/10.1021/nl4014748.

V. PUBLICATIONS ACKNOWLEDGING DOE GRANT SUPPORT — JULY 2011 TO AUGUST 2013

1. "Plasmon-Enhanced Low-Power Laser Switching of Gold::Vanadium Dioxide Nanocomposites," D. W. Ferrara, E. R. MacQuarrie, A. B. Kaye, R. F. Haglund, Jr., *Applied Physics Letters* **98**, 241112 (2011).
2. "Fabricating a dichroic plasmonic mirror in fused silica by ion implantation," R. H. Magruder, III, S. Robinson, C. Smith, A. Meldrum and R. F. Haglund, Jr., *Applied Physics A* **107**, 935-942 (2012).
3. "Selective Purcell enhancement of defect emission in ZnO thin films," B. J. Lawrie, R. Mu and R. F. Haglund, Jr., *Optics Letters* **37** (9), 1538-1540 (2012).
4. "Plasmonic Enhancement of the Vanadium-Dioxide Phase Transition Induced by Low-Power Laser Irradiation," D. W. Ferrara, E. R. MacQuarrie, V. Diez-Blanco, J. Nag, A. B. Kaye and R. F. Haglund, Jr., *Applied Physics A: Materials and Processing*, **108**, 255-261 (2012).
5. "Plasmon-exciton hybridization in ZnO-quantum well-Al nanodisc heterostructures," B. J. Lawrie, K.-W. Kim, D. P. Norton, R. F. Haglund, Jr., *Nano Letters* **12**, 6125-6157 (2012).
6. "Dynamics of band-edge Purcell enhancement in defect-rich ZnO thin films," B. J. Lawrie, R. Mu and R. F. Haglund, Jr. *Plasmonics* **8**, 693-697 (2013).
7. "Complex Polarization Response in Plasmonic Nanospirals," J. I. Ziegler and R. F. Haglund, Jr., *Plasmonics* **8**:571-579 (2013).
8. "Electron-beam deposition of VO₂ thin films for optical applications," R. E. Marvel, K. Appavoo, J. Nag, B. K. Choi and R. F. Haglund, Jr., *Applied Physics A* **111**, 975-981 (2013).
9. "Plasmon-electron coupling across the gold::vanadium dioxide interface," D. W. Ferrara, J. Nag, E. R. MacQuarrie, A. B. Kaye and R. F. Haglund, Jr., on line at *Nano Letters*, ASAP dx.doi.org/10.1021/nl401823r.
10. "Surface-plasmon-mediated photoluminescence from Ag-coated ZnO-MgO core-shell nanowires," D. C Mayo, C. Marvinney, E. Bililign, R. Mu and R. F. Haglund, Jr., under review at *Thin Solid Films*, July 2013.

PUBLICATIONS ACKNOWLEDGING DOE SUPPORT FOR WORK AT OAK RIDGE NATIONAL LABORATORY

11. "Enhanced performance of room-temperature-grown epitaxial thin films of vanadium dioxide," J. Nag, E. A. Payzant, K. L. More and R. F. Haglund, Jr., *Applied Physics Letters* **98**(25), 251916 (2011).
12. "Non-congruence of thermally driven structural and electronic transition in VO₂," J. Nag, E. A. Payzant, J. Y. Howe, Karren L. More and R. F. Haglund, Jr., *Journal of Applied Physics* **112**, 103532 (2012).

Poster Sessions

POSTER SESSION I

Monday, September 23, 7:30–9:30pm

1. Novel Temperature Limited Tunneling Spectroscopy of Quantum Hall Systems
Ray Ashoori, Massachusetts Institute of Technology
2. Microwave Spectroscopy of Electron Solids: Fractional Quantum Hall Effect and Controlled Disorder
Lloyd Engel, Florida State University
3. Quantum Electronic Phenomena and Structures
Wei Pan, Sandia National Laboratories, New Mexico
4. Emergent Phenomena in Quantum Hall Systems Far From Equilibrium
Michael Zudov, University of Minnesota
5. Complex States, Emergent Phenomena and Superconductivity in Intermetallic and Metal-Like Compounds
Sergey Bud'ko (for Canfield), Ames Laboratory
6. Digital Synthesis: A Pathway to New Materials at Interfaces of Complex Oxides
Anand Bhattacharya, Argonne National Laboratory
7. Electron Spectroscopy
Peter Johnson, Brookhaven National Laboratory
8. Quantum Materials at the Nanoscale
Peter Abbamonte, University of Illinois, Urbana-Champaign
9. Correlated and Complex Materials
Brian Sales, Oak Ridge National Laboratory
10. Electronic Complexity of Epitaxial Rutile Heterostructures
Hanno Weitering, University of Tennessee / ORNL
11. Tunneling and Transport in Nanowires
Allen Goldman, University of Minnesota
12. Novel sp²-Bonded Materials and Related Nanostructures
Alex Zettl, University of California, Berkeley / LBNL
13. Artificially Structured Semiconductors to Model Novel Quantum Phenomena
Aron Pinczuk, Columbia University
14. Competing Interactions in Complex Transition Metal Oxides
Lance De Long, University of Kentucky

- 15.** Magnetic Materials
Peter Fischer, Lawrence Berkeley National Laboratory
- 16.** Time-Resolved Spectroscopy of Insulator-Metal Transitions: Exploring Low-Energy Dynamics in Strongly Correlated Systems
Gunter Luepke, College of William and Mary
- 17.** Raman Spectroscopy of Iron Oxypnictide Superconductors
Girsh Blumberg, Rutgers University
- 18.** Investigation and Manipulation of Nanoscale Molecular Superconductivity
Saw Hla, Ohio University / Argonne National Laboratory
- 19.** Towards a Universal Description of Vortex Matter in Superconductors
Boris Majorov (for Civale), Los Alamos National Laboratory
- 20.** Probing High Temperature Superconductors with Magnetometry in Ultrahigh Magnetic Fields
Lu Li, University of Michigan
- 21.** Superconductivity and Magnetism in d- and f-electron Materials
Brian Maple, University of California, San Diego
- 22.** Non-Centrosymmetric Topological Superconductivity
Johnpierre Paglione, University of Maryland
- 23.** Probing Correlated Superconductors and Their Phase Transitions on the Nanometer Scale
Ali Yazdani, Princeton University

POSTER SESSION II

Tuesday, September 24, 7:30–9:30pm

1. Cold Exciton Gases in Semiconductor Heterostructures
Leonid Butov, University of California, San Diego
2. Magnetotransport Studies of the Low Dimensional Electron System
Ramesh Mani, Georgia State University
3. Quantum Materials
James Analytis, Lawrence Berkeley National Laboratory
4. Symmetries, Interactions, and Correlation Effects in Carbon Nanotubes
Gleb Finkelstein, Duke University
5. Spontaneous and Field-Induced Symmetry Breaking in Low Dimensional Nanostructures
Marc Bockrath (for Lau), University of California, Riverside
6. Exploring Photon-Coupled Fundamental Interactions in Colloidal Semiconductor Based Hybrid Nanostructures
Min Ouayang, University of Maryland
7. Imaging Electrons in Atomically Layered Materials
Bob Westervelt, Harvard University
8. 1/f Noise in Nanocrystal Solids
Philippe Guyot-Sionnest, University of Chicago
9. Fundamental Studies of Anisotropic Nanomagnets
Dave Sellmyer, University of Nebraska-Lincoln
10. Spin Polarized Electron Transport through Aluminum Nanoparticles
Drago Davidovic, Georgia Institute of Technology
11. Magnetic Nanostructures and Spintronic Materials
Mick Pechan, Miami University of Ohio
12. Spin-Polarized Scanning Tunneling Microscopy Studies of Nanoscale Magnetic and Spintronic Nitride Systems
Arthur Smith, Ohio University
13. Investigation of Spin Physics in Semiconductor Nanowire-Based Heterostructures
Ezekiel Johnston-Halperin (for Yang), Ohio State University
14. Experimental Studies of Correlations and Topology in Two Dimensional Electron Systems and Hybrid Structures
Adina Luican-Mayer (for Andrei), Rutgers University / Argonne National Laboratory

- 15.** Superconductivity and Magnetism
Wai-Kwong Kwok, Argonne National Laboratory
- 16.** Phase Diagram of Fe-Based Superconductors and Related Compounds at High Fields: Possible Field-Induced and Chiral Superconducting States
Luis Balicas, Florida State University
- 17.** Spectroscopic Imaging STM and Complex Electronic Matter
Séamus Davis, Brookhaven National Laboratory / Cornell University
- 18.** Experimental Study of Severely Underdoped Ultrathin Cuprate Films
Tom Lemberger, Ohio State University
- 19.** Engineering of Mixed Pairing and Non-Abelian Quasiparticle States of Matter in Chiral p-wave Superconductor Sr₂RuO₄
Ying Liu, Pennsylvania State University
- 20.** Origin of Superconductivity in Structurally Layered Materials
Athena Sefat, Oak Ridge National Laboratory
- 21.** Infrared Hall Effect in Correlated Electronic Materials
Dennis Drew, University of Maryland
- 22.** Quantum Transport in Topological Insulator Nanoelectronic Devices
Pablo Jarillo-Herrero, Massachusetts Institute of Technology
- 23.** Towards a new Quasi-Particle: Rydberg Polaritons for Quantum Materials
Jon Simon, University of Chicago

Poster Abstracts

Project title: Experimental studies of correlations and topology in two Dimensional electron systems and hybrid structures.

Principal Investigator: Eva Y. Andrei, Department of Physics and Astronomy, Rutgers University, Piscataway NJ 08855

Program Scope

The goal of this program is to discover, understand and exploit novel electronic properties that arise in two dimensional (2D) materials due to the interplay between reduced dimensionality, incomplete screening, boundaries and proximity between materials. We study atomically thin layers and interfaces including graphene, and stacked hybrid structures derived from cleavable van der Waals crystals such as hBN, MoS₂ and WS₂. These systems host novel phenomena that have no parallel in traditional electron systems: stacking-induced van-Hove singularities in the density of states; magnetically induced broken symmetry phases such as spin or charge density waves; one dimensional chiral edge states with peculiar electronic and magnetic properties. Our work addresses questions on the interplay between screening and the electronic properties; the effect of boundaries and the role of screening on chiral edge states in the integer and fractional quantum Hall regime; non-chemical routes to modifying the electronic band structure of 2D materials including twist induced tuning of the band structure in stacks of layered materials.

The experimental probes include scanning tunneling microscopy and spectroscopy (STM/STS), scanning gate spectroscopy, Landau level spectroscopy and magneto transport. Two new facilities that are currently being installed, a He-ion microscope and an aberration corrected scanning transmission electron microscope, will significantly enhance design capabilities for engineering nano-structures and for sculpting boundaries in layered materials. The ability to combine these capabilities will provide unique and powerful opportunities to access and explore new physical phenomena.

Recent Progress

We focused on thin layers and interfaces including graphene and stacked hybrid structures to study the emergence of novel electronic properties due to the interplay between reduced dimensionality, incomplete screening and boundaries. To this end we developed sample preparation and fabrication techniques and characterization tools that allowed us to probe the electronic properties of 2D electron systems and to follow their evolution with distance from an edge, with magnetic field, doping and gating. Our results are summarized below.

1. *Observation of the evolution of Landau Levels into edge states (1).* 2D electron systems support topologically ordered states in which the coexistence of an insulating bulk with conducting one dimensional chiral edge-states gives rise to the quantum Hall effect. In 2D systems confined by sharp boundaries theory predicts a unique edge-bulk correspondence which is central to proposals of QH based topological qubits. However, in conventional semiconductor based 2DES, these elegant concepts

were difficult to realize because in these systems edge-state reconstruction caused by insufficient screening destroys the edge-bulk correspondence. Our work demonstrated that edge-state reconstruction can be avoided in graphene. Using scanning tunneling microscopy and spectroscopy, we followed the spatial evolution of Landau levels (LL) towards an edge of graphene supported above a graphite substrate (Figure 1). To within one magnetic length of the edge no reconstruction was observed, in agreement with calculations based on an atomically sharp confining potential. Our results single out graphene as a system where the edge structure can be controlled and the edge-bulk correspondence preserved.

2. *Observation of an isolated charge impurity and its effect on the electronic environment in graphene in the quantum Hall effect (QHE) regime (2,3).* Charged impurities are a major source of disorder and scattering in electron systems. They produce a spatially localized signature in the density of states (DOS) which, for impurities located at the sample surface, is readily observed with scanning tunneling microscopy and spectroscopy (STS/STM). In this respect graphene, being a 2D material with its electronic states strictly at the surface, provides a unique playground for elucidating the role of impurities. Using ultra-clean gated graphene samples we have isolated a single charged impurity and studied its effect on the electronic spectrum. This allowed us to for the first time to investigate the effects of a single impurity on the 2D electronic spectrum in the QHE regime and how it is influenced by screening and the population of LLs.

- *Observation of localized and extended states (4-6).* Using STM/STS we imaged the distribution of the electronic density of states in the QHE regime as a function of energy. For energy lying in the center of LLs we showed that the electronic wave function is extended avoiding the impurity. In contrast for energies lying within the gap between LLs the wavefunction is tightly localized on the impurity. This is fully consistent with the theoretical expectation and extended electronic states in the quantum Hall effect regime in graphene and studied the transition between them.

- *Lifting the orbital degeneracy of LLs by an isolated impurity(3).* In the QHE regime where the 2D electronic spectrum is quantized into highly degenerate LLs, isolated impurities are expected to lift the local orbital degeneracy. As a result, the spectrum within each LL should split into discrete levels around a nano-scale region centered on the impurity. Thus far however these effects were not experimentally accessible due to the difficulty in attaining sufficiently clean samples to allow observing the effect of an isolated impurity. Instead, in previous experiments studying

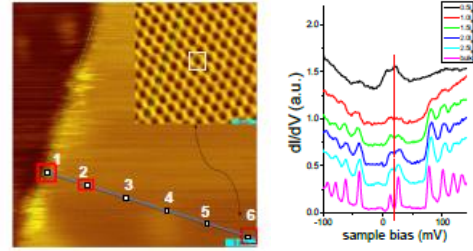


Figure 1. Evolution of LLs towards an edge in graphene. Left panel- topography image showing the edge and the positions where spectra in the right panel where taken at intervals of $0.5 l_B$ (1-6).

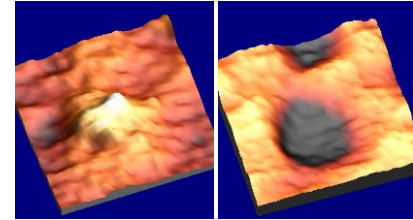


Figure 2. Density of states maps near the impurity. Left panel: energy within the gap. Right panel- Energy in the center of the LL Magnetic field 10T , image area $80 \times 80 \text{ nm}^2$.

the spatially resolved LL spectrum, tunneling between closely spaced impurity states presented a picture of “bent” levels, whose energies continuously change in space, adjusting to the local disorder potential. This behavior could be understood in the semi-classical framework, where electrons follow classical drift trajectories along the equipotential lines defined by a dense distribution of impurities.

3. *Tuning the screening properties of the 2D electron system in graphene.* Using LL spectroscopy we observed the transition between compressible and incompressible electronic states as the Fermi energy was swept by gating from one Landau level to the next. We showed that the Fermi energy remains pinned within partially filled Landau levels and scans through the localized impurity states until reaching the next landau level.

4. *Supercritical charge and atomic collapse* (2). Atomic orbitals become unstable when the nuclear charge exceeds a critical value, comparable to the inverse fine structure constant, when relativistic effects cause electrons to fall into the nucleus. Accessing this critical regime where new physics comes into play requires the creation of ultra-heavy nuclei which do not exist in nature. We demonstrated that in graphene it is possible to explore this regime by using an isolated charged impurity as the nucleus of an artificial atom together with a magnetic field and a gate voltage which define the electronic orbitals. Using scanning tunneling microscopy and spectroscopy in an ultra-clean graphene sample we showed that the effective charge of the impurity can be tuned from the subcritical to the supercritical regime by controlling the occupancy of the Landau levels with the gate voltage. We found that at low occupancy strong screening by the conduction electrons cloaks a positively charged impurity rendering it essentially invisible. At full occupancy where the impurity is unscreened it enters the supercritical regime which is identified by the appearance of a series of localized states in the negative energy sector. Our findings show that the magnetic field makes it possible to tune the strength of impurities in graphene from subcritical to supercritical providing unprecedented access to the regime of Coulomb criticality.

5. *Twist induced van-Hove singularities and slow-down of the Fermi velocity.* Our group was the first to show that the band structure of graphene can be modified and tuned by an external potential. We discovered that stacking graphene layers with a relative twist between them induces a pair of van-Hove singularities which symmetrically flank the Dirac point. We demonstrated that the separation between these singularities scales with the twist angle and that twist causes a large renormalization of the Fermi velocity and small angles.

Future Plans

1. *Towards elucidating the effect of edge reconstruction on the correspondence between bulk correlations and edge states.* Having established the absence of edge reconstruction for the case of graphene on graphite we will study edge states at the crossover between the regimes with and without edge reconstruction. To control the screening length we will vary the thickness of the dielectric spacer separating the graphene layer from the backgate using hBN flakes of variable thickness or the dielectric constant of the spacer by using gated MoS₂ flakes.

2. *Novel correlated states in twisted stacked layers.* Using the twist induced van-Hove singularities in twisted graphene layers or graphene on hBN we will explore the

possibility of inducing novel correlated states such as a charge density wave by tuning the Fermi energy into the van-Hove singularity in search of the emergence of band gaps.

References (which acknowledge DOE support)

1. Evolution of Landau Levels into Edge States in Graphene, Guohong Li , Adina Luican, Dmitry Abanin, Leonid Levitov and Eva Y. Andrei, Nature Communications,4, 1744 (2013).
2. Charged Impurities in graphene: From Cloaking to Supercriticality, Adina Luican-Mayer, Maxim Kharitonov, Guohong Li, ChihPin Lu, Ivan Skachko, Alem-Mar B. Goncalves, K. Watanabe, T. Taniguchi and Eva Y. Andrei, Nature Materials under review (2013)
3. Screening Charged Impurities and Lifting the Orbital Degeneracy in Graphene by ECMP@orise.orau.gov Populating Landau Levels, Adina Luican-Mayer, Maxim Kharitonov, Guohong Li, ChihPin Lu, K. Watanabe, T. Taniguchi and Eva Y. Andrei, Physical Review Letters, under review (2013)
4. Probing Dirac Fermions in Graphene by Scanning Tunneling Probes, Adina Luican-Mayer and Eva Y. Andrei, in “The Physics of Graphene”, editors H. Aoki and M. Dresselhaus, Springer 2013.
5. Electronic properties of graphene: a perspective from scanning tunneling microscopy and magneto-transport , E.Y. Andrei, G. Li, X. Du, Reports on Progress in Physics, 75 (2012) 056501 (Journal Cover)
6. Scanning tunneling microscopy and spectroscopy of graphene, G. Li, E.Y. Andrei, “Graphene Nanoelectronics, Metrology, Synthesis,Properties and Applications” editor H. Raza, Springer, 2012
7. Single-layer behavior and its breakdown in twisted graphene layers, A. Luican, Guohong Li and E.Y. Andrei, in print **Phys. Rev. Lett.** **106**, 126802 (2011) (**Editor's choice; Physics highlight**).
8. Self-navigation of an STM tip toward a micron sized sample, **Rev. Sci. Instrum.**, G. Li, A. Luican, E.Y. Andrei, 82 (2011) 073501.
9. Quantized Landau level spectrum and its density dependence in graphene, A. Luican, Guohong Li, and E.Y. Andrei, **Phys. Rev. B** **83** 081405(R) (2011) (**Editor's choice**)

Project Title: “*Novel Temperature Limited Tunneling Spectroscopy of Quantum Hall Systems*”

Principal Investigator: *Raymond Ashoori* (ashoori@mit.edu)

Institution: *Massachusetts Institute of Technology*

Project Scope:

Tunneling spectroscopy has long played a vital role in understanding a large number of condensed matter physics systems. For instance, study of the tunneling spectrum into BCS superconductors was one of the primary experimental signatures for validation of BCS theory. Two-dimensional electronic systems display the quantum Hall effects and a number of related remarkable phenomena. Studying these systems using tunneling to determine their “single particle spectra” can yield fundamental insights into the basic physics of these phenomena.

There have been fundamental limitations in studying tunneling into two-dimensional systems. Issues such as low conductivity of the electron layer can make it difficult to determine the energies of tunneling electrons. Moreover, the low density of electronic states in these systems often means that the tunneling electrode also gates the electronic system (changes its density). This means that any applied voltage is shared between tunneling and gating, and this distorts and complicates spectra. In scanning tunneling microscopy measurements, this phenomenon creates a local gating, and workfunction differences between the tip and the sample mean that substantial gating can be present even at zero applied tip voltage. Finally, two-dimensional and other low-dimensional systems may also particularly sensitive to heating at high electron injection energies.

This project focuses on using extremely sensitive capacitance methods for probing two-dimensional electronic systems in high magnetic fields. These capacitance methods can be used to study tunneling of electrons into and out of these systems. By determining tunneling spectra using a capacitive technique, we can circumvent *all* of the difficulties described in the paragraph above. The method, which we call “Time-Domain Capacitance Spectroscopy (TDCS), works in samples with a two-dimensional system inside of a parallel-plate capacitor and close enough to one of the plates to allow tunneling into that plate. We apply a voltage pulse across the capacitor and monitor the time dependence of charging capacitor and thereby determine the rate of charge flow to and from the 2D system via tunneling. This method requires no lateral charge flow within the 2D system, and it can, in fact, be used to study tunneling into insulators.

In semiconductors, the TDCS results have yielded unprecedented high-resolution measurements of the cold 2DES over a range of 20 meV (~200 Kelvin) above and below the Fermi surface. These measurements reveal the difficult-to-reach, beautiful, and surprising structure in this highly correlated system far from the Fermi surface. Our efforts in traditional semiconductors are currently focused on measuring samples at very low temperatures (<20 mK) and with microvolt energy resolution.

One of our major efforts in this project is to extend the use of TDCS outside of traditional semiconductors. We are currently focusing our efforts on building graphene samples using exfoliated hexagonal boron nitride (hBN) layers both as insulators and as tunnel barriers. Along the way, we have needed to understand capacitance spectra in these graphene structures. By making exquisitely sensitive capacitance measurements, we have discovered remarkable features of ultra-clean graphene in high magnetic fields (see Recent Progress section below).

Recent Progress:

We have made considerable progress in developing and making extremely sensitive capacitance measurements on high quality graphene samples. Our graphene samples are ~ 1 micron in size (see Figure 1B), and we have learned to make capacitance measurements on these samples with sub-femtoFarad resolution using excitations of less than 1 mV. Performing a systematic study of these samples, we found that the relative orientation of the hexagonal lattices on the graphene and underlying hBN has a critical impact on the electronic properties of the graphene, both at the charge neutrality point (CNP) and at specific electron densities away from the charge neutrality point. This behavior arises because the boron and nitrogen atoms in the hBN give rise to slightly different electrostatic potentials in the neighboring graphene, breaking the sublattice symmetry and giving rise to a band gap. Depending on the relative orientations of the graphene and the hBN, a moiré pattern arises with nitrogen and boron atoms alternating their positions relative to the two graphene sublattices. Figure 1B shows that there exists a wide region in gate voltage over which there is no electrical conductance, consistent with a band gap.

At zero twist angle, a superlattice appears (see Fig. 1A) due to the lattice 1.8% mismatch between graphene and hBN. The strength of the sublattice symmetry breaking thus varies with position (from zero for misalignment to a maximum value when boron and nitrogen atoms are

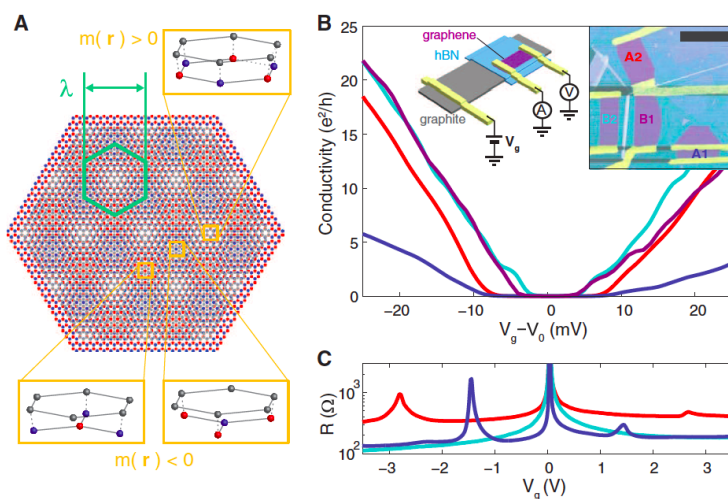


Fig. 1. Results from a graphene-hBN heterostructure. (A) Schematic of the moiré pattern for graphene (gray) on hBN (red and blue), for zero misalignment angle and an exaggerated lattice mismatch of $\sim 10\%$. The moiré unit cell is outlined in green. (B) Low-temperature ($T = 150$ mK) conductivity near charge neutrality of four heterostructure devices. Left inset: Measurement schematic. Right inset: False-color AFM image. Scale bar, 3 μm . (C) Finite-density resistance peaks indicate full filling of the lowest superlattice miniband in two of the four measured devices within the experimentally accessible density range. Adapted from Science, **340**, 1427, (2013)

respectively aligned with different sublattices). This variation was expected to reduce the width of induced bandgap. Single particle theory thus predicts a bandgap of only 5-10 meV at zero twist angle. Surprisingly, our thermal activated transport measurements display much larger bandgaps (~ 30 meV) than predicted in single particle theory, and evaluation of the effect of electron-electron interactions may be required to explain our results.

Figure 1B shows that along with the development of a band gap, we observe peaks in the sample resistivity at particular gate voltages for each sample, symmetric about the CNP. These result from the development of the “mini-gaps” arising from “mini-band” structure forming from the superlattice potential. The gate voltage positions of the resistivity peaks correlate with the observed widths of the observed gaps in gate voltage. Moreover, and STM study of our samples

shows that both the width of the gap and the gate voltage positions of the resistance peaks scale inversely with twist angle.

Our high sensitivity capacitance measurements make clear that the density of states structure in these graphene on hBN samples differs radically with that of graphene on other substrates. Figure 2 shows capacitance data from an ordinary semimetallic piece of graphene (A) compared with

insulating graphene (B). Notice that at zero magnetic field, both samples have small density of states near the CNP. However, in the ordinary structure, a large density of states peak develops as the magnetic field strength is increased, corresponding to the formation of the $v=0$ Landau level. In comparison, the insulating graphene maintains a bandgap even at high magnetic fields. Along with the band gap we observe, at high fields, capacitance and transport spectra that display clear features of the long sought Hofstadter butterfly (Science, **340**, 1427, (2013)). In future work with TDCS, we will study the details of the Hofstadter energy spectrum.

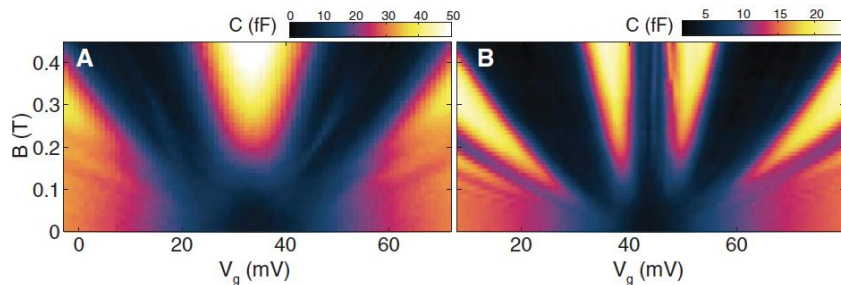


Fig. 2. Magnetocapacitance of semimetallic and insulating graphene devices. (A) Capacitance of a typical semimetallic graphene device. The zero-energy Landau level forms at ~ 0.15 T, appearing as a local maximum at the CNP ($V_g = 34.5$ mV). (B) Capacitance of an insulating graphene device under similar conditions. In contrast to (A), the density of states is at a local minimum for all fields at charge neutrality ($V_g=44$ mV). Adapted from Science, **340**, 1427, (2013)

Future Plans

TDCS of graphene samples in high magnetic fields: We are working to construct graphene samples inside of “tunnel capacitors”. This will permit an unprecedented, direct, and precise measurement of quantum Hall and Hofstadter butterfly features in graphene. We are taking two approaches to this work. As the samples we now make are small (~ 1 micron), sample capacitances are minuscule. So, we will use single electron transistors as sensors for TDCS. Another approach is to build, with collaborators, large area graphene structures (~ 20 microns) and measure them with traditional TDCS. Along the way to achieving TDCS measurements, we will continue making our ultra-sensitive capacitance measurements of a variety of monolayer and bilayer graphene systems.

Spectroscopy of the semiconductor 2DES at lower temperatures and with higher mobilities, Improvements to Experimental Apparatus and to Samples: We have recently purchased and installed a new dilution refrigerator capable of temperatures of around 5 mK and with a 16 Tesla magnetic field. We have also built a new amplifier for installation at the 1K pot of the dilution refrigerator, and we expect this to greatly diminish noise in our measurements. Finally, we have developed new higher mobility 2D electron gas samples. So, now we have ultra-clean samples, that are very cold with very low noise measurements. This combination will allow us to resolve very subtle spectral features associated with stripe and bubble phases, composite fermions, and unconventional fractional quantum Hall states. We will also continue our study of 2D hole systems and the search for spectral features associates with the 2D metal-insulator transition.

Publications 2012-2013 resulting from DOE sponsorship:

O.E. Dial, R.C. Ashoori, L.N. Pfeiffer, K.W. West, “Observations of plasmarons in a two-dimensional system: Tunneling measurements using time-domain capacitance spectroscopy” **Physical Review B (Rapid Communications)**, Vol. 85, 081306 (2012)

B. Hunt, J. D. Sanchez-Yamagishi, A. F. Young, M. Yankowitz, B. J. LeRoy, K. Watanabe, T. Taniguchi, P. Moon, M. Koshino, P. Jarillo-Herrero, R. C. Ashoori, “Massive Dirac Fermions and Hofstadter Butterfly in a van der Waals Heterostructure”, **Science**, Vol. 340, pp. 1427-1430 (2013).

A. F. Young, J. D. Sanchez-Yamagishi, B. Hunt, S. H. Choi, K. Watanabe, T. Taniguchi, R. C. Ashoori, and P. Jarillo-Herrero, “Tunable symmetry breaking along the helical edge of a graphene quantum spin Hall state”, **submitted for publication**

“Phase-diagram of Fe based superconductors and related compounds at high fields: possible field-induced and chiral superconducting states”

Luis Balicas

Condensed Matter Group

National High Magnetic Field Laboratory - Florida State University

1800, E. Paul Dirac Dr., Tallahassee – FL 32310

Program Scope

The scope of our program is broad and includes the synthesis and characterization of the bulk physical properties of a variety of unconventional superconductors. Our current program includes heavy-fermion and Fe-based superconductors, as well as the synthesis and characterization of new transition metal chalcogenides found by us to display extremely high upper critical fields relative to their superconducting transition temperature, i.e. comparable or surpassing those of the heavy-Fermion superconductors. Our current (and proposed) objectives are:

- i)** Given the evidence collected by us, as well as evidence exposed by other groups, suggesting the possibility of an additional superconducting state at high fields in the $\text{Fe}_{1+y}\text{Te}_{1-x}\text{Se}_x$ series: we proposed to expose its existence through thermodynamic measurements and map its phase diagram. Currently, we are further refining its synthesis to achieve the highest quality single-crystals.
- ii)** Given the anomalous, “magnetic like”, as opposed to a clear diamagnetic-like hysteretic response, observed in the superconducting state of LiFeAs at high fields, and which in our opinion could correspond to potential evidence for a time reversal broken superconducting state, we proposed to collect additional evidence for its existence through an array of experimental techniques. We also proposed to clarify if this state is induced by the external field. So far, we observed the de Haas van Alphen effect in three single-crystals, and all displayed this anomalous magnetic response on approaching H_{c2} . This anomalous response was absent in all those single-crystals (> 6) found by us not to display quantum oscillatory phenomena thus establishing a clear correlation between sample quality and this unconventional magnetic response.
- iii)** Similarly, given our magnetic torque data indicating the existence of phase transitions preceding H_{c2} in extreme high quality samples of URu_2Si_2 , we proposed to map its entire phase diagram as a function of field orientation and temperature by exposing its magnetic and thermodynamic properties. The wave-function of the superconducting gap of URu_2Si_2 was claimed to possess a $k_z(k_x + ik_y)$ symmetry which breaks time reversal symmetry. Our on-going study of its bulk magnetic response provides experimental evidence for such a scenario, with an anomalous magnetic response similar to the one observed by us in LiFeAs.
- v)** Given our observation of de Haas van Alphen oscillations in LiFeAs, we originally proposed to fully map the geometry of the Fermi surface of this compound in an attempt to elucidate what seemingly are strong discrepancies with band structure calculations. This would allow the development of theoretical models explaining its pairing symmetry claimed by some groups to be distinct from the proposed $s\pm$ scenario. We have just collected a very complete data set on the de Haas van Alphen effect in LiFeAs observing, for example, small Fermi surface pockets which clearly and for our greatest surprise are not two-dimensional in character (see below). This will be very difficult to model, but clearly explains the absence of itinerant magnetism in this compound.
- vi)** Given the extremely high upper critical fields (relative to its superconducting transition temperature) observed by us in $\text{Ta}_2\text{Pd}_{0.85}\text{S}_5$, we proposed to explore the possibility of observing superconductivity in other members of this family but in samples synthesized by us and subsequently map their entire phase diagram. We have just reported the observation of superconductivity in $\text{Nb}_2\text{Pd}_{0.81}\text{S}_5$, $\text{Nb}_2\text{Pd}_{0.67}\text{S}_5$, and $\text{Nb}_3\text{Pd}_{0.7}\text{Se}_7$.

Recent Progress

In such a short document it is impossible to convey the breadth of our activities undertaken under the sponsorship of the DoE. Here, we have chosen to display just some of our unpublished results, concerning in this case the Fermi surface of LiFeAs, originally proposed by us to be elucidated. We will also briefly discuss some of our recently published results, the discovery of superconductivity in new compounds. Figure 1 shows the de Haas van Alphen signal for one single-crystal from a synthesis batch whose stoichiometry was refined by us through single-crystal X-ray refinement as $\text{Li}_{0.94}\text{Fe}_{1.06}\text{As}$ with no indications for impurity phases or inclusions.

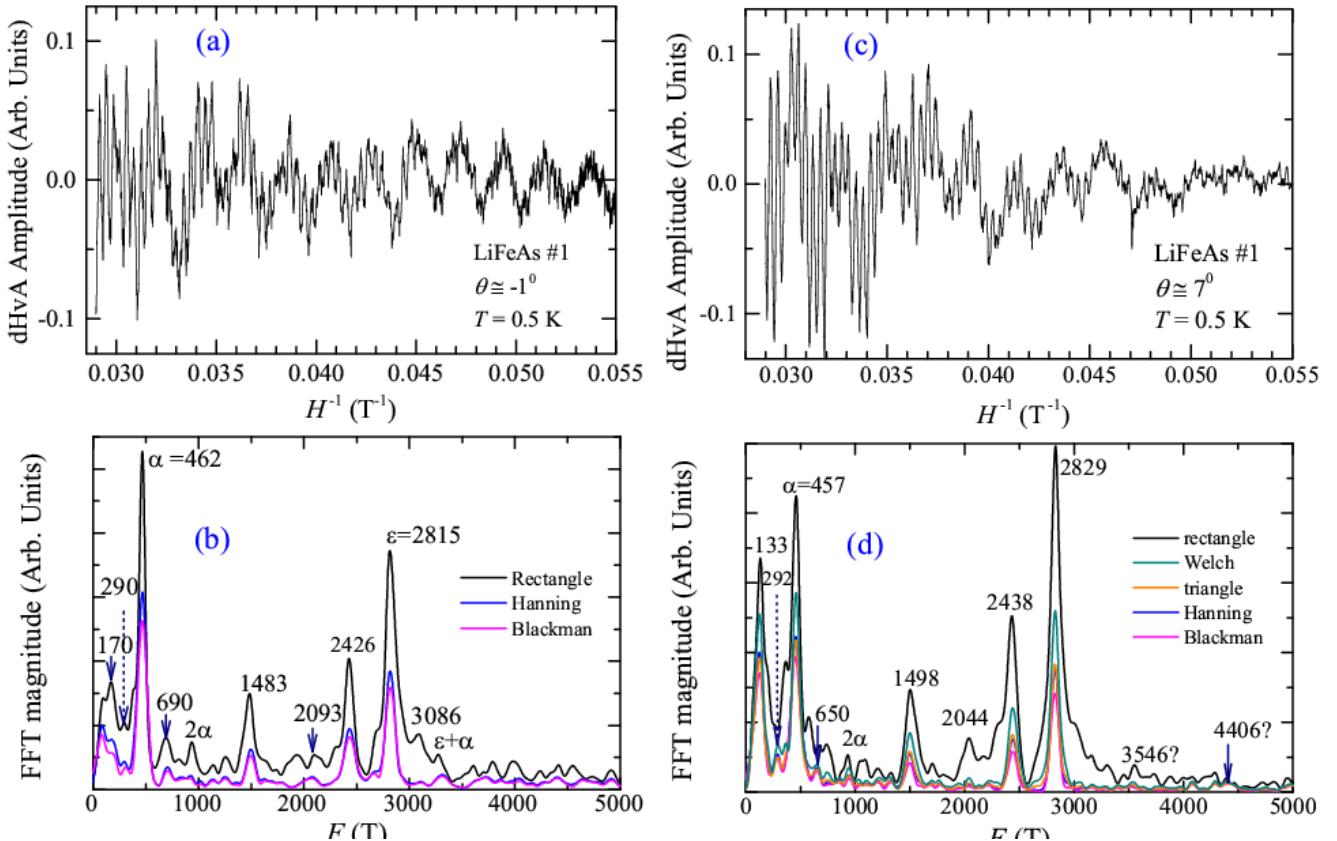
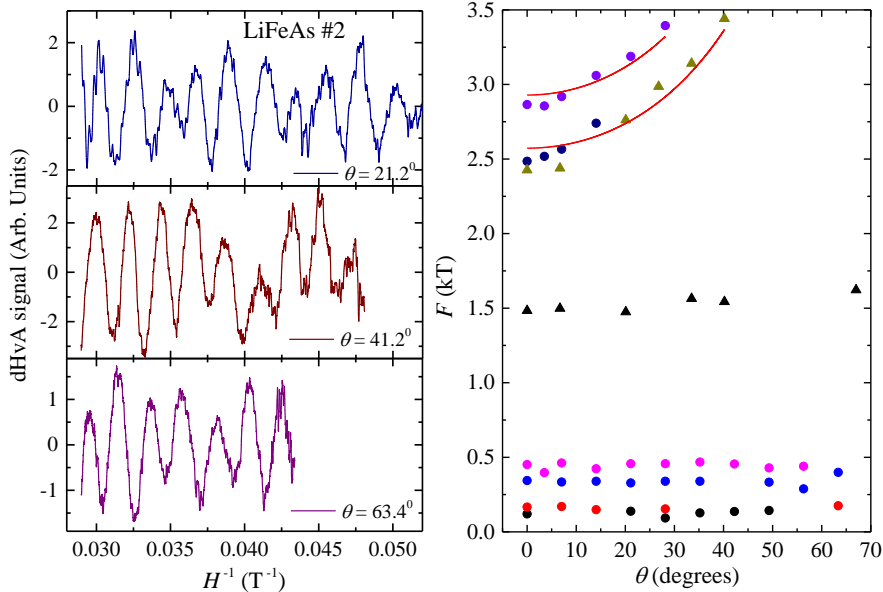


Fig. 1 (a) Oscillatory component superimposed onto the magnetic torque signal as a function of the inverse field H^{-1} , after subtraction of a paramagnetic like background, at a temperature $T = 0.5$ K and at an angle $\theta \approx -1^\circ$ between the external field and the c-axis of the crystal. (b) The fast Fourier transform of the oscillatory signal for several filters, revealing frequencies previously observed by other groups [1], namely $\delta \approx 2400$ T and $\varepsilon \approx 2800$ T, but also a number of smaller frequencies not predicted by band structure calculations. (c) Same as in (a) but for $\theta \approx 7^\circ$. (d) Same as in (b) but for $\theta \approx 7^\circ$. B. Zeng *et al.*, (unpublished).

The remarkable aspect concerning our de Haas van Alphen results is the observation of a series of much smaller frequencies, which were not predicted by current band structure calculations [1,2]. Even more perplexing is the fact that some of these frequencies, e.g. ~ 300 T and ~ 460 T are observed to be nearly isotropic as a function of the orientation of the field, see Fig. 2, thus indicating that they correspond to ellipsoids of low anisotropy, a fact that is very difficult to understand based on current band structure calculations. In fact, DFT calculations based on packages such as the WIEN2K is unable to handle off stoichiometry situations as is the case here. Although we collected our single crystal x-ray crystallographic information file at low temperatures we cannot attempt a realistic band structure calculation based on our X-ray refinements. These results present us with a conundrum: why is the experimental Fermi surface so different from the theoretically calculated one? And what are the

overall implications for the Fe based superconductors, particularly in what concerns the superconducting pairing mechanism?



Left panel: oscillatory component superimposed onto the torque signal acquired at a temperature $T = 0.3$ K and for several large angles with respect to the c-axis from a second LiFeAs single-crystal. At these larger angles the de Haas van Alphen signal is dominated by two frequencies, ~ 300 and 460 T, whose value changes very little as a function of the angle, thus indicating that they correspond to nearly isotropic Fermi surfaces in sharp contrast with band structure calculations [1, 2]. B. Zeng *et al.*, (unpublished).

Future Plans

To achieve all the objectives initially traced by us to justify this research program. Concerning the new compounds, our immediate goal is to explore the possibility of synthesizing new Fe based chalcogenides based on the experience acquired and the new superconducting phases reported in Refs. [3 and 4]. Although we have already achieved this, so far none of the Fe based compounds synthesized by us have shown superconductivity, although they seem to have interesting semiconducting properties. As of this moment, we are preparing thermal conductivity measurements down to very low temperatures with the goal of detecting potential evidence for unconventional superconductivity, e.g. nodes in the superconducting gap wave-function. We are also synthesizing a large amount of the material in order to undertake neutron scattering measurements: our goal is to study the intensity of the spin excitations in this system, or to explore the possibility that these systems might be located in close proximity to itinerant magnetism as predicted by band structure calculations. Finally, we have been actively looking for a researcher who might be interested in studying these compounds through scanning tunneling microscopy. So far the STM community in the US seems to be very focused on a variety of other projects and have not yet shown interest on these compounds (for our chagrin).

References

- [1] C. Putzke *et al.*, Phys. Rev. Lett. **108**, 047002 (2012).
- [2] D. J. Singh, Phys. Rev. B **78**, 094511 (2008).
- [3] Q. Zhang *et al.*, Sci. Rep. (UK) **3**, 1446 (2013).
- [4] Q. R. Zhang, *et al.*, Phys. Rev. B **88**, 4508 (2013).

Publications (From summer 2013 to ~ summer 2011)

- 1. Q. R. Zhang, D. Rhodes, B. Zeng, T. Besara, Siegrist, T. Siegrist, M. D. Johannes, L. Balicas, Phys. Rev. B **88**, 4508 (2013).
- 2. G. Li, G. Grisonna, B. S. Conner, F. Wolff-Fabris, C. Putzke, N. D. Zhigadlo, S. Katrych, Z. Bukowski, J. Karpinski, and L. Balicas, Phys. Rev. B (RC) **87**, 100503 (2013).
- 3. G. Li, R. R. Urbano, P. Goswami, C. Tarantini, B. Lv, P. Kuhns, A. P. Reyes, C. W. Chu, and L. Balicas, Phys. Rev. B **87**, 024512 (2013).

4. P. J. W. Moll, L. Balicas, V. Geshkenbein, G. Blatter, J. Karpinski, N. D. Zhigadlo, and B. Batlogg, Nat. Materials **12**, 134 (2013).
5. Q. Zhang, G. Li, D. Rhodes, A. Kiswandhi, T. Besara, B. Zeng, J. Sun, T. Siegrist, M. D. Johannes, and L. Balicas, Sci. Rep. (UK) **3**, 1446 (2013).
6. Y. Kohama, S. Wang, A. Uchida, K. Prsa, S. Zvyagin, Y. Skourski, R. D. McDonald, L. Balicas, H. M. Ronnow, C. Rüegg, and M. Jaime, Phys. Rev. Lett. **109**, 167204 (2012).
7. G. Li, G. Grissonnanche, J. -Q. Yan, R. W. McCallum, T. A. Lograsso, H. D. Zhou, and L. Balicas, Phys. Rev. B **86**, 054517 (2012).
8. L. Song, L. Balicas, D. J. Mowbray, R. B. Capaz, K. Storr, L. Ci, D. Jariwala, S. Kurth, S. G. Louie, A. Rubio, and P. M. Ajayan, Phys. Rev. B **86**, 075429 (2012).
9. H. D. Zhou, J. G. Cheng, A. M. Hallas, C. R. Wiebe, G. Li, L. Balicas, J. S. Zhou, J. B. Goodenough, J. S. Gardner, and E. S. Choi, Phys. Rev. Lett. **108**, 207206 (2012).
10. M. M. Altarawneh, N. Harrison, G. Li, L. Balicas, P. H. Tobash, F. Ronning, and E. D. Bauer, Phys. Rev. Lett. **108**, 066407 (2012).
11. J. G. Cheng, G. Li, L. Balicas, J. S. Zhou, J. B. Goodenough, C. Xu, and H. D. Zhou, Phys. Rev. Lett. **107**, 19720 (2011).
12. T. Gebre, G. Li, J. B. Whalen, B. S. Conner, H. D. Zhou, G. Grissonnanche, M. K. Kostov, A. Gurevich, T. Siegrist, T. and L. Balicas, Phys. Rev. B **84**, 174517 (2011).
13. G. Li, G. Grissonnanche, A. Gurevich, N. D. Zhigadlo, S. Katrych, Z. Bukowski, J. Karpinski, and L. Balicas, Phys. Rev. B **83**, 214505 (2011).
14. H. D. Zhou, S. T. Bramwell, J. G. Cheng, C. R. Wiebe, G. Li, L. Balicas, J. A. Bloxsom, H. J. Silverstein, J. S. Zhou, J. B. Goodenough, and J. S. Gardner, Nat. Commun. **2**, 478 (2011).

Program Title:

Digital Synthesis: A Pathway to New Materials at Interfaces of Complex Oxides

Principle Investigator : Anand Bhattacharya; Co-Investigator: Sam Bader

**Address: Materials Science Division,
Bldg. 223, 9700 S. Cass Ave.,
Argonne National Laboratory,
Argonne, IL 60657.**

email: anand@anl.gov

(i) Program Scope:

In our program, we seek to create, characterize and understand novel electronic and magnetic states at interfaces of complex oxides. Our technique for creating these interfaces involves synthesizing ‘digital’ heterostructures of various oxide materials in a single atomic layer-by-layer manner. This allows us to tailor interfaces with great precision and to create superlattices with very short periods, comparable or less than the length scales for charge transfer at the interfaces.

The complex oxides host a very diverse range of collective states of condensed matter. The richness of observed phenomena in these materials, which have also presented some of the greatest challenges to our understanding, are due to their strongly interacting degrees of freedom. Surfaces and interfaces between complex oxides provide a unique environment where these degrees of freedom may ‘reconstruct’ and lead to new properties that are qualitatively different from those of their bulk constituents. Thus, interfaces are a pathway for discovering new materials and phenomena. More specifically, we seek to discover and explore novel states with attributes such as tunability with external electric fields and currents, novel magnetic structures that arise as a result of broken inversion symmetry, and electronic states that arise as a result of strong spin-orbit coupling. These include multiferroic heterostructures, superconductivity at interfaces between materials that may not be superconducting themselves, non-collinear interfacial magnetic structures, and novel two-dimensional electron gases. We seek to explore materials that are known to have interesting phases, such as the manganites and cuprates, where the atoms have been ‘re-arranged’ in simple ways – for example by layering the cations in a manner such that the effects of disorder have been engineered away – to reveal new properties. We create these materials systems using state-of-the-art, ozone-assisted oxide Molecular Beam Epitaxy (MBE) at Argonne, and characterize them using the major DOE facilities for neutron and photon scattering, and at the DOE Nanoscale Science Research Centers.

(ii) Recent Progress (since 2011):

1. Tailoring polarity in a two-dimensional nickelate with single atomic layer control

Many of the 3d transition metal oxides share a common structural MO_6 building unit—a central transition metal (TM) cation octahedrally coordinated with oxygen nearest neighbors. The electronic states in these materials can be modified by tailoring the M-O bonds, which typically include the application of epitaxial strain in thin films, or pressure

and isovalent cation substitution in bulk samples. Here, we present a new route to tailor the M -O bonds without changes to the strain state or stoichiometry in two-dimensional perovskite nickelate ($n=1$ in the Ruddlesden Popper series). We do this by tailoring the dipolar electrostatic interactions at the unit cell level in nominally non-polar LaSrNiO_4 via single atomic layer-by-layer synthesis synthesis using oxide-MBE. We reconstruct the response of the crystal lattice to the induced polarity using an x-ray phase retrieval technique (COBRA). We find that the response of the O anions to the resulting local electric fields distorts the M -O bonds, being largest for the apical oxygens (O_{ap}). It also alters the Ni valence. This structural control strategy has broad implications for tailoring electronic properties in oxides that are sensitive to the M - O_{ap} bond geometry – such as superconductivity in the cuprates. This work is being done in collaboration with Dr. Hua Zhou at the Advanced Photon Source (Argonne) and Prof. James Rondinelli's group at Drexel University. (Brittany Nelson-Cheeseman et al., *in preparation*)

2. Interfacial charge transfer and long range magnetic proximity effects in nickelate/manganite superlattices.

In conventional semiconductors and metals, a mismatch between the chemical potential for charge carriers in two materials at an interface leads to charge transfer. Furthermore, an electric field develops and ‘band bending’ occurs at the interface with profound consequences. Motivated by the connection between band lineup charge transfer, we investigated the interface between two very dissimilar perovskites, LaMnO_3 and LaNiO_3 .

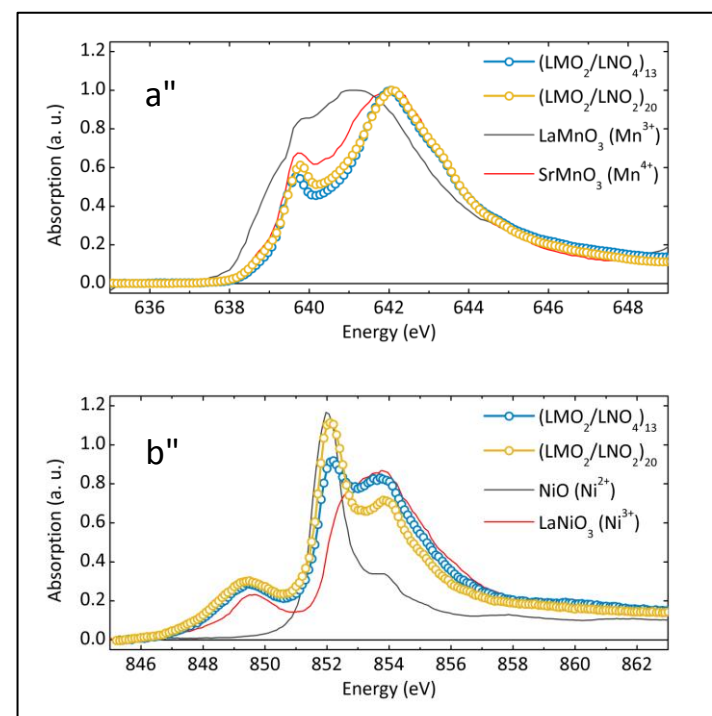


Fig. 1 Evidence for electron transfer from LaMnO_3 to LaNiO_3 in X-ray absorption spectra at the (a) Mn L -edge and the (b) Ni L -edge in $(\text{LaMnO}_3)_2/(\text{LaNiO}_3)_n$ superlattices ($n = 2, 4$). The Mn spectra resemble that for Mn^{4+} , while spectra of Ni for $n = 2$ resembles Ni^{2+} , even though Mn and Ni are nominally in the 3+ state in LaMnO_3 and LaNiO_3 .

LaMnO_3 is an antiferromagnetic orbital-ordered Mott insulator and LaNiO_3 is a paramagnetic metal. Using transport and x-ray spectroscopy (collaboration with Dr. John Freeland, Argonne), we were able to demonstrate that there is a significant charge transfer between these materials, with electrons moving from LaMnO_3 into LaNiO_3 . In superlattices of $(\text{LaMnO}_3)_2/(\text{LaNiO}_3)_n$, this leads to a metal-insulator transition as n is varied. The origin of this transition can be traced to the charge transfer between the two constituents (J. Hoffman et al., to appear in *Phys. Rev. B*).¹ This charge transfer is also linked to interfacial magnetism – the LaNiO_3 becomes magnetic over approximately the first unit cell in the vicinity of the interface. To explore this further, we

made superlattices of $(La_{2/3}Sr_{1/3}MnO_3)_m/(LaNiO_3)_n$ where we observed magnetic coupling between $La_{2/3}Sr_{1/3}MnO_3$ layers separated by $(LaNiO_3)_n$, where n was as large as 9.² This long-range magnetic coupling also leads to a non-collinear magnetic structure, which we have explored in detail using neutron reflectometry (with Dr. Brian Kirby at NIST). We are currently exploring details of magnetic and electronic instabilities in the nickelate layer brought about by proximity to the manganite. (J. Hoffman et al., *in preparation*) We also have an ongoing collaboration with Prof. Jian-Min Zuo group (UIUC) to characterize the interfacial structure and electronic properties using transmission electron microscopy (STEM EELS).

(iii) Future Plans:

a.) *Tailoring inversion symmetry materials and M-O_{ap} bond lengths:* Motivated by our results in the past few years, we have plans to create and explore a number of materials systems using the synthesis approach that has been outlined earlier. We would like to understand how broken inversion symmetries in crystal structures could be used to tailor the bond between transition metal cations and apical oxygens in layered Ruddlesden Popper materials. In particular, we plan to explore the titanates and cuprates. In the titanates we think that our approach can be used to tailor interesting metallic states made from the Ti t_{2g} manifold, where we would tailor the Rashba interaction by breaking inversion symmetry via cation ordering. In the cuprates, we hope to tailor the Cu-O_{apical} bond length in a systematic way and explore changes in properties.³

b) *Interfacial Charge Transfer and Band-lineup in Mott Insulators:* ‘Band bending’ and charge transfer are very general ideas and should occur for a broad range of oxides, beyond the nickelate/manganite interfaces that we are currently exploring. However, a general understanding of what happens at such interfaces is lacking because more often than not the 3d transition metal oxides have narrow bands where the charge carriers are strongly correlated. Here, the ideas of ‘band bending’ have to be considered in light of the dynamic nature of the bands, i.e. the sensitivity of the band structure to filling. Furthermore, interfaces have broken inversion symmetry which can have interesting consequences for interfacial magnetism. Based upon the literature on measurements of band lineup of various 3d oxides, there are systematic though empirical guides to dope materials via charge transfer at interfaces that need to be explored in a controlled manner. We plan to do this work in conjunction with theorists Prof. Andrew Millis (Columbia) and Prof. Peter Littlewood (Argonne/Chicago) who are carrying out a first principles DFT/DMFT based study of this problem.

(iv) References:

1. “Charge transfer and interfacial magnetism in $(LaNiO_3)_n/(LaMnO_3)$ superlattices”, J. Hoffman et al., *arXive:1301.7295v2*, to appear in *Phys. Rev. B* (2013).
2. A long range magnetic coupling was observed in earlier work in manganite/nickelate superlattices – “Oscillatory exchange coupling and positive magnetoresistance in epitaxial oxide heterostructures”, K.R. Nikolaev et al., *Phys. Rev. Letts.* **85**, 3728 (2000).
3. Interfacial apical oxygens can have large distortions in cuprates: "Anomalous expansion of the copper-apical-oxygen distance in superconducting cuprate

bilayers." Zhou, Hua, et al. *Proceedings of the National Academy of Sciences* **107**, 8103-8107 (2010).

(v) Publications supported by Department of Energy, Basic Energy Sciences (since 2011):

- P1. "Non-volatile ferroelastic switching of the Verwey transition and resistivity of epitaxial $\text{Fe}_3\text{O}_4/\text{PMN-PT}$ (011)", Ming Liu, J. Hoffman, J. Wang, J. Zhang, B. Nelson-Cheeseman, A. Bhattacharya, *Scientific Reports* **3**, Article No. 1876 (2013) doi:10.1038/srep01876.
- P2. Book Chapter: 'Manganites Multilayers', Anand Bhattacharya, Shuai Dong, and Rong Yu, in "Multifunctional Oxide heterostructures", Eds. E. Y. Tsymbal, E. A. Dagotto, C.-B. Eom and R. Ramesh, Oxford University Press (2012).
- P3. "Interface Magnetism in a $\text{SrMnO}_3/\text{LaMnO}_3$ superlattice", S. Smadici, B. B. Nelson-Cheeseman, A. Bhattacharya, P. A. Abbamonte, *Phys. Rev. B* **86**, 174427 (2012).
- P4. "Structurally induced magnetization in a $\text{La}_{2/3}\text{Sr}_{4/3}\text{MnO}_4$ superlattice", Amish B. Shah, Brittany B. Nelson-Cheeseman, Ganesh Subramanian, Anand Bhattacharya, and John C. H. Spence, *Phys. Status Solidi A*, 1–6 (2012) / DOI 10.1002/pssa.201127728.
- P5. "Delta Doping of Ferromagnetism in Antiferromagnetic Manganite Superlattices", T.S. Santos, B.J. Kirby, S. Kumar, S.J. May, J.A. Borchers, B.B. Maranville, J. Zarestky, S. G. E. te Velthuis, J. van den Brink, and A. Bhattacharya, *Phys. Rev. Lett.* **107**, 167202 (2011).
- P6. "Ultrathin BaTiO_3 templates for multiferroic nanostructures", X.M. Chen, S. Yang, J.H. Kim, H.D. Kim, J.S. Kim, G. Rojas, R. Skomski, H.D. Lu, A. Bhattacharya, T. Santos, N. Guisinger, M. Bode, A. Gruverman, A. Enders, *New Journal of Physics* **13**, 083037 (2011).
- P7. "Control of octahedral rotations in $\text{LaNiO}_3/\text{SrMnO}_3$ superlattices", S. J. May, C. R. Smith, J. –W. Kim, E. Karapetrova, A. Bhattacharya, P. J. Ryan, *Phys. Rev. B* **83**, 153411 (2011).
- P8. "Cation-ordering Effects in the Single layered Manganite $\text{La}_{2/3}\text{Sr}_{4/3}\text{MnO}_4$ ", B. B. Nelson-Cheeseman, A. B. Shah, T. S. Santos, S. D. Bader, J.-M. Zuo and A. Bhattacharya, *Appl. Phys. Lett.* **98**, 072505 (2011).
- P9. "Practical Spatial Resolution of Electron Energy Loss Spectroscopy in Aberration Corrected Scanning Transmission Electron Microscopy", A.B. Shah, Q.M. Ramasse, J.G. Wen, A. Bhattacharya and J.M. Zuo, *Micron* **42**, 539 (2011).

Program Title: Raman Spectroscopy of Iron Oxypnictide Superconductors
Principle Investigator: Girsh Blumberg
Mailing Address: Department of Physics & Astronomy, Rutgers University,
136 Frelinghuysen Road, Piscataway NJ 08854-8019
E-mail: girsh@physics.rutgers.edu

PROGRAM SCOPE

The objectives of this project are to investigate the manner in which charge, spin and lattice coupling and dynamics evolve through various low-temperature and doping-concentration phases of iron-pnictide superconductor materials by employing low-frequency electronic Raman (i.e., inelastic light scattering) spectroscopy, and to clarify the microscopic origin of unconventional superconductivity and magnetism in these compounds. Among the anticipated outcomes of this project are: (i) elucidation of the microscopic origin of superconductivity in the iron-pnictide family of materials; (ii) insights into how to design new materials with enhanced superconducting properties; (iii) determination of a complete spectrum of collective excitation for the new family of unconventional multi-band superconductors driven by magnetic interactions.

RECENT PROGRESS

Iron-pnictides present a new paradigm of multi-band superconductivity in proximity to a spin density wave (SDW) order. Most FeAs compounds share a common phase diagram which in the underdoped region is marked by a structural transition at temperature T_S from tetragonal to orthorhombic phase followed by an SDW transition at T_{SDW} , slightly below T_S . The orthorhombic distortion at T_S breaks C_4 rotational symmetry while the translational symmetry is broken due to doubling of the unit cell at or above T_{SDW} . The system provides exceptional setting to study coexistence or competition between superconductivity below T_C and an SDW phases, the pairing mechanism and its relation to magnetism, and the pairing symmetry.

During this project we performed multiple series of polarized low-temperature Raman scattering studies of phononic, electronic, inter-band and magnetic excitations on the following families of compounds: CaFe_2As_2 , $(\text{Sr}_2\text{VO}_3)_2\text{Fe}_2\text{As}_2$, $\text{Fe}_{1+x}(\text{TeSe})$, $\text{K}_{0.75}\text{Fe}_{1.75}\text{Se}_2$, $\text{BaFe}_{1.9}\text{Pt}_{0.1}\text{As}_2$, $\text{Ca}(\text{Co}_x\text{Fe}_{1-x})_2\text{As}_2$, $\text{Na}_{1-x}\text{FeCo}_x\text{As}$.

I will highlight the following results:

1. Evolution of the nematic fluctuations in the proximity of structural phase transition line. Evidences for new charge order below T_S .
2. Evolution of the structural and magnetic order of the parent materials. Spectroscopy of SDW gap. (See Fig. 1)

3. Evolution of the superconducting order, superconducting gaps in the multi-band materials, evidences for s+- order parameter, competition between the ordered magnetic and superconducting phases. (See Fig. 2, 3)
4. In-gap collective excitations in the superconducting phase. Evidences for sub-dominant pairing in d-wave channel. Observation of Bardasis-Schrieffer collective modes (excitons).
5. Superradiance emission by superconductor-antiferromagnetic heterostructures in $K_{0.75}Fe_{1.75}Se_2$.

FUTURE PLANS

This year we will continue spectroscopic study of the oxypnictide compounds across the phase diagram as a function of carrier concentration, temperature, and magnetic field with the following goals:

1. Evaluate the interplay between structural, magnetic, and superconducting transitions.
2. Determine the symmetry of the superconducting order parameter, the magnitude of the superconducting gaps and their evolution with doping from polarized ultra-low-frequency electronic Raman scattering.

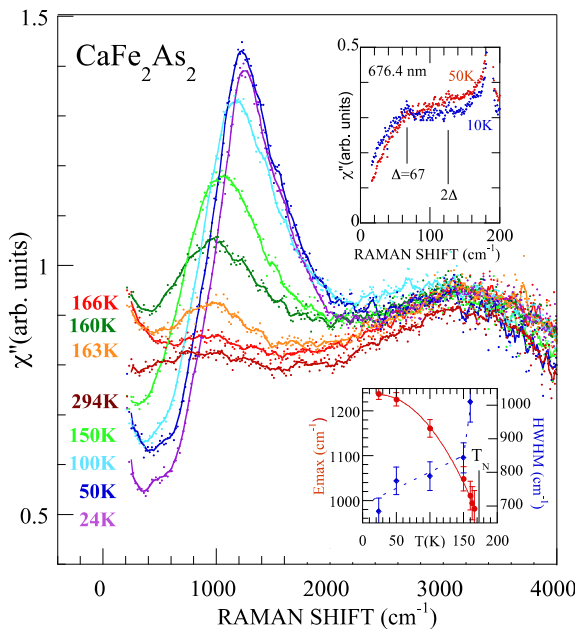


Figure 1. Raman response function showing the temperature evolution of SDW gap below T_{SDW} transition in the parent $CaFe_2As_2$ compound. Top inset depicts observation of spin gap at low temperatures.

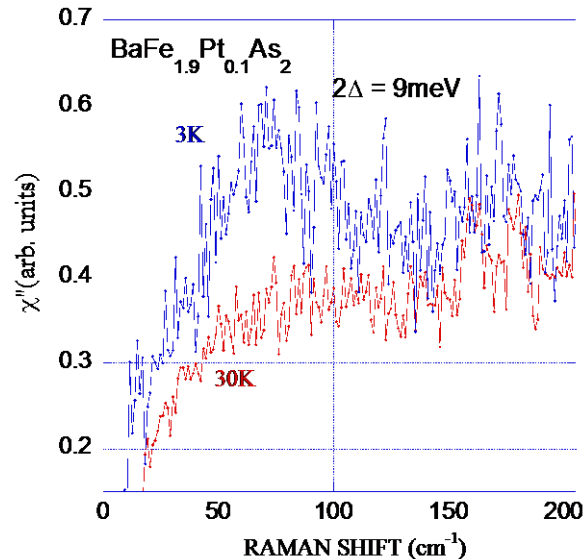


Figure 2. Low frequency Raman response from $BaFe_{1.9}Pt_{0.1}As_2$ superconductor above and below T_c . Pair breaking excitations observed with 9 meV maximum gap and about 5 meV in-gap structure.

3. Study the evolution of superconductivity with magnetic fields and determine the upper-critical fields and superconducting correlation lengths as functions of doping by magneto-Raman scattering experiments.
4. Search for the novel collective modes expected in the superconductors with multiple condensates and study their systematics.

ACKNOWLEDGMENTS

The work is done in collaboration with V.K. Thorsmolle, A. Ignatov, A. Mialitsin, C. Zhang, P. Dai, J. Paglione, N.L. Wang, Z. Yin, K. Haule. Research was supported by U.S. DOE, Office of BES, Award DE-SC0005463.

PUBLICATIONS

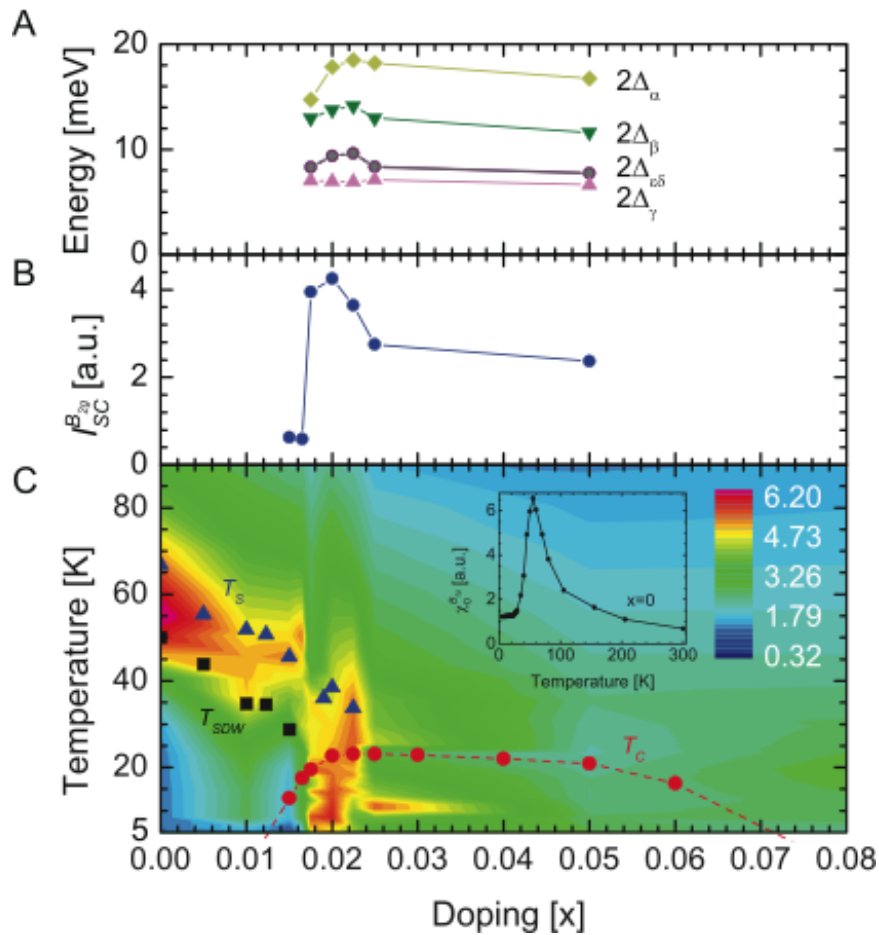


Figure 3. (A): Doping dependence of the superconducting gaps on five Fermi surfaces of $\text{Na}_{1-x}\text{FeCo}_x\text{As}$. (B): the intensity of superconducting coherence peak as function of doping. (C): Evolution of the real part of static Raman susceptibility as a function of temperature and doping. T_S , T_{SDW} , and T_C obtained by transport measurements are superimposed. A quantum critical point at about $x=0.02$ separating purely superconducting phase to the right from coexisting with SDW phase to the left is marked by enhanced Raman susceptibility. The inset shows the temperature dependence of the static Raman susceptibility for the parent compound.

1. A. Ignatov, A. Kumar, P. Lubik, R. H. Yuan, W. T. Guo, N. L. Wang, K. Rabe, and G. Blumberg, "Structural phase transition below 250 K in superconducting $K_{0.75}Fe_{1.75}Se_2$ ", Phys. Rev. **B86**, 134107 (2012).
2. V.K. Thorsmolle, C. Zhang, P. Dai, Z. Yin, K. Haule, G. Blumberg, "Phase diagram of $Na_{1-x}FeCo_xAs$ – What drives superconductivity?" In Preparation.
3. S. Ziemak, K. Kirshenbaum, S. R. Saha, R. Hu, J.-Ph. Reid, R. Gordon, L. Taillefer, A. Ignatov, D. Kolchmeyer, G. Blumberg, D. Evtushinsky, S. Thirupathaiah, S. V. Borisenko, and J. Paglione, "Observation of isotropic gap in $BaFe_{1.9}Pt_{0.1}As_2$ through multiple experimental". Preprint for Phys. Rev. B.
4. A.V. Mialitsin, I. A. Solov'yov , A. I. Toth, I. I. Mazin, A.H. Nevidomskyy, B.S. Dennis, and G. Blumberg, "Intertwined Order Parameters in a Charge-Ordered Superconductor". Submitted to PRL.
5. A.V. Mialitsin, G. Blumberg, "Pair Breaking Excitations in Superconductors – Raman Sum Rules ". In Preparation.
6. A. Ignatov, R.H. Yuan, and N.L. Wang, and G. Blumberg, "Superradiance emission by $K_{0.75}Fe_{1.75}Se_2$ superconductors." In Preparation.
7. G. Blumberg, "Raman spectroscopy of multiband superconductors." Multiband and Multiorbital Effects in Novel Materials. Cargèse, France, Aug. 1-13, 2011.
8. A. Ignatov, R.H. Yuan, and N.L. Wang, and G. Blumberg, "Phononic, magnetic, and interband Raman scattering in $K_{0.75}Fe_{1.75}Se_2$ superconductor." Contribution at APS March meeting. Boston, Massachusetts, Feb 27 - March 2, 2012.
9. G. Blumberg, "Raman spectroscopy of iron based superconductors." International Seminar and Workshop on Quantum Matter from the Nano- to the Macroscale. Dresden, Germany, June 18 - July 6, 2012.
10. S. Ziemak, K. Kirshenbaum, S.R. Saha, R. Hu, J. Paglione, J.-Ph. Reid, R. Gordon, L. Taillefer, A. Ignatov, D. Kolchmeyer, G. Blumberg, D. Evtushinsky, S. Thirupathaiah, S.V. Borisenko, "Investigation of Pairing Symmetry in Pt-Substituted $BaFe_2As_2$ " Contribution at APS March meeting. Baltimore, MD, March 18 - 22, 2013.
11. G. Blumberg, "The phase diagram of pnictide superconductors – competing orders." International Summer School on Superconductivity – Theory, Experiments, and Phenomena." Cargèse, France, August 5-17, 2013.

Cold Exciton Gases in Semiconductor Heterostructures

Leonid Butov, University of California at San Diego

Project Scope

An indirect exciton is a bound pair of an electron and a hole confined in spatially separated layers. Long lifetimes of indirect excitons allow them to cool down to low temperatures below the temperature of quantum degeneracy. This gives an opportunity to study cold exciton gases. Indirect excitons are dipoles and their energy can be controlled by voltage. This gives an opportunity to create a variety of potential landscapes for indirect excitons and use them as a tool for studying the physics of excitons. Indirect excitons have long spin relaxation times. This allows studying exciton spin transport and other spin-related phenomena. Indirect excitons can travel over large distances before recombination. This gives an opportunity to measure exciton transport by imaging spectroscopy. Within this project, we explore these properties of indirect excitons for studying cold excitons in lattices and for studying spin-related phenomena in cold exciton gases.

Recent Progress (2011-2013)

Spontaneous coherence in a cold exciton gas [1].

We observed patterns of spontaneous coherence, polarization textures, and phase singularities in a cold gas of indirect excitons. We found that spontaneous coherence of excitons emerges in the region of the macroscopically ordered exciton state and in the region of vortices of linear polarization. The coherence length in these regions is much larger than in a classical gas, indicating a coherent state with a much narrower than classical exciton distribution in momentum space, characteristic of a condensate. We found that a pattern of extended spontaneous coherence is correlated with a pattern of spontaneous polarization, revealing the properties of a multicomponent coherent state. We also observed phase singularities in the coherent exciton gas. All these phenomena emerge when the exciton gas is cooled below a few kelvin.

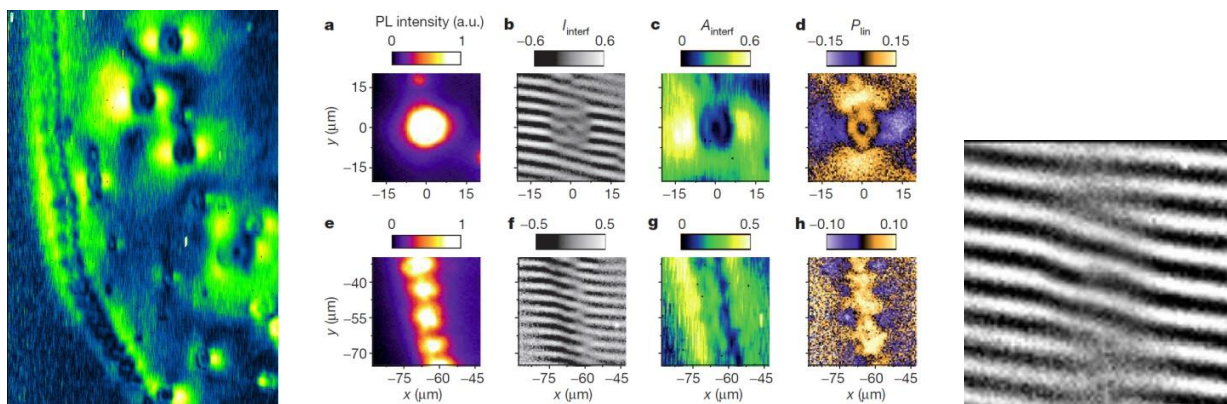


Fig. 1. Spontaneous coherence, polarization textures, and phase singularities in a cold exciton gas. (left) Pattern of spontaneous coherence. (middle) From left to right: Emission, interference, coherence, and polarization patterns in a region of a localized bright spot (upper line) and in a region of the external ring (lower line). (right) Fork-like defects in exciton interference pattern showing a phase singularity. From [1].

Spontaneous coherence and condensation of indirect excitons in a trap [2].

We observed spontaneous coherence and condensation of indirect excitons in an electrostatic trap. At low temperatures, the exciton coherence length becomes much larger than the thermal de Broglie wavelength and reaches the size of the exciton cloud in the trap. This is the key signature of exciton condensation.

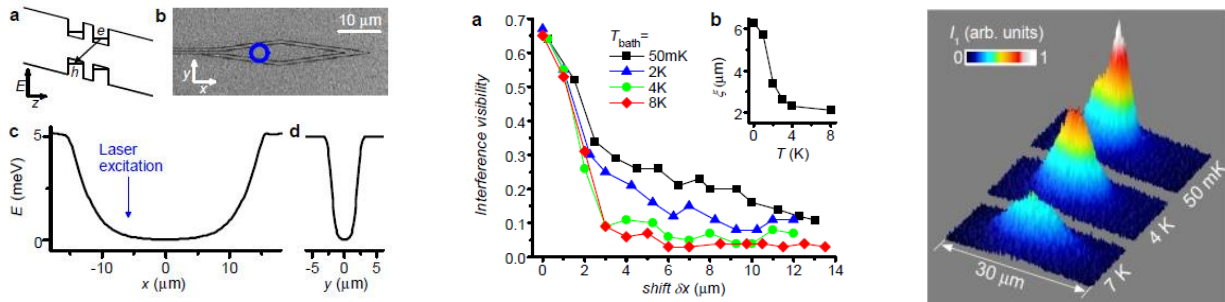


Fig. 2. Spontaneous coherence of indirect excitons in a trap. (left) (a) CQW band diagram. (b) SEM image of electrodes forming the diamond trap. The position of the laser excitation spot is indicated by the circle. (c,d) Simulation of exciton energy profile along x (c) and y (d). (middle) (a) Amplitude of interference fringes presenting exciton coherence degree for excitons in the trap. (b) Exciton coherence length as a function of temperature. (right) Exciton emission patterns. From [2].

Spin currents and spin textures in a coherent exciton gas [3].

We detected spin currents in a coherent gas of indirect excitons. The realized long-range spin currents originate from the formation of a coherent gas of bosonic pairs – a mechanism to suppress the spin relaxation. The spin currents result in the appearance of a variety of polarization patterns, including helical patterns, four-leaf patterns, spiral patterns, bell patterns, and periodic patterns. We demonstrated control of the spin currents by a magnetic field. Simulations of coherent exciton spin transport describe the observed exciton polarization patterns and indicate the trajectories of the spin currents.

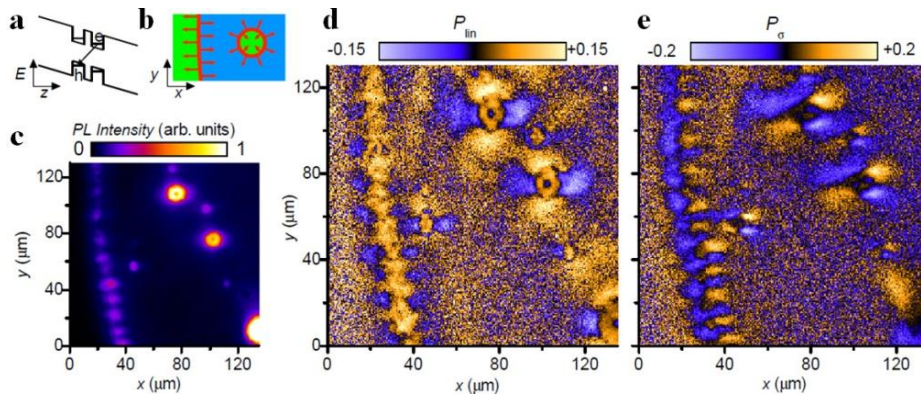


Fig. 3. Exciton polarization textures. (b) Schematic of exciton formation in the external ring (left) and LBS ring (right); Excitons (red) form on the boundary of hole-rich (blue) and electron-rich (green) areas. Exciton transport is indicated by red arrows. (c) A segment of the emission pattern of indirect excitons showing the external ring (left) and multiple LBS. (d,e) Patterns of linear $P_{\text{lin}} = (I_x - I_y)/(I_x + I_y)$ and circular $P_{\sigma} = (I_{\sigma+} - I_{\sigma-})/(I_{\sigma+} + I_{\sigma-})$ polarizations of the emission of indirect excitons in the region shown in (c). A radial source of excitons with a divergent momentum distribution in the LBS generates a helical texture of linear polarization winding around the origin (d) and a four-leaf pattern of circular polarization (e). A periodic array of beads in the MOES (c) creates periodic polarization textures (d,e). $T_{\text{bath}}=0.1$ K. From [3].

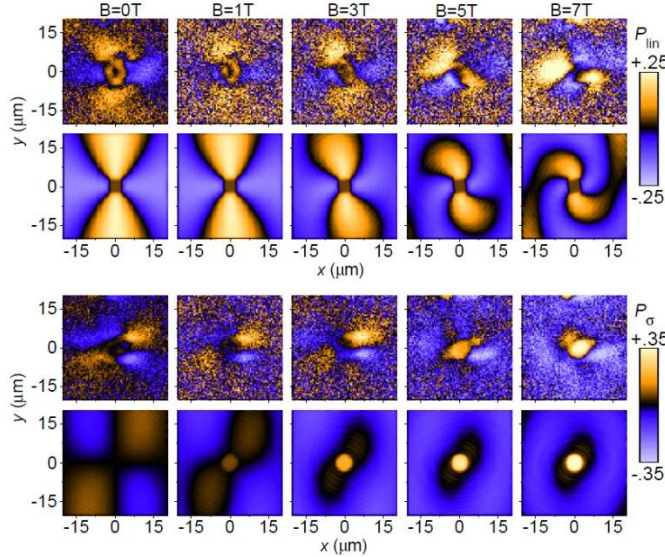


Fig. 4. Control of exciton polarization textures by magnetic field. (two top rows) Measured and simulated patterns of linear polarization of the emission of indirect excitons P_{lin} in the region of LBS vs magnetic fields B . A helical (vortex) pattern of linear polarization at $B=0$ and a spiral pattern of linear polarization at finite B are observed. (two bottom rows) Measured and simulated patterns of circular polarization of the emission of indirect excitons P_{σ} in the region of LBS vs B . A four-leaf pattern of circular polarization at $B=0$ and a bell-like pattern of circular polarization at finite B are observed. $T_{\text{bath}}=0.1$ K, the LBS is at (105,75) in Fig. 3. From [3].

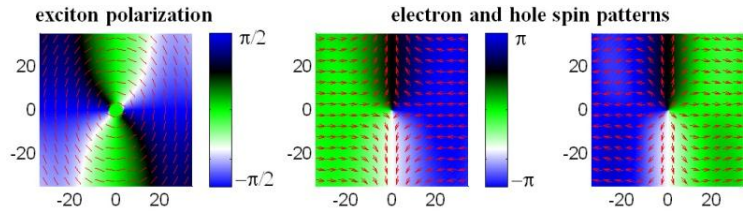


Fig. 5. Simulated in-plane exciton polarization (left) and electron and hole spin (right) patterns. The lines (arrows) and the color visualize the orientation of the linear polarization (spin, respectively). From [3].

Two-dimensional electrostatic lattices for indirect excitons [4].

We developed a method for the realization of two-dimensional electrostatic lattices for excitons using patterned interdigitated electrodes. Lattice structure is set by the electrode pattern and depth of the lattice potential is controlled by applied voltages. Exciton number per lattice site is controlled by laser excitation. We demonstrated experimental proof of principle for creating two-dimensional lattices for excitons by this method.

Future Plans

For the part of the project – excitons in lattices – we plan to continue the study of excitons in linear and two-dimensional electrostatic lattices. In particular, we plan to study exciton transport and coherence in the lattices.

In previous work, we realized moving lattices, conveyers, for indirect excitons [5]. The conveyers are created by applying AC voltages to the electrodes of the lattice. This yields a traveling lattice moving laterally across the sample. The wavelength of this moving lattice is set by the electrode periodicity, the amplitude is controlled by the applied voltage, and the speed – by the AC frequency. We plan to develop and realize stirring potentials for excitons by a modification of the exciton conveyers. While a conveyer is created by a linear set of electrodes, a stirring potential will be created by a centrally symmetric set of electrodes. Stirring potentials can be used for generation and control of exciton vortices.

For the part of the project – spin related phenomena in cold exciton gases – we plan to study the spin transport of excitons by polarization-resolved imaging. We also plan to work on the development of control of the spin transport.

Publications (2-year list of publications supported by BES)

1. A.A. High, J.R. Leonard, A.T. Hammack, M.M. Fogler, L.V. Butov, A.V. Kavokin, K.L. Campman, A.C. Gossard, Spontaneous coherence in a cold exciton gas, *Nature* **483**, 584–588 (2012).
2. A.A. High, J.R. Leonard, M. Remeika, L.V. Butov, M. Hanson, A.C. Gossard, Condensation of Excitons in a Trap, *Nano Lett.* **12**, 2605–2609 (2012).
3. A.A. High, A.T. Hammack, J.R. Leonard, Sen Yang, L.V. Butov, T. Ostatnický, M. Vladimirova, A.V. Kavokin, T.C.H. Liew, K.L. Campman, A.C. Gossard, Spin currents in a coherent exciton gas, *Phys. Rev. Lett.* **110**, 246403 (2013).
4. M. Remeika, M.M. Fogler, L.V. Butov, M. Hanson, A.C. Gossard, Two-Dimensional Electrostatic Lattices for Indirect Excitons, *Appl. Phys. Lett.* **100**, 061103 (2012).
5. A.G. Winbow, J.R. Leonard, M. Remeika, Y.Y. Kuznetsova, A.A. High, A.T. Hammack, L.V. Butov, J. Wilkes, A.A. Guenther, A.L. Ivanov, M. Hanson, A.C. Gossard, Electrostatic Conveyer for Excitons, *Phys. Rev. Lett.* **106**, 196806 (2011).

The Ames Laboratory Complex States, Emergent Phenomena and Superconductivity in Intermetallic & Metal-like Compounds FWP

PIs: P. Canfield (FWP Leader) canfield@ameslab.gov, S. Bud'ko
budko@ameslab.gov, Y. Furukawa furukawa@ameslab.gov, D. Johnston
johnston@ameslab.gov, A. Kaminski kaminski@ameslab.gov, V. Kogan
kogan@ameslab.gov, R. Prozorov prozorov@ameslab.gov, M. Tanatar
tanatar@ameslab.gov

FWP web page: <https://www.ameslab.gov/dmse/bes-projects/complex-states>

SCOPE

This FWP has been specifically assembled to create, study, and understand materials with novel electronic and magnetic ground states. It intimately links design, growth, characterization, modeling and theory within a National Laboratory setting, allowing for the rapid identification, understanding and control of systems of interest. The FWP has many powerful techniques at its disposal, ranging from a wide variety of synthetic methods, through an extensive range of thermodynamic, transport and spectroscopic measurements, to sophisticated modeling and theory. The strength of this FWP is its ability to cycle through the “think, make, measure, understand, control, think” cycle rapidly and efficiently. The goal of this FWP is the design, discovery, characterization, understanding and ultimately control over materials with complex and potentially useful properties.

RECENT PROGRESS

The priority of this FWP is the development and understanding of model systems combined with agile and flexible response to, and leadership in, a rapidly-changing materials landscape. Within this context, some of the systems that have been recently focused on include: Fe-based, and related, superconductors, and correlated electron systems with small, or vanishing, moments, because of their combined promise to serve as model systems as well as starting points for developing better, energy-relevant properties. To accomplish this goal, three highly intermeshed classes of activities will operate both in series and in parallel:

- Design and growth (Canfield, Bud'ko, Johnston, Kogan)
- Advanced Characterization (Bud'ko, Furukawa, Kaminski, Prozorov, Tanatar)
- Theory and modeling: (Johnston, Kogan, Prozorov)

During the 2011 – 13 period the FWP has been able to make significant progress in the fields of correlated electron systems, the physics associated with local moment ordering and the effects of internal and external fields on the ordered states, and, of course, superconductivity. One of the primary focii of the FWP efforts has been on the Fe-base superconductors. During the past three years we have made key contributions in the areas of:

- Detailed thermodynamic, transport, microscopic and spectroscopic studies of $\text{Ba}(\text{Fe}_{1-x}\text{TM}_x)_2\text{As}_2$ ($\text{TM} = \text{Co}, \text{Ni}, \text{Ru}, \text{Rh}, \text{Pd}, \text{Mn}$), compounds.

- Establishment of simple empirical rule between jump in specific heat and Tc for Fe-based superconductors.
- London penetration depth and thermal transport measurements across pnictide series.
- Development of post-crystal-growth annealing / quenching of pure and Co-substituted CaFe₂As₂ that allows for control of internal strain that mimics effects of externally applied pressures of up to 5 kbar and allows for ambient pressure studies of collapsed tetragonal phase.

We also continued to explore the relationship between SC and the pseudogap in cuprates. By taking a quantitative approach to ARPES measurements, we discovered a new spectroscopic signature of pair formation above T_c and demonstrated that a region commonly referred to as the “pseudogap” consists of two distinct parts: Part (1) due to pair formation, persists to an intermediate temperature $T_{\text{pair}} < T^*$ and Part (2) the “proper” pseudogap characterized by the loss of spectral weight and anomalies in transport properties that extend to T^* . T_{pair} has a value around 120–150 K even for materials with very different T_c . This likely sets a limit on the highest attainable T_c in the cuprates.

The FWP also made key discoveries in the fields of correlated electron physics as well as local moment magnetism. We advanced the fields of:

- Field and pressure induced quantum criticality, defining the phase diagrams for YbAgGe, YbBiPt and YbFe₂Zn₂₀;
- Magnetism and electronic properties of compounds related to Fe-based superconductors with detailed studies of first BaMn₂As₂ and then the Ba_{1-x}K_xMn₂As₂ series.
- Magnetic quasicrystals by discovering the first examples of local moment bearing, binary quasicrystals in the R-Cd (R = Gd – Tm, Y) system.
- ARPES by constructing a tunable, high resolution VUV laser-based spectrometer for measurements of electronic properties of novel materials. The VUV laser system utilizing a domestically-grown KBBF crystal is fully operational and delivers photons with energies tunable between 4.5 and 7 eV.
- Magnetic measurements by adapting a tunnel diode resonator (TDR) to work with a dilution refrigerator and is currently capable of taking useful data down to a temperature of 60 mK and in magnetic fields up to 16 T and by commissioning a new Mössbauer spectroscopy system that has been designed to work between 4 K and room temperature, using one cooling system, and between room temperature and 1000 K, using a separate heating system.

FUTURE PLANS

We propose to continue our efforts toward the development and understanding of model systems of complex states, emergent phenomena, and SC combined with agile and flexible responses to, and leadership in, a rapidly-changing materials landscape. We will accomplish this by creating, testing, and ultimately understanding systems that exhibit

compelling physical properties and ground states. It is our intent to organize our efforts, as an FWP and as part of the Ames Laboratory, to create and respond to new discoveries. We will broadly focus on high temperature superconductivity as well as discovery and manipulation of novel, and in some cases fragile, magnetic and electronic states. For the work on superconductors we will

- Systematically study the $\text{Ca}(\text{Fe}_{1-x}\text{T}_x)_2\text{As}_2$ ($T = \text{Co, Ni, Rh}$) systems, create temperature – strain – substitution phase diagrams, determine mechanism for strain – pressure relation, study the importance of magnetic fluctuations for formation of the superconducting state, use laser ARPES data to quantify temperature and substitution dependence of electronic structure.
- Quantify and understand the gap symmetry of Fe-based superconductors moving beyond those based solely on the AFe_2As_2 structure by use of London penetration depth and thermal conductivity measurements.
- Use the recently-developed quantitative ARPES methodology to address questions of condensation energy in CuO-based SC.
- Continue our high risk / high payoff exploratory materials physics synthesis agenda: the search for new examples of novel SC and/or other interesting ground states.

We will also study a variety of model correlated electron systems as well as systems with fragile or frustrated magnetism. These will include work on:

- CaCo_2As_2 , SrCo_2As_2 , BaCo_2As_2 , SrMn_2As_2 and other potentially correlated systems related to the Fe-based superconductors. SrCo_2As_2 in particular appears to have strong magnetic fluctuations the may drive correlated electron behavior.
- The use of NMR as well as elastic and inelastic scattering to determine the microscopic origins of quantum critical behavior in YbBiPt , YbAgGe , and $\text{YbT}_2\text{Zn}_{20}$ ($T = \text{Fe, Co, Ru, Rh, Os, Ir}$) systems.
- Further development and discovery of quantum critical systems driven either by substitution, pressure or applied field. Such systems may well feed back to our studies of superconductivity.
- The discovery of new quasicrystalline phases and the search for aperiodic systems that manifest (i) long range magnetic order, (ii) correlated electronic states, or (iii) superconductivity.
- ^{31}P -NMR measurements under high pressure on $\text{AA}'\text{VO}(\text{PO}_4)_2$ systems to systematically investigate the pressure effects on the magnetic properties of the frustrated J_1 - J_2 square spin-1/2 lattice.
- The use of our recently developed reactive / volatile multi-glove box system to develop and discover N-based materials. An initial example is highly anisotropic magnetism as well as quantum tunneling in $\text{Li}_2(\text{Li}_{1-x}\text{Fe}_x)\text{N}$.

SELECTED PUBLICATIONS (out of ~ 200 papers) FROM 2011 – 2013:

See <https://www.ameslab.gov/dmse/bes-projects/complex-states> for full list/links

“A family of binary magnetic icosahedral quasicrystals based on rare earths and cadmium”, Goldman, Alan I.; Kong, Tai; Kreyssig, Andreas; Jesche, Anton; Ramazanoglu, Mehmet; Dennis, Kevin W.; Bud'ko, Sergey L.; Canfield, Paul C. *Nature Materials* (2013), 12(8), 714-718.

“Magnetic-field-tuned quantum criticality of the heavy-fermion system YbPtBi” E. D. Mun, S. L. Bud'ko, C. Martin, H. Kim, M. A. Tanatar, J.-H. Park, T. Murphy, G. M. Schmiedeshoff, N. Dilley, R. Prozorov, and P. C. Canfield, *Phys. Rev. B* **87** (2013), 075120.

“Unusual Temperature Dependence of Band Dispersion in $\text{Ba}(\text{Fe}_{1-x}\text{Ru}_x)_2\text{As}_2$ and its Consequences for Antiferromagnetic Ordering”, R. S. Dhaka, S. E. Hahn, E. Razzoli, Rui Jiang, M. Shi, B. N. Harmon, A. Thaler, S. L. Bud'ko, P. C. Canfield, and Adam Kaminski, *Phys. Rev. Lett.* **110** (2013), 067002.

“Coexistence of Half-Metallic Itinerant Ferromagnetism with Local-Moment Antiferromagnetism in $\text{Ba}_{0.60}\text{K}_{0.40}\text{Mn}_2\text{As}_2$ ”, Abhishek Pandey, B. G. Ueland, S. Yeninas, A. Kreyssig, A. Sapkota, Yang Zhao, J. S. Helton, J. W. Lynn, R. J. McQueeney, Y. Furukawa, A. I. Goldman, and D. C. Johnston, *Phys. Rev. Lett.* **111** (2013), 047001

“Magnonlike Dispersion of Spin Resonance in Ni-doped BaFe_2As_2 ”, M. G. Kim, G. S. Tucker, D. K. Pratt, S. Ran, A. Thaler, A. D. Christianson, K. Marty, S. Calder, A. Podlesnyak, S. L. Bud'ko, P. C. Canfield, A. Kreyssig, A. I. Goldman, and R. J. McQueeney, *Phys. Rev. Lett.* **110** (2013), 177002

"Control of Magnetic, Nonmagnetic, and Superconducting States in Annealed $\text{Ca}(\text{Fe}_{1-X}\text{Co}_X)_2\text{As}_2$," S. Ran, S. L. Bud'ko, W. E. Straszheim, J. Soh, M. G. Kim, A. Kreyssig, A. I. Goldman, and P. C. Canfield, *Physical Review B* (2012), **85**, 224528

"Magnetic Susceptibility of Collinear and Noncollinear Heisenberg Antiferromagnets," D. C. Johnston, *Physical Review Letters* (2012), **109**, 077201.

"Disentangling Cooper-Pair Formation above the Transition Temperature from the Pseudogap State in the Cuprates," T. Kondo, Y. Hamaya, A. D. Palczewski, T. Takeuchi, J. S. Wen, Z. J. Xu, G. D. Gu, J. Schmalian, and A. Kaminski, *Nature Physics* **7** (2011), 21-25.

"Stabilization of an Ambient-Pressure Collapsed Tetragonal Phase in CaFe_2As_2 and Tuning of the Orthorhombic-Antiferromagnetic Transition Temperature by over 70 K Via Control of Nanoscale Precipitates," S. Ran, S. L. Bud'ko, D. K. Pratt, A. Kreyssig, M. G. Kim, M. J. Kramer, D. H. Ryan, W. N. Rowan-Weetaluktuk, Y. Furukawa, B. Roy, A. I. Goldman, and P. C. Canfield, *Physical Review B* (2011), **83**, 144517.

Program Title: Towards a Universal Description of Vortex Matter in Superconductors

Principal Investigator: L. Civale;

Mailing address: Los Alamos National Laboratory, MPA-CMMS, MS-K764, Los Alamos, NM, 87545

E-mail: lcivale@lanl.gov

Program Scope

Superconducting vortex physics has been a major field in condensed matter and statistical physics since the discovery of the oxide high temperature superconductors (HTS). The fascinating vortex phenomenology in HTS, such as their complex phase diagram in the magnetic field - temperature space and their rich non-equilibrium dynamic behavior, arises from the large influence of the thermal fluctuations, which in turn is mainly a consequence of the small superconducting coherence length (ξ) and large crystalline anisotropy (γ). It is important noticing, however, that there is no hard boundary between vortex phenomenology in HTS and conventional low temperature superconductors (LTS). A comprehensive vortex physics description should be **universal** in the sense that it should be applicable to all or at least a broad variety of SC. The present understanding of vortex matter falls far short of that goal, mostly because of the complexity of the interactions of vortices with inhomogeneities, which among other consequences are responsible for *vortex pinning*. In this project we intend to develop a general quantitative description of non-equilibrium vortex dynamics in the presence of material inhomogeneities, including flux pinning and creep phenomena, valid for all superconductors.

By comparing and contrasting systems with vastly different superconducting properties under a broad spectrum of conditions including extreme ones, and by improving and expanding existing theoretical models, we aim at establishing a general framework that could not be recognized by studying individual systems. This will drastically enhance our capability for predicting, controlling and designing the vortex matter behavior. The relevance of this study goes beyond understanding and manipulating existing materials, as any yet-to-be-discovered superconductor will share most of the vortex physics explored here.

Recent Progress

Fast, simple method to measure the absolute value of the superconducting penetration depth by magnetic force microscopy (MFM), involving no free parameters and no tip modeling [14] (Fig. 1) (Fig. 1)

The penetration depth (λ) is a characteristic parameter of a superconductor; it plays a central role in determining the vortex properties including vortex size, strength of vortex-vortex interactions, elastic constants, pinning energies, and intensity of the fluctuations that control the vortex dynamics. $\lambda(T)$ also provides important information on superconducting properties not related to vortex physics (carrier density, pairing symmetry). Several relatively simple methods had been previously developed to measure $\lambda(T)$ variations, but reliable

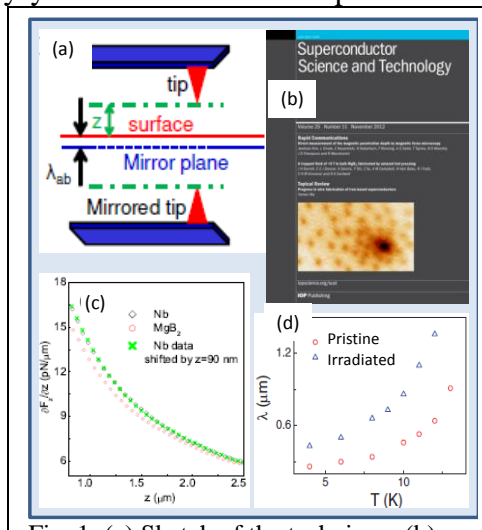


Fig. 1: (a) Sketch of the technique. (b) SuST Nov. 2012 cover. (c) use of the method to measure λ in MgB_2 [11]; (d) increase in $\lambda(T)$ in $Ca_{0.5}Na_{0.5}Fe_2As_2$ crystal due to proton irradiation [13].

determinations of λ absolute values are difficult to implement, time consuming or expensive.

The central idea of our method is to compare the MFM cantilever frequency shift due to the Meissner currents in the investigated sample and in a reference sample of known λ (Nb film), as a function of the separation between the MFM tip and the sample surface. Both curves can be superimposed by displacing one of them; the value of the displacement is the difference between the λ in both samples.

We have used the new tool to explore vortex physics in different systems, including the anomalous $\lambda(T)$ dependence in MgB₂ films due to two-band superconductivity effects [11], the increase in λ due to proton irradiation on Ca_{0.5}Na_{0.5}Fe₂As₂ single crystals [13], and the very large $\sim 1\mu\text{m}$ (indicating very low carrier density) in Ca₁₀(Pt₃As₈)₅(Fe_{1-x}Pt_x)₂As₂₅ [Ref. 9].

Realization and study of hybrid pinning landscape in iron-based superconducting films [12].

Vortex matter in iron-based superconductors exhibits a rich phenomenology that is still largely unexplored, with many shared characteristics with high T_c cuprates. One of them is that vortices are affected by strong thermal fluctuations due to the small ξ coherence length and relatively high T_c and γ . This in turn has important consequences in determining how vortices are trapped by different pinning potentials. Angular dependent critical current measurements are extremely useful to determine the nature of the effective pinning centers composed of correlated, planar and randomly distributed point-like pinning centers that comprise the pinning landscape.

Co-doped BaFe₂As₂ (Ba122) thin films show one of the strongest columnar pinning of any superconductor. They are ideal to study the interaction between columnar and point-like defects. We added point defects by 3MeV protons irradiation in consecutive doses (see Fig. 2).

We found that the addition of point defects has negative effect in the irreversibility line at fields (few T) where the columnar defects are most effective *i.e.* $\mathbf{H} \parallel c$. This is understood as a competition between columnar defects that tend to localize vortices in the columns and point defects encourage vortices meandering (de-localization). It was also observed that J_c remains unchanged (or slightly decreased) for $\mathbf{H} \parallel c$ at low fields/low temperatures (Fig. 1 a) , but at higher fields, J_c increases along the $\mathbf{H} \parallel ab$, (Fig. 2b) due to a clear anisotropic contribution to J_c coming from the point-like defects produced by the proton irradiation. Our findings indicate that there is no “magic-bullet” approach for maximizing pinning for all H and T, but that landscapes can be engineered so different defects can ‘cooperate’.

Future Plans

As a general strategy we will continue exploring vortex matter in as broad a variety of materials, properties and experimental conditions as possible. A central focus in our future work will be the understanding of the puzzling fact that the new Fe-based SC have a fast and HTS-like vortex

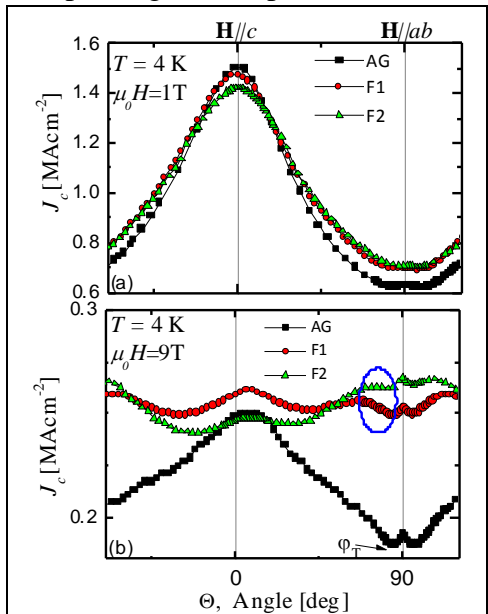


Fig. 2: Critical current density (J_c) as a function of field orientation (Θ) at T=4K and 1 and 9T, for Co-BaFe₂As₂ thin film for As Grown, and proton irradiated with F1=1x and F2=2x10¹⁶ cm⁻².

dynamics, while MgB_2 has much lower and LTS-like creep. This defines the three main groups of materials to be explored: YBCO (as representative of oxide HTS), Fe-based SC, and MgB_2 .

It also defines the key physics questions:

Is the Ginzburg number (Gi) the best parameter to quantify vortex thermal fluctuations? How is Gi affected by the disorder? How is the vortex pinning and dynamics affected by different combination of defects into complex pinning landscapes in samples with different Gi regimes?

Publications

1. “Effects of the doping on the crystalline structure and superconductivity properties in $Ca_{1-x}Na_xFe_2As_2$ single crystals”, N. Haberkorn, B. Maiorov, I.O. Usov, M. Jaime, M. Miura, G.F. Chen, W. Yu and L. Civale, *Phys. Rev. B* **84**, 064533 (2011).
2. “Strong pinning and elastic to plastic vortex crossover in Na-doped $CaFe_2As_2$ single crystals”, N. Haberkorn, M. Miura, B. Maiorov, G.F. Chen, W. Yu, and L. Civale, *Phys. Rev. B* **84**, 094522 (2011).
3. “Highly aligned carbon nanotube forests coated by superconducting NbC”, G. Zou, H. Luo, S. Baily, Y. Zhang, N. Haberkorn, J. Xiong, E. Bauer, T. McCleskey, A. Burrell, L.Civale, Y.T. Zhu, J.L. MacManus-Driscoll, and Q.X. Jia, *Nature Communications*, **2**, 428 (2011).
4. “Epitaxial superconducting δ -MoN films grown by a chemical solution method”, Y.Y. Zhang, N. Haberkorn, F. Ronning, H. Wang, N.A. Mara, M. Zhuo, C. Li, J.H. Lee, K.J. Blackmore, E. Bauer, A.K. Burrell, T.M. McCleskey, M.E. Hawley, R.K. Schulze, L. Civale, T. Tajima and Q.X. Jia,, *J. Am. Chem. Soc.* **133**, 20735 (2011)
5. “Direct observation of magnetic phase coexistence and magnetization reversal in a $Gd_{0.67}Ca_{0.33}MnO_3$ thin film”, J. Kim, N. Haberkorn, L. Civale, P. Dowden, A. Saxena, J.D. Thompson, R. Movshovich and E. Nazaretski, *Appl. Phys. Lett.*, **100**, 022407 (2012).
6. “Influence of random point defects introduced by proton irradiation on critical current density and vortex dynamics of $Ba(Fe_{0.925}Co_{0.075})_2As_2$ single crystals”, N. Haberkorn, B. Maiorov, I.O. Usov, M. Weigand, W. Hirata, S. Miyasaka, S.Tajima, N.Chikumoto, K.Tanabe and L. Civale, *Phys. Rev. B* **85**, 014522 (2012).
7. “Upper critical field and thermally activated flux flow in single-crystalline $Tl_{0.58}Rb_{0.42}Fe_{1.72}Se_2$ ”, L. Jiao, Y. Kohama, J. L. Zhang, H. D. Wang, B. Maiorov, F. F. Balakirev, Y. Chen, L. N. Wang, T. Shang, M. H. Fang and H. Q. Yuan, *Phys. Rev. B* **85**, 064513 (2012).
8. “Aligned carbon nanotubes sandwiched in epitaxial NbC film for enhanced superconductivity”, Y. Y. Zhang, F. Ronning, K. Gofryk, N. A. Mara, N. Haberkorn, G. Zou, H. Wang, J. H. Lee, E. Bauer, T. M. McCleskey, A. K. Burrell, L. Civale, Y. T. Zhu and Q.X. Jia, *Nanoscale* **4**, 2268 (2012).
9. “Large magnetic penetration depth and thermal fluctuations in a $Ca_{10}(Pt_3As_8)[(Fe_{1-x}Pt_x)_2As_2]_5$ ($x=0.097$) single crystal”, Jeehoon Kim, F. Ronning, N. Haberkorn, L. Civale, E. Nazaretski, Ni Ni, J.M. Allred, R. J. Cava, J. D. Thompson, and R. Movshovich, *Phys. Rev. B* **85**, 180504(R) (2012).
10. “High temperature change of the creep rate in $YBa_2Cu_3O_{7-d}$ films with different pinning landscapes”, N. Haberkorn, M. Miura, J. Baca, B. Maiorov, I. Usov, P. Dowden, S. R. Foltyn, T. G. Holesinger, J. O. Willis, K. R. Marken, T. Izumi, Y. Shiohara and L. Civale, *Phys. Rev. B*, **85**, 174504 (2012).

11. "Measurement of the magnetic penetration depth of a superconducting MgB₂ thin film with a large intraband diffusivity", Jeehoon Kim, N. Haberkorn, Shi-Zeng Lin, L. Civale, E. Nazaretski, B. H. Moeckly, C. S. Yung, J. D. Thompson, and R. Movshovich, Phys. Rev. B **86**, 024501 (2012).
12. "Competition and cooperation of pinning by extrinsic point-like defects and intrinsic strong columnar defects in BaFe₂As₂ thin films", B. Maiorov, T. Katase, I. O. Usov, M. Weigand, L. Civale, H. Hiramatsu, and H. Hosono, Phys. Rev. B **86**, 094513 (2012).
13. "Magnetic penetration-depth measurements of a suppressed superfluid density of superconducting Ca_{0.5}Na_{0.5}Fe₂As₂ single crystals by proton irradiation", Jeehoon Kim, N. Haberkorn, M. J. Graf, I. Usov, F. Ronning, L. Civale, E. Nazaretski, G. F. Chen, W. Yu, J. D. Thompson and R. Movshovich, Phys. Rev. B **86**, 144509 (2012).
14. "Direct measurement of the absolute magnetic penetration depth value in superconducting films", Jeehoon Kim, L. Civale, E. Nazaretski, N. Haberkorn, F. Ronning, A.S. Sefat, T. Tajima, B.H. Moeckly, J.D. Thompson and R. Movshovich, Supercond. Sci. Technol. **25**, 112001 (2012). *Selected as Editor's Highlight and issue cover (Nov. 2012)*.
15. "Theory for measurements of penetration depth in magnetic superconductors by magnetic force microscopy and scanning SQUID microscopy", S. -Z. Lin and L. N. Bulaevskii, Phys. Rev. B **86**, 014518 (2012).
16. "Josephson effect between a two-band superconductor with s++ or s± pairing symmetry and a conventional s-wave superconductor", S. -Z. Lin, Phys. Rev. B **86**, 014510 (2012).
17. "Possibility of attaining de-pairing current density in bi-axially strained thick epitaxial YBCO layers", V.F. Solovyov, Q. Li, W. Si, B. Maiorov, T.J. Haugan, H. Yao, Q.X. Jia, J.L. MacManus-Driscoll and E.D. Specht, Phys. Rev. B **86**, 094511 (2012).
18. "Nanostructured epitaxial thin films of Fe-based superconductors with enhanced superconducting properties", P. Mele, K. Matsumoto, H. Nagayoshi, K. Fujita, Y. Yoshida, Y. Ichino, T. Kiss, A. Ichinose, M. Mukaida, B. Maiorov, F.F. Balakirev, S.A. Baily and L. Civale, Mater. Res. Soc. Symp. Proc. **1434** (2012). DOI: 10.1557/opl.2012.1419
19. "Effects of density and size of BaMO₃ (M=Zr, Nb, Sn) nanoparticles on the vortex glassy and liquid phase in (Y,Gd)Ba₂Cu₃O_y films", M. Miura, B. Maiorov, J. O. Willis, T. Izumi, Y. Shiohara, K. Marken, and L. Civale, Supercond. Sci. Technol. **26**, 035008 (2013).
20. "Dissociation Transition of a Composite Lattice of Magnetic Vortices in the Flux-Flow Regime of Two-Band Superconductors", S. -Z. Lin and L. N. Bulaevskii, Phys. Rev. Lett. **110**, 087003 (2013).
21. "Stabilizing fractional vortices in multiband superconductors with periodic pinning arrays", S. -Z. Lin and C. Reichhardt, Phys. Rev. B **87**, 100508(R) (2013).
22. "Driven skyrmions and dynamical transitions in chiral magnets", S. -Z. Lin, C. Reichhardt, C.D. Batista and A. Saxena, Phys. Rev. Lett. **110**, 207202 (2013).
23. "Particle model for skyrmions in chiral magnets: dynamics, pinning and creep", S. -Z. Lin, C. Reichhardt, C.D. Batista and A. Saxena, Phys. Rev. B **87**, 214419 (2013).
24. "Role of kinetic inductance in transport properties of shunted superconducting nanowires", S. -Z. Lin and D. Roy, J. Phys.: Condens. Matter **25**, 325701 (2013).
25. "Ferromagnetic bubble clusters in Y_{0.67}Ca_{0.33}MnO₃ thin films", Jeehoon Kim, N. Haberkorn, S. Kim, L. Civale, P. C. Dowden, and R. Movshovich, Appl. Phys. Lett. **102**, 192409 (2013).
26. "Carbon nanotubes effects on the relaxation properties and critical current densities of MgB₂ superconductor", G. Pasquini, A. Serquis, A.J. Moreno, G. Serrano and L. Civale, J. Appl. Phys. **114**, 023907 (2013).

Cluster PIs:

Peter Abbamonte (abbamont@illinois.edu)
 Raffi Budakian (budakian@illinois.edu)
 James N. Eckstein (eckstein@illinois.edu)
 Laura H. Greene (lhgreen@illinois.edu)
 Anthony J. Leggett (aleggett@illinois.edu)
 Dale J. Van Harlingen (dvh@illinois.edu)

Alexey Bezryadin (bezryadi@illinois.edu)
 S. Lance Cooper (slcooper@illinois.edu)
 Eduardo H. Fradkin (efradkin@illinois.edu)
 Taylor Hughes (hughest@illinois.edu)
 Nadya Mason (nadya@illinois.edu)
 Smitha Vishveshwara (smivish@illinois.edu)

RESEARCH OVERVIEW

The central aim of the “*Quantum Materials at the Nanoscale*” (QMN) cluster is to study how collective phenomena emerge from the individual constituents of condensed matter systems on widely varying size scales. Our goals are to identify the universal features of emergent behavior, to control collective phenomena, and to create new functional behavior by manipulating the individual constituents of systems. Some highlights of our recent work are described below:

Highlight 1: Tunable superconductivity in island arrays and nanowires

Superconducting transitions in low-dimensional systems exhibit a competition between long-range correlations, localization, disorder, quantum fluctuations, and Coulomb interactions. Understanding the influence of these parameters is crucial for a variety of systems, from high temperature superconductors to superconducting qubits, but the competing influences have often proven difficult to control. Recent work by **Mason** demonstrated novel methods of tuning the parameters relevant to superconductivity in two-dimensional systems.

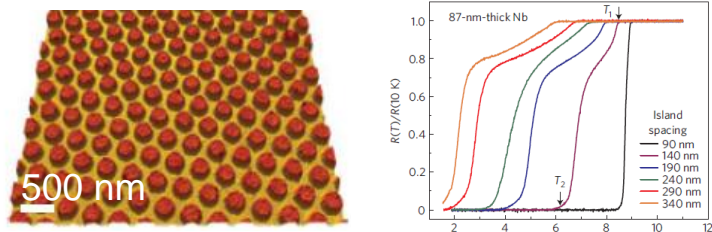


Fig. 3.A.1 (left) AFM micrograph of arrays of 87-nm thick Nb islands (red) on 10-nm thick Au underlayer (yellow). (right) Superconducting transitions in the island arrays, showing that the transitions of the islands (T_1) and the film (T_2) depend strongly on island spacing [1].

Mason studied systems of mesoscopic superconducting islands placed on normal metal films (Fig. 1 (left)). They demonstrated that these systems can behave as disordered two-dimensional superconductors [1], in which the superconducting transitions can be tuned via island size, spacing, and configuration. They performed the first systematic measurements of the dependence of the superconducting transitions on island spacing (Fig. 1 (right)), and showed that mesoscopic island arrays deviate from predictions of standard proximity theory [21]. In particular, **Mason** showed that the island systems seem to approach a quantum metallic state, a state previously thought to be precluded in 2D because of localization.

Future Work: Future studies planned for these superconducting island arrays includes performing transport measurements of vortex dynamics in superconducting island arrays, and performing scanning SQUID, MFM imaging, and microwave spectroscopy of vortex formation and dynamics in collaboration with **Van Harlingen, Budakian, and Bezryadin**. Also planned are studies of disorder effects in island arrays fabricated with controlled and correlated disorder, and investigations of vortex dynamics in aperiodic island arrays. Finally, superconducting island arrays will be fabricated on other substrates, including graphene—allowing tuning of the proximity coupling between superconducting islands via gate tuning the graphene—and topological insulators, to induce novel collective phenomena such as Majorana fermions.

Highlight 2: Two-stage orbital ordering and a pressure-tuned quantum liquid in KCuF₃

Orbital degeneracy is a pervasive phenomenon that gives rise to a wide variety of exotic quantum phenomena in condensed matter physics. The original and most widely used minimal model of orbital physics is the Kugel–Khomskii (KK) model, whose validity was first established through its explanation of the symmetry of orbital and magnetic order in KCuF₃ [22].

Recent Raman scattering measurements by **Cooper** and X-ray scattering measurements by **Abbamonte** identified a structural phase transition in KCuF₃ that cannot be explained by the KK model [2]. This transition is evident in the splitting of Raman active phonon modes (Fig. 2 (upper left)), which occurs in below $T_O = 50$ K and involves rotations of the CuF₆ octahedra, which were found to be only quasi-ordered and exhibit glassy hysteresis [2]. We proposed [2] a revised form of the KK model with a new, direct orbital exchange term that arises from a combination of electron–electron interactions and ligand distortions [Mos-2004]. Inclusion of this term creates a near degeneracy between spin/orbital configurations (Fig. 2 (right)) that dynamically frustrates the spin subsystem, but is lifted at low temperature by orbital–lattice interactions. More recent pressure-dependent Raman measurements by **Cooper** and **Abbamonte** [3] show that applied pressures above $P^* \sim 7$ kbar reverse the low temperature structural transition in KCuF₃, and causes a concomitant development of a pressure-induced fluctuational response near $T=0$ K. These results provide strong evidence for a pressure-tuned transition to a quantum liquid phase in which the CuF₆ octahedral orientations fluctuate even near $T\sim 0$ K [3].

Future Work: In future studies, pressure-dependent X-ray diffraction measurements by **Abbamonte** will be used to look for pressure-induced orbital liquid phases in KCuF₃ and other orbital-ordered systems. Pressure-dependent neutron scattering measurements of KCuF₃ by **MacDougall** will be used to investigate whether the multi-spinon excitation regime observed above 40 K under ambient pressure conditions [23] can be extended to near $T=0$ K with hydrostatic pressure, which would offer a clear signature that the emergent pressure-tuned phase in KCuF₃ is an orbital/spin liquid. Finally, **Cooper** plans to investigate whether uniaxial pressure applied along different crystallographic directions can be used to stabilize different types of orbital order in KCuF₃ and other orbital ordering materials.

Highlight 3: Fluctuations in quantum phase transitions of layered dichalcogenides

The dichalcogenides are layered systems that exhibit both superconductivity (SC) and charge density wave (CDW) ordering, and exhibit many properties reminiscent of the cuprates, including linear resistivity, coexistence and competition between superconductivity and charge order, and pseudogap effects above T_c . The dichalcogenide TiSe₂ has been known for many years to form a commensurate charge density wave (CDW), and earlier work by **Cooper** showed that pressure causes a collapse of the CDW state and the appearance of a fluctuational CDW regime prior to the complete collapse of the CDW [24]. More recently, however, it was shown that suppression of the CDW in TiSe₂—either by intercalation of Cu atoms [25] or application of hydrostatic pressure [26]—leads to the emergence of superconductivity.

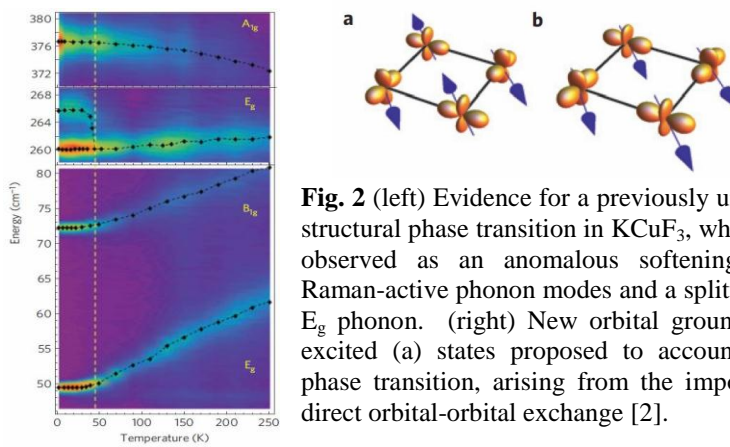


Fig. 2 (left) Evidence for a previously unobserved structural phase transition in KCuF₃, which can be observed as an anomalous softening of two Raman-active phonon modes and a splitting of the E_g phonon. (right) New orbital ground (b) and excited (a) states proposed to account for this phase transition, arising from the importance of direct orbital-orbital exchange [2].

To better understand this connection, **Abbamonte**, **Cooper**, and **Fradkin**, used high-pressure X-ray scattering to directly study and analyze the CDW order in the layered dichalcogenide TiSe_2 [4]. We succeeded in suppressing the CDW fully to zero temperature, establishing the existence of a quantum critical point at $P_c = 5.1 \pm 0.2$ GPa, which is more than 1 GPa beyond the end of the SC region. Unexpectedly, at $P = 3$ GPa we observed reentrant, weakly first order, incommensurate behavior, indicating the presence of a Lifshitz tricritical point above the superconducting dome. Our study suggests that SC in TiSe_2 may not be connected to amplitude fluctuations of the CDW, as previously believed, but to the quantum dynamics of domain walls.

Future Work: In future studies, we will combine pressure-dependent X-ray diffraction by **Abbamonte** and pressure-tuned optical spectroscopy by **Cooper** to study how the collective charge and lattice excitations evolve with pressure and intercalation towards the quantum critical point (QCP) in TiSe_2 , Cu_xTiSe_2 , TaS_2 , and Cu_xTaS_2 . **Abbamonte** will look for remnants of quantum critical scaling over a range of temperature and frequency using inelastic X-ray scattering (Fig. 4.A.7). These results will be compared to **Fradkin's** quantum mechanical generalization of the McMillan-deGennes theory of quantum phase transitions in materials with a CDW order parameter. **Van Harlingen** will use phase-sensitive Josephson tunneling and SQUID interferometry measurements to measure both the magnitude and relative phase of the superconducting order parameter within the superconducting dome regions of intercalated dichalcogenides; the goal of this effort is to study the nature of the pairing state that emerges near the quantum critical regions of these materials.

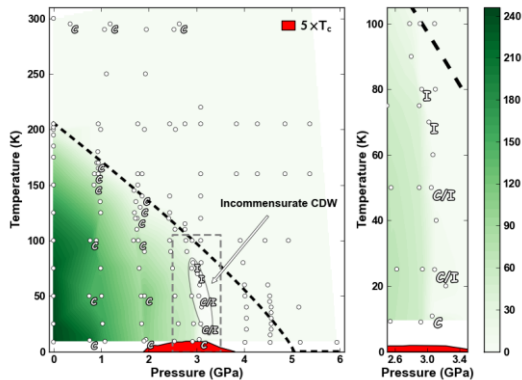


Fig. 2 Summary pressure-temperature phase diagram of TiSe_2 . (a) Broad phase diagram showing CDW ordered, normal state, and superconducting phase boundaries. The green color scale indicates the integrated intensity of CDW correlations. The superconducting T_c value has been exaggerated by a factor of 5 for visibility. Points where the precise commensurability was measured are labeled C, I, and C/I, indicating commensurate, incommensurate, or coexistence, respectively. (b) Zoom-in on the region exhibiting the transition between commensurate and incommensurate order [4].

SELECT QMN PAPERS ACKNOWLEDGING DOE SUPPORT 2012-2013

1. Eley, S., S. Gopalakrishnan, P.M. Goldbart, and **N. Mason**. "Approaching Zero-Temperature Metallic States in Mesoscopic Superconductor-Normal-Superconductor Arrays," *Nature Physics* **8**, 59 (2012).
2. Lee, J.C.T., S. Yuan, S. Lal, Y. I. Joe, Y. Gan, S. Smadici, K. Finkelstein, Y. Feng, A. Rusydi, P.M. Goldbart, **S.L. Cooper**, **P. Abbamonte**, "Two-Stage Orbital Order and Dynamical Spin Frustration in KCuF_3 ," *Nature Physics* **8**, 63 (2012).
3. Yuan, S., M. Kim, J.T. Seeley, J.C.T. Lee, S. Lal, **P. Abbamonte**, and **S.L. Cooper**, "Inelastic Light Scattering Measurements of a Pressure-Induced Quantum Liquid in KCuF_3 ," *Physical Review Letters* **109**, 217402 (2012).
4. Joe, Y.I., X.M. Chen, P. Ghaemi, K.D. Finkelstein, G. de la Pena, Y. Gan, J.C.T. Lee, S. Yuan, **S.L. Cooper**, **E. Fradkin**, and **P. Abbamonte**, "Charge Correlations Near the Quantum Critical Point in TiSe_2 ," submitted for publication, *Nature Physics* (2013).
5. Brenner, M.W., D. Roy, N. Shah, and **A. Bezryadin**, "Dynamics of Superconducting Nanowires Shunted with an External Resistor," *Physical Review B* **85**, 224507 (2012).
6. Dellabetta, B., **T.L. Hughes**, M.J. Gilbert, and B.L. Lev, "Imaging Topologically Protected Transport with Quantum Degenerate Gasses," *Physical Review B* **85**, 205442/1-205442/11 (2012).
7. **Eckstein, J.N.**, M. Zheng, X. Zhai, B. Davidson, M. Warusawithana, S. Oh, "Atomic Layer-by-Layer Molecular Beam Epitaxy of Complex Oxide Films and Heterostructures," *Molecular Beam Epitaxy*, edited by M. Henini (Elsevier), Chapter 21, pp. 509-528 (2012).

8. **Fradkin, E.** and S. Kivelson, "High-temperature Superconductivity: Ineluctable Complexity," *Nature Physics* **8**, 864-866 (2012).
9. Gan, Y., A. Kogar, **P. Abbamonte**, "Crystallographic Refinement of Collective Excitations Using Standing Wave Inelastic X-ray Scattering," *Chemical Physics* **414**, 160-167 (2013).
10. Meng, Q., **T.L. Hughes**, and **S. Vishveshwara**, "Topological Insulator Magnetic Tunnel Junctions: Quantum Hall Effect and Fractional Charge via Folding," *Physical Review Letters* **109**, 176803 (2012).
11. Aref, T., A. Levchenko, V. Vakaryuk, and **A. Bezryadin**, "Quantitative Analysis of Quantum Phase Slips in Superconducting Mo₇₆Ge₂₄ Nanowires Revealed by Switching-Current Statistics," *Physical Review B* **86**, 024507/1-7 (2012).
12. Bae, M.-H., R. C. Dinsmore, M. Sahu, and **A. Bezryadin**, "Stochastic and Deterministic Phase Slippage in Quasi-one-dimensional Superconducting Nanowires Exposed to Microwaves," *New Journal of Physics* **14**, 043014/1-15 (2012).
13. Jaafari, S. and **E. Fradkin**, "Pair-Density-Wave Superconducting Order in Two-Leg Ladders," *Physical Review B* **85**, 035104/1-19 (2012).
14. Meng, Q., **T.L. Hughes**, M.J. Gilbert and **S. Vishveshwara**, "Gate Controlled Spin-Density Wave and Chiral FFLO Superconducting Phases in Interacting Helical Liquids," *Physical Review B* **86**, 155110 (2012).
15. Meng, Q., V. Shermoggi, **T.L. Hughes**, M.J. Gilbert and **S. Vishveshwara**, "Fractional Spin Josephson Effect and Electrically Controlled Magnetization in Quantum Spin Hall Edges," *Physical Review B* **86**, 165110 (2012).
16. Uchoa, B., J.P. Reed, Y. Gan, Y.I. Joe, **E. Fradkin**, **P. Abbamonte**, D. Casa, "The Electron Many-Body Problem in Graphene," *Proceedings of the Nobel Symposium on Graphene, Physica Scripta* T146, 14014 (2012).
17. **Cooper, S.L.**, **P. Abbamonte**, **N. Mason**, C.S. Snow, M. Kim, H. Barath, J.F. Karpus, C. Chialvo, J.P. Reed, Y.I. Joe, X. Chen, D. Casa, and Y. Gan, "Raman Scattering as a Tool for Studying Complex Materials," *Optical Techniques for Solid State Materials Characterization*, edited by R.P. Prasankumar and A.J. Taylor (CRC Press, Taylor & Francis), Chapter 6, pp. 193-234 (2012).
18. Smadici, S., B.B. Nelson-Cheeseman, A. Bhattacharya, **P. Abbamonte**, "Interface Ferromagnetism in a SrMnO₃/LaMnO₃ Superlattice," *Physical Review B* **86**, 174427 (2012).
19. Chiu, C.-K., P. Ghaemi, and **T.L. Hughes**, "Stabilization of Majorana Modes in Vortices in the Superconducting Phase of Topological Insulators using Topologically Trivial Bands," *Physical Review Letters* **109**, 237009 (2012).
20. Hung, H.H., P. Ghaemi, **T.L. Hughes**, and M.J. Gilbert, "Vortex Lattices in the Superconducting Phases of Doped Topological Insulators and Heterostructures," *Physical Review B* **87**, 035401 (2013).

OTHER REFERENCES

21. Abraham, D.W., C.J. Lobb, M. Tinkham, T.M. Klapwijk, "Resistive Transition in Two-Dimensional Arrays of Superconducting Weak Links," *Physical Review B* **26**, 5268-5271 (1982).
22. Kugel, K.I. and D. I. Khomskii, "Crystal Structure and Magnetic Properties of Substances with Orbital Degeneracy," *Soviet Physics-JETP* **37**, 725 (1973).
23. Lake, B., D.A. Tennant, C.D. Frost, S.E. Nagler, "Quantum Criticality and Universal Scaling of a quantum antiferromagnet," *Nature Materials* **4**, 329-334 (2005).
24. Snow, C.W., S.L. Cooper, G. Cao, J.E. Crow, H. Fukazawa, S. Nakatsuji, and Y. Maeno, "Pressure-Tuned Collapse of the Mott-like State in Ca_{n+1}Ru_nO_{3n+1} (n = 1,2): Raman Spectroscopic Studies," *Physical Review Letters* **89**, 226401 (2002).
25. Morosan, E., H.W. Zandbergen, B.S. Dennis, J.W.G. Bos, Y. Onose, T. Klimczuk, A.P. Ramirez, N.P. Ong, and R.J. Cava, "Superconductivity in Cu_xTiSe₂," *Nature Physics* **2**, 544-550 (2006).
26. Kusmartseva, A.F., B. Sipos, H. Berger, L. Forró, E. Tutiš, "Pressure Induced Superconductivity in 1T-TiSe₂," *Physical Review Letters* **103**, 236401 (2009).

Program Title: Spin Polarized Electron Transport through Aluminum Nanoparticles

Principle Investigator: Dragomir Davidovic

Mailing Address: School of Physics, Georgia Institute of Technology

837 State Street, Atlanta, GA 30332

E-mail: dragomir.davidovic@physics.gatech.edu

Program Scope

Recently, very small ferromagnets have been incorporated in electronic circuits, leading to the field of spin-electronics or spintronics [1, 2]. Examples include giant magnetoresistance sensors, magnetic tunnel junctions, and spin-transfer torque nanopillars. As the diameter of a ferromagnetic particle decreases toward one nanometer, the particle's magnetization becomes more susceptible to perturbations by the noise in the environment. In the well known example of super-paramagnetism, the magnetization of is perturbed by thermal noise. The magnetization of a ferromagnetic particle may also be susceptible to perturbations by electron transport. At finite current through a ferromagnetic particle, the magnetization can exhibit nonequilibrium noise, much larger than the thermal noise. Further miniaturization of spintronics may be limited by this effect. For example, while hysteresis was detected in isolated magnetic molecules using magnetometry, no signs of magnetic hysteresis have been found thus far when magnetic molecules are coupled to an electric circuit [3-9]. This project investigates this fundamental limitation for the stability of magnetization in extremely small ferromagnets.

Recent Progress

1. *Sensitivity of hysteresis:* In our recent studies [10], the hysteresis loops of Cobalt particles with 1000-10000 spins are very sensitive to even a small tunneling current (10^{-11}A). The magnetic switching field is greatly reduced by the tunneling current. Those studies conclude that the magnetization of the Co particle can be excited by electron transport, and we provide a model for such a mechanism.

2. *Material dependence:* We expect that the magnetic stability boundary set by the electron transport should be material-dependent. Thus, we conduct electron tunneling experiments to study the hysteresis loops of single ferromagnetic particles composed of Cobalt, Nickel, Permalloy ($\text{Py}=\text{Ni}_{0.8}\text{Fe}_{0.2}$), and Iron, embedded in double barrier tunneling devices. Of the samples considered at $T=4.2\text{K}$, all of the Co (over one hundred) and Fe (6 samples) devices

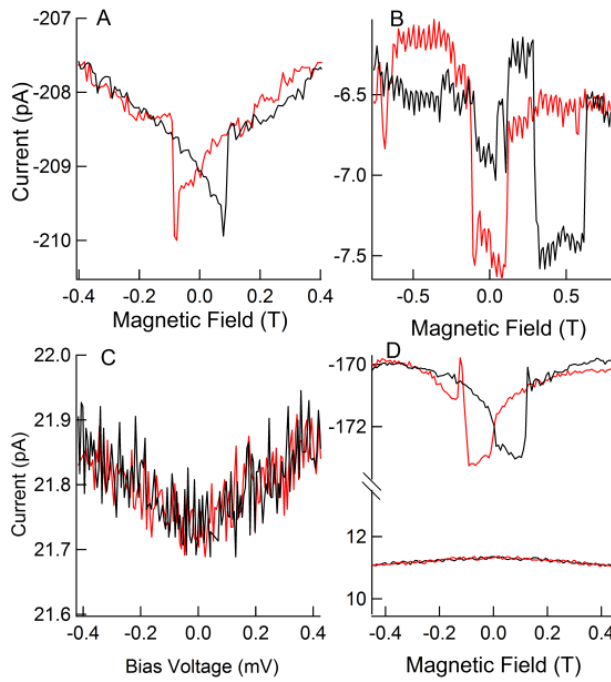


Figure 1: Hysteresis loops of (A)Co, (B)Fe, (C)Ni, and (D)Permalloy. Note the presence of hysteresis in A,B, and the upper curve of D.

Showed hysteresis. However, none of the Ni (30 samples) devices displayed hysteresis and only about half of the Py (10 samples) exhibit hysteresis (See Figure 1 for characteristic material curves). The contrast in the behaviors among various materials can be attributed to the vast difference in the magnetocrystalline and shape anisotropies in those materials.

3 *Spin-in-a-box tunnel spectra:* In order to enhance understanding of the magnetic dynamics in the ferromagnetic nanoparticles, we measure the electron tunneling spectrum of Ni particles 2-5nm in diameter at mK-temperatures. To our surprise, the tunneling spectra of Ni particles are very different from that of Co particles with similar size. In addition to the absence of hysteresis, we also observe zero-field splitting in the energy levels at low magnetic field and Zeeman splitting at high magnetic field for several Ni devices, while none of those features were present in the tunneling spectrum of Co particles (See Figure 2 for Ni spectra). The discrepancy between the tunneling spectra of Ni and Co particles has been correlated to the difference in

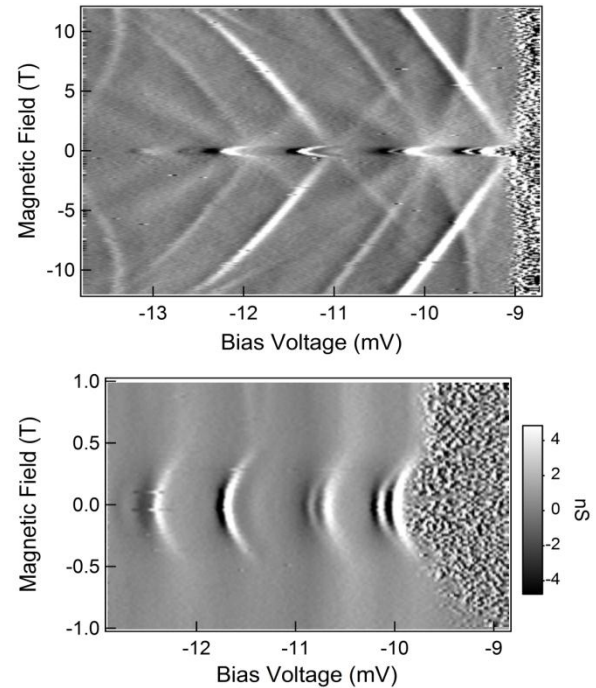


Figure 2: Differential conductance spectra of Ni samples, showing Zeeman splitting in the top image. Zero-field splitting is shown in the lower magnetic field range on the lower image

magnetization dynamics, in response to the difference in the magnetocrystalline and magnetic shape anisotropies of the two materials.

4. *Simulations.* We have developed software to simulate magnetization dynamics in single electron tunneling via discrete levels of ferromagnetic nanoparticles, using the master equation approach. This method is necessary to model the magnetization in our samples, since the conventional Landau-Lifshitz-Gilbert method does not take into account single electron tunneling events. In Fig 3, we show the motion of the magnetization statistical distribution (probability that the magnetization vector has polar angles Θ and φ) versus time, when electric current is applied at $t=0$. The blue-yellow-red scale indicates the magnetic anisotropy energy landscape versus the polar angles, while black dots indicate realizations of magnetization directions, according to the probability distributions obtained by the simulation.

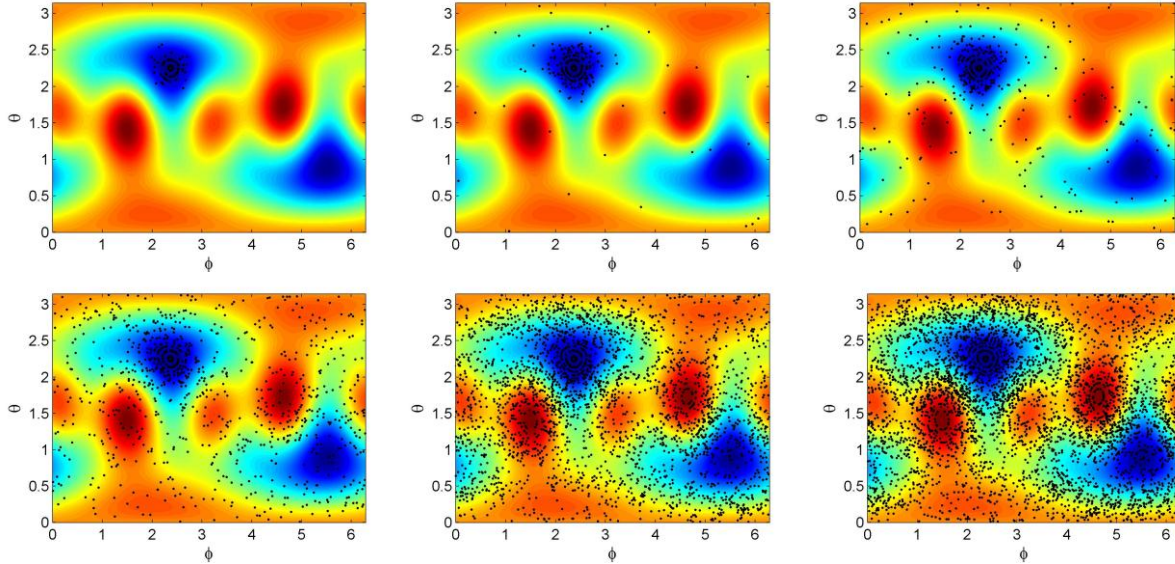


Figure 3 : Simulations of the evolution of the magnetization vector with direction angles Θ and φ in a Ni particle. The color scale represents the magnetic energy landscape in Θ and φ space. Blue (red) corresponds to low (high) magnetic energy. The black dots signify possible angle positions at the specified time for each simulation. Reading left to right, the times associated with each simulation are $1\mu\text{s}$, $2.5\mu\text{s}$, $5\mu\text{s}$, $10\mu\text{s}$, $20\mu\text{s}$, and $40\mu\text{s}$. As time progresses, the likely magnetization position is spread out over phase space and approaches an ergodic regime.

Future Plans

In future work, we plan to further study the material-dependent properties of quantum nano-magnets in order to further understand the underlying physics and potential applications of such phenomena. We will also make devices containing ferromagnetic nanoparticles with Ohmic

contacts, to understand the role of damping on magnetic stabilization. We also plan to investigate the gate voltage dependence of the observed effects.

References

1. Žutić, I., J. Fabian, and S.D. Sarma, *Spintronics: Fundamentals and applications*. Reviews of Modern Physics, 2004. **76**(2): p. 323.
2. Wolf, S., et al., *Spintronics: A spin-based electronics vision for the future*. Science, 2001. **294**(5546): p. 1488-1495.
3. Friedman, J.R., et al., *Macroscopic Measurement of Resonant Magnetization Tunneling in High-Spin Molecules*. Physical Review Letters, 1996. **76**(20): p. 3830-3833.
4. Barbara, B., et al., *Mesoscopic quantum tunneling of the magnetization*. Journal of magnetism and magnetic materials, 1995. **140**: p. 1825-1828.
5. Jo, M.-H., et al., *Signatures of molecular magnetism in single-molecule transport spectroscopy*. Nano Letters, 2006. **6**(9): p. 2014-2020.
6. Grose, J.E., et al., *Tunnelling spectra of individual magnetic endofullerene molecules*. Nature materials, 2008. **7**(11): p. 884-889.
7. Bogani, L. and W. Wernsdorfer, *Molecular spintronics using single-molecule magnets*. Nature materials, 2008. **7**(3): p. 179-186.
8. Barbara, B., *Quantum nanomagnet*. Comptes Rendus Physique, 2005. **6**(9): p. 934-944.
9. Zyazin, A.S., et al., *Electric field controlled magnetic anisotropy in a single molecule*. Nano letters, 2010. **10**(9): p. 3307-3311.
10. Jiang, W., F. Birk, and D. Davidović, *Effects of confinement and electron transport on magnetic switching in single Co nanoparticles*. Scientific reports, 2013. **3**.

Publications (which acknowledge DOE support)

- P. Gartland, F. T. Birk, W. Jiang, and D. Davidovic. Giant electron-spin g factors in a ferromagnetic nanoparticle. *Phys. Rev. B*, **88**, 075303 (2013)
- W. Jiang, P. Gartland, and D. Davidovic. Size-dependence of magneto-electronic coupling in Co nanoparticles. *J. Appl. Phys.*, **113**, 223703 (2013)
- W. Jiang, F. T. Birk, and D. Davidovic. Effects of confinement and electron transport on magnetic switching in single Co nanoparticles. *Sci. Rep.*, **3**:1200 (2013)

Spectroscopic Imaging STM and Complex Electronic Matter

J. C. Séamus Davis

CMP&MS Department, Brookhaven National Laboratory, Upton, NY 11973, USA

LASSP, Physics Department, Cornell University, Ithaca, NY 14853, USA.

Office: 607-254-8965 / Mobile: 607-220-8685 / Email: jcdavis@ccmr.cornell.edu

Program Scope

Among our long-term objectives are to understand the electronic phase diagrams and the microscopic interactions leading to strong Cooper pairing and associated higher critical temperature superconductivity. Additionally, electronic broken-symmetry states are a key area of study in condensed matter physics; our long-term goals here are to pursue the preliminary evidence that they play a fundamental role in high temperature superconductivity. The broad scientific areas of focus are: (i) DoE Grand Challenge "How do remarkable properties of matter emerge from complex correlations of atomic or electronic constituents and how can we control these properties?" and, (ii) several PRD's from BASIC RESEARCH NEEDS FOR SUPERCONDUCTIVITY (http://www.er.doe.gov/bes/reports/files/SC_rpt).

Research Progress

Significant research progress has been achieved in recent years:

Spectroscopic Imaging STM for Heavy Fermions

In a Kondo lattice, strong hybridization between electrons localized at magnetic atoms in \mathbf{r} -space and those delocalized in \mathbf{k} -space, generates exotic electronic states called ‘heavy fermions’. Their study is particularly important in the search for the mechanism of correlated superconductivity (including high- T_c) because the Cooper pairing in heavy fermion compounds is believed to be mediated by local antiferromagnetic interactions. Therefore these materials can play the role of a “hydrogen atom” for magnetic superconductivity if they can be understood. Pursuing these objectives, we introduced spectroscopic imaging STM - a technique for simultaneously visualizing the real-space (\mathbf{r} -space) and momentum-space (\mathbf{k} -space) electronic structure of a material - to the study of heavy fermions. This approach is particularly powerful for such studies because it is the strong hybridization between electrons localized in \mathbf{r} -space and those delocalized in \mathbf{k} -space that actually generates the heavy fermions.

Imaging Heavy Fermion Formation

In attempting to study heavy fermion superconductivity by SI-STM, the first challenge was to visualize the elementary heavy fermions themselves. We used SI-STM to image the temperature evolution of formation of heavy fermions in URu_2Si_2 . At low temperatures in this material we introduced heavy f-electron quasiparticle interference imaging, thereby revealing the rapid splitting of a light \mathbf{k} -space band into two new heavy fermion bands. This was the first visualization of heavy fermions in any material and paved the way to explore the possible spin fluctuation exchange mechanism of Cooper pairing in HF superconductivity; *Nature* **465**, 570 (2010).

Imaging Heavy Fermion Destruction

When, in a heavy fermion compound, a spinless atom replaces a magnetic atom, it generates a quantum state referred to as a ‘Kondo-hole’. This is dual to the ‘Kondo resonance’ at a single

magnetic atom in a metal. We achieved the first visualization of the electronic structure of a Kondo-hole at a spinless Thorium atom substituted for magnetic Uranium atom in URu_2Si_2 . Surrounding each Thorium atom we find the heavy-fermion hybridization modulations predicted to occur at Kondo-holes. By introducing the ‘hybridization gapmap’ technique to heavy fermion studies, we also observed nanoscale hybridization heterogeneity due to a combination of the randomness of Kondo-hole doping and the long-range hybridization oscillations; *PNAS* **108**, 18233 (2011).

Imaging Heavy Fermion Cooper Pairing

Most recently we completed a quite significant advance. The Cooper pairing mechanism of heavy-fermion superconductors¹⁻⁴, while long hypothesized as due to spin fluctuations⁵⁻⁷, has not been determined. It is the momentum space (k -space) structure of the superconducting energy gap $\Delta(k)$ that encodes specifics of this pairing mechanism. However, because the energy scales are so low, it has not been possible to directly measure $\Delta(k)$ for any heavy-fermion superconductor. Bogoliubov quasiparticle interference (QPI) imaging⁸⁻¹⁰, a proven technique for measuring the energy gaps of high- T_c superconductors¹¹⁻¹³, has recently been proposed¹⁴ as a new method to measure $\Delta(k)$ in heavy-fermion superconductors, specifically CeCoIn_5 ¹⁵. By implementing this method, we immediately discovered a superconducting energy gap whose nodes are oriented along $k \parallel (\pm\hat{x} \pm \hat{y})/a_0$ directions¹⁶⁻¹⁹. Moreover, we determine for the first time, the complete k -space structure of the $\Delta(k)$ of a heavy-fermion superconductor. For CeCoIn_5 , this novel information includes: the complex band structure and Fermi surface of the hybridized heavy bands, the fact that highest magnitude $\Delta(k)$ opens on a high- k band so that gap nodes occur at quite unanticipated k -space locations, and that the Bogoliubov quasiparticle interference patterns are most consistent with $d_x^2 - d_y^2$ gap symmetry. The availability of such quantitative heavy band- and gap-structure data will be critical in identifying the microscopic mechanism of heavy fermion superconductivity in general. *Nature Physics* **9**, 220 (2013)

A very rapid uptake of these new techniques to visualizing electronic structure of heavy fermion compounds is now occurring across the research community worldwide.

Future Plans

A Magnetic Cooper Pairing Mechanism

While magnetically mediated Cooper pairing is the conjectured basis of heavy-fermion superconductivity, no direct verification exists. We plan to use heavy-fermion quasiparticle interference imaging to find the kernel for the superconducting gap equations on the two heavy-fermion bands $E_k^{a,b}$. This should lead to a series of quantitative predictions about the superconducting state that will be tested by experiment. A quantitative agreement between such predictions and the measured characteristics of such superconductors could then provide strong and direct evidence that its Cooper pairing is indeed magnetically mediated.

B General Concepts of Unconventional Superconductivity

Unconventional superconductivity (SC) occurs when Cooper pair formation is dominated by repulsive electron-electron interactions, so that the symmetry of the pair wavefunction is other than isotropic s-wave. The strong, on-site, repulsive electron-electron interactions that are the proximate cause of such superconductivity are more typically drivers of commensurate

magnetism. Indeed, it is the suppression of commensurate antiferromagnetism (AF) that usually allows this type of unconventional superconductivity to emerge. Importantly, however, intervening between these AF and SC phases, “intertwined” electronic ordered phases of an unexpected nature are frequently discovered. For this reason, it has been extremely difficult to distinguish the microscopic essence of the correlated superconductivity from the oft-spectacular phenomenology of the intertwined phases. We plan a search for a model conceptual framework within which to understand the relationship between antiferromagnetic electron-electron interactions, intertwined ordered phases and correlated superconductivity.

References

- ¹ Monthoux, P., Pines, D. & Lonzarich, G. G. Superconductivity without phonons. *Nature* **450**, 1177 (2007)
- ² Norman, M. R. The challenge of unconventional superconductivity. *Science* **332**, 196 (2011)
- ³ Scalapino, D. J. A common thread: the pairing interaction for unconventional superconductors. *Rev. Mod. Phys.* **84**, 1383–1417 (2012)
- ⁴ Coleman, P. Handbook of Magnetism and Advanced Magnetic Material , Volume Fundamental Theory, eds H Kronmüller and S Parkin (Wiley and Sons, New York), pp 95–148 (2007)
- ⁵ Miyake, K., Schmitt-Rink, S., and Varma, C. M. Spin-fluctuation-mediated even-parity pairing in heavy-fermion superconductors. *Phys. Rev. B* **34**, 6554 (1986)
- ⁶ Scalapino, D. J., Loh Jr., E., and Hirsch, J. E. D-wave pairing near a spin-density-wave instability. *Phys. Rev. B* **34**, 8190 (1986)
- ⁷ Beal-Monod, M. T., Bourbonnais, C. and Emery, V. J. Possible superconductivity in nearly antiferromagnetic itinerant fermion systems. *Phys. Rev. B* **34**, 7716 (1986)
- ⁸ Wang, Q. -H., and Lee, D. -H. Quasiparticle scattering interference in high-temperature superconductors. *Phys. Rev. B* **67** 020511 (2003)
- ⁹ Capriotti, L., Scalapino, D. J., and Sedgewick, R. D. Wave-vector power spectrum of the local tunneling density of states: ripples in a d-wave sea. *Phys. Rev. B* **68** 014508 (2003)
- ¹⁰ Nunner, T. S., Chen, W., Andersen, B. M., Melikyan, A., and Hirschfeld, P. J. Fourier transform spectroscopy of d-wave quasiparticles in the presence of atomic scale pairing disorder. *Phys. Rev. B* **73**, 104511 (2006)
- ¹¹ Hoffman, J. E. *et al.* Imaging quasiparticle interference in $\text{Bi}_2\text{Sr}_2\text{CaCu}_2\text{O}_{8+\delta}$. *Science* **297**, 1148 (2002)
- ¹² Hanaguri, T. *et al.* Quasi-particle interference and superconducting gap in $\text{Ca}_{2-x}\text{Na}_x\text{CuO}_2\text{Cl}_2$. *Nature Physics* **3**, 865 (2007)
- ¹³ Allan, M. P. *et al.* Anisotropic energy-gaps of iron-based superconductivity from intra-band quasiparticle interference in LiFeAs. *Science* **336**, 563 (2012)

-
- ¹⁴ Akbari, A., Thalmeier, P., and Eremin, I. Quasiparticle interference in the heavy-fermion superconductor CeCoIn₅. *Phys Rev.* **84**, 134505 (2011)
 - ¹⁵ Petrovic, C. *et al.* Heavy-fermion superconductivity in CeCoIn₅ at 2.3 K. *J. Phys.: Condens. Matter* **13**, L337-342 (2001)
 - ¹⁶ Movshovich, R. *et al.* Unconventional superconductivity in CeIrIn₅ and CeCoIn₅: specific heat and thermal conductivity studies. *Phys. Rev. Lett.* **86** 5152 (2001)
 - ¹⁷ Izawa, K. *et al.* Angular position of nodes in the superconducting gap of quasi-2D heavy-fermion superconductor CeCoIn₅. *Phys. Rev. Lett.* **84**, 57022 (2001)
 - ¹⁸ Stock, C. *et al.* Spin resonance in the *d*-wave superconductor CeCoIn₅. *Phys. Rev. Lett.* **100**, 087001 (2008)
 - ¹⁹ An, K. *et al.* Sign reversal of field-angle resolved heat capacity oscillations in a heavy-fermion superconductor CeCoIn₅ and d_{x²-y²} pairing symmetry. *Phys. Rev. Lett.* **104**, 037002 (2010)

Program Title: Competing Interactions in Complex Transition Metal Oxides

Principal Investigator: L. E. De Long; Co-PI's: Gang Cao, J. Todd Hastings and S. S. Seo

Mailing Address: Department of Physics and Astronomy, University of Kentucky,

Lexington, KY 40506-0055

E-Mail: delong@pa.uky.edu

Program Scope

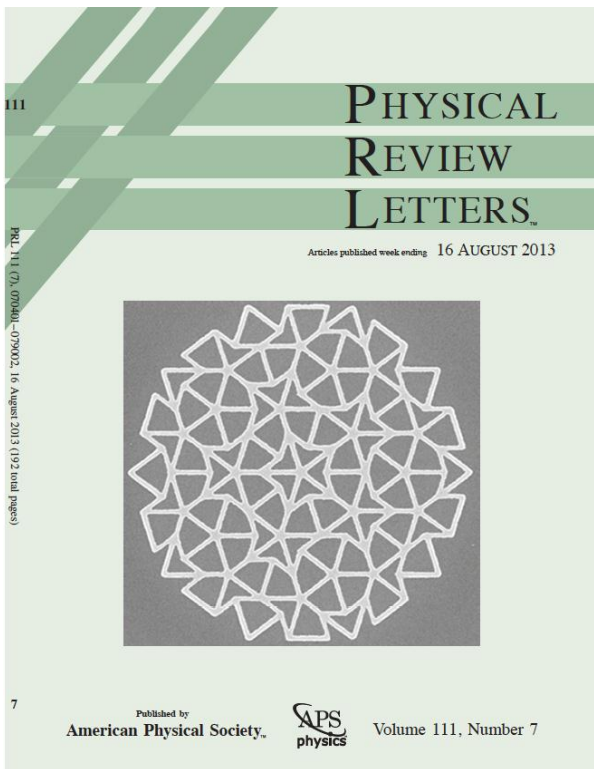
Small variations of composition, pressure or applied fields can induce drastic changes in the varied ground states exhibited by transition element (TE) oxides (ferroelectric, orbital or magnetic order, superconductivity, density waves), as well as control technologically important phenomena such as colossal magnetoresistance (CMR) and giant magnetoelectric effects (GME). We emphasize studies of the “heavy” 4d and 5d TE: These materials have more extended d-orbitals compared to 3d materials, stronger p-d hybridization, spin-orbit (SO) and electron-lattice couplings, but with reduced intra-atomic Coulomb U and crystalline electric field (CEF) interactions. These circumstances generate intriguing competitions between metallic and insulating states, paramagnetic and magnetic order, and competition between ferroelectric and magnetic ground states. We take an integrated, interdisciplinary approach to the discovery and characterization of novel TE oxides whose physical properties reflect competing interactions: We synthesize and identify novel materials, grow bulk single crystals to comprehensively study anisotropic physical properties relevant to fundamental theories, as well as fabricate and study patterned thin films and heterostructures relevant to device applications.

Our broad expertise and technical assets available in the UK Center for Advanced Materials permit comprehensive investigations of electrical transport, magnetic, dielectric and thermodynamic properties over a wide range of temperatures $0.05 < T < 1000$ K and magnetic fields $0 < \mu_0 H < 18$ T, and high-pressure electrical resistivity and magnetic moment measurements to 10 GPa. We are using National Laboratory facilities and/or external collaborators to conduct EXAFS, SEMPA, and magnetic soft X-ray and neutron scattering experiments to characterize small single crystals and thin films that are not easily studied via conventional electrical transport, magnetic or optical techniques.

Recent Progress: FMR Studies of Patterned Thin Films and Heterostructures

We have observed a remarkable degree of control of magnetic reversal and domain wall (DW) textures in the *low-field, hysteretic regime* via submicron patterning of ferromagnetic (FM) thin films [1,4,7,10]. These observations are of importance to magnetic recording and other technologies. Taking advantage of these highly interesting results, we have emphasized studies of the static and dynamic magnetic responses of FM permalloy thin films patterned with several novel types of antidot lattices (ADL). This complex program consists of four coordinated efforts in film patterning, film deposition and micromagnetic simulations done at UK, and a separate broad-band ferromagnetic resonance (BB FMR) characterization by Prof. John Ketterson and his RA, Joseph Sklenar, at Northwestern U., as described below.

High-Speed, Precision Patterning of Thin Films: We have developed techniques to optimize submicron patterning of large-area (e.g., 2 mm x 2 mm) arrays of magnetic dots or antidots in thin films. We have reduced write times for our Raith E-Line Electron Beam Lithography System by *one order of magnitude* (e.g., from 20 hours to 2 hours), which allows us to produce complex patterns with sharp features and smooth edges (**Fig. 1**).



Micromagnetic Modeling via Large-Scale Numerical Simulations: The use of sophisticated, large-scale numerical simulations is essential for understanding BB FMR and SQUID magnetometer data for patterned FM films. We have successfully implemented the NIST OOMMF micromagnetics code on the UK Supercomputer, which allows us to generate complex DC magnetization maps and hysteresis loops, as well as FMR power absorption maps and FMR mode spectra [8,15].

Fig. 1. SEM image of a 3rd generation quasicrystalline (Penrose P2 tiling) pattern in a permalloy film of thickness $t = 25$ nm. The total apical width of this decahedron is 76 microns. Bright regions correspond to permalloy, and dark regions to Si substrate. The pattern consists of two types of film segments of equal width $W = 100$ nm, and long length $d_1 = 810$ nm, and short length $d_2 = 500$ nm. See [15] for details.

Controlled Magnetic Reversal in Permalloy Films Patterned into Artificial Quasicrystals: There is a great deal of interest in understanding the propagation of spin waves (“magnonics”) and domain walls (DW) in patterned FM film media, in analogy to phonons or electrons in periodic crystals. We have extended our expertise to study the unexplored realm of quasiperiodic, Penrose tilings in FM media, which offer us a unique chance to study film patterns with long-range order and fivefold rotational symmetry, but *without periodicity*. We have recently published DC magnetization and FMR data, as well as results of numerical simulations, for novel *quasicrystalline* wire networks patterned into FM permalloy films [8,15]. An SEM image of one of our artificial quasicrystals appeared on the cover of the August 16, 2013 issue of *Physical Review Letters* (Fig. 1).

We have observed reproducible “knee” anomalies in the hysteretic, low-field data, which signal a series of abrupt transitions between ordered magnetization textures, culminating in a smooth evolution into a saturated state. The knee anomalies bear a remarkable resemblance to metamagnetic phase transitions observed in bulk magnets with complex spiral, ferromagnetic or helical orderings. Ordinarily, unpatterned FM films exhibit complex, random textures of DW within the low-field, hysteretic reversal regime. The sharp FMR spectra, clear knee anomalies in $M(H)$, and the high degree of order we observe in the simulated magnetization textures, are results of the strong shape anisotropy and exchange stiffness imposed by the patterning, in spite of the absence of periodic symmetry and substantial low-field hysteresis. Micromagnetic simulations compare well to experimental DC hysteresis loops and FMR spectra, and indicate systematic control of magnetic reversal and domain wall motion can be achieved via tiling design, offering new paradigms for *magnonic quasicrystals* and *artificial spin ice* [9,15].

Future Plans

1. Broad-Band FMR Studies at Northwestern U. We will fabricate some of the many possible varieties of quasicrystalline tilings in permalloy, and assess the control of magnetization textures. A new effort is directed at exploring the existence of phase transitions and magnon localization and propagation in patterned permalloy films.

2. Extended Micromagnetic Modeling and Simulations of Data. We will continue to implement micromagnetics codes to obtain both DC magnetization and spin maps, as well as dynamic simulations of FMR response, and develop methods to generate frequency-wavevector dispersion relations relevant to magnonics. We will implement finite-temperature micromagnetic simulations using Monte Carlo techniques.

3. SEMPA and X-Ray Scattering Studies of Domain Wall Evolution in Patterned Films. Our awarded instrument time at Oak Ridge National Lab (Dr. Gai Zheng, collaborator) was extended due to problems with the SEMPA hardware. We hope to directly image the evolution of DW for comparison to our simulations, which reveal a *remarkably reproducible DW evolution* with applied field. We are planning to complement these experiments with magnetic X-ray scattering studies of domain wall evolution and magnetic return point memory in ADL, in collaboration with Dr. S. Roy and Dr. Jeffrey Kortright of LBNL ALS.

References/Publications (September, 2011 to September, 2013)

1. "Low-Field FMR Studies of Magnetic Confinement Effects in Patterned Ferromagnetic Thin Films", V. Bhat, J. Woods, J. T. Hastings, L. E. De Long, J. Sklenar, J. B. Ketterson, O. Heinonen, K. Rivkin and V. Metlushko, Proceedings of the International Conference on Electromagnetics in Advanced Applications 2011, Torino, Italy, IEEE Explore 978-1-61284-978-2/11, pp. 718-721.
2. "Lattice-Driven Magnetoresistivity and Metal-Insulator Transition in Single-Layer Iridates", M. Ge, T. F. Qi, O. B. Korneta, L. E. De Long, P. Schlottmann and G. Cao, Phys. Rev. B **84**, 100402(R) (2011).
3. "Giant Magnetoelectric Effect in Antiferromagnetic BaMnO_{2.99} and Its Derivatives", O. B. Korneta, T. F. Qi, M. Ge, L. E. De Long, P. Schlottmann and G. Cao, J. Phys. F: Condens. Matter **23**, 435901 (2011).
4. "Broad-band FMR study of ferromagnetic thin films patterned with antidot lattices", V. Bhat, J. Woods, L. E. De Long, J. T. Hastings, V. V. Metlushko, K. Rivkin, O. Heinonen, J. Sklenar and J. B. Ketterson, Physica C **479**, 83-87 (2012). (Proceedings of the Seventh International Conference on Vortex Matter in Superconductors, Rhodes, Greece, Sept. 10-17, 2011).
5. "Strong magnetic instability in correlated metallic Bi₂Ir₂O₇", T. F. Qi, O. B. Korneta, Xiangang Wan, L. E. De Long, P. Schlottmann and G. Cao, J. Phys.: Condens. Matter **24**, 345601 (2012). Featured in *Lab Talk* of JPCM, August 2, 2012.
6. "Generating wave vector specific Damon-Eshbach spin waves in Py using a diffraction grating", J. Sklenar, V. Bhat, L. E. De Long and J. Ketterson, Appl. Phys. Lett. **101**, 52404 (2012).
7. "FMR study of permalloy films patterned into square lattices of diamond antidots", V. Bhat, J. Woods, L. E. De Long, J. T. Hastings, J. Sklenar, J. B. Ketterson and M. Pechan, Proceedings of the ICMM 2012, Kaiserlautern, Germany, IEEE Transactions on Magnetics **49**, 1029-1032 (2012).

8. "Observation of Robust FMR in Permalloy Quasiperiodic Arrays", V. Bhat, J. Woods, B. Farmer, L. E. De Long, J. T. Hastings, J. Sklenar and J. B. Ketterson, Proceedings of the MMM-INTERMAG, Chicago, IL, January, 2013, *IEEE Transactions on Magnetics* **49**, 3101-3104 (2013).
9. "Broadband Ferromagnetic Resonance Studies on an Artificial Square Spin-Ice Island Array", J. Sklenar, V. S. Bhat, L. De Long, and J. Ketterson, Proceedings of the MMM-INTERMAG, Chicago, IL, January, 2013, *J. Appl. Phys.* **113**, 17B530 (2013).
10. "Strongly Localized Magnetization Modes in Permalloy Antidot Lattices", J. Sklenar, V. S. Bhat, L. E. De Long, O. Heinonen and J. B. Ketterson, *Appl. Phys. Lett.* **102**, 152412 (2013).
11. "Tuning the $J_{\text{eff}} = \frac{1}{2}$ insulating state via electron doping and pressure in the double-layered iridate $\text{Sr}_3\text{Ir}_2\text{O}_7$ ", L. Li, P. P. Kong, T. F. Qi, C. Q. Jin, S. J. Yuan, L. E. De Long, P. Schlottmann and G. Cao, *Phys. Rev. B* **87**, 235127 (2013).
12. "Superconductivity and anomalous electrical resistivity in Single-Crystal Ir_3Te_8 ", L. Li, T. F. Qi, L. S. Lin, X. X. Wu, X.T. Zhang, K. S. J. Yuan, K. Butrouna, V. S. Cao, Y. H. Zhang, Jiangping Hu, P. Schlottmann, L. E. DeLong and G. Cao, *Phys. Rev. B* **87**, 174510 (2013).
13. "Tuning electronic structures via epitaxial strain in Sr_2IrO_4 thin films", J. Nichols, J. Terzic, E. G. Bittle, O. B. Korneta, L. E. De Long, J. W. Brill, G. Cao and S. S. A. Seo, *Appl. Phys. Lett.* **102**, 141908 (2013).
14. "Giant vertical magnetization shift induced by spin canting in a $\text{Co}/\text{Ca}_2\text{Ru}_{0.98}\text{Fe}_{0.02}\text{FeO}_4$ heterostructure", S. J. Yuan, L. Li, T. F. Qi, L. E. De Long and G. Cao, *Phys. Rev. B* **88**, 024413 (2013). Selected as a *Physical Review B Editors' Suggestion*.
15. "Controlled Magnetic Reversal in Permalloy Films Patterned into Artificial Quasicrystals", V. S. Bhat, J. Sklenar, B. Farmer, J. Woods, J. T. Hastings, S. J. Lee, J. B. Ketterson and L. E. De Long, *Phys. Rev. Lett.* **111**, 077201 (2013). Figure 1 featured on the Cover Page and Index Page of *Physical Review Letters* **111**, August 16, 2013.
16. "Anisotropic electronic properties of a-axis-oriented Sr_2IrO_4 epitaxial thin films", J. Nichols, O. B. Korneta, J. Terzic, L. E. De Long, G. Cao, J. W. Brill and S. S. A. Seo, submitted to *Applied Physics Letters* (August, 2013).
17. "The Contradictory Physical Properties and Extreme Anisotropy of $\text{Ca}_3\text{Ru}_2\text{O}_7$ ", Gang Cao L. E. De Long and P. Schlottmann, Chapter 6, in: *Frontiers of 4d- and 5d-Transition Metal Oxides*, Gang Cao and Lance E. De Long, Eds. (Singapore, World Scientific Publishing, 2013).
18. "Instability of the $J_{\text{eff}} = \frac{1}{2}$ Insulating State in $\text{Sr}_{n+1}\text{Ir}_n\text{O}_{3n+1}$ ($n = 1$ and 2)", Gang Cao and L. E. De Long, Chapter 8, in: *Frontiers of 4d- and 5d-Transition Metal Oxides*, Gang Cao and Lance E. De Long, Eds. (Singapore, World Scientific Publishing, 2013).
19. *Frontiers of 4d- and 5d-Transition Metal Oxides*, Edited by Gang Cao and Lance E. De Long (Singapore, World Scientific Publishing, 2013; ISBN 978-981-4374-85-9). This volume is a compendium of topical reviews covering physical properties of novel 4d- and 5d-transition element oxides by several expert contributors to recent research literature.

Patent: "Novel Class of Ferromagnetic Semiconductors", Larysa V. Shlyk (Inventor), Lance E. De Long, Sergiy A. Kryukov, Robert Niewa and Barbara Schüpp-Niewa (Co-Inventors), U.S. Provisional Patent Application No. 60/921,641, filed April 3, 2007. Modified and approved for issue as a Nonprovisional Application No. 12/062,076, filed April 3, 2008.

Project Title: "Infrared Hall Effect in correlated electronic materials"
Principle investigator: Dr. H. Dennis Drew
Mailing Address: CNAM, Physics Department University of Maryland
College Park, MD 20742
e-mail: hdrew@physics.umd.edu

Project Scope

The focus of our work on topological insulators is on characterizing the topologically protected surface state and examining some of its predicted unique properties. These include the spin-charge coupling and intrinsic magneto-electric effect. Thus, one prediction is a quantized Faraday rotation in zero field for a topological insulator coupled to a magnetic material to break time reversal symmetry. This is a deep signature of the topological character of this surface state. While related to the Quantum Hall Effect it is unique to topological insulators. We use cyclotron resonance, plasma excitations and other IR studies of the surface state to characterize the surface states and study their properties. At this stage in the topological insulator research little is known about the effects of potential fluctuations and other forms of disorder on the properties of the surface states and how this is related to the topological protection. One of our goals is measurements to fill this void. Because of the potential deleterious effects of scattering at surface impurities and defects passivation of the surfaces of TIs is important. Our recent work shows promise for substantially improving the mobility and repositioning the Dirac point by interface engineering with trivial insulator capping layers.

In the most promising topological insulators presently available bulk conduction obscures the clear observation of the surface state. We have used gating to mitigate this problem.

Application of an external gate changes the Fermi level in the bands near the surface. In the case of these inadvertently doped semiconductor systems, band bending occurs over a region defined by the Thomas-Fermi screening length, leading to either accumulation or depletion at the gated surface. This is illustrated in Figure 1a for Bi_2Se_3 with topological surface states. Modulation of the gate potential therefore leads to a modulation of the reflection or transmission of the sample which is sensitive to the surface states at the front surface.

In terahertz magneto-optical measurements, each conduction channel in the film has a distinct resonance response distinguishable by the sign of the charge, cyclotron mass m_c , spectral weight ne^2/m_c , and carrier scattering rate γ . Spatial location of the carrier contributions in the film are ascertained by concurrently modulating a semi-transparent top gate that spatially modulates the charge distribution in the film in a predictable (Thomas-Fermi screening) way.

Recent progress

Cyclotron resonance (CR) transmission measurements were performed on epitaxial Bi_2Se_3 thin films capped with In_2Se_3 at fixed frequencies and low temperatures with normally incident circularly polarized light as a function of applied magnetic field.

The gated terahertz cyclotron resonance measurements were enabled the spectroscopic characterization of a single topological interface state from the vicinity of the Dirac point to above the conduction band edge. The sample configuration is shown in Figure 1b. A precipitous drop in the scattering rate with Fermi energy is observed as shown in figure 2 that is interpreted as the surface state decoupling from bulk states and evidence of a shift of the Dirac point towards mid-gap. This observation opens new possibilities in tailoring Dirac cone properties in topological insulators. Near the Dirac point, potential fluctuations of 60 meV are deduced from an observed loss of differential optical spectral weight near the Dirac point. Potential fluctuations are reduced by a factor of two at higher surface Fermi levels in the vicinity of the conduction band edge inferred from the width of the scattering rate step. The passivated topological interface state attains a high mobility of $3500 \text{ cm}^2/\text{Vs}$ near the Dirac point.

The imaginary part of the complex Faraday angle $\text{Im}(\theta_F)$ (defined in Equation [Error!](#)
Reference source not found.) is related to the circular dichroism providing similar information as CR measurements, but the real part $\text{Re}(\theta_F)$ provides additional information since it is related to the reactive part of the conductivity. A quantized Faraday rotation in units of the fine structure constant is predicted for topological insulators with broken time reversal symmetry.

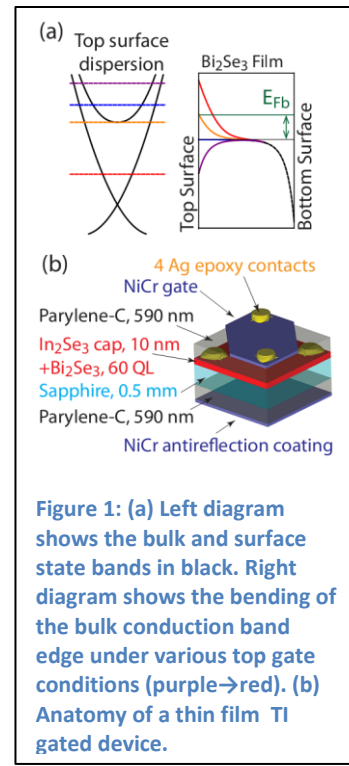


Figure 1: (a) Left diagram shows the bulk and surface state bands in black. Right diagram shows the bending of the bulk conduction band edge under various top gate conditions (purple→red). (b) Anatomy of a thin film TI gated device.

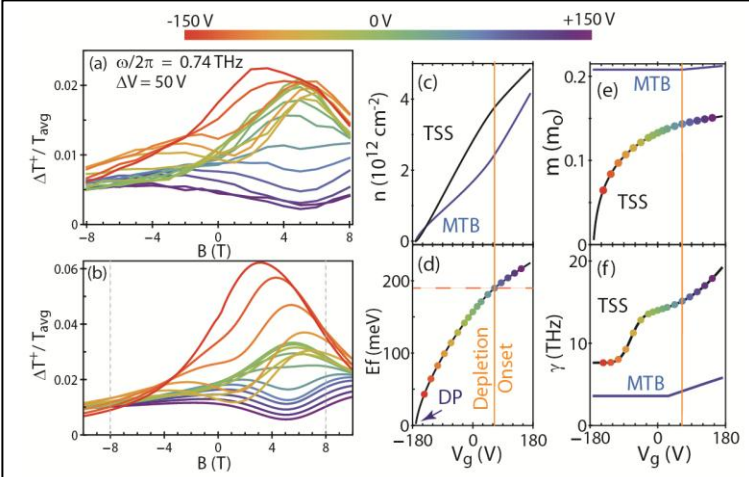


Figure 2: (a) Each plot of the Δ -CR data is transmission data taken at two gate values $V_g \pm 25\text{V}$, subtracted, and normalized to the average ($\Delta T^+ / T_{avg}$). The average gate values V_g for each plot are coded according to the colored bar at the top of the figure. (b) The optically modeled data where (c-f) are the Drude conductivity parameters of the TI surface state (TSS) and the modulated top bulk (MTB) carriers shown in black and blue, respectively. Colored dots correspond to each Δ -CR data plot.

Hall Effect. However, in topological insulators there are no edge states. Study of the quantized Faraday Effect of the TI interface state will be expanded and examined in different material systems. The quantized step evolution with temperature, applied field, and frequency will be measured to probe the fundamental nature of the quantum Hall effect in TIs. Second, the $\frac{1}{2}\alpha$ Faraday rotation quantization in zero applied field for a topological insulator with TRS broken by a magnetically ordered state will be studied. Observing such an effect would be extraordinary since no other analogous quantum Hall phenomenon exists in any other class of materials. In collaboration with Seongshik Oh we will investigate both topological insulators capped with a topologically trivial magnetic layer and topological insulators doped with magnetic ions to produce a bulk magnetic state. The Faraday rotation at zero applied magnetic field will be measured in suitable samples of these systems.

Experiments on Bi_2Se_3 capped with $(\text{In}_{(1-x)}\text{Bi}_x)_2\text{Se}_3$ alloys will study the variation of the position of the Dirac cone with the gap of the trivial insulator. This system allows easy tuning of the bandgap of the trivial insulator, where larger Dirac point shifts than those observed for In_2Se_3 are expected for smaller bandgaps. The position of the Dirac point of the surface state as a function of x will be determined. Further exploration of the passivation of the interface will also be studied.

At Fermi energies above the conduction band edge, a plateau is observed in the real part of the Faraday angle that is 80 times flatter than the step size expected from a single Landau Level, quantized in units of the fine structure constant.

Future plans

A quantized Faraday rotation for topological interface states is predicted to occur in the presence of broken time reversal symmetry (TRS). First, TRS is broken in the presence of an applied magnetic field and is related to the quantized

References (which acknowledge DOE support)

1. “*Terahertz Kerr and reflectivity measurements on the topological insulator Bi_{2}Se_3* ”, Jenkins, G. S. and Sushkov, A. B. and Schmadel, D. C. and Butch, N. P. and Syers, P. and Paglione, J. and Drew, H. D., Phys. Rev. B **82**, 125120,(2010). (The IR work was supported by DOE DE-SC0005436 [the acknowledgement in the paper was inadvertently incorrect] and the sample growth by NSF MRSEC).
2. “*Terahertz Hall measurements on optimally doped single-crystal $\text{Bi}_{2}\text{Sr}_{2}\text{CaCu}_2\text{O}_{8+x}$* ”, Jenkins, G. S., Schmadel, D. C., Sushkov, A. B., Gu, G. D., Kontani, H. and Drew, H. D., Phys. Rev. B**82**, 094518,(2010). (Primary support was DOE DE-SC0005436[the acknowledgement in the paper was inadvertently incorrect]. The early phase of this work was supported by NSF).
3. “*Topological quantization in units of the fine structure constant*” Joseph Maciejko, Xiao-Liang Qi, H. Dennis Drew, and Shou-Cheng Zhang, Phys. Rev. Letters **105**, 166803 (2010). (Drew was primarily supported by DOE DE-SC0005436 [the acknowledgement in the paper was inadvertently incorrect] with partial support from NSF MRSEC on a topological insulator seed project)
4. “*Simultaneous measurement of circular dichroism and Faraday rotation at terahertz frequencies utilizing electric field sensitive detection via polarization modulation*”, G. S. Jenkins, D. C. Schmadel and H. D. Drew, Review of Scientific Instruments **81**, 083903 (2010). (Primary support DOE DE-SC0005436[the acknowledgement in the paper was inadvertently incorrect]. Drew was partially supported by NSF MRSEC TI seed).
5. “*Terahertz Kerr and Reflectivity Measurements on the Topological Insulator Bi_2Se_3* ”, Gregory S. Jenkins, A.B. Sushkov, D.C. Schmadel, N.P. Butch, P. Syers, J. Paglione, M.-H. Kim, H.D. Drew, J.G. Analytis and I.R. Fisher, Bull. Am. Phys. Soc., **56**, 1 (2011). (The IR work was supported by DOE DE-SC0005436 [the acknowledgement in the paper was inadvertently incorrect] and the sample growth by NSF MRSEC).
6. “*The great topological expansion*” H. Dennis Drew, Nature Physics 8, 779 (2012).
7. “*Giant plateau in the terahertz Faraday angle in gated Bi_2Se_3* ”, Gregory S. Jenkins, Andrei B. Sushkov, Don C. Schmadel, M.-H. Kim, Matthew Brahlek, Namrata Bansal, Seongshik Oh, and H. Dennis Drew, PHYSICAL REVIEW B 86, 235133 (2012).
8. “*Dirac cone shift of a passivated topological Bi_2Se_3 interface state*” Gregory S. Jenkins* and Don C. Schmadel, Andrei B. Sushkov and H. Dennis Drew, Max Bichler and Gregor Koblmüller, Matthew Brahlek, Namrata Bansal, and Seongshik Oh, PHYSICAL REVIEW B **87**, 155126 (2013).

Microwave spectroscopy of electron solids: fractional quantum Hall effect and controlled disorder

Lloyd W. Engel, NHMFL/FSU

Program Scope

This program focuses on spectroscopic studies of solids of carriers in two-dimensional electron systems (2DES). These solids, related to the Wigner crystal, are stabilized by mutual repulsion of carriers, are pinned by residual disorder, and exhibit a striking resonance in their rf or microwave spectra. Understood as a pinning mode, in which pieces of the solids oscillate within the potential of the disorder, the resonance is of interest both as the signature of a solid, and as a tool for the study of these solids.

Pinning mode studies are of particular value since they provide information not available from dc transport. At low Landau filling (v), and low temperature, a 2DES is insulating and linear transport even on a high quality 2DES is highly problematic, while under the same conditions the pinning mode spectrum is easily measured. The pinning mode can distinguish between different solid phases even within the low v insulator [1]. Observation of a pinning mode also allows identification and study of a solid phase in v ranges for which it is not clear that a solid would be present, as opposed, for example to single-particle localization. Examples of this application include pinning mode resonances within the integer [2] and fractional [3] quantum Hall effects (IQHE and FQHE).

One main aspect of the program has been aimed at understanding the details of how the pinning takes place. To this end we have looked into samples with controlled alloy disorder, in the form of dilute Al in the channel where the 2DES resides

A second aspect of the program is aimed at using the pinning mode as a tool to understand exotic solid phases. In the past this has included solids composed of fractionally charged quasiparticles near Landau filling $v=1/3$ [3], crystals of skyrmions near $v=1$ [4], and bubble [5] and stripe[6] phases of higher Landau levels. Most recently, in collaboration with M. Shayegan of Princeton University, we have been investigating newly discovered solid phases near wide quantum well samples whose pinning mode spectra of such samples near $v=1$ show clear transitions between different types of Wigner solids.

Recent Progress

i. Samples with controlled Alloy disorder

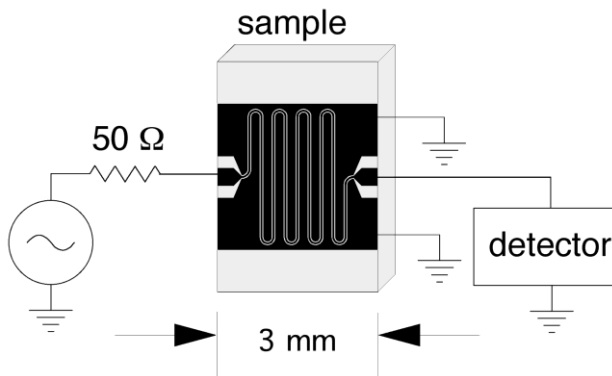


Figure 1: Schematic of experimental method. Microwave signals are sent through a transmission line of coplanar waveguide type, patterned onto the top surface of the AlGaAs/GaAs sample, a fraction of a μm above the 2DES. The transmission line couples to the 2DES capacitively, and microwave source and detector are at room temperature.

Samples with the 2DES within dilute $\text{Al}_x\text{Ga}_{1-x}\text{As}$ have been characterized [7] and shown to have the Al randomly distributed within the alloy. The Al can be modeled as spherical square wells with known depth, and size much smaller than the magnetic length for experimentally accessible magnetic fields.

We studied samples with $x=0$, 0.21, 0.33, 0.4 and 0.8%. In each of these samples fractional quantum Hall effects (FQHEs) are exhibited, and the lowest v FQHE is at $v=1/3$. On decreasing v from $1/3$ the sample enters an insulating phase, and exhibits a pinning mode. Fig. 2 shows the development of the resonance with v for several x .

Fig. 3 shows f_{pk} vs v for the pinning modes of the samples. f_{pk} for $x=0$ is much smaller than the f_{pk} for the other curves, except near the low v edge of the $1/3$ FQHE. Hence for the well-developed resonances with $x>0$ the Al dilute alloy is the main contribution to the pinning frequency. For x between 0.2 to 0.4% there is little variation in f_{pk} vs v for the several densities presented. However, on increasing x to 0.8% there is again a definite increase in f_{pk} . The relatively small change of f_{pk} between $x=0.2$ and 0.4% may be explainable by sample-to-sample variation background disorder from other sources than the deliberately introduced Al.

The f_{pk} are consistent with weak collective pinning for which the solid deformation occurs over a large enough length that deformation energy can be calculated from the shear modulus. This requires $nL^2 \gg 1$, where n is the density and L is the Larkin length, or domain size. The samples fulfill this except for the lowest v and largest x , with L calculated [8] from the (roughly accurate [9]) classical shear modulus. $f_{\text{pk}}(v)$ is not a precise fit to v^{-2} , which is the theoretical prediction [10], but the overall variation of f_{pk} over the experimental v range is roughly described by this, as shown by the red curve with $f_{\text{pk}} \propto v^{-2}$ on Fig. 3. This increase of f_{pk} as v decreases into the insulating phase is significantly faster than observed elsewhere [8,11] for samples without deliberate alloy disorder.

However, taking a carrier wave function to have the form of a lowest Landau level single particle orbital, and attempting to apply weak pinning theory [10] to these samples with the known disorder gives f_{pk} about three orders of magnitude too large. The impurity

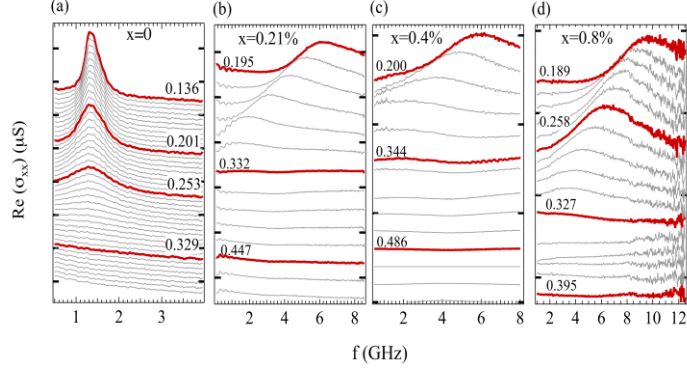


Figure 2: Microwave spectra of 2DES in $\text{Al}_x\text{Ga}_{1-x}\text{As}$, at many Landau filling factors at the onset of the insulating phase that terminates the FQHE series.

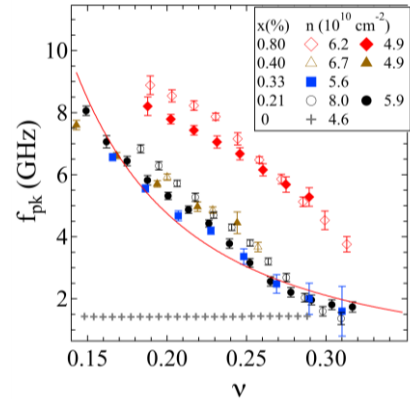


Figure 3: Resonance peak frequency, f_{pk} , vs Landau filling, v , for various Al alloy fractions x and densities n , as marked in the legend. Thin curve is $f_{\text{pk}}=0.19v^{-2}$.

energy within the volume of a carrier is comparable to the cyclotron energy, and it may be that *the carrier wave function adjusts to minimize impurity energy*.

ii. New solid phases in wide quantum wells

In wide quantum wells (WQWs), with two growth-direction subbands occupied at zero magnetic field, anomalous insulating phases of the partially filled Landau level have been observed around $v=4/5$ and $6/5$ [12] for high enough carrier densities. Fig. 4 shows series of spectra for several densities (n) for a 54 nm WQW density were changed with back and front gates adjusted to keep the growth-direction charge distribution symmetric. For the lowest n , $1.96 \times 10^{11} \text{ cm}^{-2}$, f_{pk} decreases monotonically as v moves away from 1, just as seen in earlier measurements [3,4] on samples with lower n or smaller well width. In contrast, for the higher densities in the figure, for $v < 1$, there are narrow v ranges in which the resonance moves to higher frequency as v decreases. Signs of a similar jump in resonance frequency as v increases from 1 are present in other data sets.

Fig. 5 shows traces of f_{pk} vs v for many densities. The features in the spectra appear as local maxima in f_{pk} vs v . The abrupt variation in f_{pk} vs v is interpreted as due to a transition between distinct Wigner solid phases. Within the enhanced- f_{pk} phase (the one farther from $v=1$, denoted WS2), f_{pk} continues to decrease as v moves away from 1, likely due to the quasi-hole density increasing. The enhancement in f_{pk} can mean that the effective disorder seen by the carriers is larger (perhaps from carrier distribution getting closer to interfaces), or that its shear modulus is reduced, since reduced crystal stiffness generally increases f_{pk} [10].

The pinning mode studies, also allow us to construct a phase diagram for the two solid phases which extends deep into the main IQHE range, for which low temperature dc resistivity is vanishing. For the largest n , WS2 can be identified extends quite close to $v=1$, at $v=0.92$, so that the partial filling of holes in the lowest Landau level is 0.08. It is clear that the transition is driven by the increase in the effective thickness of the wave functions at larger n or larger well width. One explanation is that the two solids may involve composite fermions of different vortex number [9].

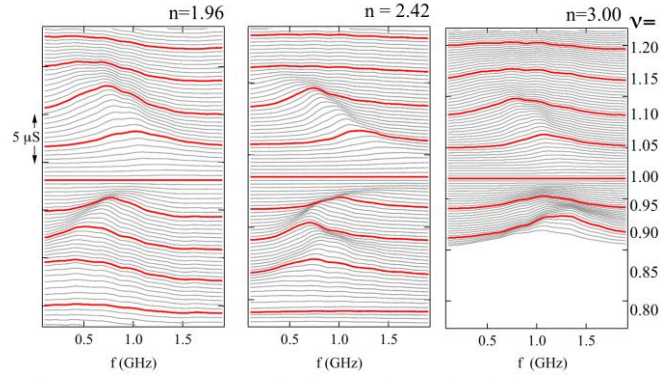


Figure 4: Spectra, real diagonal conductivity $\text{Re } \sigma_{xx}$ vs frequency (f) near $v=1$, offset vertically proportional to v for the red spectra are marked at right. Carrier densities, n , in 10^{11} cm^{-2} are marked at the top of each panel.

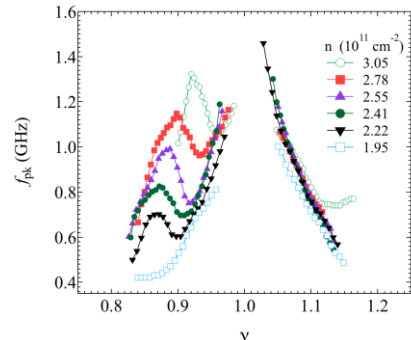


Figure 5: Resonance peak frequencies (f_{pk}) vs Landau filling v for many densities (n), for resonances within the IQHE centered at $v=1$

Future Plans

In the near term we will extend the studies of alloy-disordered samples to lower v , using high magnetic fields in resistive magnets. Low v is a particularly simple limit for quantitatively comparing the effects of varying alloy disorder. In addition we will look into the temperature dependence of the melting of the solids in the WQWs.

In the longer term we plan to investigate devices designed to study wave vector dependence of the pinning mode, in the range of ($\pi/100$ nm). We also plan studies of the undoped devices [13], whose carriers are gate-induced. These devices can allow study of extremely low density 2DES. In addition we plan to extend microwave studies of the quantum Hall effects to single and bilayer graphene.

References

1. Yong P. Chen, R. M. Lewis, L. W. Engel, D. C. Tsui, P. D. Ye, Z. H. Wang, L. N. Pfeiffer, and K. W. West Phys. Rev. Lett. **93**, 206805 (2004).
2. Han Zhu, Yong P. Chen, P. Jiang, L. W. Engel, D. C. Tsui, L. N. Pfeiffer, and K. W. West Phys. Rev. Lett. **105**, 126803 (2010).
3. Yong Chen, R. M. Lewis , L. W. Engel , D. C. Tsui , P. D. Ye , L.N. Pfeiffer and K. W. West, Phys. Rev. Lett. **89**, 016801 (2003).
4. Han Zhu, G. Sambandamurthy, Yong P. Chen, P. Jiang, L. W. Engel, D. C. Tsui, L. N. Pfeiffer, and K. W. West, Phys.Rev. Lett. **104**, 226801 (2010).
5. R. M. Lewis, P. D. Ye, L. W. Engel, D. C. Tsui, L. Pfeiffer, and K.W. West, Phys. Rev. Lett. **89**, 136804 (2002).
6. G. Sambandamurthy, R. M. Lewis, Han Zhu, Y. P. Chen, L. W. Engel, D. C. Tsui, L. N. Pfeiffer, and K. W. West Phys. Rev. Lett. **100**, 256801 (2008)
7. Wanli Li, G.A. Csáthy, D.C. Tsui, L.N. Pfeiffer, and K.W. West, Appl. Phys. Lett. **83**, 2832 (2003)
8. P. D. Ye, L. W. Engel, D. C. Tsui, R. M. Lewis, L. N. Pfeiffer, and K. West, Phys. Rev. Lett. **89**, 176802 (2002).
9. A. C. Archer, Kwon Park, Jainendra K. Jain, arXiv:1307.1892 [cond-mat.str-el] (2013).
10. R. Chitra, T. Giamarchi, and P. Le Doussal, Phys. Rev. B 65, 035312 (2001); H. A. Fertig, Phys. Rev. B **59**, 2120 (1999); M. M. Fogler, and D. A. Huse, Phys. Rev. B **62**, 7553 (2000).
11. L. W. Engel, C.-C. Li, D. Shahar, D. C. Tsui and M. Shayegan, Solid State Commun., **104** 167 (1997).
12. Y. Liu, C. G. Pappas, M. Shayegan, L. N. Pfeiffer, K. W. West, and K. W. Baldwin, Phys. Rev. Lett., **109**, 036801 (2012).
13. R. L. Willett, M. J. Manfra, L. N. Pfeiffer, and K. W. West. Applied Physics Letters **91**, 033510 (2007).

Publications

Zhihai Wang, Yong P. Chen, Han Zhu, L. W. Engel, D. C. Tsui, E. Tutuc, and M. Shayegan, “Unequal layer densities in bilayer Wigner crystal at high magnetic fields”, Phys. Rev. B 85, 195408 (2012).

B.-H. Moon, L. W. Engel, D. C. Tsui, L. N. Pfeiffer and K. W. West, “Pinning modes of high magnetic field Wigner solids with controlled alloy disorder”, *submitted* to Phys. Rev. Lett.

Program Title: Symmetries, interactions, and correlation effects in carbon nanotubes

Principle Investigator: Gleb Finkelstein

Address: Physics Department, Duke University, Durham, NC 27708

E-mail: gleb@duke.edu

i) Program Scope

Over the years, quantum impurity models have developed into one of the central subjects of the electronic transport theory. Many of them, such as the celebrated Anderson model, include only interaction at the impurity site. However, recently interest has been growing to quantum impurity models with an interacting host, and related models with dissipation [1]. It is thought that they may account for some of the exotic states observed in strongly correlated bulk compounds, such as the heavy fermion materials [2, 3]. Therefore, it seems desirable to find an experimental realization of an artificial quantum impurity with an interacting or dissipative host, based on a tunable nanoscale system.

The role of the dissipative environment in tunneling is commonly modeled by coupling the tunneling particle to an ensemble of oscillators, or a “bosonic bath” [4]. The dissipative modes generally suppress the tunneling rate, with the degree of suppression depending on the bosons’ density of states and the coupling strength [5]. Originally introduced in the context of SQUIDs, tunneling with dissipation can be also realized in a tunnel barrier contacted by resistive leads (Figure 1a). In the simplest picture, the electromagnetic excitations in the leads provide a bosonic bath with a linear density of states (Ohmic environment); the coupling strength $r = e^2 R_e / h$ is determined by the total lead (i.e. environmental) resistance R_e [6, 7].

We have recently developed a platform for studying quantum impurity systems with dissipative host [8] (Figure 1). Our samples are made from carbon nanotube quantum dots contacted by resistive leads, which provide dissipation. Tunneling properties of these leads mimics an interacting one-dimensional system, the Luttinger liquid, and the effective strength of electron interaction is easy to control by changing their resistance. By applying a gate voltage, the nanotube quantum dot can either a) mimic the single barrier behavior or b) represent a resonant level for the tunneling electron (Figure 1). In case (a), the electrical conductance ($G \equiv dI/dV$) exhibits a power law suppression $G \propto \max(k_B T, eV)^{2r}$ as a function of temperature T or bias V due to the presence of dissipation (see *e.g.* Refs. [6, 7] for a review).



Figure 1: a) Tunneling with dissipation: an electron tunneling across a tunneling junction (gray) between long resistive leads (hatched) couples to the electromagnetic environment (wavy lines). The spread of environmental modes is impeded by the high lead resistance, suppressing the tunneling rate. b) In our measurements, we replace the simple tunneling barrier with a carbon nanotube (horizontal bar), thus forming a quantum dot, which provides an intermediate state for the tunneling electrons.

ii) Recent Progress

In our DOE-supported publication “Quantum phase transition in a resonant level coupled to interacting leads” [9] we observed a quantum critical point (QCP) realized in a spin-polarized resonant level coupled to strongly dissipative electrodes (Figure 1b). Most intriguingly, we have found that for the symmetric coupling of the resonant level to the leads, the on-resonant conductance is *not suppressed* by the dissipative environment (Figure 2). Furthermore, this behavior was interpreted as manifestation of the quantum phase transition (QPT).

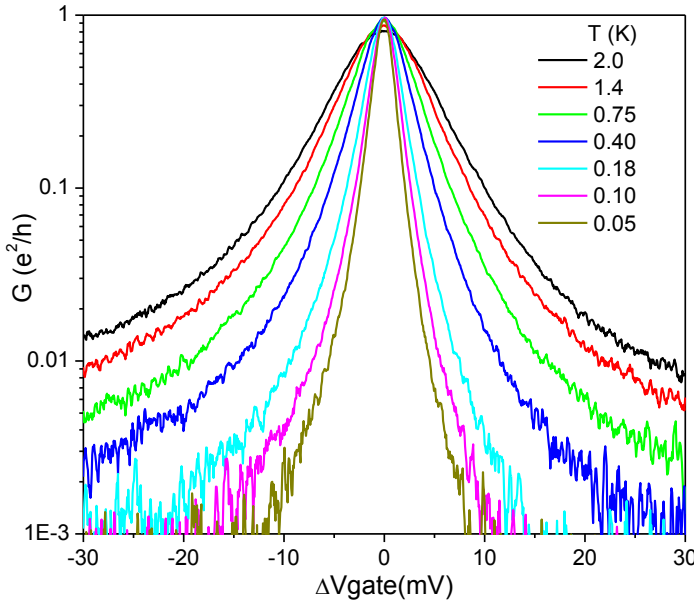


Figure 2: Shape of the resonance peak: conductance vs. gate voltage measured at several temperatures in the case of symmetric coupling of the resonant level to the two leads. The peak conductance grows with decreasing temperature, while the peak width drops. This situation corresponds to the quantum phase transition: in the limit of zero temperature, the conductance is zero everywhere except for the singular point at the center of the peak, where it reaches e^2/h (perfect transparency).

In our new paper, we investigate the exotic state of electronic matter obtained by fine-tuning the system exactly to the QCP [10]. We have measured several new transport scaling laws near and far from equilibrium, and then accounted for them theoretically (Figures 3, 4). Further, theoretical analysis performed by our collaborators revealed fractionalization of the resonant level into two quasi-independent Majorana modes: one strongly hybridized to the leads, and the other tightly bound to the quantum dot. Residual interactions involving these Majorana fermions results in a striking quasi-linear non-Fermi liquid scattering rate at the QCP, which we observe experimentally (Figure 3). Our devices constitute a viable alternative to topological superconductors as a platform for studying strong correlation effects within Majorana physics.

iii) Future Plans

- I plan to further study the quantum-critical behavior we have observed in a resonant level in dissipative environment. First, we intend to measure the critical exponents associated with the strongly coupled fixed point (*i.e.* the top of the resonance). Second, the resonant tunneling regime is predicted to disappear for strong enough dissipation, which we plan to verify. Finally, the *non-equilibrium* behavior of a resonant level with dissipation has been recently studied theoretically; we intend to probe this regime experimentally.

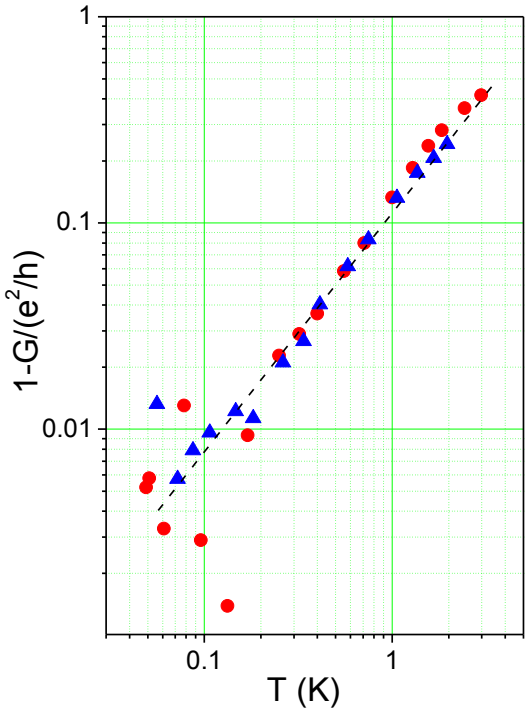


Figure 3: Temperature dependence of conductance at the QCP. Deviation of conductance from the unitary limit shows a power law dependence close to $e^2/h - G \propto T$, very different from the usual $\propto T^2$.

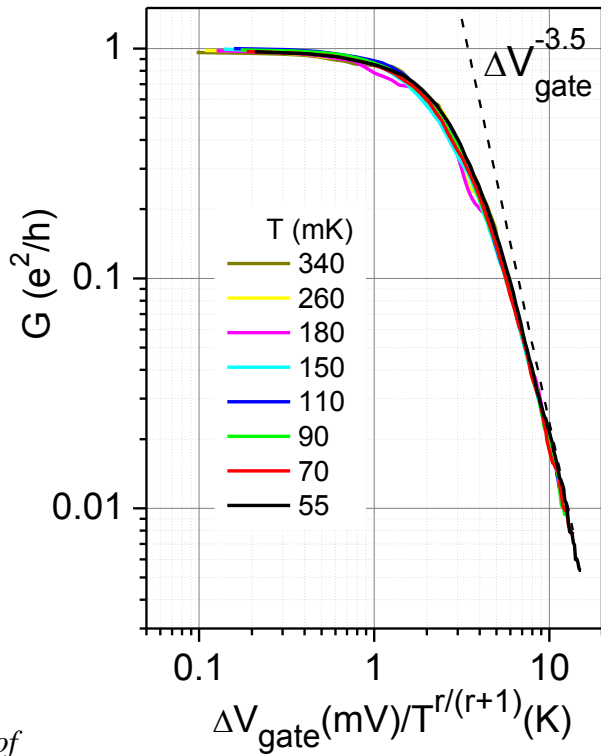


Figure 4 Peak conductance vs. scaled ratio $\Delta V_{\text{gate}}/T^{r/(r+1)}$. The data collapse on a universal curve. Dashed line: predicted asymptotic behavior.

- Tunneling with dissipation of spinful electrons. So far, we mostly studied the spin-polarized case, but multiple interesting predictions exist for the Kondo effect with Luttinger liquid leads and the (presumably similar) Kondo effect with dissipation.
- Finally, I plan to extend the (relatively) simple system described above in the following two directions: a) Non-Ohmic dissipation. We plan to realize a bosonic bath with sub-ohmic density of states, for which the analogy with the Luttinger liquid is no longer valid. b) Multi-channel resonant tunneling and Kondo effect. Dissipation in the leads prevents their hybridization, potentially allowing us to engineer multi-channel tunneling with dissipation.

iv) References

1. M. Vojta, *Impurity quantum phase transitions*. Philosophical Magazine **86**, p. 1807-1846 (2006).
2. A.C. Hewson, *The Kondo Problem to Heavy Fermions*. Cambridge Studies in Magnetism, Cambridge University Press, (1997).
3. Q. Si, S. Rabello, K. Ingersent and J.L. Smith, *Locally critical quantum phase transitions in strongly correlated metals*. Nature **413**, p. 804-808 (2001).
4. R. Feynman and F. Vernon, *The theory of a general quantum system interacting with a linear dissipative system*. Annals of physics **24**, p. 118-173 (1963).

5. A.J. Leggett, S. Chakravarty, A.T. Dorsey, M.P.A. Fisher, A. Garg and W. Zwerger, *Dynamics Of The Dissipative 2-State System*. Reviews Of Modern Physics **59**, p. 1-85 (1987).
6. G.-L. Ingold and Y.V. Nazarov, *Charge tunneling rates in ultra-small junctions*, in *Single Charge Tunneling*, M.H. Devoret and H. Grabert, Editors. 1992, Plenum Press, New York, 1992. p. 21-107.
7. K. Flensberg, S.M. Girvin, M. Jonson and D.R. Penn, *Quantum mechanics of the electromagnetic environment in the single-junction Coulomb blockade*. Physica Scripta **1992**, p. 189 (1992).
8. Y. Bomze, H. Mebrahtu, I. Borzenets, A. Makarovski and G. Finkelstein, *Resonant tunneling in a dissipative environment*. Physical Review B **79**, p. 241402R (2009).
9. H.T. Mebrahtu, I.V. Borzenets, D.E. Liu, H. Zheng, Y.V. Bomze, A.I. Smirnov, H.U. Baranger and G. Finkelstein, *Quantum phase transition in a resonant level coupled to interacting leads*. Nature **488**, p. 61-64 (2012).
10. H. Mebrahtu, I. Borzenets, H. Zheng, Y. Bomze, A.I. Smirnov, S. Florens, H.U. Baranger and G. Finkelstein, *Observation of Majorana Quantum Critical Behavior in a Resonant Level Coupled to a Dissipative Environment*. Accepted to Nature Physics (2013).

v) Publications resulting from work supported by the DOE grant in 2012-2013.

1. H. Mebrahtu, I. Borzenets, H. Zheng, Y.V. Bomze, A.I. Smirnov, S. Florens, H.U. Baranger and G. Finkelstein, Observation of Majorana Quantum Critical Behavior in a Resonant Level Coupled to a Dissipative Environment, **Nature Physics**, accepted (2013).
- 2) C.-H. Chung, K. Le Hur, G. Finkelstein, M. Vojta, and Peter Wolfle, Nonequilibrium quantum transport through a dissipative resonant level **Physical Review B** **87**, 245310 (2013).
- 3) I. Borzenets, U. Coskun, H. Mebrahtu, Y.V. Bomze, A.I. Smirnov, and G. Finkelstein, Phonon bottleneck in graphene-based Josephson junctions at millikelvin temperatures, **Physical Review Letters** **111**, 027001 (2013).
- 4) I.V. Borzenets, U.C. Coskun, H. Mebrahtu, and G. Finkelstein, Pb-graphene-Pb Josephson junctions: characterization in magnetic field, **IEEE transactions on Applied Superconductivity** (2012).
- 5) H. Mebrahtu, I. Borzenets, Yu. Bomze, and G. Finkelstein Observation of Unitary Conductance for Resonant Tunneling with Dissipation, **Journal of Physics: Conference Series** **400**, 042007 (2012).
- 6) H. Mebrahtu, I. Borzenets, D.E. Liu, H. Zheng, Y.V. Bomze, A.I. Smirnov, H.U. Baranger and G. Finkelstein, Quantum Phase Transition in a Resonant Level Coupled to Interacting Leads, **Nature** **488**, p. 61 (2012).

Program Title: Magnetic Materials

Principle Investigator: P. Fischer; Co-PIs: C.S. Fadley, F. Hellman, J.B. Kortright, W. Chao, E.H. Anderson, E.M. Gullikson, and P. Naulleau

Mailing Address: Materials Sciences Division, Lawrence Berkeley National Laboratory, Berkeley, CA 94720

E-mail: PJFischer@lbl.gov

i) Program Scope

The goals of this program are a basic understanding of novel nano- and meso-scale magnetic structures and strongly correlated magnetic materials, and the exploration of new phenomena permitting the control of spins down to fundamental magnetic length and time scales. This will not only provide answers to grand challenge questions, in particular, how new magnetic properties of matter emerge from complex correlations at the nanoscale and how those can be engineered and controlled, but how the understanding of nanoscale behavior can be used to discover new magnetic properties and phenomena at multiple length, time, and energy scales extending into meso-scales. Whereas our research is primarily knowledge-inspired, new spin-based materials, structures and phenomena can serve the development of spintronics devices with significantly enhanced functionalities, energy efficiency, and processing speed.

The main strategy to achieve our goals is to utilize a unique combination of state-of-the-art synthesis and a powerful range of characterization techniques (x-ray spectromicroscopy, photoemission, scattering, and nanocalorimetry) providing spatiotemporal imaging, elemental selectivity, depth sensitivity, and thermodynamic measurements, accompanied and supported by multiple theoretical efforts. A unique characteristic of this program is strong ties to instrument and method development, thus enabling new breakthroughs towards the goals of our program. A highly complementary and worldwide unique set of state-of-the-art characterization tools, which make extensive use of DOE facilities at LBNL constitutes the backbone of our experimental investigations.

In prototypical systems, which are synthesized both within our group and in collaboration with other groups at LBNL and elsewhere, we study the impact of surfaces and interfaces on magnetic behavior, the microscopic origins of magnetic phase transitions, the relation between heat and spin currents, magnetocaloric and spincaloritronic effects, and the spin dynamics of coupled magnetic nanostructures.

Specifically, this program addresses the following basic scientific questions:

- How do interfaces and surfaces affect or even create magnetic behavior?
- How can one control or tailor competing interactions such that desirable magnetic instabilities occur?
- Can we discover new or more efficient ways to control spins?
- How do heat currents couple to spin currents?
- How do spin fluctuations affect deterministic behavior of nano- and meso-scale magnetic processes?
- What drives magnetic phase transitions on short length and fast time scales?
- How do ultrafast dynamical spin phenomena manifest themselves with competing interactions and across interfaces?

ii) Recent Progress

A) Competing Interactions: Background

Materials with competing electronic ground states often possess first order transitions as a function of e.g. pressure, field, composition, strain, and in some cases temperature. We are interested in transitions between different magnetic states. These transitions represent an underlying electronic instability that can be controlled by application of relatively small perturbations, making them of interest for fundamental studies as well as for technological applications. The near-equatomic alloy of Fe and Rh currently is of broad interest due to its antiferromagnetic (AFM) to ferromagnetic (FM) transition near 90°C, which can be driven by magnetic field, temperature or pressure. Our expertise with thin films enables us to explore novel materials, including amorphous, multilayered and metastable compositions and designed structures, as well as strain-induced effects, e.g. for materials where pressure drives a transition. We aim to find novel meso-scale/structured materials that possess the same, or improved properties as FeRh but use more scalable materials than Rh.

Discussion of Findings

Using bulk-sensitive valence-band and core-level hard x-ray photoelectron spectroscopy with a photon energy of 5.95 keV, we measured significant changes of the electronic structure over the entire valence-band region across the first order AFM-FM transition, and interpreted the results with density-functional theory (DFT) (Anderson impurity model) [1] (Fig. 1 top). Drawing on our ability to measure an epitaxial film's heat capacity, we showed that the electronic entropy difference contributes to the transition, but the entropy associated with magnetic fluctuations is the primary driver.

We also studied the nucleation and growth of ferromagnetic domains across the transition by x-ray magnetic circular dichroism and photoemission electron microscopy (XMCD-PEEM). The coexistence of the AF and FM phases was evidenced across the broad transition and the different stages of nucleation, growth, and coalescence were directly imaged. The FM phase nucleates into single domain islands and the width of the transition of an individual nucleus is sharper than that of the transition in a macroscopic average [2] (Fig 1 bottom). Conversion electron Mössbauer spectrometry showed an unexpected spin re-orientation of the Fe moments in epitaxial FeRh films between in-plane and out-of-plane at the phase transition with perpendicular magnetic

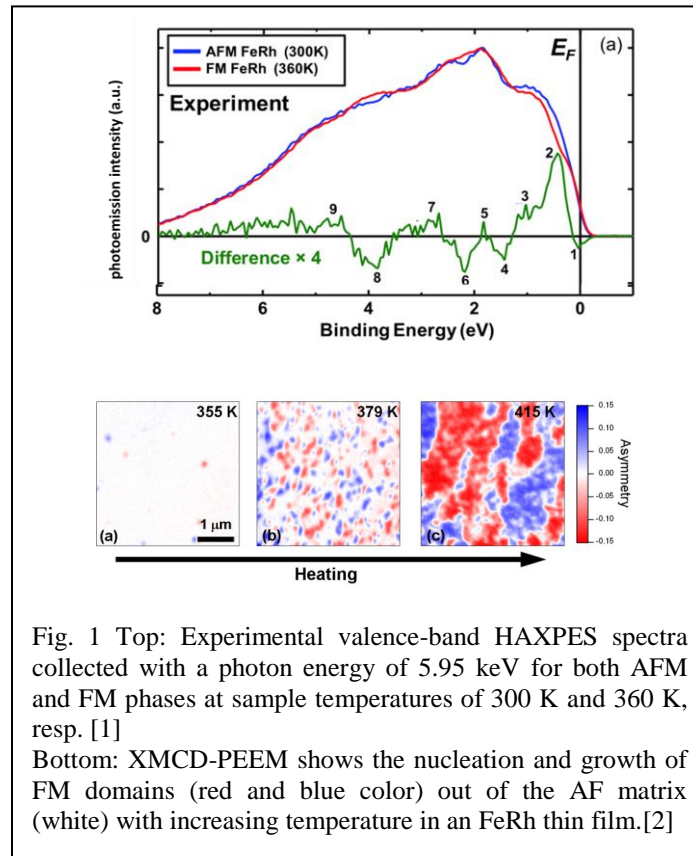


Fig. 1 Top: Experimental valence-band HAXPES spectra collected with a photon energy of 5.95 keV for both AFM and FM phases at sample temperatures of 300 K and 360 K, resp. [1]

Bottom: XMCD-PEEM shows the nucleation and growth of FM domains (red and blue color) out of the AF matrix (white) with increasing temperature in an FeRh thin film.[2]

anisotropy (PMA) possible in both phases. DFT showed that the spin re-orientation and PMA is caused by strain, and thus controllable [3].

B) New functionalities in spin textures: Background

The structure and dynamics of magnetic textures is of great interest both for fundamental and applied reasons. Magnetic vortex structures are currently discussed as new concepts for magnetic storage units, since each vortex could store four bits of information and the vortex state exhibits high stability. A fundamental understanding of the vortex state and the ability to control the vortex behavior is prerequisite for any vortex applications. Vortex states can also be seen as precursors for skyrmions, since they exhibit a half-integer skyrmion number q [4].

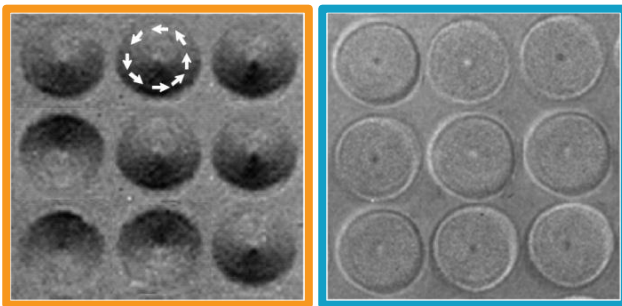


Fig. 2: Magnetic soft X-ray microscopy of circularity C (left) and polarity P (right) showed the asymmetric formation of magnetic-vortex structures in ferromagnetic nanodisks [5].

Discussion of Findings

We used magnetic full-field soft x-ray microscopy at 25nm spatial resolution to image simultaneously and directly the polarity and circularity of vortex states in large arrays of permalloy nanodisks (Fig 2.). We were able to demonstrate that the vortex nucleation process itself exhibits a non-symmetric behavior. We interpreted our observation as a result of an intrinsic Dzyaloshinskii-Moriya interaction arising from a broken inversion symmetry at the top and bottom surface/interface of the

disk. Full 3-dimensional micromagnetic simulations confirmed our experimental observation [5].

iii) Future Plans

The MSD/LBNL magnetic materials program will focus for FY14 on the following topics:

(1) Studies on FeRh: Our goal is to understand the underlying mechanisms in this prototype material for the first order FM-AF phase transition. In particular we will image with XMLD-PEEM the AF domains and we will use the bulk sensitivity of MTXM to complement the above mentioned PEEM studies with FeRh. To that end, we will deposit FeRh films by IBAD-MgO growth onto X-ray transparent substrates (Si_3N_4) and combine it with heating devices for accurate T-control. We have also started collaborations with the JILA group (Kapteyn/Murnane) to study the ultrafast dynamics response of FeRh systems.

(2) Magnetic interfaces: We are interested to see how magnetic behavior is altered at prototype interfaces using hard x-ray photoemission (HAXPES), depth-resolved ARPES using standing-wave excitation (SWARPES) [6] and XMCD. A particular topic are CoO/AZO interfaces, where magnetism emerges at the interfaces.

The PIs of the magnetism program are also involved in developing new directions for magnetism research at LBNL.

iv) References

1. A.X. Gray, D.W. Cooke, P.Krüger, C.Bordel, A.M. Kaiser, S.Moyerman, E.E Fullerton, S. Ueda, Y. Yamashita, A. Gloskovskii, C. M. Schneider, W. Drube, K. Kobayashi, **F. Hellman**, and **C. S. Fadley**, *Phys. Rev. Lett.* **108**, 257208 (2012)

2. C. Baldasseroni, C. Bordel, A. X. Gray, A. M. Kaiser, F. Kronast, J. Herrero-Albillos, C. M. Schneider, **C. S. Fadley**, and **F. Hellman**, *Appl. Phys. Lett.* **100**, 262401 (2012)
3. C. Bordel, J. Juraszek, David W. Cooke, C. Baldasseroni, S. Mankovsky, J. Minár, H. Ebert, S. Moyerman, E.E. Fullerton and **F. Hellman**, *Phys. Rev. Lett.* **109**, 117201 (2012)
4. O. A. Tretiakov and O. Tchernyshyov, *Phys. Rev. B* **75**, 012408 (2007)
5. M.-Y. Im, **P. Fischer**, Y. Keisuke, T. Sato, S. Kasai, Y. Nakatani, T. Ono, *Nature Communications* **3** 983 (2012)
6. A.X. Gray, J. Minár, **C.S. Fadley** et al. *Europh Lett*, to appear.

iv) Further publications in 2012-2013 (with DOE support)

1. M. Charilou, **F. Hellman**, *Phys Rev B* **87** 184433 (2013)
2. Z. Boekelheide, **F. Hellman**, *Appl Phys Lett* **102** 141601 (2013)
3. H.-J. Lee, C. Bordel, J. Karel, David W. Cooke, M. Charilaou, and **F. Hellman**, *Phys Rev. Lett* **110** 087206 (2013)
4. S.-H. Yang, A. X. Gray, A. M. Kaiser, B. S. Mun, B. C. Sell, **J.B. Kortright**, and **C.S. Fadley**, *J Appl Phys* **113**, 073513 (2013)
5. J. Kimling, T. Gerhardt, A. Kobs, A. Vogel, S. Wintz, M.-Y. Im, **P. Fischer**, H. P. Oepen, U. Merkt, and G. Meier, *J Appl Phys* **113**, 163902 (2013)
6. V. Uhlíř, M. Urbánek, L. Hladík, J. Spousta, M.-Y. Im, **P. Fischer**, N. Eibagi, J. J. Kan, E. E. Fullerton and T. Šikola, *Nature Nanotechnology* **8** 341-346 (2013)
7. Y.-S. Yu , D.-S. Han, M.-W. Yoo, K.-S. Lee, Y.-S. Choi , H. Jung, J. Lee, M.-Y. Im , **P. Fischer**, S.-K. Kim, *Sci. Rep.* **3**, 1301 (2013).
8. **P. Fischer**, M.-Y. Im, C. Baldasseroni, C. Bordel, **F. Hellman**, J.S Lee, and **C.S. Fadley**, *JESRP* (2013) in press DOI: 10.1016/j.elspec.2013.03.012
9. **C. S. Fadley**, *JESRP* (2013), in press DOI: 10.1016/j.elspec.2013.06.008
10. A.X. Gray, J. Minar, S. Ueda, P.R. Stone, Y. Yamashita, J. Fujii, J. Braun, L. Plucinski, C.M. Schneider, G. Panaccione, H. Ebert, O.D. Dubon, K. Kobayashi, **C.S. Fadley**, *Nat Mater* **11**, 957(2012)
11. Cooke, DW **Hellman**, F., Baldasseroni, C., Bordel, C., Moyerman, S , Fullerton, EE, *Phys Rev Lett* **109** 225901 (2012)
12. A.A.Greer, A.X.Gray, S.Kanai, A. M. Kaiser, S. Ueda, Y. Yamashita, C. Bordel, G. Palsson, N. Maejima, S.-H. Yang, G. Conti, K. Kobayashi, S. Ikeda, F. Matsukura, H. Ohno, C. M. Schneider, **J. B. Kortright**, **F. Hellman**, and **C. S. Fadley**, *Appl. Phys. Lett.* **101**, 202402 (2012)
13. Macià, F., Warnicke, P., Bedau, D., Im, M. Y., **Fischer**, P., Arena, D. A., & Kent, A. D. *Journal of Magnetism and Magnetic Materials* **324**, 3629–3632 (2012).
14. Vogel, A., Corinna Niemann, A., Stenner, C., Drews, A., Im, M.-Y., **Fischer**, P., & Meier, G., *Journal of Applied Physics* **112**, 063916 (2012).
15. Boekelheide, Z., Stewart, D., & **Hellman**, F. *Physical Review B* **86**, 085120 (2012).
16. Stone, K., Valvidares, S., & **Kortright**, J. *Physical Review B* **86**, 024102 (2012).
17. Kaiser, A. M., Gray, A. X., Conti, G., Jalan, B., Kajdos, A. P., Gloskovskii, A., Ueda, S., Yamashita, Y., Kobayashi, K., Drube, W., Stemmer, S., & **Fadley**, C. S. *Appl. Phys. Letters* **100**, 261603 (2012).
18. Jung, H., Choi, Y. S., Lee, K. S., Han, D. S., Yu, Y. S., Im, M. Y., **Fischer**, P., & Kim, S. K. *ACS Nano* **6**, 3712–3717 (2012).
19. Mesler, B. L., Buchanan, K. S., Im, M. Y., & **Fischer**, P. *Journal of Applied Physics* **111**, 07D311 (2012).
20. Boekelheide, Z., Saerbeck, T., Stampfl, A. P. J., Robinson, R. A., Stewart, D. A., & **Hellman**, F. *Physical Review B* **85**, 094413 (2012).
21. **Fischer**, P. & **Fadley**, C. S. *Nanotechnology Reviews* **1**, 5–15 (2012).
22. Im, M. Y., Bocklage, L., Meier, G., & **Fischer**, P. *Journal of Physics: Condensed Matter* **24**, 024203 (2012).

Tunneling and Transport in Nanowires (DE-FG02-02ER46004)

Allen M. Goldman, School of Physics and Astronomy, University of Minnesota, Minneapolis Minnesota

Program Scope

The goal of this program is to obtain a fundamental understanding of phenomena that might be relevant to the performance of devices and circuits at the limit of the smallest realizable feature sizes, focusing on the properties of nanowires. The approach is to study structures prepared using top-down *physical* rather than bottom-up, *chemical* or *biological* techniques. Because of the limits of lithography, all of the nano structures that are being investigated are in the mesoscopic regime of size. The smallest feature size (line width) that we can achieve is the order of 10 to 20 nanometers.

We are investigating selected properties of nanowires that are either quasi-one-dimensional (quasi-1D) or one-dimensional (1D), depending upon the size of the widths and thicknesses, or radii, characterizing the transverse dimensions of the wire relative to some characteristic length associated with a physical property that might be altered by dimensional constraint. When these lengths are smaller than the inelastic scattering, phase coherence, or superconducting coherence lengths, the wires are quasi-1D. This distinguishes them from wires for which the transverse dimensions are smaller than the Fermi wavelength and for which only the longitudinal electronic degree of freedom is relevant. For such truly 1D wires, Landau's Fermi liquid theory fails and must be replaced by Tomonaga-Luttinger Liquid (TLL) theory (Tomonaga, 1950 and Luttinger, 1962). Current projects include the study of transport properties of nanowires and nano-rings, attempts to control of the transport properties of nanowires using dissipation, and the study of the Tomonaga-Luttinger limit of ultra-narrow wires of low carrier density.

Recent Progress

Our main accomplishments to date involve experiments on quasi-1D superconducting nanowires. Our original motivation involved an effort to verify the existence of the reported superconducting "anti-proximity" effect (Tian *et al.*, 2005 and 2006), preparing quasi-1D wires in a manner different from that employed in the original work. This led to the discovery of a magnetic field restoration of superconductivity in out-of-equilibrium nanowires driven resistive by current (Chen, Snyder and Goldman, 2009, and Chen, Lin, Snyder and Goldman, 2011). At this writing there is a qualitative theoretical explanation for these observations involving dissipation (Vodolazov and Peeters, 2012), but no quantitative theory. We have new data, as yet unpublished, relating to observations of a dissipative intermediate state within the superconductor-normal metal transition regime of current-driven superconducting Zn nanowires. At the onset of this intermediate dissipative state, the system undergoes an unusual bi-stability, exhibited as repeated switching between dissipative and superconducting states. Applying a weak magnetic field leads to the collapse of the bi-stability with greatly enhanced lifetime of the

superconducting state. This provides crucial insight into the nature of the magnetic field-induced-superconductivity (Chen, Lin, Snyder, and Goldman, 2011) and the related anti-

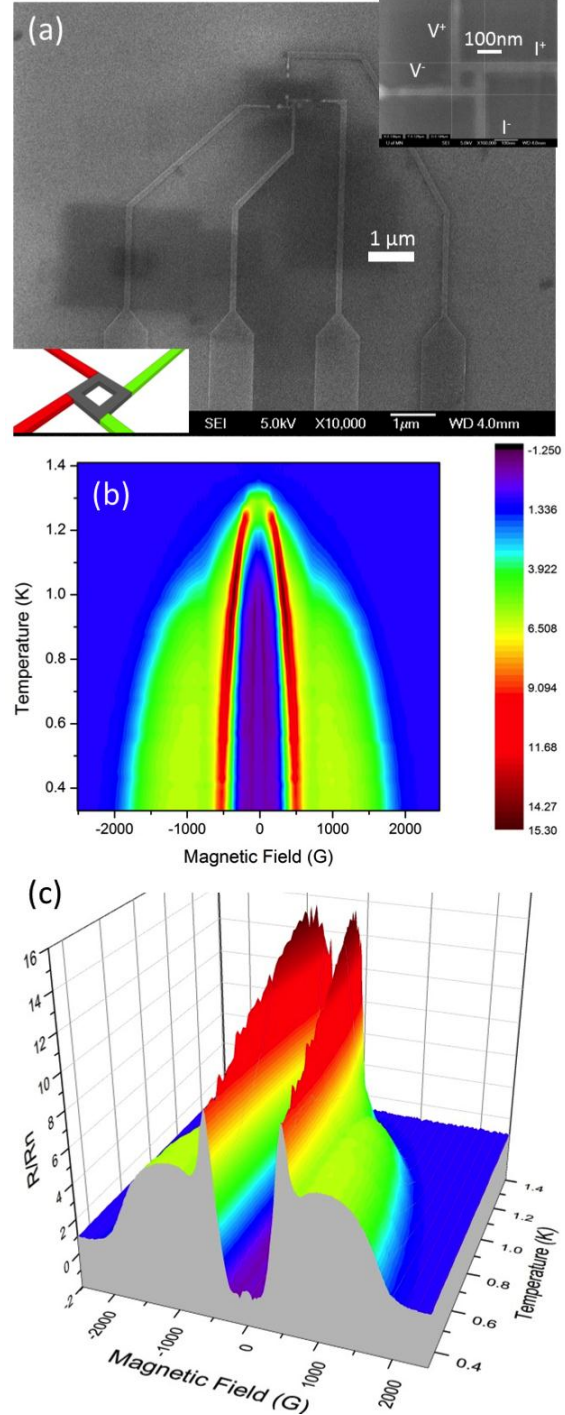


FIG. 1 (a) SEM image of loop sample. Top right inset: zoomed in image of the nano-ring with the measurement configuration. Bottom left inset: cartoon of measurement configuration with green voltage leads and red current leads. (b) Resistance color contour map (RCCM) in B-field and temperature. (c) The same data as in (b) in 3D.

proximity effect observed in superconducting nanowires. The latter were measured with averaging times that were long in comparison with the observed switching times.

Using the same fabrication technology employed to produce nanowires, we have produced ultra-small superconducting loops, which were used to investigate the prediction that for sufficiently small loops, *i.e.*, for loop dimensions less than the coherence length, the flux quantum is h/e rather than the usual $h/2e$ (Wei and Goldbart, 2008). The results of these investigations resulted in the observation of an unexpected, anomalous high-resistance state, rather than superconductivity (Snyder *et al.*, 2013). This effect, which is shown in Fig. 1, has precluded the study of h/e oscillations.

We have made progress in developing an experiment to directly control the properties of nanowires by dissipation. This involves fabricating nanowires on the surface of GaAs wafers, which have a buried, tunable two-dimensional electron gas (2DEG) not far from the surface. By changing the conductivity of the 2DEG with a back gate we should be able to control the properties of the wire.

We have also made progress in developing the technology to produce low-carrier-density nanowires that would allow us to access the Tomonaga-Luttinger liquid regime. The work involves populating an exposed narrow channel on SrTiO_3 with carriers using an electric double layer transistor configuration.

Future Plans

We are pursuing the fabrication of nanowires on top of GasAs/AlGaAs heterostructures containing buried two-dimensional electron gases (2DEGs) whose conductivities are tunable with a back gate. We are attempting to tune the superconductor-insulator transition of a nanowire. The idea behind using dissipation is that increased dissipation can dampen phase fluctuations and enhance the tendency towards superconductivity. The approach is to follow Rimberg *et al.* (1997), who presented measurements of the I-V characteristics of 2-D arrays of superconducting islands linked by Josephson junctions in close proximity (100nm) to a 2DEG. The 2DEG served as a source of variable e .

We are also pursuing the study of the superconductor-insulator transition and Tomonaga-Luttinger liquid behavior of Strontium Titanate Nanowires. The electronic double layer transistor (EDLT) technique (Lee *et al.*, 2011) is being used to alter the properties of SrTiO_3 nanowires with two goals: in the high carrier density regime to study the superconductor-insulator transition, and in the low carrier density regime to search for Tomonaga-Luttinger liquid behavior.

References

Chen, Yu, S. Snyder, and A. M. Goldman, 2009, "Magnetic Field Induced Superconductivity in Out-of-Equilibrium Nanowires," Phys. Rev. Lett. **103**, 127002.

Chen, Yu, Yen-Hsiang Lin, S. D. Snyder and A. M. Goldman, 2011, "The Stabilization of Superconductivity by Magnetic Field in Out-of-Equilibrium Nanowires," Phys. Rev. B **83**, 054505.

Lee, Yeonbae *et al.*, 2011, "Phase Diagram of Electrostatically Doped SrTiO₃," Phys. Rev. Lett. **106**, 136809.

Luttinger, J. M., 1962, "An exactly solvable model of a many-fermion system," J. Math Phys. N.Y., **4**, 1154.

Rimberg, A. J., T. R. Ho, C. Kurdak, John, Clarke, K. L. Campman, and A. C. Gossard, 1997, "Dissipation-Driven Superconductor-Insulator Transition in a Two-Dimensional Josephson-Junction Array," Phys. Rev. Lett. **78**, 2632.

Snyder, S. D., *et al.*, 2013, "High-resistance state of phase coherent nanoscale thin-film Al superconducting nanorings in magnetic fields," Phys. Rev. B **87**, 144503 (2013).

Tian, Mingliang et al., 2005, "Suppression of superconductivity in Zinc Nanowires by Bulk superconductors," Phys. Rev. Lett. **95**, 076802.

Tian, Mingliang et al., 2006, "Influence of a bulk superconducting environment on the superconductivity of one-dimensional zinc nanowires," Phys. Rev. B **74**, 014515.

Tomonaga, S., 1950, "Remark on Bloch's method of sound waves applied to many fermion problems," Prog. Theor. Phys. (Kyoto) **5**, 544.

Vodolazov, D.Y and F. M. Peeters, 2012, "Enhancement of the retrapping current of superconducting microbridges of finite length," Phys. Rev. B **85**, 024508.

Wei, Tzu-Chieh and Paul M. Goldbart, 2008, "Emergence of h/e-periodic oscillations in the critical temperature of small superconducting rings threaded by magnetic flux," Phys Rev. B **77**, 224512. (and references cited therein).

Publications

Chen, Yu, Yen-Hsiang Lin, S. D. Snyder and A. M. Goldman, 2011, "The Stabilization of Superconductivity by Magnetic Field in Out-of-Equilibrium Nanowires," Phys. Rev. B **83**, 054505.

Snyder, S. D., *et al.*, 2013, "High-resistance state of phase coherent nanoscale thin-film Al superconducting nanorings in magnetic fields," Phys. Rev. B **87**, 144503 (2013).

Lee, Yeonbae *et al.*, 2011, "Phase Diagram of Electrostatically Doped SrTiO₃," Phys. Rev. Lett. **106**, 136809. (Partially supported by the NSF)

Program Title: Conductivity and Magnetism in Strongly Coupled Quantum Dot Solids.

Principal Investigator: Philippe Guyot-Sionnest

Mailing Address: James Franck Institute, 929 E. 57th Street, The University of Chicago, Chicago, IL 60637

E-mail: pgs@uchicago.edu

Program Scope

The goal of the program is to understand and optimize charge transport in colloidal quantum dot solids and to develop magneto electrical properties. There has been much progress in the first area over the past decade. The films of colloidal quantum dots were initially insulating, and the first studies of transport investigated photocurrents which could only be observed with large extraction field. Later, by control of the Fermi level and the introduction of a simple ligand exchange procedure, films were shown to evolve dark Ohmic conduction. The introduction of FET then led to much practical interest in the characterization of the mobility in these systems. Replacement of the organic ligands by inorganic small ions has led to a paradigm change, where fully inorganic composite materials can now be made with a 3D nanostructure. Such materials are being studied by many groups, primarily for nanocrystalline solar cells or thermoelectric materials. The performances are becoming interesting. For example, although the power conversion of PbS/Se colloidal quantum dot solar cell remains low, ~ 6%, it has been shown that charge collection efficiency could be 100%, or even more with impact ionization. Over the past year, FET mobility measurements on high temperature annealed nanocrystals of the generic CdSe class have been reported in excess of $20\text{cm}^2/\text{Vs}$, lower than for crystalline inorganic semiconductors but higher than organics. Our group developed other fruitful topics. In 2009, we patented the use of Atomic Layer Deposition in multilayer films of quantum dots to tune the coupling between nanoparticles and strengthen the films. In a different project aiming for an alternative approach to tuning superconducting properties, we made a nanostructured inorganic films of Pb/PbSe nanocrystals. We observed the insulator to superconducting transition, with the same T_c as bulk Pb and about 50 times higher critical fields. More recently we developed HgTe quantum dots for mid-Infrared detection. Using the inorganic matrix As₂S₃, we obtained photoconductive devices with about 1/10 the detectivity of epitaxial materials at 3.5 microns and at higher operating temperature.

Our work from the prior grant period demonstrated solidly that the variable range hopping accounted very well for the conduction in weakly coupled quantum dots, as a function of temperature, field and charged density. However, an increasing number of publications using inorganics linkers and annealing of the nanocrystal solids report high mobility and a negative temperature coefficient, taken as evidence that the transport operates as band conduction. This is exciting but surprising. Given the large inhomogeneity and disorder in the current nanocrystals systems, band conduction would presumably require such a large coupling between particles that minibands could not form without merging together, thereby losing the quantum dot specificity. However, we concluded that the mobilities achieved in the new systems are already larger than can be explained with a simple hopping model. Therefore a question this grant will attempt to answer is the true nature of transport and density of states in these strongly coupled systems.

Recent progress

Urbach Tail in CdSe quantum dot films: The redshift seen upon a coupling procedure is often taken as a quantitative measure of the interaction between the quantum states of the quantum dots, without further inquiry. The chemical processing and annealing may however strongly alter the surface of the dots creating other possibilities. We conducted an investigation of the band edge of the CdSe quantum dots upon coupling with ammonium sulfide, a strong coupling procedure. We observed that the large redshift reported were also accompanied by extended Urbach tail, reaching well beyond the bandgap of bulk CdSe. It was concluded that the redshift, the broadening and the absorption tails of interband absorption could not be solely attributed to a strong electronic coupling between the dots. Instead, mixing of surface and core hole states was proposed to dominate the changes of the interband spectra at the absorption edge.

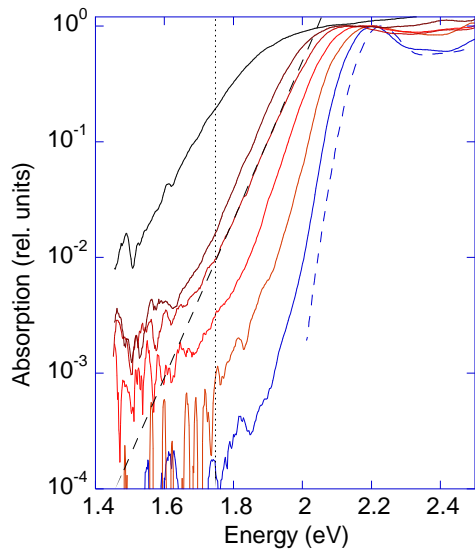


Figure 1: Absorption spectra of CdSe films processed with Ammonium sulfide and annealed at several temperatures. The dashed line is the absorption for a hexane solution. The solid lines are the absorption measured for thin films by Thermal Deflection Spectroscopy with, from right to left Heptanediamine (weak coupling), and the sulfide ions 20°C, 50°C, 100°C, 150°C, and 200°C. The dashed vertical line is at 1.75 eV, which is the bulk bandgap of CdSe. The dashed line superimposed on the 100°C spectrum is its steepest slope at 60 meV.

1/f electrical noise in Nanocrystals solids: In the weak coupling limit, nanocrystal solids are actively researched for sensors, such as chemically sensitive resistors and photoconductive detectors. In these systems, electrical noise limits the performances. In particular, the nanocrystal systems can exhibit large excess 1/f noise. For our HgTe infrared detectors, the 1/f noise limits the Detectivity below 1 kHz. 1/f noise is often attributed to charges moving into different states with a wide range of tunneling distance or activation energies, and these charges affect the transport by either contributing to the number of mobile charges or modulating the mobility. We therefore initiated a study to determine if the 1/f noise could be reduced by film processing, by the choice of the materials comprising the nanocrystals, and by the choice of the matrix. It seemed to us obvious that, just as for bulk materials, we would be able to strongly affect the noise level by using different materials. We did find that diminishing the prevalence of cracks in the films was effective in lowering the 1/f noise, and this was expected. However, our results show also some universal 1/f noise floor with all the materials studied, with a noise scaling as the number of nanocrystals in the system, i.e. extensive as for bulk systems, and approximately proportional to the interdot conductance, irrespective of the materials. We qualitatively conclude that the noise is an intrinsic effect of the disorder of the granularity in conduction, where charges moving in part

of the network act to modify transport in the higher conductivity, and better connected part of the network, yielding effectively a noise mechanism that only depends on the interdot conductance and not on the nature of the material.

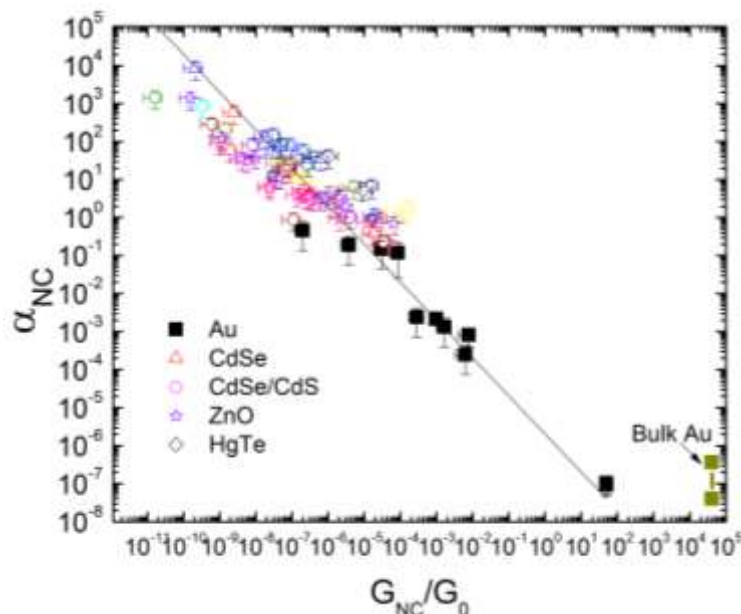


Fig. 2: Comparison between gold nanoparticle (black squares) and the semiconductor nanocrystal films. They both show universal scaling of the noise per nanocrystal, with interdot conductance. All the data in hopping regime were taken under 1V bias , corresponding to ~0.3-0.6 mV/nanocrystal.

Future plans

FET vs Bulk mobility: FET data of quantum dot solids have shown very high mobility ($> 10 \text{ cm}^2/\text{Vs}$) and very weak or even negative temperature dependence. Bulk conductivity data based on electrolyte or ion gel gating show instead rather low mobility ($< 1 \text{ cm}^2/\text{Vs}$) and temperature dependence consistent with hopping transport. These materials need however to be porous which may reasonably introduce additional barriers and disorder for transport. We plan therefore to test the bulk mobility of the materials that have the exceptional FET mobilities. This will be done by time of flight methods and photoexcitation.

Magnetotransport: although magnetic doping of semiconductor quantum dot has much progressed in the past decade, there have been no significant results concerning the magnetotransport. Our own investigations have so far indicated that the dominant effects are the spin-blockade, effective only in the very weak coupling limit, and the wavefunction squeezing. However, the large effective g-factor and the magnetic polarons seen in the quantum dots have so far failed to lead to significant magnetoresistance in our experiments. It may be that strong coupling is required for these effects to appear, and this will be the subject of future investigations.

References (which acknowledge DOE support)

- Mott and Efros-Shklovskii Variable Range Hopping in CdSe Quantum Dots Films, Liu H, Pourret A, Guyot-Sionnest P, **ACS Nano 4, 5211-5216 (2010)**
- n- and p-Type HgTe Quantum Dot Films, Liu Heng; Keuleyan Sean; Guyot-Sionnest P **J. Phys. Chem. C 116, 1344-1349 (2012)**
- A “mirage” study of CdSe colloidal quantum dot films, Urbach tail and surface states, Guyot-Sionnest P, Lhuillier E., Liu H., **J. Chem. Phys. 137, 154704 (2012)**

Electrical Transport in Colloidal Quantum Dot Films, by Guyot-Sionnest P. **J. Phys. Chem. Lett.**
3, 1169-1175 (2012)

Universal 1/f noise in nanocrystal solids, Heng Liu, Emmanuel Lhuiller, P. Guyot-Sionnest,
Submitted.

Program Title: Investigation and Manipulation of Nanoscale Molecular Superconductivity

Principal Investigator: Saw Wai Hla

Mailing Address: 251B Clippinger Lab, Physics & Astronomy Department, Ohio University, Athens, OH 45701.

Email: hla@ohio.edu

Program Scope

This project focuses on atomic level investigations of *nanoscale* molecular superconductors formed by charge transfer based donor-acceptor systems on metallic surfaces using scanning tunneling microscopy, tunneling spectroscopy, and atomic and molecular manipulation at low temperatures in an ultrahigh vacuum environment. We are advancing the molecular superconductivity research in two critical areas; 1) fundamental properties, and 2) manipulation of charge states of molecular superconductors. In the first part, we measure superconducting gaps, explore superconductor-metal phase transitions, and investigate proximity effects at superconductor-metal boundary. In the second part, we manipulate the charge state of the molecular superconductors by adding additional donor and acceptor molecules locally. The effect of substrate electron confinement on the superconductivity will also be studied using hybrid cluster-quantum corral devices. Our project includes both conventional and innovative components, and the achievements will impact on fundamental understanding of nanoscale superconductivity and its potential applications in energy sciences.

Recent Progress

We have made significant progresses in a number of fronts. For the fundamental properties of nanoscale superconductors on metal surfaces, we have measured proximity effect at the superconductor-metal boundary at the atomic scale, have investigated charge transfer at the molecule-substrate and molecule-molecule interfaces, and have identified metallic state of the molecular clusters before their transition to the superconducting state. A part of the results is described in ‘I’. In addition, we have recently completed the study of a new superconducting structure formed by molecular chains on Ag(111). Here, we have investigated superconductor-metal phase transition, size dependent superconductivity (coherent length), and mechanical properties of superconducting clusters by STM manipulation. We have also determined interaction of surface state electrons with the new superconducting structure and proximity effects at the molecule-metal boundary. For the manipulation of charge state, we are pursuing hybrid molecular structures formed by molecular superconductors and magnetic molecules. A part of the studies related to magnetic molecular machine is described in ‘II’.

I. Atomic scale proximity effects of a nanoscale molecular superconductor on a Ag(111) surface

Interfaces generate the most intriguing phenomena in nature. In materials science, novel interfacial phenomena have been discovered in materials ranging from metals, semiconductors, superconductors, to topological insulators. How a superconductor interacts with two dimensional electron gas at the interface with a metal, especially at the atomic scale, is an intriguing question but has yet to be explored. Here we investigate charge transfer at a superconductor-metal interface, and electronic structural evolutions at a superconductor-metal boundary between $(\text{BETS})_2\text{-GaCl}_4$ nanoscale superconducting clusters and a Ag(111) surface at the atomic scale.

Charge transfer based molecular superconducting system formed by $(\text{BETS})_2\text{-GaCl}_4$ on a Ag(111) surface exhibits a superconducting gap even at the small chains composed of just four molecular pairs [1]. However, the charge transfer mechanism in $(\text{BETS})_2\text{-GaCl}_4$ clusters adsorbed on a Ag(111) surface is not at all clear. For instance, the charge transfer at the molecule-metal interface may also play a role in the observed superconductivity. Our density functional theory (DFT) calculations show that the Ag(111) surface injects 0.22 electronic charge to the donor BETS through the low lying surfer (S) atoms. The acceptor GaCl_4 is slightly elevated from the surface and it still acquires the desired charge amount of 0.84 electron from the BETS molecules. Each BETS loses 0.22 electronic charge to the acceptor GaCl_4 thereby the outermost BETS orbital becomes partially filled leading to a metallic state. In accord with the DFT results, the dI/dV - V tunneling spectroscopy measurements reveal that the highest occupied molecular orbital of $(\text{BETS})_2\text{-GaCl}_4$ clusters crosses over the surface Fermi level (Fig. 1a, 1b). Therefore we directly identify the partially filled band of BETS, and the metallic state of molecular clusters on Ag(111). The metallic state is an essential condition for the superconducting transition of the molecular clusters below the critical temperature of $\sim 10\text{K}$.

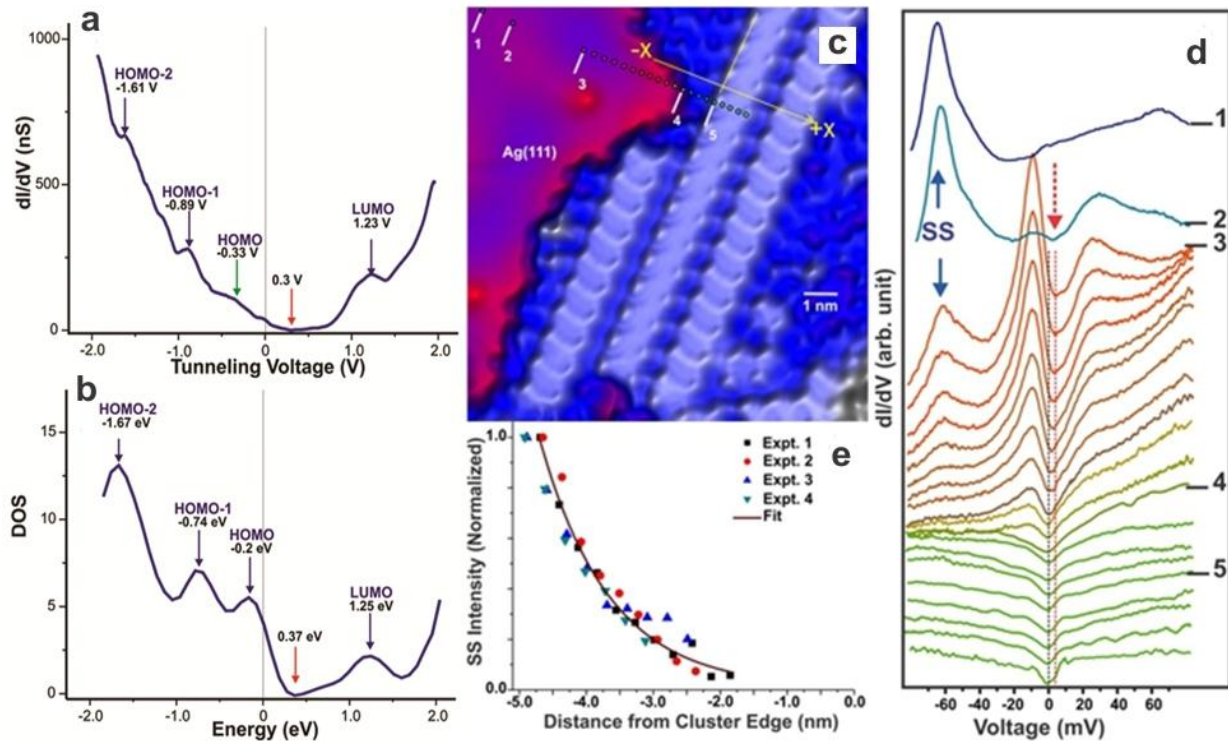


Fig. 1. (a) dI/dV - V spectroscopy and (b) calculated density of state of $(\text{BETS})_2\text{-GaCl}_4$ reveals Fermi level crossing of HOMO. (c) An STM image of superconducting clusters (blue) next to a bare surface area (red). Tunneling spectra are measured along ‘-x’ axis. (d) Tunneling spectroscopy data measured at the locations indicated with dots in (c). The black-dotted line indicates the Fermi level while the red-dotted line shows the minimum energy location of the observed state on Ag(111) terrace. (e) Normalized surface state intensity as a function of lateral positions measured for four sequences show an exponential decrease of the surface state intensity. Here, ‘0’ is the superconductor-metal boundary and it is located at ‘5’ in (c).

For the proximity effects, the tunneling spectroscopy measurements across the superconducting-metal boundary reveal that the intensity of surface state rapidly decreases following an exponential decay, and it is completely quenched at $\sim 1.5\text{ nm}$ distance from the boundary (Fig. 1c-1e). By comparing with surface state intensity near the Ag(111) step-edge and random BETS- GaCl_4 clusters at higher temperatures, we show that the observed phenomenon can be found only at the superconductor-metal interface. Moreover, a gap-like state is observed near the Fermi level on Ag(111) surface that transforms to the superconducting gap over the molecular clusters. This again highlights how superconducting gap is

formed at the metal-superconductor boundary and therefore valuable for the understanding of superconducting phenomena across the board.

II. Controlled clockwise and counterclockwise rotational switching of a molecular motor

Molecule containing magnetic atoms may be able to use doping of the $(\text{BETS})_2\text{-GaCl}_4$ molecular superconductor to change its charge state. We chose a molecule containing 4 Fe atoms for this study, which also functions as a standalone molecular motor. This motor is a piano-stool complex [$\eta^5\text{-}1\text{-}(4\text{-tolyl})\text{-}2,3,4,5\text{-tetra(4-ferrocenylphenyl)}\text{ cyclopentadienyl hydrotris [6-((ethylsulfanyl)methyl)indazol-1-yl] borate ruthenium(II)}$] consisting of a five-arm *rotator* mounted on a molecular tripod *stator* (Fig. 2a). Rotation of the *rotor* is enabled by the central *Ru* atom acting as an atomic ball bearing between the *stator* and the central 5-membered ring in the *rotor*. Four of the *rotor* arms have a ferrocene group attached at their ends while the fifth arm is truncated beyond the phenyl ring. This provides a structural dissymmetry to help in the detection of discrete rotation steps of the *rotor* relative to the *stator*. Ferrocene groups have been chosen for their electro-activity, which enable them to act as reversible electron relays. Moreover, by injecting electrons from STM tip, a charged ion state can be induced in the ferrocene, which will be used as a dopant to the molecular superconductors.

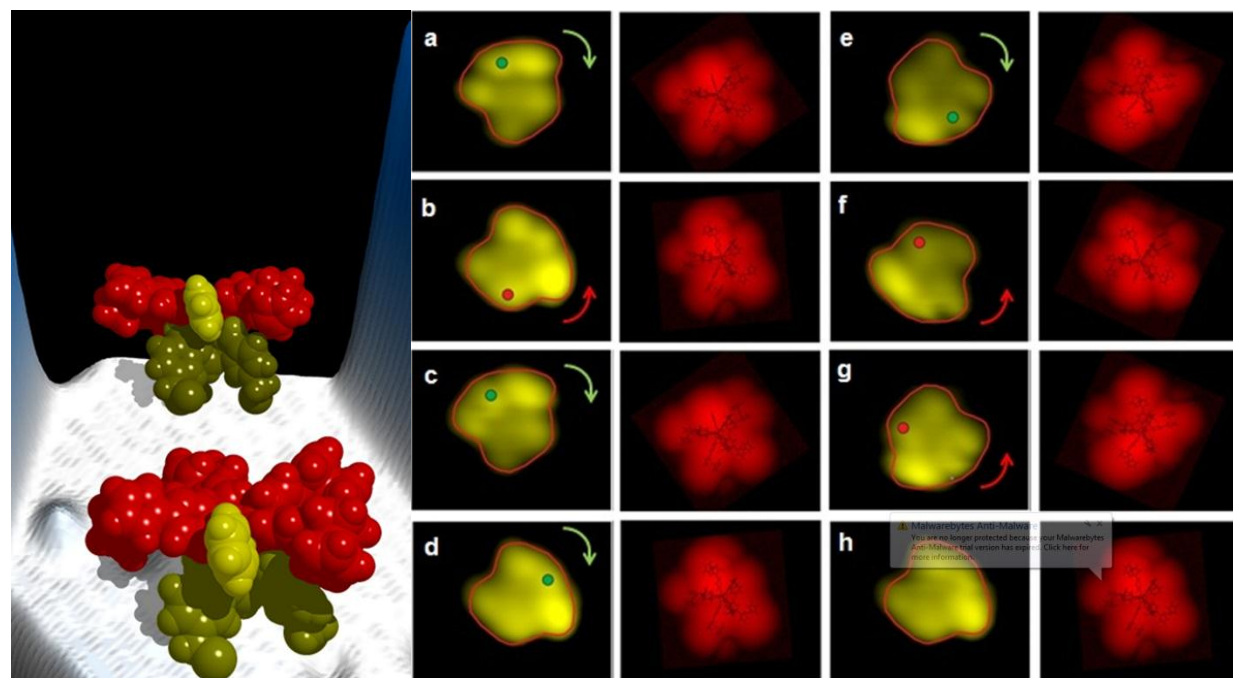


Fig. 2. (Left) 3-D illustration of molecular motors. (Right) (a-h) A sequence of STM images (yellow) and calculated structures (red) showing controlled step-wise rotation of the motors.

We use STM manipulation and spectroscopy schemes to explore rotation of individual molecular motors on a Au(111) surface. It is found that a single standalone molecular motor can be made to rotate in a clockwise or counterclockwise direction by selective inelastic electron tunneling through different sub-units of the motor. The electron injection into truncated arm results in clockwise rotation while electron injection into any of the ferrocene arm causes counter clockwise rotation. The directional rotation originates from saw-tooth-like rotational potentials, which are solely determined by the internal molecular structure and are independent of the surface adsorption site. This finding will further accelerate the development of complex and automated nano machineries that can be operated on a material surface, in addition to our primary goal of forming hybrid magnetic molecule-molecular superconductor structures.

Future Plans

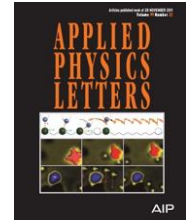
Our finding of extended gap state on metallic surface near superconductor-metal boundary opens further questions; The minimum energy location of this gap-like state is shifted towards positive energy, and the gap appears larger than the superconducting gap. In most cases, pseudo gaps near the metal-superconductor region appear smaller than the superconducting gap itself. This indicates that the observed gap state might be of different origin than a pseudo-gap. For instance, similar gap-like state has been recently reported on NbSe₂ system [2] where it is explained as due to the charge density waves. We plan to pursue further investigations of this effect using spin-polarized STM set-up. This will also be extremely useful for understanding the spin contributions in the observed gap state.

Another research direction being pursued is the formation of hybrid superconductor-magnetic molecule systems by mixing superconducting molecular systems with other interesting molecular systems. This can also be considered as local doping of the superconductors. We are also investigating other types of charge transferred based molecular superconductors as well.

List of Publications Acknowledging Current DOE Grant

Published:

- Deshpande, K.-F. Braun, & S.-W. Hla, "Determination of Chemical Specific Atomic Interaction with Scanning Tunneling Microscope", *Appl. Phys. Lett.* **99**, (2011) 221902. [**DOE-ER46012-20**]
- U.G.E. Perera, F. Ample, H. Kersell, Y. Zhang, G. Vives, J. Echeverria, M. Grisolia, G. Rapenne, C. Joachim, & S.-W. Hla. *Controlled Clockwise and Anticlockwise Rotation of a Molecular Motor*. *Nature Nanotechnology* **8** 46-51 (2013). [**DOE-ER46012-31**]



Submitted:

- S.-W. Hla. *Atomic Level Assembly*. [**DOE-ER46012-32**]
- K. Clark, R. Rankin, K.Z. Latt, S. Khan, A. Hassanien, J. Greeley, & S.-W. Hla. *Atomic scale proximity effects of a nanoscale molecular superconductor on a Ag(111) surface*. [**DOE-ER46012-29**]

Other References:

1. K. Clark, A. Hassanien, S. Khan, K.-F. Braun, H. Tanaka, & S.-W. Hla. *Superconductivity in Just Four Pairs of (BETS)₂-GaCl₄ Molecules*. *Nature Nanotechnology* **5**, (2010) 261-265. [**DOE-ER46012-24**]
2. Soumyanarayanan, A. et al. *Quantum phase transition from triangular to stripe charge order in NbSe₂*. *Proc. Nat. Acad. Sci.* **110**, (2013) 1623-1627.

Project Title: Quantum Transport in Topological Insulator Nanoelectronic Devices

PI: Prof. Pablo Jarillo-Herrero

Mailing address: 77 Massachusetts Avenue, 13-2017.

Massachusetts Institute of Technology. Cambridge, MA 02139.

Email: pjarillo@mit.edu

(i) Program Scope

This project aims to investigate electronic transport in Topological Insulators (TIs) devices. TI-based electronic devices are attractive as platforms for spintronic applications¹, and for detection of emergent properties such as Majorana excitations², electron-hole condensates³ and the topological magnetoelectric effect⁴. Most of these theoretical proposals envision experimental geometries consisting of a planar TI device integrated with materials of varying physical phases. Their implementation remains a challenge due to the ubiquitous presence of bulk carriers and the surface degradation under device fabrication. In the past, we have addressed these challenges by developing two alternative device fabrication approaches: the first approach is based on contacting Bi_2Se_3 flakes exfoliated from a single crystal, which we employed for establishing that the surface channel supports electronic transport⁵, that its density is tunable by a gate voltage, and that the surface-state's spin-helicity allows for a polarization-dependent photocurrent⁶. The second approach is based on patterned thin-films of Bi_2Se_3 grown in an ultra-high vacuum chamber, where we investigated the nature of coherent transport in the TI system⁷, where weak antilocalization (WAL) emerges as a consequence of the surface-state's non-trivial Berry's phase.

(ii) Recent Progress

Our recent work has focused on developing surface-sensitive probes which include capacitance and tunneling. These are implemented in both thin film and exfoliated devices. In the latter case, we have developed an advanced fabrication technique based on exfoliated thin film transfer, which allows us to integrate TI layers into heterostructures including hexagonal Boron-Nitride (hBN) and graphene.

Capacitance measurements

Capacitance is a valuable probe for the study of TI surface states: It is sensitive to the ground-state density of States (DOS) which is manifested as a correction to the total capacitance, called "quantum capacitance". Since a gate electrode only affects a system as far as its electric field penetrates, the capacitance measurement is free of most of the bulk effects present in in-plane transport studies.

We have performed capacitance measurements on patterned Bi_2Se_3 thin film devices capped by HfO_2 dielectric (Fig. 1, green). A clear minimum in the capacitance is observed, and is associated with the surface state Dirac point. The capacitance signal is symmetric, while the conductance (blue) is asymmetric due to contribution of bulk carriers. Furthermore, capacitance and transport minimum value do not appear at the same voltage, and remain offset even when accounting for contributions of the bulk. This

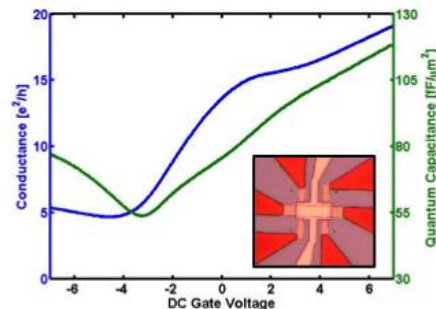


Figure 1: A comparison of device conductance (blue) and approximate quantum capacitance (green), which is proportional to density of states, featuring minima in both quantities.

result is surprising, as both minima would naively be associated with the surface Dirac point. The conductance minimum, however, may shift relative to the Dirac point due to the details of the band structure and disorder potential, as suggested by recently published theory⁸ which we find consistent with our data.

Gated Exfoliated Devices

The next project we report is the development of a TI device architecture where both surfaces are separately controlled by gates (Fig. 2(a)). Full control over both surfaces will allow us to study the interplay between quantum oscillations on both surfaces, effects of Coulomb interactions between two TI surfaces, and potentially exciton condensations. Furthermore, recent calculations⁹ suggest that full bulk depletion should be reachable in realistic devices. To avoid doping during the dielectric deposition, as occurs during the process of Atomic Layer Deposition (ALD) of HfO₂ or Al₂O₃⁵, we developed a novel approach to interfacing Bi₂Se₃ with flakes of transferred hexagonal Boron-Nitride (hBN)¹⁰. This is a promising direction, because the transfer process is mechanical, requiring no chemistry at the interface, and hBN could be effective in encapsulating the underlying layer from contamination and reactions later in the fabrication process. Fig. 2(b, c) show examples of such devices, and Figure 2(d) shows field effect measurements taken on a 60 nm thick device, which exhibits significant modulation when $V_{TG} < 0$, with a field effect mobility exceeding 1000 cm²/V/s. The applied back-gate voltage V_{BG} appears to increase the effective top-gate field-effect mobility (Fig. 2(e)), suggesting finite field penetration through the bulk carriers.

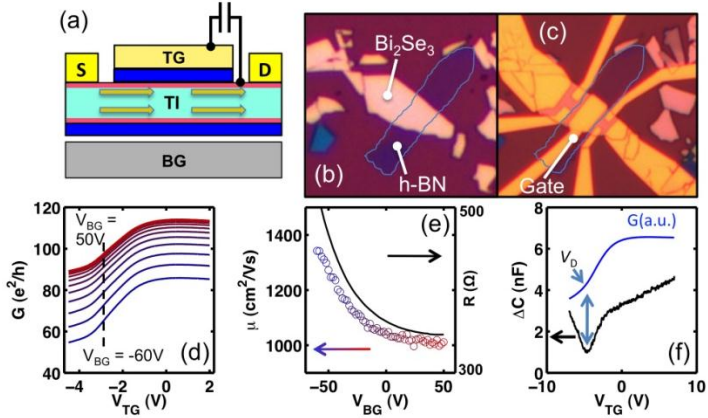


Figure 2: h-BN gated TI devices. (a) Side-view schematic of a double-gated TI device. (b) Transferred h-BN (dark purple) on Bi₂Se₃ (bright pink). The h-BN flake is few nm thick and its outline is highlighted. (c) Same device, with evaporated contacts and gate. (d) G vs. V_{TG} of double-gated Bi₂Se₃ device, taken at different V_{BG} . (e) Left axis: Peak field effect mobility from (d) taken at $V_{TG} = -3$ V vs. V_{BG} . Right axis: R (Ω) vs. V_{BG} . (f) C and G vs. V_{TG} in another top-gated device with h-BN dielectric. Minimum in capacitance coincides with “kink” in resistance.

We are also able to measure capacitance on similar devices: Figure 2(f) shows a C vs. V_{TG} trace (left axis), which exhibits a pronounced minimum at $V_{TG} = -4.5$ V, associated closely with the Dirac point. The conductance trace (right axis) taken on the same device, similar to other h-BN top gated devices (Fig. 2(d)), does not exhibit a conductance minimum – likely due to the large contribution of bulk carriers to in-plane transport.

TI-Graphene Devices

A new research direction we have initiated this year is the study of graphene-TI hybrid devices. One motivation to study such a device relates to the effect of the TI on the graphene channel, which is expected to gain an enhanced spin-orbit interaction due to the proximity to the TI¹¹. Another motivation is to use the TI-Graphene system as a spintronic device, with the TI surface serving as a spin injector or detector contact, having the advantage that the spins are oriented in-plane without requiring an external magnetic field to polarize them. A typical device appears in the inset to Fig. 3(a). It

consists of a graphene flake exfoliated onto a Si/SiO₂ substrate, onto which a Bi₂Se₃ flake is subsequently deposited using the transfer technique described earlier. The differential conductance dI/dV, measured in a 4-probe geometry is plotted vs. the Bi₂Se₃-graphene voltage drop V_{TI}. The dI/dV signal agrees strikingly well with STM measurements of Bi₂Se₃¹², suggesting that electronic transport between the two flakes is dominated by tunneling. This is an exceptionally good tunnel-junction, sustaining voltage biases exceeding 0.5V while keeping the current stable. We can also tune the graphene density by applying a back-gate voltage (Fig. 3(b)). The gate-dependent dI/dV curves exhibit a rich spectrum of excitations, some of which evolve with density (arrows on top and bottom) and some which do not (vertical dashed line, bottom traces). A similar pattern is observed in STM studies on back-gated graphene, in which the non-dispersive and dispersive features are associated with phonons^{13,14} and density-dependent plasmons¹⁴, respectively. The most prominent non-dispersive feature found in our data, at ± 63 meV, agrees well with features measured by STM, associated with the out-of-plane graphene phonon. The phonon provides the necessary momentum for injected electrons to access states at the K and K' points. The role of momentum-conservation in the tunneling process is fundamental, since spin-momentum locking suggests that conserved momentum would be tied to conserved spin and hence to the potential use of Bi₂Se₃ as a source of spin-polarized electrons in graphene.

(iii) Future plans

TI Graphene Continuation

We will address some of the questions raised by our results this year: what is the role of momentum in the tunneling process, and does the tunneling process conserve spin? We will address these questions by studying the effect of magnetic fields on the junction's tunneling conductance and by seeking signatures of spin-precession in a double-junction geometry. Furthermore, we will test potential of the graphene-TI junction as a generic tunnel junction for studying proximity-induced superconductivity in Bi₂Se₃.

TI Tunneling Devices

The use of a thin dielectric deposited on the top of Bi₂Se₃ has another application: When the dielectric is thin enough, it can serve as a tunneling barrier and allow the study of the tunneling spectrum of the TI surface states under diverse conditions. We will experiment with a broad range of potential dielectric barriers, including h-BN, MoS₂, WSe₂, and similar transition metal dichalcogenides, which, having a narrower band-gap than h-BN, are better suited to serve as tunnel-barriers.

(iv) References

1. *Spin Polarization and Transport of Surface States in the Topological Insulators Bi₂Se₃ and Bi₂Te₃ from First Principles*. O. V. Yazyev, J. E. Moore & S. G. Louie. **Physical Review Letters** 105, 266806 (2010).

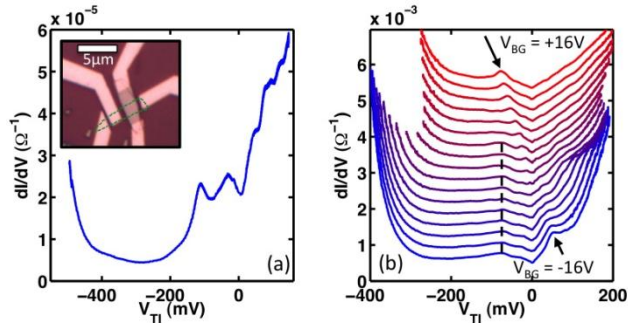


Figure 3: Graphene-TI junctions (a) Differential conductance of junction in inset (“Device 1”) measured in 4-probe. V_{TI} is bias applied from TI side. Inset: Junction device. Graphene (outlined in green) is on the bottom, Bi₂Se₃ on top. (b) Differential conductance of Device 2 vs. applied back-gate voltage. Non-dispersing features at V_{TI} = -63 meV are marked by vertical dashed line. The arrows mark a gate-dispersive feature.

2. *Superconducting Proximity Effect and Majorana Fermions at the Surface of a Topological Insulator.* L. Fu & C. L. Kane. **Physical Review Letters** 100, 096407 (2008).
3. *Exciton Condensation and Charge Fractionalization in a Topological Insulator Film.* B. Seradjeh, J. E. Moore & M. Franz. **Physical Review Letters** 103, 066402 (2009).
4. *Time-Reversal-Invariant Topological Superconductors and Superfluids in Two and Three Dimensions.* X.-L. Qi, T. L. Hughes, S. Raghu & S.-C. Zhang. **Physical Review Letters** 102, 187001 (2009).
5. *Surface state transport and ambipolar electric field effect in Bi_2Se_3 nanodevices.* H. Steinberg, D. Gardner, Y. Lee & P. Jarillo-Herrero. **Nano Letters** 10, 5032-5036 (2010).
6. *Control over topological insulator photocurrents with light polarization.* J. W. McIver, D. Hsieh, H. Steinberg, P. Jarillo-Herrero & N. Gedik. **Nature Nanotechnology** 7, 96-100 (2012).
7. *Electrically tunable surface-to-bulk coherent coupling in topological insulator thin films.* H. Steinberg et al., **Physical Review B** 84 (2011).
8. *Two-dimensional transport and screening in topological insulator surface states.* S. Adam, E. H. Hwang & S. Das Sarma. **Physical Review B** 85 (2012).
9. *Weak localization and antilocalization in topological insulator thin films with coherent bulk-surface coupling.* I. Garate & L. Glazman. **Physical Review B** 86 (2012).
10. *Boron nitride substrates for high-quality graphene electronics.* C. R. Dean et al. **Nature Nanotechnology** 5, 722-726 (2010).
11. *Proximity-induced giant spin-orbit interaction in epitaxial graphene on a topological insulator.* K.-H. Jin & S.-H. Jhi. **Physical Review B** 87, 075442 (2013).
12. *STM Imaging of Impurity Resonances on Bi_2Se_3 .* Z. Alpichshev et al. **Physical Review Letters** 108, 206402 (2012).
13. *Giant phonon-induced conductance in scanning tunnelling spectroscopy of gate-tunable graphene.* Y. Zhang et al. **Nature Physics** 4, 627-630 (2008).
14. *Observation of carrier-density-dependent many-body effects in graphene via tunneling spectroscopy.* V. W. Brar et al. **Phys Rev Lett** 104, 036805 (2010)

(v) Publications acknowledging DOE support

- (1) *Photon helicity dependent currents in an optically driven topological insulator.* J. W. McIver, D. Hsieh, H. Steinberg, P. Jarillo-Herrero & N. Gedik. **Nature Nanotechnology** 7, 96 (2011).
- (2) *Measurement of Intrinsic Dirac Fermion Cooling on the Surface of the Topological Insulator Bi_2Se_3 Using Time-Resolved and Angle-Resolved Photoemission Spectroscopy.* Y. H. Wang, et al. **Physical Review Letters** 109, 127401 (2012).

Program Title: Electron Spectroscopy

Principle Investigator: P.D. Johnson; Co-PIs: C. Homes and P.D. Johnson

**Mailing Address: Condensed Matter Physics and Materials Science Department,
Brookhaven National Laboratory, Upton, NY 11973**

E-mail: pdj@bnl.gov

Program Scope:

The Electron Spectroscopy Group (ESG) examines the role of dimensionality, competing orders, disorder and inhomogeneities in strongly correlated materials through studies of a variety of materials including topological insulators, the high T_c superconductors and two-dimensional graphene. The primary techniques used by the group include high resolution photoemission and optical spectroscopy, both laboratory and facility based. In the latter case, the instruments are based at the *National Synchrotron Light Source* (NSLS). The techniques complement each other in that both provide information on scattering rates and hence the self-energy. In fact the ESG has played a world leadership role by redefining the way that scattering rates are determined in photoemission studies.

The group is also actively involved in developing new instrumentation. Most recently such activities include the development of a new instrument for ultra high-resolution photoemission using time resolved techniques. The latter will be combined with a new facility under construction that will allow both direct laser based photoemission and two photon photoemission capabilities involving the use of both femtosecond and picoseconds lasers. While most of the current experiments are carried out at the NSLS, with some collaborations involving the CFN, the group is also very much involved with the development of plans for the next generation light source, NSLS II. Indeed the group has participated in the development of two beamline proposals for the latter facility.

Recent Progress:

In the area of Topological Insulators we have shown that topological surface states on topological insulators remain fully spin polarized and coherent at room temperature, indicating that they may support dissipationless spin and charge transport at room temperature. This is crucially important for possible wide-spread spintronic applications (ref. [3,22 in the Publication list below]). We have shown that the scattering selection rules on surfaces of topological crystalline insulators (TCI) are more relaxed and that the states are more sensitive to disorder than those on TIs (ref. [1]). We have measured detailed spin-and angle- resolved electronic structure of a newly discovered topological insulator with the superlattice structure, Bi₂-Bi₂Se₃, a material with two different surface terminations and two types of topological surface states (ref. [2,12]). We have further resolved the spin structure of quantum well-like states formed with the surface doping of a topological insulator and explored the role of spin in the scattering mechanism (ref. [10]). We have shown that the topological surface states on TIs can effectively carry supercurrents in a process that it is remarkably robust against disorder (ref. [12]).

In the area of graphene we have shown that graphene-derived electrons in graphite intercalation compounds couple strongly to graphene-derived phonons, making the graphene

sheets responsible for superconductivity in GICs (ref. [24]). We have also studied the mechanism and dynamics of the intercalation process of Cs in graphene on Ir(111) and established some general principles important for any intercalation process (ref. [8]).

Optical conductivity studies have recently demonstrated that organic superconductors follow the same scaling relationship as that previously demonstrated for the high T_c superconductors. (ref.[6]). The temperature dependence of the complex optical properties of the three-dimensional topological insulator Bi₂Te₂Se has been determined for light polarized in the a-b planes at ambient pressure, as well as the effects of pressure at room temperature. This material displays a semiconducting character with a bulk optical gap of E_g similar or equal to 300 meV at 295 K. In addition to the two expected infrared-active vibrations observed in the planes, there is an additional fine structure that is attributed to either the removal of degeneracy or the activation of Raman modes due to disorder.(ref.[11])

Low-temperature scanning tunneling microscopy has been used to study a one-dimensional system that undergoes a charge-density-wave (CDW) instability on a metallic substrate, in particular a self-assembled monatomic chain of Co atoms aligned by the steps on a vicinal Cu(111) surface. The measured CDW instability is assigned to ferromagnetic interactions along the chain.(ref.[7]) A microscopic scaling relation linking the normal and superconducting states of the cuprates in the presence of a pseudogap is derived using angle-resolved photoemission spectroscopy. This scaling relation, complementary to the bulk universal scaling relation embodied by Homes' law, explicitly connects the momentum-dependent amplitude of the *d*-wave superconducting order parameter at $T \sim 0$ to quasiparticle scattering mechanisms operative at $T \gtrsim T_c$.(ref.[27])

Future plans

We will continue to work on TIs and TCIs - in particular we want to explore the interaction of magnetism and superconductivity with the topological states. In this direction, we will study ferromagnetic bulk samples doped with magnetic impurities and search for the signatures of an anomalous quantum Hall state in ARPES and transport. In collaboration with several MBE groups, we will also study artificial superlattices made of TIs and magnetic layers. We will also try to synthesize and study the structures involving TIs and "trivial" materials and TIs and superconductors.

It is intended to initiate photoemission studies of the heavy-fermion systems to complement the recent STM studies carried out at BNL. We have also initiated a program to explore the universality of the viscosity/entropy ration in strongly correlated systems. In particular we are exploring this phenomena in the strongly correlated cuprates as a model system.

We also plan to continue our studies of epitaxial graphene grown on different substrates and to explore the ways of its transfer to the device-ready substrates.

In the area of optical conductivity the complex optical properties of the Fe based superconductors, iridates and osmium materials will be studied in detail.

Publications in the last two years:

1. *Quasiparticle interference on the surface of topological crystalline insulator Pb_{1-x}Sn_xSe*, A. Gyenis, I. K. Drozdov, S. Nadj-Perge, O. B. Jeong, J. Seo, I. Pletikosic, T. Valla, G. D. Gu, and A. Yazdani, submitted to Phys. Rev. B, Rapid Comm.

2. *Termination dependent topological surface states of the natural superlattice phase Bi₄Se₃*, Q.D.Gibson, L.M.Schoop, A.P. Weber, Huiwen Ji, S.Nadj-Perge, I. K. Drozdov, H. Beidenkopf, J. T. Sadowski, A. V. Fedorov, A.Yazdani, T.Valla and R.J. Cava, submitted to Phys. Rev. Lett.
3. *Persistent coherence and spin-polarization of topological surface states on topological insulators*, Z.-H. Pan, E. Vescovo, A. V. Fedorov, G. D. Gu, and T. Valla, Phys. Rev. B **88**, 041101(R) (2013).
4. *Three-dimensional Dirac fermions in quasicrystals as seen via optical conductivity*, T. Timusk, J. P. Carbotte, C. C. Homes, D. N. Basov, and S. G. Sharapov, Phys Rev B.87, 235121 (2013)
5. *Evidence of a full gap in LaFeAsO_{1-x}F_x thin films from infrared spectroscopy*, Xiaoxiang Xi, Y. M. Dai, C. C. Homes, M. Kidszun, S. Haindl, and G. L. Carr, Phys Rev B 87,180509 (2013)
6. *Do organic and other exotic superconductors fail universal scaling relations?*, S.V. Dordevic, D.N. Basov, C.C. Homes, Scientific Reports, 3, 1713 (2013)
7. *Experimental observation of spin-exchange-induced dimerization of an atomic one-dimensional system*, Nader Zaki, Chris A. Marianetti, Danda P. Acharya, Percy Zahl, Peter Sutter, Junichi Okamoto, Peter D. Johnson, Andrew J. Millis, and Richard M. Osgood, Phys Rev B 87,161406 (2013)
8. *How to sweep under the thinnest rug: Caesium intercalation of epitaxial graphene*, M. Petrovic, I. Srut, S. Runte, C. Busse, J. T. Sadowski, P. Lazic, I. Pletikosic, Z.-H. Pan, M. Milun, P. Pervan, N. Atodiresei,R. Brako, D. Sokcevic, T. Valla, T. Michely and M. Kralj, submitted to Nature Communications.
9. *Symmetry Protected Josephson Supercurrents in Three-Dimensional Topological Insulators*, S.J. Cho, B. Dellabetta, A. Yang, J. Schneeloch, Z. J. Xu, T. Valla, G. Gu, M.J. Gilbert, N. Mason, Nature Communications **4**, 1689 (2013),
10. *Spin Configuration and Scattering Rates on the Heavily Electron-Doped Surface of Topological Insulator Bi₂Se₃*, Z.-H. Pan, E. Vescovo, A. V. Fedorov, B. Sinkovic, D. R. Gardner, S. Chu, Y. S. Lee, G. D. Gu and T. Valla, submitted to EPL,
11. *Optical properties of Bi₂Te₂Se at ambient and high pressures*, A. Akrap*, M. Tran, A. Ubaldini, J. Teyssier, E. Giannini, and D. van der Marel, Phys Rev B. 86, 235207 (2012)
12. *Topological Semimetal in a Bi-Bi₂Se₃ Infinitely Adaptive Superlattice Phase*, T. Valla, Huiwen Ji, L. M. Schoop, A. P. Weber, Z.-H. Pan, J. T. Sadowski, E. Vescovo, A. V. Fedorov, A. N. Caruso, Q. D. Gibson, L. Muchler, C. Felser and R. J. Cava, Phys. Rev. B **86**, 241101(R) (2012),
13. *Optical spectroscopy shows that the normal state of URu₂Si₂ is an anomalous Fermi liquid*, U. Nagel, T Uleksin, T Rõõm, R.P.S.M. Lobo, P Lejay, C.C. Homes, J.S. Hall, A.W. Kinross, S.K. Purdy, T. Munsie, T.J. Williams, G.M. Luke, and T. Timusk, Proc. Nat. Acad. 109, 19161 (2012)
14. *Orbital characters and near two-dimensionality of Fermi surfaces in NaFe_{1-x}Co_xAs*, Z.-H. Liu, P. Richard, Y. Li, L.-L. Jia, G.-F. Chen, T.-L. Xia, D.-M. Wang, J.-B. He, H.-B. Yang, Z.-H. Pan, T. Valla, P. D. Johnson, N. Xu, H. Ding, and S.-C. Wang, Appl. Phys. Lett. **101**, 202601 (2012).
15. *Probing the bulk electronic states of Bi₂Se₃ using nuclear magnetic resonance*, Ben-Li Young, Zong-Yo Lai, Zhijun Xu, Alina Yang, G. D. Gu, Z.-H. Pan, T. Valla, G. J. Shu, R. Sankar and F. C. Chou, Phys. Rev. B **86**, 075137 (2012).

16. *Angle-Resolved Photoemission from Cuprates with Static Stripes*, T. Valla, Physica C **481**, 66 (2012).
17. *Effective medium approximation and the complex optical properties of the inhomogeneous superconductor K_{0.8}Fe_{2-y}Se₂* , C. C. Homes, Z. J. Xu, J. S. Wen, and G. D. Gu, Phys Rev B. 86, 144530 (2012)
18. *n(s)-T-c Correlations in Granular Superconductors*, Y. Imry, M. Strongin, and C. C. Homes, Phys Rev Lett.109. 067003 (2012)
19. *Photoemission band mapping with a tunable femtosecond source using nonequilibrium absorption resonances*, M.B. Yilmaz, J.I. Dadap, K.R. Knox, N. Zaki, Z. Hao, P.D. Johnson, and R.M. Osgood, J. Vac. Sci. Tech. A 30, 041403 (2012)
20. *Optical conductivity of superconducting K_{0.8}Fe_{2-y}Se₂ single crystals: Evidence for a Josephson-coupled phase*, C. C. Homes*, Z. J. Xu, J. S. Wen, and G. D. Gu, Phys Rev B.85.180510 (2012)
21. *Phonon Energy Gaps in the Charged Incommensurate Planes of the Spin-Ladder Sr₁₄Cu₂₄O₄₁ Compound by Raman and Infrared Spectroscopy*, V. K. Thorsmølle, C. C. Homes, A. Gozar, G. Blumberg, J. L. M. van Mechelen, A. B. Kuzmenko, S. Vanishri, C. Marin, and H. M. Rønnow, Phys Rev Lett.108. 217401 (2012)
22. *Measurement of an Exceptionally Weak Electron-Phonon Coupling on the Surface of the Topological Insulator Bi₂Se₃ Using Angle-Resolved Photoemission Spectroscopy*, Z.-H. Pan, A. V. Fedorov, D. R. Gardner, S. Chu, Y. S. Lee and T. Valla, Phys. Rev. Lett. **108**, 187001 (2012)
23. *Determination of the optical properties of La_{2-x}Ba_xCuO₄ for several dopings, including the anomalous x=1/8 phase*, C. C. Homes*, M. Hücker, Q. Li, Z. J. Xu, J. S. Wen, G. D. Gu, and J. M. Tranquada, Phys Rev B.85.134510 (2012)
24. *Reply to Comment on “Electronic structure of superconducting KC8 and non-superconducting LiC6 graphite intercalation compounds: Evidence for a graphene-sheet-driven superconducting state”*, Z.-H. Pan, A. V. Fedorov, C. A Howard, M. Ellerby and T. Valla, Phys. Rev. Lett. 108, 149702 (2012).
25. *Photoemission Spectroscopy of Magnetic and Nonmagnetic Impurities on the Surface of the Bi₂Se₃ Topological Insulator*, T. Valla, Z.-H. Pan, D. Gardner, Y. Lee, S. Chu, Phys. Rev. Lett. **108**,117601 (2012).
26. *The ESM beamline at NSLS-II: a Wide Photon-Energy Range, Micro-Focusing Beamline for Photoelectron Spectro-Microscopies*, R. Reininger, S. Hulbert, P. D. Johnson, J. Sadowski, D. Starr, O. Choubard, T. Valla, and E. Vescovo, Review of Scientific Instruments **83**, 023102-023102-8 (2012).
27. *“ Evidence for a Universal Scaling of Length, Time and Energy in the Cuprate High-Temperature Superconductors ”*, J.D. Rameau, Z.-H. Pan, H.-B. Yang, G.D. Gu, and P.D. Johnson, Physical Review B, 84, 180511, (2011).

Program Title: Superconductivity & Magnetism

Principle Investigators: W. -K. Kwok, **Co-PIs:** U. Welp, A. E. Koshelev, V. Vlasko-Vlasov, G. W. Crabtree, Z. L. Xiao

Mailing Address: Materials Science Division, Argonne National Laboratory, 9700 S. Cass Ave., Argonne IL 60439

E-mail: wkwo@anl.gov

Program Scope

This program undertakes experimental and theoretical investigations of novel superconducting and magnetic materials that are important for fundamental physics and applications. It explores new physical phenomena associated with superconductivity and its interplay with magnetism and determines the origins of these phenomena to promote use-inspired innovations. We investigate materials from macroscopic to nanoscale samples and heterostructures using a wide range of sophisticated thermodynamic and dynamic characterization tools. One area of pursuit is devoted to the thermodynamic studies of the new iron-based superconductors, which embody a new opportunity in the search for an *isotropic* high temperature superconductor. Another area is to develop novel strategies for controlling vortex dynamics by creating unique vortex pinning landscapes to tailor the electromagnetic behavior of type II superconductors. In addition, we are also pursuing research into the spectral character of THz radiation from high temperature superconducting crystal micro-mesas, which have the potential for a new compact and portable continuous THz source. We maintain leading programs in experiment and theory, with each deriving strong benefit from close mutual cooperation.

Recent Progress

- Tuning the Superconducting Anisotropy in Iron-based Superconductors: The iron-based superconductors are unique in their multi-band, multi-gap character and versatility for chemical doping while achieving relatively high superconducting transition temperatures. One interesting aspect of these superconductors is their rather low superconducting anisotropy, making them desirable for potential applications in superconducting coils and rotating machinery, where the orientation of the applied magnetic field is critical to performance. $\text{SmFeAsO}_{0.8}\text{F}_{0.15}$ is of great interest because it has the highest transition temperature among all the iron-based superconductors and relatively high critical currents. However, it also has the largest anisotropy, $\Gamma \sim 8$, a detriment for many applications. Fig. 1 shows the temperature dependence of the specific heat of a $\text{SmFeAsO}_{0.8}\text{F}_{0.15}$ crystal before and after irradiation with 1.4GeV Pb-ions to a dose of $1.9 \times 10^{11} \text{ ions/cm}^2$. Our results demonstrate that the thermodynamic superconducting anisotropy can be halved by particle irradiation. We developed an impurity scattering theory rooted in anisotropic electron scattering that predicts that the superconducting anisotropy can be tailored via correlated defects in semi-metallic, fully gapped type II superconductors.

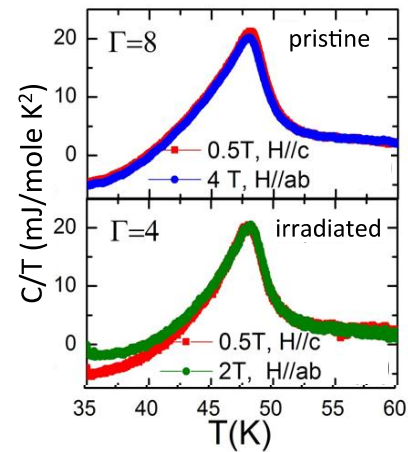


Figure 1 Temperature dependent specific heat at fixed fields for $H \parallel c$ and $H \parallel ab$ to determine the superconducting anisotropy Γ . The ratio of the two orthogonal fields for which the C/T curves coincide is the anisotropy Γ [1].

- Enhancing critical current with the vortex ice state through jamming: The motion of vortices is the main source of dissipation in superconductors. They can be pinned or trapped by defects such as nano-holes created by nano-lithography, hence mitigating their motion and resulting in higher current carrying capacity. We demonstrated the creation of a novel ‘vortex ice’ state to jam the flow of vortices [2].

In conventional water/ice, the arrangement of oxygen and hydrogen atoms follows the so-called ‘two atoms in, two atoms out’ ice rule: each oxygen atom has four neighboring hydrogen atoms with two forming the H_2O molecule and two hydrogen atoms of neighboring water molecules. Artificial ice systems that have properties similar to atomic spin ices have been gaining tremendous interest in recent years in areas ranging from solid-state systems to magnetism and soft matter. Using hole-pairs arranged in a square lattice patterned into a superconducting MoGe thin film, we obtained the ground state of an artificial square vortex ice which follows the ‘two vortices in, two vortices out’ rule at each vertex, where the state of each hole-pair site is defined as ‘in’ if the vortex sits close to the vertex and ‘out’ otherwise (Fig. 2). Magnetotransport measurements reveal that such a vortex-ice configuration can enhance the critical current even higher than in zero field due to vortex jamming as illustrated by the Ginzburg-Landau (GL) simulations.

- Controlling vortex dynamics in superconducting / ferromagnetic hybrid structures: Magnetic pinning of vortices provides a new platform to augment conventional vortex core pinning. We studied the effect of soft ferromagnetic patterns on vortex dynamics in superconducting niobium bridges using thin Py stripes oriented parallel (\parallel) and perpendicular (\wedge) to the current direction (Fig. 3). From IV measurements, we found that the Py stripes act as a strong barrier (\parallel stripes) or an easy channel (\wedge stripes) for vortex flow. Furthermore, for short Py stripes at $\sim 45^\circ$ to the bridge, forming arrays of funnel

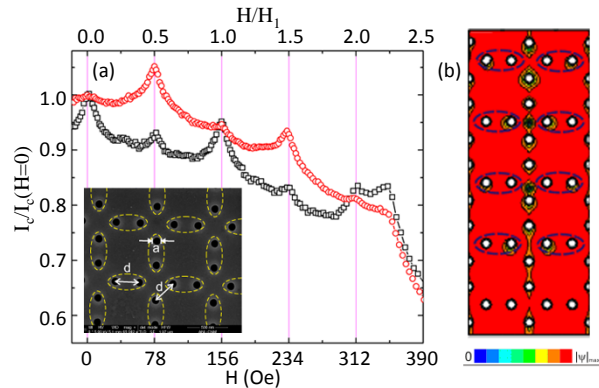


Figure 2 (a) Critical current vs. magnetic field at different temperatures. (Inset) SEM image of the sample. Hole diameter $a = 102$ nm and inter-hole spacing $d = 300$ nm. (b) GL simulation of vortex jamming in the central column area by vortices arranged in square ice configuration, highlighted by the dashed blue ellipses [2].

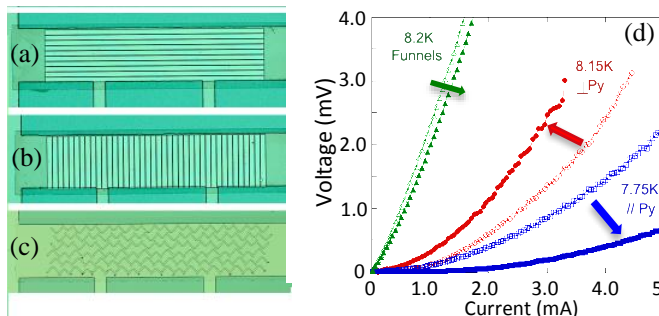


Figure 3 Top view of $100 \mu\text{m}$ wide Nb bridges, with deposited $9 \mu\text{m}$ wide Py stripe structures (a) parallel and (b) perpendicular to the bridge with a thin SiO_2 spacer between the Nb and Py. (c) $2 \times 10 \mu\text{m}$ Py stripes arranged in the shape of ‘funnels’. (d) Comparison of the VI characteristics induced by vortex dynamics. (open symbols = reference Nb bridge)

structures, we detected enhanced vortex motion at low temperature and retardation at high temperature compared to a reference Nb film. The effect can be explained by the jamming of vortices, similar to that we reported in patterned YBCO crystals [3].

- Emission of powerful monochromatic THz-radiation from BSCCO resonators: The Josephson effect occurring intrinsically between the CuO₂-bilayers in Bi₂Sr₂CaCu₂O_{8+δ} (BSCCO) enables the fabrication of compact sources of coherent cw THz radiation [4]. When the Josephson frequency matches an electromagnetic cavity resonance inside the sample high-frequency electric fields are strongly enhanced resulting in strong emission (top inset, Fig. 4). Excessive self-heating and constraints in sample fabrication limit the power from current single resonators to ~50 μW. Using simulations [5] of the electromagnetic fields in arrays of parallel rectangular BSCCO resonators patterned onto a common base crystal, we demonstrated that strong coupling between the resonators arises when their spacing equals their width (lower inset, Fig. 4). In an array of 60-μm wide resonators we find that the emission power increases approximately as the square of resonator number [6], the hallmark of synchronized emission into an unmatched load, reaching 0.6 mW at a frequency of 0.5 THz for three resonators (Fig. 4). This power is large enough for novel applications in THz spectroscopy and imaging.

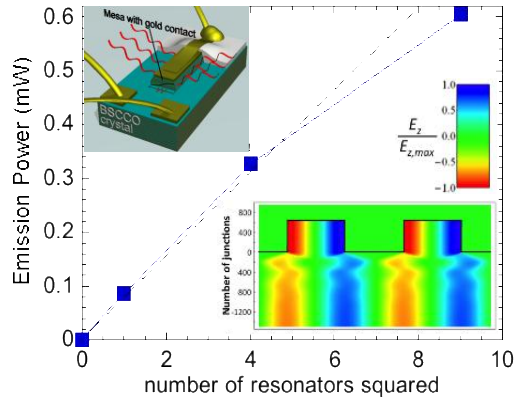


Figure 4 Total emission power at 0.5 THz as function of number of resonators squared. Upper inset shows a schematic of emission (red waves) from a single resonator. Lower inset shows simulations of the c-axis electric field in a cross-section of two resonators.

Future Plans

- Phase diagram and superconducting mechanism of iron-pnictide superconductors: We propose to measure the angular dependent specific heat, thermal conductivity, and normal state resistivity to probe the quasiparticle density of states and the scattering rate in particle irradiated samples. The experimental results will be analyzed in the context of theoretical work to understand the density of states, the symmetry of the order parameter and the effect of scattering centers that mix targeted bands via interband scattering and the appearance of Anderson-localized electronic states.
- Vortex dynamics in nano-structured pinscapes: We recently explored a novel conformal mapped hole array as an effective pinscape for interstitial vortices and achieved a large enhancement of the critical current at high magnetic fields [7]. We plan to extend our studies to a new type of composite pinning array by placing holes at the vertices of an Archimedean tiling composed of square, triangular and/or hexagonal plaquettes. We expect novel phenomena from the competition of the different plaquette types.
- Direct imaging of vortex dynamics in hybrid SC/FM structures: We will image vortices in Nb/striped-Py bridges with magnetic force microscopy to record vortex redistribution due to current pulses to elucidate the effect of the Py stripes on the critical current.
- THz-emission – synchronization of large-scale intrinsic Josephson junctions: The non-linear collective states that arise from the interplay between the synchronization of large arrays of Josephson junctions and non-uniform temperature distributions [8] will be explored experimentally and in large-scale simulations. Their relation to high-power THz emission will be investigated to enable the synchronization of larger resonator arrays.

References

- [1] L. Fang, Y. Jia, V. Mishra, C. Chaparro, V. Vlasko-Vlasov, A. E. Koshelev, U. Welp, G. W. Crabtree, S. Zhu, S. Katrych N. D. Zhigadlo, J. Karpinski, W. K. Kwok, Huge Critical Current Density and Tailored Superconducting Anisotropy in $\text{SmFeAsO}_{0.8}\text{F}_{0.15}$ by Low Density Columnar-Defect Incorporation. *Nature Commun.* (pending).
- [2] M. L. Latimer, G. R. Berdiyorov, Z. L. Xiao, F. M. Peeters, W. K. Kwok, Realization of Artificial Ice Systems for Magnetic Vortices in a Superconducting MoGe Thin Film with Patterned Nanostructures. *Phys. Rev. Lett.* **111**, 067001 (2013).
- [3] V. K. Vlasko-Vlasov, T. M. Benseman, U. Welp, W. K. Kwok, Jamming of superconducting vortices in a funnel structure. *Supercond. Sci. Technol.* **26**, 075023 (2013).
- [4] U. Welp, K. Kadowaki, R. Kleiner, Superconducting emitters of THz radiation. *Nature Photonics* **7** (Aug. 29, 2013, in press).
- [5] S.- Z. Lin, A. E. Koshelev, Synchronization of Josephson oscillations in a mesa array of $\text{Bi}_2\text{Sr}_2\text{CaCu}_2\text{O}_{8+\square}$ through the Josephson plasma waves in the base crystal. *Physica C* **491**, 24 (2013).
- [6] T. M. Benseman, K. E. Gray, A. E. Koshelev, W. K. Kwok, U. Welp, H. Minami, K. Kadowaki, T. Yamamoto, Powerful terahertz emission from $\text{Bi}_2\text{Sr}_2\text{CaCu}_2\text{O}_{8+\square}$ mesa arrays. *Appl. Phys. Lett.* **103**, 022602 (2013).
- [7] Y. L. Wang, M. L. Latimer, Z.L. Xiao, R. Divan, L. E. Ocola, G. W. Crabtree, W. K. Kwok, Enhancing the critical current of a superconducting film in a wide range of magnetic fields with a conformal array of nanoscale holes. *Phys. Rev. B* **87**, 220501 (2013).
- [8] T. M. Benseman, K. E. Gray, A. E. Koshelev, W. K. Kwok, U. Welp, V. K. Vlasko-Vlasov, K. Kadowaki, H. Minami, C. Watanabe, Direct imaging of hot spots in $\text{Bi}_2\text{Sr}_2\text{CaCu}_2\text{O}_{8+\square}$ mesa terahertz sources. *Journ. Appl. Phys.* **113**, 133902 (2013).

Other Select Publications out of 27 supported by BES:

- [9] L. Fang, Y. Jia, . J. Miller, M. L. Latimer, Z. L. Xiao, U. Welp, G. W. Crabtree, W. K. Kwok, Catalyst-Free Growth of Millimeter-Long Topological Insulator Bi_2Se_3 Nanoribbons and the Observation of the pi-Berry Phase. *Nano Letters* **12**, 6164 (2012).
- [10] G. R. Berdiyorov, M. V. Milosevic, M. L. Latimer, Z. L. Xiao, W. K. Kwok, F. M. Peeters, Large Magnetoresistance Oscillations in Mesoscopic Superconductors due to Current-Excited Moving Vortices. *Phys. Rev. Lett.* **109**, 057004 (2012).
- [11] C. Chaparro, L. Fang, H. Claus, A. Rydh, G. W. Crabtree, V. Stanev, W. K. Kwok, U. Welp, Doping dependence of the specific heat of single-crystal $\text{BaFe}_2(\text{As}_{1-x}\text{P}_x)_2$. *Phys. Rev. B* **85**, 184525 (2012).
- [12] V. K. Vlasko-Vlasov, A. Buzdin, A. Melnikov, U. Welp, D. Rosenmann, L. Uspenskaya, V. Fratello, W. K. KwokDomain structure and magnetic pinning in ferromagnetic/superconducting hybrids. *Phys. Rev. B* **85**, 064505 (2012).
- [13] T. M. Benseman, A. E. Koshelev, W. K. Kwok, U. Welp, K. Kadowaki, J. R. Cooper, G. Balakrishnan, The ac Josephson relation and inhomogeneous temperature distributions in large $\text{Bi}_2\text{Sr}_2\text{CaCu}_2\text{O}_{8+\square}$ mesas for THz emission. *Supercond. Sci. Technol.* **26**, 085016 (2013).

Spontaneous and Field-Induced Symmetry Breaking in Low Dimensional Nanostructures

PI: Chun Ning (Jeanie) Lau

co-PI: Marc Bockrath

Department of Physics and Astronomy, University of California, Riverside, CA 92521

Program Scope

Electron-electron interactions can strongly modify the qualitative properties of low-dimensional materials. For example, one-dimensional (1D) systems exhibit Luttinger liquid behavior instead of Fermi liquid behavior, while two-dimensional (2D) systems exhibit the fractional quantum Hall effect. The goal of this program is to investigate and understand strongly correlated electron behavior using carbon nanotubes and graphene, which has emerged as archetypal 1D and 2D nanostructures. These systems will be studied via low temperature transport experiments and nanoelectromechanical measurements. The research program consists of 3 key projects: (1). symmetry-broken phases and quantum phase transitions in ultra-clean bilayer graphene (BLG); (2). symmetry-breaking, phase diagrams and stacking-order dependent transport of trilayer graphene (TLG); and (3). momentum-conserved tunneling between 2D graphene and 1D carbon nanotubes. Taken together, these proposed experiments will provide an in-depth investigation of how electron-electron interactions affect the properties of these exciting materials.

The first 2 projects are motivated by the instability of few-layer graphene to the formation of a correlated electron ground state. A variety of states with different properties have been theoretically proposed[1-11], such as a gapped anomalous Hall state[2, 3, 12], a layer antiferromagnetic state[3-5, 10, 11, 13, 14] and a current loop state[15] that break time-reversal symmetry and gapless nematic states which alter the Dirac point structure and reduce rotational symmetry[1-11, 13]; however, the exact nature of the ground state is under intense experimental and theoretical debate[12, 14, 16, 17]. We plan to investigate and establish the nature of the ground state in BLG and TLG, using dual-gated suspended devices with mobility as high as $300,000 \text{ cm}^2/\text{Vs}$. The devices' electrical properties will be measured as functions of electric field, perpendicular and parallel magnetic fields, charge density, disorder and temperature. Furthermore, since the various correlated states are in principle energetically comparable, we plan to explore possible quantum phase transitions among the phases and systematically map the phase diagram. A related direction is to search for fractional quantum Hall effect and Wigner crystal states in these atomic membranes. Finally, while transport experiments can yield much information about the properties of the electron systems, some information, such as the presence of spontaneous layer polarization is difficult to obtain. We propose to measure the layer polarization directly in BLG and TLG using the graphene layers as nanomechanical elements. Utilizing both top and bottom gates, we plan measure the surface potential of the membranes via a technique akin to Kelvin probe microscopy, thus realizing a which-layer probe.

For TLG, the presence of an extra layer affords additional symmetry and an intriguing parameter – stacking order[18][15][16]. We have recently demonstrated that ABA-stacked TLG remains metallic at the Dirac point, whereas ABC-stacked TLG develops a spontaneous gap due to interactions[19]. We plan to explore the different ground states and phase diagrams in TLG with both stacking orders and transport across stacking domains. Comparison of the results with those found in BLG will provide us with fundamental insight into correlated electron phenomena in low dimensions.

Recent Progress

Since submission of the proposal, we have made significant progress in our studies of ultra-clean low dimensional nanostructures, focusing on ultra-clean graphene devices that are either suspended or supported on hexagonal BN substrates, as outlined below.

Transport Spectroscopy of a Spontaneous Gapped State in Ultra-Clean Bilayer Graphene

Using source-drain bias as a spectroscopic tool, we resolve a gap of ~ 2 meV in ultraclean double-gated BLG at the charge neutrality point. The gap can be closed by a perpendicular electric field of strength ~ 15 mV/nm, but it increases monotonically with magnetic field, with an apparent particle-hole asymmetry above the gap. We are able to provide the first spectroscopic mapping of the ground states in BLG in the presence of both electric and magnetic fields. This work was published by *Nature Nanotechnol.*[14].

Moreover, by systematically investigating a large number of BLG devices, we observe a bimodal distribution of CNP minimum conductivities σ_{min} . Although $\sigma_{min} \sim 2-3 e^2/h$ for most BLG devices, it is ~ 0 in devices with both high mobility and low extrinsic doping. The insulating state in the latter samples appears below a transition temperature $T_c \sim 5$ K, and develops an energy gap of ~ 3 meV. Transitions between these different states can be tuned by adjusting disorder or carrier density. This work was published by *Proc. Natl. Acad. Sci.*[20].

Broken Symmetry Quantum Hall States in Dual-Gated ABA Trilayer Graphene

In the quantum Hall (QH) regime, we able to completely lift the 12-fold degeneracy of the lowest Landau levels (LL). Under a perpendicular electric field E_\perp , we observe degeneracy breaking and transitions between QH plateaus. This work was recently published by *Nano Letters*[21].

Spontaneous Gapped State in ABC-Stacked Trilayer Graphene

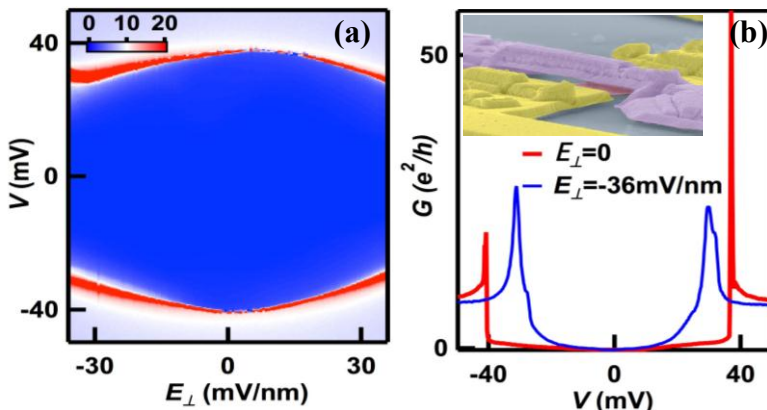


Fig. 1. (a) Conductance (color) in units of e^2/h vs. source-drain bias (vertical axis) and applied electric field E_\perp (horizontal axis). The dark blue region represents an insulating gap, which is being closed symmetrically by E_\perp . (b). $G(V)$ line traces at $E_\perp=0$ and -36 mV/nm, respectively. Inset: an SEM image of a graphene sheet (red) suspended between electrodes (yellow) below a top gate (purple)

ABC-stacked TLG, which is found in $\sim 15\%$ of all TLG sheets, has an unusual *cubic* dispersion relation, with the energy $E \sim k^3$, where k is the wavevector. This produces a very high density of states at the charge neutrality point, making it highly unstable to electronic interactions. Such inclination towards interaction-induced phases with broken symmetries is similar to, but even more so than that in bilayer graphene. However, observation of such symmetry-broken phase(s) entails obtaining ultra-clean dual-gated ABC-stacked TLG, which is challenging and has not been hitherto achieved.

Recently we have been able to fabricate dual-gated suspended ABC-stacked TLG devices

(Fig. 1b inset) with mobility up to 150,000 cm²/Vs. We found a strongly insulating state at the charge neutrality point, with a gap \sim 30–40 meV. This gap is reduced by an applied out-of-plane electric field E_{\perp} of either polarity (Fig. 1) (but not yet completely closed by the largest E_{\perp} that we are able to apply). Such a large interaction-induced gap is exceedingly interesting for condensed matter physics, and may also be useful for THz technologies.

Future Plans

Apart from the experiments outlined in the first section, our immediate plans for the upcoming year are:

Spontaneous Symmetry Breaking in Charge Neutral Bilayer Graphene

The exact nature of the symmetry-broken state in charge neutral BLG has been under intense debate for the past several years, though a consensus is emerging (based partly on our experimental data) that such a state is gapped and insulating. On the other hand, the most likely candidate, a layer antiferromagnetic state, remains to be experimentally verified. Another intriguing possibility is to stabilize BLG, via applied strain or other parameters, into different symmetry-broken states, such as the anomalous Hall or spin Hall states. Our plan is to systematically investigate the various phases in BLG, and map the phase diagram as a function of strain, temperature, disorder, electric field, charge density and magnetic field, and determine whether the transitions are first or second order, or simply represent cross-over behavior.

Symmetry-Broken Quantum Hall States

In the quantum hall regime, the competing spin, valley and orbital symmetries in BLG states allow various ordering possibilities and transitions via externally controlled parameters. This underlies exciting new quantum Hall (QH) and many body physics afforded by BLG. Yet, the nature of the symmetry-broken states is poorly understood and often under intense theoretical debate. Also, many of the QH states are expected to be layer polarized, yet studies of their evolution under electric field have never been performed, partly due to the difficulty of fabricating dual-gated devices. We plan to investigate the integer QH states in BLG, explore their energy gaps and inter-Landau level transitions at different magnetic and electric fields. Finally, improved mobility and device geometry should allow us to observe fractional quantum Hall states and examine their evolution with temperature and magnetic and electric fields.

Spontaneous Gapped State in ABC-Stacked Trilayer Graphene

To ascertain the nature of the spontaneous gapped state observed in ABC-stacked TLG (Fig. 1), we will perform further measurements at different temperatures, bias, sample mobility, in-plane and out-of-plane magnetic fields, and working with Dr. Paco Guinea (a collaborator on the program) to ascertain the exact nature of this gap.

Transport across stacking ABA-ABC stacking domains

Using Raman spectroscopy mapping, we are able to map and identify ABA-ABC stacking domains in individual TLG sheets. We would be able to fabricate devices to study transport across the stacking domain soon.

References

- [1] H. Min, G. Borghi, M. Polini, and A. H. MacDonald, Pseudospin magnetism in graphene, *Phys. Rev. B* **77** (2008).

- [2] R. Nandkishore, and L. Levitov, Quantum anomalous Hall state in bilayer graphene, *Phys. Rev. B* **82** (2010).
- [3] F. Zhang, J. Jung, G. A. Fiete, Q. A. Niu, and A. H. MacDonald, Spontaneous quantum Hall states in chirally stacked few-layer graphene systems, *Phys. Rev. Lett.* **106** (2011).
- [4] J. Jung, F. Zhang, and A. H. MacDonald, Lattice theory of pseudospin ferromagnetism in bilayer graphene: Competing interaction-induced quantum Hall states, *Phys. Rev. B* **83** (2011).
- [5] F. Zhang, H. Min, M. Polini, and A. H. MacDonald, Spontaneous inversion symmetry breaking in graphene bilayers, *Phys. Rev. B* **81** (2010).
- [6] Y. Lemonik, I. L. Aleiner, C. Toke, and V. I. Fal'ko, Spontaneous symmetry breaking and Lifshitz transition in bilayer graphene, *Phys. Rev. B* **82** (2010).
- [7] O. Vafek, and K. Yang, Many-body instability of Coulomb interacting bilayer graphene: Renormalization group approach, *Phys. Rev. B* **81** (2010).
- [8] E. V. Castro, N. M. R. Peres, T. Stauber, and N. A. P. Silva, Low-density ferromagnetism in biased bilayer graphene, *Phys. Rev. Lett.* **100** (2008).
- [9] I. Martin, Y. M. Blanter, and A. F. Morpurgo, Topological confinement in bilayer graphene, *Phys. Rev. Lett.* **100** (2008).
- [10] M. Kharitonov, Canted antiferromagnetic phase of the v=0 quantum Hall state in bilayer graphene, *Phys. Rev. Lett.* **109** (2012).
- [11] F. Zhang, and A. H. MacDonald, Distinguishing Spontaneous Quantum Hall States in Graphene Bilayers, *Phys. Rev. Lett.* **108** (2012).
- [12] R. T. Weitz, M. T. Allen, B. E. Feldman, J. Martin, and A. Yacoby, Broken-symmetry states in doubly gated suspended bilayer graphene, *Science* **330** (2010).
- [13] M. Kharitonov, Antiferromagnetic state in bilayer graphene, *Phys. Rev. B* **86** (2012).
- [14] J. Velasco, L. Jing, W. Bao, Y. Lee, P. Kratz, V. Aji, M. Bockrath, C. N. Lau, C. Varma, R. Stillwell, D. Smirnov, F. Zhang, J. Jung, and A. H. MacDonald, Transport spectroscopy of symmetry-broken insulating states in bilayer graphene, *Nature Nanotechnol.* **7** (2012).
- [15] L. Zhu, V. Aji, and C. M. Varma, Ordered Loop Current States in Bilayer Graphene, *Phys. Rev. B* **87** (2013).
- [16] F. Freitag, J. Trbovic, M. Weiss, and C. Schonenberger, Spontaneously gapped ground state in suspended bilayer graphene, *Phys. Rev. Lett.* **108** (2012).
- [17] A. S. Mayorov, D. C. Elias, M. Mucha-Kruczynski, R. V. Gorbachev, T. Tudorovskiy, A. Zhukov, S. V. Morozov, M. I. Katsnelson, V. I. Fal'ko, A. K. Geim, and K. S. Novoselov, Interaction-driven spectrum reconstruction in bilayer graphene, *Science* **333** (2011).
- [18] K. F. Mak, J. Shan, and T. F. Heinz, Electronic structure of few-layer graphene: experimental demonstration of strong dependence on stacking sequence, *Phys. Rev. Lett.* **104** (2010).
- [19] W. Bao, L. Jing, Y. Lee, J. V. Jr., P. Kratz, D. Tran, B. Standley, M. Aykol, S. B. Cronin, D. Smirnov, M. Koshino, E. McCann, M. Bockrath, and C. N. Lau, Stacking-Dependent Band Gap and Quantum Transport in Trilayer Graphene, *Nat. Phys.* **7** (2011).
- [20] W. Bao, J. Velasco, Jr., F. Zhang, L. Jing, B. Standley, D. Smirnov, M. Bockrath, A. H. MacDonald, and C. N. Lau, Evidence for a spontaneous gapped state in ultraclean bilayer graphene, *Proc. Nat. Acad. Sci.* **109** (2012).
- [21] Y. Lee, J. V. Jr., D. Tran, F. Zhang, W. Bao, L. Jing, K. Myhro, D. Smirnov, and C. N. Lau, Broken symmetry quantum Hall states in dual gated ABA trilayer graphene *Nano Lett.* **13** (2013).

Program Title: Experimental Study of Severely Underdoped Ultrathin Cuprate Films

Principle Investigator: Thomas R. Lemberger

Mailing Address: Dept. of Physics, The Ohio State University, Columbus, OH 43210

E-mail: TRL@physics.osu.edu

Program Scope

The main goal of this research is to understand the nature of superconductivity in ultrathin, severely underdoped cuprate films, near the super-to-insulator quantum phase transition. In this regime, quantum and thermal phase fluctuations combine to produce a unique environment. This research complements and advances studies of severely underdoped thick films and single crystals which probe 3-D fluctuations.

We have already made and published superfluid density measurements on 3-D and 2-D underdoped YBCO films. We have recently made analogous measurements on several-unit-cell thick underdoped Bi-2212 films that are in quantitative agreement with YBCO in terms of 2-D scaling of T_c with superfluid density at T = 0.[1,2] There is an important outstanding issue: these Bi-2212 films do not show 2-D thermal phase fluctuations near T_c, even though they exhibit 2-D quantum fluctuations. For context, two-unit-cell-thick YBCO films show 2-D quantum and thermal fluctuations. We are working to grow similarly thin Bi-2212 films (i.e., one-unit-cell, or equivalently, two-CuO₂-bilayers thick) that remain superconducting. On the other hand, clean underdoped YBCO crystals and “thick” films show 3-D quantum fluctuations but not 3-D thermal fluctuations.

The strategy is to continue a broader suite of transport measurements both below and above T_c to look for evidence of fluctuations in other quantities.

Recent Progress

Our most interesting advance over the past 18 months is development of a two-coil technique for determining the superconducting coherence length, ξ . This effort involved development of the experimental apparatus, underlying theory, computer programs for taking and analyzing data, and measurements on test cases, i.e., two well-known conventional superconductors (pure Nb and amorphous MoGe alloy). An experimental paper describing the latter has been submitted to PRB.[0] Two supporting theoretical papers have been published in PRB [4,5], and a third paper is in preparation.[-1] While the superfluid density is determined by measurements in the low-magnetic-field regime where the Meissner screening supercurrent is linearly proportional to the applied 50 kHz magnetic field, the coherence length is determined by data in the high-field regime where the applied field generates lots of vortices and antivortices. The really nice thing is that “high-field” means tens of gauss rather than the tens of teslas typically needed to determine $B_{c2}(T) \equiv \Phi_0 / 2\pi\xi^2$ from resistance measurements. The key physics is that vortices and antivortices originate as bound vortex-antivortex pairs which break apart when the superfluid momentum associated with the Meissner supercurrent is close to \hbar/ξ .

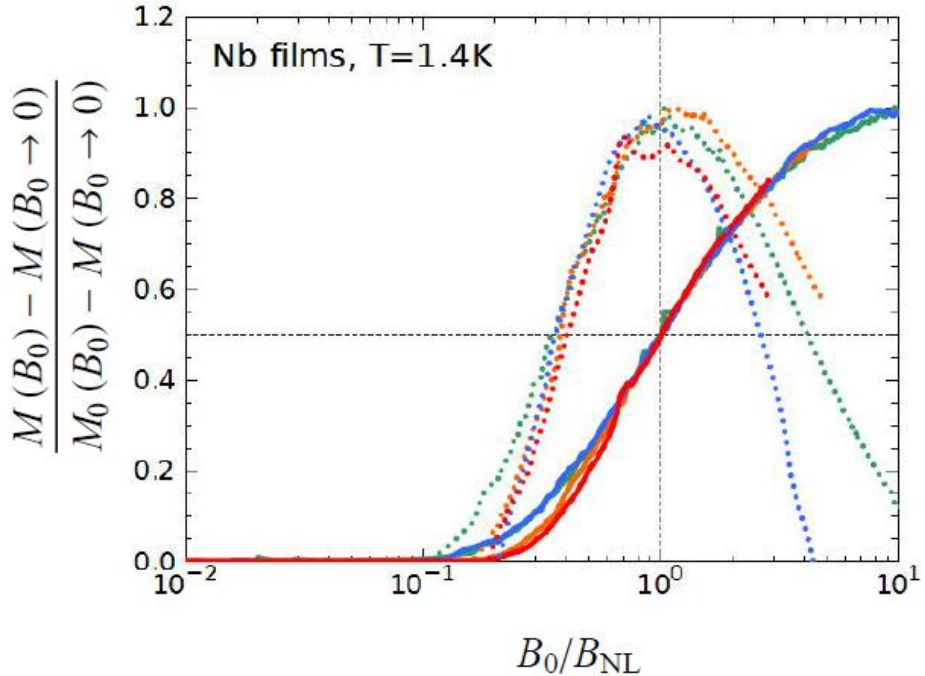


Fig. 1. Real (solid) and imaginary (dotted) parts of the mutual inductance of drive and pick-up coils on opposite sides of thin Nb films, as functions of the normalized applied magnetic field at the center of the film.

Figure 1 shows the increase in coupling between drive and pick-up coils when the amplitude of the applied ac field exceeds a certain threshold. “ B_{NL} ” is defined from the midway point between the coupling at low field and the normal-state coupling. We determine ξ from B_{NL} using the value of the magnetic penetration depth taken from measurements at low applied field.

Figure 2 shows the expected and measured dependence of B_{NL} on R/Λ , where R is the radius at which the applied field changes sign and Λ is the two-dimensional magnetic penetration depth. Squares are data on Nb films; circles on a-MoGe. We assume that ξ for Nb is nearly the same for all films, independent of thickness. We assume that ξ for a-MoGe is inversely proportional to T_c . The data are in good agreement with the solid theoretical curve. Quantitative values of ξ for Nb and a-MoGe are in factor-of-two agreement with values obtained from our measurements of $B_{c2}(T)$.[0]

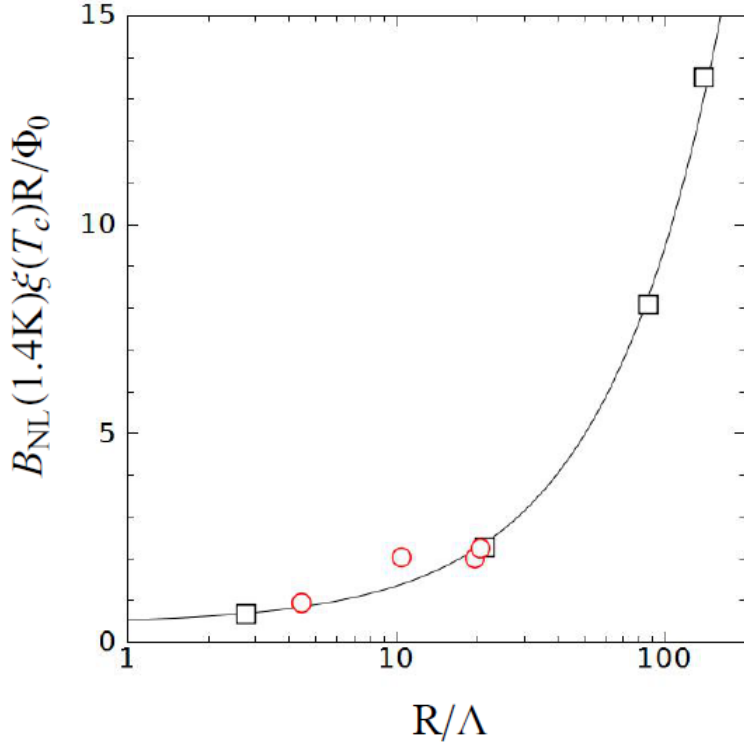


Fig. 2. “Non-linear” magnetic field, B_{NL} , defined as shown in Fig. 1, vs. R/Λ .

Plans

We are measuring penetration depths and coherence lengths of a variety of thin and thick cuprate films, and other materials, to assess the general applicability of the technique. We are making resistivity and Hall measurements as well to assess the extent of fluctuations above T_c .

References/Publications acknowledging DoE support

- 1. “Model of Low-frequency Vortex Dynamics in a Two-dimensional Superconductor Exposed to a Non-uniform Magnetic Field”, T. R. Lemberger et al., in preparation for Phys. Rev. B.
- 0. “Measuring the superconducting coherence length in thin films using a two-coil experiment”, J. Draskovic, T. R. Lemberger, Brian Peters, Fengyuan Yang, Jaseung Ku, A. Bezryadin, and Song Wang, subm. to Phys. Rev. B, Aug. 2013.
- 1. “Comparison of 2-D Quantum and Thermal Critical Fluctuations of Underdoped $\text{Bi}_2\text{Sr}_2\text{Ca}\text{Cu}_2\text{O}_{8+\delta}$ with Ultrathin $\text{YBa}_2\text{Cu}_3\text{O}_{7-\delta}$ ”, M. J. Hinton, J. Yong, Stanley Steers and T. R. Lemberger, J. Supercond. Nov. Magn. **26**, 2617–2620 (2013).

2. “Evidence of two-dimensional quantum critical behavior in the superfluid density of extremely underdoped Bi₂Sr₂CaCu₂O_{8+x}”, J. Yong, M. J. Hinton, A. McCray, M. Randeria, M. Naamneh, A. Kanigel, and T. R. Lemberger, Phys. Rev. B **85**, 180507(R) (2012).
3. “Robustness of the Berezinskii-Kosterlitz-Thouless transition in ultrathin NbN films near the superconductor-insulator transition”, J. Yong, Jie Yong, T. R. Lemberger, L. Benfatto, K. Ilin and M. Siegel, Phys. Rev. B **87**, 184505 (2013).
4. “Upper limit of metastability of the vortex-free state of a two-dimensional superconductor in a nonuniform magnetic field”, T. R. Lemberger and Adam Ahmed, Phys. Rev. B **87**, 214505 (2013).
5. “Theory of the lower critical magnetic field for a two-dimensional superconducting film in a nonuniform field”, T. R. Lemberger and J. Draskovic, Phys. Rev. B **87**, 064503 (2013).

Program Title: Probing High Temperature Superconductors with Magnetometry in Ultrahigh Magnetic Fields

Principle Investigator: Lu Li

Mailing Address: University of Michigan, 450 Church St, Ann Arbor, MI 48109

E-mail: luli@umich.edu

Program Scope

The goal of the program is to investigate the high-field magnetic properties of high temperature superconductors, materials that conduct electricity without loss. High temperature superconductivity discovered in Fe-based [1, 2] and Cu-based materials [3] has been a treasure trove for condensed matter physicists. The relatively high transition temperature T_c , critical field, and critical currents indicate many possible applications in energy transfer and conservation. More importantly, the investigation of the origin of the superconductivity leads to various breakthroughs in fundamental physics. Currently, many key issues are under debate: for cuprates, whether they are a normal Fermi liquid with a hidden ordering state or an exotic phase coming out of a doped Mott Insulator; for Fe-based materials, what catches the essential physics in the parent compound - the “bad metal” seen in early discovered materials or the “Mott Insulator”? Direct answers to these questions will essentially determine the right approach to understanding the superconducting mechanism, i.e. whether it is a weak-coupling phenomenon or a strongly correlated effect. Moreover, in both cuprates and Fe-based materials, superconductivity arises by doping an antiferromagnetic state. Precise measurement of the magnetization M in ultrahigh magnetic fields will shed light on the magnetic ground state, the superconducting property, and the interaction between them.

To achieve the goal, torque magnetometry will be adapted to ultrahigh magnetic field up to 100 T in the pulsed magnetic field facilities in Los Alamos National Laboratory (LANL). Major challenges for research in the pulsed field facilities are 1) the vibrational and electrical noise, 2) difficulty stabilizing temperatures in elevated temperature ranges, and 3) short magnetic field pulses as narrow as milli-seconds. These conditions exclude some common approaches based on resonating oscillators or piezo resistors. Even the method using commercial capacitance bridge to track the cantilever deflection is challenging, since the measurement frequency of the commercial bridge is barely fast enough to catch the torque change in the milli-second pulse width. We propose several technical innovations to advance the high frequency capacitance bridge technique to precisely measure the magnetic torque in pulsed magnetic fields. The major innovations include, 1) home-built capacitance bridge working the best from 10 kHz to 10 MHz measurement frequencies, and 2) cold amplifier near the sample to eliminate the large shunt capacitance and to greatly enhance the bridge balancing signal.

Recent Progress

(1). Resolving magnetic torque of high temperature superconductors in the 60 T generator-based pulsed magnet

In our recent experiment in LANL, we succeeded in measuring the magnetic torque of underdoped ortho-II YBCO in a 1 second wide 60 T generator-based pulsed magnet.

We first measured the magnetic torque of a current-generated magnetic moment. As shown in the insert of the left panel of Fig. 1, we attached a current loop on the top plane of the insulating cantilever. A small DC current is passed through the loop to generate the magnetic moment. This method provides an *in situ* measurement of the spring constant of the cantilever, as well as a direct test of the linearity of the cantilever response. We passed a small DC current through the wire loop to generate a constant magnetic moment. An example of magnetic torque is shown in Fig. 1, in which the magnetic moment is around $2 \times 10^{-8} \text{ A.m}^2$. The torque is linear with field H , within noise. We also varied the magnitude and the sign of the DC current to verify the magnetic torque scales with the current.

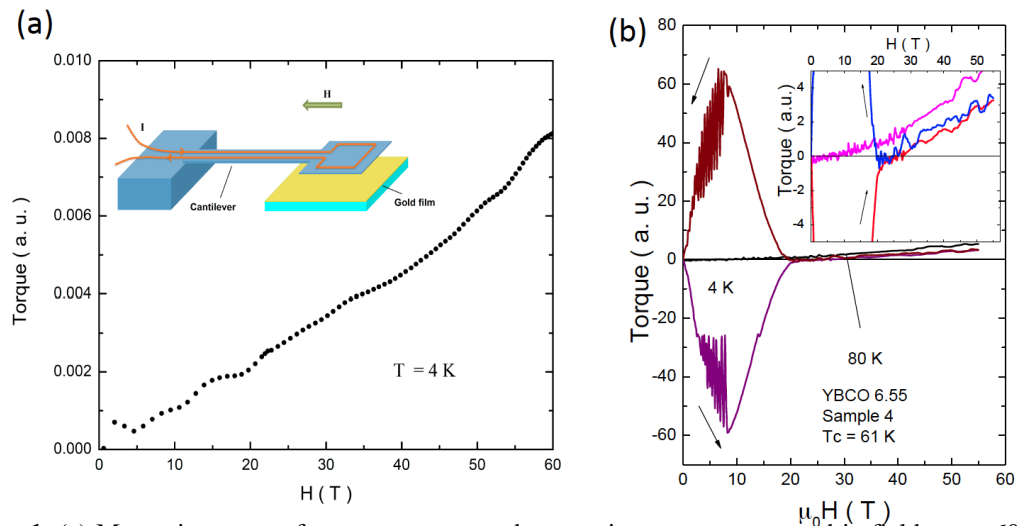


Figure 1. (a) Magnetic torque of a current-generated magnetic moment measured in field up to 60 T. The magnetic moment is about $2 \times 10^{-8} \text{ A.m}^2$. The insert is a sketch of the cantilever setup without sample loaded. (b) Magnetic torque of underdoped ortho-II YBCO at oxygen content 6.55. The insert shows the comparison of the high field response at expanded scale to emphasize the negative contribution of the diamagnetism of the superconducting fluctuation in surviving well above the close of the hysteresis loop.

We further succeeded in measuring the magnetic torque of high temperature superconductors. Fig. 1(b) shows an example of the magnetic torque τ of an underdoped $\text{YBa}_2\text{Cu}_3\text{O}_x$ (YBCO) single crystal in magnetic field H up to 55 T. The oxygen content x is 6.55, the doping where quantum oscillation has been observed in electrical transport properties. We compare the $\tau - H$ curve deep in the superconducting state ($T = 4 \text{ K}$) with that at the normal state ($T = 80 \text{ K}$). At H below 20 T, the $\tau - H$ curve is hysteretic, as a result the flux pinning of the vortex solid. The end of the hysteresis loop marks the melting of the vortex solid. Above the melting field 20 T, the $\tau - H$ curve becomes reversible. More importantly, above 20 T the magnetic torque at 4 K is much smaller than that in the 80 K normal state. Therefore, even though the YBCO is not in the vortex solid state at $H > 20 \text{ T}$, there is still considerably large diamagnetic signal coming from the moving vortices, i.e., the vortex liquid state with surviving superconductor pairing [4,5].

(2). Quantum oscillations in heavy fermion Kondo insulator SmB_6

Torque magnetometry is a powerful tool to uncover the quantum oscillation from Landau Level quantization in correlated materials [6]. Torque magnetometry is extremely sensitive to the quantized free energy of electrons, since magnetization is a derivative of

the free energy. We recently demonstrated the power of probing the hidden state with torque magnetometry and quantum oscillations in correlated Kondo insulator SmB_6 [8].

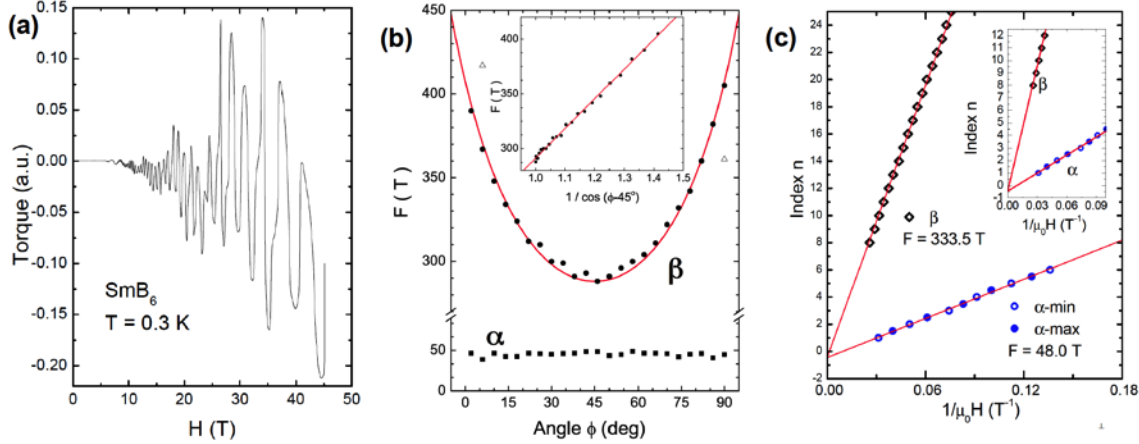


Figure 2. Signature of 2D Dirac electronic state in quantum oscillations in SmB_6 . (a) Quantum oscillations in the magnetic torque curves of SmB_6 measured up to 45 T. (b) The Landau Level index plot finds the infinite field limit is $-1/2$, a Berry phase contribution of Dirac dispersion as in graphene.

Kondo insulators are based on rare earth elements where f-shell electrons generally provide localized magnetic moment and strong interaction. The hybridization between itinerant electrons and localized orbitals opens a gap and makes the material insulating. The ground state electronic structure in the strongly correlated system can be mapped to a rather simple electronic state that resembles a normal topological insulator. As a result, in the ground state of the Kondo insulator there exists a bulk insulating state and a conductive surface state, named as topological Kondo insulator [7]. The experimental verification of topological Kondo insulator is exciting, this will be the first example of interaction-driven topological phases in correlated materials.

Our result on topological Kondo insulator SmB_6 confirms the existence of 2D surface state [8]. Quantum oscillation is observed in the magnetic torque in H up to 45 T, shown in Fig. 2(a). As shown in Fig. 2(b), the Fermi surface cross section determined from quantum oscillations is found to follow $1/\cos(\phi - 45^\circ)$, indicating the electronic state is indeed 2D. The infinite field limit Landau level, shown in Fig. 2(c), turns out to be $-1/2$, a Berry phase factor due to Dirac dispersion, as demonstrated in graphene and Bi-based topological insulators.

Future Plan

(1). Solve the cantilever ringing problem with active feedback

From the 60 T generator-based long pulse to the 100 T magnetic field, there would be rather short interval (~ 20 ms) of high field regime (60T – 100 T). An issue of cantilever ringing arises in such a rapid field-changing environment. At 4 K, the ringing frequency is typically between 500 Hz and 1 kHz, dependent on the sample weight. This suggests the response time is around 1 – 2 ms. For the short pulse we used, the rising time is about 8 ms, and the discharging time is about 22 ms. Therefore, the response time is fast enough, especially during the discharge. However, the cantilever ringing strongly distorts the torque trace.

The cantilever ringing starts as the rapidly changing magnetic torque creates large acceleration. To solve the problem, we propose to use the current loop to cancel this acceleration and to keep the cantilever static. We will accomplish this by feeding back the change of the torque to a PID control circuit and connecting the control output to balance the cantilever. This process is similar to the topology mapping of scanning tunneling microscopy (STM) in which the tip height is controlled to keep the tunneling current constant. In our setup, the ringing frequency is slightly less than 1 kHz. That means if we can get a feedback control circuit as fast as 10 kHz, we can control the torque to near zero and make the cantilever roughly non-moving. Given the small loop resistance (\sim 50 ohms including the probe leads) and relative small shunt capacitance (\sim 200 pF), such feedback is easy to setup. Since the required current-generated magnetic moment balances the sample magnetic torque, we can use the recorded balancing current to track the magnetic torque.

(2). Search for quantum oscillations in the underdoped Fe-based and Cu-doped high temperature superconductors.

One key problem towards understanding the high temperature superconducting mechanism is determining the electronic state behind the superconducting phase. Is it a normal metal or correlated Mott state? It is very important to search for quantum oscillations in Fe-based and Cu-based high temperature superconductors. Our result on SmB₆ provides an example of the power of high field torque magnetometry uncovering quantum oscillations. We plan to work with collaborators to optimize the sample growth to search for quantum oscillations in high temperature superconductors.

References

- [1] Y. Kamihara et al. "Iron-based layered superconductors La[O_{1-x}F_x]FeAs (x = 0.05-0.12) with T_c = 26 K", J. Am. Chem Soc. 103, 2396.
- [2] X. H. Chen et al, "Superconductivity at 43 K in SmFeAsO_{1-x}F_x" Nature 453, 761.
- [3] Bednorz & Muller. "Possible High T_c Superconductivity in the Ba La Cu O System", Z. Phys. B 64, 189.
- [4] L. Li, J. G. Checkelsky, S. Komiya, Y. Ando, and N. P. Ong, "Low-temperature vortex liquid in La_{2-x}SrxCuO₄," *Nature Physics*, vol. 3, pp. 311-314, 2007.
- [5] L. Li, Y. Wang, S. Komiya, S. Ono, Y. Ando, G. D. Gu, and N. P. Ong, "Diamagnetism and Cooper pairing above T_c in cuprates," *Phys. Rev. B*, vol. 81, pp. 054510-054510, 2010.
- [6] L. Li, J. G. Checkelsky, Y. S. Hor, R. J. Cava, C. Uher, A. F. Hebard, and N. P. Ong, "Phase transitions of Dirac electrons in bismuth," *Science*, vol. 321, pp. 547-550, 2008.
- [7]. M. Dzero, K. Sun, V. Galitski, and P. Coleman, "Topological Kondo Insulators," *Physical Review Letters*, vol. 104, 2010.
- [8]. G Li, Z Xiang, F Yu, T Asaba, B Lawson, P Cai, C Tinsman, A Berkley, S Wolgast, YS Eo, Dae-Jeong Kim, C Kurdak, JW Allen, K Sun, XH Chen, YY Wang, Z Fisk, Lu Li, Quantum oscillations in Kondo Insulator SmB₆", arXiv:1306.5221 (2013).

Publications acknowledging DOE-BES support

G Li, Z Xiang, F Yu, T Asaba, B Lawson, P Cai, C Tinsman, A Berkley, S Wolgast, YS Eo, Dae-Jeong Kim, C Kurdak, JW Allen, K Sun, XH Chen, YY Wang, Z Fisk, Lu Li, Quantum oscillations in Kondo Insulator SmB₆", arXiv:1306.5221 (2013).

Project Title: Engineering of mixed pairing and non-Abelian quasiparticle states of matter in chiral *p*-wave superconductor Sr₂RuO₄

Principal Investigator: Ying Liu

Institution: Department of Physics, Pennsylvania State University, 104 Davey Laboratory, University Park, PA 16802

Email: liu@phys.psu.edu

1. Project Scope

This project is focused on the study of pure Sr₂RuO₄ and related Ru-Sr₂RuO₄ eutectic phase. Sr₂RuO₄, believed to be a chiral *p*-wave superconductor, which is expected to feature novel topological quantum states of matter, including half-flux-quantum Abrikosov vortices (half vortices) that host a Majorana mode in its normal that carries non-Abelian statistics. On the other hand, a novel mixed pairing superconducting state is expected at the Ru/Sr₂RuO₄ interface in the eutectic phase. Majorana modes are the building block for constructing a topological quantum computer that is expect to be robust against decoherence.

Strong evidence for $p_x \pm ip_y$ superconductivity has been obtained in pure Sr₂RuO₄ in the past couple of decades. Half vortices are expected to form in a $p_x \pm ip_y$ superconductor because of the availability of charge neutral spin supercurrent in addition to the normal supercurrent. In the eutectic phase of Ru-Sr₂RuO₄, which is interesting because of the enhancement of superconducting transition temperature (T_c) to nearly twice of bulk Sr₂RuO₄, an atomically sharp interface between Sr₂RuO₄ and *s*-wave superconductor Ru was found. Therefore, at the interface region, both *p*- and *s*-wave pairs should form and condense into a novel superconducting state marked by a mixed pairing symmetry.

Evidence for half flux quantum states was found in mesoscopic samples of Sr₂RuO₄, which can be viewed as coreless half vortices, suggesting that half vortices may indeed be present in Sr₂RuO₄. However, the existence of half vortices and the associated non-Abelian statistics of the Majorana mode has not been established. For eutectic phase of Ru-Sr₂RuO₄, the T_c enhancement has been associated, unexpectedly, to the presence of dislocation. On the other hand, evidence for the mixed pairing state has not been found.

In the past couple of years, we have pursued the preparation and the measurements of microstructures of Sr₂RuO₄ including mesoscopic rings to search for the half-flux states through quantum oscillations and clarify the physical origin of the unexpected T_c enhancement near dislocations found in Sr₂RuO₄. In the future we plan to 1) search for half vortices and the associated Majorana modes; 2) explore ways to detect the presence of domains and domain walls, and that of chiral edge currents; and finally, 3) carry out tunneling spectroscopy studies of the Ru-Sr₂RuO₄ interface region to obtain evidence for the mixed pairing state.

2. Recent Progress

In the past couple of years we pursued the fabrication and measurements of various Sr₂RuO₄ microstructures to facilitate the exploration of the mixed pairing and non-Abelian Majorana states. Towards this goal, we established a process prepare thin flakes of pure Sr₂RuO₄ and Ru-Sr₂RuO₄ eutectic phases and characterized them by scanning micro Raman spectroscopy, scanning transmission electron microscope (STEM) and electron energy loss spectroscopy

(EELS); Motivated by the recent observation of half-height magnetization steps in a cantilever magnetometry measurement of doubly connected mesoscopic samples of Sr_2RuO_4 in the presence of an in-plane magnetic field¹, which suggests the presence of a half-flux-quantum ($\Phi_0/2 = h/4e$) state; we also fabricated mesoscopic superconducting rings of Sr_2RuO_4 and carried out Little-Parks resistance oscillation measurements. The Little-Parks experiment will provide not only additional evidence for the presence of a half-flux states but also insight into its physical origin by tracing out the landscape for the system. We found anomalously large resistance oscillation of full-flux quantum ($h/2e$) without the presence of an in-plane field; currently we're working on the same measurements with the application of an in-plane field, aiming at obtaining additional evidence for the half flux states. We worked on tunneling into the interface region in the Ru- Sr_2RuO_4 eutectic phase to search for mixed pairing states.

Because superconducting films of Sr_2RuO_4 are not yet available, our samples are fabricated using superconducting sub-micron thin flakes of Sr_2RuO_4 prepared by mechanical exfoliation from bulk single crystals. We use photolithography to prepare the leads needed for the Little-Parks resistance oscillation and focused ion beam (FIB) for cutting the ring. Applying a magnetic field perpendicular to the plane of the ring (along the c axis) without the in-plane magnetic field revealed resistance oscillations of a full-flux quantum ($h/2e$) period.

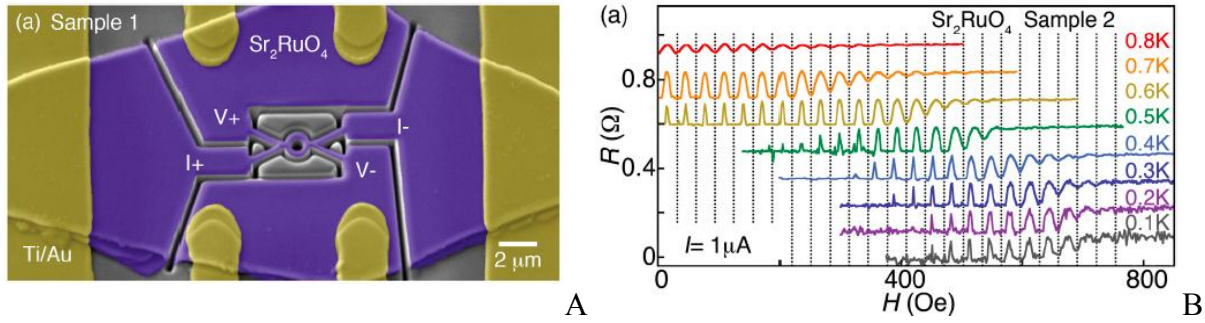


Figure 1. A) An SEM image of a mesoscopic ring of Sr_2RuO_4 prepared by photolithography and FIB; B) Measured Little-Parks resistance oscillations of the Sr_2RuO_4 ring at various temperature. T mid-point diameter of the ring is $0.9 \mu\text{m}$ and the wall thickness, w , is 160 nm on the top and 240 nm at the bottom. The observed oscillation period, $\Delta H \approx 31.4 \text{ Oe}$.

The enhanced T_c seen in the eutectic phase of Ru- Sr_2RuO_4 was attributed originally to the capillary effect at the Ru/ Sr_2RuO_4 interface. In a recent study, we found that dislocations in Sr_2RuO_4 , which can form easily near the Ru/ Sr_2RuO_4 interface (Fig. 2a), may also be able to produce an enhancement in T_c in this material system². This is surprising for Sr_2RuO_4 as it was found previously that superconductivity in Sr_2RuO_4 is particularly sensitive to the presence of disorder. In fact the T_c of Sr_2RuO_4 was found to be suppressed completely when the concentration of non-magnetic impurities of Al reaches 50 ppm.

We formulated a phenomenological theory that focuses on the consequences of the loss of four-fold symmetry near a dislocation in a spin-triplet superconductor having a two-component order parameter. Our phenomenological theory indeed predicts an enhanced T_c with its value depending on the parameters characterizing the symmetry reduction strengths (Fig. 2d). Furthermore, the magnitudes of the two components of the superconducting order parameter near a dislocation are strongly temperature dependent. We carried out measurements on Sr_2RuO_4 flakes that are free of Ru islands (the presence of a Ru island can be detected by SEM or TEM, see Fig. 2b), and therefore Ru/ Sr_2RuO_4 interfaces as well, and found an enhanced T_c . Some of these measurements were studied by TEM after all low-temperature transport measurements

were carried out, which yielded evidence for the presence of dislocations in the sample, thus establishing a direct link between the enhanced T_c and the presence of dislocations. The microscopic origin of the T_c enhancement as well as the implications of this work on other topological defects in other unconventional superconductors are currently being explored.

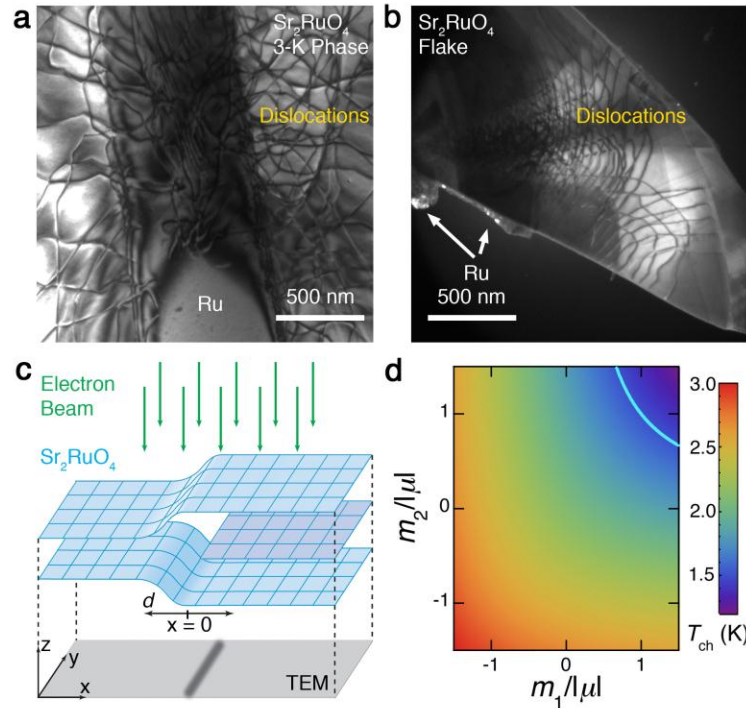


Figure 2. (a) TEM image of a Sr_2RuO_4 -Ru eutectic crystal showing a Ru island in the middle and large numbers of dislocations. (b) TEM image of a Sr_2RuO_4 single-crystal flake, showing dislocations and nanodomains of Ru on the edge. The dislocation lines are the superposition of many layers. (c) Schematic of an edge dislocation caused by an extra layer (purple) in a Sr_2RuO_4 lattice. (d) T_{ch} plotted as a function of various parameter used in the phenomenological theory showing that an enhanced T_c can indeed be expected.

3. Future Plans

Half flux states. In the coming year our top priority is to complete the experiment on the detection of half flux states in mesoscopic rings of Sr_2RuO_4 through the Little-Parks resistance oscillation measurements. We're also in the process of setting up a ^3He scanning SQUID that will measure directly the flux trapped in a mesoscopic ring of Sr_2RuO_4 and image half-flux Abrikosov vortices. The PI arranged an Agreement for Joint Study between IBM and Penn State that has allowed the scanning SQUID built by Dr. John Kirtley to be on loan to PI's lab. Little-Parks resistance oscillation measurements with the presence of an in-plane field have been carried out. Preliminary results do seem to indicate that half-flux-quantum Little-Park oscillations may indeed be there.

Domain and domain walls. Even though there is strong evidence for p -wave superconductivity in Sr_2RuO_4 and that for a time-reversal symmetry breaking superconducting state from μSR and polar Kerr rotation measurements, domains and domain walls expected in a chiral p -wave superconductor have not yet been observed directly in this material. Therefore, further experimental studies that can detect and manipulate domains and domain walls are highly

desired. We plan to carry out experiments on microstructures of Sr₂RuO₄ and detect the presence of domains and domain walls in Sr₂RuO₄ using Josephson effect based phase-sensitive measurements. We plan to prepare Au_{0.5}In_{0.5}/Sr₂RuO₄ SQUIDs for controlling and detecting domains in Sr₂RuO₄. Small magnetic field coils prepared by photo lithography can be used to create conditions favoring the formation of two domains opposite chiralities during a slow field cool. Quantum oscillation patterns obtained in zero-field and finite-field cools will be compared to see if there are signs for the present of domains. Essentially, with and without the presence of the domain correspond to a 180-degree intrinsic phase shift, which will in turn lead to a shift in the minimum position in the quantum oscillation. In addition, we will also explore the physical behavior of the flakes when their sizes become smaller and smaller. In sufficiently small flakes only a single domain exist as the domain wall is expected to be around 1 μm wide, which will show feature not present in flakes that can host multiple domains.

Mixed pairing state: Previously we carried out measurements on tunnel junctions prepared on a single Ru island recently. However, Ru islands chosen for this study, found on a polished surface of the Ru-containing Sr₂RuO₄ single crystal, feature a relatively rough surface, which may prevent the detection of the mixed pairing state. We plan to minimize the amount of the disorder on the surface of Ru island and prepare tunnel junctions on Ru island by FIB followed by low-energy ion milling to remove the damaged surface layer. Mixed pairing state is expected, which should be detected in both transport and tunneling measurement.

4. Publications resulting from DOE sponsored research (2011-2013)

- 1) Y. A. Ying, Y. Liu, T. He, and R. J. Cava, "Magnetotransport properties of BaRuO₃: Observation of two scattering rates," **Phys. Rev. B** 84, 233104 (2011).
- 2) X. Cai, Y. A. Ying, N. E. Staley, Y. Xin, D. Fobes, T. Liu, Z. Q. Mao, and Y. Liu, "Quantum oscillations in small rings of odd-parity superconductor Sr₂RuO₄," **Phys. Rev. B Rapid Comms.**, 87, 081104(R) (2013).
- 3) Y. A. Ying, N. E. Staley, Y. Xin, K. Sun, X. Cai, D. Fobes, T. J. Liu, Z. Q. Mao, and Y. Liu, "Dislocations and the enhancement of superconductivity in odd-parity superconductor Sr₂RuO₄," accepted for publication for **Nature Communications** (2013). arXiv:1205.3250

¹ J. Jang, D. G. Ferguson, V. Vakaryuk, R. Budakian, S. B. Chung, P. M. Goldbart, and Y. Maeno, "Observation of Half-Height Magnetization Steps in Sr₂RuO₄," [Science 331, 186 \(2011\)](#).

² Y. A. Ying, Y. Xin, B. W. Clouser, E. Hao, N. E. Staley, R. J. Myers, L. F. Allard, D. Fobes, T. Liu, Z. Q. Mao, and Y. Liu, "Suppression of proximity effect and the enhancement of *p*-wave superconductivity in the Sr₂RuO₄-Ru system," **Phys. Rev. Lett.** 103, 247004 (2009).

Time-Resolved Spectroscopy of Insulator-Metal Transitions: Exploring Low-Energy Dynamics in Strongly Correlated Systems

Gunter Luepke

**Department of Applied Science, College of William & Mary,
Williamsburg, VA 23187, email: Luepke@wm.edu**

Program Scope

The research program focuses on the study of the large interfacial magneto-electric (ME) coupling effect and coherent spin dynamics in complex multiferroic (MF) oxide heterostructures using interface-specific and time-resolved nonlinear-optical techniques. The goal of these studies is to elucidate the static and dynamic magnetic interactions and their correlations with the electronic structure and strain states at the valence and lattice mismatched interfaces, which can be artificially engineered. Building on key advances of the previous award period, our program concentrates on two major themes: (i) to determine the interfacial ME coupling mechanism and its correlation with charge transfer, orbital states and strain states induced by the substrate or film thickness using the interface-specific magnetization-induced second-harmonic generation (MSHG) technique, and (ii) to investigate its effect on the coherent spin precession in these strongly correlated systems as a new path for fast magnetic switching utilizing the time-resolved magneto-optical Kerr effect (MOKE) technique. The science addresses issues of energy dissipation and the coupling between electronic and magnetic order in such advanced materials, of fundamental importance to our understanding of solid-state properties and has numerous applications.

Recent Progress

Charge Control of Interface Magnetization at Oxide Heterointerface

The complex oxide heterointerface is key to the development of emerging multiferroic and spintronic technologies with new functionality. Even so, direct characterization of the interfacial spin state is missing, which prevents further interpretation of the coupling between spin and other ordering parameters at such oxide heterointerfaces, and impedes the development of future interface-based devices. Here we use the interface-specific MSHG technique to investigate the interfacial magnetic state of the MF heterostructure $\text{PbZr}_{0.52}\text{Ti}_{0.48}\text{O}_3$ / $\text{La}_{0.67}\text{Sr}_{0.33}\text{MnO}_3$ (PZT/LSMO) and its dependence on the charge state. We observe a gradual transition from ferromagnetic (FM) to canted anti-ferromagnetic (AFM) phase in the first unit cell layer at the heterointerface with increasing hole doping. Moreover, the exchange coupling between interface and bulk is weak, independently of the carrier filling. Our results provide new insight into the interface spin system of MF heterostructures, and have

implications for developing electric field control of spin switches and magnetic tunneling junctions.

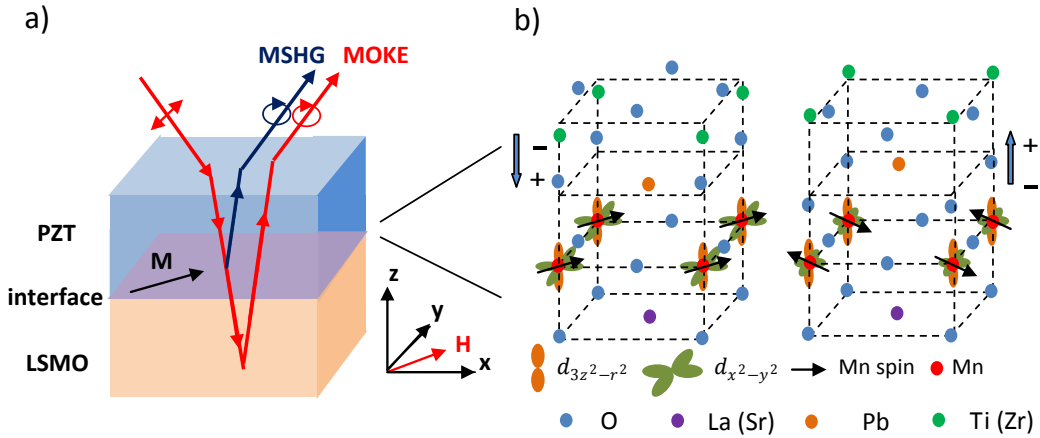


Figure 1: Schematic of magneto-optical measurements (a), and model of interfacial charge, spin, and orbital states under different polarization orientations of PZT/LSMO (b)

To investigate the interfacial magnetic state of the PZT/LSMO heterostructure, we use the MSHG technique, which probes specifically the magnetization at surfaces and interfaces where both spatial and time reversal symmetry are broken. The MSHG signal is sensitive only to the magnetic state of the first unit cell layer of LSMO at the PZT/LSMO interface. For comparison, MOKE measurements are carried out to probe the magnetic state of the LSMO bulk layer, using a similar experimental configuration as for MSHG, as depicted in Fig. 1(a).

Figure 1(b) shows a schematic model of screening charge accumulation, spin and orbital state for 3d electrons of Mn ions at the PZT/LSMO interface, responding to opposite ferroelectric polarization orientations in the PZT layer. The polarization follows the relative displacement along the z direction of the metal cations (Pb, Zr and Ti) with respect to their neighboring oxygen anions in the same formal (001) plane. At the same time, screening electrons will accumulate or deplete at the LSMO side of the interface to compensate for the charge on the PZT side. As a result, the hole doping level of LSMO at the interface can be effectively modulated.

Figure 2 (a) displays the change of interfacial magnetization with applied gate voltage probed with MSHG. It is clear that the magnetization of the

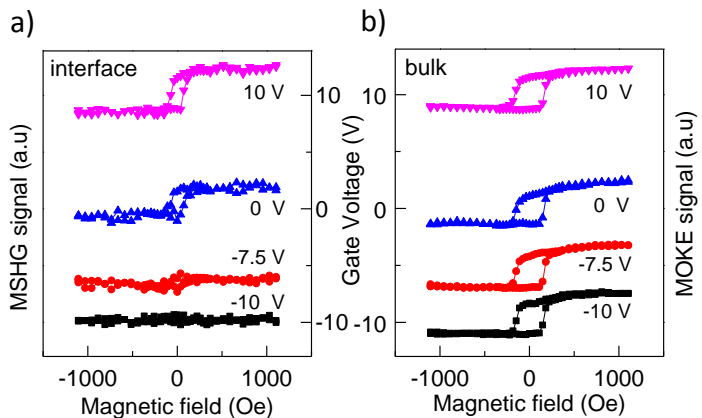


Figure 2: Interface (a) and bulk (b) magnetization responding to external gate voltage on PZT/LSMO heterostructure

interfacial layer can be modulated by the electric field. As the gate voltage on PZT/LSMO heterostructure increases, e_g electrons are depleted away from the interface layer, which causes a reduction of magnetization. As for the bulk magnetization of LSMO probed with MOKE shown in Fig. 2(b), it is not sensitive to the modulation of gate voltage. The screening charge mainly accumulates at the LSMO interface layer, while the LSMO bulk remains almost at the same doping level.

Figure 3(a) displays the ferroelectric behavior of the PZT/LSMO heterostructure. Figure 3(b) shows the relationship between interfacial magnetization and applied gate voltage exhibiting a hysteresis-loop-like shape instead of a butterfly shape. This is consistent with the polarization vs. electric field behavior of PZT (Fig. 3(a)). This directly proves that the interfacial ME coupling in this heterostructure is

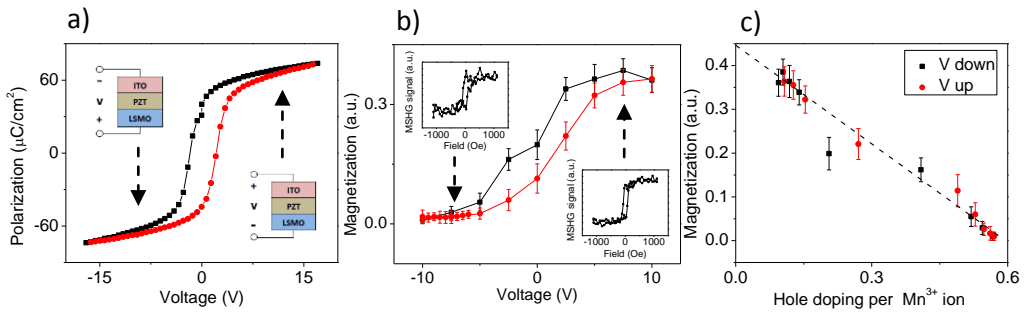


Figure 3: Ferroelectric behavior of PZT/LSMO heterostructure (a), and the dependence of interface magnetization on gate voltage (b) and hole doping level (c) per Mn^{3+} ion

governed by the charge mediated mechanism but not by strain, since the latter shows a “butterfly-shape” dependence on gate voltage according to the piezoelectric behavior of PZT.

We attribute the diminishing positive magnetic contrast with increasing hole doping to the appearance of a canted AFM spin alignment in the first unit cell layer at the PZT/LSMO interface, where spins are AFM coupled on x-y plane as depicted in Fig 1(b). When the ferroelectric polarization is pointing towards the LSMO layer, electrons accumulate at the LSMO surface as a result of the charge screening effect. The electrons fill into the 3d e_g bands of Mn ions and due to the strong Double Exchange (DE) effect their spins align parallel with other Mn ion spins, which in turn enhances the FM exchange interaction with respect to the Super-Exchange (SE) induced AFM interaction. Both, bulk and interfacial LSMO are rich in quasi-free e_g electrons and are in FM phase. When the ferroelectric polarization of PZT is pointing away from the LSMO layer, holes accumulate at the surface of LSMO, which depletes the 3d e_g electrons from Mn ions and to some extent limits the hopping of quasi-free e_g electrons. According to the phase diagram of LSMO, the electron depleted interface region becomes AFM phase, while bulk is not affected by such hole injection and stays in FM phase.

Figure 3(c) shows the dependence of interfacial magnetization M on hole doping p of Mn^{3+} ions. The dependence of M on p falls into a linear correlation for the entire modulation region. We use the effect of hoping electrons on canted AFM model to explain such linear dependence. This AFM canting spin model is consistent

with our observation that the magnetization of the first LSMO unit cell layer at the interface is proportional to the Zener carrier concentration, starting from anti-parallel spin alignment at $p \approx 0.6$ to parallel spin alignment at $p \approx 0.1$ (Fig 1(b)). From the least-square linear fit for such dependence, the magnetization will become zero at $p=0.59$, and the interfacial single-unit-cell layer will be in AFM phase.

In conclusion, we have investigated the interfacial spin state of PZT/LSMO heterostructure and its dependence on ferroelectric switching with magnetic second-harmonic generation. The cross-coupling between ferroelectric and ferromagnetic behavior at interface layer is purely electronic, due to charge injection. Different degrees of carrier filling can modulate the spin alignment at interface from FM to AFM exchange coupled. As a result, the interface saturated magnetization is linear proportional to the concentration of Zener carriers, while the coercivity is unrelated. We believe our results will help promote the development of new interface-based functionalities and device concepts.

Future Plans

In the future we will address the effect of the interfacial ME coupling on the coherent spin precession in the manganite layer with the time-resolved MOKE technique. The dynamic response of such structures based on ME coupling is not well investigated. Considering the future of ME coupling in magnetic storage, it is still a crucial question how fast magnetic states can response to a triggering E field for the purpose of switching. A coherent manipulation of the magnetization enhances the operational speed of these devices. The time-domain measurements also provide directly the damping constant which is a very important parameter in designing fast precessional switching devices. We plan to elucidate the mechanism of spin scattering by correlating the damping constant with the magnetic structure and interactions.

Publications

1. X. Ma, A. Kumar, S. Dussan, H. Zhai, F. Fang, H. B. Zhao, J. F. Scott, R. S. Katiyar, and G. Lüpke, Charge Control of Interface Magnetization at Oxide Heterointerface, submitted to Nature Nanotechnology (2013).
2. Y. Fan, X. Ma, F. Fang, J. Zhu, Q. Li, T. P. Ma, Y. Z. Wu, Z. H. Chen, H. B. Zhao, and G. Lüpke, Photo-induced Spin Angular Momentum Transfer into Antiferromagnetic Insulator, submitted to Phys. Rev. Lett. (2013).
3. P. He, X. Ma, J. W. Zhang, H. B. Zhao, G. Lüpke, Z. Shi , and S. M. Zhou, Quadratic scaling of intrinsic Gilbert damping with spin-orbital coupling in L10 FePdPt films, Phys. Rev. Lett. 110 (2013), 077203.
4. Wei Zheng, and Gunter Lüpke, Photoelastic lensing effect in Ti:Sapphire crystal pumped by high energy pulses, Appl. Opt. 51 (2012), 1945-1949.
5. H. B. Zhao, D. Talbayev, X. Ma, Y. H. Ren, A. Venimadhav, Qi Li, and G. Lüpke, Coherent Spin Precession via Photoinduced Antiferromagnetic Interactions in La_{0.67}Ca_{0.33}MnO₃, Phys. Rev. Lett. 103 (2011), 207205.

Program Title: Magnetotransport studies of the low dimensional electron system

Principle Investigator: R. G. Mani

Mailing Address: Dept. of Physics & Astronomy, Georgia State University, Atlanta, GA 30303

E-mail: rmani@gsu.edu

Program Scope

Magneto-transport studies of low dimensional electron systems have contributed to exciting advances in condensed matter physics such as the discoveries of the integral and fractional quantum Hall effects in the Si-MOSFET and the GaAs/AlGaAs heterostucture systems, and the identification of Dirac fermions in sheets of carbon known as graphene. Such magneto-transport studies have mostly examined the equilibrium properties of low dimensional electron systems. This research is concerned with comparing the equilibrium properties with non-equilibrium magneto-transport realized under steady-state microwave- and terahertz- photoexcitation of the GaAs/AlGaAs and graphene low dimensional electron systems. An aim of this research is to uncover novel emergent phenomena in the far-from-equilibrium photoexcited electronic system. Another aim of the research is to elucidate the electronic properties using photo-excited transport in the near-to-equilibrium context.

Recent Progress

1. Resistively detected spin resonance and zero-field pseudo spin splitting in epitaxial graphene:

The work described here represents the first instance of resistive detection of spin resonance in epitaxial graphene, and the first ESR based measurements of the g-factor, the spin relaxation time, and the pseudo-spin (valley - degeneracy)-splitting at zero-magnetic-field in nanoscale graphene.

Transport studies were carried out in the $B \perp c$ -axis configuration on p-type epitaxial graphene Hall bar specimens. The specimen was immersed in pumped liquid Helium, and irradiated with microwaves over the frequency range $10 \leq f \leq 50$ GHz. Figure 1(a) exhibits the diagonal resistance, R_{xx} , vs. B , for a trilayer sample. At $T = 1.5$ K (blue curve, Fig. 1(a)), the sample exhibits a cusp in R_{xx} near null magnetic field, i.e., Weak Localization (WL), followed by positive magnetoresistance at $B > 0.2$ T. In Fig. 1(a), an increase in T (red curve, Fig. 1(a)) produces a positive displacement of the

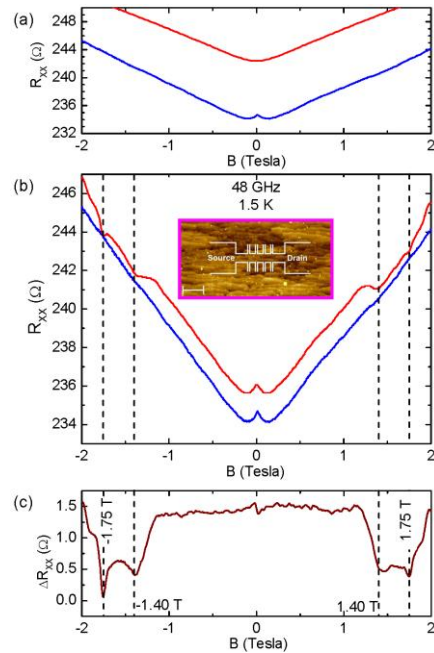


Figure 1) This figure illustrates resistively detected microwave-induced spin-resonance at $f = 48$ GHz in a three layer epitaxial graphene specimen. (a) The diagonal resistance, R_{xx} , is exhibited vs. the magnetic field, B , at temperatures $T = 90$ K (red trace) and $T = 1.5$ K (blue trace). The upward displacement of the $T = 90$ K curve with respect to the $T = 1.5$ K curve shows that R_{xx} increases with the temperature, i.e., $dR_{xx}/dT \geq 0$. (b) R_{xx} is exhibited vs. B without microwave excitation (blue trace), and under constant $f = 48$ GHz microwave excitation at $P = 4$ mW (red trace), at $T = 1.5$ K. The photo-excited (4 mW) R_{xx} trace exhibits a uniform upward shift with respect to the dark R_{xx} curve for $B < 1$ T. At higher B , resonant reductions in the R_{xx} are observed in the vicinity of $B = \pm 1.4$ T and $B = \pm 1.75$ T, where R_{xx} approaches the dark value. Inset: An AFM image of the EG/SiC surface with the device superimposed upon it. (c) The change in the diagonal resistance, ΔR_{xx} , between the photo-excited and dark conditions in panel (b), i.e., $\Delta R_{xx} = R_{xx}(4 \text{ mW}) - R_{xx}(\text{dark})$, is exhibited vs. B . Note the valleys in ΔR_{xx} in the vicinity of $B = \pm 1.40$ T and $B = \pm 1.75$ T.

R_{xx} vs. B trace, i.e., $dR_{xx}/dT > 0$ at $B = 0$ Tesla, along with the quenching of WL. Fig. 1(b) illustrates the influence of microwave-excitation at $f = 48$ GHz. Here, for $B < 1$ Tesla, microwave excitation (red trace) seems to produce electron heating in these graphene specimens. However, at $B > 1$ Tesla, R_{xx} exhibits resonant resistance-valleys as the photo-excited curve approaches the dark (blue) curve, similar to reducing T. To highlight associated resonances, $\Delta R_{xx} = R_{xx}(4 \text{ mW}) - R_{xx}(\text{dark})$, is exhibited vs. B in Fig. 1(c). Fig. 1(c) shows two noteworthy features: a high magnetic field resonance at $|B| = 1.75$ Tesla, and a low magnetic field feature at $|B| = 1.4$ Tesla. Similar resonances were also observed in monolayer graphene specimens and followed as a function of frequency. Figure 2(a) presents a plot of the microwave frequency, f , vs. the resonance magnetic fields, B , for trilayer graphene and a pair of monolayer graphene specimens. Remarkably, Fig. 2(a) shows that the resonance B-values for the three specimens collapse onto two lines: a gold-colored line in Fig. 2(a), which represents the high B-field resonances of Fig. 1, follows $f(\text{GHz}) = 27.2 B(\text{T})$, with the ordinate-intercept at the origin. Another line shown in magenta in Fig. 2(a), which represents the low-B resonances of Fig. 1, follows $f(\text{GHz}) = 10.76 + 26.9 B(\text{T})$. The observed slopes, $df/dB = 26.9 \pm 0.4 \text{ GHz/Tesla}$ ($df/dB = 27.2 \pm 0.2 \text{ GHz/Tesla}$) for the low (high) field resonance correspond to spin resonances with $g_{\parallel} = 1.92 \pm 0.028$ ($g_{\parallel} = 1.94 \pm 0.014$). The g-factors measured here are comparable to the g-values obtained from traditional ESR-studies of graphite, which have indicated that the g-factor for $B \parallel c$ -axis, g_{\parallel} , increases from 2.05 at 300 K to 2.15 at 77 K, while, at $T = 300$ K, the g-factor for B perpendicular to the c-axis, $g_{\perp} = 2.003$. The reduced g_{\parallel} observed here relative to g_e , the free electron g-factor, are consistent with expectation for holes.

2. Microwave reflection and transport in the microwave photo-excited high mobility GaAs/AlGaAs two-dimensional electron system

The GaAs/AlGaAs two-dimensional electron system (2DES) exhibits microwave-induced zero-resistance states, and strong magnetoresistance oscillations with nodes at cyclotron resonance and harmonics thereof, at liquid helium temperatures, see refs. 1,2,5-8. The magnetoresistance oscillations are understood in terms of the displacement and inelastic models for photo-excited transport in the 2DES. In order to identify the relative contributions, we correlate transport measurements and concurrent “remote sensing” measurements of the 2DES.

Thus, transport measurements were carried out on high mobility GaAs/AlGaAs heterostructure devices with a microwave sensor immediately above the Hall bar, as the device was subjected to microwave photo-excitation with $25 \leq f \leq 110$ GHz, as illustrated in the top inset of Fig. 3. Here, the sensor resistance, R_s , with its strong temperature sensitivity and negative

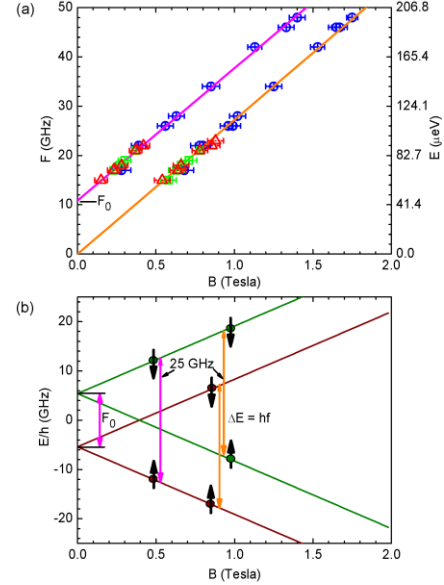


Figure 2) The figure exhibits the observed relation between the microwave frequency, f , and the resonance magnetic fields, B , in epitaxial graphene, and the model used to explain the observed resonances. (a) The plot shows that the high B-field resonance in Fig. 1 follows $f(\text{GHz}) = 27.2 B(\text{T})$, with an intercept at the origin, while the low B-field resonance follows $f(\text{GHz}) = 10.76 + 26.9 B(\text{T})$, with $f_0 = 10.8 \text{ GHz}$. (b) A four-fold degeneracy is lifted in the absence of a magnetic field to produce a pair of spin-degenerate levels (doublets) separated by $E/h = f_0$. Zeeman splitting then lifts the spin-degeneracy of the upper and lower doublets. Microwave photo-excitation induces spin-flip transitions between the spin-levels of the lower- or upper doublet, as shown in gold. Such transitions require vanishing photon energy in the $B \rightarrow 0$ limit. On the other hand, the transition shown in magenta requires non-vanishing photon energy in the limit of $B \rightarrow 0$.

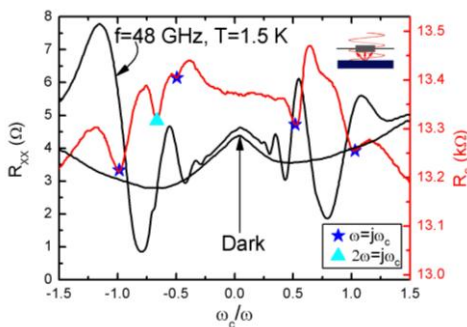


Figure 3) The diagonal resistance R_{XX} (black curve) and sensor resistance R_S (red curve) are plotted vs. ω_c/ω for a high mobility GaAs/AlGaAs 2DES under 48 GHz microwave excitation at 1.5 K. The colored symbols point out the minima of R_S . The inset on the top right schematically shows the experimental configuration.

and two photon excitations, $2\omega=j\omega_c$, where j is an integer, and (b) comparing the 2DES reflection results with Lei *et al.*'s previous calculations [X. L. Lei and S. Y. Liu, Phys. Rev. B **72**, 075345 (2005)] of the absorption properties of the irradiated 2DES. In brief, the results indicate that it is possible to remotely sense the radiation-induced transport of the microwave photo-excited high mobility 2DES.

Future Plans

- We have thus far observed hole spin resonance since we have measured p-type material, see ref. 4. Is it possible also to electrically detect electron spin resonance in graphene? In graphite, the g-factor, g_{\parallel} , is reduced below the free electron value, $g_e = 2.0023$, for holes in the $B \perp c$ -axis configuration, consistent with our report, and enhanced above g_e for electrons. Theory attributes this g-factor change to an effective field arising from the spin-orbit interaction in graphite and, therefore, the shift in the g-factor is associated with the mean value of this field, which is related to the orbital susceptibility of the carriers. Further experiments can help to show whether $g_{\parallel} > g_e$ for electrons in graphene in the $B \perp c$ -axis configuration.
- Carry out comparative studies of photo-excited transport in CVD and epitaxial graphene examining the relative importance of electron heating in the two systems. Seek out electrically detected spin resonance in CVD graphene.
- Carry out further studies of the role of the microwave polarization in radiation-induced transport in the GaAs/AlGaAs system, see refs. 5, 6, 11. The published results thus far have shown that the amplitude of the microwave radiation-induced oscillations changes dramatically when the polarization angle is rotated with respect to the Hall bar axis. Further, we have observed a finite phase shift, θ_0 , for maximal response with respect to the device axis, and, curiously, this phase shift depends upon the extrema in question and the sign of the magnetic field. The questions to be addressed include: (i) what is the

temperature coefficient, served to detect changes in the incident microwave power over the course of magnetic-field-sweep studies of the diagonal resistance, R_{XX} , under microwave photo-excitation. In the typical experiment, R_{XX} showed microwave induced magneto-resistance oscillations, as R_S exhibited correlated features under microwave excitations, at all microwave frequencies. As microwave frequency is increased from 35 GHz to 110 GHz, both the R_{XX} oscillations and the associated R_S features expanded on the magnetic field scale. We closely examined R_S for cyclotron resonance related features by plotting R_S versus ω_c/ω , see Fig. 3, where $\omega_c=B/e/m^*$ is the cyclotron resonance frequency and $\omega=2\pi f$ is the angular frequency of microwave. It is clear from the figure, that when $\omega_c/\omega=\pm 1, \pm 1/2$ and $-2/3$, R_S exhibits a local minimum, which indicates that the carbon sensor experiences enhanced heating due to maximal microwave reflection from the specimen. Such reflection behavior of the 2DES can be understood by (a) invoking both single photon excitation, $\omega=j\omega_c$,

physical origin of the phase shift? (ii) Why do different extrema exhibit different phase shifts? And, (iii) why does the phase shift depend upon the sign of the magnetic field?

References (which acknowledge DOE support)

1. Terahertz photovoltaic detection of cyclotron resonance in the regime of the radiation-induced magnetoresistance oscillations, R. G. Mani, A. N. Ramanayaka, T. Ye, M. S. Heimbeck, H. O. Everitt, and W. Wegscheider, Phys. Rev. B 87, 245308 (2013).
2. Remotely sensed transport in microwave photoexcited GaAs/AlGaAs two-dimensional electron system, T. Ye, R. G. Mani, and W. Wegscheider, Appl. Phys. Lett. 102, 242113 (2013).
3. Mesoscale scanning electron and Tunneling microscopy study of the surface morphology of thermally annealed copper foil for graphene growth, Chem. of Materials 25, 1643 (2013).
4. Observation of resistively detected hole spin resonance and zero-field pseudo spin splitting in epitaxial graphene, R. G. Mani, J. Hankinson, C. Berger, and W. A. de Heer, Nature Comm. 3, 996 (2012).
5. Effect of rotation of the polarization of linearly polarized microwaves on the radiation-induced magnetoresistance oscillations, A. N. Ramanayaka, R. G. Mani, and W. Wegscheider, Phys. Rev. B 85, 205315 (2012).
6. Observation of linear-polarization-sensitivity in the microwave-radiation-induced magnetoresistance oscillations, R. G. Mani, A. N. Ramanayaka, and W. Wegscheider, Phys. Rev. B 84, 085308 (2011).
7. Microwave-induced electron heating in the regime of the radiation-induced magnetoresistance oscillations, Phys. Rev. B 83, 165303 (2011).
8. Comparative study of microwave radiation-induced magnetoresistance oscillations in GaAs/AlGaAs devices, R. G. Mani and W. Wegscheider, IEEE Trans. On Nanotechnology, 10, 170 (2011).
9. Hall effects in doubly connected specimens, A. Kriisa, R. G. Mani, and W. Wegscheider, IEEE Trans. On Nanotechnology, 10, 179 (2011).
10. Electron heating due to microwave photoexcitation in the high mobility GaAs/AlGaAs two dimensional electron system, A. N. Ramanayaka, R. G. Mani, and W. Wegscheider, in the Proceedings of the 31th International Conference on the Physics of Semiconductors, (to be published).
11. Observation of linear-polarization-sensitivity in the microwave-radiation-induced magnetoresistance oscillations, R. G. Mani, A. N. Ramanayaka, and W. Wegscheider, in the Proceedings of the 31th International Conference on the Physics of Semiconductors, (to be published).
12. Study of reflection and transport in the microwave photo-excited GaAs/AlGaAs two dimensional electron system, T. Ye, R. G. Mani, and W. Wegscheider, in the Proceedings of the 31th International Conference on the Physics of Semiconductors, (to be published).
13. Topological Hall insulator, A. Kriisa, R. G. Mani, and W. Wegscheider, in the Proceedings of the 31th International Conference on the Physics of Semiconductors, (to be published).

Program Title: Superconductivity and magnetism in d- and f-electron materials**Principal Investigator: M. Brian Maple****Mailing Address: Department of Physics, University of California, San Diego, La Jolla, CA 92093****Email: mbmaple@ucsd.edu****Program Scope**

The primary emphasis of this project is on the physics of strongly correlated electron phenomena in novel transition metal, rare earth, and actinide based oxides and intermetallic compounds with a focus on the growth of high quality single crystals. These phenomena include superconductivity, novel types of magnetic and charge order, heavy fermion behavior, non-Fermi liquid behavior, quantum criticality, etc. The types of materials investigated include Fe-pnictide high temperature superconductors, unconventional U-based superconductors, magnetically ordered rare-earth compounds, heavy fermion *f*-electron materials, transition metal oxides and intermetallic compounds.

The approach involves the synthesis and characterization of bulk and thin film materials, with emphasis on single crystals, coupled with the investigation of their transport, thermal, and magnetic properties as a function of temperature, magnetic field and pressure. This approach completes the feedback loop between materials synthesis and properties measurement and thereby facilitates efforts to identify underlying mechanisms of correlated electron phenomena in new materials and modify materials of interest to optimize their properties. A wide variety of sample synthesis techniques are employed including solid-state reaction, arc-melting, pulsed laser deposition, optical floating zone growth, Czochralski crystal growth, and molten metal flux growth. Electrical/thermal transport, specific heat, and magnetization measurements can be performed in our laboratory at UCSD to temperatures as low as 0.01 K, in magnetic fields up to 10 T, and pressures into the megabar range. More specialized measurements to study electronic and magnetic structure and excitations are carried out in the laboratories of collaborators and at national laboratory facilities for high magnetic field, synchrotron light source and neutron scattering research.

The compounds that are investigated are correlated electron materials, which comprise a vast reservoir of unconventional phenomena. This family of materials includes both oxides (e.g., cuprates, iron-pnictogen oxides, bismuth-sulfur oxides) and intermetallics (e.g., heavy fermion *f*-electron compounds) where transition metal, rare earth, and actinide elements with partially-filled *d*- or *f*-electron shells promote unconventional behavior. Common characteristics include: unstable *f*-electron shells, reduced dimensionality, large unit cells, molecular units/clusters, oversize atomic cages with filler ions, light elements, and unusual metal/metalliod ratios. In these materials, competing interactions can often be “tuned” via the variation of a control parameter such as composition, magnetic field, or pressure, yielding a variety of novel ground states and complex temperature vs. control parameter phase diagrams. For example, unconventional superconductivity is often found in the vicinity of other ordered phases (e.g., magnetic, quadrupolar, SDW, CDW, insulating, “stripe” phases, etc.). In some cases, superconductivity occurs in the vicinity of a quantum critical point (QCP) where a second order phase transition is suppressed to 0 K by varying a control parameter. This has lead to the view that order parameter fluctuations in the vicinity of a magnetic QCP may mediate superconducting electron pairing.

Recent Progress

Our recent research has focused on several topics, which include: Correlated electron phenomena in noncentrosymmetric $Ln_2T_{12}Pn_7$ compounds; superconductivity in Fe-pnictide and Bi-sulfide compounds [6-8]; interrelation of valence fluctuations, quantum criticality, and superconductivity in the $Ce_{1-x}Yb_xCoIn_5$ system [4,9]; superconductivity and magnetism in LnT_4X_{12} filled skutterudites; interplay of weak ferromagnetism and superconductivity in UCoGe based materials [5]; and hidden order, magnetism, and superconductivity in URu_2Si_2 [2,3]. In the following, we focus on highlights in three of these areas.

- *Correlated electron behavior in noncentrosymmetric $Ln_2T_{12}Pn_7$ compounds*

A large family of noncentrosymmetric intermetallic compounds with the chemical formula $M_2T_{12}Pn_7$, where $M = \text{Zr, Hf, Ce-Lu, Th, U}$; $T = \text{Fe, Co, Mn, Ni}$, and $Pn = \text{P and As}$, constitutes a vast reservoir of correlated electron phenomena and novel magnetism. These compounds crystallize in the hexagonal $\text{Zr}_2\text{Fe}_{12}\text{P}_7$ -type structure, which contains chains of M atoms separated by large distances that are filled with T and Pn atoms. Examples include intermediate valence in $\text{Ce}_2\text{Fe}_{12}\text{P}_7$, heavy fermion ferromagnetism in $\text{Sm}_2\text{Fe}_{12}\text{P}_7$, and local moment antiferromagnetism in $\text{U}_2\text{Fe}_{12}\text{P}_7$, making them well suited for investigating the interplay between magnetic frustration and strong electronic correlations. A particularly interesting example we studied in earlier work is $\text{Yb}_2\text{Fe}_{12}\text{P}_7$. This compound exhibits some type of magnetic order below 0.9 K and has an unusual temperature-magnetic field (T - H) phase diagram with an extended region of NFL behavior at low T . Here, $\square(T)$ exhibits NFL behavior in the magnetically ordered phase at low fields. The magnetic order is suppressed upon increasing the magnetic field, yielding a disordered state that also shows NFL characteristics, but with different exponents. This observation indicates that $\text{Yb}_2\text{Fe}_{12}\text{P}_7$ may form some novel kind of metallic state. We have further investigated the novel ground state of $\text{Yb}_2\text{Fe}_{12}\text{P}_7$ via thermal expansion measurements and have extended the magnetic phase diagram to high magnetic fields up to 60 T. Recent experiments on single crystals of $\text{Yb}_2\text{Ni}_{12}\text{P}_7$ suggest that Yb has an intermediate valence, while the behavior of $\square(T)$ and $C(T)$ indicate a crossover from NFL to FL behavior below ~ 2 K, suggesting that $\text{Yb}_2\text{Ni}_{12}\text{P}_7$ is in close proximity to an unidentified QCP. Experiments on $\text{Hf}_2\text{Fe}_{12}\text{P}_7$ revealed a nonmagnetic ground state in which $\square(T)$ has a nearly linear NFL T -dependence between 0.05 and 4.5 K, consistent with NFL behavior. Measurements of $C(T)$ on $\text{Nd}_2\text{Ni}_{12}\text{P}_7$ indicate an enhanced Sommerfeld coefficient $\gamma \approx 340 \text{ mJ/mol K}^2$, suggesting the presence of strong electronic correlations.

- *Hidden order, magnetism, and superconductivity in URu_2Si_2*

The compound URu_2Si_2 is one of the most interesting heavy fermion compounds. It exhibits a so-called “hidden order” (HO) phase that occurs below 17.5 K whose order parameter has eluded identification for nearly three decades. The HO phase forms a gap over about 40% of the Fermi surface and coexists with superconductivity below $T_c \approx 1.5$ K. Large moment antiferromagnetic order (LMAFM), large moment ferromagnetic order (LMFM), novel non-Fermi liquid ground states, and quantum critical behavior are found when the delicate balance between competing interactions in URu_2Si_2 is “tipped” by chemical substitution, magnetic fields, and pressure. In previous work, we discovered a two-fold enhancement of the HO/LMAFM phase boundary $T_0(x)$ in the $\text{URu}_{2-x}\text{Fe}_x\text{Si}_2$ system. The $T_0(P_{ch})$ curve, obtained by converting x to “chemical pressure” P_{ch} is strikingly similar to the $T_0(P)$ curve, where P is applied pressure for URu_2Si_2 – both exhibit a “kink” at 1.5 GPa and a maximum at ~ 7 GPa. This similarity suggests that the HO-LMAFM transition at 1.5 GPa in URu_2Si_2 occurs at $x \approx 0.2$ ($P_{ch} \approx 1.5$ GPa) in $\text{URu}_{2-x}\text{Fe}_x\text{Si}_2$. Recently, we discovered a similar and larger enhancement of $T_0(x)$ in the $\text{URu}_{2-x}\text{Os}_x\text{Si}_2$ system, suggesting that a phase transition from the HO phase to another phase whose identity has not yet been determined, but is likely to be a LMAFM phase. This study reveals that both Fe and Os isoelectronic substitutions for Ru in URu_2Si_2 , yield an enhancement of $T_0(x)$. In contrast to the $\text{URu}_{2-x}\text{Fe}_x\text{Si}_2$ system, where the unit cell volume decreases with x , in the $\text{URu}_{2-x}\text{Os}_x\text{Si}_2$ system, the unit cell volume increases with x . Thus, the enhancement of the HO/LMAFM transition temperature cannot be solely due to an increase of chemical pressure.

Single crystal specimens of URu_2Si_2 and $\text{URu}_{2-x}\text{Re}_x\text{Si}_2$ were prepared and investigated by means of neutron scattering and ultrasound measurements in an effort to gain information about the identity of the HO phase and the onset of LMAFM and LMFM phases. Inelastic neutron scattering measurements in the HO state of $\text{URu}_{2-x}\text{Re}_x\text{Si}_2$ with $x = 0.1$ show that the effect of Re doping is to weaken, but surprisingly, not destroy the HO on approach to the quantum phase transition to LMFM, in contrast to the enhancement LMAFM and destruction HO by Rh doping.

- *Superconductivity in new layered LnOBiS_2 compounds containing F and Th substituents and subjected to pressure*

We recently reported the synthesis and measurements of $\square(T)$, $\square(T)$, and $C(T)$ on F-substituted $LnO_{0.5}F_{0.5}BiS_2$ ($Ln = La, Ce, Pr, Nd, Yb$) compounds. These materials belong to a new family of BiS_2 -based superconductors, which have layered crystal structures similar to those of high- T_c cuprate and Fe-based superconductors. Measurements of $\square(T)$ reveal semiconducting behavior that gives way to superconductivity at $T_c = 3.1$ K, 1.9 K, 4.3 K, 4.4 K, and 5.3 K for $Ln = La, Ce, Pr, Nd, Yb$, respectively. These were the first reports of superconductivity for the compounds $LnO_{0.5}F_{0.5}BiS_2$ ($Ln = Ce, Pr, Nd, Yb$). Superconductivity and magnetic order appear to coexist below ~ 2.7 K in $YbO_{0.5}F_{0.5}BiS_2$.

A new method of inducing superconductivity in the BiS_2 -based compound $LaOBiS_2$ was discovered. This involves increasing the charge-carrier density (electron doping) via the substitution of tetravalent Th^{+4} , Hf^{+4} , Zr^{+4} , and Ti^{+4} for trivalent La^{+3} (rather than substituting F^{-1} for O^{-2}). The $LaOBiS_2$ and $ThOBiS_2$ parent compounds, which behave as bad metals, can be rendered superconducting by electron doping with T_c values reaching 2.85 K.

Measurements of $\square(T)$ between 1 K and 300 K at various pressures up to ~ 3 GPa were performed on the superconducting compounds $LnO_{0.5}F_{0.5}BiS_2$ ($Ln = La, Ce, Pr, Nd$). For each compound, a pressure-induced transition from a low T_c to a high T_c phase was observed. This transition correlates with a suppression of the semiconducting behavior with pressure to metallic, or nearly metallic, behavior.

Future Plans

Some of our future research plans are briefly described in the following:

- We plan to continue our systematic investigation of noncentrosymmetric “2-12-7” $Zr_2Fe_{12}P_7$ -type crystals to search for new correlated electron ground states and phenomena and study the interplay between magnetic frustration and strong electronic correlations. A large polycrystalline sample of $U_2Fe_{12}P_7$ has been synthesized for neutron diffraction measurements at low temperatures, which will soon be carried out. We have succeeded in synthesizing some of the corresponding Ni-As based 2-12-7 compounds, and will investigate their properties. Depending on the transition metal that occupies the T -site of $Ln_2T_{12}P_7$, the T sub-lattice may exhibit long-range FM order ($T = Co$) or non-magnetic behavior ($T = Fe$ or Ni). In two substitution studies, specifically, $Hf_2(Fe_{1-x}Co_x)_{12}P_7$ and $Yb_2(Fe_{1-x}Co_x)_{12}P_7$, we have shown that the FM order can be continuously suppressed by replacing Fe with Co, allowing for the possibility of an FM QCP. In the case of $Yb_2(Fe_{1-x}Co_x)_{12}P_7$, in which the Yb-ions order magnetically as well, we will continue our investigation of the possible interplay of these two magnetic sublattices in the vicinity of the possible QCP.
- We plan to continue our investigation of valence fluctuations, quantum criticality, and unconventional superconductivity in the $Ce_{1-x}Yb_xCoIn_5$ system. In addition, we have embarked on an investigation of the related system $Ce_{1-x}Yb_xRhIn_5$ to establish whether the correlated electron state is stabilized by cooperative behavior involving the unstable valences of the Ce and Yb and to study the properties of this system at low temperature and high pressure.
- We hope to exploit the similarity of the $T_0(P_{ch})$ curve, where P_{ch} is “chemical pressure,” of the $URu_{2-x}Fe_xSi_2$ system to the $T_0(P)$ curve of URu_2Si_2 to perform experiments to study HO and other phenomena at ambient pressure on the $URu_{2-x}Fe_xSi_2$ system that would difficult or impossible to carry out on URu_2Si_2 under pressure. Examples of techniques that could provide new insights into the HO include neutron scattering, IR spectroscopy, STM, ARPES and PCS. In order to pursue this direction, we have embarked on a major program to prepare single crystal specimens of $URu_{2-x}Fe_xSi_2$, which we will plan to study in detail by means of transport, thermal, and magnetic measurement, in addition to the spectroscopic measurements mentioned above. Currently, high field magnetization and neutron scattering studies on several $URu_{2-x}Fe_xSi_2$ compounds are in progress. In addition, we are exploring the effect of other transition metal T substitutions for Ru in URu_2Si_2 to obtain information about HO, magnetic order, and quantum critical behavior encountered in the $URu_{2-x}T_xSi_2$ systems.

- We plan to continue our research on high temperature superconducting materials. We will follow up our studies of LaFeAsO single crystals by means of magnetotransport measurements and electrical resistivity measurements under high pressure to 30 GPa, with similar studies of single crystals of other LnFeAsO compounds (Ln = Ce, Pr, Nd, Sm, Eu, Gd) which, when doped with F or O vacancies have the highest values of T_c of any of the Fe-pnictide superconductors. Thus far, we have not observed any evidence of pressure-induced superconductivity in LaFeAsO single crystals, in contrast to research reported several years ago on polycrystalline samples of LaFeAsO. We will continue our efforts to synthesize new BiS₂-based superconductors and study their normal and superconducting state properties at ambient and high pressure.

Selected Publications (which acknowledge DOE support)

1. T. Keiber, F. Bridges, R. E. Baumbach, and M. B. Maple, "Unusual local disorder in NdOs₄Sb₁₂ and PrOs₄Sb₁₂ skutterudites," *Phys. Rev. B* **86**, 174106 (2012).
2. T. J. Williams, Z. Yamani, N. P. Butch, G. M. Luke, M. B. Maple, and W. J. L. Buyers, "Neutron scattering study of URu_{2-x}Re_xSi₂ ($x=0.10$): Driving order towards quantum criticality," *Phys. Rev. B* **86**, 235104 (2012).
3. P. Das, R. E. Baumbach, K. Huang, M. B. Maple, Y. Zhao, J. S. Helton, J. W. Lynn, E. D. Bauer and M. Janoschek, "Absence of a static in-plane magnetic moment in the 'hidden-order' phase of URu₂Si₂," *New J. Phys.* **15**, 053031 (2013).
4. T. Hu, Y. P. Singh, L. Shu, M. Janoschek, M. Dzero, M. B. Maple, and C. C. Almasan, "Non-Fermi liquid regimes with and without quantum criticality in Ce_{1-x}Yb_xCoIn₅," *Proc. Nat. Acad. Sci.* **110**, 7160 (2013).
5. K. Huang, J. J. Hamlin, R. E. Baumbach, M. Janoschek, N. Kanchanavatee, D. A. Zocco, F. Ronning, and M. B. Maple, "Ferromagnetic quantum critical point in UCo_{1-x}Fe_xGe," *Phys. Rev. B* **87**, 054513 (2013).
6. D. Yazici, K. Huang, B. D. White, A. H. Chang, A. J. Friedman, and M. B. Maple, "Superconductivity of F-substituted LnOBiS₂ ($Ln = La, Ce, Pr, Nd, Yb$) compounds," *Phil. Mag.* **93**, 673 (2012).
7. D. Yazici, K. Huang, B. D. White, I. Jeon, V. W. Burnett, A. J. Friedman, I. K. Lum, M. Nallaiyan, S. Spagna and M. B. Maple, "Superconductivity induced by electron doping in La_{1-x}M_xOBiS₂ ($M = Ti, Zr, Hf, Th$)," *Phys. Rev. B* **87**, 174512 (2013).
8. C. T. Wolowiec, D. Yazici, B. D. White, K. Huang, and M. B. Maple, "Pressure-induced enhancement of superconductivity and suppression of semiconducting behavior in the LnO_{0.5}F_{0.5}BiS₂ ($Ln = La, Ce$) compounds," *Phys. Rev. B* **88**, 064503 (2013).
9. B. D. White, J. J. Hamlin, K. Huang, L. Shu, I. K. Lum, R. E. Baumbach, M. Janoschek, and M. B. Maple, "Insensitivity of the pressure dependence of characteristic energy scales in Ce_{1-x}R_xCoIn₅ ($R = Yb, Y, Gd$) to rare earth ion electronic configuration," *Phys. Rev. B: Rapid Commun.* **86**, 100502(R) (2012).

Program Title: Quantum Materials

Principle Investigator: Joseph W. Orenstein; **Co-PIs:** Robert Birgeneau Edith Bourret, Alessandra Lanzara, Dung-Hai Lee, Joel Moore, Ashvin Vishwanath, Ramamoorthy Ramesh, James Analytis.

Mailing Address: Materials Science Division, Lawrence Berkeley National Lab, Berkeley, CA 94720

E-mail: janalytis@lbl.gov

Program Scope

The goal of Quantum Materials (QM) is to understand, manipulate, and control interacting forms of quantum order in condensed matter systems. This work will lead to the understanding of the fundamental properties of complex many-body systems and to the design of new generations of materials where emergent quantum properties can be utilized.

Our program carries out research that has interpenetrating and complementary aspects: probing and understanding novel quantum phases and the transitions between them both in single crystals and epitaxial thin-film heterostructures. The QM team focuses on two areas: (1) High-T_c superconductivity, with the goal of identifying the key interactions that lead to Cooper pairing in unconventional superconductors in order to progress towards room temperature superconductivity, and (2) Spin-orbit coupled electronic systems, with the goal of discovering new phases and phenomena that arise when spin and charge degrees of freedom are entangled by correlations and spin-orbit interactions. The focal point of this abstract will be in the second of the two areas. We have combined experiment and theory in order to understand complex spin-orbit interactions; how the spin texture of a topological insulator (TI) surface state can be manipulated (Lanzara)[1], how exotic "Weyl" fermions can emerge in pyrochlore iridates (Vishwanath)[2] and understood the dynamics of emergent helical magnons in binary metallic magnets (Orenstein, Vishwanath)[3].

Theoretically, the iridium based oxides are the simplest realizations of spin-1/2 quantum magnetism and these materials are a focal point of the QM program. We have recently synthesized thin films of the perovskite SrIrO₃ and discovered that different amounts of biaxial strain can tune these materials from magnetic insulators to unconventional metals (Ramamoorthy, Vishwanath) [4,5]. We have furthermore developed a theoretical understanding of how these thermodynamic transitions can be driven by structural and chemical modifications (Vishwanath) [6]. Our strategy is to build on this experimental and theoretical foundation by synthesizing new 5d transition metal materials manifesting magnetic interactions that lead to the emergence of exotic quantum ground states.

Recent Progress

We have synthesized the first single crystals of a new structural motif of Li₂IrO₃, shown in Figure 1A.

Background: In the honeycomb iridates $A_2\text{IrO}_3$ (A is an alkali), an exotic kind of anisotropic exchange emerges which maps these structures onto a remarkable theoretical model pioneered by Kitaev [6]. This supports a novel state of matter known as the quantum spin liquid (QSL), which is characterized by the emergence of chargeless, spinful fermions with fractional statistics. The layered honeycomb structure is composed of octahedrally

coordinated Ir⁴⁺, bonded together their O₂ edges. The exchange pathway between spin-1/2 Ir, is across these bonds and is predicted to be highly anisotropic due to the spin-orbit coupling. The idealized case where these satisfy the Kitaev model, relies on the ideal symmetry of the octahedral environment, and the present focus on Li₂IrO₃, is due to its small octahedral distortion as compared to that of Na₂IrO₃ [8].

Results and Discussion: Our best structural refinement achieves an *R*-value of <4%. In stark contrast to the monoclinic structure of the layered iridate, we find that these materials are orthorhombic, with lattice parameters *a* = 5.92 Å, *b* = 8.45 Å, *c* = 17.85 Å. The likely structure (shown in Figure 1B and 1C) contains two symmetry related honeycomb planes. Each Ir atom is co-ordinated by three others with D_{3h} symmetry and is locally identical to the layered system. The three dimensional nature of this structure arises because the three-fold coordinated iridium can continue a honeycomb in one plane or twist to form a honeycomb in the symmetry related plane. Perfect octahedral symmetry will constrain the angle between the honeycomb planes to cosφ₀=1/3, namely φ₀≈70°. This 70° geometry is evident in the crystalline morphology (compare Figure 1A and 1B) and is manifest in the high temperature magnetic properties. The local magnetism of the Ir can be described by two components of susceptibility χ_{//} and χ_⊥, parallel and perpendicular to each honeycomb plane (colored triangles in Figure 2A). At temperatures well above the energy scale of the dominant exchange interaction, the orthorhombic susceptibility are simple ratios of each other since they are all composed of χ_{//} and χ_⊥. The magnetic anisotropy extracted from the torque measurements, is shown in Figure 2C. We find that at sufficiently high temperature the ratio of the anisotropic susceptibilities α_{ij}/α_{ik} saturate to exactly the simple fractional values suggested by the above argument (1,1/2,-1/2).

The remarkable structure of our compound is composed of simple building blocks - a repeating pattern along the *c*-axis, one link in the same honeycomb plane (an *S*-link), followed by one that rotates to the other honeycomb plane (a *R*-link).

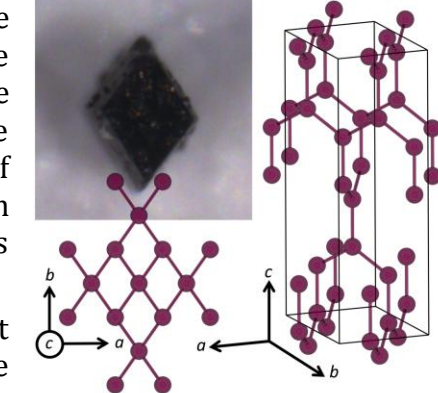


Figure 1: (A) The first single crystals of {1}-HHC. (B) and (C) the likely crystal structure showing only the Ir positions but for one Li at the center of a honeycomb plaquette [Analytis, Vishwanath, unpublished].

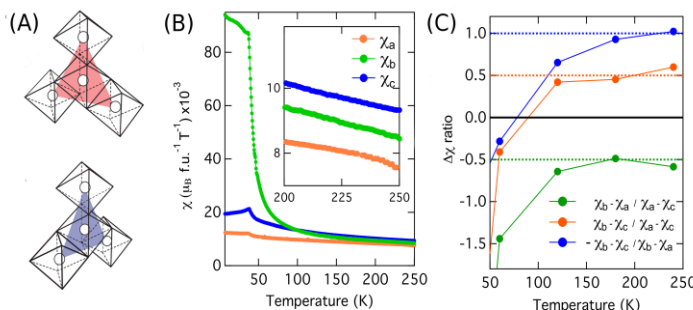


Figure 2: (A) Two HHC planar orientations which determine high T properties. (B) Magnetic susceptibility along three different crystallographic directions. (C) Magnetic anisotropy determined by torque magnetometry [Analytis, Vishwanath, unpublished].

In this compound the principle components of susceptibility tend to diverge as temperature is lowered with the inverse susceptibilities extrapolating to a negative temperature intercept, indicating predominantly antiferromagnetic exchange interactions. The spin

anisotropy of the exchange interactions leads to a large deviation from Curie-Weiss behavior, highlighted by a striking reordering of the principle components of susceptibility: α_{bc} changes sign at $T \approx 75K$. This is in stark contrast to spin-isotropic Heisenberg exchange systems where the low temperature susceptibility reflects the g-factor anisotropy observed at temperatures greater than the energy of the dominant exchange interactions. The change of sign of α_{bc} arises because χ_b softens, becoming an order of magnitude greater than χ_a . This ten fold increase χ_b is not driven by the geometry of the local iridium environment (which is constrained by our high temperature determination), and is hence evidence for highly spin anisotropic exchange.

The next important discovery that immediately followed the above structural determination is theoretical. The Kitaev model could now be applied in three-dimensions (3D) and remains solvable, yielding a 3D QSL. To our knowledge, this is the first fully 3D system with this solution. The key experimental consequence is that, unlike the two-dimensional case of the layered honeycomb, the 3D Kitaev spin liquid phase survives to finite temperatures, undergoing an entropy-driven phase transition at finite temperature to a classical paramagnet.

To understand whether the magnetic exchange pathway is indeed Kitaev-like, we consider the low temperature characteristics (Figure 2B). At $T=38K$ the system undergoes a magnetic phase transition. As this temperature is approached on cooling, the simple geometric relationship between the components of the susceptibility at high T breaks down. χ_b appears to diverge, becoming ten times larger than χ_a before it finds some long-range ordered state. This kind of anisotropy cannot be explained by an isotropic Heisenberg exchange mechanism. Indeed, comparing this direction with the crystal structure, it is apparent that the *b*-axis is associated with one specific Ir-O₂-Ir bond – just one plane where a Kitaev-like mechanism might be expected. These anisotropies are a smoking-gun for an exotic type of exchange mechanism, driven by correlations in these strongly spin-orbit coupled materials.

Future Directions

Infrared studies of spin-orbit coupled magnetism (Orenstein, Analytis, Vishwanath): One example of the physics we anticipate in these materials is the emergence of exotic magnon modes. The degree of octahedral distortion is reflected in the honeycomb planar angle ϕ_0 . A lattice softening associated with this angle would be directly related to the anisotropic magnetic mechanism – perhaps an exotic magnon mode emerging from spin-orbit coupled magnetic exchange.

Magnetic order and magnetic fluctuations (Birgeneau, Analytis, Vishwanath): A key step will be to reveal how the local moments order. This information is critical for understanding the nature the magnetism in these materials and how closely it is related to the correlated electron physics. We will perform Magnetic Resonant X-ray Scattering and Neutron scattering (available at the ALS, Argonne and Oakridge respectively) to uncover the magnetic lattice. Improvements in the synthesis will soon yield crystals large enough for inelastic neutron experiments, which can reveal the excitation spectrum of the fluctuations around the magnetic transition.

Thin-film and bulk single crystal synthesis (Ramamoorthy, Analytis, Vishwanath): Our long term goals are to synthesize different members of the {N}-HHC series. Our first strategy will be the careful tuning of our present single crystal methods to favor one phase over another. We have recently synthesized single-phase of the first $\{\infty\}$ -HHC by adjusting our flux-based growth procedures – this alone suggests other phases are likely to be stable. Our other strategy is thin film synthesis. We anticipate for example, that growing these materials on the [111] STO substrate will stabilize $\{\infty\}$ -HHC, due to the commensurability of the honeycomb lattice, while a [100] STO substrate will stabilize lower {N}-HHC phases.

Doped materials and the theory of unconventional spin-orbit magnetic metals (Analytis, Ramamoorthy, Vishwanath): Our final direction will be to synthesize doped versions of these materials. This is an exciting direction, because the octahedral distortion is directly tied to the kind of transition metal and the kind of alkali. This fact will directly influence the stability of a specific {N}-HHC phase. In addition, the addition of holes or electrons into this strongly magnetic lattice, could lead to exotic new states of matter, including topological superconductivity [Liu2012]. The properties of the new materials can then be connected to the theory of these emergent phases.

References with DOE support

- [1] Photoelectron spin-flipping and texture manipulation in a topological insulator, Chris Jozwiak, Cheol-Hwan Park, Kenneth Gotlieb, Choongyu Hwang, Dung-Hai Lee, Steven G. Louie, Jonathan D. Denlinger, Costel R. Rotundu, Robert J. Birgeneau, Zahid Hussain, and Alessandra Lanzara, *Nature Physics* 9, 293-298 (2013).
 - [2] Topological semimetal and Fermi-arc surface states in the electronic structure of pyrochlore iridates, Xiangang Wan, Ari M. Turner, Ashvin Vishwanath, and Sergey Y. Savrasov, *Phys. Rev. B* 83, 205101 (2011)
 - [3] Observation of Coherent Helimagnons and Gilbert damping in an Itinerant Magnet J. D. Koralek, D. Meier, J. P. Hinton, A. Bauer, S. A. Parameswaran, A. Vishwanath, R. Ramesh, R. W. Schoenlein, C. Pfleiderer, J. Orenstein, *Phys. Rev. Lett.* 109, 247204 (2012)
 - [4] Epitaxy-distorted spin-orbit Mott insulator in Sr₂IrO₄ thin films, C. Rayan Serrao, Jian Liu, J.T. Heron, G. Singh-Bhalla, A. Yadav, S.J. Suresha, R. J. Paull, D. Yi, J.-H. Chu, M. Trassin, A. Vishwanath, E. Arenholz, C. Frontera, J. Železný, T. Jungwirth, X. Marti, and R. Ramesh, *Phys. Rev. B* 87, 085121 (2013).
 - [5] Tuning the electronic properties of $J_{eff}=1/2$ correlated semimetal in epitaxial perovskite SrIrO₃, Jian Liu, J.-H. Chu, C. Rayan Serrao, D. Yi, J. Koralek, C. Nelson, C. Frontera, D. Kriegner, L. Horak, E. Arenholz, J. Orenstein, A. Vishwanath, X. Marti, R. Ramesh, arXiv:1305.1732
 - [6] Doping a spin-orbit Mott Insulator: Topological Superconductivity from the Kitaev-Heisenberg Model and possible application to (Na₂/Li₂)IrO₃, Yi-Zhuang You, Itamar Kimchi, Ashvin Vishwanath, *Phys. Rev. B* 86, 085145 (2012)
- Other authors' work relevant to the N-hyper-honeycomb series**
- [7] A. Yu. Kitaev, *Ann. Phys.* 321, 2 (2006)
 - [8] Yogesh Singh, S. Manni, J. Reuther, T. Berlijn, R. Thomale, W. Ku, S. Trebst, P. Gegenwart, *Phys. Rev. Lett.* 108, 127203 (2012)

Program Title: Exploring Photon-Coupled Fundamental Interactions in Colloidal Semiconductor Based Hybrid Nanostructures

Principle Investigator: Min Ouyang

Institution: University of Maryland – College Park

Email: mouyang@umd.edu

Program Scope

This new BES project (starting this year) is aimed at gaining an improved understanding of emerging fundamental photon-coupled processes at the nanoscale with particular emphasis on spin-related interfacial coupling of semiconductor by integrating various far-field time-resolved optical spectroscopy with recent materials advance of precisely tailored zero-dimensional (0D) semiconductor based hybrid nanostructures possessing different functionality. Far-field ultrafast all-optical spectroscopy is applied to probe *ensemble* spin dynamics of semiconductor and its coupling with plasmons, magnet and phonon within various pre-designed 0D hybrid nanostructures, involving Groups *II-VI* and *III-V* semiconductors that can be chemically synthesized with precisely tailored structural and physical properties.

The research work involves precise control of bottom-up novel hybrid nanoscale materials with desired coupling interactions among plasmon, magnetism and exciton, ultrafast and sensitive optical spectroscopy and instrumentation development.

Current Status

The interplay between photon and matter is the basis of many fundamental processes and various applications [1]. Harnessing light-matter or even more exotic light-matter-spin interactions can allow new underlying physical principles as well as technologies of solid-state quantum information processing: for example, the a.c. optical Stark effect (OSE) has enabled coherent quantum control schemes of exciton and spin in semiconductors, with the potential for achieving opto-quantum devices [2]. Importantly, when size of matter is reduced to nanoscale in range of Bohr radius (typically below tens of nanometers), strong quantum confinement effect starts manifesting, and their charge, spin and phonon could respond differently to external stimuli such as photon, leading to novel physical phenomena and fundamental photon coupling processes. A few progresses that are closely related to this new BES project are summarized below:

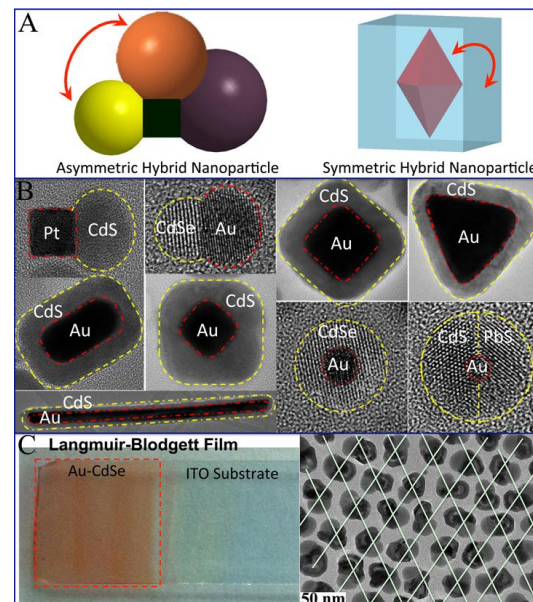


Figure 1. (A) Schematic hybrid nanostructures; (B) Exemplary hybrid nanostructures as synthesized; (C) Solid assembly of hybrid nanostructures (unpublished).

Precise Control of Hybrid Nanostructures: In order to study photon-assisted spin-coupling processes at the nanoscale, we have developed novel non-epitaxial chemical synthesis to rationally design high quality 0D hybrid nanostructures with tunability of their structure and functionality [3]. A hybrid nanostructure is defined as a well-defined nanostructure that can integrate different functional subunits (e.g., metallic, semiconducting, magnetic) with different structural symmetry (Fig.1A). As a result, this new type of nanostructures can allow to introduce and to engineer spin-related coupling from the bottom-up. Briefly, in a non-epitaxial synthesis, growth of hybrid nanostructures consisting of monocrystalline semiconductor is based on a Lewis acid-base mechanism directed cation exchange process, where the reaction is spatially confined by an amorphous matrix either surrounding core (core-shell configuration) or side-by-side anchoring to a distinct components (dumbbell configuration). Chemical thermodynamics of reaction needs to be controlled in order to provide enough positive energy for initiating and directing monocrystalline growth of semiconductor component. Because monocrystalline growth process of semiconductor is confined within an amorphous matrix that is independent of other components, it can circumvent limitations imposed by epitaxial strategies. Our non-epitaxial synthesis has been demonstrated to allow control of crystallinity, size and shape of distinct subunits in a hybrid nanostructure, with a few examples highlighted in Figure 1B [3-5]. Further importantly, we have applied different assembly approaches, such as Langmuir-Blodgett assembly, to organize and achieve nanostructure solids (Fig.1C), which can facilitate low temperature optical measurements in the project.

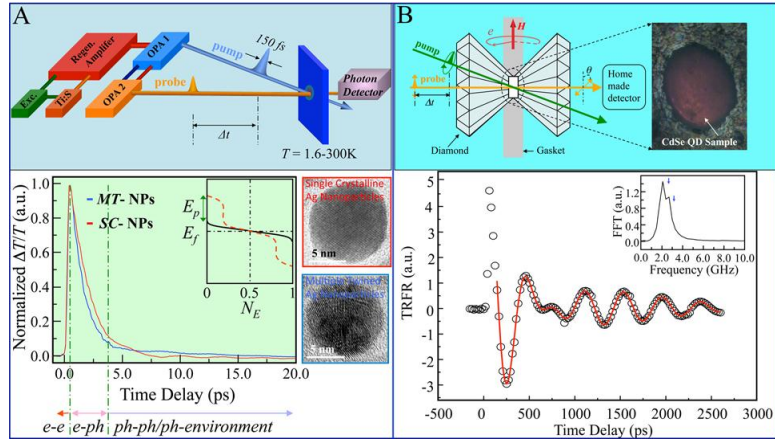


Figure 2. Ultrafast optical measurement of (A) charge and phonon dynamics of Ag nanoparticles, and (B) spin dynamics of semiconductor quantum dots under high pressure.

All optical measurement and manipulation of spin dynamics at nanoscale: In order to perform measurements of spin and spin-dependent process in ultrafast time domain, we apply an ultrafast optical orientation based technique to initialize spin polarization (spin “up” and “down” eigen-states, or their superposition states) and to measure spin evolution in a very fast time domain (femto- to nano- seconds). Such optical measurement can provide valuable information of charge and spin dynamics, including lifetime, decay length and Lande g-factors. We have demonstrated all-optical ultrafast techniques to different nanoscale systems, with two examples shown in the Figure 2 of charge and phonon dynamics of metal nanoparticles (Fig.2A) and spin dynamics of semiconductor quantum dots at high pressure (Fig.2B), respectively [6,7].

Novel light-matter-spin interactions at the nanoscale: We have combined our materials

expertise with ultrafast optical spectroscopy to explore a few new underlying physics of photon-assisted spin related process. Figure 3A and 3B illustrates our first observation of resonant plasmon-exciton coupling that is realized by finely tailoring band structures of metal and semiconductor subunits in a core-shell hybrid nanostructure [8]. A signature of plasmon-exciton coupling is the existence of a substantially red-shifted and broadened hybrid exciton peak with a long absorption tail at the low energy regime. Importantly, plasmon-exciton resonant coupling has led to a clear observation of enhanced (ac) OSE with evidence of blue shift of exciton energy under virtual excitation by a sub-resonant laser (Fig.3B). Such resonant coupling phenomena were clearly absent in a different hybrid structure of Ag-CdSe, in which localized surface plasmon resonance of Ag nanoparticles was off-resonant with exciton energy of CdSe shell. We have also demonstrated for the first time that dependence of OSE- energy shift on polarization of sub-resonant photons suggested that plasmon enhanced OSE could offer a viable mechanism for creation of a pseudo-magnetic field (H_{Stark}) (Fig.3C). This novel optical induced ultrafast pseudo magnetic field can offer a new route for coherent manipulation of exciton spin at the nanoscale at ~2K (Fig.3D).

Future Plans

This new BES project is just starting this year. In this research program, we systematically will investigate nature of new plasmon-exciton-spin resonant coupling, including roles of energy resonance, temperature and anisotropy. Enabled by plasmon-exciton-spin resonant coupling as demonstrated in the Figure 3, we will further explore all-optical spin-echo scheme with colloidal semiconductor nanostructures, which can allow a comprehensive understanding of intrinsic spin physics at the nanoscale. A few other effects, including nanoscale ferromagnetic imprinting and phonon-assisted spin dechoerence process, will be also investigated at the ensemble level.

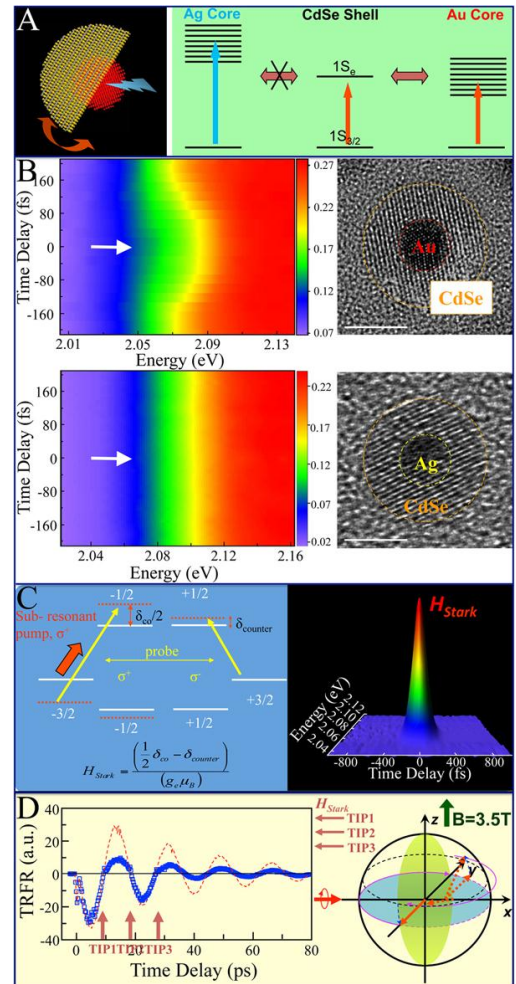


Figure 3. (A) Model of resonant plasmon-exciton coupling in a hybrid nanostructure; (B) Experimental observation of OSE in Au-CdSe via resonant plasmon-exciton coupling; OSE was not observed in off-resonant condition; (C) Ultrafast light-induced magnetic field by polarization dependent OSE; (D) Coherent spin manipulation in colloidal Au-CdSe nanostructures enabled by H_{Stark} .

References

1. J. Weiner and P.-T. Ho, Light-Matter Interaction: Fundamentals and Applications, Wiley & Sons, New York (2003).
2. D.D. Awschalom, L.C. Bassett, A.S. Dzurak, E.L. Hu and J.R. Petta, Quantum Spintronics: Engineering and Manipulating Atom-Like Spins in Semiconductors, *Science* **339**, 1174-1179 (2013).
3. J. Zhang, Y. Tang, K. Lee and M. Ouyang, Nonepitaxial growth of hybrid core-shell nanostructures with large lattice mismatches, *Science* **327**, 1634-1638 (2010).
4. K. Lee, H.Z. Bai, J.T. Zhang and M. Ouyang, Anisotropic control and mechanically driven monocrystalline growth of hybrid nanostructures, *Science* (under review, 2013).
5. L. Weng, H. Zhang, A.O. Govorov and M. Ouyang, Hierarchical synthesis of hybrid NanoOligomers and enabled hot-plasmon driven photocatalysis, *Science* (under review 2013).
6. Y. Tang, A.F. Goncharov, V.V. Struzhkin, R.J. Hemley and M. Ouyang, Spin of semiconductor quantum dots under hydrostatic pressure, *Nano Lett.* **10**, 358-362 (2010).
7. Y. Tang and M. Ouyang, Tailoring properties and functionalities of metal nanoparticles through crystallinity engineering, *Nature Materials* **6**, 754-759 (2007).
8. J. Zhang, Y. Tang, K. Lee and M. Ouyang, Tailoring light-matter-spin interactions in colloidal hetero- nanostructures, *Nature* **466**, 91-95 (2010).

Project Title: Non-Centrosymmetric Topological Superconductivity
Principal Investigator: Johnpierre Paglione
Institution: University of Maryland
Email address: paglione@umd.edu

Project Scope

Topological insulator (TI) materials are distinguished from ordinary insulators by the so-called Z_2 topological invariants associated with the bulk band structure [1]. Several intriguing and potentially technologically useful properties make the TI states of particular interest beyond fundamental curiosities. In particular, TIs possess a surface state with a Dirac electronic dispersion similar to graphene, topologically protected against localization by time-reversal-invariant (i.e. non-magnetic) disorder. Spin and momentum are perfectly coupled in the chiral TI surface state, leading to novel magnetoelectric effects and much potential for advanced applications [2,3]. Furthermore, the realization of a condensed-matter version of Majorana quasiparticles, fermions that are their own anti-particle [4], has driven an entire field of interest in coupling TI states with superconductivity. First shown by Kitaev in the context of spinless $p_x + ip_y$ superconducting quantum wire [5], the possibility of localizing Majorana fermions at the boundaries of a topological superconductor – for instance at the edges of a wire or inside a vortex core – has great potential in realizing the next generation of fault-tolerant quantum computation [6].

The major experimental efforts over the past several years have been conducted primarily these non-interacting bismuth-based “first generation” TI materials, and have focused on refining both growth and measurement techniques in order to detect signatures of surface states. Large families of new topological materials are waiting to be discovered in small-gap semiconductor systems and semimetals with high-Z elements [7], and true materials exploration is the only route to finding them. To move beyond the problems of the first generation of TI materials, a new approach is absolutely necessary to overcome the current physical, chemical and materials science problems. This Proposal outlines a unique research program focused on the synthesis, characterization and optimization of a new family of topological superconductors to help elucidate the scientific and technological potential of this second generation of topological insulator materials, as well as provide new routes to realizing exotic phenomena such as Majorana fermion physics. We have identified a new family of superconducting topological insulator compounds in the ternary half-Heusler system (Fig. 1) that not only show promise to realize TI states in stable, stoichiometric materials, but also to combine non-trivial topologies of both electron band structure and odd-parity superconducting states to produce a truly new realm of topological materials. Combining this with intrinsic coupling to collective modes such as magnetism and superconductivity, these materials hold great promise for harboring new and exotic electronic states that couple the traditional symmetry-breaking phases of condensed matter with exotic topologically classified states.

A non-trivial band structure that exhibits band ordering analogous to that of the known 2D and 3D TI materials was predicted in a variety of 18-electron half-Heusler compounds using first principles calculations [8,9]. The band structures of these compounds are very sensitive to the electronegativity difference of the constituents, resulting in semiconducting band gaps that can vary from zero (LaPtBi) to 4 eV (LiMgN) [8]. A subset of these compounds possess an inverted band structure, with the top of an s -type orbital-derived valence band lying below a p -type conduction band, with both centered at the high-symmetry Γ point and with no other bands crossing the Fermi level elsewhere in the Brillouin zone. Because such a band inversion changes the parity of the wavefunction, it provides the proper condition

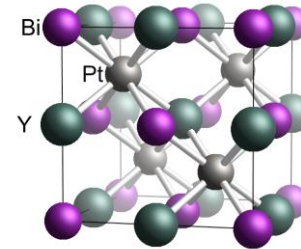


Figure 1: non-centrosymmetric nature of half-Heusler structure, shown for YPtBi .

for the TI state, yielding a handy indicator of the potential for specific compounds to be TIs. This can be quantified by calculating the band structure and measuring the degree of band inversion, shown as the separation in energy between bands with Γ_6 and Γ_8 symmetries. Plotting as a function of lattice constant or spin-orbit coupling strength (represented by nuclear charge) as shown in Figure 2, reveals a sensitive tuning of band inversion present in a host of these ternary half-Heusler materials. With the ability to tune the energy gap and set the desired band inversion by appropriate choice of compound with appropriate hybridization strength (i.e., lattice constant) and magnitude of spin-orbit coupling (i.e., nuclear charge), the half Heusler family shows much promise for realizing the next generation of TI materials.

Superconductors are among the most fascinating systems for realizing topological states, either via a proximity effect, or intrinsically via an odd-parity, time-reversal-invariant pairing state. Alongside the usual signature supercurrents arising from Cooper pair coherence, a direct analogy exists between superconductors and insulators: since the Bogoliubov-de Gennes (BdG) Hamiltonian for the quasiparticles of a superconductor is essentially analogous to that of a band insulator, one can consider the interesting possibility of TI surface states arising due to a superconducting “band gap”. Similar to TI systems, a topological superconductor (TSC) thus has a fully gapped bulk band structure and gapless surface Andreev bound states. Thus the search for TSCs in materials with strong band inversion is a promising direction. In the case of time-reversal-invariant (centrosymmetric) systems, a material is a TSC if it is an odd-parity, fully gapped superconductor and its Fermi surface encloses an odd number of time-reversal-invariant momenta in the Brillouin zone [10].

Superconductors without inversion symmetry, or non-centrosymmetric superconductors, promise a much more robust route to realizing TSC states. With inversion symmetry being one of two key symmetries for Cooper pairing (time reversal being the other), its absence has profound implications on the formation of Cooper pairs. With a non-trivial topology of the Bogoliubov quasiparticle wavefunction resulting in protected zero-energy boundary states analogous to those of TI systems, the promise of TSC in NC superconductors is very strong. With strong band inversion, the RPtBi and RPdBi ternary half-Heusler compounds are candidate TI systems as explained above. As NC superconductors, they also have the potential to harbor mixed-parity states and are therefore unique in that they are simultaneously both TI and TSC candidate systems.

Recent Progress

We have recently begun to explore the family of rare earth-bismuthide half-Heusler compounds, synthesizing high-quality crystalline specimens (Fig. 3) and fully characterizing their normal, superconducting and magnetic states in an effort to reveal their potential for realizing the next generation of topological insulators and superconductors. In addition to ongoing work on the RPtBi series, preliminary work on the Pd-based version of this compound has revealed another family of superconducting compounds in the RPdBi (R=La to Lu) series. These include non-metallic transport, low

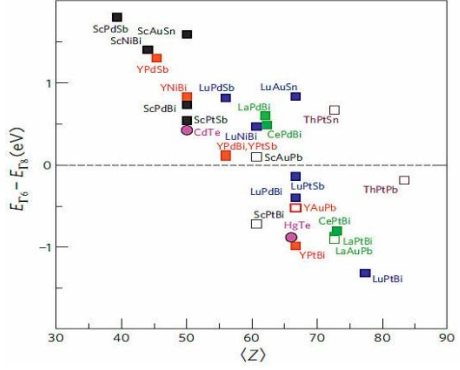


Figure 2: Calculated band inversion strength in ternary half-Heusler compounds plotted as a function of spin-orbit coupling strength, represented by average nuclear charge $\langle Z \rangle$ (from [8]).

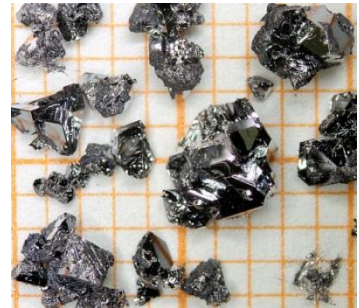


Figure 3: single-crystal synthesis of the RPdBi series grown via flux techniques.

carrier densities, unconventional magnetoresistance, magnetism and superconductivity. We have just begun to explore this family of materials, revealing a host of interesting properties that span several traditional areas of interest: unconventional superconductivity, low-carrier density metals, topological insulators and the newly combined field of topological superconductivity. Preliminary measurements on the RPtBi and RPdBi series of compounds have been performed down to 20 mK temperatures, and include resistivity, AC susceptibility and heat capacity. Intriguingly, our preliminary results on the RPdBi compounds indicate that superconductivity in this series onsets at a higher transition temperature than in the Pt-based series as shown 4 for LuPdBi (Fig. 4), which enters the superconducting state at $T_c = 1.6$ K. Furthermore, superconductivity may coexist with long-range magnetic order, as determined by neutron scattering experiments on TbPdBi (Fig. 4), which undergoes an antiferromagnetic ordering transition near 2 K before entering a superconducting state at a lower temperature of 1.6 K. These results have been confirmed by AC susceptibility measurements and continue to be probed by specific heat measurements, which are challenging owing to extremely low carrier densities ($\sim 10^{18}$ cm $^{-3}$).

Future Plans

We plan to explore the unusual normal and superconducting state properties of this family of compounds to understand the nature of the normal and superconducting states, using our full arsenal of probes in combination with a systematic growth program aimed at comparing properties of the RPtBi series. The peculiar normal state properties will be studied by probing their sensitivity to crystalline and sample surface quality by using different growth and treatment techniques (flux/melt growth, Bridgman temperature gradient growth, arc melting growth, annealing, acid etching, high-temperature quench, etc.). Furthermore, with the availability of various rare earth substituents at our disposal, we plan to substitute varying amounts of magnetic and non-magnetic rare earth elements (e.g., $Y_{1-x}R_xPtBi$) to study the effects of magnetic impurities on both the TI surface states as well as the superconducting state. Pushing the limits of valence stability will be pursued by aliovalent chemical substitutions in different positions of the unit cell, for instance substituting small amounts of Ti^{4+} for Y^{3+} will allow for controlled study of electron doping and its effect on the normal state, superconducting and topological surface state properties.

Future experiments will include neutron scattering measurements to refining the structure of lattice and magnetic order, as well as the energy landscape (i.e. crystal field levels) in order to fully understand the role of magnetism in the RPtBi and RPdBi series. We plan to continue work with Nuh Gedik (MIT), who has recently developed a unique ARPES setup to both characterize novel TI materials and study the dynamical coupling between charge and spin degrees of freedom. Work with H. Dennis Drew (UMD) will measure the THz cyclotron resonance in these materials to determine charge densities, carrier type and effective masses of the bulk and surface state carriers. Work with Ruslan Prozorov (Iowa State/Ames) will continue a series of penetration depth measurements on the RPtBi series using the tunnel-diode resonator technique to determine the unconventional nature of the superconducting state.

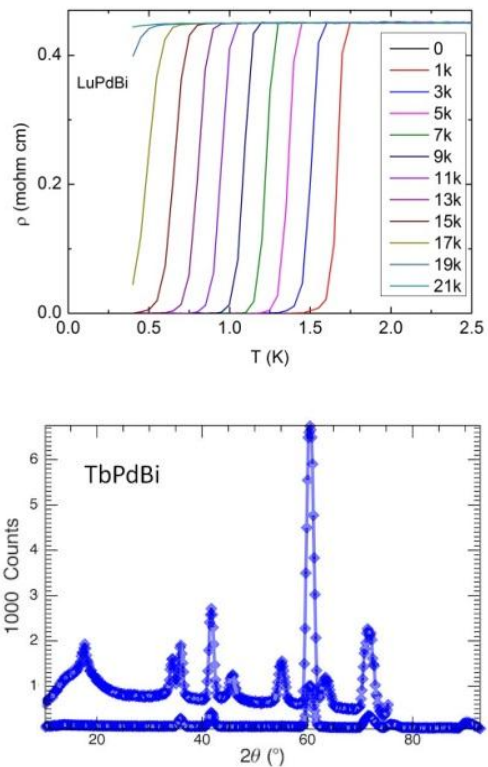


Figure 4: superconductivity in LuPdBi (top), and preliminary neutron diffraction data for TbPdBi with magnetic order [unpublished].

References

1. C. L. Kane and E. J. Mele, "Z2 Topological Order and the Quantum Spin Hall Effect," Phys. Rev. Lett. 95, 146802 (2005); L. Fu and C. L. Kane, "Time reversal polarization and a Z2 adiabatic spin pump," Phys. Rev. B 74, 195312 (2006).
2. J. E. Moore, "The birth of topological insulators," Nature 464, 194 (2010).
3. M. Z. Hasan and C.L. Kane, Topological insulators, Rev. Mod. Phys. 82, 3045 (2010); X.-L. Qi and S.-C. Zhang, Topological insulators and Superconductors, Rev. Mod. Phys. 83, 1057 (2011).
4. F. Wilczek, "Majorana returns," Nature Phys. 5, 614 (2009).
5. A. Y. Kitaev, "Unpaired Majorana fermions in quantum wires", Phys.-Usp. 44, 131 (2001).
6. C. Nayak, S. H. Simon, A. Stern, M. Freedman, S. Das Sarma, "Non-Abelian anyons and topological quantum computation," Rev. Mod. Phys. 80, 1083 (2008).
7. B. Yan, S.-C. Zhang, "Topological Materials," Rep. Prog. Phys. 75, 096501 (2012).
8. S. Chadov, X. Qi, J. Kübler, G. H. Fecher, C. Felser, S. C. Zhang, "Tunable multifunctional topological insulators in ternary Heusler compounds," Nature Mater. 9, 541 (2010).
9. H. Lin, L. A. Wray, Y. Xia, S. Xu, S. Jia, R. J. Cava, A. Bansil, M. Z. Hasan, "Half-Heusler ternary compounds as new multifunctional experimental platforms for topological quantum phenomena," Nature Mater. 9, 546 (2010); D. Xiao, Y. Yao, W. Feng, J. Wen, W. Zhu, X.-Q. Chen, G. M. Stocks, Z. Zhang, "Half-Heusler Compounds as a New Class of Three-Dimensional Topological Insulators" Phys. Rev. Lett. 105, 096404 (2010); W. Feng, D. Xiao, Y. Zhang, Y. Yao, "Half-Heusler topological insulators: A first-principles study with the Tran-Blaha modified Becke-Johnson density functional," Phys Rev B 82, 235121 (2010); W. Al-Sawai, H. Lin, R. S. Markiewicz, L. A. Wray, Y. Xia, S.-Y. Xu, M. Z. Hasan, A. Bansil, "Topological electronic structure in half-Heusler topological insulators," Phys Rev B 82, 125208 (2010).
10. L. Fu, E. Berg, "Odd-Parity Topological Superconductors: Theory and Application to Cu_xBi₂Se₃", Phys. Rev. Lett. 105, 097001 (2010).

Publications

This project commenced in September 2013, so there are as of yet no publications stemming from this funding.

Program Title: Quantum Electronic Phenomena and Structures

Principle Investigator: W. Pan; Co-PIs: M.P. Lilly, J.L. Reno, G.T. Wang, R.

Prasankumar, E.A. Shaner, and D.C. Tsui

Mailing Address: P.O. Box 5800, MS 1086, Sandia National Labs, Albuquerque, NM 87185

E-mail: wpan@sandia.gov

Program Scope

An important goal of nanoscience and nanotechnology is to take novel quantum behaviors occurring at the nanoscale and propagate them upward into the macroscopic realm. Thus, it is necessary to probe and understand the quantum electronic phenomena not just at the macroscopic scale, but more deeply at the nanometer scale which is governed by the laws of quantum mechanics.

The focus of this project is to study the physics of novel quantum electronic phenomena, induced by strong electron-electron interactions and the interplay between electron and disorder interactions, in low dimensional quantum systems. The project includes ongoing research in quantum transport studies, electron dynamics, ultrafast optical studies in single nanowires, and high quality nanostructure materials growth. New exciting directions, such as the impact of disorder in many-body ground states, topological properties in strong spin-orbit coupling systems, quantum dopant effect in high quality Si electron systems, and electron dynamics in graphene systems, will be explored. The research topic presented in this program is at the frontier of the field of condensed matter physics, integrates well with the expertise and interests of the participating personnel and institutions, and further extends their work in exciting new directions.

The research activities are categorized in three synergistically integrated tasks. **Task 1, Quantum Transport in Structured Semiconductors**, seeks to nano-engineer new types of quantum electronic structures and to discover and understand novel collective electron states and their quantum properties in low-dimensional systems. The ability to investigate electron physics at the nanometer scale that occurs due to strong electron-electron and electron-disorder interactions will undoubtedly yield new discoveries and new understanding. **Task 2, Electronic and Optical Properties in III-Nitride Nanowires**, seeks to probe novel quantum electronic and optical phenomena in freestanding III-nitride (III-N) based heterostructured nanowires. GaN/AlGaN based core-shell nanowires will serve as a key materials platform for this task. InN based nanowires will also be investigated in the context of spin-orbital coupling properties. Key to achieving our research goals is our top-down nanowire fabrication process, newly developed during our last three-year budget period, which gives us the capability to fabricate heterostructure nanowires with a high degree of control over the nanowire dimensions, material quality, growth orientation, doping, composition, and layer thicknesses. This capability, unique to Sandia, will allow us to explore high quality, novel heterostructure nanowires not easily realized by standard bottom-up nanowire synthesis methods. The long term vision of **Task 3, Electron Dynamics of Low Dimensional Quantum Systems**, is to seek new phenomena and to understand the frequency and time domain dynamics of charge transport in many types of clean low-dimensional quantum correlated systems.

Recent Progress

Non-Abelian quantum Hall physics: Spin transition in the fractional quantum Hall liquids in the second Landau level (Papers #5 and 13).

Background

The non-Abelian fractional quantum Hall effect (FQHE) states have attracted a great deal of current interest due to their potential application in topological quantum computation. Extensive research has been carried out to examine non-Abelian statistics and probe their exotic properties in the most celebrated non-Abelian FQHE state, the 5/2 state. Recent theoretical developments have identified possible non-abelian ground state in several fractional quantum Hall states that have been extensively studied for years, for example, the 8/3 state in the second Landau level. This is expected to open a new chapter in our understanding of the fractional quantum Hall effect and could impact topological quantum computation. In light of this new theoretical development, we believe that systematic research on the 8/3 state should be revisited. The outcome may have important impact on our understanding of non-Abelian physics. Besides the 8/3 state, some quantum Hall states in the lowest Landau level, for example, the 3/8 and 4/11 states, are also believed to be non-Abelian and their properties may be more exotic than that of the 5/2 state.

Results and Discussions

Unlike the odd-denominator FQHE state in the first Landau level, where most of them are well understood within the picture of either the hierarchical model or weakly-interacting CF model, the nature of the odd-denominator FQHE states in the second Landau level remains largely unsettled. On the other hand, it can be expected that a deep understanding of the FQHE in the second Landau level will lead to much exciting many-body physics.

In a recent experiment, we studied the spin polarization of the 7/3 and 8/3 states as a function of electron density (n). Figure 1a shows the R_{xx} trace at an electron density of $n=0.77 \times 10^{11} \text{ cm}^{-2}$. Well-developed FQHE is observed at $v=5/2$ at a low magnetic field of $\sim 1.3\text{T}$. Figure 1b shows the density dependence of the 8/3 energy gap. It is observed that in the density range between 0.5×10^{11} and $3 \times 10^{11} \text{ cm}^{-2}$, the energy gap of the 8/3 state ($\Delta_{8/3}$) first decreases with increasing density, nearly disappears at $n \sim 0.8 \times 10^{11} \text{ cm}^{-2}$. Beyond this density, $\Delta_{8/3}$ increases with increasing density. This density dependence of $\Delta_{8/3}$ clearly signals a spin transition at this filling factor. For comparison, the energy gap of the 7/3 state ($\Delta_{7/3}$) shows a monotonic density dependence (not shown here), supporting a spin polarized state down to $0.5 \times 10^{11} \text{ cm}^{-2}$. Results from this work were published in Phys. Rev. Lett. [Paper #5].

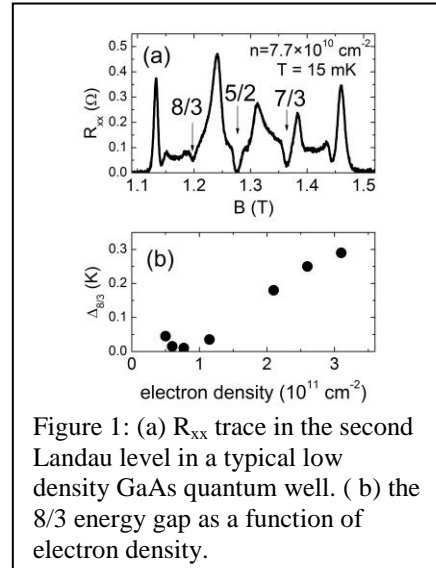


Figure 1: (a) R_{xx} trace in the second Landau level in a typical low density GaAs quantum well. (b) the 8/3 energy gap as a function of electron density.

The observation of a spin transition at 8/3 is unexpected. It has been theoretically argued that the 8/3 state should remain spin polarized even at vanishingly small Zeeman energy. This is because the more repulsive effective interactions in the second Landau level force electrons to occupy the maximum spin state. Our results now clearly show that the Zeeman energy, which was

considered unlikely to be relevant, does play an import role in the ground states in the second Landau level. More experimental and theoretical studies are needed to examine whether the 8/3 state is a two-component non-Abelian state or a boundary state between the Abelian and non-Abelian states.

Future Plans

For the 8/3 state, we plan to carry out edge tunneling experiments in quantum point contact devices and, possibly, interference measurements in quantum cavity devices. These types of measurements should allow us to obtain the effective charge of the quasi-particles of the 8/3 state and its interaction parameter. Comparison between the experimentally measured values with theoretical prediction should allow us to gain a better understanding of this unique state. We also plan to study magneto-resistance fluctuations in narrow channels in the FQHE regime in the second Landau level. This experimental technique has been widely used in the past to study the FQHE in the lowest Landau level. To our knowledge, it is for the first time that this technique is proposed to the FQHE states in the second Landau level. It can be expected that this experiment should also be able to provide useful information on the quasi-particles of the FQHE states in the second Landau level.

Research on the 3/8 and 4/11 states (as shown in Figure 2) is sparse, partially due to two conflicting requirements in a quantum Hall device, i.e., low electron density (due to the limitation in magnetic field) and high electron mobility (which tends to be lower at low electron density). Now, this hurdle has been overcome by Loren Pfeiffer at Princeton, who has successfully grown high quality and low density GaAs quantum wells. Indeed, in a recent study of the spin transition in the 8/3 fractional quantum Hall effect, well developed FQHE was observed at $v=8/3$, $5/2$, and $7/3$ in the second Landau level at a very low density of $4 \times 10^{10} \text{ cm}^{-2}$. With those high quality, low density samples, we plan to revisit the 4/11 and 3/8 state in these newly grown quantum wells, utilizing Sandia's dilution refrigerator (with a base temperature of 10mK) cooling, the nuclear demagnetization refrigerator cooling and in-situ sub-milliKelvin sample rotating in Gainesville by collaborating with research staff at the high B/T facility. Our main goal is to provide clear experimental verification whether these two states are indeed a candidate of anti-Pfaffian pairing of composite fermions (CFs) in the lowest Landau level. To this goal, we will examine whether these two states are spin polarized, predicted in the p-wave pairing theory of CF's. We propose the following two experiments in which the spin state of a FQH liquid can be revealed through the competition between the Coulomb energy E_c and Zeeman energy E_z of the 2D system: 1) tilt magnetic field dependence at nuclear demagnetization refrigerator temperatures; 2) density evolution of 4/11 and 3/8 states.

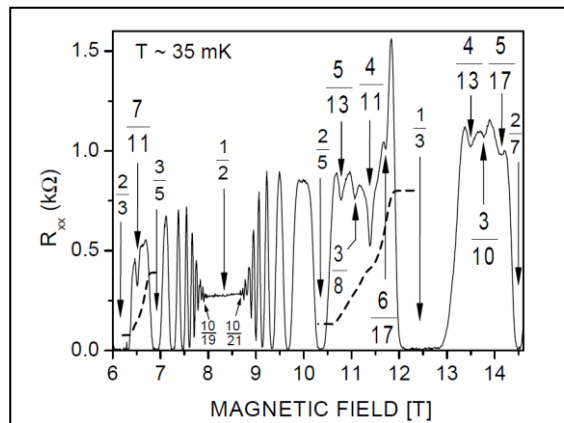


Figure 2: R_{xx} in the regime of $2/3 > v > 2/7$ at $T \sim 35 \text{ mK}$. Major fractions are marked by arrows. Dashed traces are the Hall resistance R_{xy} around $v = 7/11$ and $v = 4/11$.

FY 2012 and 2013 Journal Publications:

- 1) Nonlinear transport in a two-dimensional electron gas with a periodically modulated potential, S.K. Lyo and W. Pan, Phys. Rev. B **84**, 195320 (2011).
- 2) Quantitative examination of the collapse of spin splitting in the quantum Hall regime, W. Pan, K.W. Baldwin, K.W. West, L.N. Pfeiffer, and D.C. Tsui, Phys. Rev. B **84**, 161307 (2011).
- 3) Coulomb drag in vertically integrated one-dimensional quantum wires, D. Laroche, G. Gervais, M. P. Lilly and J. L. Reno, Nature Nanotechnology **6**, 793 (2011).
- 4) The influence of radial heterostructuring on carrier dynamics in gallium nitride nanowires, A. Kar, Q. Li, P. C. Upadhyay, M. A. Seo, J. Wright, T. S. Luk, G. T. Wang, R. P. Prasankumar, Appl. Phys. Lett. **101**, 143104 (2012).
- 5) Spin Transition in the $\nu=8/3$ Fractional Quantum Hall Effect, W. Pan, K.W. Baldwin, K.W. West, L.N. Pfeiffer, and D.C. Tsui, Phys. Rev. Lett. **108**, 216804 (2012).
- 6) Transmission line theory of collective plasma excitations in periodic two-dimensional electron systems: finite plasmonic crystals and tamm states, Greg Aizin and G. C. Dyer, Phys. Rev. B **86**, 235316 (2012).
- 7) Chaotic Quantum Transport near the Charge Neutrality Point in Inverted Type-II InAs/GaSb Field-Effect Transistors, W. Pan, J.F. Klem, J.K. Kim, M. Thalakulam, M.J. Cich, and S.K. Lyo, Appl. Phys. Lett. **102**, 033504 (2013).
- 8) Quantum control of a Landau-quantized two-dimensional electron gas in a GaAs quantum well using coherent terahertz pulses, T. Arikawa, X. Wang, D.J. Hilton, J.L. Reno, W. Pan, J. Kono, Phys. Rev. B **84**, 241307 (2011).
- 9) Tuning the Surface Charge Properties of Epitaxial InN Nanowires, S. Zhao, S. Fathololoumi, K. H. Bevan, D. P. Liu, M. G. Kibria, Q. Li, G. T. Wang, H. Guo, Z. Mi, Nano Lett. **12**, 2877 (2012).
- 10) Understanding the role of Si doping on surface charge and optical properties: Photoluminescence study of intrinsic and Si-doped InN nanowires, S. Zhao, Z. Mi, M. G. Kibria, Q. Li, G. T. Wang, Physical Review B **85**, (2012).
- 11) Understanding ultrafast carrier dynamics in single quasi-one-dimensional Si nanowires, M. A. Seo, S. A. Dayeh, P. C. Upadhyay, J. Martinez, B. S. Swartzentruber, S. T. Picraux, A. J. Taylor, and R. P. Prasankumar, Appl. Phys. Lett. **100**, 071104 (2012).
- 12) Mapping carrier diffusion in single silicon core-shell nanowires with ultrafast optical microscopy, M. A. Seo, J. Yoo, S. A. Dayeh, S. T. Picraux, A. J. Taylor, and R. P. Prasankumar, Nano Lett. **12**, 6334 (2012).
- 13) Spin polarization of the $\nu=12/5$ fractional quantum Hall state, C. Zhang, H. Chao, J.S. Xia, N.S. Sullivan, W. Pan, K.W. Baldwin, K.W. West, L.N. Pfeiffer, and D.C. Tsui, Phys. Rev. B **85**, 241302 (2012).
- 14) Inducing an Incipient Terahertz Finite Plasmonic Crystal in Coupled Two Dimensional Plasmonic Cavities, G. C. Dyer, G. R. Aizin, S. Preu, N. Q. Vinh, S. J. Allen, J. L. Reno, and E. A. Shaner, Phys. Rev. Lett. **109**, 126803 (2012).
- 15) Fractional quantum Hall effect of two-dimensional electrons in high mobility Si/SiGe field-effect transistors, T.M. Lu, W. Pan, D.C. Tsui, C.H. Lee, C.W. Liu, Phys. Rev. B **85**, 121307 (2012).
- 16) Magnetoplasmons in quasineutral epitaxial graphene nanoribbons, J.M. Pumirol, W. Yu, X. Chen, C. Berger, W.A. de Heer, M.L. Smith, T. Otha, W. Pan, M.O. Goerbig, D. Smirnov, and Z. Jiang, Phys. Rev. Lett. **110**, 246803 (2013).

Program Title: Magnetic Nanostructures and Spintronic Materials

Principle Investigator: Michael Pechan

**Mailing Address: 620 E. Spring Street, 17 Culler Hall, Miami University, Oxford, OH
45056-3653**

E-mail: pechanmj@muohio.edu

Program Scope

Nanoscale systems are the basis for a wealth of novel phenomena in condensed matter magnetism. Of particular significance are effects arising from epitaxial and otherwise laterally constrained systems, which include spintronic systems, exchange biased structures and patterned nano-structures. In all such systems ferromagnetic resonance is becoming an increasingly significant probe of anisotropy and magnetic relaxation. For example, both anisotropy and relaxation of the magnetization to equilibrium are key parameters in recording technology and knowledge of anisotropy, precession frequency and damping are crucial in the development of devices based upon spin torque phenomena. Pechan's group explores magnetodynamics and magnetostatics in spintronic related materials, coupled nanostructures, bio-related nanoparticles and single crystal transition metals. A more powerful and sensitive microwave source has been installed for the technique of ferromagnetic resonance. Pechan works in collaboration with scientists from other universities and industrial and national laboratories.

Recent Results

Tunable Resonance in Nanoscale Multilayers

Recently, in collaboration with Eric Fullerton at UCSD, we reported remarkable resonance tunability in Fe films (thickness 2, 4 and 6 nm) sandwiched between Co/Pd multilayers with strong perpendicular magnetic anisotropy. The films were grown by dc magnetron sputtering with the following structures: Ta₄/Pd₄[Co_{0.3}/Pd_{0.7}]_{x5} Fe_x/Pd_{0.7} [Co_{0.3}/Pd_{0.7}]_{x5}Ta₄, where the thicknesses are in nm. Magnetization measurements (not shown) reveal the overall in-plane anisotropy, but with an out-of-plane component strongly dependent upon Fe thickness. Ferromagnetic resonance (FMR) measurements were made on a broadband co-planar waveguide with field applied normal to the film plane at frequencies ranging from 2 to 16 GHz. As seen in Fig. 1, resonant fields varied linearly with frequency three for the samples when measured above the saturation field. All have approximately the same slope (400 Oe / GHz) indicative of a well-defined Fe resonance. For an isolated Fe layer the expected zero frequency intercept will be the shape anisotropy field ($4\pi M_s$). However the measured field intercepts decreases dramatically with decreasing Fe thickness. The lower field intercepts for the thinner Fe layers indicates the presence of an out-of-plane effective field (or anisotropy) arising from the interfacial coupling that is counteracting the shape anisotropy. The interfacial coupling or exchange is given by $J_{\text{exchange}} = 2\pi M_s(M_s - H_{\text{intercept}})d_{\text{Fe}}$, the value of which is a rather large 3.4 erg/cm² in this system and is the source of the significant resonance tunability.

Spintronic Materials In collaboration with Casey Miller at the University of South Florida, we are investigating the temperature dependence of spin polarized Fe₃O₄ epitaxially grown on (100) MgO substrates with an overlayer of Ag. The Fe₃O₄ layers were fixed at 350 nm thick, while the Ag thicknesses ranged from 0 to 500 nm. FMR measurements at 9.2 GHz were carried out with the sample film normal to the applied magnetic field in the temperature range 30 to 295 K. The focus of the investigation is spin damping and pumping, which is reflected in the FMR linewidth. Linewidths for all samples remain fairly constant with decreasing temperature until the Verwey transition ($T_V \sim 110$ K), below which damping increases dramatically (Fig. 2). The abrupt transition at the expected temperature confirms the optimal stoichiometry in these thin film samples. At and below T_V the Ag manifests its strongest influence. As shown in the Figure, the rate of change in the linewidth and its ultimate low temperature value vary dramatically with Ag overlayer thickness, reaching peak value at approximately 100 nm. While not yet fully understood, this phenomena shows promise to for probing the spin pumping in Fe₃O₄ and magnetodynamics associated with perplexing nature of the Verwey transition itself.

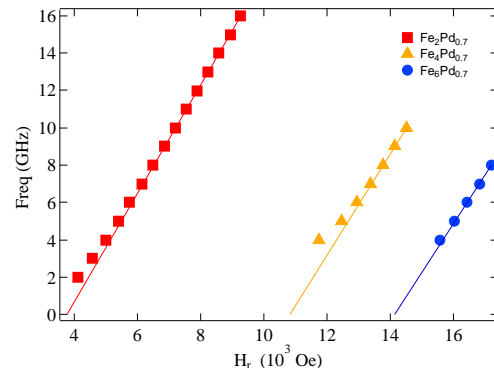


Fig. 1. Field/frequency dispersion for samples measured. Magnetic field is applied normal to the film surface.

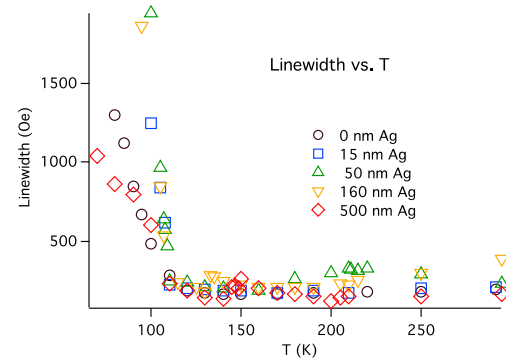


Fig. 2. Fe₃O₄ linewidth vs. temperature and Ag thickness.

Developing Work and Future Plans

Spin Polarized Heuslers We are investigating anisotropy and spin damping in the Heusler alloy Co₂MnSi in collaboration with Chris Palmstrom's group at UC – Santa Barbara. The Heusler films ($x = 3, 5$ and 10 nm) are grown epitaxially on GaAs (100) with an 8 nm ScErAs buffer layer and a 2 nm Al cap layer. Two additional samples were measured, one with 5 nm of Cr between the Heusler and the Al and another with 2 nm of MgO separating 5 and 10 nm of the Heusler. Preliminary results are shown in Fig. 3, where one clearly observes the expected 4-fold symmetry. Interesting to note is the dependence of both the in-plane anisotropy amplitude and out-of-plane effective anisotropy (mean of the 4-fold oscillation) upon Heusler thickness. We also observed well resolved double resonance for the Heusler films separated by MgO, which is promising as a method for investigating coupling. Based upon these results, additional samples are being prepared for further study.

Hard/Soft, Shell/Core Nanoparticles We are collaborating with Josep Nogues from Barcelona on Mn₃O₄/Fe₃O₄, core/shell nanoparticles. FMR measurements are being done at both 9 and 35 GHz on these powdered samples. Preliminary results clearly show the effect of the hard Mn₃O₄ ordering (~ 40 K) on the resonance field. Figure 4 shows the deviation from room temperature resonances for core/shell samples, as well as a pure Fe₃O₄ sample for comparison. We are continuing with the measurements to ascertain the nature of the core/shell coupling.

Magnetostatics and Magnetodynamics in Transition Metal Thin Films We have two projects involving epitaxial transition metal films. The first is on single crystal Ni grown on (110) and (100) MgO in collaboration with Caroline Ross and Carl Thompson at MIT. Here we are investigating the effects of system strain on the highly magnetostrictive Ni and its relation to dewetting as reported by Thompson's group in *Acta Materialia* (2010). Second we are investigating damping effects in relation to transport in single crystal Fe in collaboration with Dan Dahlberg at the University of Minnesota. Preliminary FMR on sputtered films show great epitaxy and signal strength, but less than ideal damping data.

CoO/ZnO Multilayers Discussions with Frances Hellman at UC – Berkeley resulted in my group making FMR measurements on electron mediated oxide multilayers [PRL 110, 087206 (2013)]. Resonances observed thus far are weak and quite broad indicating very short magnetic relaxation times. Further studies will be necessary to determine if this is intrinsic or arises from inhomogeneities.

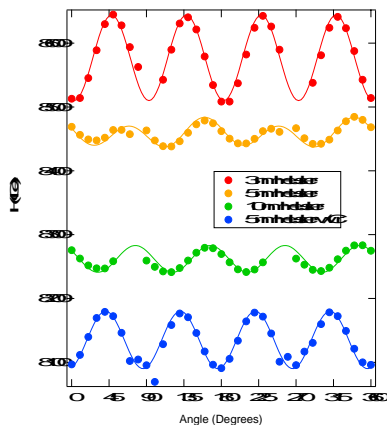


Fig. 3. FMR resonance fields as a function of in-plane angle.

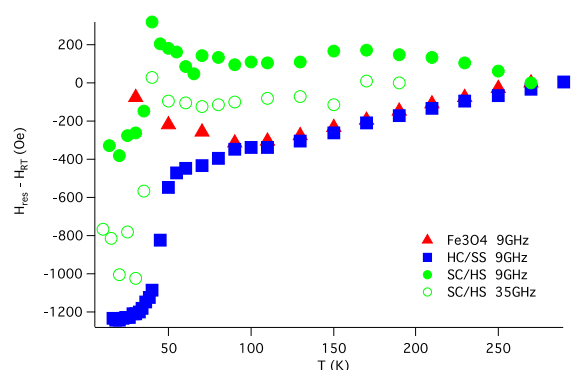


Fig. 4. Core/shell FMR field relative to room temperature values at both 9 and 35 GHz. Fe₃O₄ nanoparticle sample included for reference.

References (which acknowledge DOE support)

1. “Tunable resonant properties of perpendicular anisotropy [Co/Pd]/Fe/[Co/Pd] multilayers”, Jian Dou, Michael J. Pechan, E. Shipton, N. Eibagi and E. E. Fullerton. *J. Appl. Phys.*, **113**, 17C115 (2013).
2. “Exchange-coupling modified spin wave spectra in the perpendicularly magnetized permalloy nanodot chain arrays”. Jian Dou, Sarah C.Hernandez *, Chengtao Yu, Michael J. Pechan, Liesl Folks, Jordan A Katine, Matthew J.Carey. *J. Appl. Phys.* **107**, 09B514 (2010).
3. “Enhancing remote controlled heating characteristics in hydrophilic magnetite nanoparticles via facile co-precipitation”. Reynolds A. Frimpong, Jian Dou, Michael Pechan and J.Z. Hilt. *J. Magn. Magn. Mat.* **322** 326–331 (2010).
4. “Mechanisms of exchange bias in $\text{DyFe}_2/\text{YFe}_2$ exchange-coupled superlattices”. M. R. Fitzsimmons, C. Dufour, K. Dumesnil, Jian Dou and Michael Pechan. *Phys. Rev. B* **79**, 144425 (2009).
5. “Exchange-coupled suppression of vortex formation in permalloy nanodot chain arrays”. Sarah Hernandez, Jian Dou, Chengtao Yu, Michael Pechan, Liesl Folks, Jordan Katine and Matthew Carey. *J. Appl. Phys.* **105**, 07C125 (2009).

Program Title: Artificially Structured Semiconductors to Model Novel Quantum Phenomena

Principal Investigator: A. Pinczuk; Co-PIs: S.J. Wind and V. Pellegrini

Mailing Address: Department of Physics, Columbia University, New York, NY 10027

E-mail: ap359@columbia.edu

Program Scope

In this project we seek the design and exploration of novel collective electron states in controllable artificial structures that are realized in semiconductor quantum heterostructures by advanced nanofabrication methods. Beyond the challenges in fabrications, we strive to uncover new collective states of strongly interacting electrons in artificial potential energy patterns of tunable geometry.

The fabricated devices belong to a class of scalable quantum simulators of novel quantum states in which the main actors are many electron systems in high quality semiconductor structures. The primary goals of these studies seek to reveal striking interplays between fundamental electron interactions and geometrical constraints (topology). These interactions should be venues for novel quantum states that could, eventually, lead to new device concepts. To achieve milestones in this research we strive to advance the state-of the-art of nanofabrication of patterns superimposed on semiconductors. The honeycomb topology, or ‘artificial graphene’ (AG), is a benchmark of the proposed research [1,2]. In AG lattices an assembly of quantum dots are in a honeycomb pattern so that electron entanglement occurs via inter-dot interactions. AG should support Dirac fermions with interactions that are tunable by design and by external fields. Recent experimental results obtained by us from honeycomb patterns defined on two-dimensional electron gases (2DEGs) in GaAs structures offer exciting evidence that AG structures can be realized in the laboratory [2,3]. These seminal results reveal unique low-lying collective excitations, such as ‘anomalous spin waves’, in spectra of inelastic light scattering [3].

In this project we aim at the uncovering of novel quantum behavior and phases of electrons that emerge in semiconductor structures designed and fabricated with ‘exquisite’ precision. The preliminary and initial studies have focus on the construction of lattices with honeycomb symmetry. We seek here to achieve electron systems that display the linearly dispersing energy states that characterize Dirac fermions. Reaching this milestone leads to research goals that we describe as creation and study of “fermion quantum fluids in a semiconductor chip of high perfection”.

The proposed research is carried out jointly between the groups at Columbia University and at the Istituto Nanoscienze of the Italian National Research Council (CNR) in Pisa. At Columbia Dr. Shalom Wind will lead on nanofabrication with a new 100keV e-beam nanolithography that is currently being employed in tests of fabrication of the semiconductor artificial lattices. Prof. Aron Pinczuk will lead on optical experiments that can be carried out at high magnetic fields and low temperature reaching to below 50mK. High quality modulation doped GaAs/AlGaAs quantum wells are the starting material for the fabrication of artificial lattices. These structures, made by molecular-beam-epitaxy, are from our partners Prof. Loren Pfeiffer (Princeton

University) and Prof. Michael Manfra (Purdue University). We envision that much of the proposed work will be with samples processed from n-type wafers GaAs/AlGaAs heterostructures grown along the (001) direction that host 2DEGs of very high-mobility. Our partners at Princeton and at Purdue are enthusiastic about participation in the research proposed here. The reactive ion etching (RIE) and other processing will be carried at Columbia, at Princeton and in Pisa. We will seek access to processing facilities available at the Brookhaven National Laboratory's Center for Functional Nanomaterials, as needed and depending on availability of the resources.

The research in this project relies on fabrication capabilities to create high quality semiconductor structures patterned at the nanoscale by means of e-beam nanolithography and dry etching. Methods developed in past years by the Columbia PI and the Pisa co-PI were applied to the fabrication of nanopatterns that created multiple quantum wires [4,5] and multiple quantum dots [6-8]. Figure 1 describes the typical steps involved. The works using this procedure have demonstrated the realization of patterns that support high quality low dimensional electron systems [2,3,5-8]. The original quality of the electron system is to a great extent preserved in these protocols because the RIE processing does not cut through the doping layer.

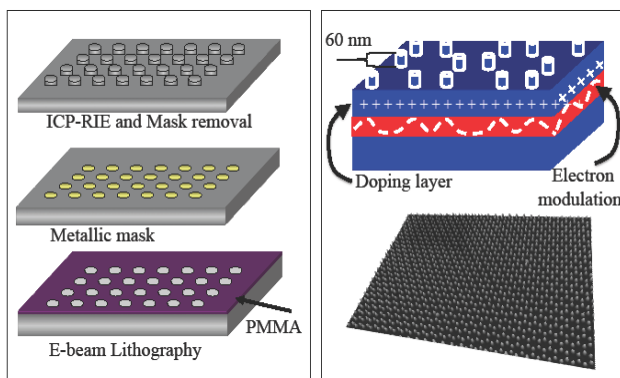


Figure 1. Left panel. Schematic rendition of the sequential steps in the fabrication of a nanoscale pattern in GaAs/AlGas quantum structures by use of e-beam lithography, followed by the deposition of a metal mask (nickel in typical cases), and followed by inductively-coupled-plasma reactive-ion dry etching (ICP-RIE) and mask removal. The ICP-RIE etch is shallow, reaching to less of 100nm below the sample surface. This final step (top drawing in the right panel) results in a pattern like the one shown in the lower picture of the right panel. In a modulation doping GaAs structure the etched pattern creates electron density and electric potential profiles (not shown in this figure).

Preliminary results of nanofabrication and spectroscopy indicate the feasibility of the proposed venues to study quantum simulators in nanofabricated artificial lattices in semiconductors. Figure 2 shows results for a honeycomb pattern with period $a=90\text{nm}$ obtained by our collaborators in Pisa. The upper panel in Fig. 2 shows a SEM picture of the honeycomb lattice. The lattice fabricated on top of a one-side modulation-doped $25\text{nm Al}_{0.1}\text{Ga}_{0.9}\text{As/GaAs}$ quantum well as described in Fig. 1. The lower panel shows the results of measurements of low-lying excitation modes by resonant inelastic light scattering. In addition to the mode at the cyclotron energy, there is a mode identified as intra-Landau level excitation between interaction-induced states of the Hubbard model that describes the artificial lattice with honeycomb symmetry.

While there is much room for major improvement, the low level of disorder achieved in these lattices (as evidenced by the narrow bands measured in the light scattering experiments) could be sufficient to prevent electron localization due to random fluctuations. In current results, and in

spite of likely presence of random residual-disorder, we find that the electrons display unusual collective behavior that is driven by the Coulomb interaction terms that are due to

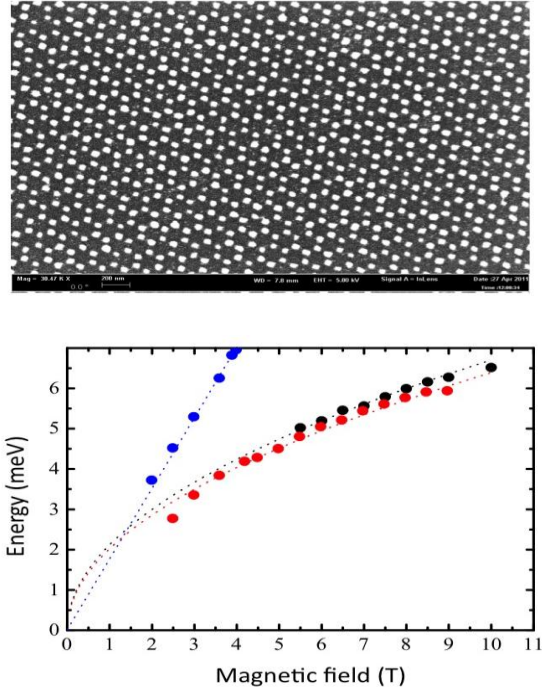


Figure 2. Upper panel. Scanning electron microscopy (SEM) images of a nanofabricated lattice with honeycomb geometry. The artificial lattice is realized on GaAs quantum structures by e-beam lithography and dry etching. The bright dots are the GaAs pillars that have been protected from dry etching. Lower panel. The blue dots are the evolution of the cyclotron mode $h\omega_c$. The Hubbard modes $h\omega_{HB}$ in the artificial honeycomb lattice are shown as red dots for a lattice spacing of $a=130\text{nm}$ [3], and as black circles for $a=90\text{nm}$. The temperature is $T=1.7\text{ K}$. The dashed blue line is a linear fit with the bulk electron mass GaAs $m^*=0.067m_e$ (m_e is the bare electron mass). The red and black dashed lines are fits with $E=\alpha\sqrt{B[T]}$ ($\alpha \approx 2\text{ meV}$), where B is the perpendicular magnetic field.

the superimposed artificial lattice potential. These interaction terms can be tuned at will to probe diverse regimes of the interplay between topology and interactions in quantum physics.

Recent Progress

Theoretical estimates indicate that well-defined linearly dispersing Dirac fermions already occur in AG lattices of period below 60nm. The goal in our initial work is to achieve high quality artificial honeycomb patterns of about 50nm. We are currently exploring the nanofabrication of AG lattices (the honeycomb topology) on GaAs surfaces. Patterns with sub-50nm pitch imprinted on pmma (poly-methylmethacrylate) and HSQ (hydrogen silsesquioxane) using the new 100keV e-beam writer at Columbia should be attained shortly. Given that random defects due to processing by ICP-RIE could play a role, we will study the impact of residual disorder in samples with 50nm period. In the longer term we expect to achieve artificial lattices with periods reaching to 20nm.

Future Plans

This project starts on September 1st, 2013. Initially we will focus on AG lattices. The initial characterizations of the nanofabricated specimens, and of determinations of the Hubbard gap will be carried out by optical experiments. Going beyond this stage, we will focus on studies of the new states in magnetic fields and explore the impact of spin-orbit coupling. In our grant requests (in the fall of 2011) we have indicated that AG lattices in semiconductor quantum well

heterostructures based on GaAs, that have significant spin-orbit coupling strength, could be hosts to exciting new states with remarkable topological properties. Short pitch (below 50nm) AG lattices patterned on 2DEG's in high quality GaAs quantum structures will be examined to establish the occurrence of Dirac fermion states that have linear momentum dispersion. The simultaneous presence of linearly dispersing electron states in 2D with significant spin-orbit strength may lead to novel topological states. Phases of topological insulating states have been recently predicted in the states of valence band holes of laterally patterned semiconductors such as those in GaAs quantum wells [9]. Our search will be carried out in the conduction states of the AG lattices. On the basis of the spin-splitting observed in 2DEG's in conduction band states of GaAs [10], we expect that novel topological states will emerge for AG patterns with periods of 50nm and below.

References (which acknowledge DOE support)

There are no references citing this award because its start date is September 1st, 2013.

Other References

1. Making Massless Dirac Fermions from a Patterned Two-Dimensional Electron Gas, Cheol-Hwan and Steven G. Louie, *Nano Letters* **9**, 1793-1797 (2009).
2. Engineering Artificial Graphene in a Two-dimensional Electron Gas, Marco Gibertini, Achintya Singha, Vittorio Pellegrini, Marco Polini, Giovanni Vignale, Aron Pinczuk, Loren N. Pfeiffer, and Ken W. West, *Physical Review B* **79**(R), 241406 (2009).
3. A. Singha, M. Gibertini, B. Karmakar, S. Yuan, M. Polini, G. Vignale, M.I. Katsnelson, A. Pinczuk, L.N. Pfeiffer, K.W. West, and V. Pellegrini, "Two-dimensional Mott-Hubbard Electrons in an artificial honeycomb lattice", *Science* **332**, 1176-1179 (2011).
4. One-dimensional Plasmon Dispersion and Dispersionless Intersubband Excitations in GaAs Quantum Wires, A. R. Goni, A. Pinczuk, J. S. Weiner, J. M. Calleja, B. S. Dennis, L. N. Pfeiffer, and K. W. West, *Physical Review Letters* **67**, 3298-3301 (1991).
5. Inelastic Light Scattering by Spin-density, Charge-density, and Single-particle Excitations in GaAs Quantum Wires, A. Schmeller, A.R. Goni, A. Pinczuk, J.S. Weiner, J.M. Calleja, B.S. Dennis, L.N. Pfeiffer, and K.W. West, *Physical Review B* **49**, 14778-14781 (1994).
6. Evidence of Strong Correlation in Spin Excitations of Few-electron Quantum Dots, C.P. Garcia, V. Pellegrini, A. Pinczuk, M. Rontani, G. Goldoni, E. Molinari, B.S. Dennis, L.N. Pfeiffer, K.W. West, *Physical Review Letters* **95**, 266806 (2005).
7. A Molecular State of Correlated Electrons in a Quantum Dot, S. Kalliakos, M. Rontani, V. Pellegrini, C. P. Garcia. A. Pinczuk, G. Goldoni, E. Molinari, L. N. Pfeiffer, and K. West, *Nature Physics* **4**, 467-471 (2008).
8. Correlated Electrons in Optically Tunable Quantum Dots: Building an Electron Dimer Molecule, A. Singha, V. Pellegrini, A. Pinczuk, L. N. Pfeiffer, K. W. West, and M. Rontani, *Physical Review Letters* **104**, 246802 (2010).
9. Topological Insulating States in Laterally Patterned Ordinary Semiconductors, O.P. Sushkov and A. H. Castro Neto, *Physical Review Letters* **110**, 186601 (2013).
10. Zero-Magnetic-Field Spin Splitting in the GaAs Conduction Band from Raman Scattering on Modulation-Doped Quantum Wells, B. Jusserand, D. Richards, H. Peric, and B. Etienne. *Physical Review Letters*, **69**, 848-851 (1992).

Program Title: Correlated and Complex Materials

Principle Investigator: B. C. Sales; Co PIs: D. Mandrus, M. A. McGuire, C. Cantoni, L. A. Boatner

Mailing Address: Materials Sciences and Technology Division

Oak Ridge National Laboratory, Oak Ridge TN, 37831-6056

Email: salesbc@ornl.gov

Program Scope

The ultimate aim of our research is to attain a predictive understanding of the behavior of correlated and complex materials. This research program uses the experimental tools of materials synthesis, compositional tuning, and crystal growth to address cutting edge issues in the physics of these systems, with particular focus on the discovery and investigation of novel cooperative phenomena and new forms of order in complex transition-metal compounds. Phenomena such as charge and orbital ordering, coupling of magnetism and ferroelectricity, unconventional superconductivity, low carrier density helimagnetism, and anharmonic phonons in thermoelectric materials are studied. A substantial fraction of the effort is devoted to the discovery of innovative materials and the growth of large single crystals of fundamental interest to material physics. The composition of these materials are carefully controlled, and the effects of compositional tuning on the basic physics of the materials are studied using X-ray and neutron diffraction, magnetization, specific heat, and electrical and thermal transport measurements. Once the materials have been prepared and characterized, in-depth experiments such as inelastic neutron scattering, photoemission, scanning transmission electron microscopy and scanning tunneling microscopy are performed in order to obtain a deeper understanding of the relevant physics. Some of the materials investigated are promising for energy-related applications such as superconductors for grid applications, and permanent magnets and thermoelectrics for energy conversion.

This program focuses on science driven synthesis, that is, the identification and synthesis of single crystals that have the potential to address specific scientific questions. The exact compositions to be investigated are determined by crystal chemistry “rules” and guidance from electronic structure calculations. Calculations connect properties to the atomic scale and provide understanding of origins and trends but they require idealizations; measurements are the acid test and are essential in material design. Single crystals are prepared using a variety of techniques, including flux growth, vapor transport, and optical-floating-zone growth.

This program interacts strongly with most of the materials science programs at ORNL (both experimental and theoretical) and involves extensive collaborations with scientists at universities and other national laboratories.

Recent Progress

Much of our recent work has focused on some unusual relationships among magnetism, superconductivity and thermal conductivity. To illustrate some of the progress made over the past 2 years, four examples of unexpected and surprising results will be summarized.

Giant Seebeck Effect in CrSb₂ Single Crystals. In some materials magnetic excitations can carry large amounts of heat. This effect is largest in compounds where the magnetic energy scale, J, in at least one direction, is larger than the Debye energy. CrSb₂ is an unusual narrow gap semiconductor ($E_{\text{gap}} \approx 0.1$ meV) with very strong magnetic interactions in one direction ($J_c \approx 35$ meV) and weak interactions in the other two ($J_a \approx J_b \approx 1$ meV), as proved by inelastic neutron scattering (Ref.1). If magnetic excitations carry heat in CrSb₂ the thermal conductivity should be larger along the c direction, which was indeed found to be the case. (Ref.1 and 2). An unexpected

finding, however, was a giant maximum in the magnitude of Seebeck coefficient that attained a value of $-4500 \mu\text{V/K}$ at 18 K, independent of the orientation of the crystal (Fig 1). Analysis of CrSb_2 Hall and resistivity data show that a phonon-drag mechanism is the likely origin of the giant Seebeck effect. This conclusion is important since it implies a similar origin for the large thermopower in FeSb_2 , which had been touted in the literature as a potential low temperature thermoelectric material driven by strong correlations. In CrSb_2 strong correlations are not needed to account for the data.

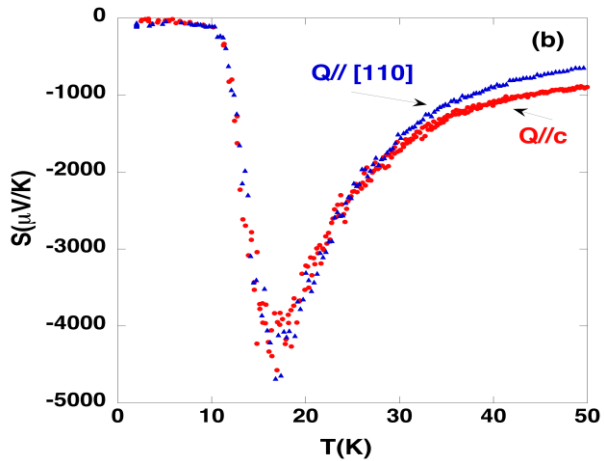


Fig 1. Thermopower of CrSb_2 single crystal with heat flow along two directions.

Thermal Conductivity Near T_c : A Screening Tool for Unconventional Superconductivity One of the challenges in studying complex materials is identifying new materials that will potentially exhibit new phenomena or effects, and will provide additional insight into the underlying physics. In phonon-mediated superconductors the thermal conductivity, κ , decreases just below T_c since electrons in the superfluid state carry no heat. By contrast, in all of the unconventional superconductors, of which we are aware, the thermal conductivity always increases just below T_c . This observation suggests that a relatively simple thermal conductivity measurement may be a way of identifying superconductors with an unusual pairing mechanism. Although this does not help identify new superconductors, it may help determine which materials have the potential for a much higher T_c . A careful investigation was made of the thermal conductivity of electron-doped $\text{Ba}(\text{Fe}_{1-x}\text{Co}_x)_2\text{As}_2$ single crystals with an emphasis on the behavior near the magnetic and superconducting transition temperature (Ref 3). An enhancement of the in-plane thermal conductivity, κ_{ab} , was observed below T_c for all samples, with the greatest enhancement near optimal doping. The observed trends are consistent with the scattering of heat carriers by low energy excitations. Upon entering the superconducting state, the formation of a spin gap leads to reduced scattering and an enhancement in $\kappa(T)$. A similar enhancement of κ was observed for polycrystalline BaFe_2As_2 below the magnetic transition, but surprisingly in single crystals there was no detectable change in κ_{ab} below T_N . This result suggests remarkably strong anisotropic scattering in BaFe_2As_2 .

Nanoscale probe of orbital occupancy and local structure in iron-based superconductors Over the past two years we have investigated in detail the local electronic and chemical structure of a large number of Fe-based superconductors (FBS) using aberration-corrected scanning transmission electron microscopy (STEM) coupled with electron energy loss spectroscopy (EELS) at room temperature. We observe a universal behavior between the magnitude of the local dynamic magnetic moment and hole concentration across different families of FBS. All of the parent compounds have the same number of electrons in the Fe 3d bands; however the local magnetic moment varies due to different orbital occupancy. In addition we directly measured how both the local magnetic moment and hole concentration changed as a function of Co-doping in a series of $\text{Ba}(\text{Fe}_{1-x}\text{Co}_x)_2\text{As}_2$ crystals. After initially decreasing with increasing x , the dynamic magnetic moment at room temperature inferred from EELS data shows a dome-like maximum

near optimal doping- which was not expected (Fig 2) (Ref. 4). This result directly implies that certain types of magnetic fluctuations are good for superconductivity. Another surprise from this work is that the structure of BaFe₂As₂ is not tetragonal at room temperature, but has a small distortion (≈ 0.01 nm) and is composed of domains of order 10-12 nm (Ref 5).

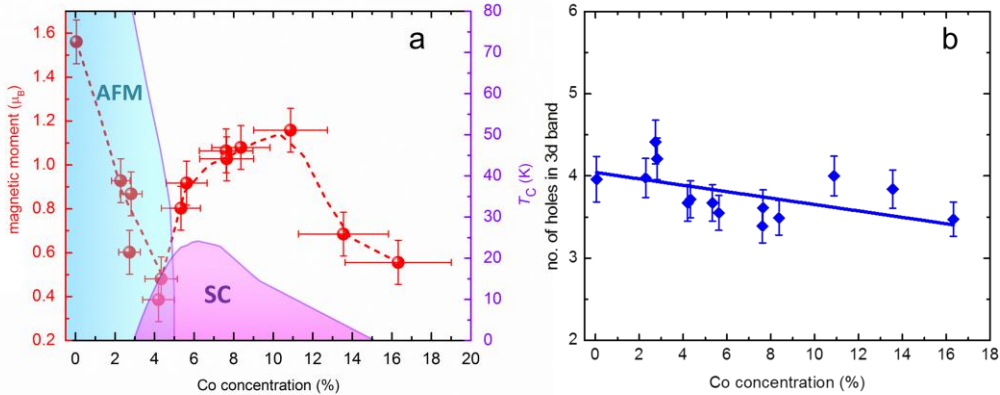


Fig 2. Inferred local Fe magnetic moment and total number of holes in the 3d orbitals in $\text{Ba}(\text{Fe}_{1-x}\text{Co}_x)_2\text{As}_2$ as function of the local Co concentration as determined from room temperature EELS data (Ref 4)

Future Plans

Our future research will focus on identifying, synthesizing (often in single crystal form) and studying model material systems that will improve our understanding of the interrelationships among magnetism, superconductivity and thermal conductivity. A new theme that we plan to undertake is to identify model systems that will provide a clearer understanding of the role of spin-orbit coupling in condensed matter physics- from the rich spin structures and dynamics created by the Dzyaloshinsky-Moriya interaction to the ability to design better permanent magnets. This new theme will involve a close coupling among crystal growth, neutron scattering and theory.

Publications

Over the past 2 years (August 2011-August 2013) 72 Journal Papers were published including: 6 PRL, 2 Advanced Materials, 1 Nat. Mat., 1 Nat. Nano, 1 Nat. Comm., 2 PNAS, 1 JACS, 1 ACS nano and 39 PRBs. Most of these publications involved strong collaborations with other MSED programs and facilities at ORNL. The publications referenced in the abstract and some of our most interesting papers are listed below.

1. M. B. Stone, M. D. Lumsden, S. E. Nagler, D. J. Singh, J. He, B. C. Sales, and D. Mandrus, "Quasi-One-Dimensional Magnons in an Intermetallic Marcasite," *Phys. Rev. Lett.* **108**, 167202 (2012).
2. B. C. Sales, A. F. May, M. A. McGuire, M. B. Stone, D. J. Singh, and D. Mandrus, "Transport, thermal, and magnetic properties of the narrow-gap semiconductor CrSb₂," *Phys. Rev. B* **86**, 235136 (2012).
3. A. F. May, M. A. McGuire, J. E. Mitchell, A. S. Sefat, and B. C. Sales, "Influence of spin fluctuations on the thermal conductivity in superconducting $\text{Ba}(\text{Fe}_{1-x}\text{Co}_x)_2\text{As}_2$," *Phys. Rev. B* **88**, 064502 (2013).

4. C. Cantoni, J. E. Mitchell, A. F. May, A. S. Sefat, M. A. McGuire, J. C. Idrobo, M. F. Chisholm, W. Zhou, S. J. Pennycook and B. C. Sales- submitted to Nature Physics
5. C. Cantoni *et al.*- in preparation
6. J. Ma, O. Delaire, A. F. May, C. E. Carlton, M. A. McGuire, L. H. VanBebber, D. L. Abernathy, G. Ehlers, T. Hong, A. Huq, W. Tian, V. M. Keppens, Y. Shao-Horn, and B. C. Sales, "Glass-like phonon scattering from a spontaneous nanostructure in AgSbTe₂," *Nat. Nanotechnology*, **8**, 445 (2013).
7. W. Lin, Q. Li, B. C. Sales, S. Jesse, A. S. Sefat, S. V. Kalinin, and M. Pan, "Direct Probe of Interplay between Local Structure and Superconductivity in FeTe_{0.55}Se_{0.45}," *ACS Nano* **7**(3), 2634–2641 (2013).
8. A. F. May, M. A. McGuire, H. Cao, I. Sergueev, C. Cantoni, B. C. Chakoumakos, D. S. Parker, and B. C. Sales, "Spin Reorientation in TlFe_{1.6}Se₂ with Complete Vacancy Ordering," *Phys. Rev. Lett.* **109**, 077003 (2012).
9. O. Delaire, J. Ma, K. Marty, A .F. May, M .A. McGuire, M. H. Du, D. J. Singh, A. Podlesnyak, G. Ehlers, M .D. Lumsden, and B. C. Sales, "Giant Anharmonic Phonon Scattering in PbTe," *Nature Materials* **10**, 614 (2011).
10. J. Cheng, W. Tian, J. Zhou, V. M. Lynch, H. Steinfink, A. Manthiram, A. F. May, V. O. Garlea, J. C. Neufeind, and J. Yan, "Crystal and Magnetic Structures and Physical Properties of a New Pyroxene NaMnGe₂O₆ Synthesized under High Pressure," *J. Am. Chem. Soc.* **135**, 2776 (2013).
11. W. Siemons, M. A. McGuire, V. R. Cooper, M. D. Biegalski, I. N. Ivanov, G. E. Jellison, L. A. Boatner, B. C. Sales, and H. M. Christen, "Dielectric-Constant-Enhanced Hall Mobility in Complex Oxides," *Adv. Mater.* **24**, 3965 (2012).
12. Paolo Vilmercati, Alexei Fedorov, Federica Bondino, Francesco Offi, Giancarlo Panaccione, Paolo Lacovig, Laura Simonelli, Michael A. McGuire, Athena S. M. Sefat, David Mandrus, Brian C. Sales, Takeshi Egami, Wei Ku, and Norman Mannella, "Itinerant electrons, local moments, and magnetic correlations in the pnictide superconductors CeFeAsO_{1-x}F_x and Sr(Fe_{1-x}Co_x)₂As₂," *Phys. Rev. B* **85**, 220503(R), (2012).
13. J.-Q. Yan, M. A. McGuire, A. F. May, H. Cao, A. D. Christianson, D. G. Mandrus, and B. C. Sales, "Flux growth and physical properties of Mo₃Sb₇ single crystals," *Phys. Rev. B* **87**, 104515 (2013).
14. G. J. MacDougall, D. Gout, J. L. Zarestky, G. Ehlers, A. Podlesnyak, M. A. McGuire, D. Mandrus, and S. E. Nagler, "Kinetically Inhibited Order in a Diamond-Lattice Antiferromagnet," *PNAS* **108**(38), 15693–15698 (2011).
15. N. J. Ghimire, M. A. McGuire, D. S. Parker, B. Sipos, S. Tang, J.-Q. Yan, B. C. Sales, and D. Mandrus, "Magnetic phase transition in single crystals of the chiral helimagnet Cr_{1/3}NbS₂," *Phys. Rev. B* **87**, 104403 (2013).
16. K. Marty, A. D. Christianson, A. M. dos Santos, B. Sipos, K. Matsubayashi, Y. Uwatoko, J. A. Fernandez-Baca, C. A. Tulk, T. A. Maier, B. C. Sales, and M. D. Lumsden, "Effect of pressure on the neutron spin resonance in the unconventional superconductor FeTe_{0.6}Se_{0.4}," *Phys. Rev. B* (Rapid Communications) **86**, 220509(R) (2012).
17. M. A. McGuire, A. F. May, and B. C. Sales, "Crystallographic and Magnetic Phase Transitions in the Layered Ruthenium Oxyarsenides TbRuAsO and DyRuAsO," *Inorg. Chem.* **51**, 8502 (2012).
18. C. Cantoni, J. Gazquez, F. M. Granozio, M. P. Oxley, M. Varela, A. R. Lupini, S. J. Pennycook, C. Aruta, U. S. di Uccio, P. Perna, and D. Maccariello, "Electron Transfer and Ionic Displacements as the Origin of the 2D Electron Gas at the LAO/STO Interface: Direct Measurements with Atomic-Column Spatial Resolution," *Adv. Mater.* **24**, 3952 (2012).

Program Title (ECA): Origin of Superconductivity in Structurally Layered Materials

Principle Investigator: Athena S. Sefat

Mailing Address: Materials Sciences and Technology Division, Oak Ridge National Laboratory, P. O. Box 2008, 1 Bethel Valley Road, Oak Ridge, TN, 37831-6056

Email: sefata@ornl.gov

Project Scope:

The overarching goal of the program is to lay a foundation for predicting superconducting materials by documenting similarities and differences between the two high-temperature superconducting classes through focused studies. The understanding of the fundamental nature of the superconducting state and the ultimate design improved superconductors are of crucial importance, if superconductive materials are to fulfill their promise for widespread use in energy-related needs such as wind-power generation. This project involves (a) a strong synthesis component for the design of known and potentially improved iron- and copper-based materials, and also the design of those without such 3d-elements, in addition to (b) strong materials characterization efforts involving determination of lattice/magnetic structures and thermodynamic/transport measurements, and also other specialized characterization (ARPES, pressure, STEM, TEM, inelastic scattering, etc.) techniques and theoretical calculations that are done through extended collaborations (other DOE programs at ORNL, universities, other national labs). Because the mechanism of high-temperature superconductivity remains unknown, this project focuses on tackling several specific queries such as: Are there specific structural features that stabilize a superconducting state? Can local structure greatly affect/explain bulk superconducting properties? What are the roles of chemical substitutions or certain non-hydrostatic applied pressures? What is the role of Fe or Cu 3d electrons, or other magnetic ions, in relation to superconducting charge carriers? Is there a relationship between bulk structure and superconducting critical temperature?

Recent Progress: Below is a brief outline of *two* of our *2013 publications*.

Publication 1: B. Saparov, D. J. Singh, V. O. Garlea, & A. S. Sefat, “Crystal, magnetic, and electronic structures, and magnetic properties of new BaMnPnF ($Pn = As, Sb, Bi$),” *Scientific Reports* **3** (2013), 2154.

New manganese-based ‘1111’ materials with chemical composition of BaMnPnF ($Pn = As, Sb, Bi$) were synthesized, and found to be high-temperature antiferromagnets, similar to the iron-based superconducting parents. Because these new ‘1111’ materials are found to have the well-known tetragonal ZrCuSiAs-type structure (similar to LaFeAsO) with manganese (not iron), and also show high-temperature antiferromagnetic ordering with the magnetic ordering wave-vector of the iron-based superconducting parents, the hope was to have them form a new class of high-temperature superconductor based on manganese (not iron or copper). However, electrical resistivity results give semiconducting behavior, unlike the spin-density-wave behavior in LaFeAsO. In addition, electronic structures of BaMnPnF show differences to those of iron-based superconducting parents. In conclusion, even though BaMnPnF may not show superconductivity upon doping of holes or electrons, these new manganese-based 1111 phases should demonstrate interesting variation of electrical and magnetic properties with chemical substitutions and upon applied pressure.

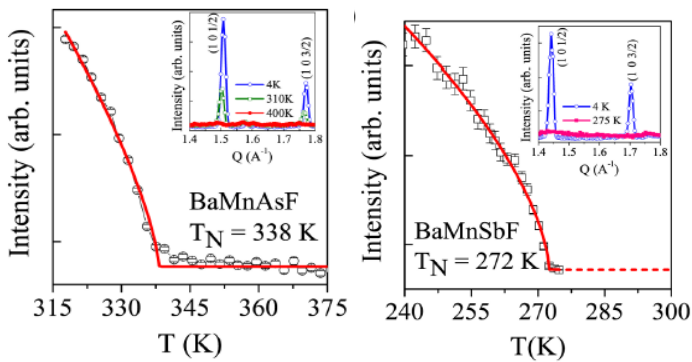


Figure 1: Temperature-dependence of the intensity of (1 0 1/2) magnetic peak for the new Mn-based 1111 materials, showing evidence for high antiferromagnetic ordering temperature.

Publication 2: B. Saparov, & A. S. Sefat “Crystals, magnetic and electronic properties of a new ThCr_2Si_2 -type BaMn_2Bi_2 and K-doped compositions,” *J. Solid State Chem.* **204** (2013), 32.

New non-iron-based ‘122’ ternary transition-metal pnictide of BaMn_2Bi_2 is crystallized from bismuth flux. BaMn_2Bi_2 adopts ThCr_2Si_2 -type structure ($I4/mmm$) with $a = 4.4902(3)$ and $c = 14.687(1)$ Å. This study was motived by (a) identifying new 122 classes of non-Fe-based materials for their possible superconductivity, and hopes that (b) the heavier pnictides of antimonides and bismuthides may have higher T_C compared to the smaller arsenide and phosphide analogs. Although high-temperature magnetization results show that magnetic ordering temperature is $T_N \sim 400$ K, electrical resistivity and heat capacity confirmed insulating ground state in BaMn_2Bi_2 . With limited amount of K-doping (<3%), down-turns in electrical resistivity and low-field magnetization data are seen below 4 K, with no sign of zero resistance or diamagnetism.



Figure 2: As-grown single crystals of BaMn_2Bi_2 , from flux.

Future Plans:

This project is focused on the chemistry and physics of superconductivity. It will continue to synthesize & characterize: (a) already-known (or improved) materials in order to extend the understanding of a certain physical behavior that is related to the superconducting state (e.g. magnetism, spin excitations, etc.); (b) new materials that are somehow structurally-related to known-superconductors, in order to find if certain chemistry is crucial, or if high-temperature superconductivity in non Fe or Cu related materials is possible. In addition to the iron-based superconductors, the PI is planning to relook at some of the high- T_C Tl-based cuprates in order to answer certain open questions. As a side project, the PI will investigate possible superconductivity in 3D non-layered structures – this project was just funded through an ORNL LDRD project.

Publications:

From **July 2011 to the present time**, this project has published **40** scientific manuscripts in journals such as *Phys. Rev. Lett.* (5), *Phys. Rev. X* (1), *MRS Bulletin* (1), *ACS Nano* (1), *Inorganic Chem.* (1), *Supercon. Sci. Tech.* (2), *Scientific Reports* (1), and *Rep. Prog. Phys.* (1). The full list is below.

- 1) Uhoya, W. O.; et al. "Structural phase transitions in EuFe₂As₂ superconductor at low temperatures and high pressures," *J. Physics: Condens. Matter* 23 (2011), 365703.
- 2) Frontzek, M.; et al. "Magnetic excitations in the geometric frustrated multiferroic CuCrO₂," *Phys. Rev. B* 84 (2011), 094448.
- 3) Arsenijevic, S.; et al. "Pressure effects on the transport coefficients of Ba(Fe_{1-x}Co_x)₂As₂," *Phys. Rev. B* 84 (2011), 075148.
- 4) Schafgans, A. A.; et al. "Phonon splitting and anomalous enhancement of infrared-active modes in BaFe₂As₂," *Phys. Rev. B* 84 (2011), 052501.
- 5) Sales, B. C.; et al. "Unusual phase transitions and magnetoelastic coupling in TlFe_{1.6}Se₂ single crystals," *Phys. Rev. B* 83 (2011), 224510.
- 6) Sefat, A. S.; et al. "Chemistry and electronic structure of iron-based superconductors," *MRS Bulletin* 36 (2011), 614.
- 7) Sefat, A. S. "Pressure effects on two superconducting iron-based families," *Rep. Prog. Phys.* 74 (2011), 124502.
- 8) Sefat, A. S.; et al. "Effect of molybdenum 4d hole substitution in BaFe₂As₂," *Phys. Rev. B* 85 (2012), 024503.
- 9) Saparov, B.; et al. "Spin glass and semiconducting behavior in one-dimensional BaFe_{2-δ}Se₃ ($\delta \approx 0.2$) crystals," *Phys. Rev. B* 84 (2011), 234132.
- 10) Niedziela, J. L.; et al. "Phonon softening near the structural transition in BaFe₂As₂ observed by inelastic x-ray scattering," *Phys. Rev. B* 84 (2011), 224305.
- 11) Clancy, J. P.; et al. "High-resolution x-ray scattering studies of structural phase transitions in Ba(Fe_{1-x}Cr_x)₂As₂," *Phys. Rev. B* 85, 054115.
- 12) Sefat, A. S.; et al. "Effect of molybdenum 4d hole substitution in BaFe₂As₂," *Phys. Rev. B* 85 (2012), 024503.
- 13) Dhital, C.; et al. "Effect of uniaxial strain on the structural and magnetic phase transitions in BaFe₂As₂," *Phys. Rev. Lett.* 108 (2012), 087001.
- 14) Cao, H.; et al. "Evolution of the nuclear and magnetic structures of TlFe_{1.6}Se₂ with temperature," *Phys. Rev. B* 85, 054515.
- 15) Saparov, B.; et al. "Metallic properties of Ba₂Cu₃P₄ and BaCu₂Pn₂ (Pn = As, Sb)," *J. Solid State Chem.* 191 (2012), 213.
- 16) Saparov, B.; et al. "Properties of Binary Transition-Metal Arsenides (TAs)," *Supercond. Sci. Tech.* 25 (2012), 084016. (invited)
- 17) Schafgan, A. A.; et al. "Electronic correlations and unconventional spectral weight transfer in the high-temperature pnictide BaFe_{2-x}Co_xAs₂ superconductor using infrared spectroscopy," *Phys. Rev. Lett.* 108 (2012), 147002.
- 18) Vilmercati, P.; et al. "Itinerant electrons, local moments, and magnetic correlations in the pnictide superconductors CeFeAsO_{1-x}F_x and Sr(Fe_{1-x}Co_x)₂As₂," *Phys. Rev. B* 85 (2012), 220503(R).
- 19) Vilmercati, P.; et al. "Direct probe of the variability of Coulomb correlation in iron pnictide superconductors," *Phys. Rev. B* 85 (2012), 235133.
- 20) Ballinger, J.; et al. "Magnetic properties of single crystal EuCo₂As₂," *J. Appl. Phys.* 111 (2012), 07E106.
- 21) Li, G.; et al. "Coupled structural and magnetic antiphase domain walls on BaFe₂As₂," *Phys. Rev. B* 86 (2012), 060512(R).

- 22) Kim, J. S.; et al. "Specific heat to H_{c2} : Evidence for nodes or deep minima in the superconducting gap of underdoped and overdoped $\text{Ba}(\text{Fe}_{1-x}\text{Co}_x)_2\text{As}_2$," *Phys. Rev. B* **86** (2012), 014513.
- 23) Moon, S. J.; et al. "Infrared measurement of the pseudogap of the P-doped and Co-doped high-temperature BaFe_2As_2 superconductors," *Phys. Rev. Lett.* **109** (2012), 027006.
- 24) Saparov, B.; et al. "Properties of Binary Transition-Metal Arsenides (TAs)," *Supercond. Sci. Tech.* **25** (2012), 084016. (invited)
- 25) Uhoya, W. O.; et al. "High-pressure structural phase transitions in chromium-doped BaFe_2As_2 ," *J. Phys.: Conf. Ser.* **377** (2012), 012016.
- 26) Mitchell, J. E.; et al. "Temperature-composition phase diagrams for $\text{Ba}_{1-x}\text{Sr}_x\text{Fe}_2\text{As}_2$ ($0 \leq x \leq 1$) and superconducting $\text{Ba}_{0.5}\text{Sr}_{0.5}(\text{Fe}_{1-y}\text{Co}_y)_2\text{As}_2$ ($0 \leq y \leq 0.141$)" *Phys. Rev. B* **86** (2012), 174511.
- 27) Fu, M.; et al. "NMR search for spin nematic state in a LaFeAsO single crystal," *Phys. Rev. Lett.* **109** (2012), 247001.
- 28) Tsoi, G. M.; et al. "Pressure-induced superconductivity in $\text{Ba}_{0.5}\text{Sr}_{0.5}\text{Fe}_2\text{As}_2$," *J. Phys.: Condens. Matter* **24** (2012), 495702.
- 29) Moon, S. J.; et al. "Interlayer coherence and superconducting condensate in the c -axis response of optimally doped $\text{Ba}(\text{Fe}_{1-x}\text{Co}_x)_2\text{As}_2$ high- T_C superconductor using infrared spectroscopy," *Phys. Rev. Lett.* **110** (2013), 097003.
- 30) Xu, N.; et al. "Electronic band structure of BaCo_2As_2 : A fully doped ferropnictide analog with reduced electronic correlations," *Phys. Rev. X* **3** (2013), 011006.
- 31) Yeon, J.; et al. "Crystal growth, structural characterization, and magnetic properties of new uranium (IV) containing mixed metal oxalates: $\text{Na}_2\text{U}_2\text{M}(\text{C}_2\text{O}_4)_6(\text{H}_2\text{O})_4$ ($\text{M} = \text{Mn}^{2+}, \text{Fe}^{2+}, \text{Co}^{2+}$, and Zn^{2+})," *Inorganic Chem.* **52** (2013), 2199.
- 32) Lin, W.; et al. "Direct probe of the interplay between local structure and superconductivity in $\text{FeTe}_{0.55}\text{Se}_{0.45}$," *ACS Nano* **7** (2013), 2634.
- 33) Mohanty, D.; et al. "Investigating phase transformation in the $\text{Li}_{1.2}\text{Co}_{0.1}\text{Mn}_{0.55}\text{Ni}_{0.15}\text{O}_2$ lithium-ion battery cathode during high-voltage hold (4.5 V) via magnetic, X-ray diffraction and electron microscopy studies," *J. Mater. Chem. A* **1** (2013), 6249.
- 34) Mohanty, D.; et al. "Structural transformation in a $\text{Li}_{1.2}\text{Co}_{0.1}\text{Mn}_{0.55}\text{Ni}_{0.15}\text{O}_2$ lithium-ion battery cathode during high-voltage hold," *RSC Advances* **3** (2013), 7479.
- 35) Sergueev, I.; et al. "Effect of pressure, temperature, fluorine doping, and rare earth elements on the phonon density of states of LFeAsO studied by nuclear inelastic scattering," *Phys. Rev. B* **87** (2013), 64302.
- 36) Saparov, B.; et al. "Crystals, magnetic and electronic properties of a new ThCr_2Si_2 -type BaMn_2Bi_2 and K-doped compositions," *J. Solid State Chem.* **204** (2013), 32.
- 37) Christianson, A. D.; et al. "Doping dependence of the spin excitations in the Fe-based superconductors $\text{Fe}_{1+y}\text{Te}_{1-x}\text{Se}_x$," *Phys. Rev. B* **87** (2013), 224410.
- 38) Yeon, J.; et al. "Crystal growth, structure, polarization, and magnetic properties of cesium vanadate, $\text{Cs}_2\text{V}_3\text{O}_8$: A structure-property study," *Inorg. Chem.* **52** (2013), 6179.
- 39) Saparov, B.; et al. "Crystal, magnetic, and electronic structures, and magnetic properties of new BaMnPnF ($Pn = \text{As}, \text{Sb}, \text{Bi}$)," *Scientific Reports* **3** (2013), 2154.
- 40) May, A. F.; et al. "Influence of spin fluctuations on the thermal conductivity in superconducting $\text{Ba}(\text{Fe}_{1-x}\text{Co}_x)_2\text{As}_2$," *Phys. Rev. B* **88** (2013), 064502.

Program Title: Fundamental Studies of Anisotropic Nanomagnets

Principal Investigator: David J. Sellmyer; Co-PI: Ralph Skomski, in collaboration with George Hadjipanayis

Mailing Address: Nebraska Center for Materials and Nanoscience and Department of Physics, University of Nebraska, Lincoln, NE 68588-0298

E-mail: dsellmyer@unl.edu

Program Scope

The *goal* of this research is to advance through fundamental research our understanding of a key class of materials important in magnetism and nanoscience. The work is directly relevant to several grand challenges in nanomagnetism including: (a) quantum understanding of spin-polarized matter at the 1-10 nm scale, (b) complex fabrication and integration of top-down and self-assembled nanomagnetic structures, (c) ultra-strong permanent magnets, (d) extremely high-density information storage, (e) magnetologic, spintronic and spin-qubit devices, (f) magnetic cooling materials, and (g) nanoscale biomagnetic and other sensors. The length scale involved requires advanced quantum and simulational approaches because it spans the gap between molecular and macroscopic levels. In nanoscale magnets, novel structures, not existing in the bulk, may be formed, and surface and interface phenomena assume critical importance. Another important aspect is that synthesis and fabrication advances are as critical to progress as theoretical, structural and characterization discoveries.

The *significance* of our research is its high potential for understanding and controlling magnetization and magnetic anisotropy, whose practical importance in energy-related technologies cannot be overestimated. Advancement in key areas such as permanent magnetism, information storage and future electronic devices require new materials and structures with tunable coercivity, Curie temperature, magnetization and other properties. Our research focuses on these goals through a critical combination of experimental and theoretical magnetism and nanoscience approaches. *Innovative aspects* of the work include creation of new magnetic nanostructures through special fabrication techniques. The *unifying concept* underlying this proposal is *nanometer-length-scale* and *real-structure control* as a precondition for highly anisotropic and highly coercive nanostructures. This larger perspective provides a coherent theme for all of the nanomaterials and subprojects in our research.

Our research focuses on nanoscale and submicron magnets with characteristic dimensions $1 \text{ nm} \leq d \leq 500 \text{ nm}$, and with high anisotropy constants $K \geq 10 \text{ Merg/cm}^3$. The reasons for this are several. First, this length scale spans the typical important dimensions of exchange lengths and domain-wall widths, which means that significant control of magnetic properties can be had by varying grain or particle dimensions. High anisotropy is significant for applications including extremely high-density data storage, high-energy exchange-coupled permanent magnets and ultra-small spintronic devices such as current-induced switching in perpendicular magnetic tunnel junctions [MTJ]. For future data storage at 10 Tb/in^2 , a

thermal-stability parameter $\xi \equiv K_1 V/k_B T \geq 50$ is required for 10-year storage, where grain diameter $d \approx V^{1/3} \approx 4$ nm. Regarding future high-energy exchange-coupled permanent magnets, one requires $J_s = 4\pi M_s$ (or $\mu_0 M_s \approx 15$ kG), and coercivity $H_c = 2K_1/M_s - NM_s \geq 10$ kOe. Thus high K_1 values (≥ 10 Merg/cm³) are required. Similarly, in ultra small spin-valve or MTJ devices based on FePt or CoFeB/MgO, the thermal stability factor must be in the range of 40-50, which requires high anisotropy.

The research is based on a continuing collaboration in experimental and theoretical research between groups at the Universities of Nebraska and Delaware. A broad set of experiments is performed including structural characterization by x-ray diffraction, analytical and high-resolution electron microscopy, and magnetic measurements between 4.2 and 1000 K. The results are correlated with theoretical work on analytical and simulational nanomagnetism to study magnetization reversal mechanisms, anisotropies, and magnetic interactions [1-15].

Recent Progress

Background: Our recent research has focused on synthesis and properties of nanomagnets and nanostructures that can be formed only by non-equilibrium processes such as cluster formation, sputtering and rapid quenching from the melt. These processes often result in novel structures, properties, and phenomena. Below we discuss examples of recent research in high-anisotropy transition-metal-based nanoclusters and physics of novel high-anisotropy nanostructured materials.

1. Nanocluster Research [1-7]

Discussion: We have succeeded in producing uniaxially aligned HfCo₇ nanoparticles and HfCo₇:Fe-Co nanocomposites at room temperature using a single-step cluster-deposition method. Structural analysis indicates that HfCo₇ crystallizes in an orthorhombic structure. HfCo₇ nanoparticles exhibit H_c (4.4 kOe), K_1 (~ 10 Mergs/cm³), and J_s (10.8 kG) at 300K, which are comparable with the magnetic properties of rare-earth alloy nanoparticles. An enhancement of J_s to as high as 16.6 kG was observed in HfCo₇:Fe-Co nanocomposites on varying Fe-Co concentration to 39 vol. %, although the coercivity is reduced as compared to HfCo₇ nanoparticles. In addition, we have demonstrated the synthesis of new rare-earth-free Zr₂Co₁₁ nanoparticles having high coercivity and magnetic moment using cluster-deposition, which are suitable as building blocks for rare-earth-free permanent-magnet materials. This method permits the direct ordering of high-anisotropy rhombohedral-structure nanoparticles without the requirement of a subsequent high-temperature annealing, alignment of the easy axes prior to deposition, and co-deposition of soft Fe-Co phase having high magnetization to fabricate exchange-coupled nanocomposites. The result is an assembly of a dense nanostructured rare-earth-free material in which a substantial magnetic remanence and coercivity are achieved, as well as the highest energy product for a non-rare-earth material, *viz.*, 19.5 MGoe.

Significance: Nanostructured Zr₂Co₁₁-based and related materials, which remain to be fabricated in bulk forms, in due course can be useful in applications where magnets with energy products in the intermediate range between alnico and RE-containing magnets are

required. Thus, the result reported in this study is an important step in mitigating the critical-materials aspects of rare-earth elements and satisfying the ever-increasing demand for permanent magnets.

2. Nanostructured Materials [8-15]

Discussion: Films of aligned $L1_0$ -structure $(\text{Fe},\text{Co})\text{Pt}$ with fcc $\text{Fe}(\text{Co},\text{Pt})$ are synthesized by co-sputtering Fe, Co, and Pt on an (001) MgO substrate with *in situ* heating at 830 °C. The nanostructures and magnetic properties of the films are characterized by X-ray diffraction (XRD), transmission electron microscopy (TEM), and superconducting quantum interference device (SQUID). The compositions of the samples $(\text{Fe},\text{Co})_x\text{Pt}_{1-x}$ are designed to maintain an atomic Fe: Co ratio of 65: 35 while increasing the Fe,Co content in each successive sample. The XRD patterns confirm the formation of $L1_0$ -ordered $(\text{Fe},\text{Co})\text{Pt}$ and its epitaxial growth on MgO. TEM shows that the $(\text{Fe},\text{Co})\text{Pt}$ films form isolated magnetic grains of about 100 nm in diameter. Hysteresis-loop measurements show that the increase of the Fe,Co concentration from 57.3 to 68.3 at% enhances the saturation magnetization M_s from 1245 emu/cm³ to 1416 emu/cm³, and the coercivity decreases from 32 kOe to 8.9 kOe. The nominal maximum energy product per grain is 64 MGOe. In addition we have recently studied several non-equilibrium structures including Mn_yGa ($1 < y < 2$), Mn_{3-x}Ga , and cubic Mn_3Ga . These structures exhibit coupled structural and magnetic phase transitions, and the latter (Mn_3Ga) shows a Kondo-like resistance minimum at low temperature. The properties are compared with first-principles DFT calculations.

Significance: The compounds studied in this research generally have high anisotropy and can have significant magnetization and spin-polarization values. Detailed characterization may lead to new materials for spintronic and information-storage applications.

Future Plans

We have only uncovered a small number of new transition-metal-based nanoclusters, so a huge space exists for further studies. We intend to investigate new systems with high potential for enhanced magnetic anisotropy, including FeNi , SmCo_4B , and related phases. We have purchased a second cluster source from Mantis that is being added to our cluster-deposition system, which will give greatly expanded opportunities for studies of nanocomposite systems consisting of alloy or compound constituents.

In the area of new nanostructured materials, we will explore compounds with the form: Mn_2XY , where X = Ti, V, Cr, Fe and Y = Si, Ga, Sn. Theoretical predictions have indicated a high degree of spin polarization in several of these, and we will synthesize samples by thin-film and rapid quenching from the melt. The potential for magnetoelectronic or other applications will be studied.

References Acknowledging DOE Support

1. B. Balamurugan, R. Skomski, X. Li, S. Valloppilly, J. Shield, G.C. Hadjipanayis, D.J. Sellmyer, "Cluster Synthesis and Direct Ordering of Rare-Earth Transition-Metal

- Nanomagnets," *Nano Lett.* **11**, 1747-1752 (2011); doi: 10.1021/nl200311w.
2. O. Akdogan, W. Li, G.C. Hadjipanayis, D.J. Sellmyer, "Synthesis of Single-Crystal Sm-Co Nanoparticles by Cluster Beam Deposition," *J. Nanoparticle Res.* **13**, 7005-7012 (2011); doi: 10.1007/s11051-011-0612-8.
 3. B. Balasubramanian, R. Skomski, X.Z. Li, G. C. Hadjipanayis, and D. J. Sellmyer, "Magnetism of Directly Ordered Sm-Co Clusters," *J. Appl. Phys.* **111**, 07B527 (3 pages) (2012); doi:10.1063/1.3677668.
 4. B. Balasubramanian, R. Skomski, B. Das, X.Z. Li, S. Valloppilly, P. Manchanda, A. Kashyap, and D. J. Sellmyer, "Magnetism of Dilute Co(Hf) and Co(Pt) Nanoclusters," *J. Appl. Phys.* **111**, 07B532 (3 pages) (2012); doi: 10.1063/1.3678582.
 5. B. Balamurugan, B. Das, V. R. Shah, R. Skomski, X. Z. Li, and D. J. Sellmyer, "Assembly of Uniaxially Aligned Rare-Earth-Free Nanomagnets," *Appl. Phys. Lett.* **101**, 122407 (2012); doi: 10.1063/1.4753950.
 6. O. Akdogan, W. Li, B. Balasubramanian, D.J. Sellmyer, and G.C. Hadjipanayis, "Effect of Exchange Interactions on the Coercivity of SmCo₅ Nanoparticles Made by Cluster Beam Deposition," *Adv. Funct. Mater.* 2013, DOI: 10.1002/adfm.201201353.
 7. B. Balasubramanian, B. Das, R. Skomski, W.Y. Zhang, and D.J. Sellmyer, "Novel Nanostructured Rare-Earth-Free Magnetic Materials with High Energy Products," *Adv. Matls.* (2013), doi: 10.1002/adma201302704.
 8. Y. Liu, T.A. George, Ralph Skomski and D.J. Sellmyer, "Aligned and Exchange-Coupled FePt-Based Films," *Appl. Phys. Lett.* **99**, 172504 (3 pages) (2011); doi:10.1063/1.3656038.
 9. Y. Liu, T. A. George, R. Skomski, and D. J. Sellmyer, "Aligned and Exchange-Coupled L1₀ (Fe,Co)Pt-Based Magnetic Films," *J. Appl. Phys.* **111**, 07B537 (3 pages) (2012); doi: 0.1063/1.3679099.
 10. O. Akdogan, W. Li, G.C. Hadjipanayis, R. Skomski, and D.J. Sellmyer, "One-Step Fabrication of L1₀ FePt Nanocubes and Rods by Cluster Beam Deposition," *J. Appl. Phys.* **111**, 07B535 (3 pages) (2012); doi: 10.1063/1.3679085.
 11. P. Kharel, P. Thapa, P. Lukashev, R.F. Sabirianov, E. Y. Tsymbal, D.J. Sellmyer, and B. Nadgorny, "Transport Spin Polarization of High Curie Temperature MnBi Films," *Phys. Rev. B* **83**, 024415 (1-6) (2011); doi: 10.1103/PhysRevB.83.024415.
 12. P. Kharel, R. Skomski, P. Lukashev, R. Sabirianov, and D.J. Sellmyer, "Spin Correlations and Kondo Effect in a Strong Ferromagnet," *Physical Review B* **84**, 014431 (1-5) (2011); doi: 10.1103/PhysRevB.84.014431.
 13. P. Kharel, R. Skomski, and D.J. Sellmyer, "Spin Correlations and Electron Transport in MnBi:Au Films," *J. Appl. Phys.* **109**, 07B709 (1-3) (2011); doi: 10.1063/1.3537952.
 14. P. Kharel and D.J. Sellmyer, "Anomalous Hall Effect and Electron Transport in Ferromagnetic MnBi Films," *J. Phys. Cond. Matt.* **23**, 426001(1-5) (2011); doi: 10.1088/0953-8984/23/42/426001.
 15. Y. Huh, P. Kharel, V. R. Shah, X. Z. Li, R. Skomski and D. J. Sellmyer, "Magnetism and Electron Transport of Mn_yGa (1<y<2) Nanostructures," *J. Appl. Phys.* **114**, 013906 (1-5) (2013); doi: 10.1063/1.4812561.

Spin-Polarized Scanning Tunneling Microscopy Studies of Nanoscale Magnetic and Spintronic Nitride Systems

Arthur R. Smith and Jeongihm Pak, Ohio University, Nanoscale & Quantum Phenomena Institute, Athens, OH 45701

Program Scope: The scope of this project is to investigate the properties of nanoscale magnetic and spintronic nitride systems. Of particular interest is to investigate nitride surfaces such as wurtzite gallium nitride coated with magnetic layers. As our central experimental technique, we utilize ultra-high vacuum (UHV) scanning tunneling microscopy (STM) and spin-polarized scanning tunneling microscopy (SP-STM). Both room temperature and low-temperature STM systems are employed in this project in order to address key questions regarding the magnetic and spintronic properties at the nanometer and atomic length scales. Samples investigated are prepared using molecular beam epitaxy (MBE) and transferred *in-situ* to the adjoining UHV-STM chambers for investigation.

Recent Progress: Over the last two years, we have made significant progress studying magnetic Mn-containing layers grown heteroepitaxially on GaN, and also with manganese nitride layers such as MnN and Mn₃N₂ grown on MgO(001). A central thrust has been the study of ferromagnetic MnGa layers on GaN. It has been found in the case of the Ga-polar GaN(0001) substrate, that ferromagnetic MnGa ultra-thin films can grow epitaxially and with little or no atomic diffusion from the film into the substrate. This results in high quality MnGa(111) layers growing under step-flow-type growth conditions.

Atomic MnGa (111)-oriented layers are separated by single atomic steps 2.2 Å in height. Using STM, different reconstructions are observed on the surfaces including 1×2, 2×2, and 2×3, as seen in Fig. 1. In order to determine appropriate atomic models for these structures and to compare the STM images with theoretical simulations, we have collaborated with theoreticians from the *Universidad Nacional Autónoma de México*. Based on their first-principles, density functional theory calculations, we have been able to determine that the 1×2 structure is the stoichiometric surface, whereas the 2×2 is Mn-rich with a 3:1 surface Mn:Ga concentration. But since much of the surface has the 2×2 structure and not the 1×2 structure, this result is in apparent contradiction with the fact that the layer growth was carried out under only slightly Mn-rich growth conditions (Mn:Ga flux ratio = 1.09). However, Rutherford backscattering on the same film carried out by the group of Prof. David Ingram, our local collaborator at *Ohio University*, has resolved the issue by revealing that the film's bulk stoichiometry is actually on the slightly Ga-rich side (Mn:Ga = 0.99). Therefore, it indicates that there is a tendency for Mn to segregate towards, or accumulate in, the top surface layer during growth under slightly Mn-rich growth conditions. **These results are currently out for review in a manuscript to *Applied Physics Letters*, including both the experimental and theoretical results.**

On the N-polar, GaN(0001) surface, deposition of Mn onto the Ga-rich surface has been found to result in a qualitatively different growth mode. Namely, rather than forming a uniform film everywhere, quantum-height MnGa islands several hundred nanometers across are formed with two characteristic (quantum) heights (9.3 Å and 11.3 Å), the difference being one atomic layer. Structurally, the lateral MnGa lattice constant of these islands is stretched (increased) to coherently fit the GaN substrate *in-plane* spacing, while the *out-of-plane* MnGa lattice constant is correspondingly reduced, resulting in layer spacing of ~ 1.9 Å. But the cause of the special heights of these islands cannot be explained using any strain argument. Rather, it is due to the existence of a preferred thickness, which is attributed to the quantum size effect (QSE). QSE-driven growth modes have been observed for a handful of other systems such as Ag/GaAs(110) and Pb/Si(111).[1,2] In our case, we observe a QSE-driven growth mode for ferromagnetic material (MnGa) on wide band-gap GaN, which has not been seen before. **These results were published in an article in *Applied Physics Letters* (2012).**

On the topic of manganese nitride, we have made a major finding recently concerning the magnetic properties of Mn₃N₂ (001). This is a layer-wise anti-ferromagnetic material in bulk. Our results concern with the surface magnetism, as accessed using SP-STM. Because of the 3:2 Mn:N stoichiometry, every two MnN layers are separated from the next two by an intervening Mn layer. At the (001) surface, these Mn layers can be distinguished from the two neighboring MnN layers in a 3-layer super-periodicity. The sequence of layers is accessed easily due to the formation of a 3-dimensional *spin pyramid* morphology. Electronically, using normal W tips, the Mn layers are easily distinguished from the MnN layers in dI/dV maps as either brighter (at negative sample bias) or darker (at positive sample bias). Magnetically, the two MnN layers have opposite spin directions, and this is easily resolved using magnetic (Fe-coated) W tips having *in-plane* magnetization. However, the magnetic direction of the Mn layers could not be resolved using the *in-plane* oriented Fe-coated W tips. Rather, we found that consecutive Mn

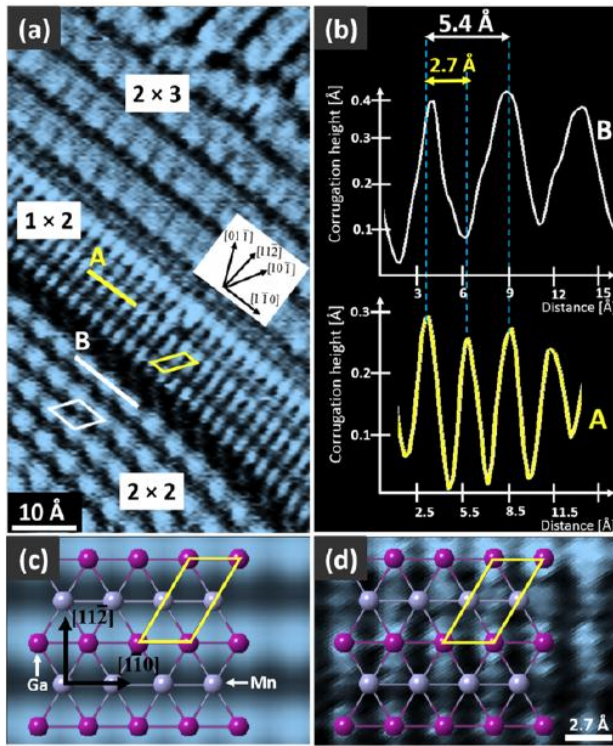


Fig. 1. (a) STM image of MnGa(111) surface. Three different reconstructions are seen - 1×2, 2×2, and 2×3. Scanning parameters: Vs = -6.2 mV, It = 293 pA. (b) line profiles for the 1×2 (A) and 2×2 (B) showing the double spacing of the 2×2 compared to the 1×2. (c) and (d) are simulated and experimental STM images for the stoichiometric 1×2, corresponding to the bias voltage Vs = -6.2 mV. The theoretical 1×2 model was overlaid on both images.

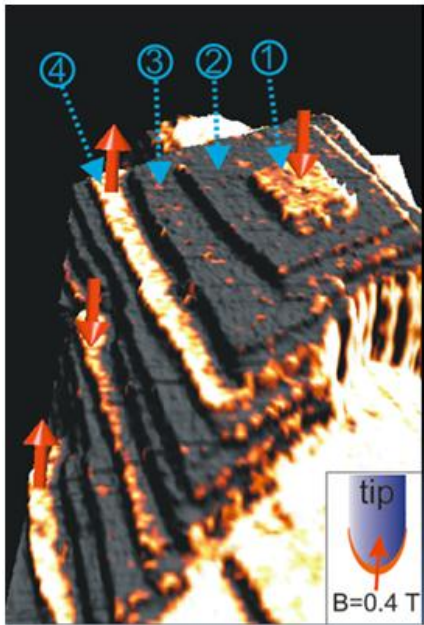


Fig. 2. SP-STM image of $\text{Mn}_3\text{N}_2(001)$ nano-pyramid in 3-D rendering, with contrast level suppressed, in which one can see the magnetic contrast on the consecutive Mn layers indicated by red arrows, with *out-of-plane* magnetic field turned on. Layers (1), (2), (3), and (4) correspond to Mn (spin \downarrow), MnN , MnN , and Mn (spin \uparrow) layers.

work on chromium nitride, which has very controversial electronic properties as a function of temperature, to include spin magnetic measurements at low temperature.

In the case of the smooth MnGa films on Ga-polar GaN substrates, we are planning to probe how the magnetic properties change locally as a function of the reconstruction (1×2 , 2×2 , 2×3). We anticipate the stoichiometric 1×2 regions to have the expected ferromagnetic behavior, whereas the Mn-rich regions to have antiferromagnetic behavior. In the case of the MnGa quantum-height islands on the N-polar GaN substrates, due to the changed lattice parameters within these coherently strained islands, we expect their magnetization directions may be modified quite dramatically as compared to the unstrained MnGa layers. While speculation can often be wrong in magnetic systems, we also expect to find unusual magnetic behavior for these islands due to their discreet QSE-driven heights.

Future plans also include initial work to look at rare earth-doped GaN surfaces such as Gd-doped GaN(0001) as well as GdN itself at low temperatures and under applied magnetic fields.

layers could be distinguished magnetically only by applying a small *out-of-plane* magnetic field, rotating the tip magnetization vector into an *out-of-plane* direction, as seen in Fig. 2. This then allowed us to show that the Mn layers at the growth surface possess orthogonal spin ordering relative to the MnN layers. Moreover, the *out-of-plane* spin ordering of the Mn layers was linked to the formation of a $c(2\times 4)$ reconstruction in which every 4 surface Mn atoms combine into tetramer units. The bond distortion upon tetramer formation is clearly linked to the surface spin reorientation from *in-plane* (for bulk) to *out-of-plane* (for the surface). **This work was published in Nano Letters (2012).**

Future Plans: Our recent work has set the stage for spin magnetic measurements for a variety of magnetic nitride-based systems. As discussed, we obtained spin magnetic results already for the $\text{Mn}_3\text{N}_2(001)$ spin pyramids, finding unexpected *out-of-plane* orthogonal spin ordering. We are currently planning to continue probing the magnetic properties of these systems using both our RT-STM and LT-STM systems under applied magnetic fields. In particular, we hope to uncover further insight into the unusual surface spin reorientation. Alongside the manganese nitride work, we will soon expand our previous

References

- [1] A. R. Smith, K. J. Chao, Q. Niu, and C. K. Shih, *Science* **273**, 226 (1996).
- [2] T.-L. Chan, C. Z. Wang, M. Hupalo, M. C. Tringides, and K. M. Ho, *Phys. Rev. Lett.* **96**, 226102 (2006).

Publication List (2011-13):

- 73. [Heteroepitaxial Growth and Surface Structure of L₁₀-MnGa\(111\) Ultra-thin Films on GaN\(0001\)](#), Andrada-Oana Mandru, Reyes Garcia Diaz, Kangkang Wang, Kevin Cooper, Muhammad Haider, David C. Ingram, Noboru Takeuchi, and Arthur R. Smith, **submitted to Applied Physics Letters (2013)**.
- 72. [Manganese 3x3 and sqrt3 x sqrt3-R30° Structures and Structural Phase Transition on w-GaN\(000-1\) Studied by Scanning Tunneling Microscopy and First-principles Theory](#), Abhijit V. Chinchore, Kangkang Wang, Meng Shi, Andrada Mandru, Yinghao Liu, Muhammad Haider, Arthur R. Smith, Valeria Ferrari, Maria Andrea Barral, and Pablo Ordejon, **Physical Review B** **87**, 165426 (2013).
- 71. [Formation of Manganese Delta-doped Atomic Layer in Wurtzite GaN](#), Meng Shi, Abhijit Chinchore, Kangkang Wang, Andrada-Oana Mandru, Yinghao Liu, and Arthur R. Smith, **Journal of Applied Physics** **112**, 053517 (2012).
- 70. [Three-Dimensional Spin Mapping of Antiferromagnetic Nanopyramids Having Spatially Alternating Surface Anisotropy at Room Temperature](#), Kangkang Wang and Arthur R. Smith, **Nano Letters** **12**(11) (<http://dx.doi.org/10.1021/nl204192n>), (2012).
- 69. [Spontaneous Formation of Quantum Height Manganese Gallium Islands and Atomic Chains on N-polar Gallium Nitride\(000-1\)](#), Abhijit Chinchore, Kangkang Wang, Meng Shi, Yinghao Liu, and Arthur R. Smith, **Applied Physics Letters** **100**, 061602 (2012).
- 68. [The effect of growth parameters on CrN thin films grown by molecular beam epitaxy](#), Yinghao H. Liu, Kangkang Wang, Wenzhi Lin, Abhijit Chinchore, Meng Shi, Jeongilm Pak, Arthur R. Smith, and Costel Constantin, **Thin Solid Films** **520**, 90 (2011), 10.1016/j.tsf.2011.06.052.
- 66. [A Modular Designed Ultra-High-Vacuum Spin-Polarized Scanning Tunneling Microscope with Controllable Magnetic Fields for Investigating Epitaxial Thin Films](#), Kangkang Wang, Wenzhi Lin, Abhijit V. Chinchore, Yinghao Liu, and Arthur R. Smith, **Review of Scientific Instruments** **82**, 053703 (2011).
- 65. [Structural Controlled Magnetic Anisotropy in Heusler L₁₀-MnGa Epitaxial Thin Films](#), Kangkang Wang, Erdong Lu, Jacob W. Knepper, Fengyuan Yang, and Arthur R. Smith, **Applied Physics Letters** **98**, 162507 (2011).
- 64. [Two-Dimensional Mn Structure on the GaN Growth Surface and Evidence for Room-Temperature Spin Ordering](#), Kangkang Wang, Noboru Takeuchi, Abhijit Chinchore, Wenzhi Lin, Yinghao Liu, and Arthur R. Smith, **Phys. Rev. B** **83**, 165407 (2011).

Program Title: Electronic complexity of epitaxial rutile heterostructures

Principal Investigator: H.H. Weitering
Co-PIs: P.C. Snijders and P.R.C. Kent

Mailing Address: Oak Ridge National Laboratory, PO Box 2008 MS-6056
Oak Ridge, TN 37831-6056

Email: hanno@utk.edu

Program scope

This is a new program that will commence in FY 2014. The overarching goal of the new work is to understand and tailor the electronic complexity of epitaxial rutile heterostructures. Our focus will center on exploiting quantum mechanical confinement to tailor the electronic structure and orbital order of epitaxial rutile heterostructures. Tuning parameters include film thickness, dielectric properties of the quantum mechanical boundaries, and chemical doping.

Complex transition metal oxide exhibit a plethora of fascinating broken symmetry states that emerge from the intricate interplay between the various quantum mechanical degrees of freedom of these materials, including electronic and/or spin excitations, orbital ordering, and cooperative lattice deformation. While most investigations to-date have focused on complex perovskite systems and related heterostructures, rutile heterostructures offer a particularly unique and hitherto almost unexplored perspective for tuning electronic complexity and emergent properties in complex oxides. In particular, the presence of edge-shared MO_6 octahedra (M=metal cation) and formation of direct cation-cation bonds in rutile tends to lower the effective dimensionality of the electronic structure, compared to corner-shared perovskite systems, and greatly facilitates the growth of non-polar (001) and (110)-oriented heterostructures. The existence of two stable growth orientations, along with the extreme anisotropy of the metal-metal σ -bonds, offers a unique opportunity to vary the occupation of selected $3d\text{-}t_{2g}$ orbitals via quantum confinement, and their coupling to the other degrees of freedom (see Figure 1) [1].

The new investigations aim to understand and tailor the electronic, orbital, and spin degrees of freedom of quantum-confined rutile heterostructures, and explore the existence of recently-predicted and/or other competing quantum matter phases for select heterostructures [2]. Our approach will involve epitaxial synthesis via Molecular Beam Epitaxy, in-situ electron spectroscopy, scanning tunneling microscopy (or spectroscopic STM), ab-initio density functional theory (DFT) and post-DFT calculations. Fundamental knowledge that will be gleaned from these studies will broaden and deepen our understanding of complexity and spontaneous symmetry breaking in correlated electron systems, and elucidate how collective materials properties can be controlled through manipulation of the electronic and orbital degrees of freedom.

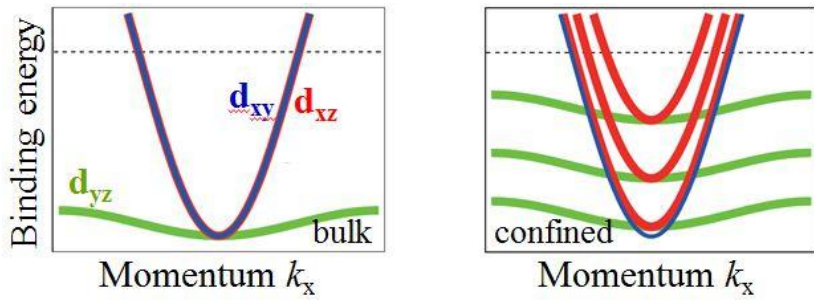


FIG 1. Orbital selective quantization: of the degenerate d_{xy} and d_{xz} orbitals in the bulk, only the d_{xz} quantizes upon confinement along the z-direction. 2D subband quantization pushes some of the subbands above the Fermi level, meaning that charge will have to be transferred to the in-plane d -orbitals with consequences for the orbital ordering in these systems. Adapted from Ref. [1].

References:

- [1] K. Yoshimatsu, K. Horiba, H. Kumigashira, T. Yoshida, A. Fujimori, and M. Oshima, “Metallic quantum well states in artificial structures of strongly correlated oxide,” Science **333**, 319 (2011).

- [2] V. Pardo, and W.E. Pickett, “Metal-insulator transition through a semi-Dirac point in oxide nanostructures: VO₂(001) layers confined within TiO₂,” Phys. Rev. B **81**, 035111 (2010).

Program Title: Imaging Electrons in Atomically Layered Materials

Principal Investigator: R.M. Westervelt

Mailing Address: School of Engineering & Applied Sciences, Harvard University, Cambridge MA, 02138

E-mail: westervelt@seas.harvard.edu

Program Scope

The objective of this work is to combine high-resolution transmission electron microscope (TEM) sculpting of nanoscale devices with cooled scanning probe microscope (SPM) imaging to study electron motion and the energy of electron states in atomically layered materials: graphene (G), hexagonal boron nitride (BN), and molybdenum disulfide (MoS_2).

These revolutionary new materials have layers that are atomically thin, opening the way to atomic-scale devices that promise to transform electronics. They change the rules: In graphene, electrons move as massless particles at a constant speed, which is 1/300 the speed of light, opening the way for ultrafast electronics; BN serves as an insulating atomic layer, and MoS_2 provides few-atom-thick semiconducting layers for flexible electronics and switches.

Project Description: By combining TEM and cooled SPM techniques, the PIs make, image, study and understand atomic-scale structures and devices made from atomically layered materials. Using a Zeiss Libra TEM in *Harvard's Center for Nanoscale Systems* (CNS), **David Bell** can make and image atomic-scale structures by sculpting the material with the electron beam. Our goal is to find stable atomic configurations, which could serve as building blocks for atomic electronics. **Robert Westervelt** plans to use custom-made cooled SPM instruments to image electrons inside atomic-scale structures, building on his previous imaging electron flow in GaAs 2DEGs. Westervelt plans to use the SPM tip as a movable gate to do Coulomb blockade spectroscopy of electron states inside quantum dots sculpted by the TEM electron beam, and as a movable scatterer to image electron motion. The analysis will be guided through a close collaboration with theorist **Eric Heller**.

Potential Impact: The radical behavior of electrons in atomically layered materials was only discovered eight years ago, leading to the Nobel prize for Andre Geim and Konstantin Novoselov and creating an exciting research environment. Atomically thin materials offer transformative new approaches to sensing and signal processing that offer new ways to make electronics, like silicon devices did fifty years ago. By developing new ways to make atomic-scale structures and image how electrons move through them, we hope to make important steps along this path.

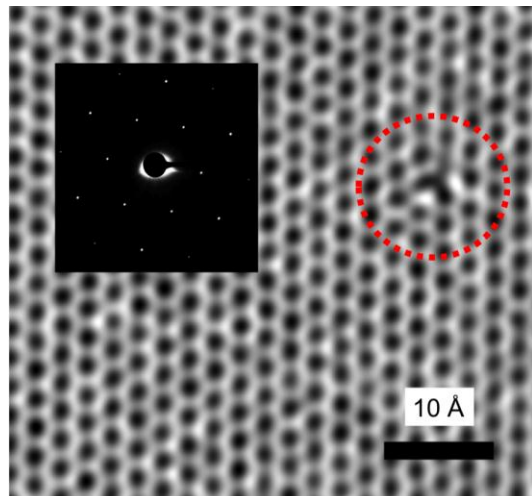


Fig. 1 CNS Zeiss Libra TEM image of suspended single atomic layer graphene sheet; insert: electron diffraction pattern. A single missing C atom is circled.

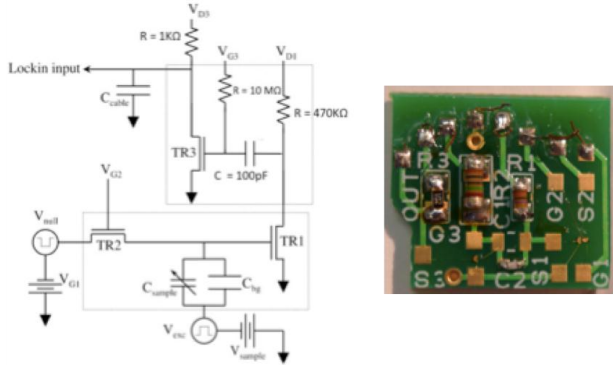


Fig. 2 Cooled charge preamplifier circuit (Steele 2006) and 13x14 mm² circuit board with wire-bonded HEMT transistors.



Fig. 3 New cooled SPM head with coarse positioning when cooled.

Recent Progress

Cooled Scanning Probe Microscope Additions and Improvements Over the past two years, we have carried out important additions and improvements for our cooled scanning probe microscope laboratory: 1) cooled charge preamplifier, 2) cooled SPM head with mechanical coarse positioning, 2) completion of two cooled scanning probe microscopes, one equipped with a superconducting solenoid for magnetic field measurements and one with a closed He-3 cooler to reach temperatures below $T \sim 0.5$ K. We describe these additions below.

Cooled Charge Preamplifier - A circuit diagram and photo of the cooled charge amplifier is shown in Fig. 2. The circuit, originally designed by Gary Steele in Ashoori's group (Steele 2006), is based on a low capacitance, high electron mobility transistor (Fujitsu FHX35X) that is available in an unpackaged format. The input is a capacitance bridge, with the small capacitance formed by a depleted HEMT, labeled TR2. To minimize the input capacitance, the charge amp is positioned very near the SPM cantilever inside the SPM head. The tested performance at low temperatures is excellent.

Rebuilt SPM Head - The SPM head (Fig. 3) was redesigned by DOE student Sagar Bhandari to allow mechanical coarse positioning of the SPM tip, while the unit is cold. This permits the study of many devices during a single cool down.

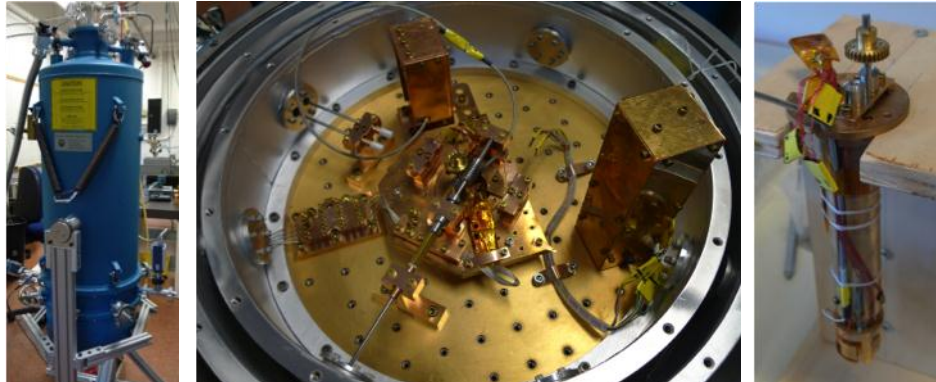


Fig. 4 Liquid He cooled SPM equipped with superconducting solenoid. A second SPM has closed liquid He-3 cooling to 0.5K.

Liquid He Cooled SPM Systems - We have completed the construction of two new liquid He cooled SPM systems (Fig. 4). The dewar, shown on left, is equipped with a cold plate to allow the SPM head to operate in a vacuum, to preserve the sample surfaces. To gain access to the cold plate, one rotates the dewar on pivots, and removes a 'top hat' vacuum chamber head, and two radiation shields. A close-up of the SPM head is on the right. One SPM system is equipped with a superconducting solenoid, to permit SPM imaging in strong magnetic fields. The other has a closed liquid He-3 cooler to permit measurements at temperatures ~ 0.5 K.

Atomic Scale Ripples in Few Layer Graphene - By combining high-resolution images of few layer graphene sheets with theoretical simulations of the electron system Wei Li Wang was able to measure atomic scale ripples in suspended sheets of few-layer graphene, shown in Fig. 13 (Wang et al. 2012). The ripples are made visible by the changes they make in atomic scale images of suspended graphene sheets. Wang converted the observed changes to angular deflection of the sheet through computer simulations of electrons in graphene. The measured deflection vs. position is shown in Fig. 5.

Future Plans

Nanosculpting and Imaging Graphene Structures at the Atomic Scale

The electron beam in a TEM or a STEM provides an excellent way to cut and shape suspended graphene sheets into atomic scale structures (Fischbein and Drndic 2008; Girit *et al.* 2009). This approach is powerful, because the same instrument can be used to image the structure immediately after it was formed.

In our proposed research, we plan to use the CNS Zeiss Libra STEM and TEM instruments in as powerful tools to sculpt and image atomic layered materials at the atomic scale. Experiments on the materials science of atomic scale structures to find stable shapes and atomic configurations will be carried out inside the TEM and STEM. We also plan to sculpt samples for imaging and probing using our cooled SPMs, as described below.

The capability of CNS TEM and STEM instruments is demonstrated in Fig. 1 - a TEM image of a suspended

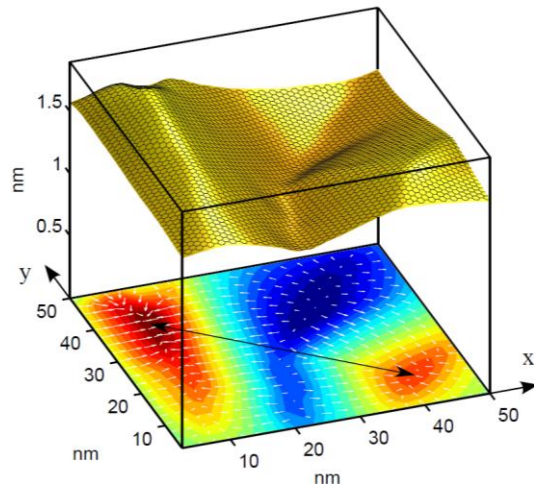


Fig. 5 Topography reconstruction of a suspended graphene surface via theoretical analysis of TEM images; amplitude 0.5 nm, typical width 45 nm (Wang et al. 2012).

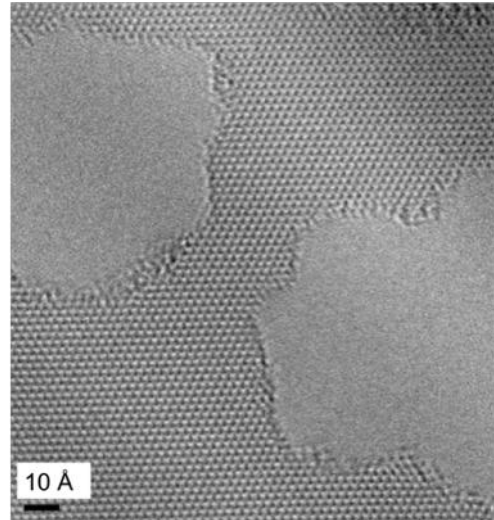


Fig. 6 TEM image of a graphene bridge in a suspended graphene sheet formed by nanosculpting (Bell CNS).

single-atomic-layer graphene sheet. The quality of the sample and instrument is illustrated in the diffraction pattern inset. It is remarkable that a single missing C atom can be identified, marked by a red circle.

Figure 6 shows a TEM image of an atomic scale structure made by nanosculpting a suspended graphene film with the electron beam of the CNS Zeiss TEM instrument. By creating two nearby holes, a narrow ribbon is formed. It's interesting that the atoms reconfigure their arrangement along the sides of the ribbon, preferring the zig-zag atomic configuration, which also shows up in the ribbon's shape. Using our cooled SPMs we plan to image electron flow through such structures, using electrons injected from the conducting tip, or image electrons capacitively attracted to the structure, as described below.

By sculpting three or more nearby apertures, one can create a quantum dot. The graphene bridges that support the dot from quantum point contacts with widths less than half the electron wavelength as demonstrated by Stampfer et al. (2008). Using the conducting SPM tip as a movable gate, and the cooled preamp as a charge sensor, we plan to do Coulomb blockade spectroscopy measurements on graphene quantum dots with different atomic configurations.

References

Michael Fischbein and Marija Drndic, "Electron beam nanosculpting of suspended graphene sheets," *App. Phys. Lett.* **93**, 113107 (2008).

Çaglar Ö. Girit, Jannik C. Meyer, Rolf Erni, Marta D. Rossell, C. Kisielowski, Li Yang, Cheol-Hwan Park, M. F. Crommie, Marvin L. Cohen, Steven G. Louie, A. Zettl, "Graphene at the Edge: Stability and Dynamics," *Science* **323**, 1705 (2009).

C. Stampfer, E. Schurtenberger, F. Molitor, J. Guttinger, T. Ihn and K. Ensslin, "Tunable Graphene Single Electron Transistor," *Nano Letters* **8**, 2378 (2008).

Gary A. Steele "Imaging Transport Resonances in the Quantum Hall Effect," PhD Thesis, MIT (2006).

Publications (supported by DOE grant over previous 2 years)

Keith A. Brown, Kevin J. Satzinger, and Robert M. Westervelt, "High spatial resolution Kelvin probe force microscopy with coaxial probes," *Nanotechnology* **23**, 115703 (2012).

Keith A. Brown, Ben Yang and R.M. Westervelt, "Self-driving capacitive cantilevers for high frequency dynamic AFM," *Appl. Phys. Lett.* **100**, 053110 (2012).

Wei L. Wang, Sagar Bhandari, Wei Yi, David C. Bell, Robert Westervelt, and Efthimios Kaxiras, "Direct imaging of atomic-scale ripples in few-layer graphene," *Nano Lett.* **12**, 2278-82 (2012).

Keith A. Brown and Robert M. Westervelt, "Triaxial AFM probes for non-contact trapping and manipulation," *Nano Lett.* **11**, 3197-3201 (2011).

Keith A. Brown, Jesse Berezovsky, and R.M. Westervelt, "Coaxial atomic force microscope probes for imaging with dielectrophoresis," *Appl. Phys. Lett.* **98**, 123109 (2011).

Project Title: Investigation of Spin Physics in Semiconductor Nanowire-Based Heterostructures

PI: Fengyuan Yang
Department of Physics, The Ohio State University
Email: fyyang@physics.osu.edu

Co-PI: Ezekiel Johnston-Halperin
Department of Physics, The Ohio State University
Email: ejh@physics.osu.edu

Project Scope:

The central goal of this DOE project is to investigate spin relaxation, spin transport, and coupling of spins in nanostructures enabled by semiconductor nanowires using a variety of optical techniques. We have been using metal-organic chemical vapor deposition (MOCVD) for the growth of heterostructured III-V semiconductor nanowires with the capability to grow nanowires (e.g. GaAs) with precisely controlled dimension, carrier type and concentration, as well as an epitaxial shell (e.g. AlGaAs) with dielectric and lattice matching. The *in-situ* growth of the shell also greatly minimizes the density of defect states at the GaAs/AlGaAs interface, which is critically important for their spintronic performance.

This abstract describes the recent progresses of this project in three parts: (1) understanding the correlation between MOCVD growth aspects and optical/electronic quality of the core/shell structured GaAs/AlGaAs nanowires; (2) electrical characterization of individual GaAs wires embedded in AlGaAs using conducting atomic force microscopy; and (3) spin lifetime measurements using pump-probe time-resolved Kerr rotation techniques. In addition, we discuss our plan for ferromagnetic resonance (FMR) driven spin pumping from a ferromagnet into semiconducting nanostructures.

Recent Progress

1. Control of MOCVD nanowire growth for optimal optoelectronic quality

Spin relaxation and optical properties in semiconductor nanowires are sensitive to defect states in nanowires. The growth conditions in MOCVD systems greatly affect the density and nature of these defect states in semiconductor nanowires. However, a good understanding of how the MOCVD growth process affects the electronic and optical properties of nanowires is still lacking. We performed a systematic study of the growth parameters and the resulting nanowire topography and optical quality using photoluminescence (PL) spectroscopy.

Nanowire growth requires a balance between the pyrolysis of the organometallic precursors, the solid solubility of the group III and group V atoms in the Au colloid, and the diffusion of atomic species on the substrate and nanowire surface. As a result, accurate and reproducible measurement of the substrate temperature during growth is essential. We use a pyrometer (accurate above 480°C) in our MOCVD system to measure the real sample temperatures, from which we extrapolate the calibration of the thermocouple in the sample heater to achieve accurate control of the growth temperature for GaAs nanowires between 400°C and 450°C. The estimated error of the growth temperature is $\pm 0.5^\circ\text{C}$, leading to a growth-to-growth variation of up to $\pm 2^\circ\text{C}$ for nominally identical growth conditions.

Figures 1a and 1b, are SEM images of nanowires grown on GaAs(100) and (111)B at growth temperatures of 410°C and 431°C, respectively. Wires grown on the (111)B surfaces are normal to the surface and those grown on a (100) surface make an angle of $\sim 35^\circ$ with the substrate surface. The desired morphology is a straight wire with smooth sides. Wires grown at the lower end of the temperature range have negligible tapering in

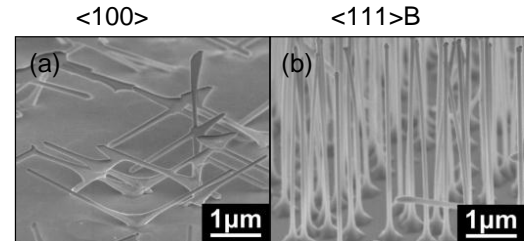


Fig. 1. SEM image for nanowires grown on (a) GaAs $<100>$ and (b) GaAs $<111>\text{B}$ for growth temperatures of (a) 410°C and (b) 431°C. For clarity, the image in (a) was intentionally taken in an area of low density. Both images are from the perspective of 52° from the surface normal.

diameter, but a higher probability of having rough sides, kinking and growing in different directions. At the higher end of the range, the wires show smooth walls and a larger tapering, indicating a higher rate of growth on the side.

As shown in the PL spectra in Fig. 2, a sharp near-band-edge emission centered at 819 nm is observed at a growth temperature of 410°C for wires on the (100) substrate and 430°C for the (111)B substrate. This dominance of near-band-edge emission in the PL spectrum is an indication of high optical quality and low defect density. As the growth temperature increases, both substrates show a gradual shift in the spectral weight from the band edge emission at 819 nm toward 830 nm which is commonly associated with carbon impurity luminescence in MOCVD-grown GaAs.

The maximum growth rate is found to be approximately 440°C +/- 4°C for wires grown on both substrates (Figs. 3a and 3b). The mechanism for decreasing axial growth rate with increasing growth temperature in the range of 440 – 472°C is attributed to a shift in the dominant growth mode from the vapor-liquid-solid (VLS) to a thin film growth mode. Figs. 3c and 3d show the relative PL intensity of the 819 nm band edge peak compared to the 830 nm defect peak measured on transferred nanowires to separate the nanowire PL emission from the GaAs substrate. This ratio, $I_{819\text{nm}}/I_{830\text{nm}}$, is calculated by integrating the photoluminescence at 819 nm and 830 nm with a bandwidth of 4 nm, which provides a density-independent measure of nanowire optical quality.

In this temperature regime, lowering the growth temperature decreases the dominance of the 830 nm peak hence increasing the peak ratio, likely because the VLS growth mode dominates over sidewall growth and leads to reduced defect states at the GaAs surface. In contrast, the peak ratio at temperatures below the maximum growth rate exhibits opposite trends on the different substrates. While the peak ratio levels off with decreasing growth temperature down to 410°C on the (100) surface, wires grown on the (111)B surface exhibit a decrease in peak ratio with decreasing temperature.

2. Electrical characterization of individual GaAs nanowires embedded in AlGaAs

In the process of exploring the impact of shell thickness on optical properties, we have developed a novel growth mode that we believe has the potential for significant impact in both charge based and spin based applications. Specifically, we have developed the capability to embed the GaAs nanowires in a

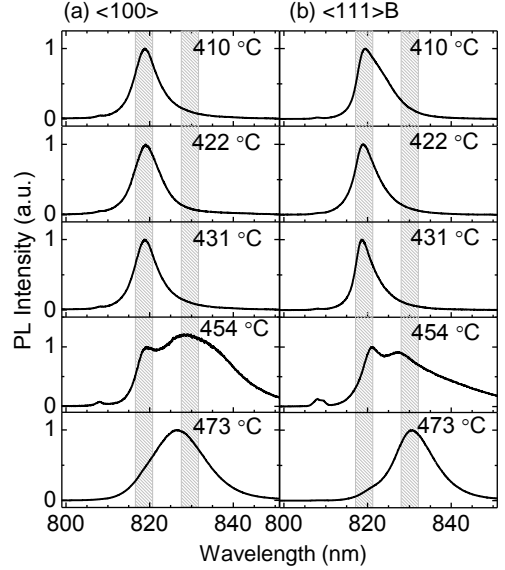


Fig. 2. PL spectra at 5 K of GaAs nanowires grown at various temperatures on (a) GaAs $<100>$ and (b) GaAs $<111>B$. As growth temperature increases the spectral weight shifts from 819 nm (band edge luminescence) toward 830 nm (impurity related PL).

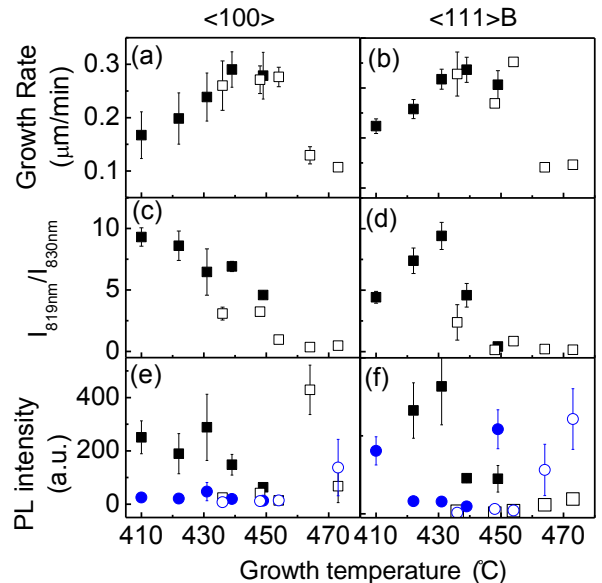


Fig. 3. Nanowire growth rate as a function of substrate temperature on (a) GaAs $<100>$ and (b) GaAs $<111>B$. Panels (c) and (d) are plots of the ratio of intensities of the 819 nm band edge peak to the 830 nm defect peak. Panels (e) and (f) are plots of PL intensities of both the 819 nm (squares) and 830 nm peaks (circles) as a function of growth temperature. The solid and open markers represent samples from two series of growths.

fully coalesced AlGaAs shell, resulting in a 2D film that is compatible with both traditional device fabrication and epitaxial regrowth. We use a combination of mechanical polishing and reactive ion etching to planarize and etch the sample to expose the GaAs nanowires for direct electrical contact.

Using a combination of traditional and conducting atomic force microscopy (AFM), we verify first that the planarization is effective in producing flat films (Fig. 4a) and second that we can electrically access individual GaAs nanowires (conducting AFM in Fig. 4b). More detail of the electronic structure can be seen in Fig. 4c, wherein current-voltage (I - V) characteristics for both a GaAs NW (black line) and the AlGaAs matrix (red line) show classic Schottky response with a turn-on voltage of roughly 1.5 V and 3.5 V, respectively, commensurate with the bandgaps of the two materials.

These results demonstrate the capability to perform *in situ* planarization with a lattice matched insulating material, allowing for the smooth transition from 2D to quasi-1D materials. The planarization and etching allows for top contacts to small ensembles of nanowires to be deposited using standard lithographic techniques. For example, the improved strain tolerance of the NW geometry should make it possible to produce light emitting diodes whose spectral range (and hence lattice constant) are simply not possible with 2D growth. These diodes can then be processed using established fabrication techniques. Of more direct relevance for spintronics, this planar geometry will allow for the integration of planar ferromagnetic end contacts to our nanowires, removing the potential complications of shape induced anisotropies and domain formation that can significantly complicate spin transport in lateral contact geometries. In addition, with further optimization we believe it may be possible to regrow additional, epitaxial 2D structures on top of the planarized nanowires. This will allow for truly novel 2D-1D-2D heterostructures wherein one can take advantage of the relative strengths of each growth mode, for example high mobility lateral transport in 2D GaAs/AlGaAs quantum wells and the increased strain tolerance in 1D structures described above. We are currently preparing these first results for publication.

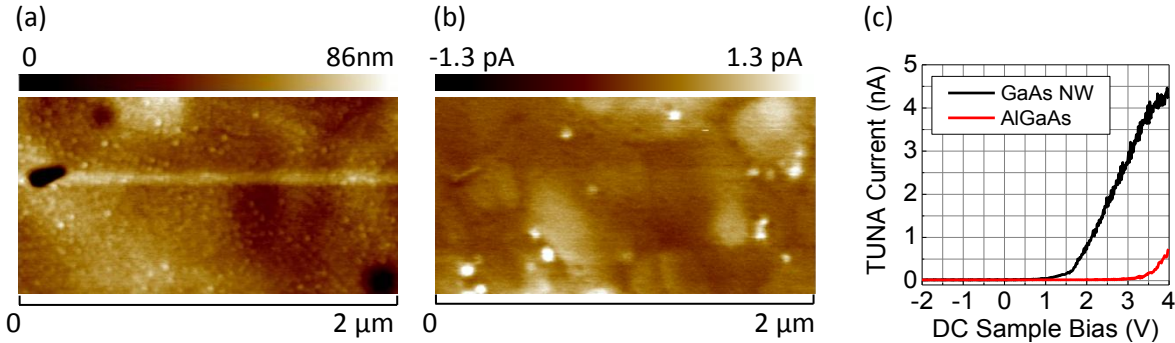


Fig. 4. (a) Topographic AFM image of the polished surface of GaAs nanowires with coalesced AlGaAs shell. (b) Conducting AFM image taken at a bias of +3 V. Nanowires show up as bright spots that are uncorrelated with topography. (c) Tunneling AFM I - V curves for the conducting tip positioned both over a NW (black line) and over the AlGaAs matrix (red line), demonstrating Schottky behavior with turn-on voltage commensurate with the difference in bandgap.

3. Spin lifetime measurements using pump-probe time-resolved Kerr rotation technique

Based on the foundation of these novel materials, we have continued our pursuit of realizing time domain spin lifetime measurements in 1D and quasi-1D systems. Using similar sample structures to those described above, we have developed the ability to grow samples with isotropic dielectric response on a lattice-matched InGaP layer (Fig. 5a, left panel). The matching dielectric environment is necessary to mitigate the effects of polarization anisotropy due to the 1D nature of the nanowires (see publication [2]) and the InGaP is used as an etch-stopping layer for removing the GaAs substrate. Finally, the epitaxial, lattice-matched AlGaAs shell is highly effective in passivating the nanowire surface defects.

As can be seen in the right hand panel of Fig. 5a, this structure so far shows no time-resolved spin signal. In diagnosing this problem, we have generated a series of control samples consisting of a bulk

GaAs epilayer grown on similar InGaP stop-etch layers, and have found that the most likely reason for the lack of TRKR signal in NW samples in Fig. 5a is that the InGaP (1 μm) etch-stop layer is too thick. Even though the excitation light is nominally sub-bandgap the presence of residual absorption due to defects or the tail of the band edge apparently suppresses our excitation over the 2 μm path length (1 μm in and 1 μm out). This hypothesis is borne out by the calibration sample shown in Fig. 5b wherein the thickness of the InGaP layer has been reduced to 184 nm and where the coherent oscillations of the spins in the GaAs epilayer are clearly visible. We are presently working to fabricate appropriate nanowire membrane samples to translate this geometry to our primary measurement.

Future Plans

In a separate project, Yang and Johnston-Halperin have worked to develop the technique of ferromagnetic resonance (FMR) driven spin pumping from ferromagnets to normal metals. While this work is yielding fundamental insights into the spin pumping process, that science lies well beyond the scope of this project. We mention it here because of the potential for strong technical leveraging and synergy with the studies of spin injection and transport in nanostructures that are the focus of this DOE BES program. Specifically, this technique realizes one of the “holy grails” of spin injection, spin transfer in the absence of a charge current. This synergy presents the opportunity to add a third technique to our investigations, supplementing optical and charge based spin injection with FMR driven spin transfer.

The key technical challenge is the fact that all spin pumping experiments to date rely on the inverse spin-Hall effect (ISHE) to monitor the injected spin current, and as the induced voltage is proportional to the length of the sample (and only reaches 10’s of microvolts in millimeter sized samples), it is not appropriate for nanoscale materials. We propose to overcome this limitation by using established *optical detection* techniques to probe the FMR-injected spin current. Specifically, circularly polarized luminescence due to spin polarized carriers is a direct measure of spin polarization in semiconductors. The zero background nature of a PL measurement makes this technique a natural fit for probing optically active nanostructures. As a result, we are working to develop a measurement based on microwave excitation of FMR in a layer of Fe deposited directly on a GaAs epilayer within our optical cryostat, allowing for simultaneous polarization resolved PL studies.

List of publications

1. Dongkyun Ko, Xianwei Zhao, Kongara Reddy, Oscar Restrepo, Nandini Trivedi, Wolfgang Windl, Nitin Padture, Fengyuan Yang, and Ezekiel Johnston-Halperin, “Role of defect states in charge transport in semiconductor nanowires,” *J. Appl. Phys.* **114**, 043711 (2013).
2. Lei Fang, Xianwei Zhao, Yi-Hsin Chiu, Dongkyun Ko, DongSheng Li, Nitin Padture, Fengyuan Yang, and Ezekiel Johnston-Halperin, “Controlling the polarization anisotropy through oxide coating in InP and ZnO nanowires,” *Appl. Phys. Lett.* **99**, 141101 (2011).

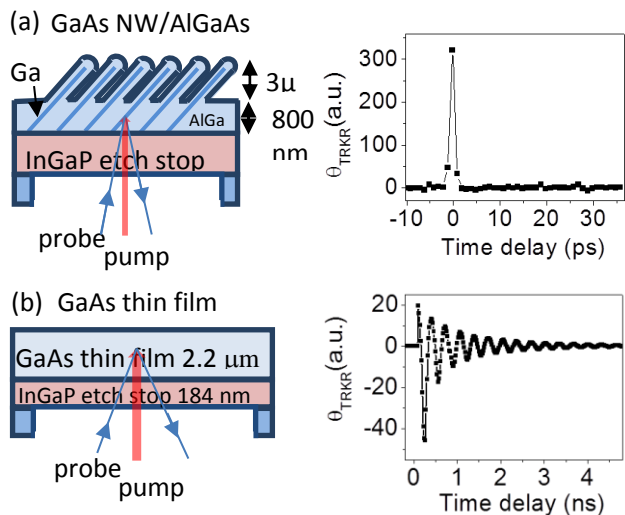


Fig. 5. (a) Left panel: schematic of NW core/shell growth on an InGaP etch-stop layer, chemical selective allows for membrane fabrication and back side illumination. Right panel: time resolved Kerr rotation (TRKR) from NW sample. (b) Left panel: similar structure with NWs replaced by a bulk GaAs epilayer and a much thinner InGaP layer. Right panel: TRKR showing coherent spin precession in the GaAs epilayer measured through the InGaP layer.

While this work is yielding fundamental insights into the spin pumping process, that science lies well beyond the scope of this project. We mention it here because of the potential for strong technical leveraging and synergy with the studies of spin injection and transport in nanostructures that are the focus of this DOE BES program. Specifically, this technique realizes one of the “holy grails” of spin injection, spin transfer in the absence of a charge current. This synergy presents the opportunity to add a third technique to our investigations, supplementing optical and charge based spin injection with FMR driven spin transfer.

The key technical challenge is the fact that all spin pumping experiments to date rely on the inverse spin-Hall effect (ISHE) to monitor the injected spin current, and as the induced voltage is proportional to the length of the sample (and only reaches 10’s of microvolts in millimeter sized samples), it is not appropriate for nanoscale materials. We propose to overcome this limitation by using established *optical detection* techniques to probe the FMR-injected spin current. Specifically, circularly polarized luminescence due to spin polarized carriers is a direct measure of spin polarization in semiconductors. The zero background nature of a PL measurement makes this technique a natural fit for probing optically active nanostructures. As a result, we are working to develop a measurement based on microwave excitation of FMR in a layer of Fe deposited directly on a GaAs epilayer within our optical cryostat, allowing for simultaneous polarization resolved PL studies.

Probing Correlated Superconductors and their Phase Transitions on the Nanometer Scale

Ali Yazdani

Department of Physics

Princeton University, Princeton, NJ 08544

yazdani@princeton.edu

Program Scope:

Our experimental program provides an atomic scale perspective of unconventional superconductivity — how it evolves from an unconventional conducting state, and how it competes with other forms of order in correlated electronic systems. Such phenomena are at the heart of some of the most debated issues in condensed matter physics, and their understanding is an intellectual driver for many of the DOE-BES projects for the development of novel materials, including search for higher temperature superconductivity. Our aim is to provide a microscopic view of these exotic materials and their phase transition into the superconducting state using some of the most sophisticated scanning tunneling microscopy (STM) and spectroscopy techniques. The results of the experiments proposed here provide important evidence that will help constrain theoretical models of unconventional superconductivity, the normal states from which it emerges from, and electronic states with which it competes.

The proposed program is divided into three parts. The first part will focus on examining how heavy electron states emerge in compounds in which f orbital interact with more itinerant electronic states and the process by which such heavy electronic states give rise to unconventional superconductivity. Although heavy fermions do not superconduct at very high temperatures, their transition temperature is a substantial fraction of the heavy electron state bandwidth, hence making these materials among the most strongly correlated superconductors discovered to date. More importantly, the parallels between the puzzles in heavy fermions and high- T_c cuprates superconductors suggest that heavy fermions might provide important clues to a more general understanding of correlated electronic states and their superconductivity. For example, like cuprates or Fe-based superconductors, superconductivity in heavy fermion system is often found in vicinity of anti-ferromagnetism in the phase diagrams of these systems.

The second part of the proposed program focuses on how charge ordering competes with superconductivity in high- T_c cuprates. One of the key questions is to determine whether there is universality in the way charge ordering occurs in doped Mott insulators and the connection between different forms of charge ordering now observed in different cuprate families. Overall, the precise determination of charge ordering in Bi-based compounds as a function of field and temperature examined in our program, and contrasting the results of such studies with experiments on other cuprates, will establish what aspects of charge ordering in the cuprates are universal and what aspects are material dependent. The third and more exploratory part of this program is to focus on the development of techniques for local Josephson tunneling with superconducting STM tips at millikelvin temperatures. Development of such a technique can provide important details about the nature of the superfluid response and phase of the superconducting order parameter on the nanoscale, with broad applicability for the study of superconductivity in a wide range of materials. The three components of the proposed program provide a broad attack on some of the most important problems in the physics of correlated materials and the emergence of superconductivity in these systems.

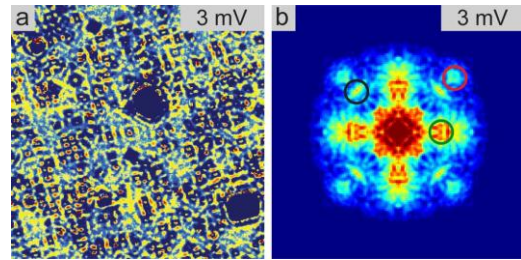


Figure 2. (a) Real space and (b) momentum space spectroscopic mapping of heavy quasi-particle states in Ce-115 family of compounds with STM.

Recent Progress:

Visualizing Heavy Fermions Emerging in a Quantum Critical Kondo Lattice—Nature (2012) [1]

In solids containing elements with f -orbitals, the interaction between f -electron spins and those of itinerant electrons leads to the development of low-energy fermionic excitations with a large effective mass. These excitations are fundamental to the appearance of unconventional superconductivity and non-Fermi liquid behavior observed in actinide- and lanthanide-based compounds. During the last three years, our group has succeeded in applying scanning tunneling microscopy (STM) techniques to study the heavy fermion systems and their superconductivity for the first time. Three years ago, we had a major breakthrough in the study of heavy fermion states and their phase transition into the so-called “hidden order” state in URu_2Si_2 , (Aynajian et al. *PNAS* 2010). Last year, we made an even more exciting advance in the study of heavy fermion compounds by using spectroscopic mapping with the STM to detect the emergence of heavy excitations upon lowering the temperature in a prototypical family of Ce-based heavy fermion compounds, (*Nature* 2012, [1]). The Ce-based compounds are particularly exciting to work on as they show a remarkably similar phase diagram to high-temperature cuprate superconductors. This system can be tuned between an anti-ferromagnetic ground state and an unusual high temperature non-Fermi liquid state, which when cooled exhibits unconventional superconductivity.

In this project we have demonstrated the sensitivity of the tunneling process to the composite nature of these heavy quasiparticles that arises from a quantum entanglement of itinerant conduction and f -electrons. Scattering and interference of the composite quasiparticles in the Ce-based 115 systems is used to resolve their energy-momentum structure and to extract their mass enhancement, which develops with decreasing temperature. This is the first time the energy-momentum structure of a generic heavy fermion state has been measured, as previous angle-resolved experiments have not had enough energy resolution to perform such studies.

Visualizing Nodal Heavy Fermion Superconductivity—Nature Physics (2013) & covered in News and Views [2]

Following our last year’s study of heavy quasi-particles formation in f -electron system, we have had a major breakthrough this year by performing the first STM experiment to study the emergence of heavy electron superconductivity with lowering of temperature. Through this study, we have uncovered the first direct spectroscopic and spatial resolve evidence for $d_{x^2-y^2}$ gap symmetry in a heavy fermion system. These experiments, which were also carried out on CeCoIn_5 , are made possible by our recent development of an advance ultralow temperature high magnetic field UHV STM system, also supported by DOE-BES.

STM can probe the symmetry of the superconducting order parameter through scattering of quasi-particle from impurities as well as when the impurity is strong enough to trap a localized quasi-particle state in its immediate vicinity. We have preformed comprehensive STM measurements probing the interplay between quasi-particles and impurities in Ce-115 system in both superconducting and its normal state. For weak impurities, probing symmetry of the superconducting order parameter, requires understanding of the interference of quasi-particle scattering from the impurities—a task that requires assumption about the band structure and the way in which pairing gaps the Fermi surface of the superconductor. The complex three-dimensional Fermi surface of CeCoIn_5 makes such an analysis unreliable. In contrast, if the impurity is strong enough to trap an electron-like or hole-like quasi-particle,

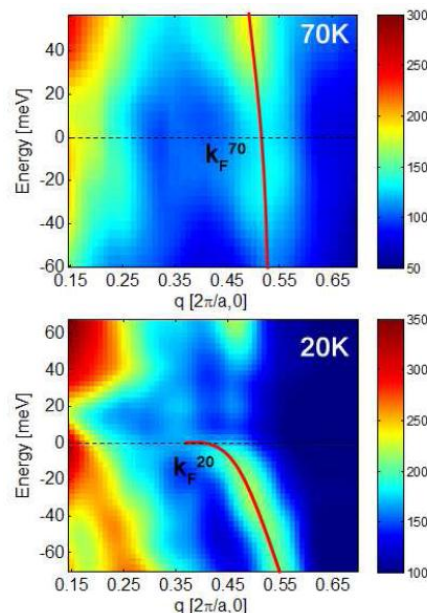


Figure 1. Transition from a small to large Fermi surface in CeCoIn_5 showing the development of the heavy fermion state with decreasing temperature detected by spectroscopic mapping with the STM.

direct mapping of this impurity bound state provide direct visual evidence for the pairing symmetry. The results of such experiments on CeCoIn₅ are shown in Figure 3. As shown in this figure the electron-like component of the impurity bound state leaks out away from the impurity along the minima of pairing potential, thereby pinpointing the nodes to occur at diagonal to the crystal axis in $d_{x^2-y^2}$ form. This behavior is further confirmed by imaging the hole component of the same impurity state, showing it to be spatially complementary to the electron component as is expected.

These experiments firmly establish its pairing symmetry in CeCoIn₅ to be similar to that of the high- T_c cuprate superconductors and extend for the first time the power of the STM to another class of extraordinary superconductors, the heavy fermions. In fact, the parallels to the high- T_c goes even further as our spectroscopy reveals the superconductivity gap to develop within a depression of the density of states near the Fermi level that persists above T_c and above the critical magnetic field. Further experiments are required to fully understand the interplay between our discovery of a “pseudogap” and other electronic correlation in this heavy fermion system.

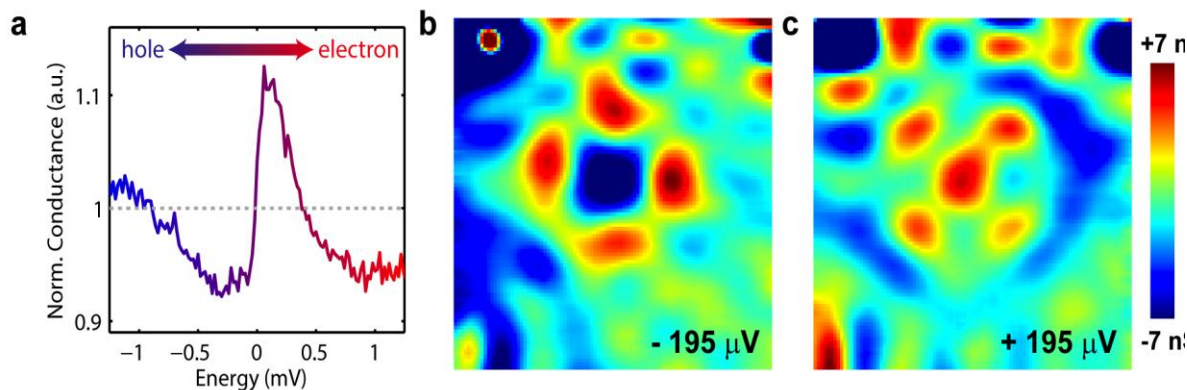


Figure 2. An impurity in an unconventional superconductor locally disturbs the Cooper pairs of the electron sea. In a), we determine that this particular impurity attracts the electron component of the Cooper pair as its spectrum shows an enhancement at positive energies relative to the spectrum far away from it. The characteristic energy-dependent spatial patterns of how this impurity locally perturbs superconductivity (shown for negative and positive energy in b) and c), respectively) directly reveal the symmetry of unconventional Cooper pairing in this compound.

Incipient Charge Order & its Interplay with High Temperature Superconductivity in Cuprates

Our group continues to probe the electronic states of the high- T_c cuprates superconductors in their pseudogap and superconducting states. In a series of recent experiments (reported by Parker *et al.*, *Nature* 2010), we have reported that the onset of pseudogap behavior in Bi-based cuprates coincides with the appearance of real space electronic modulations with near 4-lattice constant spacing. Recently, we have focused on understanding the interplay between this ordering phenomena and superconductivity in the cuprates. Through a series of more recent on going experiments we have been able to confirm for the first time that such charge organization is indeed competing with pairing in the cuprates. In addition, we have recently examined the claims that in addition to these modulated patterns electronic states in cuprates develop neumatic order and breaks C4 symmetry on the atomic scale. Through a set of comprehensive experiments, we have established that the likely cause of these neumatic signatures in STM studies is not due to neumatic electronic ordering but rather due to anisotropy of the STM tips used in typical experiments [3].

New Instrumentation: Spin Polarized & Ultra-low Temperature High magnetic field STM

Through a supplementary DOE instrumentation grant, we have been developing a spin polarized STM capable of performing spin resolved experiments on correlated materials. We have have finished the construction of this new instrument and have successfully had several runs with spin-polarized tip. Currently, we are focused on developing more reliable methods for fabrication of anti-ferromagnetic tips

than previously reported in the literature. A key advantage of such tips is that they do not alter the magnetic properties of the sample during the measurements and are not sensitive to application of an external field that alters the magnetic texture of the sample. A likely first candidate for the new machine is the study of anti-ferromagnetism in the heavy fermion 115 compounds, for which we have already obtained STM results without spin-polarized tips.

In addition to the development of an instrument dedicated to spin-polarized measurements, our group has completed developing the capabilities for STM measurements at millikelvin temperatures and in magnetic fields of up to 14 Tesla. Our instrument is already functional and used in the studies described above. Such capability will be critical to study heavy electron systems as well as to probe correlated systems generically with high resolutions. In addition, this instrument will be used for the development of atomic scale Josephson microscopy in which we will use a superconducting tip and probe its Josephson coupling with a superconducting sample on the atomic scale.

Future Plans:

We will continue to explore the physics of correlated superconductors through various experiments on heavy fermion and cuprate superconductors, with an emphasis on understanding the competition between superconductivity and other types ordering phenomena that is possible in these systems. We are also in the process of developing our Josephson STM capability using our newly constructed dilution fridge ultra low temperature STM.

Publication Supported by the DOE-BES (2011-August 2013):

In addition to publications directly related to DOE-BES projects, the DOE funds that support the instrumentation in our lab have assisted other projects. The publications from these projects benefiting from DOE support are also included in the list below (marked as partially supported by DOE).

1. P. Aynajian, E. H. da Silva Neto, A. Gynis, R. E. Baumbach, J. D. Thompson, Z. Fisk, E. D. Bauer, and A. Yazdani, "Visualizing heavy fermions emerging in a quantum critical Kondo lattice," *Nature* **486**, 201 (2012). Fully supported by DOE.
2. B. Zhou, S. Misra, E. H. da Silva Neto, P. Aynajian, R. E. Baumbach, J. D. Thompson, E. D. Bauer, and A. Yazdani, "Visualizing Nodal Heavy Fermion Superconductivity," *Nature Physics* **9**, 474 (2013). (Covered in News & Views) Fully supported by DOE.
3. E. H. da Silva Neto, P. Aynajian, R. E. Baumbach, E. D. Bauer, J. Mydosh, S. Ono, and A. Yazdani, "Detection of electronic nematicity using scanning tunneling microscope," *Physical Review B* **87**, 161170 (2013). (Editors choice). Fully supported by DOE.
4. S. Misra, L. Urban, M. Kim, G. Sambandamurthy, and A. Yazdani, "Measurements of the Magnetic-Field-Tuned Conductivity of Disordered Two-Dimensional Mo₄₃Ge₅₇ and InO_x Superconducting Films: Evidence for a Universal Minimum Superfluid Response," *Physical Review Letters*, **110**, 037002 (2013). *Partially supported by the DOE.*
5. E. H. da Silva Neto, C. V. Parker, P. Aynajian, A. Pushp, J. Wen, Zhijun Xu, G. Gu, and A. Yazdani, "Scattering from incipient stripe order in the high-temperature superconductor Bi₂Sr₂CaCu₂O_{8+d}," *Physical Review B* **85**, 104521 (2012). Fully supported by DOE.
6. E. H. da Silva Neto, C. V. Parker, P. Aynajian, A. Pushp, J. Wen, Z. Xu, G. Gu, and A. Yazdani, "Detecting incipient stripe order in the high-temperature superconductor Bi₂Sr₂CaCu₂O_{8+d}," *Physica C* **481**, 153 (2012). Fully supported by DOE.
7. H. Beidenkopf, P. Roushan, J. Seo, L. Gorman, I. Drozdov, Y. S. Hor, R. J. Cava, and A. Yazdani, "Spatial Fluctuations of Helical Dirac Fermions on the Surface of Topological Insulators," *Nature Physics* **7** 939 (2011). Partially supported by the DOE.

AProgram Title: Novel Sp₂-Bonded Materials and Related Nanostructures

Principal Investigator: A. Zettl; Co-PIs: C. Bertozzi, M.L. Cohen, M. Crommie, A. Lanzara, S. Louie; Other Collaborator: F. Wang

**Mailing Address: Department of Physics, University of California, Berkeley, CA 94720
E-mail: azettl@berkeley.edu**

Program Scope

This project concerns the design, synthesis, characterization, and evaluation for technological application, of novel materials based primarily on sp²-bonding configurations and nominally of nanoscale dimensions. The sought-after characteristics of the materials, composed largely of lightweight but strong covalent-bonding upper-row elements of the period table (including carbon, nitrogen, and boron), include exceptional electronic, optical, thermal, and mechanical properties. The research approach consists of closely coordinated efforts of theoretical predictions of new materials, structures, and electronic and electromechanical devices; experimental synthesis of such materials and systems using a variety of techniques including non-equilibrium plasma growth, laser ablation, CVD, high pressure synthesis, wet chemistry methods and biological functionalization, and atomic-scale manipulation; and characterization of the materials and devices on the atomic, molecular, and macroscopic scale using microscopy, photoemission, optical response, general transport, and mechanical properties measurements. The materials, devices, and associated systems are evaluated for technological applications. Planar and high-curvature sp²-bonded structures are useful building blocks for a host of new materials with unique properties relevant to the BES scientific/technical mission, including materials with high elastic modulus, high thermal conductivity, molecular-scale electronic functionality and chemical and biological sensor capability, and superior gas-adsorption. The project merges a tailor-made theoretical prediction platform with advanced and demonstrated synthesis and characterization capabilities. The project relies heavily on specialized resources available at LBNL including the National Center for Electron Microscopy, the Molecular Foundry, the National Energy Research Scientific Computing Center, and the Advanced Light Source.

Recent Progress

Progress in Theoretical Studies Theory efforts have focused on the electronic, structural and optical properties of novel sp²-bonded materials, with emphasis on close collaborations with the experimental activities in this program to provide basic understandings and guidance. *ab initio* calculations have been performed on properties of quasiparticles (dispersion and lifetimes) in graphene systems treating electron-electron and electron-phonon interactions in equal footing, which have explained ARPES and STS measurements.¹ Predictions have been made on magnetic edge states in chiral graphene nanoribbons which have been seen in STS measurements.² A possible route to the separation of zigzag graphene nanoribbons was proposed.³ New Dirac Fermions were predicted in periodically modulated bilayer graphene.⁴

A theory was developed to explain the tunable phonon-exciton Fano phenomenon in the optical spectrum of bilayer graphene observed experimentally^{5,6}. Novel and tunable properties associated with excitons in biased bilayer graphene were predicted⁷. Theoretical calculations on the structure and properties topological defects (dislocations and grain boundaries) in graphene were carried out⁸ leading to discovery of novel transport effects through grain boundaries. Theoretical explanation to several important experiments performed in the program including

charging and screening of adatoms on graphene⁹ and the structure and dynamics of atoms on graphene edges and point defects on BN sheet¹⁰ was provided. *ab initio* calculations and detailed theoretical studies of the optical properties of over 200 single-walled carbon nanotubes

[SWCNTs] were preformed, leading to the construction and systematic understanding of the family behaviors of the atlas of SWCNTs,¹¹ and a theory was developed to explain the orientation angle dependence of the Raman spectra of rotated double-layer graphene as observed experimentally (Fig. 1).¹²

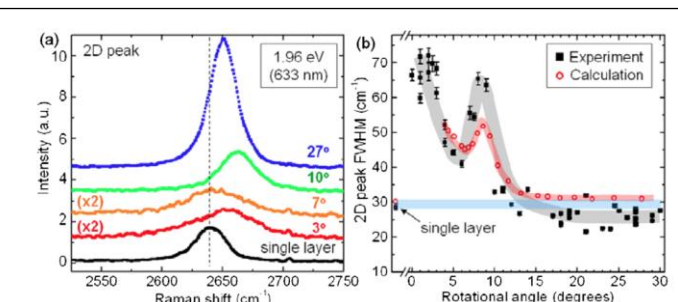


Fig. 1. Comparison between theory and experiment of Raman spectrum of rotated double-layer graphene. (a) Raman intensity of 2D peak and (b) comparison of theory vs experiment of 2D peak intensity.

potassium doped C_{60} chain encapsulated in a boron nitride nanotube are studied¹³.

Progress in Experimental Studies A new synthesis method has been developed for the growth of epitaxial graphene on a SiC substrate.¹⁴ With respect to other existing methods, this growth method is quite simple and provides a good control of the graphene thickness and sample quality. Sample thickness and quality have been monitored by ARPES. Using new functionalization chemistries multifunctional imaging probes have been developed based on single-walled carbon nanotubes for *in vivo* applications. Carbon nanotubes were functionalized with dibenzoazacyclooctyne (DIBAC) moieties to target them to metabolically labeled cell-surface sialic acid residues *in vivo*.

A new graphene liquid cell has been invented that allows *in-situ* atomic resolution TEM investigation of nanostructures suspended in liquids¹⁵ [Fig. 2]. Initial studies on Pt nanocrystals using the TEAM microscope at the National Center for Electron Microscopy reveal details on nanocrystal growth, fusing, active crystallographic faces, and dynamics within the fluid. A new technique of Dirac point mapping was developed by integrating gated graphene devices with low temperature STM spectroscopy. Measurements were performed on individual Co atoms deposited onto back-gated graphene devices. It was discovered that the electronic structure of Co adatoms can be tuned by application of the device gate voltage, and that individual Co atoms can be reversibly ionized.¹⁶ It was found that BN substrates result in extraordinarily flat graphene layers that display microscopic Moire patterns and a significant reduction in local microscopic charge inhomogeneity compared to graphene on SiO_2 .¹⁷ Using cryogenic STM spectroscopy, a direct measurement was carried out of the nanoscale response of Dirac fermions to individual Coulomb potentials placed on a gated graphene device. This work allowed a confirmation of predictions regarding how Dirac fermions behave near subcritical Coulomb potentials, as well as a determination of graphene's intrinsic interband dielectric constant: $\epsilon = 3.0 \pm 1.0$.¹⁸

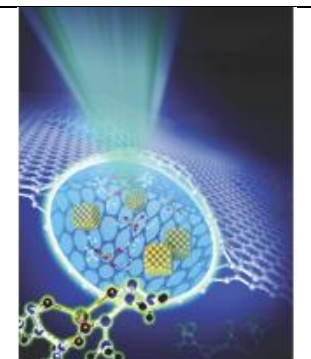


Fig. 2. Artists rendition of graphene liquid cell for use in TEM imaging.

Photoemission has been used to gain an understanding of the quantum many-body interactions in graphene, such as the Coulomb interaction among electrons (electron-electron interaction) and the electron-phonon interaction, as well as the interplay between them.¹⁹ When the dielectric screening was changed through the substrate, it was found that that the nonlinearity and the velocity of the energy spectrum become dramatically enhanced, with values as high as $\sim 2.5 \times 10^6$, which is at least 2.3 times higher than graphene on any other substrate, when the electron-electron interaction is increased. ARPES measurements, performed at the Advanced Light Source, can be used to directly measure the phase of the band wave-function and the sign of matrix elements for non equivalent orbitals of both single and double layers graphene.²⁰ In a coupled theory-experiment effort, the Berry's phase and the sign of the hopping integral between nonequivalent orbitals in graphene (a quantity never measured for any material before) were extracted.

The built-in electrical potential of bi-phase nanocrystals has been measured directly using specialized electrostatic force microscopy. These crystals have photovoltaic relevance. Graphene and narrowly-defined metal fingers have been used to realize externally gate tunable pn junctions in silicon and other semiconductors.²¹ Graphene membranes have been mechanically distressed until rupture; details of the atom geometry at the tears are investigated via atomic resolution TEM using the TEAM microscope at the National Center for Electron Microscopy. Armchair and zigzag edges are clearly resolved at the ruptures.²² In graphene, where charge carriers behave as massless relativistic particles, it has been predicted that highly charged impurities should exhibit resonances corresponding to atomic collapse states. The formation of such resonances has been observed²³ around artificial nuclei (clusters of charged calcium dimers) fabricated on gated graphene devices via atomic manipulation with a scanning tunneling microscope (STM).

Future Plans

Because of strong many-electron interaction effects, the optical oscillator strengths of excitons in the full class range of nanotubes have not been elucidated. This project seeks to carry out *ab initio* GW-BSE calculations and extend Hubbard Hamiltonian studies to obtain basic understanding and analytical, quantitative scaling relations of the diameter and family dependences of the excitation energies and oscillator strengths of the dominant exciton transitions in arbitrary SWCNTs.

TEM studies of nanoparticles in liquid using graphene liquid cell (GLC) technology will be expanded. Some of this work will be performed at the National Center of Electron Microscopy. Of particular interest will be the formation of nanoscale metal alloys. Graphene (and BN-based) sandwiches and veils will be constructed from magnetic and optically active nanostructures and explored via appropriate spin-polarized STM, photoemission, optics, and transport measurements. Higher-order BNNT and CNT structures adapted for specific function, including coupling to plasmonic nanocrystals, mated to graphene and hBN, and mated to cell surface glycans will be explored, including using hydrophobic adsorption and covalent crosslinking approaches.

This project will explore the behavior of spin and spin-orbit impurities on graphene and graphene based nanostructures. Phenomena such as the Kondo effect will be investigated using high-resolution low temperature STM spectroscopy.

References and Publications (which acknowledge DOE support)

1. C-H. Park, F. Giustino, C.D. Spataru, M.L. Cohen, and S.G. Louie. Inelastic carrier lifetime in bilayer graphene. *Appl. Phys. Lett.* **100**, 032106 (2012)
2. O.V. Yazyev, R.B. Capaz, S.G. Louie. Theory of magnetic edge states in chiral graphene nanoribbons. *Phys. Rev. B* **84**, 115406 (2011)
3. H.K. Lee, M.L. Cohen, and S.G. Louie. Selective functionalization of halogens on zigzag graphene nanoribbons: A route to the separation of zigzag graphene nanoribbons. *Appl. Phys. Lett.* **97**, 233101 (2010)
4. L.Z. Tan, C-H. Park, and S.G. Louie. New Dirac fermions in periodically modulated bilayer graphene. *Nano Lett.* **11** 2596 (2011)
5. T-T. Tang, Y. Zhang, C-H. Park, B. Geng, C. Girit, Z. Hao, M.C. Martin, A. Zettl, M.F. Crommie, S.G. Louie, Y.R. Shen, and F. Wang. A tunable phonon-exciton fano system in bilayer graphene. *Nature Nanotech.* **5**, 32 (2010)
6. B.S. Geng, J. Horng, Y.B. Zhang, T.T. Tang, C-H. Park, C. Girit, Z. Lao, M. Martin, A. Zettl, M.F. Crommie, S.G. Louie, and F. Wang. Optical spectroscopy of bilayer graphene. *Phys. Status Solidi B* **247**, 2931 (2010)
7. C-H. Park and S.G. Louie. Tunable excitons in bilayer graphene. *Nano Lett.* **10**, 426 (2010)
8. O.V. Yazyev, R.B. Capaz, and S.G. Louie. One-dimensional structural irregularities in graphene chiral edges and grain boundaries. *J. Physics: Conference Series* **302**, 012016 (2011)
9. V.W. Brar, et al. Gate-controlled ionization and screening of cobalt adatoms on a graphene surface. *Nature Physics* **7**, 43 (2011)
10. N. Alem, et al. Probing the out-of-plane distortion of single point defects in atomically thin hexagonal boron nitride at the picometer scale. *Phys. Rev. Lett.* **106**, 126102 (2011)
11. K. Liu, et al. *Nature Nanotech.* **7**, 325 (2012)
12. K. Kim, et al. *Phys. Rev. Lett.* **108**, 246103 (2012)
13. T. Koretsune, S. Saito, and M.L. Cohen. One-dimensional alkali-doped C₆₀ chains encapsulated in BN nanotubes. *Phys. Rev. B* **83**, 193406 (2011)
14. X.Z. Yu, et al. *Journal of Electron Spectroscopy and Related Phenomena* **184**, 100-106 (2011)
15. J.M. Yuk, et al. High-resolution EM of colloidal nanocrystal growth using graphene liquid cells. *Science* **336**, 61-64 (2012)
16. V. W. Brar, et al. Gate-controlled ionization and screening of cobalt adatoms on a graphene surface. *Nature Physics* **7**, 43-47 (2011)
17. R. Decker, et al. *Nano Lett.* **11**, 2291-2295 (2011)
18. Y. Wang, et al. Mapping Dirac quasiparticles near a single coulomb impurity on graphene. *Nature Physics*, (2012)
19. D.A. Siegel, C.G. Hwang, A.V. Fedorov, and A. Lanzara. Electron-phonon coupling in highly screened graphene. *New Journal of Physics* (2012)
20. C. Hwang, et al. Direct measurement of quantum phases in graphene via photoemission spectroscopy. *Phys. Rev. B* **84**, 125422 (2011)
21. W. Regan, et al. Screening-engineered field-effect solar cells. *Nano Lett.* (**web**) (2012)
22. K. Kim, et al. Ripping graphene: preferred directions. *Nano Lett.* **12**, 293–297 (2011)
23. Y. Wang, et al. Observing subatomic collapse in artificial nuclei on graphene. *Science (express)* **1234320** (2013)

Emergent Phenomena in Quantum Hall Systems Far From Equilibrium

Michael Zudov

School of Physics and Astronomy, University of Minnesota - Twin Cities, Minneapolis, MN 55455, USA

E-mail: zudov@physics.umn.edu Web: <http://groups.physics.umn.edu/zudovlab/>

Program Scope

The project focuses on magnetotransport phenomena in semiconductor nanostructures driven away from equilibrium by microwave and sub-THz radiation. The main objective of the proposal is to advance our understanding of how these phenomena originate from the behavior of individual electrons due to their interactions with high frequency photons in quantizing magnetic fields. The research expands upon the area of non-equilibrium quantum transport in very high Landau levels [1] of two-dimensional electron systems (2DES), originated by discoveries of microwave-induced resistance oscillations (MIRO) [2] and zero-resistance states [3] about a decade ago. The project explores *new* fundamental phenomena emerging in *separated Landau levels* of non-equilibrium 2DES focusing on (i) *giant microwave photoresistance effects* in the vicinity of the cyclotron resonance and its second harmonic, (ii) *microwave photoresistance in the regime of Shubnikov-de Haas oscillations*, (iii) search for *non-equilibrium phenomena in the quantum Hall effect regime and other 2D systems*, and (iv) search for *interference effects in photocurrent and photoresistance*.

Recent Progress

Giant photoresistance effects near cyclotron resonance at sub-Terahertz frequencies. Extending experiments on photoresistance of ultra-high mobility 2DES to higher radiation frequencies allows to enter regimes of Shubnikov-de Haas oscillations (SdHO) or even of quantum Hall effect, which remain largely unexplored but are likely to reveal interesting physics and novel nonequilibrium phenomena.

We have recently investigated microwave photoresistance at radiation frequencies ranging from

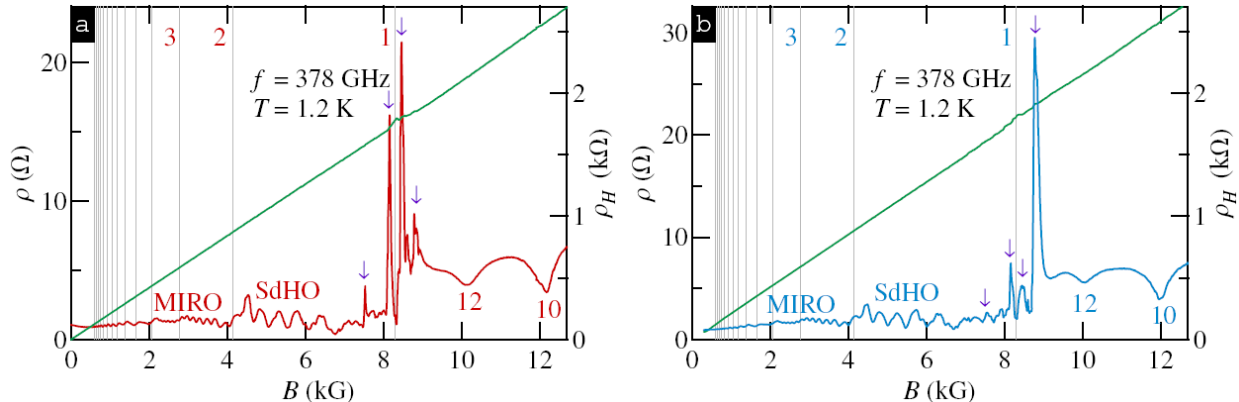


Fig. 1: Longitudinal $\rho(B)$ (left axes) and Hall $\rho_H(B)$ (right axes) magnetoresistivities obtained in (a) positive and (b) negative sweep direction of the magnetic field. The magnetic field sweep rate was 0.2 T/min. Vertical lines in are drawn at the harmonics (marked by 1, 2, 3) of the cyclotron resonance. SdHO minima are marked by filling factor $v = 10, 12$. Sharp photoresistance spikes near the cyclotron resonance are marked by \downarrow . The microwave frequency and temperature were $f = 378$ GHz and $T = 1.2$ K, respectively.

200 to 400 GHz. An example of the photoresponse measured at frequency $f = 378$ GHz and temperature $T = 1.2$ K is presented in Fig. 1. Here, the data in panel (a) [(b)] were obtained as the magnetic field was swept in the positive [negative] direction at a rate of 0.2 T/min. In both cases one observes giant photoresistance signal in the vicinity of the cyclotron resonance (see vertical line marked by “1”), which reveals *a series* of very sharp peaks which exceed dark resistivity by an order of magnitude. Remarkably, direct comparison of the data in Fig. 1(a) and Fig. 1(b) shows that the height of these peaks (marked by ↓) depends sensitively on the sweep direction. Furthermore, the photoresponse in the longitudinal resistance near the cyclotron resonance is accompanied by a concomitant photo-induced structure in the Hall resistivity. We have also found that this giant photoresistance effect appears to be extremely sensitive to the radiation intensity, exhibiting strongly superlinear power dependence. Another interesting aspect of these data is that even at this high frequency, MIRO are clearly resolved, persisting up to the 20-th order, while coexisting with SdHO over a wide range of magnetic fields.

(ii) **Microwave photoresistance in the regime of Shubnikov-de Haas oscillations** Using lower radiation intensity allows to extend photoresistance measurements to considerably lower temperatures, at which magnetotransport is usually dominated by prominent Shubnikov-de Haas oscillations. We have recently performed such measurements which revealed unexpected new features. Figure 2 shows longitudinal magnetoresistivity, obtained at the same microwave frequency as the data shown in Fig. 1, but at a considerably lower power and temperature $T = 0.38$ K. In contrast to higher-power, higher-temperature data shown in Fig. 1, giant photoresistance peaks in the vicinity of the cyclotron resonance are no longer observed. Instead, the data reveal strong suppression of the SdHO amplitude near the cyclotron resonance; the SdHO minimum at $\nu = 14$ is considerably weaker than the lower- B minimum at $\nu = 16$, while the minimum at $\nu = 12$ is barely visible. Similar observations can be made for the neighboring SdHO maxima at odd filling factors, i.e. at $\nu = 15, 13$. In addition to the suppression near the cyclotron resonance, the data also reveal suppression of the SdHO amplitude near its harmonics. The most interesting feature of the data shown in Fig. 5(a) is what at first glance appears as noise near the cyclotron resonance. However, this fine structure turned out to be highly reproducible and its strength was found to depend sensitively on microwave power. A closer look at this

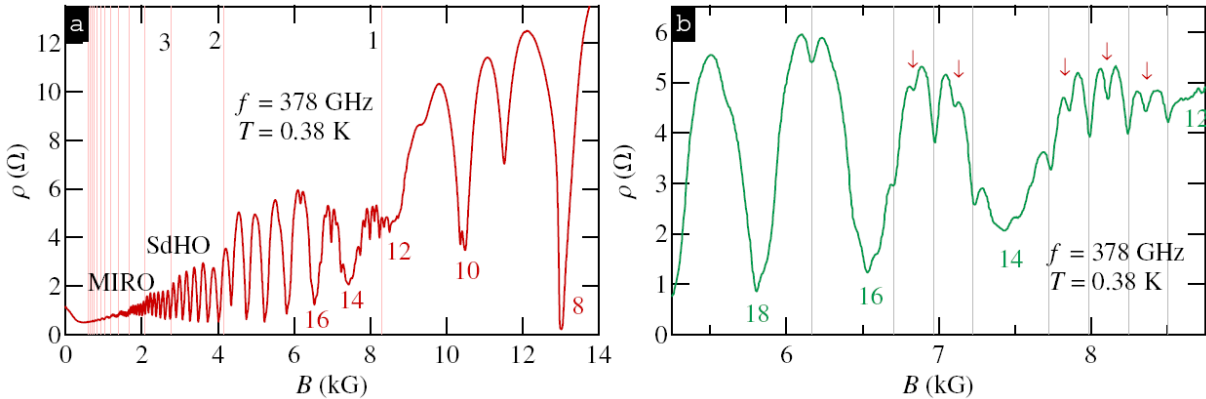


Fig. 2: (a) Magnetoresistivity $\rho(B)$ under microwave irradiation of frequency $f = 378$ GHz measured at temperature $T = 0.38$ K. Vertical lines in (a) are drawn at the harmonics (marked by 1, 2, 3) of the cyclotron resonance. SdHO minima are marked by filling factor $\nu = 8, 10, 12, 14, 16$. (b) Zoomed-in part of the data shown in (a) near the cyclotron resonance. A series of “deep” radiation-induced minima is marked by vertical lines, separated by $\delta B = 0.26$ kG. A series of “shallow” radiation-induced minima is marked by ↓.

structure, presented in Fig. 2(b), reveals that it is a series of extrema, which are roughly equally spaced in magnetic field. The extrema appear to be more pronounced near the SdHO maxima, i.e., near odd filling factors $\nu = 17, 15$ and especially, near $\nu = 13$. In contrast to giant photoresistance peaks discussed above, this oscillatory structure appears to be insensitive to the magnetic field sweep direction and exhibits no hysteresis. More careful examination of this structure near $\nu = 13$ reveals that there are, in fact, two series of radiation-induced minima. Indeed, there exists a series of “deep” minima, marked by vertical lines (separated by $\delta B = 0.26$ kG) and a series of “shallow” minima, marked by ↓, which appear roughly in the middle between neighboring “deep” minima. Similar observations can be made near $\nu = 15$ and one “deep” minimum can also be seen near $\nu = 17$. While the “deep” minima in the close vicinity of $\nu = 15$ and $\nu = 17$ appear at the same magnetic fields where one expects to see minima due to spin splitting (such as the minimum at $\nu = 9$), the features under consideration are considerably sharper and are clearly caused by microwave radiation. Understanding the origin of this oscillatory structure remains a subject of future studies.

Future Plans

Our future plans include experiments which will:

- (i) search for phase-sensitive contributions in photocurrent and photoresistance under bichromatic irradiation
- (ii) establish the origin of radiation-induced suppression of SdHO near the harmonics of the cyclotron resistance
- (iii) study the effects of dc electric field on giant photoresistance effects near the cyclotron resonance and its second harmonic [4-6].
- (iv) search for nonequilibrium effects in other 2D systems, such as graphene, and in the quantum Hall effect regime

References

- [1] I. A. Dmitriev, A. D. Mirlin, D. G. Polyakov, and M. A. Zudov, “Nonequilibrium phenomena in high Landau levels”, *Rev. Mod. Phys.* **84**, 1709 (2012).
- [2] Zudov *et al.*, *Phys. Rev. B* **64**, 201311(R) (2001), Ye *et al.*, *Appl. Phys. Lett.* **79**, 2193 (2001)
- [3] Mani *et al.*, *Nature* **420**, 646 (2002), Zudov *et al.*, *Phys. Rev. Lett.* **90**, 046807 (2003), Willett *et al.*, *Phys. Rev. Lett.* **93**, 026804 (2004), Smet *et al.*, *Phys. Rev. Lett.* **95**, 116804
- [4] Dai *et al.*, *Phys. Rev. Lett.* **105**, 246802 (2010).
- [5] Hatke *et al.*, *Phys. Rev. B* **83**, 121301(R) (2011).
- [6] Hatke *et al.*, *Phys. Rev. B* **83**, 201301(R) (2011).

Publications

- (i) Q. Shi, M. Khodas, A. Levchenko, and M. A. Zudov, “I Phase-sensitive bichromatic photoresistance in a two-dimensional electron gas” (2013) (submitted)
- (ii) A. Bogan, A. T. Hatke, S. A. Studenikin, A. S. Sachrajda, M. A. Zudov, L. N. Pfeiffer, and K. W. West, “Effect of an in-plane magnetic field on microwave photoresistance and

- Shubnikov-de Haas effect in high-mobility GaAs/AlGaAs quantum wells”, *Journal of Physics: Conference Series* **456**, 012004 (2013) (published)
- (iii) A. T. Hatke, M. A. Zudov, J. D. Watson, M. J. Manfra, L. N. Pfeiffer, and K. W. West, “Effective mass from microwave photoresistance measurements in GaAs/AlGaAs quantum wells”, *Journal of Physics: Conference Series* **456**, 012040 (2013) (published)
 - (iv) A. T. Hatke, M. A. Zudov, L. N. Pfeiffer, and K. W. West, “Shubnikov-de Haas oscillations at very high tilt angles”, *Journal of Physics: Conference Series* **456**, 012041 (2013) (published)
 - (v) A. T. Hatke, M. A. Zudov, J. D. Watson, M. J. Manfra, L. N. Pfeiffer, and K. W. West, “Evidence for effective mass reduction in GaAs/AlGaAs quantum wells”, *Physical Review B – Rapid Communications* **87**, 161307(R) (2013) (published)
 - (vi) I. A. Dmitriev, A. D. Mirlin, D. G. Polyakov, and M. A. Zudov, “Nonequilibrium phenomena in high Landau levels”, *Reviews of Modern Physics* **84**, 1709 (2012) (published)
 - (vii) A. Bogan, A. T. Hatke, S. A. Studenikin, A.S. Sachrajda, M.A. Zudov, L.N. Pfeiffer, and K.W. West, “Microwave-induced resistance oscillations in tilted magnetic fields”, *Physical Review B* **86**, 235305 (2012) (published)
 - (viii) A. T. Hatke, M. A. Zudov, L. N. Pfeiffer, and K. W. West, “Nonlinear response in overlapping and separated Landau levels of GaAs quantum wells”, *Physical Review B – Rapid Communications* **86**, 081307(R) (2012) (published)
 - (ix) A. T. Hatke, M. A. Zudov, L. N. Pfeiffer, and K. W. West, “Shubnikov-de Haas oscillations in tilted magnetic fields”, *Physical Review B – Rapid Communications* **85**, 241305(R) (2012) (published)
 - (x) A. T. Hatke, M. A. Zudov, J. D. Watson, and M. J. Manfra, “Magnetoplasmon resonance in a two-dimensional electron system driven into a zero-resistance state”, *Physical Review B–Rapid Communications* **85**, 121306(R) (2012) (published)
 - (xi) A. T. Hatke, M. A. Zudov, J. L. Reno, L. N. Pfeiffer, and K. W. West, “Giant negative magnetoresistance in a high-mobility 2DES”, *Physical Review B – Rapid Communications* **85**, 081304(R) (2012) (published)
 - (xii) M. A. Zudov, A. T. Hatke, H. -S. Chiang, L. N. Pfeiffer, K. W. West, and J. L. Reno “Nonequilibrium transport in very high Landau levels”, *Journal of Physics: Conference Series* **334**, 012007 (2011) (published)
 - (xiii) A. T. Hatke, M. A. Zudov, L. N. Pfeiffer, and K. W. West, “Microwave photoresistance in a 2D electron gas in separated Landau levels”, *Physical Review B – Rapid Communications* **84**, 241304(R) (2011) (published)
 - (xiv) A. T. Hatke, M. A. Zudov, L. N. Pfeiffer, and K. W. West, “Non-linear response of a high mobility two-dimensional electron system near the second harmonic of the cyclotron resonance”, *Physical Review B - Rapid Communications* **83**, 201301 (R) (2011) (published).
 - (xv) A. T. Hatke, M. A. Zudov, L. N. Pfeiffer, and K. W. West, “Giant microwave photoresistivity in a high-mobility quantum Hall system”, *Physical Review B – Rapid Communications* **83**, 121301(R) (2011) (published).
 - (xvi) A. T. Hatke, M. A. Zudov, L. N. Pfeiffer, and K. W. West, “Resistance oscillations induced by the Hall field in tilted magnetic fields”, *Physical Review B – Rapid Communications* **83**, 081301(R) (2011) (published).

Author Index

Abbamonte, Peter	233
Adams, Philip W.	123
Analytis, James	317
Anderson, E. H.	261
Andrei, Eva Y.....	201
Aronson, M. C.	65
Ashoori, Raymond	205
Bader, Sam	213
Balicas, Luis	209
Basov, D. N.	185
Bawendi, Moungi	181
Bell, C.	3
Bertozzi, C.	373
Bezryadin, Alexey	233
Bhattacharya, Anand.....	213
Bird, Jonathan.....	135
Birge, Norman O.	175
Birgeneau, Robert	317
Biswas, Rana	109
Blumberg, Girsh	217
Boatner, L. A.	341
Bockrath, Marc	289
Bourret, Edith	317
Buchanan, Kristen	51
Bud'ko, S.	225
Budakian, Raffi	233
Butov, Leonid.....	221
Canfield, P.	77, 225
Cantoni, C.	341
Cao, Gang	245
Chao, W.	261
Chi, M.	15
Christen, Hans M.	15
Civale, L.....	229
Cohen, M. L.	373
Cooper, S. Lance	233
Crabtree, G. W.	285
Crespi, Vincent	47
Crommie, M.	373
Csathy, Gabor.....	145
Dai, P.	77
Davidovic, Dragomir	237
Davis, J. C. Séamus	241
De Long, L. E.	245
Dobrovitski, Viatcheslav.....	109
Drew, H. Dennis	249
Du, Rui-Rui	149
Eckstein, James N.	233
Engel, Lloyd W.....	253
Eom, Chang-Beom	7
Eres, G.....	15
Eskildsen, M. R.	77
Fadley, C. S.	261
Feldman, L. C.	113
Field, Stuart	159
Finkelstein, Gleb.....	257
Fischer, P.	261
Fradkin, Eduardo H.	233
Furukawa, Y.	225
Goldhaber-Gordon, D.	59
Goldman, Allen M.	265
Gray, K. E.	69
Greene, Laura H.	233
Greven, M.	77
Gullikson, E. M.	261
Guyot-Sionnest, Philippe	269
Hadjipanayis, George C.	55, 349
Haglund, Jr., Richard F.	189
Halperin, W. P.	77
Harrison, N.	171
Hastings, J. Todd	245
Hellman, F.	261
Heremans, Jean J.	127
Hikita, Y.	3
Hla, Saw Wai.....	273
Ho, Kai-Ming	109
Hoffmann, Axel	131
Homes, C.	281
Hughes, Taylor	233
Hwang, H. Y.	3
Jaime, M.	171
Jarillo-Herrero, Pablo	277
Jiang, Zhigang	95
Johnson, P. D.	281
Johnston, D.	225
Johnston-Halperin, Ezekiel	365
Kaminski, A.	225
Kapitulnik, A.	77
Kent, P.R.C.	357
Kim, B. J.	69
Kim, Philip	99
Kogan, V.	225

Kono, Junichiro	87
Kortright, J. B.	261
Koshelev, A. E.	285
Kwok, W.-K.	285
Lanza, Alessandra	317, 373
Lau, Chun Ning (Jeanie).....	289
Lee, Dung-Hai	317
Lee, H. N.	15
Lee, Minhyea.....	43
Leggett, Anthony J.	233
Lemberger, Thomas R.	293
Li, Lu	297
Li, Qi.....	163
Lilly, M.P.	329
Liu, Ying.....	301
Louie, S.	373
Lüpke, G.....	113, 305
Mandrus, D.	341
Manfra, Michael	145
Mani, R. G.	309
Manoharan, H. C.	59
Maple, M. Brian	313
Mascarenhas, Angelo.....	105
Mason, Nadya.....	233
McDonald, R. D.	171
McGuire, M. A.	341
Millis, Andy	21
Mitchell, J. F.	69
Moore, Joel	317
Musfeldt, Janice L.	37
Natelson, Douglas.....	25
Naulleau, P.	261
Novotny, Lukas	83
Orenstein, Joseph W.	59, 317
Osgood, R. M.	21
Ouyang, Min	321
Paglione, Johnpierre	325
Pak, Jeongihm	353
Pan, W.	329
Pechan, Michael	333
Pellegrini, V.	337
Pinczuk, A.	337
Prasankumar, R.	329
Pratt, Jr., William P.	175
Prozorov, R.	225
Raghu, S.	3
Ramesh, Ramamoorthy.....	317
Reno, J. L.	329
Rokhinson, Leonid P.	153
Rosenbaum, Thomas F.	119
Rouleau, C. M.	15
Sales, B. C.	341
Samarth, Nitin.....	47
Schiffer, Peter	47
Schuller, Ivan K.	33
Sefat, Athena S.	345
Sellmyer, David J.	55, 349
Seo, S. S.	245
Shaner, E. A.	329
Shayegan, M.	141
Shinar, Joseph.....	109
Singleton, J.	171
Skomski, Ralph	349
Smirnov, Dmitry	95
Smith, Arthur R.	353
Smith, Kevin E.	29
Snijders, P.C.	357
Soukoulis, Costas.....	109
Stewart, G. R.	73
Tanatar, M.	225
Thomas, John E.	167
Tolk, N. H.	113
Tsui, D. C.	329
Van Harlingen, Dale J.	77, 233
Vishveshwara, Smitha	233
Vishwanath, Ashvin	317
Vlasko-Vlosov, V.	285
Wang, Feng	91, 373
Wang, G. T.	329
Ward, T. Z.	15
Weitering, H.H.	357
Wells, Barrett O.	11
Welp, U.	285
Westervelt, R. M.	361
Wind, S. J.	337
Xiao, Z. L.	285
Yang, Fengyuan.....	365
Yazdani, Ali	369
Zapf, V.	171
Zettl, A.	373
Zhang, S.-C.....	59
Zudov, Michael.....	377

Participant List

Participant List

Name	Organization	E-Mail Address
Abbamonte, Peter	University of Illinois, Urbana-Champaign	abbamonte@mrl.illinois.edu
Adams, Philip	Louisiana State University	adams@phys.lsu.edu
Analytis, James	Lawrence Berkeley National Laboratory	janalytis@lbl.gov
Aronson, Meigan	Brookhaven National Laboratory	maronson@bnl.gov
Ashoori, Raymond	Massachusetts Institute of Technology	ashoori@mit.edu
Balicas, Luis	Florida State University	balicas@magnet.fsu.edu
Basov, Dmitri	University of California, San Diego	dbasov@ucsd.edu
Bawendi, Moungi	Massachusetts Institute of Technology	mgb@mit.edu
Bhattacharya, Anand	Argonne National Laboratory	anand@anl.gov
Bird, Jonathan	University at Buffalo	jbird@buffalo.edu
Birge, Norman	Michigan State University	birge@pa.msu.edu
Blumberg, Girsh	Rutgers University	firsh@physics.rutgers.edu
Bockrath, Marc	University of California, Riverside	marc.bockrath@ucr.edu
Buchanan, Kristen	Colorado State University	kristen.buchanan@colostate.edu
Bud'ko, Sergey	Ames Laboratory	budko@ameslab.gov
Butov, Leonid	University of California, San Diego	lvbutov@ucsd.edu
Christen, Hans	Oak Ridge National Laboratory	christenhm@ornl.gov
Click, Tammy	Oak Ridge Institute for Science and Education	Tammy.Click@orau.org
Crockett, Teresa	U.S. Department of Energy	Teresa.Crockett@science.doe.gov
Csathy, Gabor	Purdue University	gcsathy@purdue.edu
Davenport, James	U.S. Department of Energy	james.davelport@science.doe.gov
Davidovic, Dragomir	Georgia Institute of Technology	dragomir.davidovic@physics.gatech.edu
Davis, JC Séamus	Brookhaven National Laboratory	jcdavis@ccmr.cornell.edu
De Long, Lance	University of Kentucky	delong@pa.uky.edu
Drew, Howard	University of Maryland	hdrew@physics.umd.edu
Du, Rui-Rui	Rice University	rrd@rice.edu
Engel, Lloyd	Florida State University	engel@magnet.fsu.edu
Eom, Chang-Beom	University of Wisconsin-Madison	eom@engr.wisc.edu
Fecko, Christopher	U.S. Department of Energy	Christopher.Fecko@science.doe.gov
Field, Stuart	Colorado State University	field@lamar.colostate.edu
Finkelstein, Gleb	Duke University	gleb@phy.duke.edu
Finnemore, Douglas	Ames Laboratory	finnemor@ameslab.gov
Fischer, Peter	Lawrence Berkeley National Laboratory	pjfischer@lbl.gov
Fitzsimmons, Tim	U.S. Department of Energy	tim.fitzsimmons@science.doe.gov
Goldhaber-Gordon, David	SLAC / Stanford University	goldhaber-gordon@stanford.edu

Name	Organization	E-Mail Address
Goldman, Allen	University of Minnesota	goldman@physics.umn.edu
Guyot-Sionnest, Philippe	University of Chicago	pgs@uchicago.edu
Hadjipanayis, George	University of Delaware	hadji@udel.edu
Haglund, Richard	Vanderbilt University	richard.haglund@vanderbilt.edu
Halperin, William	Northwestern University	w-halperin@northwestern.edu
Harrison, Neil	Los Alamos National Laboratory	nharrison@lanl.gov
Hellman, Frances	University of California, Berkeley / Lawrence Berkeley National Laboratory	fhellman@berkeley.edu
Heremans, Jean J.	Virginia Polytechnic Institute and State University	heremans@vt.edu
Hla, Saw Wai	Ohio University / Argonne National Laboratory	hla@ohio.edu
Hoffmann, Axel	Argonne National Laboratory	hoffmann@anl.gov
Horwitz, James	U.S. Department of Energy	james.horwitz@science.doe.gov
Hsieh, David	California Institute of Technology	dhsieh@caltech.edu
Hwang, Harold	SLAC / Stanford University	hyhwang@stanford.edu
Jarillo-Herrero, Pablo	Massachusetts Institute of Technology	pjarillo@mit.edu
Jiang, Zhigang	Georgia Institute of Technology	zhigang.jiang@physics.gatech.edu
Johnson, Peter	Brookhaven National Laboratory	pdj@bnl.gov
Johnston-Halperin, Ezekiel	Ohio State University	johnston-halperin.1@osu.edu
Kaminski, Adam	Ames Laboratory	kaminski@ameslab.gov
Kim, Philip	Columbia University	pk2015@columbia.edu
Kono, Junichiro	Rice University	kono@rice.edu
Kwok, Wai-Kwong	Argonne National Laboratory	wkwok@anl.gov
Lee, Minhyea	University of Colorado Boulder	minhyea.lee@colorado.edu
Lemberger, Thomas	Ohio State University	tri@physics.osu.edu
Li, Lu	University of Michigan	luli@umich.edu
Li, Qi	Pennsylvania State University	qil1@psu.edu
Liu, Ying	Pennsylvania State University	liu@phys.psu.edu
Luepke, Gunter	College of William and Mary	Luepke@wm.edu
Luican-Mayer, Adina	Rutgers University / Argonne National Laboratory	luican-mayer@anl.gov
Maiorov, Boris	Los Alamos National Laboratory	maiorov@lanl.gov
Manfra, Michael	Purdue University	mmanfra@purdue.edu
Mani, Ramesh	Georgia State University	rmani@gsu.edu
Maple, M. Brian	University of California, San Diego	mbmaple@ucsd.edu
Mascarenhas, Angelo	National Renewable Energy Laboratory	angelo.mascarenhas@nrel.gov
Mason, Nadya	University of Illinois, Urbana-Champaign	nadya@illinois.edu

Name	Organization	E-Mail Address
Mitchell, John	Argonne National Laboratory	mitchell@anl.gov
Musfeldt, Jan	University of Tennessee	musfeldt@utk.edu
Natelson, Douglas	Rice University	natelson@rice.edu
Novotny, Lukas	University of Rochester	lnovotny@ethz.ch
Osgood, Richard	Columbia University	osgood@columbia.edu
Ouyang, Min	University of Maryland	mouyang.umd.edu
Paglione, Johnpierre	University of Maryland	paglione@umd.edu
Pan, Wei	Sandia National Laboratories, New Mexico	wpan@sandia.gov
Pechan, Michael	Miami University	pechanmj@miamiOH.edu
Pinczuk, Aron	Columbia University	aron@phys.columbia.edu
Rokhinson, Leonid	Purdue University	leonid@purdue.edu
Rosenbaum, Thomas	University of Chicago	t-rosenbaum@uchicago.edu
Sales, Brian	Oak Ridge National Laboratory	salesbc@ornl.gov
Schiffer, Peter	University of Illinois, Urbana-Champaign	pschiffe@illinois.edu
Schuller, Ivan	University of California, San Diego	ischuller@ucsd.edu
Schwartz, Andrew	U.S. Department of Energy	andrew.schwartz@science.doe.gov
Sefat, Athena	Oak Ridge National Laboratory	sefata@ornl.gov
Sellmyer, David	University of Nebraska-Lincoln	dsellmyer@unl.edu
Shayegan, Mansour	Princeton University	shayegan@princeton.edu
Shinar, Joseph	Ames Laboratory	shinar@ameslab.gov
Simon, Jonathan	University of Chicago	simonjon@uchicago.edu
Smirnov, Dmitry	Florida State University	smirnov@magnet.fsu.edu
Smith, Arthur	Ohio University Nanoscale & Quantum Phenomena Institute	smitha2@ohio.edu
Smith, Kevin	Boston University	ksmith@bu.edu
Stewart, Greg	University of Florida	stewart@phys.ufl.edu
Thiyagarajan, Pappannan	U.S. Department of Energy	p.thiyagarajan
Thomas, John	North Carolina State University	jethoma7@ncsu.edu
Tolk, Norman	Vanderbilt University	norman.tolk@vanderbilt.edu
Wang, Feng	University of California, Berkeley	fengwang76@berkeley.edu
Weitering, Hanno	University of Tennessee / Oak Ridge National Laboratory	hanno@utk.edu
Wells, Barrett	University of Connecticut	wells@phys.uconn.edu
Westervelt, Robert	Harvard University	westervelt@seas.harvard.edu
Wilson, Lane	U.S. Department of Energy	Lane.wilson@science.doe.gov
Yazdani, Ali	Princeton University	yazdani@princeton.edu
Zettl, Alex	University of California, Berkeley	azettl@physics.berkeley.edu
Zudov, Michael	University of Minnesota	zudov@physics.umn.edu